UNIVERZITA PALACKÉHO V OLOMOUCI

Přírodovědecká fakulta

Katedra biochemie

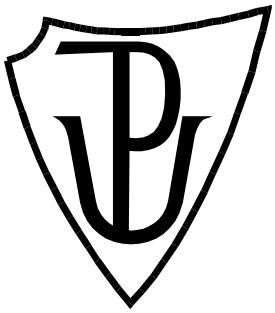

Analýza proteomu pomocí nanoLC-MALDI-TOF/TOF MS a MS/MS

DISERTAČNÍ PRÁCE

Mgr. Zdeněk Perutka

Olomouc

Prohlašuji, že jsem disertační práci vypracoval samostatně s vyznačením všech použitých pramenů a spoluautorství. Souhlasím se zveřejněním disertační práce podle zákona č. 111/1998 Sb., o vysokých školách, ve znění pozdějších předpisů. Byl jsem seznámen s tím, že se na moji práci vztahují práva a povinnosti vyplývající ze zákona č. 121/2000 Sb., autorský zákon, ve znění pozdějších předpisů.

V Olomouci dne Mgr. Zdeněk Perutka

Poděkování

Rád bych touto cestou poděkoval především svému školiteli prof. Mgr. Marku Šebelovi, Dr. za odborné vedení, možnosti zapojit se do zajímavých projektů, vyzkoušet spousty laboratorních technik a poznat spousty skvělých lidí, stejně jako za trpělivost a cenné rady, které mi během práce věnoval a za čas, který obětoval. Dále bych poděkoval Mgr. René Lenobelovi, Ph.D, z Laboratoře růstových regulátorů, PřF UP v Olomouci, za mnoho skvěle provedených analýz na q-TOFu a nespočet poskytnutých užitečných rad, informací a technickou podporu nejen v oblastech hmotnostní spektrometrie a kapalinové chromatografie. Děkuji také za spolupráci Ing. Beátě Petrovská, Ph.D z Ústavu experimentální botaniky AV ČR Olomouc. Za poskytnutí vzorků netradičního vína a spolupráci děkuji panu prof. Ing. Miroslav Strnad, CSc. DSc. a Miloslavu Šufeislovi, Velké poděkování za ochotu kdykoli pomoci patří všem spolupracovníkům z bývalého Oddělení biochemie proteinů a proteomiky (CRH) a Katedry biochemie PřF UP v Olomouci. Dále bych chtěl poděkovat prof. Martině Marchetti-Deschmann, Ph.D za možnost strávit 2 měsíční stáž na Ústavu chemických technologií a analytiky Technické univerzity ve Vídni. Za měsíc spolupráce v Krakově na Jagelonské univerzitě děkuji Dr. Robertu Koniecznemu a jeho kolegům. Nakonec bych chtěl poděkovat rodině a přátelům za podporu během studia.

Bibliografická identifikace

Jméno a příjmení autora	Mgr. Zdeněk Perutka
Název práce	Analýza proteomu pomocí nanoLC-MALDI-TOF/TOF MS a MS/MS
Typ práce	Disertační
Pracoviště	Oddělení biochemie proteinů a proteomiky, Centrum regionu Haná pro biotechnologický a zemědělský výzkum; Katedra biochemie PřF UP v Olomouci
Vedoucí práce	prof. Mgr. Marek Šebela, Dr.
Rok obhajoby práce	2022

Abstrakt

Hmotnostní spektrometrie ve spojení s nanoprůtokovou kapalinovou chromatografií (nLC-MS) je zavedená technika pro analýzu peptidů z komplexních směsí proteinových digestů. V této práci byla využita technika nLC MS ve spojení s ionizací a desorpcí laserem s pomocí matrice (MALDI) a komplementární analýza pomocí elektrospreje, a to pro identifikaci proteinů rozdělených gelovou elektroforézou z rozličných vzorků. Tato práce nejprve demonstruje aplikaci proteasy pseudotrypsinu, málo známé proteoformy hovězího trypsinu, nejběžněji používaného enzymu pro proteomické experimenty. Pseudotrypsin byl izolován z autolyzátu trypsinu pomocí chromatografie na kationtoměniči a následně použit pro štěpení proteinových extraktů z jader ječmene. Odlišná specifičnost pseudotrypsinu umožňující štěpení za aromatickými aminokyselinami a leucinem navíc k jeho tryptické aktivitě, vede ke vzniku unikátních peptidů a následně identifikaci odlišných proteinů při proteomických experimentech. S využitím standardu hovězího sérového albuminu a izotopově značených peptidových standardů byla srovnána účinnost štěpení připraveného pseudotrypsinu s komerčními trypsiny.

V návaznosti na práci s jádry ječmene byla provedena proteomická analýza mitotických chromozomů izolovaných technikou průtokové cytometrie. Získaná data byla následně vyhodnocena pomocí bionformatických nástrojů a stanovena možná původní buněčná lokalizace nalezených proteinů a provedena jejich relativní kvantifikace.

V dalším experimentu byly pomocí nLC-MS hledány proteiny a enzymy trávící tekutiny masožravé rostliny *Drosery capensis.* Po štěpení trypsinem nebo chymotrypsinem byly nalezeny proteiny podobné těm používaným rostlinami pro jejich obranu. Jako hlavní skupiny proteinů sekretomu rosnatky kapské byly identifikovány proteolytické enzymy a chitinasy.

V nejrozsáhlejší studii zahrnuté do této práce bylo využito technik nLC-MS pro charakterizaci variability proteinového zastoupení jako možné příčiny neodstranitelného zákalu experimentálního vína připraveného z hrozna částečně napadeného *Botrytis cinerea*. Pro porovnání proteinových profilů SDS-PAGE a nLC-MS analýzou byly pomocí dialýzy a ultrafiltrace izolovány proteiny z komerčních bílých vín a hroznové šťávy. Proteinové zastoupení v analyzovaných vzorcích bylo následně zhodnoceno s ohledem na původ a charakteristiky vína jako pH, barva a teplotní stabilita případně viditelný zákal. Byl pozorován fenomén vysokého obsahu prolinu v proteinech nalezených v testovaných vínech. Vybrané proteiny *V. vinifera* s touto charakteristikou byly izolovány a otestovány, zda mohou významně přispívat k teplotní nestabilitě a vzniku zákalu vína. Tato hypotéza se nepotvrdila. Ve vzorcích vín byla nalezena opakovaně se vyskytující thiolová proteasa, která byla následně částečně charakterizována.

Klíčová slova Hmotnostní spektrometrie, identifikace proteinů, pseudotrypsin, proteasa, proteom, jaderné proteiny, chromozom, víno, zákal, *Drosera*, trávící šťáva, *Botrytis*

Počet stran 111

Počet příloh 8

Jazyk Český

Bibliographical identification

Autor's first name and surname	Mgr. Zdeněk Perutka
Title	Proteome analysis by nanoLC-MALDI-TOF / TOF MS and MS / MS
Type of thesis	Disertation
Department	Department of Protein Biochemistry and Proteomics, Centre of the Region Haná for Biotechnological and Agricultural Research Department of Biochemistry, Faculty of Science, Palacký University Olomouc
Supervisor	prof. Mgr. Marek Šebela, Dr.
The year of presentation	2022

Abstract

Nanoflow liquid chromatography coupled to mass spectrometry (LC-MS) is well established technique for analysis of complex peptide mixtures. In this work, the nLC-MS technique in conjunction with matrix-assisted laser ionization and desorption (MALDI) and complementary electrospray analysis were used to identify proteins from various kinds of samples separated by gel electrophoresis. First, this work convincingly demonstrates the application of the protease pseudotrypsin, a little-known proteoform of bovine trypsin, the predominantly used enzyme for proteomic experiments. Pseudotrypsin was isolated from trypsin autolysate by cation exchange chromatography and subsequently used for barley nuclear proteins digestion. The cleavage specificity of pseudotrypsin allows protein hydrolysis behind aromatic amino acids and leucine in addition to its prime tryptic activity. This leads to the formation of unique peptides and allows identification of different proteins after its application. The cleavage efficiency of the isolated pseudotrypsin was compared with commercial trypsins using a bovine serum albumin and prepared isotopically labeled peptide standards. Proteomic analysis of mitotic

chromosomes isolated by flow cytometry was performed, following the work with barley nuclei. The obtained data were subsequently evaluated using bioinformatics tools. Label-free quantification of proteins was counted and possible original cellular localization of proteins was predicted. In another experiment, digestive fluids of the carnivorous plant *Drosera capensis* were searched for proteins and enzymes using LC-MS. Proteins similar to those produced by plants for their defense were discovered after secretome extract digestion by trypsin or chymotrypsin. Proteolytic enzymes and chitinases have been identified as the major components of Cape sundew digestive fluid. As the last part, an unusual protein representation as a possible cause of experimental wine turbidity prepared from grapes partially infected with Botrytis cinerea was investigated by the nLC-MS technique. Wine proteins were isolated from commercial white wines and grape juice by dialysis and ultrafiltration. Wine protein profiles were compared by gel electrophoresis and LC-MS analysis. The protein content in the analyzed samples was evaluated with regard to the wine origin and characteristics including pH, color, temperature stability and visible haze. The frequent presence of proteins high in proline was typically observed among the tested wines. Three V. vinifera proteins with this characteristic were isolated and tested to prove they possible contribution to wine thermal instability and turbidity. This hypothesis has not been confirmed. Novel thiol protease was repeatedly found in the samples of the analyzed wines and was therefore partially characterized.

Keywords Mass spectrometry, protein identification, pseudotrypsin, protease, proteome, nuclear proteins, chromosome, wine, turbidity, drosera, botrytis, digestive juice

Number of pages 111

Number of appendices 8

Language Czech

CÍLE PRÁCE

1) Příprava literární rešerše k řešeným tématům.
2) Příprava a izolace pseudotrypsinu a jeho aplikace pro identifikaci proteinů z jader ječmene.
3) Proteomická analýza proteinů z mitotických chromozomů ječmene a stanovení jejich lokalizace pomocí bioinformatických nástrojů a databazí.
4) Proteomická analýza trávící tekutiny rosnatky kapské (*Drosera capensis*) technikami nLC MS.
5) Proteomická analýza experimentálního vína se zákalem a komerčních vín a následná izolace a otestování vybraných proteinů *v. vinifera* jako možných původců teplotní nestability vína. Izolace a charakterizace nalezené cysteinové proteasy *V. vinifera*.

Obsah

1. ÚVOD 1

2. PROTEOMIKA 1

2.1 Hmotnostní spektrometrie v proteomice 3

2.1.1. Ionizace elektrosprejem 4

2.1.2. MALDI ionizace 4

3. PSEUDOTRYPSIN – izolace, vlastnosti, aplikace 9

3.1. Struktura a vlastnosti trypsinu a pseudotrypsinu 9

3.2 Vznik a příprava pseudotrypsinu 10

3.3. Jádro a jaderné proteiny 11

3.2.1. Jaderné útvary a významné proteiny 12

3.2.1.1. Jadérko 12

3.2.1.2. Cajalovo tělísko 12

3.2.1.3. Jaderné speckle 12

3.2.1.4. Obal jádra 13

3.2.1.4. Jaderné póry 13

3.2.1.5. Jaderný transport 14

3.2.1.6. Genetická informace v jádře 15

3.3.1. Proteiny rostlinných chromozomů 15

3.4. Chromozomální proteiny *H. vulgare* 17

3.5. Výsledky – pseudotrypsin 21

3.5.1. Izolace pseudotrypsinu 21

3.5.2. Srovnání štěpení pseudotrypsinu a trypsinu pomocí MALDI-TOF MS 22

3.5.2. Aplikace pseudotrypsinu pro štěpení jaderných proteinů 24

3.6. Diskuse 26

4. IDENTIFIKACE PROTEINŮ TRÁVÍCÍ ŠŤÁVY *D. capensis* 29

4.1. Karnivorní syndrom 29

4.2. Proteiny a trávení masožravých rostlin 30

4.2.1. Trávení kořisti 31
4.2.2. Enzymy v trávících šťávách MR 32
4.2.3. Příjem živin 36
4.3. Ostatní látky obsažené v šťávách MR – sekundární metabolity 37
4.4. *Dionea muscipula* – modelová masožravá rostlina 38
4.3. Výsledky: Proteiny trávící šťávy rosnatky kapské 40
4.4. Diskuse: Proteiny trávící šťávy rosnatky kapské 44
5. PROTEINY BOHATÉ NA PROLIN JAKO MOŽNÍ PŮVODCI ZÁKALU VÍNA 46
5.1. Senzorické defekty vína 46
5.2. Proteinogenní defekty vína 47
5.2.1. Nestabilita vinných proteinů 47
5.2.2. Enzymová oxidace vína 48
5.3. Proteiny ve víně 49
5.3.1. Proteiny podobné thaumatinu 49
5.3.2. Chitinasy 50
5.3.3. β-D-glykosidasy 50
5.3.4. Lipid transfer proteiny 50
5.3.5. Proteasy vína 51
5.3.6. Exogenní proteiny vína 51
5.4. Metody číření vína 53
5.4.1. Bentonit 53
5.4.2. Čiření vína pomocí proteinů a enzymů 54
5.4.3. Ostatní čiřící prostředky 55
5.5. Izolace a stanovení proteinů ve víně 55
5.6. Výsledky – proteiny vína 58
5.6.1. Charakteristiky porovnávaných vín 58

5.7. Cysteinové proteasa vína 60
5.8. Diskuse – proteiny vína 63
6. PŘEHLED POUŽITÝCH METOD 65
6.1. Využití pseudotrypsinu pro identifikace jaderných proteinů 65
6.1.1. Příprava pseudotrypsinu 65
6.1.2. Izolace ψ-trypsinu 65
6.1.3. Srovnání štěpění pseudotrypsinu a trypsinu pomocí MALDI TOF MS 67
6.1.4. Příprava extraktů proteinů z jader ječmene 68
6.1.5. SDS-PAGE 68
6.1.6. Štěpení proteinů v gelu a odsolení peptidů 69
6.1.7. Odsolení vzorků před nLC MSMS analýzou 70
6.1.8. nLC MALDI TOF-TOF MSMS analýza peptidů 70
6.1.9. nLC ESI qTOF MSMS analýza peptidů 71
6.2. Extrakce proteinů z trávící šťávy *D. capensis* 71
6.3. Zpracování vína a extrakce proteinů 72
6.3.3. Stanovení pH vína 72
6.3.4. Stanovení stability vína a měření zákalu 72
6.3.5. Izolace proteinů vína pomocí gelové permeační chromatografie 73
6.3.6. Štěpení proteinů z vína v roztoku 73
6.3.7. Zpracování dat z MS analýz vína 73
6.3.8. nLC ESI-ion trap MSMS analýza peptidů 74
7. ZÁVĚR 75
SEZNAM ZKRATEK 77
SEZNAM LITERATURY 79
Příloha 1: i
Příloha 2: xxix
Příloha 3: xlviii

Příloha 4: livv

Příloha 5: lxix

Příloha 6: vlxxxiv

Příloha 7: vixciii

Příloha 8: viicii

SEZNAM PŘÍLOH

Příloha 1: Perutka, Z., Šebela, M. (2018) Basis of Mass Spectrometry: Technical Variants. In *The Use of Mass Spectrometry Technology (MALDI-TOF) in Clinical Microbiology* (pp. 19-45). Academic Press.

Příloha 2: Perutka, Z., Kaduchová, K., Chamrád, I., Beinhauer, J., Lenobel, R., Petrovská, B., Bergougnoux, V., Vrána, J., Pečinka, A., Doležel, J., Šebela, M., 2021. Proteome Analysis of Condensed Barley Mitotic Chromosomes. *Frontiers in Plant Science* 12, 1716.

Příloha 3: Seznam nově identifikovaných proteinů z jader ječmene na základě peptidů získaných po štěpení proteinových extraktů pseudotrypsinem.

Příloha 4: Perutka Z., Šebela M., 2018. Pseudotrypsin: a little known trypsin proteoform. *Molecules* 23, 2637.

Příloha 5: Perutka Z., Šufeisl M., Strnad M., Šebela M., 2019. High-proline proteins in experimental hazy white wine produced from partially botrytized grapes. Biotechnol. Applied Biochemistry and Biotechnology 66, 398-411.

Příloha 6: Seznamy proteinů identifikovaných ve vínech a informace o obsahu prolinu v nalezených proteinech. Výsledková příloha k Perutka *et al.,* 2019

Příloha 7: Perutka, Z., Šebela, M., 2020. Mass spectrometry of peptides and proteins using digestion by a grape cysteine protease at pH 3. *Journal of Mass Spectrometry* 55, e4444.

Příloha 8: Perutka, Z., Voženílek, V., Šebela, M. (2021) Wine Contaminations and Frauds From the Bioanalytical and Biochemical Points of View. In *Comprehensive Foodomics* Vol. 3, (pp. 104-116). Elsevier.

1. ÚVOD

Proteomika hraje ústřední roli při identifikaci proteinů, charakterizaci posttranslačních modifikací, nebo při objevování biomarkerů a interakcí. Tyto studie obvykle využívají techniku kapalinové chromatografie (LC) spojenou s detekcí hmotnostní spektrometrií (MS). Proteomické experimenty používají jednoduchou LC pro čištění vzorku, tak pro zvýšení dynamického rozsahu analýzy pomocí chromatofokusace a separace analytů. Kombinace techniky MALDI-MS s LC je výkonným nástrojem pro analýzu malých peptidů i velkých molekul proteinových komplexů. Široká škála použitelných matric a samotná měkká ionizace MALDI (ionizace a desorpce laserem za účasti matrice) poskytuje kvalitní a jednoduchá hmotnostní spektra. Díky depozici vzorku, LC eluentu, na destičku může být také analýza MALDI-MS prováděna nezávisle na pořadí eluce nebo retenčním čase (Chen *et al.*, 2005). Proteomika založená na MS je zaměřena na peptidy a spoléhá na proteasy specificky hydrolyzující proteinovou směs. Znalost vlastností použité proteasy je proto klíčová, jak pro samotné štěpení, tak pro identifikaci hmotnostních spekter získaných peptidů (Vandermarliere *et al.*, 2013). Proteiny mají klíčovou roli v procesech udržování a přenosu genetické informace buňky. Dosud byly u rostlin popsány proteiny z izolovaných jader a jejich suborganel (Petrovská *et al.*, 2015). Bližší charakterizace proteinů interagujících a izolovaných přímo ze struktur chromozomů a chromatinu byly omezeny na živočišné buňky (Ohta *et al.*, 2010). Proteomické studie zaměřené na víno pomáhají nejen porozumět fyziologickým mechanismům a reakcím rostliny na stres, ale také k identifikaci proteinových markerů plísňové infekce. Pomocí proteomiky tak lze na úrovni proteinů sledovat reakce ovoce na chemické nebo fyzikální změny probíhající během zrání a dalšího zpracování (Kambiranda *et al.*, 2014). Fyziologie, netradiční způsob získávání potravy a metabolické produkty s antimikrobiálními účinky staví do popředí zájmu poznání masožravé rostliny. Účelová sekrece proteinů a dalších látek těmito rostlinami vybízí k možnému využití těchto mechanismů pro tvorbu rekombinantních proteinů a jejich podrobnějšímu studiu (Athauda *et al.*, 2004).

2. PROTEOMIKA

Proteomika je vědní obor zabývající se studiem proteinů se zaměřením na jejich samotnou identifikaci, kvantifikaci, strukturu a funkci v daném místě a čase (Chmelík, 2005). Jako první proteomické studie mohou být klasifikovány experimenty využívající

technik dvoudimensionální elektroforetické separace využívané od 80. let, kdy bylo možno pomocí optimalizovaných postupů rozlišit až řádově stovky proteinů na jednom gelu (Rabilloud *et al.*, 2010). Zásadní komplikací té doby představovaly omezené možnosti identifikace. Dostupným řešením se stalo štěpení izolovaného proteinu na charakteristicky končící a překrývající se kratší peptidy a následné přečtení aminokyselinové sekvence těchto částí pomocí sekvenátoru (Aebersold *et al.,* 1987). Významného posunu bylo dosaženo zavedením technik hmotnostní spektrometrie pro studium proteinů (Aebersold a Mann, 2003). Pro všechny informace o proteinech získaných pro konkrétní organismus byl zaveden termín proteom, toho času označující výlučně soubor proteinů odpovídající genomu (Willkins *et al.*, 1996). Od prvního užití pojmu proteom se jeho význam vyhranil a dnes je pod tímto označením možno očekávat dočasný specifický proteinový komplement odpovídající genomu pouze v místě tkáně a zahrnující všechny proteiny včetně jejich modifikací vzniklých během translace nebo i později (Graham *et al.*, 2005). Studium proteinů tak dnes v mnoha ohledech kopíruje studium genů. Výchozím bodem pro proteomiku se však stává identifikovaný protein a cílem podmět a gen odpovědný za jeho produkci. Proteomika v současné době využívá metody tzv. „bottom-up" analýzy hmotnostní spektrometrie (Chait *et al.*, 2006, Hughes *et al.*, 2010). „Bottom-up" analýza MS zahrnuje štěpení proteinů na kratší 5–20 AK obsahující úseky (obvykle proteasou trypsinem), ionizaci výsledných peptidů, separaci iontů podle jejich poměru hmotnost/náboj (*m/z*) a poté detekci iontů (Resing a Ahn, 2005). Přístup analyzující peptidové směsi pocházející z komplexního proteinového extraktu pomocí spojení vysoce účinné kapalinové chromatografie a hmotnostní spektrometrie se označuje jako „shotgun" analýza. Pro identifikaci proteinů hmotnostní spektrometrií jsou tradičně používány techniky ionizace elektrosprejem (ESI) nebo MALDI a přístroje umožňující fragmentaci a přečtení aminokyselinové sekvence analyzovaných peptidů (Chait *et al.*, 2006). Alternativně lze zjednodušit složení peptidové směsi před její ionizací v hmotnostním spektrometru použitím kompatibilní separační techniky, často kapalinové chromatografie (Valaskovic *et al.,* 1996, Chait *et al.*, 2006). Získané sekvence a molekulové hmotnosti peptidů jsou následně prohledány proti proteinové databázi za pomoci nástrojů umožňující zahrnout do srovnávání s *in-silico* databázemi i modifikace očekávatelné pro analyzované peptidy (Resing a Ahn, 2005). Takto identifikované peptidy jsou nakonec spojeny s odpovídajícím proteinem nebo proteinovou rodinou, pokud není možné na základě shody sekvence

identifikovaných peptidů s více proteiny mezi těmito proteiny rozlišit (Resing a Ahn, 2005).

Další způsob využití MS v proteomice představují „top-down“ metody (TD). Pomocí TD MS mohou být na základě velmi přesného určení molekulové hmotnosti identifikovány přímo jak celé proteiny, tak i jejich fragmenty (Chait *et al.*, 2006). Pomocí hmotnostního spektrometru je tak na počátku analyzována celá molekula proteinu, která je až následně fragmentována. Tento přístup umožňuje získat celistvou informaci o proteinové sekvenci a charakterizovat přítomné proteoformy (Smith a Kelleher, 2013). Značné omezení je dáno maximální velikost proteinů, které je technikami pro TD MS možno fragmentovat (Siuti a Kelleher, 2007).

Kombinací přístupů „bottom-up“ a TD proteomiky využívající MS vzniká prostor pro střední cestu tzv. „middle-down“ přístup. Tato metodologie zahrnuje studium středně dlouhých peptidů, ideálně 20–100 AK (Laskay *et al.*, 2013, Cristobal *et al.*, 2017). K produkci takovýchto štěpů je využíváno časově limitované aplikaci proteasy, kombinace méně aktivních přísně specifických enzymů nebo chemické činidlo (Laskay *et al.*, 2013; Cristobal *et al.*, 2017,). V porovnání s „bottom-up“ proteomikou je takto získáno méně unikátních peptidů, které však mohou být lépe popsány, a to včetně postranslačních modifikací (Laskay *et al.*, 2013).

Proteomický výzkum poskytuje skrze možnosti MS a další techniky ucelený pohled na dění v buňce na úrovni proteinů (Beynon, 2005). Podle zaměření a aplikace můžeme studium proteomiky rozdělit do několika oblastí. Proteomika je tak nejčastěji zaměřena k důkazu přítomnosti a kvantifikaci proteinů a jejich stavů jako proteomika expresní. Pro porovnávání více vzorků na proteinové úrovni slouží diferenční proteomika. Hlubší studium jednotlivých bílkovin lze zařadit do proteomiky strukturní a funkční. Dále lze pomocí proteomických metod sledovat interakce mezi jednotlivými proteiny, jejich komplexy a dalšími biomolekulami.

2.1 Hmotnostní spektrometrie v proteomice

Techniky hmotnostní spektrometrie jsou založeny na principu stanovení poměru náboje k hmotnosti detegované částice. Tento princip poprvé dokumentoval Thomson v roce 1911, když objevil elektron a později stanovil jeho hmotnost (Griffiths, 2008). Neméně důležitý je i příspěvek Dempstera (1925) popisující ionizaci plynu pomocí protonu po aplikaci vysokého napětí. K rozdělení nabitých částic bylo následně využíváno kombinace elektrického a magnetického pole (Thomson, 1911). Techniku MS

použili Bieman *et al.*, 1959 k identifikaci derivátů aminokyselin. Analýza makromolekul bez jejich destrukce během procesu ionizace byla umožněna technikou FAB (Fast Atom Bombardment) ionty Ar^+ popsaná v práci Barber *et al.*, 1981 a využita pro sekvenční analýzu peptidů (Morris *et al.*, 1981). Následně byly na obdobném principu stvořeny tzv. měkké ionizační techniky pro biomolekuly a to MALDI a ESI (Karas a Hillekampf, 1988, Fenn *et al.*, 1989). Základní součásti hmotnostního spektrometru jsou iontový zdroj se vstupem pro vzorek, hmotnostní analyzátor, detektor a systém pro záznam a zpracování dat. Nepostradatelnou součástí je systém pro udržování vysokého vakua (Perutka a Šebela, 2018). Ionty vznikají po převedení vzorku do plynné fáze v iontovém zdroji. K rozdělení, analýze, dochází na základě rozdílných vlastností iontů v analyzátoru. Po průchodu analyzátorem jsou přítomné ionty zaznamenány pomocí detektoru, jako vzniklý elektrický signál. Signál z detektoru je následně zpracován a vizualizován, běžně jako závislost intenzity signálu jednotlivých iontů ku poměru jejich velikosti a nábojového čísla (příloha č. 1, Perutka a Šebela, 2018).

2.1.1. Ionizace elektrosprejem

Ionizace elektrosprejem je nejběžnější technikou pro analýzu kapalných vzorků pomocí hmotnostní spektrometrie. Předností ESI je možnost přímého spojení se separačními technikami jako je kapalinová chromatografie nebo kapilární elektroforéza. Při ESI v iontovém zdroji dochází ke vzniku iontů na výstupu z vodivé kapiláry, na kterou je přivedeno vysoké napětí. Vzniklé kapky chromatografického rozpouštědla obsahující molekuly analytu jsou sušeny proudem inertního plyn, často dusíku. Tím dochází k odpařování rozpouštědla a zmenšování objemu kapiček čímž se na jejich povrchu koncentruje náboj. Jakmile překonají odpudivé síly mezi molekulami povrchové napětí kapky, praskne a nabité molekuly jsou uvolněny pro vstup do analyzátoru (Bruins, 1998). Charakteristickými vlastnosti ESI je vznik vícenásobně nabitých iontů. To je výhodné pro analýzu velkých molekuly v analyzátorech s omezeným hmotnostním rozsahem (např. kvadrupóly) nebo pro analýzu intaktních proteinů (Fenn *et al.*, 1989).

2.1.2. MALDI ionizace

Předpokladem pro ionizaci pomocí MALDI je přítomnost UV-absorbující složky, matrice, ve vzorku ozařované pulsy paprsků laseru odpovídající vlnové délky. Začleněním analytu do struktury matrice absorbující energii laseru umožňuje přenos energie z matrice na analyt, sublimaci zahřáté matrice s analytem z pevné fáze do plynné a ionizaci molekul analytu (Gimon *et al.*, 1992, Yates, 1998, Zenobi a Knochenmuss

1998). Alternativní teorie principu MALDI o tzv. „Lucky survivors“ předpokládá přítomnost nabitých molekul analytu už v matrici spolu s opačně nabitými ionty. Tyto klastry jsou rozděleny po desorbci způsobené ozáření laserem zpět na ionty. Přítomné ionty jejichž náboj není neutralizován absorbcí fotelektronů nebo elektronů z kovového terčíku jsou následně detegovatelné jako „Lucky survivors“ (Jaskolla a Karas, 2011). Vznik převážně 1× nabitých iontů a jejich jasné oddělení v MALDI MS spektru je devízou této ionizační techniky (Yates, 1998).

2.1.2.1. Matrice pro MALDI

Vlastnosti matrice a schopnost kokrystalovat a ionizovat vzorek jsou zásadní pro kvalitu MS analýzy (Zenobi a Knochenmuss, 1998). První technika MALDI využívala jako matrici ultrajemný kovový prášek v glycerolu (a poskytovala asi 10 x vyšší citlivost, při aplikaci vzorku v množství 10 μg, pro detekci intaktních proteinů než SDS-PAGE nebo gelová permeační chromatografie (Tanaka *et al.,* 1987). Karas a Hillemkapf, 1988 po aplikaci kyseliny nikotinové jako matrice dosáhli citlivosti okolo 0,5–1 $\mu g \times \mu l^{-1}$ a jejich přístup je základem dnešních MALDI aplikací. Nejběžnější matrice pro MALDI analýzu proteinů a peptidů jsou aromatické organické kyseliny a jejich deriváty a ostatní aromatické sloučeniny, jako α-kyano-4-hydroxyskořicová kyselina (HCCA nebo CHCA), sinapová kyselina (SA), a 2,5-dihydroxybenzoová kyselina (DHB), 2,4,6-trihydroxyacetofenon (THAP) nebo 1,5-diaminonaftalen (DAN). Výběr vhodné matrice pro MALDI analýzu záleží také na její schopnosti přijímat energii laseru a následně sublimovat a desorbovat analyt z povrchu terčíku. Matrice tak lze rozlišit na tzv. studené (např. DHB) a horké, přičemž u horkých matric, jako je CHCA, je potřeba počítat s možnou nežádoucí fragmentací analytu po aplikaci vysoké energie laseru (Zenobi a Knochenmuss, 1998). Lepší ionizace, protonizace analytu může být dosaženo použitím halogenderivátů běžných matric, např. kyseliny 2,4-difluoro-α-kyanoskořicové (DiFCCA) charakteristických svou nižší afinitou k vazbě protonu (Dreisewerd, 2014).

2.1.2.2. MALDI v analýze proteinů a peptidů

Aplikace MALDI MS v proteomice představuje snadno použitelnou a dostatečně citlivou techniku tolerantní i k nižší kvalitě vzorku (Aebersold a Goodlett, 2001). Pro analýzu proteinů pomocí MALDI se tradičně používala technika tzv. peptidového mapování (PMF, „*peptide mass fingerprinting*“), srovnávající signály z hmotnostního spektra specificky hydrolyzovaného proteinu s databází proteinových štěpů vzniklých teoreticky při znalosti specifičnosti štěpení (Pappin *et al.,* 1993; Webster a Oxley, 2012).

Informaci o sekvenci proteinu je možné získat pomocí technik fragmentace v iontovém zdroji („in-source decay“, ISD) nebo za ním („post-source decay“, PSD). Aminokyselinová sekvence získaná PSD nebo ISD fragmentací je většinou nekompletní, na druhou stranu pro tyto experimenty není třeba dalšího zpracování vzorku (Suckau a Cornett, 1998). Běžně jsou již pro proteomické analýzy a sekvenční analýzu peptidů využívány přístroje s MALDI ionizací a fragmentační celou pro kolizí indikovanou disociaci prekurzorových iontů proudem inertního plynu (CID) nebo je k fragmentaci využita vysoká energie laseru (LID). Tyto techniky umožnují MALDI MS/MS experimenty využitelné pro sekvenční analýzu biomolekul (Yergey *et al.*, 2002; Suckau *et al.*, 2003). Omezení daná limitujícím množstvím vzorku aplikovatelným na MALDI terčík a jeho následné spotřebovávání ablací laserem je řešeno spojením MALDI MS/MS s kapalinovou chromatografií (LC-MALDI) (Suckau *et al.*, 2003; Hattan *et al.*, 2005). Technicky je LC-MALDI řešeno mísením vzorku, eluátu z kapalinového chromatografu s vhodně zvoleným množstvím matrice těsně před depozicí této směsi na MALDI terčík pomocí automatizovaného robota (Suckau *et al.*, 2003; Hattan *et al.*, 2005). LC-MALDI poskytuje alternativní řešení v oblasti „shotgun“ proteomiky k LC-ESI, přičemž kombinací obou technik lze docílit značné reprodukovatelnosti a překryvu identifikovaných peptidů převyšující 60 %, tak i získat unikátní peptidy charakteristické pro každý typ ionizace (Bodnar *et al.*, 2003; Staples a Barofsky, 2004). Imobilizace vzorku na MALDI terčík umožňuje navíc omezeně opakování celého měření nebo cílenou MS/MS analýzu vybraných prekurzorů (Chen *et al.*, 2005).

2.1.2.3. MALDI imaging

Technologie MALDI MS může být použita také ke dvourozměrnému zobrazení zastoupení molekul v tenkém vzorku (Caprioli *et al.*, 1997). Zobrazování pomocí MALDI, tzv. MALDI „imaging“ (MALDI MSI) je založen na analýze vzorku metodou rastrování, postupné analýzy sousedních ploch s rozlišením jednotek μm (Kompauer *et al.*, 2017). Následným skládáním takto získaných iontových snímků např. tenkých řezů větší živočišné buňky nebo části tkáně může být vytvořen obraz zastoupení biomolekul v prostoru (Dueñas *et al.*, 2017). Vzorek pro MALDI MSI je připraven jako tenký řez, pomocí mikrotonu, který je umístěn na vodivou podložku, typicky pokovené sklíčko, a pokryt matricí. Klíčovými kroky MALDI MSI analýzy jsou volba matrice a technika jejího nanesení na vzorek (Baker *et al.*, 2017). Specifické matrice pro MALDI MSI představují kvercetin – použitelný pro analýzu lipidů v pozitivním módu (Wang *et al.*,

2013) DAN nebo deriváty kys. anthranilové – pro analýzu lipidů v negativním i pozitivním módu (Thomas *et al.*, 2012; Huang *et al.*, 2020) nebo kurkumin – vhodný pro analýzu malých molekul léků, lipidů, peptidů i malých proteinů (Francese *et al.*, 2013). Aplikace MALDI a MALDI MSI pro analýzu malých molekul je limitována ionty vznikající z matrice, které mohou být isobarické s cílovými analyty. Toto lze překonat dostatečnou rozlišovací schopností analyzátoru a oddělit matricové ionty a ionty analytu. Kromě toho mohou ionty matrice sloužit jako interní referenční standardy pro přesná měření hmotnosti (Cornett *et al.*, 2008). Signály iontů matrice lze také potlačit přidáním aditiv jako je cetrimoniumbromid nebo LiCl (Guo *et al.*, 2003; McCombie a Knochenmuss, 2004). Matrice je pro MALDI MSI nanášena na vzorek typicky pomocí sprejování nebo napařováním za sníženého tlaku a následně je rekrystalována promytím vhodným rozpouštědlem (Hankin *et al.*, 2007; Yang a Caprioli, 2011; Mounfield a Garrett, 2012). Aplikace MALDI MSI zahrnuje hledání a vizualizaci biomarkerů chorob, sledování metabolismu léčiv nebo studium chování patogenů (Holzlechner *et al.*, 2016; Vaysse *et al.*, 2017).

2.1.2.4. Kvantifikace pomocí MALDI

MALDI MS může poskytnout také kvantitativní informaci o analyzovaném vzorku. Klíčové faktory pro úspěšnou MALDI kvantifikaci zahrnují jednak technické možnosti přístroje, ale zejména srovnatelnou kvalitu vzorků a použité matrice (Albrethsen, 2007, Wang *et al.*, 2016). MALDI kvantifikace vyžadují také precizní kalibraci (Rzagalinski a Volmer, 2016). Benefitem tohoto přístupu je možnost přímé kvantifikace molekul z rozmanitých vzorků, nebo např. tkání v případě MALDI MSI, bez nutnosti jejich dalšího zpracování (Rzagalinski a Volmer, 2016). Kvůli omezené možnosti opakovat měření ze stejného místa MALDI terčíku je vhodné při MALDI kvantifikaci využít data z co největšího počtu měření stejného analytu při co nejvíce různých koncentracích. Jako vhodné se jeví také pro jednotlivá měření využít průměr spekter získaný z více výstřelů na větší ploše vzorku (Wang *et al.*, 2016). Optimální volbou v případě MALDI kvantifikace je využití interního izotopově značeného standardu (Mirgorodskaya *et al.*, 2000).

2.1.2.5. MALDI „biotyping“

MALDI TOF technologie je už více než 10 let široce využívána pro identifikaci mikroorganismů na základě srovnávání jejich unikátních proteinových profilů s databází pomocí MALDI „biotypingu“ (Claydon *et al.*, 1996; Fenselau a Demirev, 2001). Tímto

přístupem jsou mikroorganismy identifikovány pomocí proteinů uvolnitelných z jejich povrchu nebo buněčných extraktů, obdobně jako jsou identifikovány proteiny PMF metodou, avšak na úrovni proteinů. Velikost sledovaných signálů biomarkerů při MALDI „biotypingu“ nepřesahuje 20 kDa (Fenselau a Demirev, 2001). Srovnávaná MALDI-TOF MS spektra těchto vysoce hojných často neustále produkovaných proteinů, jsou dobře reprodukovatelná a většinou nezávislá na podmínkách kultivace mikroorganismu (Valentine *et al.,* 2005; Wunschel *et al.*, 2005). Přesnost identifikace jednotlivých druhů mikroorganismů může být zvýšena aplikací extenzivnějších procesů extrakce nebo např. specifickou hydrolýzou daného extraktu což vede k získání většího množství rozlišitelných signálů (Gekenidis *et al.,* 2014). Při srovnání klasické technologie klasifikace na základě metod molekulární biologie je technologie MALDI „*biotypingu*“ citlivá, ekonomická a hlavně rychlá (Claydon *et al.*, 1996, Pranada *et al.,* 2016). MALDI-TOF MS je tak využívána pro řadu účelů, nejen pro mikrobiální identifikace a typizace kmenů, ale i epidemiologické studie, detekce biologických bojových látek, detekce patogenů ve vodě a potravinách, stanovení míry rezistence patogenů vůči antibiotikům nebo klinická vyšetření (Singhal *et al.*, 2015, Pranada *et al.*, 2016).

2.1.2.6. MALDI v analýze nukleových kyselin

MALDI TOF MS je vhodnou technikou pro analýzu krátkých úseků DNA i RNA (Gao *et al.*, 2012). Pro MALDI MS analýzu NK lze využít jednoduché MALDI TOF analyzátory, tak i pokročilé přístroje umožňující cílenou fragmentaci nebo vysoké rozlišení (Kellersberger *et al.*, 2004; Honisch *et al.*, 2017). Jako matrice je pro analýzu NK často využívána HPA (Gao *et al.*, 2012). Rozlišení SNP („single nucleotide polymorphism“) na základě hmotnostní změny umožňuje rychlou identifikaci těchto odlišnostní i laboratorní diagnostiku pro řetezce NK o délce až 50 bází *(*Honisch *et al.*, 2017). Vzorky pro NK pro analýzu SNP jsou připravovány pomocí PCR, kdy je v první fázi amplifikován sledovaný úsek DNA, následně jsou odstraněny zbývající volné báze a pomocí specifických primerů je amplifikován úsek končící právě sledovaným místem SNP. Výsledkem je stanovení rozdílu *m/z* mezi amplifikovanými produkty odpovídající záměně jedno nukleotidu (Gao *et al.*, 2012). Další aplikace MALDI pro analýzu NK nabízí detekce, identifikace, kvantifikace a sledování přenosu virů *(*Honisch *et al.*, 2017), prenatální diagnostika (Zhong a Holzgreve, 2009), sledování změn a struktrury RNA nebo charakterizace endonukleas *(*Thomas a Akoulitchev, 2006; Douthwaite a Kirpekar, 2007; Joyner *et al.*, 2012).

3. PSEUDOTRYPSIN – izolace, vlastnosti, aplikace

Štěpení proteinů pomocí charakteristicky specifické proteasy je klíčovým krokem v typickém proteomickém experimentu využívajícím hmotnostní spektrometrii. Nejrozšířenější použití doznává díky vysoké specifičnosti trypsin vytvářející ideálně dlouhé peptidy o 9–15 AK s molekulovou hmotnostní do 3000 Da vhodné pro LC-MS experimenty (Vandermarliere *et al.*, 2013, Tsiatsiani a Heck, 2015). Specifičnost tryptického štěpení poskytující bazické AK (R nebo K) na C-konci peptidů navíc zlepšuje ionizaci v pozitivním módu MS analýzy (Tsiatsiani a Heck, 2015). V případě hovězího trypsinu mohou autolytickým štěpením vznikat další proteoformy s odlišnou specifičností štěpení, což vede ke vzniku odlišných peptidů (Keil-Dlouhá *et al.*, 1971a; Lacerda *et al.*, 2014, Dyčka *et al.*, 2015). Negativním výsledkem vysoké aktivity trypsinu je tvorba malých peptidů, obtížně zachytitelných a detekovatelných LC-MS, což může vést k identifikaci méně peptidů (Swaney *et al.*, 2010, Hildonen *et al.*, 2014). Za účelem částečného nebo úplného vynechání použití trypsinu byly charakterizovány další velmi specificky štěpící proteolytické enzymy např. AspN, GluC (Tsiatsiani a Heck, 2015, Giansanti *et al.*, 2016). Pro dosažení lepšího pokrytí proteinových sekvencí a získaní více peptidů jsou také popsány metody vhodně kombinující proteasy a způsoby digesce vedoucí k ideálním množství vzniklých a využitelných peptidů pro MS analýzu (Tsiatsiani a Heck, 2015; Dau *et al.*, 2020).

3.1. Struktura a vlastnosti trypsinu a pseudotrypsinu

Trypsin patří mezi serinové endoproteasy a vzniká z neaktivní proformy trypsinogenu autolyticky nebo činností enterokinasy ve dvanáctníku (Kunitz, 1939, Kay a Kassell, 1971). V bazickém pH aktivní β-trypsin je vytvořen po odštěpení 15 AK signálního a 6 AK dlouhého aktivačního peptidu z N-konce trypsinogenu (Keil, 1971; Vandermarliere *et al.*, 2013). U lidské formy trypsinogenu je mutace na počátku aktivačního peptidu spojena s projevy chronické pankreatidy (Witt *et al.*, 1999). Autolytickým štěpením mezi Lys 131-Ser 132 vzniká α-trypsin (Keil, 1971). Dalším štěpením α-trypsinu, držícím dohromady 3 disulfidovými vazbami spojujícími oba AK řetězce, mezi Lys 176-Asp 177 vzniká 3 řetězcová struktura stále proteolyticky aktivního ψ-trypsinu (Smith a Shaw, 1969). Molekulová hmotnost β-trypsinu byla pomocí ESI-MS stanovena na 23 294 Da (Ashton *et al.*, 1994). V případě ψ-trypsinu hodnota 23 330 Da přesně odpovídá predikci a 2 hydrolýzám za Lys 131 a 176 (Dyčka *et al.*, 2015). Struktura trypsinu je tvořena 2 β-barely stabilizovanými 6 disulfidovými můstky. Aktivní místo

enzymu tvořené Asp 102, Asp 57 a Ser 195 je umístěny mezi β-barely (Sandler *et al.*, 1998). Pro vlastní aktivitu je pro trypsin nezbytná vazby vápenatého iontu (Bode a Schwager, 1975). Prostorová struktura ψ-trypsinu nebyla dosud vyřešena.

Rozvolněnější struktura uděluje ψ-trypsinu oproti β a α formě odlišné vlastnosti, projevující se zejména změnou afinity a širší specifičnosti štěpení. Odlišné chování ψ-trypsinu pozorovali po jeho purifikaci Smith a Shaw, 1969, když po inkubaci s běžným chromogenním substrátem trypsinu N^{α}-benzoyl-D,L-arginin-4-nitroanilidem nedetegovali produkt reakce. Aktivita však byla prokázána reakcí s radioaktivně značeným diisopropylfluorofosfátem a jeho vazbou do aktivního místa enzymu (Smith a Shaw, 1969). Následně byla enzymová kinetika ψ-trypsinu studována dalšími autory. Afinita ψ-trypsinu k umělým substrátům N^{α}-benzoyl-L-arginin-ethylesteru, N^{α}-*p*-tosyl-L-arginin-methylesteru je oproti α-trypsinu i více než 1000× nižší (Smith a Shaw, 1969; Foucault *et al.*, 1971). Podobně velké rozdíly byly zjištěny i při srovnání aktivity ψ-trypsinu a nefrakcionovaného trypsinu, směsi α a β formy (Smith a Shaw, 1969; Inagami a Sturtevant, 1960). Schopnost ψ-trypsinu štěpit N^{α}-acetyl-L-tyrosin-ethylester ukazuje specifičnost podobnou chymotrypsinu (Smith a Shaw, 1969). Zásadním rozdílem v reaktivitě je netečnost ψ-trypsinu vůči ireverzibilnímu inhibitoru trypsinu N^{α}-*p*-tosyl-L-lysin-chloromethylketonu (TLCK, Smith a Shaw, 1969). Keil-Dlouhá 1971b prokázala schopnost ψ-trypsinu štěpit i za aromatickými AK a jeho specifičnost podobnou chymotrypsinu. Jako modelové substráty byly zvoleny heptapeptid GFFYTPK z β-řetězce insulinu a glukagon. Analýza produktů ψ-tryptického digestu glukagonu dokázala specifičnost odpovídající α i β formě, ale také přítomnost peptidů vzniklých po štěpení za Phe a Trp. Heptapeptid z inzulinu nebyl při kontrolních experimentech štěpen žádnou formou trypsinu ani chymotrypsinem (Keil-Dlouhá *et al.*, 1971a; Keil-Dlouhá *et al.*, 1971b). Schopnost ψ-trypsinu štěpit za rezidui aromatických AK byla potvrzena pomocí MALDI-MS analýzy peptidů vzniklých z čistých standardních proteinů i komplexní proteinové směsi (Dyčka *et al.*, 2015).

3.2 Vznik a příprava pseudotrypsinu

Popsané metody přípravy hovězího ψ-trypsinu jsou založeny na použití řízené autolýzy čistého trypsinu za podmínek inkubace v pufru pH 8, přítomnosti vápenatých iontů a teplotě 25 °C po dobu 6,5h. Hlavní produkty směsi obsahující zejména α a β formu plus ψ-trypsin jsou následně inhibovány přidaným TLCK. Autolýzou vzniklé peptidy a polypeptidy byly před separací trypsinů odstraněny gelovou filtrací (Smith a Shaw,

1969). Jednotlivé trypsiny jsou poté rozděleny na iontoměniči Sulfoethyl (SE)-Sephadex C-50 nebo HemaBio 1000SB koloně isokratickou elucí 100 mM Tris-HCl pufrem, pH 7.1 s 20 mM $CaCl_2$ (Smith a Shaw, 1969; Dyčka *et al.*, 2015). Pro odstranění možné kontaminace výchozí směsi chymotrypsinem, může být alternativně přidán jeho inhibitor *N*-*p*-tosyl-L-fenylalanin-chloromethylketon (TPCK) směs krátce inkubována v ideálních podmínkách aktivity trypsinu. Nadbytek TPCK je odstraněn dialýzou (Dyčka *et al.*, 2015). Trypsiny byly z kolony eluovány vždy v pořadí ψ a poté TLCK inhibovaná α a β proteoforma. (Smith a Shaw 1969; Dyčka *et al.*, 2015). Komerční preparát ψ-trypsinu není dostupný.

3.3. Jádro a jaderné proteiny

Jádro je vlastní membránou uzavřená organela a jeho přítomnost je charakteristickým znakem eukaryotických organismů (Hertzer *et al.*, 2005). Jádro je zodpovědné za procesy organizace, replikace a dělení chromozomů, spouštění a vypínání genů a další činnosti nezbytné pro fungování buňky (Shaw a Braun., 2004). Umístění celého jádra v rámci buňky je aktivně řízeno a upravováno dle potřeby (Gundersen a Worman, 2013). Součástí mnoha buněčných procesů je migrace celého jádra (Gundersen a Worman, 2013). Struktura jádra je velmi dobře organizovaná a jeho nejdůležitější součástí je genom. Na periferiích jádra, vázána na jadernou laminu a proteiny vnitřní jaderné membrány, je lokalizována neaktivní kondenzovaná genetická informace ve formě heterochromatinu (Solovei *et al.*, 2013). Méně kondenzovaný euchromatin s aktivními geny se obvykle nalézá blíže pomyslného středu jádra (Zulo *et al.*, 2012). Největší strukturou uvnitř jádra je jadérko, místo vzniku ribozomů (Shaw a Braun., 2004). Další jaderné struktury představují Cajalovo tělísko a jaderné „speckles“ (Shaw a Braun., 2004). U rostlin lze nalézt také specifické jaderné kompartmenty jako „dicing“ tělíska procesující mikroRNA nebo útvary reagující na světlo (Petrovská *et al.*, 2015). Specifickým znakem rostlinných jader je variabilita jejich tvaru a velikosti související s typem pletiva a buňky v níž se nacházejí (Meier *et al.*, 2016). Studium jaderných tělísek a specifických útvarů často zahrnuje analýzu jejich proteomu pomocí MS. Nejrozsáhlejší studie popisující rostlinný jaderný proteom náleží k *A. thaliana,* když bylo identifikováno přes 1500 proteinů a ječmeni s více než 2400 jadernými proteiny (Blavet *et al.* 2017, Goto *et al.*, 2019).

3.2.1. Jaderné útvary a významné proteiny

3.2.1.1. Jadérko

Jadérko je místem kde dochází k transkripci a zpracování ribozomálních RNA (rRNA) a jejich sestavení do ribozomálních podjednotek před exportem do cytoplazmy (Pendle *et al.,* 2005). V jadérku lze nalézt ribozomální proteiny, faktory biogeneze ribozomů a proteiny potřebné pro export ribozomálních podjednotek přes komplex jaderných pórů do cytoplazmy (Fatica a Tollervey, 2002). Podle práce Pendle *et al.,* 2005 je značný rozdíl mezi známými lidskými a rostlinnými proteiny z jadérka, když nalezli homology jen pro 18 % identifikací z celkových 217 proteinů původem z *A. thaliana* (Pendle *et al.*, 2005). Ke struktuře jadérka se také váže chromatin a slouží jako centrum replikace (Pontvianne *et al.*, 2016). Charakteristickým markerem jadérka je protein nukleolin (Pontvianne *et al.,* 2016).

3.2.1.2. Cajalovo tělísko

V rostlinných buňkách jsou s jadérkem většinou těsně spojena 1-2 Cajalova tělíska (CT), bezmembránové útvary a místa tvorby a metabolismu ribonukleoproteinů (Love *et al.*, 2017). Základní strukturní složkou CT je protein koilin umožňující interakci mezi ostatními proteiny CT a molekulami RNA (Collier *et al.,* 2006; Matera *et al.,* 2006). Důležitá se zdá být u rostlin role coilinu a CT při virové patogenezi a odpovědi na abiotický stres (Shaw *et al.,* 2014; Love *et al.,* 2017).

3.2.1.3. Jaderné speckle

Jaderné „speckles“ (skvrny) slouží jako místo koncentrace faktorů pro sestřih, „splicing“, pre-mRNA a nachází v prostoru interchromatinu (Reddy *et al.,* 2011). Mezi „splicing“ faktory patří proteiny bohaté na serin a arginin (SR proteiny), jejichž lokalizace ve „specklích“ je regulována pomocí fosforylace (Ali *et al.,* 2003). V případě *A. thaliana* byla pozorována nezávislá lokalizace jednotlivých typů SR proteinů v rámci jaderných skvrn, což může ukazovat na specifičnost těchto proteinů k pre-mRNA (Lorkovic *et al.,* 2008). V jaderných skvrnách rostlin se vyskytují také proteiny tzv. „polycomb“ represivních komplexů zprostředkovávající epigentickou genovou regulaci prostřednictvím histonmethyltransferasy nebo vazbou přímo na histony (Hohenstatt *et al.,* 2018). V místech poškození DNA vznikají v jádře tělíska tvořená opravnými faktory jako „chromatin remodeling“ faktor RD54 (Rothkamm *et al.,* 2015; Hirakawa a Matsunaga, 2019). Specifický typ „speckles“ vzniká v jádře reakcí na světlo a asociací fytochromů

(Ronald a Davis, 2019). Přímou souvislost mezi kryptochromy z těchto tělísek a působením modrého světla vedoucí k modulaci cirkadiálního rytmu rostlin popsali Wang *et al.*, 2021. Ke zpracování a biogenezi miRNA dochází v jádře rostlinných buněk v „D-bodies“, obsahujících proteiny jako HYL vázající dvouvláknovou RNA a „zincfinger serrate protein“ (Liu *et al.*, 2011, Wang *et al.*, 2019).

3.2.1.4. Obal jádra

Obal jádra v eukaryotických buňkách sestává z vnější jaderné membrány, která je úzce spojena s endoplazmatickým retikulem obklopujícím jádro a vnitřní jaderné membrány propojené k vnější prostřednictvím jaderných pórů. Jaderný obal má kromě ohraničení a ochrany vnitřního obsahu jádra řadu funkcí. Tyto zahrnují regulaci transportu z jádra a opačným směrem, zajištění fyzického umístění jádra v buňce, signalizaci a buněčné dělení (Graumann *et al.*, 2010).

Na organizaci vnitřní struktury jádra a jeho spojení s cytoskeletem rostlinné buňky se mohou podílet proteiny jako KAKU4 nebo tzv. proteiny tvořící jadernou matrici (Ciska a Moreno Díaz de la Espina, 2014, Goto *et al.*, 2014). Homology laminu tvořící kostru jádra živočišných buněk nebyly dosud v žádném rostlinném genomu nalezeny (Ciska a Moreno Díaz de la Espina, 2014). Fyzické spojení mezi jádrem a cytoskeletem zajišťuje v živočišných buňkách LINC komplex složený z oligomerních proteinů se SUN doménami lokalizovaných ve vnitřní jaderné membráně a proteinů tvořících KASH domény nalézající se ve vnější jaderné membráně a intereagující se SUN v mezimembránové jaderné lumen (Rothballer a Kutay, 2013). Spojení mezi rostlinnými SUN1 a SUN2 proteiny s cytoplazmatickou strukturou aktinu a myosinu je zprostředkováno WIP a WIT nebo SINE proteiny, plnící funkci živočišných KASH oligomerů (Graumann *et al.*, 2010; Zhou *et al.*, 2014). Umístění jádra v rámci rostlinné buňky umožňují pohybem po mikrotubulech motorové proteiny kinesinu a unikátní kinesiny mající calponinovou doménu zastávající funkci dyneinu (Yamada a Goshima, 2018).

3.2.1.4. Jaderné póry

Jaderné póry (JP) představují hlavní spojení pro transport makromolekul mezi jádrem a okolím. Struktura jaderných pórů je obdobná mezi všemi eukaryotickými organismy a je tvořena prstencem 8 proteinových komplexů nukleoporinů (NUP) (Tamura a Haranishimura, 2014). Proteiny JP mohou být podle umístění a funkce rozděleny do skupin. Na vnější straně jádra se nachází NUP cytoplazmatické oblasti

a další asociované proteiny. Analog živočišného Nup214 proteinu, u *A. thaliana* produkt LNO1, je nezbytný pro embryogenezi a vývoj semen (Braud *et al.*, 2012). Na okraji jádra se nachází dále Gle1 interagující s LOS4 proteinem, ovlivňujícím citlivost buněk na chlad. LOS4 se může vázat i k Nup214. Na okraji jaderného obalu jsou umístěny NUP tzv. komplexu Y. Funkce Nup160 z této oblasti je spojena s působením auxinu a resistencí buněk (Robles *et al.*, 2012). Vnitřní část JP je tvořena NUP s opakujícími se úseky Phe a Gly ovlivňující selektivitu JP a dále NUP komplexy Nic96. Ze skupiny Phe-Gly NUP je popsán Nup62 protein nalézající se také v cytoplazmatické oblasti JP a interagující s Ran import faktorem NTF2 (Boeglin *et al.,* 2016). MOS7 analog živočišného Nup88 patřící do Nic96 komplexu ovliňuje buněčnou imunitu a hromadění imunoreceptoru snc1 v jádře (Cheng *et al.*, 2009). Spojení mezi jadernou membránou a ostatními NUP zajišťují transmembránové NUP. Gu popsal působení transmembránového CPR5 komplexu ovlivňující jaderný transport změnou selektivity interagujících Phe-Gly NUP (Gu *et al.*, 2016). Uvnitř jádra se na JP nalézají proteiny tvořící jaderný koš. Jednou z jeho částí je Nup136, spojovaný s vnitřní organizací jádra a možný analog živočišného Nup153, který je vázán na strukturu jaderné laminy (Tamura a Hara-Nishimura, 2011).

3.2.1.5. Jaderný transport

Transport malých látek skrze jaderný pór může probíhat pasivní difuzí. Molekuly větší než 40 kDa však musí využít proteinový komplex jaderného póru a dalších specifických transportních proteinů (Grossman *et al.*, 2012). Zásadní pro transport mezi jádrem a cytoplazmou, ale také opačným směrem je rozpoznání přenášeného nákladu pomocí proteinů karyopherinů, zahrnující importiny a exportiny. Jaderné Importiny α zprostředkovávají spojení mezi molekulami mířícími do jádra, mající specifickou signální AK sekvenci pro lokalizaci právě v jádru. Importiny β interagují s komplexem NUP tvořící JP (Marfori *et al.*, 2011). Specifické adaptorový protein Snurpotin1 pro jaderný import využívají proteiny tvořící spliceosom (Marfori *et al.*, 2011). Studie na živočišných buňkách také prokazují, že velké molekuly jako ribozomální podjednotky nebo Cdk/cyclin komplex nevyžadují pro vstup do jádra adaptorový protein a váží se přímo k importinu β (Marfori *et al.*, 2011). Rostlinný importin SAD2 je zapojen do přenosu transkripčních faktorů regulující odezvu buňky na k. abscisovou (ABA) a k. jasmonovou (JA) (Tamura a Nishimura, 2014). Pro přenos fytochromů do jádra je nezbytná jejich vazba k interakčním faktorům nebo zprostředkovatelům např. k PIF3 nebo FHY1

(Pfeiffer *et al.*, 2012). Transport molekul importiny je řízen pomocí „Ras-related nuclear protein“ GTPasy, tj. Ran GTPase, zprostředkovávající v nukleoplazmě oddělení jednotky importinu α a uvolnění přenášeného nákladu od importinu β jeho vazbou k Ran GTPase (Stewart, 2007).

3.2.1.6. Genetická informace v jádře

U rostlin a ostatních eukaryotických organismů je většina DNA umístěna v jádře a organizována pomocí histonů do struktury chromatinu. Chromatin a interagující proteiny se následně účastní procesů využívajících DNA jako jsou replikace, transkripce a genová regulace. Tyto děje jsou ovlivňovány signálními dráhami přinášejícími informace z prostředí vedoucí k přeprogramování transkripce (Eberharter a Becker, 2002). K tomu na úrovni chromatinu dochází díky jeho struktuře umožňující interakci přítomných proteinů nebo specifických úseků DNA. Interakce následně může vést k rozvolnění nebo naopak bránit dalším proteinům v přístupu k DNA. Za tímto účelem působí na chromatin komplexy proteinů nazvané remodelátory chromatinu (Bannister a Kouzarides, 2011, Hohenstatt *et al.*, 2018). Protein DDM1 *A. thaliana* náležící mezi SWI/SNF typ modulátorů umožňuje methyltransferasam a dalším enzymům přístup k DNA na nukleosomech a její methylaci (Zemach *et al.*, 2013). Při chladovém stresu je organizace chromatinu znepřístupněna zvýšením činnosti histondeacetylasy 6 (Luo *et al.*, 2012). Dalším příkladem je DEK3 protein interagující s DNA topoisomerasou ovlivňující růst *A. thaliana* v prostředí se zvýšeným obsahem solí (Waidman *et al.*, 2014).

Necílené studie nukleoproteomu a metody izolace rostlinných jaderných proteinů přehledně shrnuli Narula *et al.*, 2013 a Petrovská *et al.*, 2015. Soudobé směry studia nukleoproteomu představuje sledování postranslačních modifikací a výskyt zájmových proteinů v závislosti působení vnějších faktorů (Yin a Komatsu, 2015; Li *et al.*, 2015; Mazur *et al.*, 2017). Dalším směrem je zacílení výzkumu přímo na s DNA interagující proteiny chromatinu nebo zmíněných jaderných kompartmentů (Goto *et al.*, 2019; Tang *et al.*, 2020, Veléz-Bermúndez a Schmidt, 2021; Perutka *et al.*, 2021).

3.3.1. Proteiny rostlinných chromozomů

Růst rostlin je výsledkem koordinované interakce mitotického buněčného dělení a expanze buněk. Stejně jako u ostatních eukaryotických organismů se buněčný cyklus rostlin skládá ze čtyř fází: G1 (postmitotická interfáze), S (fáze syntézy DNA), G2 (předmitotická interfáze) a M (mitóza/cytokineze). Průběh a přechod mezi jednolivými fázemi buněčného cyklu je řízen cyklin-dependentními kinázami (CDK) a cykliny (Qi a

Zhang, 2020). Pro úspěšný průběh buněčného dělení jsou kromě správného načasování a lokalizace zásadní také proteiny nukleoplazmy a cytoplazmy interagující s jaderným obalem. U vyšších rostlin se při dělení buněk jaderný obal rozpadá, aby se mitotické vřeténko mohlo spojit s chromozomy. V tomto okamžiku se genetický materiál buňky nachází v cytoplazmě a k dokončení buněčného dělení je nezbytné přetvoření jaderného obalu (Graumann *et al.,* 2010, Pradillo *et al.,* 2019). Pro regulaci aktivity genomu eukaryot je klíčové sbalení DNA do formy chromatinu a kompaktních jednotek nukleozomů. Modifikací nebo výměnou histonů tvořící nukleozomy, modifikací bazí DNA nebo malé RNA lze ovlivňovat stav chromatinu ve výsledku umožňující přepis jiných částí DNA vedoucí k odlišným produktům transkripce (Berger, 2007). Pro rostlinné genomy jsou charakteristické značné rozdíly v jejich velikosti a úroveň ploidie, počtu homologních sad chromozomů. Chromozomy eukaryot se mohou lišit také tvary, složením DNA, proteinů a RNA (Schubert, 2007). Tvar monocentrických chromozomů je určen polohou centromery, která rozděluje chromozom na ramena. Velikost chromozomu v metafázi může být menší než 1 μm, ale i větší než 10 μm (Schubert, 2007). Počet chromozomů rostlin se obvykle pohybuje v rozmezí 5–20. Například každý ze 7 chromozomů diploidního genomu ječmene *H. vulgare* obsahuje v průměru přibližně 14% část z úplného 5,1 gigapárů bazí velkého genomu (Doležel *et al.,* 2014). Pro srovnání genomy *A. thaliana*, kukuřice *Z. mays* a člověka mají velikost 5,1 megaparů bazí rozprostřených na 5 haploidních chromozomech (Initiative, 2000), 2,4 gigapárů bází na 10 haploidních chromozomech v případě kukuřice (Hake a Walbot, 1980) a 3,1 gigapárů bází na 23 haploidních chromozomech u člověka (International Human Genome Sequencing Consortium, 2001). Pro zajištění replikace a stability během buněčného dělení obsahují chromozomy 3 základní struktury: centromery, telomery a počátky replikace DNA (Gill *et al.,* 2008). Proteiny nezbytnými pro udržení sesterských chromatid pohromadě během mitozy a meiózy jsou komplexy strukturní údržby chromozomů („structural maintenance of chromosome“, SMC). Jednou ze složek těchto komplexů představuje kohesin, duležitý také pro aktivitu SWI/SNF komplexů po poškození DNA (Meisenberg *et al.,* 2019; Bolaños-Villegas, 2021). Typickým chromozomálním proteinem je centromerově specifický histon H3, vázající se je na opakující se sekvence DNA právě v centromerách a interagující s tubuliny kinetochor při segregaci chromozomů (Simon *et al.,* 2015). Interakce s histonem H2A je popsána pro fibrilarin fungující jako DNA methyltransferasa (Loza-Muller *et al.,* 2015).

3.4. Chromozomální proteiny *H. vulgare*

Na základě spolupráce s Ústavem experimentální biologie AV ČR Olomouc byla provedena proteomická analýza extraktů z mitotických chromozomů ječmene izolovaných technikou průtokové cytometrie (Doležel *et al.*, 2012). Cílem experimentu bylo identifikovat proteiny nalezající se ve struktuře izolovaných chromozomů nebo nacházejících se s nimi v kontaktu. Pomocí nLC ESI MSMS analýzy byla provedena „label-free" kvantifikace přítomných proteinů a jejich množství porovnáno na základě NSAF („normalized spectral abundance factor"). Pomocí kombinace výsledků z bioinformatických nástrojů predikující buněčnou lokalizaci a proteinové domény byl zjištěn předpokládaný původ identifikovaných proteinů. Pro ověření nabohacení o specifické proteiny ve vzorcích chromozomů byly jako kontroly analyzovány vzorky buněčného lyzátu nerozdělené průtokovou cytometrií a také nechromozomální frakce „debris" zůstavající po izolaci chromozomů.

Výchozím materiálem pro experimenty bylo vždy 10 milionů chromozomů nebo odpovídající množství „debris" a buněčného lyzátu obsahující 4 μg proteinů. Pro extrakci proteinů z dodaných vzorků byl použit protokol vycházející z práce Jany Beinhauer, Ph.D a Ivo Chamráda Ph.D, zahrnující odstranění formaldehydu použitého k fixaci buněk kořenových špiček ječmene, denaturaci proteinů a rozvolnění DNA aplikací benzonasy a následné štěpení v roztoku trypsinem. Ke zvýšení počtu identifikací bylo použito rozdělení peptidové směsi pomocí mikroseparace v gradientu acetonitrilu v bazickém pH. Data získaná MSMS analýzou byla prohledána softwarem PEAKS Studio 10 (Bioinformatics Solutions) s limitem FDR<1 % na úrovni, spekter, peptidů i proteinů. Informace o lokalizaci proteinů ječmene z databáze UniProt KB byly doplněny o informace odpovídající podobným proteinům *A. thaliana* vyhledaným pomocí NCBI protein-protein Blast (Altschul *et al.*, 2005). Další informace o možné lokalizaci a funkci nalezených proteinů ječmene byly získany analýzou jejich AK sekvencí nástroji Localizer, NucPred, CELLO2GO a WegoLoc (Brameier *et al.*, 2007, Chi a Nam, 2012, Yu *et al.*, 2014, Sperschneider *et al.*, 2017). Tyto nástroje poskytují informaci o možné jaderné lokalizace proteinů, která byla předpokládána. K analýze funkčních proteinových domén byl využit nástroj CD-Search (Marchler-Bauer a Bryant, 2004). Data získaná ze zmíněných nástrojů byla následně připojena k identifikovaným proteinům pomocí Perseus v.1.6.10.45 (Tyanova *et al.*, 2016). Proteiny identifikované ze vzorků chromozomů, pro které byla v UniprotKB zadána jaderná lokalizace a stejnou informaci

nebo přímo chromozomální lokalizaci předpovídaly i nástroje analyzující AK sekvence byly označeny jako jaderné/chromozomální. Obdobně byla vytvořena i skupina nejaderných proteinů z dat ze vzorků „debris“. Těmto skupinám proteinů odpovídaly i proteinové domény jejichž distribuce byla zaznamenána a pro každou doménu bylo vypočteno pravděpodobnostní skóre výskytu mezi jadernými nebo cytosolárními proteiny (Ohta *et al.*, 2010). Kombinace informací o lokalizaci z UniprotKB, jaderná/chromozomální lokalizace předpovídaná predikčními nástroji a informace o doménovém zastoupení byly využity jako tzv. klasifikátory určující pravděpodobnost přiřazení proteinu do skupin dle zvolených parametrů (Ohta *et al.*, 2010). Postup stanovení jaderné/chromozomální lokalizace pomocí klasifikátorů byl aplikován i na dříve získaná data z analýz provedených Janou Beinhauer, Ph.D, kdy bylo pro předseparaci peptidů využito vícekrokové eluce ze silného kationtoměniče (SCX) v uspořádání „stage-tip“ a data z analýzy chromozomálních proteinů separovaných pomocí SDS-PAGE s navazující identifikací pomocí MS.

Výsledkem provedených analýz a vyhodnodnocení byla identifikace 4139 proteinových rodin z nichž pro 837 je předpokládána jaderná/chromozomální lokalizace. Pro přiřazení lokalizace proteinů podle charakteristických domén z nástroje CD-Search bylo na základě lokalizace v UniprotKB shodující se se softwarovými prediktory vytvořena databáze čítající 869 domén a jejich pravděpodobnost výskytu v cytosolu nebo jádru. Obohacení proteinů zařazených mezi jaderné bylo vyšší u vzorků předseparovaných na SCX dosahující v průměru 44 % (8 vzorků) oproti 36 % (3 vzorky) zastoupení u vzorků z mikrogradientové separace. Kvalitativní proteinové zastoupení však bylo opačné, v průměru 257 oproti 231 zástupcům ve prospěch mikrogradientu. Možným vysvětlením je obohacení vzorků z SCX o peptidy z abundantních bazických proteinů jako jsou histony. Ve vzorcích izolovaných chromozomů bylo na základě NSAF vypočteno obohacení pro skupiny jaderných/chromozomálních proteinů nalezených nejméně ve 2 biologických replikátech o více než 140 % oproti kontrole představující původní buněčný lyzát kořenových špiček ječmene. Využitím průtokové cytometrie je tak možné i z fixovaných preparátu buněčného lyzátu ječmene efektivně izolovat obohacenou chromozomální frakci včetně proteinů. Identifikované proteiny označené jako jaderné byly porovnány s databází UncleProt (Blavet *et al.*, 2017). Za tímto účelem byla zdrojová data UncleProt prohledána stejným způsobem a se shodnými parametry a databází jako experimentální data z analýz chromozomů. Výsledkem byla shoda ve 311

proteinových rodinách z 837 srovnávaných. GO analýzou („gene ontology") nástrojem DavidGO (Huang *et al.*, 2009) byly pro více než 60 % proteinů z chromozomů označených jako jaderné/chromozomální přiřazeny GO kategorie „jádro“, „chromozom“, „telomera“ nebo „centromera“ dokládající funkčnost použité klasifikační strategie. Pomocí nástroje Panther GO, umožňující převést vložený dataset mezi organismy, byly proteiny označené jako jaderné seskupeny do tříd dle funkce. V tomto případě byl pro anotaci více zástupců převeden omezeně popsaný set proteinů z ječmene na dataset *Arabidopsis* s lepší anotací. Po rozřazení rozpoznaných proteinů do tříd bylo v případě SCX experimentů označeno 60 % z nich, jako interagující s nukleovými kyselinami (z toho 59 % s DNA, a zbytek s RNA, při použití mikrogradientu bylo takto zařazeno dohromady 56 % popsaných zástupců).

Mezi identifikovanými proteiny s popsanou jadernou nebo přímo chromozomální lokalizací převládaly histony. Z 837 jaderných proteinů bylo nalezeno 114 resp. 137 zástupců popsaných přímo v databázi Uniprot pro ječmen a *A. thaliana*. Hlavní podíl mezi nalezenými proteiny tvořily histony i dle NSAF. Kromě bežných histonů H2 a H3 euchromatinu byl nalezeny i formy z heterochromatinu H3.1 nebo H1.2 zastoupené v obou případech 14×. Identifikován byl také histon centromery CENH3 označený jako A0A287TWS5 pro *H. vulgare*. Po analýze dat pomocí nástroje Panther GO, byla vyčleněna skupina 10 proteinů souvisejících s chromatinem zahrnující podjednotky komplexů SWI/SNF (A0A287QVR1 a A0A287TEF2) remodelujících chromatin a ovlivňujících přepis DNA (Zemach *et al.*, 2013). Pro dynamiku a údržbu chromatinu má zásadní význam protein NAP1 („Nucleosome assembly protein 1“) přenášející do jádra histony a podílející se na sestavování nukleosomů, který je homologní k nalezeným proteinům F2DVK7 a A0A287GF83 (Park a Luger, 2006). Dále do této skupiny byly zařazeny podjednotky SPT16 komplexu FACT („FAcilitates Chromatin Transcription“, A0A287H1F1, A0A287H1F8, M0Z854) u rostlin interagující s RNA polymerasou 2 (Grasser, 2020). Nalezené proteiny A0A287JVQ6 a A0A287EES7 podobné Sin3 proteinu hrají důležitou roli jako nástupní proteiny pro další komponenty korepresorového komplexu umlčující transkripci mezi proliferací a diferenciací buněk (Spronk *et al.*, 2000). Posledním proteinem z vyčleněné skupiny je možný analog RSA1 (A0A287P3E5) u *A. thaliana* zastávající funkci jaderného receptoru vázající Ca^{2+} a reagující na vnější stress způsobený zasolením (Guan *et al.*, 2013). Dále bylo nalezeno 15 zástupců skupiny MCM proteinů („Mini-chromosome maintenance“). MCM proteiny

tvoří heterohexamerní komplex složený z MCM2-MCM7 a všechny tyto komponenty byly v tomto experimentu identifikovány (Tuteja *et al.*, 2011). Tvorba MCM komplexu a jeho aktivace CDK je nezbytným krokem k zahájení replikace DNA (Tuteja *et al.*, 2011). SMC proteiny zajišťující strukturu chromozomů byly nalezeny pro komplex kohesinu obsahující SMC3 a SMC1 a komplex kondensinu zahrnující SMC2 a SMC4. Proteiny SMC5 a SMC6 tvořící vlastní komplex SMC5/6 nebyly identifikovány (Schubert, 2009). Skupinu zahrnující 127 zástupců tvoří mezi proteiny označenými jako jaderné/chromozomální zástupci skupin vázající RNA nebo označení jako ribozomální proteiny. Mezi těmito zástupci převládají 40S a 60S ribozomální podjednotky. Mezi proteiny vázající RNA náleží idenfitikovaná β podjednotka DNA řízené RNA polymerasy 2. Fibrilarin 1 (FIB1) zastávající funkci rRNA 2'-O-methyltransferasy procesuje pre-ribozomální RNA. Proteomická data zařazující FIB1 jako jaderný/chromozomální protein byla potvrzena experimentem dokládající jeho přítomnost, po původní lokalizaci v jadérku také na povrchu chromozomů v průběhu mitózy buněk. Za tímto účelem byla kolegy z ÚEB a Oddělení molekulární biologie CRH PřF UP, připravena transgenní linie ječmene produkující fuzní protein EYFP-FIB1. Jeho přítomnost byla ověřena mikroskopickým pozorováním na struktuře izolovaných chromozomů. Zároveň byla také dokázána asociace tohoto proteinu k chromozomům prostřednictvím přítomné RNA, po jejímž odstranění RNAasou byl ztracen i signál EYFP-FIB1. Kompletní data a detailní popis použitých metod lze nalézt v publikaci Perutka *et al.*, 2021 uvedené jako příloha č. 3 této práce.

3.5. Výsledky – pseudotrypsin

3.5.1. Izolace pseudotrypsinu

Autolýzou trypsinu a následnou separací na kationtoměniči byla získána frakce obsahující proteoformu ψ-trypsin. Podle záznamu chromatografické separace na HemaBio 1000 SB koloně byla předpokládána přítommnost ψ-trypsinu v jedné z frakcí s elučními časy 19,5, 24,5 a 25,5 min. Po dialýze těchto frakcí z původních objemů (8,5, 7,5 a 6,0 ml) na objem 1 ml bylo pomocí MALDI-TOF MS zjištěna přítomnost ψ-trypsinu ve frakci eluované v 19,5 min (Obr. 1). Nejlepší separace na koloně Hema Bio 1000 SB bylo dosaženo při snížení obsahu $CaCl_2$ z koncentrace 20 mM na 10 mM v mobilní fázi 50 mM Tris-HCl pufru o pH 7,1. Obsah proteinů v této frakci byl stanoven na 0,5 $mg \cdot ml^{-1}$. Při použití UNO S12 kolony byl ψ-trypsin identifikován ve frakci eluované v čase 30 min od začátku separace při použití stejného pufru a lineárně vzrůstající koncentraci 1M NaCl do celkového obsahu 30 % v mobilní fázi (Obr. 1, dole). Podmínky pro opakovatelnou chromatografickou separaci jednotlivých proteoforem trypsinu při použití kombinace MonoS5 a UnoS1 kolony v sériovém spojení se nepodařilo optimalizovat.

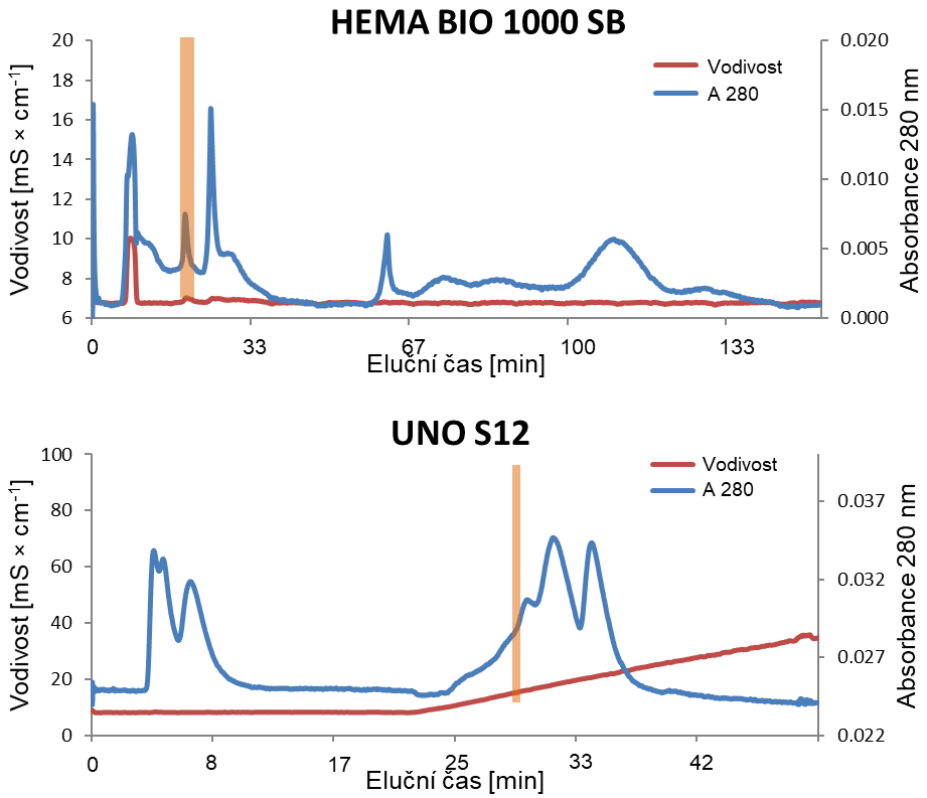

Obr. 1 Chromatogramy separace autolyzátu trypsinu na koloně Hema Bio 1000SB (nahoře) a UnoS12 Frakce obsahující ψ-trypsin jsou vyznačeny oranžově.

Přítomnost ψ-trypsinu ve vyznačených frakcích byla potvrzena analýzou MALDI-TOF MS. V hmotnostním spektru lze vidět kontaminaci běžnými formami α- a β-trypsinu. Signály těchto kontaminantů odpovídají součtu jejich MW a vazbě v nadbytku přidaného ireverzibilního inhibitoru TLCK, který není vázán pouze ψ-trypsinem. Dále lze pozorovat adukty inhibovaných enzymů s použitou matricí SA (Obr. 2). Obsah ψ-trypsinu v preparátu byl stanoven na 20 % vzhledem k zjištěné kontaminaci inhibovanými formami.

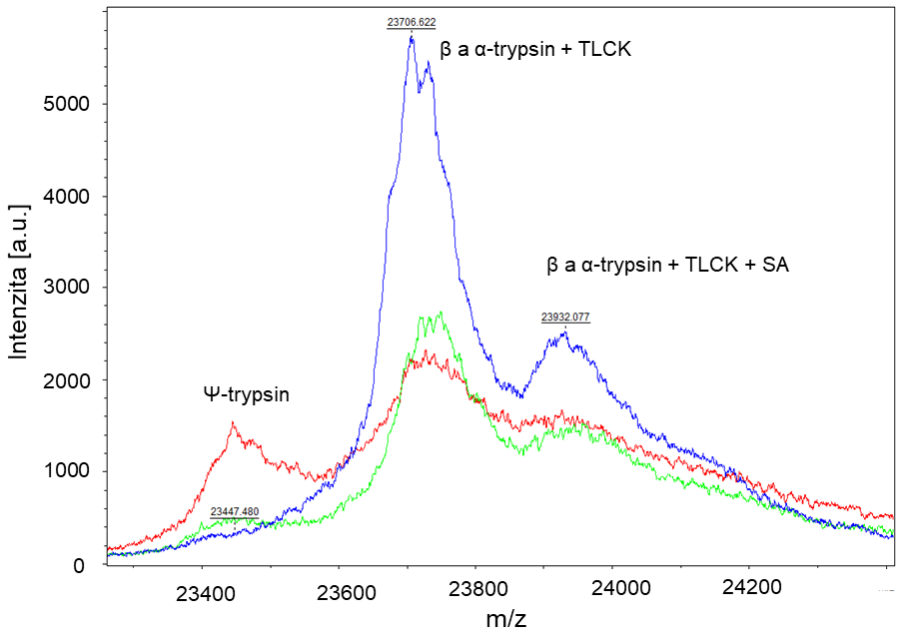

Obr. 2 MALDI TOF Hmotnostní spektra frakcí po separaci autolyzátu trypsinu na Hema Bio 1000SB koloně. Použita matrice SA. Barvy spektra, červená – eluce v 19,5 min, modrá – eluce v 24,5 min, zelená – eluce v 25,5 min.

3.5.2. Srovnání štěpení pseudotrypsinu a trypsinu pomocí MALDI-TOF MS

Po vyhodnocení MALDI-TOF MS spekter směsných vzorků digestů BSA s RafBT (rafinosou modifikovaný hovězí trypsin) připravených ve vodě $H_2{}^{18}O$ s produkty štěpení ostatních trypsinů bylo nalezeno 5 peptidů poskytující při všech kombinacích dostatečně izotopově rozlišená spektra pro vzájemná porovnání (Tab. 1).

Tabulka 1. Peptidy vznikající enzymovým štěpením standardu BSA všemi porovnávanými trypsiny a ψ-trypsinem. Koeficienty izotopového zastoupení korelující velikosti plochy píků (*m/z* +2 Da a *m/z* +4 Da) „f3“ a „f5“ jednotlivých peptidů (Mirgorodskaya *et al.*, 2000; Obr. 3).

Peptid BSA		koeficienty izotopového zastoupení	
sekvence	*m/z*	f3	f5
LVNELTEFAK	1163.6	0.2470	0.0150
FKDLGEEHFK	1249.7	0.2901	0.0197
HLVDEPQNLIK	1305.7	0.2990	0.0211
SLHTLFGDELCK (Cys_CAM)	1419.7	0.3877	0.0427
RPCFSALTPDETYVPK (Cys_CAM)	1880.9	0.6145	0.1002

Na základě výpočtu bylo zhodnoceno relativní množství jednotlivých peptidů ve vzorcích.

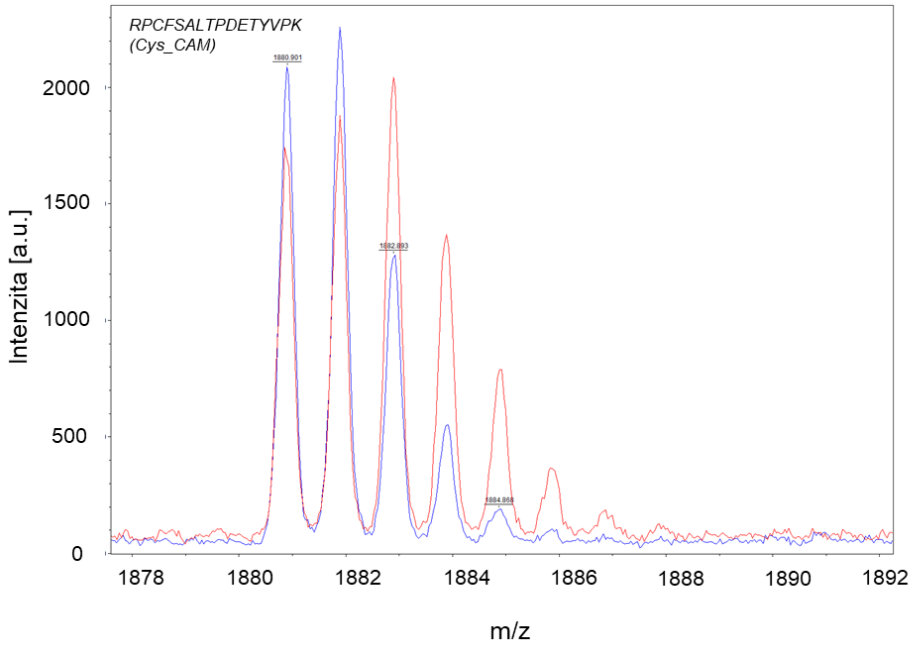

Obr. 3 MALDI TOF MS spektrum peptidu značeného ^{18}O a neznačeného peptidu. Spektrum peptidu *RPCFSALTPDETYVPK (Cys_CAM)* s *m/z* 1880,9 původem z 500 fmol BSA naštěpeného ψ-trypsinem (modrá) a směsi ½ množství stejného digestu s odpovídajícím množství RafBT digestu BSA v ^{18}O pufru (červená).

Poměr mezi obsahem peptidů BSA po naštěpení RafBT v pufru s ^{18}O vodou a běžným digestem BSA stejným enzymem byl pro srovnání s dalšími trypsiny normalizován a brán

jako shodný. Největší obsah sledovaných peptidů poskytoval oproti značenému standardu vždy vzorek digestu BSA a trypsinu izolovaného z prasečího pankreatu a modifikovaného pomocí reduktivní metylace od fy. Serva. Relativně nižší množství peptidů bylo pozorováno u vzorků s ψ-trypsinem a i u vzorku štěpeném hovězím trypsinem od fy. Roche (Obr. 4). Míra účinnosti štěpení Serva trypsinu oproti standardu RafBT byla až o více než 10 % vyšší. V případě ψ-trypsinu bylo naopak štěpení méně efektivní, a to v průměru o 10 %.

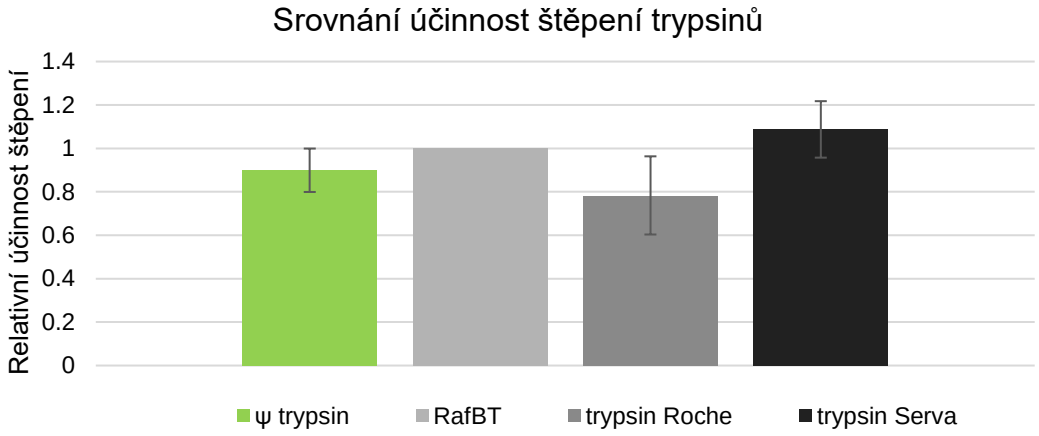

Obr. 4 Srovnání účinnosti štěpení trypsinů. Srovnání relativní účinnosti štěpení trypsinů včetně izolovaného ψ-trypsinu na základě porovnání množství vybraných peptidů, kvantifikovaných dle ploch jejich píku v MALDI-TOF MS spektrech vzhledem k izotopově značenému standardu.

3.5.2. Aplikace pseudotrypsinu pro štěpení jaderných proteinů

Analýzou pomocí nLC MALDI MSMS bylo ve vzorcích proteinů extrahovaných z jader ječmene (Obr. 5), rozdělených pomocí gelové elektroforézy a následně po frakcích štěpených pomocí ψ-trypsinu bylo identifikováno více než 15 % peptidů vzniklých nespecifickým štěpení za W, Y, F, L/I (Obr. 6). Na úrovni proteinů bylo pomocí nLC MALDI MSMS identifikováno od 90 do 140 proteinů (příloha č. 1), z nichž vždy nejméně 10 % bylo nových, neidentifikovaných pomocí štěpení pouze RafBT ani při použití nLC ESI analýzy (Tab. 2).

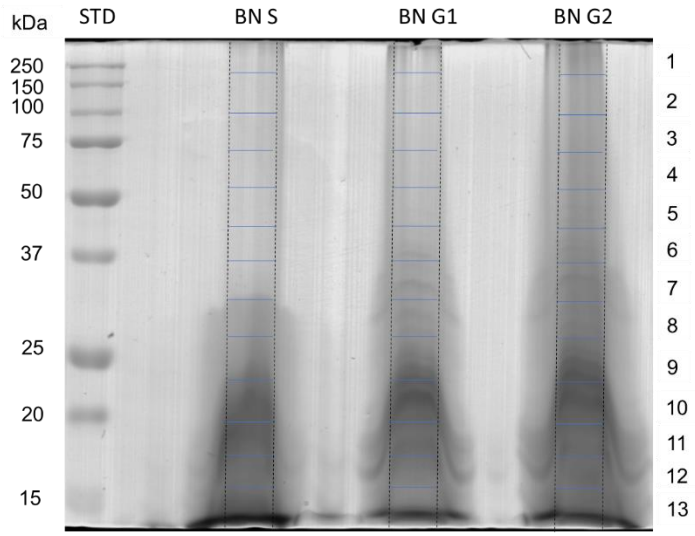

Obr. 5 SDS-PAGE separace proteinů z 10 milionů jader ječmene z fáze S, G1, a G2 buněčného cyklu. Vyznačené linie označují rozdělení gelu na frakce 1–13, které byly zpracovány vždy jako 2 shodné části (pravá/levá) pro paralelní štěpení RafBT a ψ-trypsinem (výsledky uvedeny v příloze č. 4). Gel byl barven Coomassie Bio-Safe (Bio-Rad). Vlevo vyznačeny standardy MW Precision Plus Protein Standards *(*Bio-Rad).

Tab. 2 Počty proteinových rodin identifikovaných po štepení ψ-trypsinem.
Počty proteinů jsou redukovány na počty proteinových rodin po analýze dat softwarem Peaks Studio 8, při FDR <1 %, a přítomnosti min. 1 unikátního peptidu.

vzorek	nLC MALDI MSMS			nLC ESI MSMS		
proteiny	celkem	nové	%	celkem	nové	%
G1	102	18	*19*	460	47	*10*
G2	141	17	*12*	558	59	*10*
S	91	13	*16*	346	44	*13*

Analýzou vzorků pomocí nLC ESI bylo identifikováno vždy nejméně 20 % peptidů vzniklých aktivitou ψ-trypsinu. Kompletní seznam nově identifikovaných proteinů pomocí nLC MALDI a nLC ESI MSMS technik je uveden jako příloha č. 3.

Po odečtení proteinů identifikovaných duplicitně mezi vzorky z jednotlivých fází buněčného cyklu ječmene bylo nalezeno celkem 133 a 42 nových proteinových rodin po analýzách nLC-ESI-MSMS a nLC-MALDI-MSMS (viz. příloha č.3). Na základě identifikovaných peptidů byla stanovena specifičnost štěpení ψ-trypsinu. Nejčastěji byly

identifikovány tryptické peptidy s C-koncovým R nebo K tvořící okolo 80 % celkového počtu. Štěpné produkty odpovídající specifičnosti ψ-trypsinu dále tvoří 10–15 % zastoupení peptidů (Obr. 7).

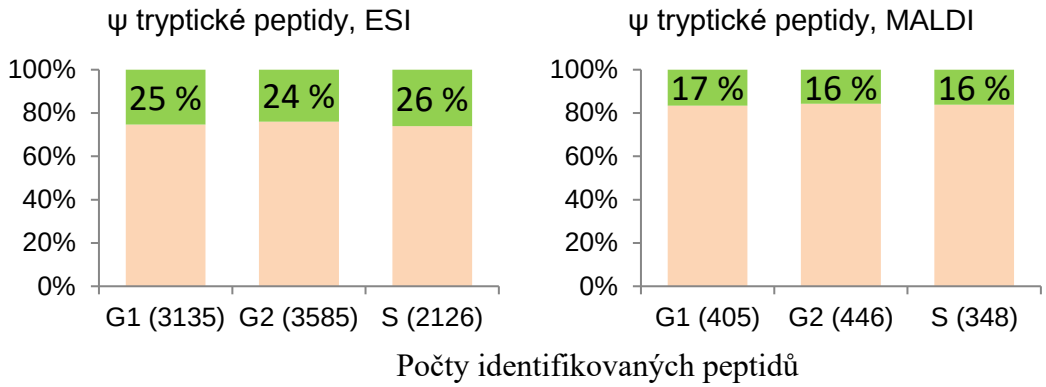

Obr. 6 Sloupcové grafy zobrazující poměry peptidů vzniklých aktivitou ψ-trypsinu a detegovaných sekvenční analýzou pomocí nLC-MALDI-MSMS a nLC-ESI-MSMS.

P1 AK	G	A	V	L	I	M	P	F	W	S
MALDI	2.0%	0.9%	0.5%	2.2%	0.1%	0.9%	0.3%	2.1%	0.4%	0.7%
ESI	1.1%	0.9%	0.5%	4.4%	0.3%	0.8%	0.3%	4.8%	0.8%	0.6%

P1 AK	N	Q	T	Y	C	K	R	H	D	E
MALDI	1.1%	0.4%	0.6%	4.2%	0.0%	32.7%	49.2%	0.4%	1.2%	0.1%
ESI	0.8%	0.4%	0.3%	5.2%	0.0%	37.0%	39.6%	0.5%	1.1%	0.4%

Obr. 7 Specifičnost štěpení. Grafické znázornění procentuálního zastoupení peptidů vzniklých po štěpení ψ-trypsinu za C-koncovou (P1 pozice) aminokyselinou.

3.6. Diskuse

Pseudotrypsin získaný autolýzou hovězího trypsinu vykazoval při stanovení jeho specifičnosti štěpení velmi podobné preference jako publikovali Dyčka *et al.*, 2015. Při aplikaci pseudotrypsinu pro 12 hodinové štěpení připraveného standardu BSA v roztoku, je jeho relativní účinnost srovnatelná s komerčními trypsiny. Překvapivě nižší výtěžky

sledovaných peptidů z BSA u trypsinu fy. Roche byly zřejmě způsobeny špatnou přípravou, rozpuštěním tohoto enzymu v nevhodném skladovacím pufru, kdy mohlo dojít k jeho autolýze. Otestované metody separace autolyzátu trypsinu, nebo standardu trypsinu obsahující α a β proteoformu, jsou použitelné i pro izolaci ψ-trypsinu. Výtěžek izolace ψ-trypsinu z autolyzátu je však velmi nízký dosahující jen 1-5 % hmotnosti vzhledem v původnímu materiálu. Nízký obsah ψ-trypsinu vzniklého autolýzou se neshoduje s výsledky Smith a Shaw, 1969, kteří získali i přes 40 % žádaného produktu. Klíčovým faktorem ovlivňující množství vzniklého pseudotrypsinu a výtěžek jeho přípravy, tak zřejmě bude čistota vstupního materiálu bez přítomnosti zbytků chymotrypsinu. Dostatečná účinnost a specifičnost pseudotrypsinu umožnila jeho použití pro štěpení komplexních proteinových směsí jaderných proteinů a identifikaci nových proteinů dosud neidentifikovaných v experimentech využívajících běžný trypsin (Blavet *et al.,* 2016). Mezi nově identifikovanými proteiny z jader ječmene byla nalezena například tRNAasa Z (M0XD10_HORVD), endonukleasa upravující 3´-konec prekurzorových tRNA molekul (Vogel *et al.*, 2005). Dle prohledání NCBI Blast je tento protein téměř shodný se stejným enzymem ječmene a obdobnými rostlinnými enzymy lokalizovanými v mitochondriích. Jaderná lokalizace a vazba k DNA je uváděna pro „SAP domain-containing protein“ (M0WPB1_HORVD). Proteiny s touto doménou jsou zapojeny do organizace chromozomů a oprav DNA (Aravind *et al.*, 2000). Methylace cytosinu DNA je hlavním způsobem metylace DNA mající zásadní roli v regulaci genové exprese. V rostlinné říši je tento proces spojen s růstem listů, vývojem semen nebo zráním plodů (Li *et al.*, 2018). Mezi enzymy zprostředkovávající tuto modifikaci patří identifikované DNA-cytosin-5-metyltransferasy (M0UHH0_HORVD, M0UHG9_HORVD, M0YKC8_HORVD a M0YKD6_HORVD) s předpokládanou jadernou lokalizací. Protein M0WJV7_HORVD bohatý na glycin se dle analogie může nespecificky vázat na molekuly RNA i DNA. U rostlin byla tato schopnost popsána u semen *A. thaliana*. Iniciátorem interakce může byl enviromentální stres a následkem opožděné klíčení (Kwak *et al.*, 2005). Podařilo se identifikovat i součást jaderného póru NUP133 protein (M0YGC4_HORVD). Transkripční faktor WRKY6 je u *A. thaliana* spojován s obrannými procesy, senescencí. Funkce nalezeného „WRKY6-like“ proteinu (M0YE09_HORVD) z kořene ječmene by na základě analogie mohla souviset s obsahem dostupného fosfátu a jeho transportérem PHO1 (Chen *et al.,* 2009). V jadérku je lokalizován identifikovaný „SAM_MT_RSMB_NOP domain-containing“ protein (M0WTL8_HORVD), methyltransferasa zapojená do biogeneze ribozomů. Dále se

podařilo zachytit β-1 podjednotku importinu (M0UKH1_HORVD) pro přenos proteinů do jádra (Marfori *et al.*, 2011). Nalezený protein (M0XWY3_HORVD) obsahující HIRAN doménu by mohl být SWI2/SNF2 nebo Rad5 remodelátor chromatinu (Zemach *et al.*, 2013).

4. IDENTIFIKACE PROTEINŮ TRÁVÍCÍ ŠŤÁVY *D. capensis*

Masožravé rostliny (MR) jsou schopny lákat, lapat a následně trávit svou kořist s cílem získat a aktivně využít živiny, které jejich oběti představují (Givnish *et al.*, 2018). Specifickou adaptací těchto rostlin pro zachycení kořisti se staly jejich listy, které se morfologicky přeměnily na pasti (Givnish *et al.*, 2015). Tato dovednost umožnila MR osídlit a obývat velmi slunná, suchá nebo příliš vlhká a temná, na živiny chudá stanoviště (Givnish *et al.*, 2018). V současnosti lze nalézt okolo 800 druhů MR rozdělených do 5 řádů a 20 rodů krytosemenných rostlin (Givnish, 2015; Ellison a Adamec, 2017). Kořist MR představuje většinou drobný hmyz. Masožravost se u rostlin vyvinula navzájem nezávisle a vznikla tak řada specializovaných pastí (Givnish, 2015).

Podle způsobu použití a možností pohybu lze pasti MR rozdělit na aktivní a pasivní. Aktivní pasti lze rozdělit na sklapovací, podtlakové nebo měchýřkové a aktivní lepivé pasti (Givnish, 2015). Pasivní pasti, tedy nástrahy, kterými MR oběť zachytí pasivně bez investice další energie pro aktivní pohyb mohou fungovat na principu přilepení, adheze nebo jako spádová past, láčka, do které oběť sama spadne a lepivá tekutina na dně v kombinaci s kluzkými stěnami ji neumožní uniknout (Givnish, 2015). Netradiční typy pastí představují tzv. jednosměrné pasti u MR rodu *Genlisea* a rostliny *Sarracenia psittacina*, kdy je drobný hmyz nalákán a zachycen ve stále se zužující chodbě vystlané orientovanými chloupky umožňující pouze jednosměrný pohyb (Givnish, 2015). Pasti připomínající láčky využívají MR z rodů *Brocchinia* nebo *Catopsis*, ve kterých je kořist trávena v prostoru uprostřed listové růžice, kam je z listů sekretována trávící tekutina (Givnish, 2015). Trávení kořisti MR probíhá po zachycení kořisti do pasti zejména pomocí hydrolas. Spouštěcími mechanismy pro zvýšenou sekreci těchto enzymů a zahájení trávení jsou buďto specifické látky uvolněné z těla obětí nebo mechanický stimul (Mithöfer *et al.*, 2014; Böhm *et al.*, 2016). Uvolněné živiny z kořisti jsou následně rostlinou aktivně vstřebávány (Hedrich a Neher, 2018). Vysoká specializace a zřejmá podobnost těchto pochodů a mechanismů s již známými metabolickými procesy běžných rostlin (Pavlovič a Mithöfer *et al.*, 2019) vystavuje MR intenzivnímu zájmu studia na úrovni genů i proteinů.

4.1. Karnivorní syndrom

Rostliny klasifikované jako masožravé musí splňovat několik podmínek souhrnně označovaných jako tzv. „syndrom masožravosti“. Hlavní podmínkou je odchyt kořisti pomocí k tomu uzpůsobené pasti, dále musí být MR schopna uvolněné látky z kořisti

absorbovat a konečně je musí také využít pro vlastní růst a vývoj (Givnish *et al.*, 1984, Adamec *et al.*, 1997, Ellison a Adamec, 2017). Všechny typy pastí masožravých rostlin se vyvinuly přeměnami listů. Příjem látek povrchem listů MR vedl k omezení fotosyntetického aparátu v těchto částech, což je důvodem jejich pomalejšího růstu oproti běžným autotrofním rostlinám (Adamec, 2010). Dodatečný zisk živin z kořisti kompenzuje MR omezený přísun kořeny, které jsou vzhledem k velikosti celé rostliny redukovány a mohou tvořit i jen 3 % těla rostliny (Adamec *et al.*, 1997, Adamec *et al.*, 2002). Tato adaptace je běžná pro téměř všechny MR typicky obývající kyselé, bažinaté nebo podmáčené půdy s výjimkou rusnolistu lusitánského (*Drosophyllum lusitanicum*) adaptovaného pro růst v prostředí pískovcových skal jižní Evropy a Maroka (Adlassnig *et al.*, 2006). Kořist je pro MR významným zdrojem základních makroprvků N a P běžně získávaných rostlinami kořeny. Charakteristickou vlastností je pro masožravé rostliny schopnost reutilizace, znovu využití látek z vlastních starých odumírajících částí (Adamec *et al.*, 1997). Takto mohou některé rostliny znovu zužitkovat až 99 % materiálu (Adamec, 2002).

4.2. Proteiny a trávení masožravých rostlin

Kořist zachycená v pasti MR většinou stimuluje sekreci trávících šťáv rostliny. Signál k těmto dějům je zprostředkován pomocí rostlinných hormonů nebo látek jim podobných. V případě prostudovaného mechanismu mucholapky podivné (*Dionaea muscipula*) je zavření pasti a následná sekrece trávící šťávy spuštěna až opakovaným podrážděním senzorových chloupků uvnitř pasti. Podráždění následně vede ke vzniku a šíření signálu pomocí Ca^{2+} iontů (Nakamura *et al.*, 2013). K produkci trávících šťávy u mucholapky dochází po zachycení signálu z kořisti. Externími signálními molekulami mohou v tomto případě být jasmonáty, nebo konjugát k. jasmonové s Leu a strukturní analog této látky koronatin, které po indukci rostlina sama produkuje a hromadí se v pletivu pasti. Zdrojem coronatinu může být rostlinný patogen *Pseudomonas syrringae*, který je hmyzem přenášen (Nakamura *et al.*, 2013). Jasmonáty, zejména kyselina oxylipin-12-oxofytodienová (OPDA) jsou přitom akumulovány i v ostatních pastech, které se stávají citlivější na aktivaci kořistí (Escalante-Pérez *et al.*, 2011). Stejné působení bylo pozorováno i u *Drosera capensis* (Obr. 8). Akumulace jasmonátů v listu na kterém

došlo k zachycení kořisti a vedlo k jeho pozvolnému ohybu, který je nutný aby se kořist dostala do kontaktu s trávící šťávou (Mithöfer *et al.*, 2014).

Obr. 8 Makrofotografie listu rosnatky kapské v čase 12 h po zachycení kořisti hmyzu. (převzato z Nakamura *et al.*, 2013)

Dalším typem indukce a stimulace MR k lovu může být mechanismus založený na obraně proti patogenním houbám, který je znám z říše rostlin i živočichů. Elicitorem je chitin z buněčné stěny houby. Protein vázající se k oligosacharidovým fragmentům chitinu byl charakterizován jako 41 kDa glykopeptid obsahující 2 LysM motivy (Kaku *et al.*, 2006). Srovnáním proteinových profilů trávící šťávy *N. khasiana* ze zavřených láček po indukci čistým chitinem byly pozorovány 4 nové pásy po SDS-PAGE a zesílení signálu u 2 odpovídajícím profilu bez indukce chitinem. Proteiny tvořící tyto signály nebyly identifikovány (Eilenberg *et al.*, 2006). K výraznému zvýšení sekrece hydrolas do trávící šťávy došlo po přidání NH_4Cl do láčky *S. purpurea* (Gallie a Chang, 1997). Přidání NaCl způsobilo minimální změnu aktivity sledovaných enzymů. Po indukci sekrece hydrolytických enzymů bylo pozorováno postupné okyselování trávící šťávy (Gallie a Chang, 1997).

4.2.1. Trávení kořisti

Trávení kořisti v pasti MR obstarávají k tomu produkované enzymy. Hlavní roli v procesu rozkladu kořisti zaujímají proteolytické enzymy, chitinasy, fosfatasy, glukanasy, nukleasy, lipasy a zřejmě také oxidasy a další typy hydrolas (Scala *et al.*, 1969; Heslop-Harrison a Knox, 1971; Robins a Juniper, 1980; Athauda *et al.*, 2004; Eilenberg *et al.*, 2006; Hatano a Hamada, 2008; Mithöfer 2011; Schulze *et al.*, 2012; Nishimura *et al.*, 2013; Lee *et al.*, 2016; Rottloff *et al.*, 2016; Fukushima *et al.*, 2017; Krausko *et al.*, 2017; Kocáb *et al.*, 2020). Sekrece trávících enzymů je konstitutivní nebo indukovaná

(Pavlovič a Mithöfer *et al.*, 2019). Spouštěčem pro expresi trávících enzymů může být mechanický nebo chemický stimul (Pavlovič *et al.*, 2014, Saganová *et al.*, 2018).

4.2.2. Enzymy v trávících šťávách MR

Trávící šťávy masožravých rostlin obsahují směs hydrolytických enzymů umožňující rozklad biologických polymerů jako je celulosa nebo u hmyzu chitin. K rozložení proteinů, obsahující pro rostlinu důležitý dusík jsou v trávících šťávách přítomny kyselé proteasy. Některé druhy masožravých rostlin vlastní trávící enzymy neprodukují a jsou závislé na činnosti mikroorganismů žijících v jejich pastech nebo zavlečených tam kořistí.

4.2.2.1. Chitinasy

Chitinasy jsou hydrolasy štěpící beta-1,4 vazbu mezi *N*-acetyl-glukosaminovými monomery tvořící chitin (Grover, 2012). Pro rostliny jsou chitinasy důležitým obranným prostředkem proti napadení houbami. Rozkladem chitinové buněčné stěny hub, potlačují rostliny jejich růst. Chitinasy mohou štěpit na koncích nebo uvnitř řetězce chitinu, lze tak rozlišit endo- a exochitinasy. Exochitinasy se dále odlišují podle toho, zda odštěpují 1 nebo 2 monomery *N*-acetylglukosaminu (Grover, 2012). Chitinasy jsou rozděleny do 5 tříd mezi 2 rodiny glykosidas. Chitinasy s lysozomální aktivitou, kam náleží i enzymy masožravých rostlin patřící do III třídy chitinas zahrnutých mezi glykosidasy rodiny č. 18 (Cohen-Kupiec a Chet, 1998). Pro mucholapku je hlavním nástrojem pro hydrolýzu vnější kostry hmyzu chitinasa 1 patřící mezi extracelulární chitinasy třídy Ib schopná štěpit chitin v rozpustné i krystalické formě (Paszota *et al.*, 2014). Transkripce genu pro tento 33,2 kDa velký enzym byla zaznamenána vždy, jak po mechanickém, tak po chemické stimulaci a výhradně jen v buňkách sekretujících trávící štávu. Optimální podmínky pro aktivitu chitinasy-1 mucholapky jsou 50 °C a pH 5. Odolnost vůči vlastním proteasám je zvýšena přítomností nejméně 4 disufidových vazeb a vysokým obsahem prolinu (7,8 %) v kompaktní struktuře tohoto enzymu (Paszota *et al.*, 2014). K zvýšení její transkripce dochází do 48 hodiny po stimulaci a zavření pasti mucholapky. Mezi 48-68 hodinami po stimulaci převládá tento enzym v trávící šťávě mucholapky (Schulze *et al.*, 2012). U láčkovek (*Nepenthes*) jsou dlouhé polymery chitinu štěpeny chitinasami III třídy a fragmenty následně dále hydrolyzovány chitinasami z třídy IV (Hatano a Hamada, 2012). Srovnáním sekvencí cDNA byly u této čeledi nalezeny geny pro chitinasy třídy I. obsahující C-koncovou signální sekvenci pro transport do vakuoly, ale i geny pro chitinasy třídy I. sekretované extracelulárně, do láčky, nemající signální sekvenci

(Eilenberg *et al.*, 2006). Chitinasa třídy III, také sekretovaná do apoplastu *Nepentehs* má N-koncový signální peptid (Rottloff *et al.*, 2011). Extracelulárně sekretované chitinasy oproti vakuolárním obsahují ve struktuře více Pro, zejména v oblasti „Hinge" domény (Renner a Specht, 2012). Exprese extracelulárních chitinas roste při stimulaci receptorů pasti MR. Chitinasy s vakuolární signální sekvencí jsou tvořeny konstitutivně u všech druhů rostlin. Teplotní optimum pro aktivitu enzymů produkovaných do láčky u *Nepenthes* je 40–50 °C, při hodnotách pH 3–5. Pro chitinasu IV *Nepenthes alata* bylo zjištěno optimální pH 5,5 a největší aktivita zaznamenány při teplotách okolo 60 °C (Ishisaki *et al.*, 2012). Naopak v trávící šťávě *S. purpurea* nebyla chitinasova aktivita zaznamenána (Gallie a Chang, 1997). In vitro byla studována struktura genu pro chitinasu u rosnatky okrouhlolisté (*Drosera rotundifolia*) obsahující 2 exony (Durechová *et al.*, 2019).

4.2.2.2. Glukanasy

Beta-1,3-glukanasy obsažené v trávících šťávách MR hydrolyzují beta-1,3-glukany, hlavní složku buněčné stěny patogenních hub. Stejnou funkci mohou plnit i proteiny podobné thaumatinu (Grenier *et al.*, 1999). Glukanasy umožňují karnivorním rostlinám získat živiny kromě hmyzu i z jiných objektů zachycených v pastech rostlin. Těmito zdroji jsou např. pylová zrna a spory hub bohaté na β-glukany. Tyto struktury jsou glukanasami rozloženy na menší jednotky, které jsou absorbovány povrchem listů, pastí rostliny a podílí se tedy přímo na trávení „ulovené" kořisti (Michalko *et al.*, 2013).

4.2.2.3. Oxidoreduktasy

V trávících štávách mucholapky (*Dionea*) a láčkovky (*Nepenthes*) byly identifikovány proteiny patřící mezi oxidoreduktasy. U obou zmíněných rostlin byly nalezeny peroxidasy (Hatano a Hamada, 2012; Schulze *et al.*, 2012). Kořist MR je těmito enzymy pravděpodobně oxidována a posléze rozkládána hydrolasami (Schulze *et al.*, 2012). Stejně jako chitinasy jsou oxidoreduktasy řazeny mezi PR („pathogenesis related") proteiny, chránící rostlinu proti enviromentálnímu stresu.

4.2.2.4. Proteasy

Nepenthesiny jsou nejdéle známé proteasy MR identifikované v trávících šťávách láčkovek (*Nepenthes*). V této čeledi rostlin mají aspartátové proteasy hlavní roli v degradaci proteinů kořisti (Stephenson a Hogan, 2006; Buch *et al.*, 2015). Z trávící šťávy *Nepenthes distillatoria* byla částečně purifikována a charakterizována kyselá

peptidasa nazvaná nepenthesin podílející se na trávení kořisti. Ideální podmínky pro působení tohoto enzymu jsou při pH 4,5 a teplotě 55 °C. Molekulová hmotnost byla pomocí SDS-PAGE stanovena na 50 kDa. Možná specifičnost působení byla popsána po hydrolýze oxidovaného beta řetězce insulinu trávícími šťávami různých druhů *Nepenthes* (An *et al.*, 2002). Syntetický substrát PFU-093 (FITC(Ahx)-Val-Val-LysDbc) byl štěpen nepenthesiny v trávící šťávě z *N. mirabilis* a *N. alata* za valinem (Buch *et al.*, 2015). Byly také charakterizovány purifikované nepenthesiny I a II, izolované z trávící šťávy *Nepenthes distillatoria*. Oba tyto enzymy obsahují ve struktuře 12 Cys, což umožňuje formaci 6 disulfidových můstků. Nepethesin I. obsahuje navíc 6 možných *N*-glykosylačních míst oproti pouze 1 u nepenthesinu II. Nepethesin II z *N. gracilis* neobsahuje žádná glykosylační místa. Enzymy jsou velmi stabilní i při 50 °C a aktivní v širokém rozmezí pH od 3 do 10 (Athauda *et al.*, 2004). Aspartatové proteasy podobné nepenthesinům byly identifikovány i v trávící šťávě mucholapky (*Dionea*). Nalezeny zde byly 4 isoformy, z nichž 2 jsou aktivní a podílí se na trávení kořisti. Analogické názvy aktivních enzymů jsou dionaesin 1 a 2 (Schulze *et al.*, 2012). Dionainy byly identifikovány jako hlavní složka trávící šťávy mucholapky (*D. muscipula*). Dionainy patří mezi Cys-proteasy podrodiny C1A. Hlavním zástupcem této skupiny je papain, kterému dionainy strukturně odpovídají. U dionainů se předpokládá autoaktivace v kyselém prostředí odštěpením peptidu z N-konce. Největší aktivita byla zaznamenána v mírně kyselém prostředí v oblasti pH 5–7 (Takahashi *et al.*, 2011). Podle podobnosti s papainem by dionainy měly hydrolyzovat peptidové vazby bazických AK, dále Gly, Leu a velkých hydrofobních AK (Polgar, 1989). Dionain 1, hlavní proteasa mucholapky trávící proteiny kořisti, byla charakterizována Takashi *et al.*, 2011 a později studována jako rekombinantní produkt (Risør *et al.* 2016). Enzym o velikosti 45 kDa byl uměle vytvořen včetně signálního propeptidu v *P. pastoris*. Velikost proformy obsahující obsazené *N*-glykosylační místo v autokatalyticky odštěpitelné prodoméně dosahovala cca 50–66 kDa. Specifičnost tohoto enzymu je podobná papainu, přičemž autoaktivace je možná pouze v kyselém prostředí o pH 3,5-3,8 (Risør *et al.*, 2016). Aktivita cysteinových proteas při hydrolýze proteinů kořisti je v trávící šťávě pasti mucholapky detegovatelná už první den po sekreci a tyto enzymy zde lze nalézt v různých formách (Schulze *et al.*, 2012; Libiakova *et al.*, 2014, Gergely *et al.*, 2018). Dionain1 není inhibován pepstatinem jako Asp-proteasy (Takahashi *et al.*, 2012). V trávící štávě rosnatky indické (*Drosera Indica*) jsou zřejmě přítomny nejméně 2 isoenzymy endopeptidasy dionainu pojmenované analogicky jako droserainy (Takahashi, 2012). Aktivita odpovídající

cysteinovým proteasám byla zjištěna i u láčkovky *Nepenthes ventricosa* (Stephenson a Hogan, 2006). Další skupinu hydrolytických enzymů MR tvoří serinové proteasy nalezené v trávící šťávě mucholapky (*Dionea*). Byla identifikována Ser-karboxypeptidasa patřící do rodiny S10 aktivní v kyselém prostředí (Schulze *et al.*, 2012). Dosud neznámý katalytický mechanismus využívá na prolin specifická proteasa neprosin z *Nepenthes ventrata* (Lee *et al.*, 2016).

4.2.2.5. Další proteiny účastnící se trávení kořisti

Významným zdrojem fosforu jsou pro masožravé rostliny nukleové kyseliny kořisti, což potvrzuje přítomnost ribonukleas v jejich trávících šťávách. Tyto enzymy, „S-like“ ribonukleasy (RNasy) slouží běžným rostlinám k reutilizaci fosforu ze starých orgánů v období senescence nebo při poranění. U masožravých rostlin jsou využity k získávání fosforu z RNA kořisti a obraně před zavlečenými viry (Okabe *et al.*, 2005). Exprese „S-like“ RNas může být také aktivována jasmonáty (LeBrasseur *et al.*, 2002). U karnivorních rostlin dochází ke konstitutivní nebo indukované expresy genů pro RNasy homologní k „S-like“ RNasám. V případě *D. muscipula* k indukci dochází po zachycení kořisti. Regulaci exprese genů pomocí methylace promotoru pro tyto enzymy popsal Nishimura a kolektiv u druhů *D. muscipula, D. Adelae* a *C. follicularis* (Okabe *et al.*, 2005; Nishimura *et al.*, 2013). U *D. Adalae* RNase DA1 o velikosti 22 kDa tvoří 1,2 % proteinové složky trávící šťávy. Neaktivní enzym obsahující signální 18 AK sekvenci pro sekreci má MW 24,9 kDa (Okabe *et al.*, 2005). Struktura RNas z trávící šťávy MR obsahuje 5 disulfidových vazeb, což je charakteristické i pro „S-like“ RNAsy běžných rostlin (Nishimura *et al.*, 2013). Vedle sekrece ribonukleas dochází zřejmě u některých druhů MR i tvorbě DNA hydrolas sekretovaných do trávící šťávy (Gallie a Chang, 1997).

Fosfatasy jsou enzymy schopné hydrolyzovat monoesterové vazby a uvolnit anorganický fosfát ze substrátu. Fosfor je jedním z nejdůležitějších makroprvků pro všechny druhy organismů (Dick *et al.*, 2011). Fosfatasová aktivita byla zjištěna v trávící šťávě mucholapky *D. muscipula,* kde byla její přítomnost dokázána pomocí proteomické analýzy obsahu této šťávy hmotnostní spektrometrií. Rostlina tak za působení dalších hydrolas může získávat fosfát z nukleových kyselin kořisti a fosfoproteinů, jak naznačují Schulze *et al.* (2012). Fosfát může *Dionaea* získávat i z fosfolipidů působením fosfolipasy v trávící šťávě (Schulze *et al.*, 2012). Přítomnost fosfatas byla pomocí fluorescenčně značeného substrátu prokázána u 46 druhů masožravých rostlin včetně druhů označovaných jako protokarnivorní, u kterých se

vlastní hydrolytická aktivita nepředpokládala (Płachno *et al.,* 2006). K aktivaci proteolytických enzymů MR může přispívat H^+ ATPasa plasmatické membrány snižující pH v láčce u *Nepenthes alata*. Tento mechanismus by také mohl umožňovat absorpci živin do buněk pomocí H^+ gradientu (An *et al.,* 2001). Mikroorganismy žijící v láčce *N. hybrida* produkují lipasy schopné fungovat v kyselém prostředí trávící šťávy a umožňují rostlině trávit tučnou kořist (Morohoshi *et al.,* 2011). Přítomnost enzymů, esteras, zkracujících alifatické uhlíkové řetězce na C8 a C4 sloučeniny byla popsána u stejného druhu rostlin i ve šťávě z neotevřených láček, což naznačuje, že rostlina tyto enzymy sama sekretuje (Higashi *et al.,* 1993).

4.2.3. Příjem živin

Masožravé rostliny chytáním a trávením kořisti, hlavně hmyzu, doplňují přísun živin, který probíhá hlavně kořeny. Studie provedená na rosnatce okrouhlolisté (*Drosera rotundifolia*) ukázala, že při dostatku dusíku v půdě roste jeho příjem rostlinou skrze kořeny. Autoři také potvrdili dřívější poznatky, že příjem fosforu oproti dusíku naopak závisí na dostatku kořisti, z níž je získáván (Millett *et al.,* 2015). Příjem draslíku je listy (pastmi) limitován a musí být přijímán kořeny (Adamec, 1997). Dusík a fosfor nemohou být přijímány z tekutiny uvnitř pasti masožravých rostlin, pokud zde není jejich nadbytek z trávené kořisti. Rostliny naopak tyto prvky do trávící šťávy mohou doplňovat, aby podpořili růst mikroorganimů podílejících se na trávení, což bylo pozorováno u vodního druhu *Utricularia* (Adamec, 2013). Transport látek z pastí do floemu se děje hlavně apoplasticky. Pokud tato cesta není možná, transport musí probíhat symplasticky pomocí kanálů a transportérů mechanismem podobným příjmu živin kořeny. Geny pro transportní enzymy a přenašeče pro peptidy, amonné ionty a aminokyseliny byly identifikovány u *N. alata* (Schulze *et al.,* 1999). Pokusy na *D. capensis.*, která byla krmena mravenci, ukázaly na změny v koncentraci jednotlivých AK a vybraných sekundárních metabolitů, zejména fenolů v listech rostliny a trávených tělech hmyzu. Po 3 a 21 dnech trávení rostlinou byl zaznamenán vysoký obsah volných AK ve zbytcích těl trávených mravenců. Obsah rozpustných dusíkatých látek naopak poklesl. Oproti tomu přítomnost kořisti neměla vliv na koncentraci fenolů a flavonoidů v listech *D. capensis* (Kováčik *et al.,* 2012).

Příjem látek obsahující dusík probíhá u masožravých rostlin skrze bifunkční sekreční žlázy (Parsons a Sunley, 2001). U *Nepenthes* je obsah amonných iontů v trávící štávě láčky asi 250 $\mu mol \cdot l^{-1}$. Zdroji NH_4^+ jsou natrávená kořist a bakterie fixující dusík žijící v láčce (Prankevicius a Cameron, 1991). U *D. muscipula* je dusík uvolňován ve

formě NH_4^+ z glutaminu v reakci zprostředkované glutamindeaminasou (Scherzer *et al.*, 2013). Amonné ionty jsou rostlinou vstřebávány prostřednictvím kanálků (*Dionaea muscipula* amonium transportérový kanál, DmATM1) umožňující vstup NH_4^+ do žlázových buněk. Afinita těchto kanálků roste při působení OPDA a jejich derivátu, coronatinu a také při vyšší koncentraci NH_4^+. Zajimavé je, že citlivost těchto kanálků k amonným iontům roste až během procesu trávení, po stimulaci a sekreci trávících šťáv.

Změny koncentrace jiných kationů, zejména protonů v silně kyselé trávící šťávě mucholapky aktivitu těchto transportérů neovlivňují (Scherzer *et al.*, 2013). Absorpce draselných iontů z potravy u *D. muscipula* je zprostředkována pomocí kotransportéru DmHAK5 K^+/H^+ a DmKT1 kanálem. Oba transportní proteiny jsou regulovány fosforylací komplexem Ca^{2+}-dependentní kinasy CBL/CIPK. Kooperace obou transportérů umožňuje příjem K^+ z pasti za podmínek jeho snížené koncentrace po trávení kořisti prostřednictvím symportu DmHAK5 po gradientu H^+. Snížení pH trávící šťávy v pasti na začátku trávícího procesu vede ke změně membránového potenciálu žlázových buněk obsahující DmKT1, který se za těchto podmínek otevírá a umožňuje jednosměrný tok K^+ do těchto buněk rostliny (Scherzer *et al.*, 2015).

4.3. Ostatní látky obsažené v šťávách MR – sekundární metabolity

Sekundární metabolity jsou látky produkované organismy, sloužící jim jako konkurenční výhoda k zajištění vlastního přežití v daných podmínkách. Mnoho z těchto látek nebo jejich derivátů je dnes využíváno terapeuticky nebo preventivně (Bourgaud *et al.*, 2001; Cragg a Newman, 2013). Molekuly s velmi rozmanitými účinky byly izolovány z běžně člověkem konzumovaných rostlin. Velký potenciál nabízejí také rostliny nejedlé využívané v tradiční medicíně. K této skupině mohou být zařazeny i MR, zejména *Nepenthes* a *Drosera* (Kováčik *et al.*, 2012). K hojení ran jsou používány listy tučnic (*Pinguicula*). Odvar z mucholapky (*Dionea*) slouží k léčbě dýchacích obtíží. Čerstvá šťáva z listů rosnatky (*Drosera*) je používána na bradavice (Gaascht *et al.*, 2013). V severní Americe byly indiány tradičně používány extrakty ze špirlice nachové (*Sarracenia purpurea*, Arndt *et al.*, 2012). Čerstvá šťáva z láčkovky (*Nepenthes khasiana*) je indickými domorodci používána k léčbě žaludečních potíží (Gaascht *et al.*, 2013). Obsáhlou skupinu sekundárních metabolitů tvoří fenolové sloučeniny, plnící u rostlin např. ochrannou funkci před UV zářením nebo hmyzem. Fenoly slouží také jako molekuly chránící rostliny před oxidativním stresem a slouží jako signální molekuly. Biosyntéza těchto látek je regulována prostřednictvím fenylalaninamoniaklyasy (PAL).

U masožravých rostlin se předpokládá, že aktivita tohoto enzymu je závislá na obsahu využitelného dusíku. Při nedostatku může být dusík rostlinou uvolňován právě z Phe prostřednictvím zvýšené aktivity PAL a zbylá uhlíková kostra je využita pro syntézu fenolových sloučenin (Kováčik *et al.,* 2012). V trávících šťávách mucholapky byla objevena dosud jinde nenalezená sloučenina patřící mezi naftochinony nazvaná diomuscipulon (Gaascht *et al.,* 2013). Ve velkém množství je mucholapkou produkovaný plumbagin a jeho obsah v listech pasti dosahuje až 0,5 % hmotnosti. Hlavní funkcí je ochrana rostliny před predátory a patogeny. Těkavost spolu s vysokým redoxním potenciálem stimulují bakteriální dýchací řetězec. Toto působení vede k tvorbě superoxidu a je hlavním mechanismem působení této sloučeniny (Tokunaga *et al.,* 2004). Plumbagin byl identifikován i u *N. khasiana*. Byl nalezen v extraktu z horní částí láčky, obsahující krystaly vosku a nektar lákající kořist. Plumbagin byl nalezen i v ostatních částech rostliny, nebyl však prokázán v trávící šťávě. Nárůst koncentrace plumbaginu byl zaznamenán ve všech částech láčkovky po indukci roztokem koloidního chitinu (Raj *et al.,* 2011). Další naftochinony prvně identifikované u rosnatky, droseron a 5-metyldroseron, byly naopak nalezeny pouze v trávící šťávě *N. khasiana* (Raj *et al.*, 2011). Odlišná lokalizace těchto derivátů plumbaginu může být způsobena dostupností jeho prekurzorů (Raj *et al.,* 2011). V láčkách *Heliamphora heterodoxa a H. tatei* byly identifikovány terpeny sarracenin a cineron. Nalezen byl také erucamid, v průmyslu používaný, jako antiadhezivní přípravek a estery palmitové a linolové kyseliny (Jaffé *et al.*, 1995). Dále byla popsána přítomnost alkaloidů koniinu a reserpinu (Ghate *et al.*, 2015). Koniin objevený v pasti špirlice žluté (*S. flava*) paralyzuje nervový systém kořisti (Mody *et al.,* 1976).

4.4. *Dionea muscipula* – modelová masožravá rostlina

Čeleď rosnatkovitých patří mezi nejlépe prostudovanou skupinu MR. Do této čeledi náleží všechny druhy rosnatek *Drosera sp.*, mucholapka podivná (*Dionea muscipula*) a vodní druh aldrovandka měchýřkatá (*Aldrovanda vesiculosa*). Proteomickou analýzu trávící šťávy mucholapky provedli Schulze a kolektiv na základě dříve získaných cDNA dat (Schulze *et al.*, 2012). Během tohoto experimentu bylo prokázáno, že hlavní třídu proteolytických enzymů *D. muscipula* tvoří cysteinové proteasy (Schulze *et al.*, 2012). Dále byla identifikována aspartátová i serinová proteasa a proteiny ze skupiny PR-proteinů jako chitinasy, peroxidasy, LTP proteiny a osmotin (Schulze *et al.*, 2012). Charakteristickým znakem této rostliny jsou sklapovací pasti,

jejichž zavření a iniciaci trávení je možno simulovat aplikací jasmonátů (methyljasmonátu (MeJA), popř. koronatinu) imitujících prvotní elektrochemický impuls vznikající ohnutím vlásků spouštěcího mechanismu uvnitř pasti (Escalante-Pérez *et al.*, 2011). Fyziologicky je reakce spuštěna až po druhém, opakovaném kontaktu kořisti se citlivými vlásky pasti v krátkém časovém intervalu, indukce sekrece trávící šťávy je spuštěna až po 3 stimulu (Escalante-Pérez *et al.*, 2011; Libiaková *et al.*, 2011; Böhm *et al.*, 2016). Zajímavostí je, že ačkoli dochází na listech mucholapky k sekreci trávící šťávy, po indukci nenastává rychlé zavření pasti jako pří mechanické stimulaci, ale pouze k pozvolnému pohybu. Popsán byl i vliv přítomnosti uměle zvýšené koncentrace auxinů u mucholapky, které způsobují menší citlivost pasti na mechanické podráždění (Escalante-Pérez *et al.*, 2011). Největší obsah enzymů pro rozklad kořisti v pasti mucholapky je zaznamenáván 3-4 den trávení (Scala *et al.*, 1969). Jako atraktant pro kořist slouží barevné vyvedení vnitřní části pasti i chemické stimulanty produkované rostlinou (Kreuzwieser *et al.*, 2014). Následný přenos hydrolyzované potravy je zprostředkován řadou specifických mechanismů (Scherzer *et al.*, 2013; Scherzer *et al.*, 2015). Podle energetické potřeby jsou hlavní složky potravy N a C využity k růstu, respektive je C spotřebován během respirace (Pavlovič *et al.*, 2010, Kruse *et al.*, 2014, Fasbender *et al.*, 2017).

4.3. Výsledky: Proteiny trávící šťávy rosnatky kapské

Po rozdělení extraktu proteinů z trávící šťávy rosnatky pomocí SDS-PAGE a vizualizaci byly pozorovány proteinové pásy v oblasti pod 70 kDa (Obr. 9). Celkem bylo identifikováno 43 proteinů, z toho 19 pomocí nLC MALDI MSMS a 39 nLC ESI MSMS technikou. Největší zastoupení proteinů je v oblasti od 40 do přibližně 10 kDa, představující spodní okraj gelu. Nejmenším identifikovaným proteinem dle databázové hmotnosti 13,2 kDa je lipid transfer protein (gi|1130872420) původně z příbuzného druhu *D. adelae*. Největším zaznamenaným enzymem je analog k nukleotidfosfatase (gi|1002635122) *N. mirabilis* s předpokládanou velikostí okolo 70 kDa (Tab. 2). Pro proteiny s identifikátory gi|1226791974, gi|902236137, gi|1219112697, gi|870863687 se nepodařilo najít podobné zástupce s popsanou funkcí. Všechny tyto neznámé proteiny byly identifikovány pouze na základě jednoho popsaného peptidu.

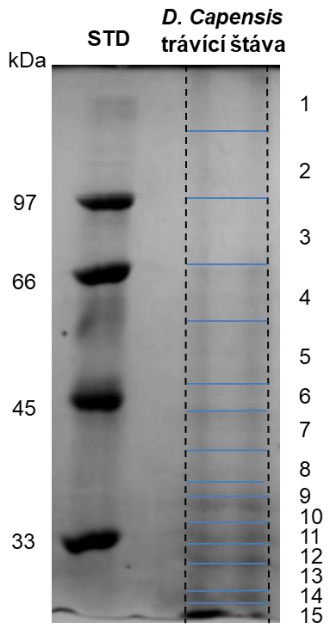

Obr. 9 Proteiny trávící tekutiny *D. capensis*. SDS-PAGE separace proteinů z 100 µl extraktu z trávící šťávy rosnatky kapské. Gel byl obarven Coomassie Brilliant Blue R250. Vyznačené oblasti na gelu byly zpracovány pro MS analýzu.

Sekvence identifikované Asp-proteasy NEP_DCAP (dle Butts *et al.*, 2016a), byla srovnána s ověřenou sekvencí nepenthesinu 1 z *N. gracilis* dle UniProtKB Q766C3 (NEP1_NEPGR, Obr. 10). Identifikované Cys-proteasy byly vzájemně rozlišeny pomocí vyhledávacího programu PEAKS Studio X a rozřazeny do proteinových rodin. Sekvence prvních zástupců z těchto rodin byly srovnány do fylogramu (Obr. 11). Z výsledku srovnání je patrná odlišnost těchto enzymů oproti modelovému příkladu papainu (zástupci C1A skupiny Cys-proteas).

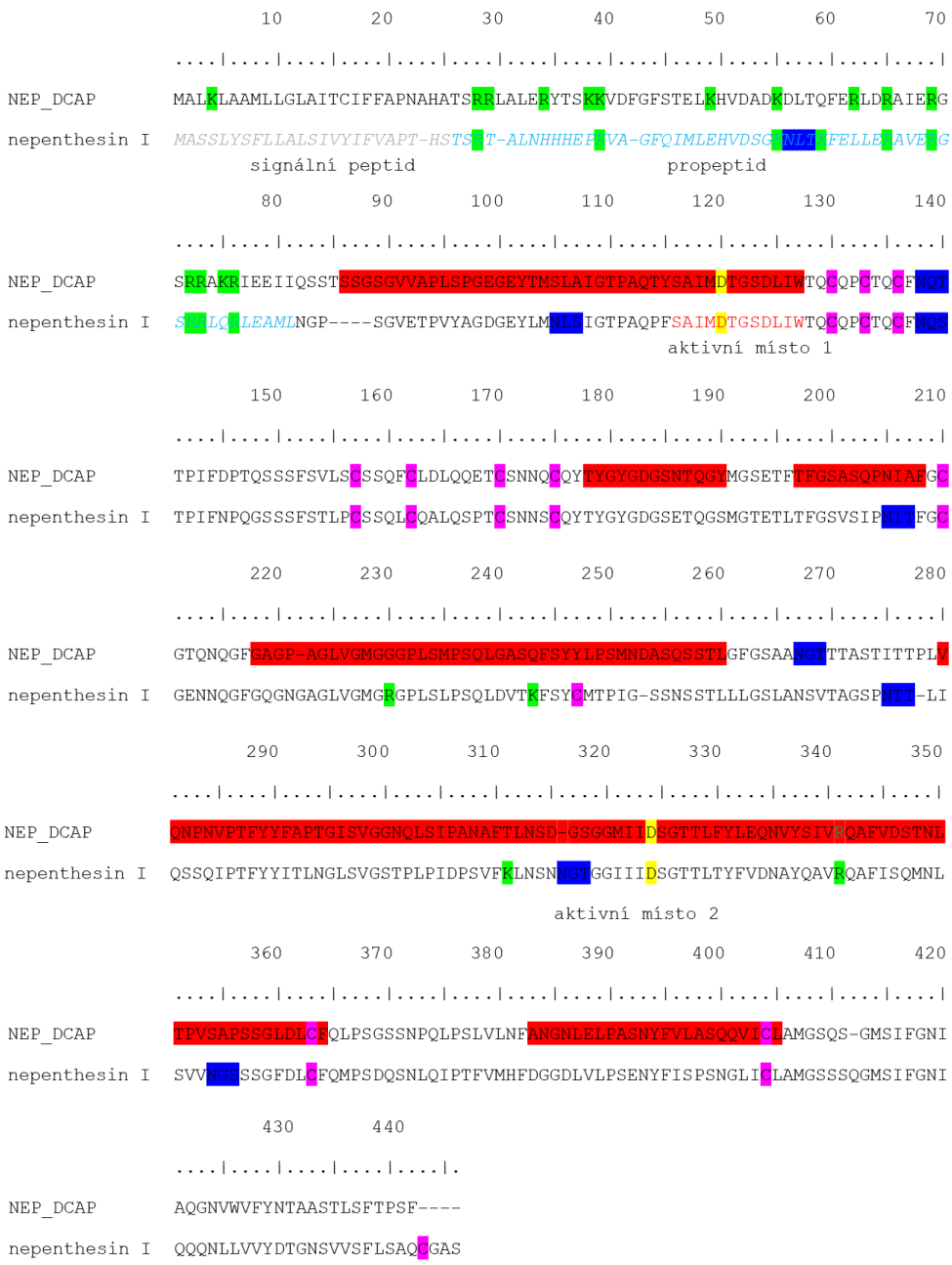

Obr. 10 Srovnání proteinových sekvencí Asp-proteasy (NEP_DCAP) rosnatky kapské a nepenthesinu1. Uvedeny jsou sekvence Asp proteasy rosnatky kapské NEP_DCAP (Butts et a., 2016a) a nepenthesinu 1 (Q766C3, UniProtKB). Aminokyseliny aktivního místa jsou vyznačeny žlutě, zeleně jsou označeny Lys, Arg. Modře vyznačena jsou místa možné *N*-glykosylace pro nepenthesin 1 dle UniProtKB, pro NEP_DCAP dle predikce na Asn pokud je v rámci sekvence Asn-Xaa-Ser/Thr. Cysteiny z disulfidových vazeb (C130-C133, C136-C210, C157-165, C162-170, C247-444, C363-404) jsou vyznačeny růžově.

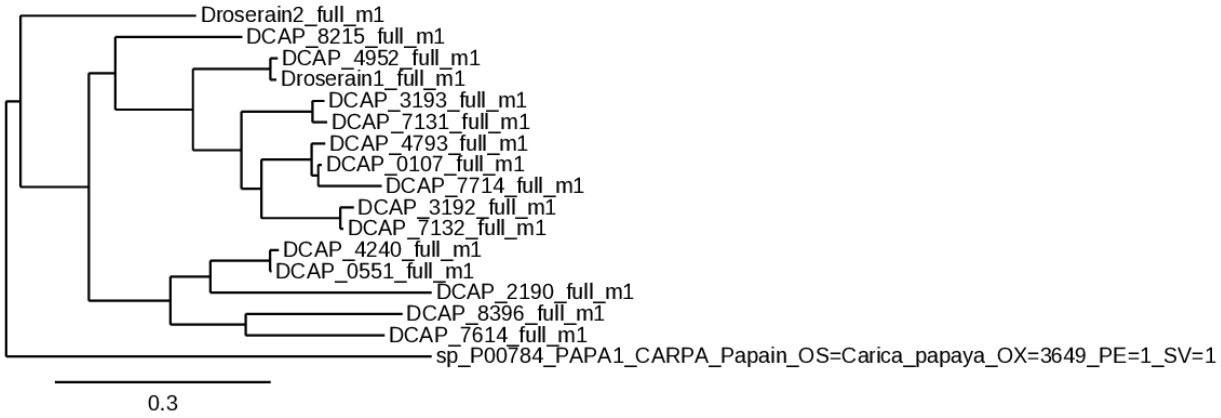

Obr. 11 Fylogenetický strom srovnání identifikovaných cysteinových proteas trávící šťávy *D. capensis*. Pro srovnání je vložena sekvence papainu (UniProtKB P00784). Fylogram byl vytvořen pomocí nástroje http://www.phylogeny.fr, délka ramen spojení mezi jednotlivými uzly a sekvencemi značí jejich vzájemnou míru podobnosti (Deeper *et al.*, 2008).

Tab. 3 Proteiny trávící šťávy rosnatky kapské.

Seznam proteinů identifikovaných pomocí nLC MALDI MSMS a nLC ESI MSMS. Proteiny trávící šťávy *D. capensis* byly separovány pomocí SDS-PAGE a štěpeny trypsinem modifikovaným rafinosou (T) nebo chymotrypsinem (Ch). Pozitivní identifikace proteinu v experimentu je vyznačena hvězdičkou. Prohledání dat bylo provedeno pomocí Peaks Studio 8 při použití vlastní databáze složené z obsažených proteinových sekvencí NCBInr Carryophyllales a dat extrahovaných z publikací Butts *et al.*, 2016a; Butts *et al.*, 2016b; Unhelkar *et al.*, 2016; Duong *et al.*, 2018. Databáze celkem zahrnovala 285743 záznamů včetně běžných kontaminantů. Parametry prohledání dat byly FDR na úrovni přiřazených spekter peptidů <1 %, tolerance pro vyhledávání pro prekurzory - 50 ppm, tolerance pro fragmenty - 0,05 Da pro ESI a 0,5 Da pro MALDI analýzy. Data byla vyhledávacím softwarem automaticky rekalibrována. Oxidace Met a acetylace N-konce proteinů byly nastaveny jako variabilní modifikace. Karbamidomethylace cysteinu byla nastaveno jako trvalá modifikace. Pro prohledání po štěpení chymotrypsinem bylo povoleno 5 možných vynechaných štěpných míst, v případě trypsinu 3 a povoleno vyhledávání peptidů vzniklých nespecifickou aktivitou zadaných proteas.

nLC ESI		nLC MALDI		Gel protein band	Protein	-10lgP	Pokrytí sekvence (%)	Počet peptidů	Unikátní peptidy	MW	Funkce proteinu	
Ch	T	Ch	T									
	*			3	gi|1226791974	35.26	2	1	1	71592	probable leucine-rich repeat receptor-like protein kinase At1g35710 [Spinacia oleracea]	*X*
*		*		4	gi|1002635122	64.35	3	2	2	70712	putative nucleotide pyrophosphatase/phosphodiesterase [Nepenthes mirabilis]	fosfatasa
	*			4	gi|902236137	20.48	5	1	1	31120	hypothetical protein SOVF_017840 [Spinacia oleracea]	*X*
	*			5	gi|1002635113	25.84	2	1	1	47270	putative alpha-galactosidase 2 [Nepenthes mirabilis]	α-galaktosidasa
*		*		6	NEP_DCAP	201.74	49	33	33	46349	NEP_DCAP_full_m1	Asp-proteasa
	*	*	*	6	gi|1002635124	66.18	9	3	3	35878	putative peroxidase 27 [Nepenthes mirabilis]	peroxidasa
			*	6	gi|902138077	29.04	4	1	1	35626	hypothetical protein SOVF_199100 [Spinacia oleracea]	peroxidasa
*	*			7	DCAP_4952	174.35	44	13	1	30247	DCAP_4952_full_m1	Cys-proteasa
*	*		*	7	Droserain1_full_m1	172.54	29	14	2	36070	Droserain1_full_m1	Cys-proteasa
*	*		*	7	gi|1552058024	110.43	14	5	2	34216	endochitinase [Drosera capensis]	chitinasa, F19
*		*	*	7	DCAP_5513	108.04	17	5	1	30994	Chtitinase_mmc26	chitinasa class I, F19
*				7	gi|1114672837	83.97	14	4	1	37755	dionain 2 [Dionaea muscipula]	Cys-proteasa
*				7	Droserain2__full_m1	74	4	3	1	38415	Droserain2__full_m1	Cys-proteasa
	*			7	gi|1219112697	25.02	1	1	1	83311	cysteine-rich receptor-like protein kinase 25 isoform X2 [Chenopodium quinoa]	*X*
*	*	*		8	DCAP_4240	109.84	25	11	4	37554	DCAP_4240_full_m1	Cys-proteasa
	*		*	8	DCAP_0533	100.26	13	4	4	49825	Chtitinase_mmc24	chitinasa class IV, F19
	*		*	8	DCAP_0551	99.16	16	8	1	36096	DCAP_0551_full_m1	Cys-proteasa
	*			9	DCAP_7714	55.22	8	3	1	37084	DCAP_7714_full_m1	Cys-proteasa
*	*			9	gi|787035404	52.36	9	3	3	38380	glucanase [Drosera adelae]	Glukanasa
		*		9	gi|1130872412	44.89	6	2	2	36720	beta-1 3-glucanase [Drosera adelae]	β-1,3-glukanasa
*	*		*	10	DCAP_4793	174.53	39	16	2	36608	DCAP_4793_full_m1	Cys-proteasa
*				10	DCAP_0107	170.23	32	15	1	36714	DCAP_0107_full_m1	Cys-proteasa
*	*			10	DCAP_7131	152.53	20	9	1	36737	DCAP_7131_full_m1	Cys-proteasa
*				10	DCAP_3193	148.96	20	8	1	36858	DCAP_3193_full_m1	Cys-proteasa
*				10	gi|1130872414	60.3	11	3	3	36611	beta-1 3-glucanase [Drosera adelae]	beta-1,3-glukanasa
	*			10	DCAP_8215	41.74	8	2	2	34841	DCAP_8215_full_m1	Cys-proteasa
*				10	gi|1130872436	21.45	3	1	1	42569	C-terminal peptidase [Nepenthes alata]	proteasa (Neprosin)
*	*		*	11	DCAP_7132	193.89	42	15	5	37230	DCAP_7132_full_m1	Cys-proteasa
*				11	DCAP_3192	171.88	40	12	3	37294	DCAP_3192_full_m1	Cys-proteasa
*	*	*	*	11	DCAP_7614	124.67	38	13	13	38111	DCAP_7614_full_m1	Cys-proteasa
*				11	DCAP_2209	65.56	23	5	5	27516	Chtitinase_mmc12	chitinasa, F18
			*	11	gi|902043096	37.72	19	1	1	8544	hypothetical protein SOVF_215330 partial [Spinacia oleracea]	tubulin
*	*	*	*	12	DCAP_2190	171.87	47	26	24	38356	DCAP_2190_full_m1	Cys-proteasa
*	*			12	DCAP_8396	112.12	30	13	12	37857	DCAP_8396_full_m1	Cys-proteasa
*	*			13	gi|71611076	48.05	10	2	1	24880	ribonuclease [Drosera adelae]	ribonukleasa
	*		*	14	gi|1842103754	44.55	11	2	2	23406	thaumatin-like protein [Drosera adelae]	thaumatin-like protein
			*	14	gi|870863687	27.29	3	1	1	43741	hypothetical protein BVRB_3g065650 [Beta vulgaris subsp. vulgaris]	*X*
*				14	gi|778204087	27.07	2	1	1	54084	cyclo-DOPA 5-O-glucosyltransferase [Amaranthus tricolor]	glukosyltransferasa
	*			14	gi|1130872440	21.91	5	1	1	23871	thaumatin-like protein [Nepenthes alata]	thaumatin-like protein
*				15	gi|1130872418	71.33	21	4	3	23717	thaumatin-like protein [Drosera adelae]	thaumatin-like protein
*			*	15	gi|165292438	65.26	7	1	1	23859	thaumatin like protein [Nepenthes alata]	thaumatin-like protein
*				15	gi|1130872420	58.91	15	3	3	13271	lipid-transfer protein [Drosera adelae]	lipid transfer protein
*				15	gi|870860818	28.45	6	1	1	24091	hypothetical protein BVRB_5g100770 [Beta vulgaris subsp. vulgaris]	thaumatin-like protein

4.4. Diskuse: Proteiny trávící šťávy rosnatky kapské

Pomocí imitace kořisti na pastech rosnatky aplikací JA byla úspěšně vyvolána sekrece trávící šťávy, která byla odebrána a podrobena proteomické analýze. K úspěšné identifikaci rozmanité sady produkovaných proteinů výrazně napomohla jejich separace pomocí SDS-PAGE, když došlo i k oddělení různých forem jednotlivých enzymů a dalších proteinů. Dle počtů a typů identifikovaných proteinů lze vyvodit, že trávící mechanismus *D. capensis* není založen na digesci pomocí Asp-proteas, ale stejně jako u *D. muscipula* mají hlavní zastoupení proteasy cysteinové. Přítomna je zřejmě také na endopeptidasa specifická pro prolin a podobná neprosinu z *Nepenthes ventrata* (Lee *et al.*, 2016). Hydrolýzu tělesných schránek hmyzu zajišťují nejméně 3 chitinasy. Ostatní polysacharidy mohou být štěpeny alfa-1,3-glukosidasou nebo 1,3-glukanasami hydrolyzující ochranné glukany původně bránící působení chitinas na bakteriální buněčnou stěnu. U běžných rostlin mohou houby z mykorhizy pomocí oligochitinových fragmentů indukovat zvýšení Ca^{2+} koncentrace v epidermálních buňkách kořene (Hu *et al.,* 2009). Rostlina následně podle délky oligochitinových řetězců pozná, zde jde o parazita nebo symbiotický organismus (Sanchez-Vallet *et al.* 2015). Rostlinné patogeny se naučily tento signalizační mechanismus omezovat a sekretují proteiny vázající se na chitin a bránici působení rostlinných chitinas (Kaku *et al.*, 2006). Indukce obranné reakce oligosacharidy chitinu může vést u rostlin ke tvorbě ROS (Kaku *et al.,* 2006). Změna a zvýšeni koncentrace Ca^{2+} je potřebná pro tvorbu jasmonátů a dalších sekundárních metabolitů. Při exogenní aplikaci JA byl tento iniciační krok vedoucí i k sekreci trávící šťávy rosnatky přeskočen (Krausko *et al.,* 2017). Po reanalýze dat proti velmi dobře in-vitro přeloženým sekvencím proteas a chitinas z genomu rosnatky, lze rozlišit různé formy těchto hydrolas (Butts *et al.,* 2016a; Butts *et al.,* 2016b; Unhelkar *et al.,* 2016; Duong *et al.*, 2018). Nevšedním enzymem trávicí šťávy rosnatky je chitinasa třídy IV (DCAP_0533) obsahující ve své struktuře 2 vazebná místa pro chitin. Tento enzym byl dosud predikován jen dle DNA a podobný protein v rostlinné říši není znám (Unhelkar *et al.*, 2016). Nalezená Asp-proteasa (NEP_DCAP) podobná nepenthesinům byla dle původního vyhodnocení identifikovaná pouze podle jednoho unikátního peptidu z okolí aktivního místa (překryv s protilátkou použitou pro detekci enzymu westernblotem; Krausko *et al.*, 2017). Při použití aktualizované databáze data prokázala, že enzym byl přítomen zřejmě v hojném zastoupení a MSMS technikami po jeho naštěpení chymotrypsinem byla potvrzena shoda na téměř 60 % aktivní sekvence. Sekvence enzymu je pro proteomickou analýzu s využitím trypsinu dokonale nepřístupná díky

přítomnosti pouze jedné bazické AK (R341). Tato extrémní adaptace může také významně prodloužit životnost droserasinu (NEP_DCAP) v trávící šťávě rosnatky po jeho aktivaci a působení spolu s převládajícími thiolovými proteasami. Oproti nepenthesinu 1 z láčkovky (NEP1_NEPGR), zřejmě ve struktuře enzymu rosnatky chybí jedna disulfidová vazba mezi C247 a C444. Toto spojení může mít zásadní vliv na vlastnosti tohoto enzymu, jelikož u nepenthesinu 1 drží C-konec proteinu kompaktně přiložený ke zbytku struktury. *N*-glykosylace droserasinu na aktivní části proteinu je předpokládána jen na 2 místech oproti 6 u nepenthesinu 1. Zastoupení Cys-proteas v trávící šťávě rosnatky je velmi rozmanité a enzymy se vyskytují v několika velmi blízkých formách podobných prvnímu popsanému zástupci droserainu (Takahashi *et al.*, 2012). Z identifikovaných Cys-proteas není také žádná podobná enzymům běžných rostlin z více než 65 % AK sekvence. Přítomnost různých forem Cys-proteas může být teoreticky výsledkem různého zpracování původní genetické informace (Stephenson a Hogan, 2006). Hydrolýzu biopolymerů z kořisti mohou oxidací usnadňovat přítomné peroxidasy (Hatano a Hamada, 2012). Identifikace fosfatasy a ribonukleasy dokládá, že rosnatka kapská je vybavena i pro aktivní rozklad nukleových kyselin mechanismy původně sloužící k obraně před viry (Okabe *et al.*, 2005, Nishimura *et al.*, 2013). Na základě geonomických dat byly publikovány modelové struktury lipas a esteras rosnatky kapské (Duong *et al.*, 2018). Ze získaných proteomických dat nebyl žádný z těchto enzymů v trávící štávě zaznamenán. K trávení kořisti může přispívat i schopnost některých „thaumatin-like“ proteinů rozkládat β-1,3-glukany a zvyšovat prostupnost membrán, která byla pozorována při jejich interakci s patogenními hubami (Grenier *et al.*, 1999). Výskyt „thaumatin-like“ proteinů a lipid transfer proteinu v trávící šťávě nemusí souviset z masožravostí a může dokládat jen původ celého mechanismu trávení v obranné strategii rostlin, které jsou tyto proteiny součástí (Pavlovič a Mithöfer *et al.*, 2019).

5. PROTEINY BOHATÉ NA PROLIN JAKO MOŽNÍ PŮVODCI ZÁKALU VÍNA

Výroba vína tradiční cestou z hrozna s sebou nese rizika vzniku senzorických vad. Ve většině případů jsou příčinou fyzikálně a chemicky nestabilní sloučeniny, případně toxické látky snižující kvalitu samotného vína a způsobující tak ekonomické ztráty jeho prodejci nebo výrobci. Původ většiny vad vína je v současnosti znám a rutinně jsou aplikovány postupy a prostředky předcházející vzniku nebo projevu těchto nedokonalostí. Nástroje pro boj s defekty vína představují chemické přípravky, využívání inertních materiálů v technologii, šlechtěné živé kultury kvasinek a jiných mikroorganismů nebo proteinové přípravky, často enzymy (Palmisano *et al.*, 2010, Gaspar *et al.*, 2019, Sui *et al.*, 2020). Prostředky investované jen proti potlačení zákalu vína celosvětově představují více než 1 miliardu dolarů ročně, odpovídající asi 0,5 % hodnoty celkového trhu s vínem (Robinson *et al.*, 2012). Překážkou při výrobě vína mnohokrát není způsob, jak danou vadu odstranit, ale jak ji odstranit beze změny dalších charakteristik (Lambri *et al.*, 2010). Při výrobě vína se uplatňují preventivní opatření mající za cíl zabránit vzniku a projevu možných vad před konečným stáčením do lahví a následně uchovat kvalitu nápoje při možné nepřízni vnějších podmínek změn teplot a vystavení světlu (Marangon *et al.*, 2011). Vady a nedostatky vína mohou být dle vlivu na kvalitu rozděleny na senzorické vizuální, chuťové nebo pachy a vady představující nebezpečí pro konzumaci.

5.1. Senzorické defekty vína

Běžným defektem vína je přítomnost krystalků vinanů objevujících se při překročení meze jejich rozpustnosti (Lasanta a Gómez, 2012). V případě červených vín může docházet k nežádoucí změně barevnosti nebo srážení pigmentů odvozených od anthokyaninů (Alcalde-Eon *et al.*, 2014). Zvětralá příchuť vína je projevem vysoké hladiny acetaldehydu (60, resp. 300 $mg \cdot l^{-1}$ pro bílá a červená vína) vznikajícího enzymovou oxidací ethanolu nebo oxidací vzdušným kyslíkem např. při delším skladování vína (Sheridan a Elias, 2015). Nepříjemná kyselost vína je důsledkem vysokého obsahu (nad 700 $mg \cdot l^{-1}$) kyseliny octové tvořené aerobními bakteriemi během fermentace prováděné za nevhodných podmínek (Vilela-Moura *et al.*, 2011). Vysoký obsah ethylacetátu, běžně poskytující příjemné ovocné aroma, se negativně projevuje na hořkosti vína (Lilly *et al.*, 2006). Diacetyl (2,3-butandion) vznikající během jablečno-mléčného kvašení je původcem máslového nebo mléčného zápachu vína (Guth, 1997).

Řada senzorický projevů je pro víno zcela nepůvodní. Kvasinky rodu *Brettanomyces* nebo *Dekerra* jsou schopné tvořit charakteristicky vonící vinylfenoly z běžných fenolových kyselin (Milheiro *et al.*, 2017). Stejné druhy mikroorganismů jsou zodpovědné i za tzv. „zápach myšiny“ vína způsobený deriváty pyrrolinu a pyridinu (Snowdon *et al.*, 2006). Chuť korku ve víně je projevem 2,4,6-trichloroanisolu tvořeným běžnými houbovými plísněmi *Penicillium* a *Aspergillus* z biocidních přípravků obsahující chlorofenoly prostupujících do materiálu korkových zátek (Simpson a Sefton, 2007). Nepříjemné pachy thiolů a H_2S jsou produkty hladovějících kvasinek v pozdějších stádiích fermentace vína (Ugliano *et al.*, 2009).

5.2. Proteinogenní defekty vína

Proteom vína je tvořen majoritně rostlinnými PR-proteiny, odolávající snižujícímu se pH i celému průběhu fermentace. Vedle těchto proteinů lze v hotovém vínu nalézt proteiny původem z kvasinek, případně dalších mikroorganismů, které se dostaly s vínem do kontaktu během jeho výroby. Běžnými vizuálními vadami souvisejícími s proteiny obsaženými ve víně jsou změny barevnosti a průzračnosti objevující se po stáčení. Původcem těchto změn bývají sraženiny vzniklé agregací nestabilních složek vína nebo oxidační produkty (Esteruelas *et al.*, 2011, Lambri *et al.*, 2013, van Sluyter *et al.*, 2015, Cosme *et al.*, 2020).

5.2.1. Nestabilita vinných proteinů

Projevem přítomnosti nestabilních proteinů ve víně je vznik pozorovatelného zákalu v celém objemu tekutiny nebo sedliny na dnu láhve (Esteruelas, 2009, Cosme *et al.*, 2020). Proteiny podílející se na vzniku agregátů tvořící zákal jsou běžně výhradně rostlinné PR-proteiny a invertasa (E.C. 3.2.1.26) původem ze *S. cerevisiae* (Falconer *et al.*, 2010). Další složkou proteinogenního zákalu tvoří hydroxysloučeniny, snadno adsorbující na struktury bohaté na prolin (Siebert, 1996, McRae *et al.*, 2015, Obr. 12). Stabilitu proteinů ve víně ovlivňuje faktor teploty a iontové síly, kdy jejich změnou dochází ke strukturním změnám. Obsah alkoholu ve víně stabilitu vinných proteinů neovlivňuje (Sarmento *et al.*, 2000). Strukturní změny vinných proteinů jsou za běžných podmínek reverzibilní (Marangon *et al.*, 2011). Van-Sluyter *et al.*, 2015 popsal vznik zákalu jako třífázový proces takto, v prvním kroku musí dojít k rozvolnění struktury proteinů, což následně umožní jejich vzájemnou agregaci, nakonec může dojít ke spojení mezi těmito proteinovými agregáty a dalšími komponenty vína. Zásadní roli v tomto procesu zřejmě hraje obsah siřičitanů, dříve označovaných jako komponenta zákalu „*X*“

(Pocock *et al.*, 2007, Marangon 2011, Chagas *et al.*, 2016). Podle modelu autorů Chagas *et al.*, 2016 právě ionty HSO_3^- a zvýšená teplota umožňují rozrušení intramolekulárních disulfidových vazeb i u nejodolnějších „thaumatin-like" proteinů (TLP) a tím jejich vzájemnou interakci. Následná interakce s dalšími složkami vína vede až ke vzniku pozorovatelných agregátů projevujících se jako zákal (Chagas *et al.*, 2016). Proteiny z hrozna podílející se na tvorbě zákalu figurují také jako možné alergeny vína. Hlavní alergeny v hotovém vínu představují chitinasa 4A a lipid transfer proteiny (LTP), pro které je možné najít analogy u broskve a třešně (Pastorello *et al.*, 2003, Schäd *et al.*, 2004).

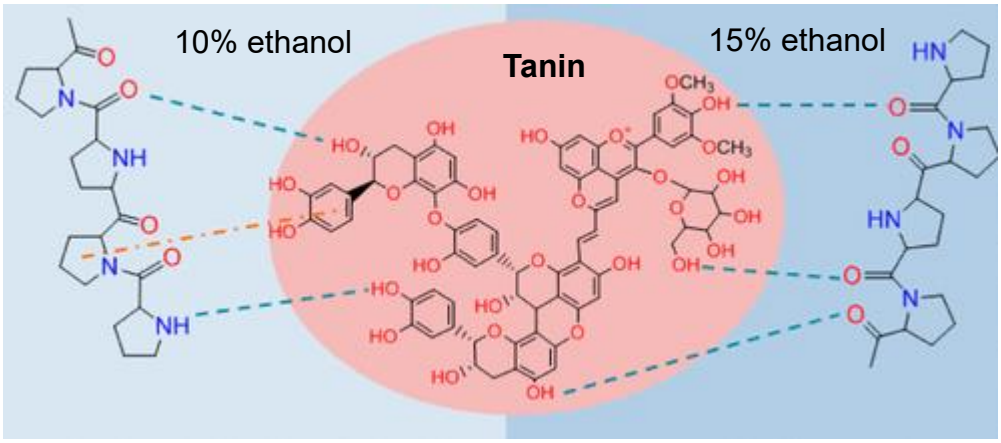

Obr. 12 Předpokládaný model interakce taninu s polypeptidy bohatými na Pro. V prostředí s nižším obsahem ethanolu dochází kromě možných vazeb prostřednictvím vodíkových můstků (přerušovaná modrozelená ještě k interakci mezi Pro a taninem zprostředkovaným hydrofobními interakcemi (přerušovaná oranžová). Převzato a upraveno z McRae *et al.*, 2015.

5.2.2. Enzymová oxidace vína

Předčasná oxidace vína projevující se zhnědnutím způsobuje znehodnocení mladých bílých vín. V případě červených vín je mírná oxidace naopak žádoucí (Chinnici *et al.*, 2013). Enzymová oxidace fenolových sloučenin je nastartována během lisování vína a uvolnění polyfenoloxidas ze slupky hrozna (Fronk *et al.*, 2015). Činností zejména tyrosinasy (E.C. 1.14.18.1) jsou následně přeměňovány monofenolové a difenolové sloučeniny na reaktivní chinony, které oxidují další sloučeniny (Fronk *et al.*, 2015). Oxidované chinony se projevují hnědým zabarvením, kdežto katechiny tvoří po oxidaci žluté struktury (Guyot *et al.*, 1996). Analogií tohoto projevu je hnědnutí vína v důsledku aktivity lakasy (EC 1.10.3.2) sekretované dovnitř hrozna patogenem *B. cinerea*. Substráty lakasy jsou kyseliny gallová, ferulová, kávová nebo resveratrol (Fronk *et al.*, 2015; Claus

et al., 2014). Využívání molekulového kyslíku oběma zmíněnými enzymy umožňuje jejich činnost potlačit použitím tzv. síření pomocí SO_2 (Cheynier *et al.*, 1989).

5.3. Proteiny ve víně

Obsah proteinů v hotovém víně se může značně lišit dle použité odrůdy a stavu hrozna, běžně je udáváno rozmezí 10-500 $mg \cdot l^{-1}$ (Ferreira *et al.*, 2001, Pocock *et al.*, 2007). Popsané extrahovatelné množství proteinů v hroznech nepřesahuje 800 $mg \cdot l^{-1}$, přičemž až 2/3 tvoří proteiny semen (Ferreira *et al.*, 2000, Kambiranda *et al.*, 2014). Pocock *et al.*, 1998 prokázali, že počáteční množství proteinů v hroznech před zpracováním může ovlivnit míra jejich poškození během sběru a doba prodlevy, než dojde k jejich zpracování. Dvojnásobný obsah proteinů byl zaznamenán v extraktu z hroznů sklizených nešetrně mechanicky oproti extraktu z ovoce sklízeného manuálně nebo mechanicky s minimálním poškození bobulí (Pocock *et al.*, 1998). Obsah vinných proteinů klesá o 60-90 % během fermentace vlivem proteolýzy a denaturace (Ndlovu *et al.*, 2019). Odolnost vinných proteinů lze demonstrovat jejich přítomností v kvasném octu (Di Girolamo *et al.*, 2011). Největší podíl mezi proteiny hrozna i vína zaujímají chitinasy a TLP (Giribaldi *et al.*, 2007).

5.3.1. Proteiny podobné thaumatinu

„Thaumatin-like“ proteiny vína jsou řazeny mezi PR-5 proteiny. Velikost TLP je okolo 24 kDa. Ve víně lze najít 2 hlavní isoformy označené VvTLP1 a VvTLP2 lišící svým obsahem v závislosti na stavu hrozna. Zatímco VvTLP1 je produkován konstitutivně, forma VvTLP2 je ve zdravých hroznech výrazně méně zastoupena (Tattersall *et al.*, 1997, Pocock *et al.*, 2000). Thaumatiny a osmotiny z hrozna identifikovali Monteiro *et al.*, 2003 jako příčinu rezistence vína vůči působení a růstu patogenů *Botrytis cinerea, Uncinula necator* (padlí revové) a *Phomopsis viticola* (černá skvrnitost révy). Yan *et al.*, 2017 identifikovali z 33 VvTLP genů 6, které byly ve zvýšené míře přepisovány po inokulaci rostlin hrozna *B. cinerea* a *Erysiphe necator* (padlí). Struktura TLP je známa pro původní thaumatin z *Thaumatococcus daniellii* (Ogata *et al.*, 1992), a analogy z banánu, rajčete, jablka a dalších (Leone *et al.*, 2006; Ghosh *et al.*, 2008). Strukturu rostlinných TLP tvoří tři domény stabilizované disulfidovými vazbami (Min *et al.*, 2004). Prostorovou strukturu tří vinných TLP proteinů vyřešili Marangon *et al.*, 2014 po jejich izolaci z hroznové šťávy *V. vitifera* odrůdy Sauvignon Blanc. Pouze F2/4JRU z těchto TLP, lišící se zejména v oblasti centrální a zároveň největší domény I,

byl schopný se podílet na zákalu vína po provedení teplotního testu stability vína (Marangon *et al.* 2014).

5.3.2. Chitinasy

Chitinasy (EC 3.2.1.14) jsou hydrolytické enzymy rozkladající chitin - polymer *N*-acetylglukosaminu propojený β-1,4 glykosidovými vazbami. Chitinasy patří mezi glykosidhydrolasy rodin 18 a 19, přičemž rodina 19 se vyskytuje hlavně u rostlin (Grover, 2012). Pro *V. vinifera* bylo nalezeno 42 genů pro chitinasy. Po infekci patogenem *B. cinerea* byly významně zvýšena exprese 4 genů, z nichž 3 jsou v listech a 1 v hroznu (Zheng *et al.*, 2020). Na úrovni proteinů byla popsána inhibice růstu *B. cinerea* vinnými chitinasami ze třídy I, II a IV (Saito *et al.*, 2011). Obsah chitinasy IV byl stanoven v rozmezí 10–45 $mg \cdot l^{-1}$ v hroznech Sauvignon blanc, Semillon a Manzoni Bianco (van Sluyter *et al.*, 2009; Vincenzi *et al.*, 2014). Optimální teplota pro aktivitu tohoto enzymu je 30–40 °C při pH 4,5–6 (Saito *et al.*, 2011, Vincenzi *et al.*, 2014). Při vyšších teplotách dochází k prudkému poklesu aktivity souvisejícímu s omezenou stabilitou tohoto enzymu (Falconer *et al.*, 2010). Za podmínek fermentace (pH 3,2 a 25 °C) je aktivita tohoto enzymu jen okolo 12 % oproti ideálním podmínkám (Vincenzi *et al.*, 2014), což je výhodné pro růst kvasinek, který tak není negativně potlačován.

5.3.3. β-D-glykosidasy

Aroma a chuť vína jsou ovlivněny činností další skupiny hydrolytických enzymů, β-D-glykosidas (EC 3.2.1.21). Senzoricky výrazné látky mohou být v hroznu přítomny ve formě glykosidů a aby se vlastnosti aglykonů projevily, musí být uvolněny aktivitou β-D-glykosidas nebo kyselou hydrolýzou (Zhu *et al.*, 2014). Malá aktivita glykosidas a inhibice volnou glukosou je příčinou pomalého rozkladu glykosidů v prostředí vína, což konečně způsobuje méně intenzivnější aroma mladých vín, která stále obsahují velký podíl těchto látek v původní formě (Cabaroglu *et al.*, 2003). Umělá aplikace různě specifických β-D-glykosidas je tak možnou cestou k výrobě aromatičtějších vín (van Rensburg a Pretorius, 2000).

5.3.4. Lipid transfer proteiny

Nespecifické přenašeče lipidů jsou malé proteiny mající zásadní roli v obranné reakci rostlin, procesu tvorby lipidové dvojvrstvy kutikuly nebo suberinu a mnoha dalších procesech (Salminen *et al.*, 2016; Edqvist *et al.*, 2018). Charakteristickými vlastnostmi LTP je vysoký obsah Cys a bazických AK a velikost do 12 kDa (Gomés *et al.*, 2003). Pro

LTP byla ověřena odolnost procesům vinifikace, tolerance k nízkému pH, obsahu alkoholu do 13,5 % a lze je proto najít i v hotovém víně (Okuda *et al.*, 2006; Jaeckels *et al.*, 2013). Množství LTP ve víně je zřejmě spojeno s jeho barvou, kdy více LTP bylo detekováno v červených vínech (Jaeckels *et al.*, 2013, Wigand *et al.*, 2009). Možné vysvětlení nabízí známá lokalizace LTP majoritně ve slupce a semenech hrozna a předpokládaná snadná adsorpce na bentonit při procesu čiření bílých vín (Wigand *et al.*, 2009; Edqvist *et al.*, 2018).

5.3.5. Proteasy vína

V hroznu je předpokládána přítomnost proteolytických enzymů podobných subtilisinu zastávajících obrannou funkci proti houbovým patogenům (Cao *et al.*, 2014; Figueiredo *et al.*, 2016). Byl prokázán klíčový vliv serinových a cysteinových proteas v listech hrozna proti infekci patogenu *Plasmopara viticola* Gindro *et al.*, 2012. Serinová proteasa byla na modelu buněčné kultury *V. vinifera* indukovaná aplikací methylovaných cyklodextrinů (Martinez-Esteso *et al.*, 2009). Přítomnost a pětinásobně zvýšený obsah serinové proteasy (gi 297744927) zaznamenala Dadáková *et al.*, 2015 po infekci buněčné kultury *V. vinifera* šedou plísní *B. cinerea*. Serinové proteasy mohou mít význam pro tvorbu fyzické bariéry zabraňující invazi patogenů (Martinez-Esteso *et al.*, 2009). Enzymová aktivita Cys-proteasy byla detekována na listech révy vinné po indukci MeJA (Řepka *et al.*, 2013). Hydrolasa s chováním odpovídající thiolové protease byla izolována z hroznové štávy (Expósito *et al.*, 1991). Přítomnost a funkce aspartátových proteas může být u *V. vinifera* dedukována pouze na základě expresních profilů a genomických dat (Guo *et al.*, 2013).

5.3.6. Exogenní proteiny vína

Proteom hrozna potažmo moštu a vína odráží vnější prostředí, kvalitu hrozna případně použitá čiřící činidla (Giribaldi *et al.*, 2007; D´Amato *et al.*, 2010). Specifické exogenní proteiny vína jsou produkovány vinnými patogeny *B. cinerea, Plasmopara viticola, Penicillium expansum* nebo *Erysiphe necator*. Plíseň šedá (*B. cinerea*) napadá bobule vína během zrání a způsobuje primárně jejich sesychání. Přítomnost padlí (*E. necator*) odhaluje bílo-šedý povlak na povrchu hrozna a lístů. Peronospora (*P. viticola*) napadá všechny orgány révy. Infekce peronospory se projevuje přítomností olejovitých skvrn na povrchu listů nebo bobulí vína a může vést až k zasychání listů, hrozna, případně celé rostliny. Fyziologické změny bobulí způsobené patogeny vína jsou menší velikost, blednutí barvy slupky, urychlené změkčení tkáně a zejména kratší trvanlivost v případě

stolního hrozna a menší výnosy pro výrobu vína (Cantoral *et al.*, 2011). Houbová infekce hrozna je popisována jako proces se čtyřmi fázemi představujícími prvotní záchyt patogena na rostlině, následné rozmnožení umožňující infekci vedoucí ke kolonizaci a dalšími šíření patogena (Li *et al.*, 2019). Proteiny sekretované patogeny cílí na vnější ochranou bariéru buňky, jedná se tedy o polygalakturonasy/pektinasy, pektinlyasy a kutinasy hydrolyzující rostlinné pletivo a umožňující šíření a virulenci infekce na rostlině (Kars *et al.*, 2005; Zhang a van Kan, 2013). Pro *B. cinerea* jde zejména o polygalakturonasy Bcpg1 a Bcpg2 produkované konstitutivně během infekce (ten Have *et al.*, 2001; Haile *et al.*, 2020). Dalšími produkty plísně ovlivňující kvalitu vína jsou pro *B. cinerea* proteolytické enzymy. Proteolytická aktivita *B. cinerea* negativně ovlivňuje obsah jak rostlinných proteinů, tak i množství proteinů z kvasinek (Girbau *et al.*, 2004, Marchal *et al.*, 2006, Cilindre *et al.*, 2007, Cilindre *et al.*, 2008, Marchal *et al.*, 2020). Po napadení hrozna padlím byl naopak zaznamenán nárůst obsahu vinných PR-proteinů ve šťávě i víně (Girbau *et al.*, 2004). Produkce a aktivita aspartátových proteas byla u *B. cinerea* prokázána jen při pH 3.0–4.0 vnějšího prostředí (Manteau, 2003). Schopnost těchto hydrolas štěpit i odolné vinné PR-proteiny je využívána v případě BcAP8 proteasy, která je dnes uměle přidávána jako čiřící činidlo pří výrobě vína (van Sluyter *et al.*, 2013). Jako biomarker botrytického původu dezertních vín může sloužit důkaz přítomnosti sekretovaných oxidas a to lakasy 2 (*BcLCC2*) a lakasy 3 (*BcLCC7*, Ployon *et al.*, 2020).

Nejběžnějšími mikroogranismy používanými k fermentaci hroznové šťávy na víno jsou pekařské neboli vinné kvasinky *S. cerevisiae*. V průmyslové výrobě vína převládá použití vyšlechtěných kmenů odolávajících uměle sníženým teplotám během fermentace a vykazujících dostatečnou toleranci k očekávanému obsahu cukru a množství tvořeného ethanolu. Tyto vlastnosti umožňují *S. cerevisiae* během fermentace přerůst ostatní mikroorganismy přítomné již na povrchu hrozna a výroba vína tak probíhá řízeným opakovatelným způsobem (Bauer a Pretorius, 2000). Kvasinky k adaptaci na ztěžující se růstové podmínky během fermentace sekretují řadu proteinů, které lze následně identifikovat ve víně (Ferreira *et al.*, 2002). Nezanedbatelný obsah glykoproteinů z kvasinek uvolňujících se do vína během kvašení zaznamenal Dambrouck, 2003. Vincenzi *et al.*, 2011 detegoval přítomnost mannoproteinů původem z kvasinek v moštu již po měsíci fermentace. Uvolňování mannoproteinů z usazených kvasinek také přispívá k jejich obohacení a díky své stabilitě a schopnosti vázat taniny vylepšují kvalitu vína (Rowe *et al.*, 2010). Mezi první identifikované zástupce patří *N*-glykosylované proteiny HPF1 a HPF2 („haze protective factor“) a cukerná invertasa. HPF

proteiny byly testovány jako účinné protektory vzniku zákalu vína po vystavení změnám teplot (Moine-Ledoux a Debourdieu, 1999, Dupin *et al.*, 2000, Brown *et al.*, 2007. Ostatní proteiny sekretované kvasinkami nebo z nich uvolněné jsou spojeny s růstovými stresy. Na úrovni genů je dobře charakterizována rodina 24 Pau proteinů kvasinek, z nichž Pau5 je silně indukován nedostatkem kyslíku a nízkou teplotou (Luo *et al.*, 2009). Přítomnost *O*-glykosylovaného Pau5 proteinu byla korelována s tendencí samovolného vypěnění šumivých vín (Kupfer *et al.*, 2017). Během fermentace dochází u kvasinek k významným úpravám metabolismu dusíku a tvorbě permeas a přenašečů AK k jejich transportu (Beltran *et al.*, 2005). K detoxifikaci iontů mědi z na hrozno aplikovaných postřiků vytvářejí kvasinky metalothioneiny (Warringer *et al.*, 2011).

5.4. Metody číření vína

Stabilizace vína pomocí čířících činidel je běžným postupem k dosažení vysoké kvality zejména bílých vín zahrnující příjemnou barvu a vyvážený organoleptické profil (Cosme *et al.*, 2012). Pomocí čiřících činidel jsou z vína záměrně odstraňovány částice odpovědné za zákal, zejména fenolické látky tvořící koloidní shluky a proteiny způsobující tepelnou nestabilitu (Falconer *et al.*, 2010, van Sluyter *et al.*, 2015, Cosme *et al.*, 2020) Částečně také čiřidla redukují a změkčují chuť třísloviny a usnadňují filtrovatelnost vína (Castillo-Sánchez *et al.*, 2008, Chagas, 2012).

5.4.1. Bentonit

Nejběžnější technikou čiření vín představuje přidávání suspenze bentonitu. Bentonitový prášek (obsah 60-80 % minerálu montmorillonitu) funguje jako silný kationtoměnič a při nízkém pH vína na sebe váže kladně nabité proteiny zejména z hrozna (Lambri *et al.*, 2010; Jaeckels *et al.*, 2017). Největší efektivita adsorpce na bentonit byla prokázána pro menší proteiny do 30 kDa bez výrazného vlivu rozdílů pH vína. Obecně však s klesajícím pH účinnost čiření bentonitem klesá. Bentonity s vysokým obsahem Ca^{2+} jsou nejméně účinné pro odstranění proteinů původem z hrozna (Dordoni *et al.*, 2015). Jako nejsnáze adsorbující protein na bentonit byla identifikována endo-1,3-β-glukosidasa z hrozna mající oproti ostatním proteinům vína vyšší hodnotu p*I* než okolní prostředí vína (Jaeckels, 2015). Velmi efektivně jsou bentonitem odstraňovány i rostlinné chitinasy (Jaeckels, 2017). Nespecifické působení bentonitu nejen na proteiny může negativně ovlivnit obsah dalších molekul, hlavně polyfenolů a anthokyanidinů ovlivňujících aroma a barvu vína (Pretorius, 2000; Granato *et al.*, 2010; Lambri *et al.*, 2010, He *et al.*, 2020). Běžně používané koncentrace bentonitu aplikovaného do vína

nepřesahují 1 $g \cdot l^{-1}$, což vede až k 85% snížení proteinového obsahu a ukazuje tak bentonit jako nejúčinnější běžně užívané deproteinační činidlo aplikované ve vinařství (Sauvage *et al.*, 2010; Chagas *et al.*, 2012; van Sluyter *et al.*, 2015). Negativem po použití bentonitu je ztráta běžně asi 10% části čiřeného vína tvořící sedlinu a tzv. bentonitový kal (Waters *et al.*, 2005).

5.4.2. Čiření vína pomocí proteinů a enzymů

Další skupinu čiřících činidel představují živočišné proteiny a proteinové extrakty. Nejběžněji jsou využívány vaječný albumin, hovězí kasein nebo vyzina („isinglass“) (Wigand *et al.*, 2009; D´Amato *et al.*, 2010, Chagas *et al.*, 2012, van Sluyter *et al.*, 2015). Podle nařízení evropské komise (2007/68/EC) však musí tyto přidané látky být na hotovém výrobku deklarovány, zvláště pokud jde o známé alergeny. Po aplikaci zmíněných proteinových čiřidel běžně následovalo další ošetření vína bentonitem k jejich odstranění. Technický pokrok umožnil tyto alergeny snadno detegovat a lze tak předpokládat minimalizaci a odklon od jejich nadměrné aplikace (D´Amato *et al.*, 2010, Rizzi *et al.*, 2016). K efektivnímu potlačení vzniku zákalu přispívají silně glykosylované mannoproteiny (viz. kapitola 5.3.6.), polysacharidy a hydrolytické enzymy tvořené kvasinkami. K praktické aplikaci tak lze použít extrakty ze *S. cerevisiae* nebo inokulovat kvasinky (*Saccharomycces japonicus*), které mannoproteiny tvoří ve zvýšeném množství (Dupin *et al.*, 2000; Pozo-Bayón *et al.*, 2009; Gaspar *et al.*, 2019; Millarini *et al.*, 2020). Snadnější uvolnění mannoproteinů z buněčné stěny autolyzujících kvasinek je možné podnítit aplikací slabých elektrických impulzů (Martinéz *et al.*, 2016). Aplikace tohoto přístupu přímo po fermentaci vína však nebyla testována.

Přímou cestou k odstranění teplotně nestabilních proteinů tvořících zákal je již při výrobě vína aplikace proteolytických enzymů. V kombinaci se zvýšenou teplotou je účinné použití aspergillopepsinů I a II (EC 3.4.23.18 a EC 3.4.23.19) vedoucí až k 80% snížení obsahu proteinů ve vínu fermentovaném z hroznové šťávy ošetřené rychlou pasterizací (75 °C, 1 min) a následným přidání proteasy v množství 15 $mg \cdot l^{-1}$ (Marangon *et al.*, 2012). Proteolytickou aktivitou při fermentaci vykazuje i vakuolární proteinasa A (saccharomycin, EC 3.4.23.25) uvolňující se do vína po autolýze samotných kvasinek (Younes *et al.*, 2011; Song *et al.*, 2017). Vinné PR-proteiny jsou účinně hydrolyzovány zmíněnou rekombinantní proteasou BcAp8 původem z *B. cinerea* (van Sluyter *et al.*, 2013). V laboratorním měřítku bylo testováno snížení obsahu

proteinů a zvýšení stability vína za použití imobilizovaného bromelainu nebo papainu v míchaném a průtokovém mikroreaktoru (Benucci *et al.*, 2014, 2016, 2020).

5.4.3. Ostatní čiřící prostředky

Polyvinylpolypyrrolidon (PVPP) umožnuje nejefektivnější snížení obsahu polyfenolů ve víně což může přispět k vyšší teplotní stabilitě takto ošetřených vín (Pocock *et al.,* 2007; Esteruelas *et al.,* 2011; Chagas *et al.*, 2012). Menší ztráty objemu byly popsány po aplikaci přírodních zeolitů namísto bentonitu (Mierczynska-Vasilev *et al.*, 2019). Alternativně je k čiření vína možné použít také chitosan nebo chitin (Vincenzi *et al.,* 2005; Chagas *et al.*, 2012). Účinně lze proteiny z vína odstranit pomocí přírodního kappa-karagenanu (Ratnayake *et al.,* 2019). Pro čiření vína se dále studují možnosti aplikace extraktů získaných přímo z pecek hrozna, aplikace magnetických nanočástic nebo například systém afinitní filtrace s cílem stabilizovat víno a zároveň zachovat nebo potlačit ostatní senzorické vlastnosti méně než použitím tradičních technik (Gazzola *et al.*, 2017; Dumitriu *et al.*, 2017; Mierczynska-Vasilev *et al.*, 2019).

5.5. Izolace a stanovení proteinů ve víně

Ve vinařské praxi je stanovení obsahu proteinů prováděno nepřímo a interpretováno jako pozorovatelný nebo měřitelný zákal. Principem těchto metod je sledování zákalu a sraženiny vzniklé po vystavení vína změně teploty nebo přidání s proteiny interagujících nebo srážecích činidel. Nenáročnou metodu predikce míry stability vína je pozorování trvanlivosti pěny a míry pěnivosti po jeho intenzivním promíchání (Hodeček, 2016).

Kvantitativnímu stanovení proteinů z vína pomocí běžných biochemických metod předchází jejich izolace a nabohacení pomocí technik dialýzy, ultrafiltrace, srážení, nebo fázové extrakce (Tab. 4). Pro první proteomickou studii proteinů hrozna využívající MS aplikovali Sarry *et al.*, 2004 precipitaci homogenátu acetonem s 12,5 % TCA a přídavkem β-merkaptoethanolu. Analýzou proteinů zejména z mezokarpu hrozna, získaných šetrnou manuální homogenizací, bylo u všech vzorků po separaci 2D-elektroforézou rozlišeno více než 200 signálů (Sarry *et al.*, 2004). U zralých bobulí bylo také pozorováno kvalitativně největší zastoupení PR-proteinů (Sarry *et al.*, 2004). První identifikaci proteinů z vína Sauvignon Blanc pomocí nLC MSMS a SDS-PAGE separace publikoval Kwon, 2004. Po zakoncentrování proteinů vína ultrafiltrací s následným vysolením se autorovi podařilo identifikovat 20 proteinů převážně původem z kvasinek (Kwon, 2004). Pro zpracování hrozna pro proteomickou analýzu byl popsán postup využívající

homogenizaci v suchém ledu a v tekutém dusíku (Vincent *et al.*, 2006, Giribaldi, 2010, Martines Esteso, 2010).

Tab. 4 Přehled publikovaných analýz vína popisující inovativní metody extrakce a izolace proteinů. (TCA – trichloroctová kyselina; UF X kDa – ultrafiltrace, X značí velikost póru v kDa; EtOH – ethanol; SCX-LC kapalinová chromatografie na kationtoměniči; PVPP – polyvinylpolypyrrolidon; LSB – Laemmliho pufr pro elektroforézu; DTT – dithiothreitol, 2-ME - merkaptoethanol)

publikovaná práce	odrůda vína	materiál	zpracování vzorku	kvantifikace proteinů	metoda separace proteinů	MS analýza	proteiny [n]
Sarry et al., 2004	komerční vína	hrozno	homogenizace, filtrace, precipitace 12,5 % TCA aceton s merkaptoetanolem	Bradford	2D ELFO	MALDI MS	67
Kwon, 2004	Sauvignon Blanc	víno	UF 5 kDa, vysolení 80 % síran amonný	Bradford	SDS-PAGE	nLC MSMS	20
Vincent et al., 2006	Cabernet Sauvignon	hrozno	drcení se suchým ledem následně tekutým dusíkem	EZQ kit - fuorescence	2D ELFO	nLC MSMS	11 - 44
Okuda et al., 2006	Chardonnay	víno	odpaření 40 °C 10× konc., precipitace do 80 % síran amonný, dialýza, lyofilizace	vážení lyofilizované frakce	2D ELFO	N-term sekv.	8
Vanrell et al., 2006	komerční vína	víno	dialýza 12 kDa, lyofilizace	A280	FPLC, ASX, SEC, ConA	X	X
Negri et al., 2008	Barbera	hrozno	drcení v tekutém dusíku, homogenizace s acetonem, filtrace, vysušení, extrakce, precipitace MeOH/aceton	2D Quant kit	2D ELFO	nLC MSMS	69
Cillindre et al., 2008	Chardonnay	víno	dialýza, UF 10 kDa, precipitace EtOH + 15% TCA	vážení lyofilizované frakce	2D ELFO	Western Blot	37
Weber et al., 2009	komerční vína	víno + kasein	lyofilizace, 150× konc., UF 35,5 kDa, dialýza, lyofilizace	X	SDS-PAGE	X	X
Batista et al., 2009	Arinto	víno	UF 3 kDa, odsolení Sephadex G-25M, lyofilizace, SCX LC, lyofilizace	Lowry	X	X	X
Grimplet et al., 2009	Cabernet Sauvignon	hrozno	drcení v tekutém dusíku, fenolová extrakce, precipitace MeOH	EZQ kit - fuorescence	2D ELFO	MALDI MSMS	1047
Esteruelas et al., 2009	Sauvignon	exp. víno	dialýza 3,5 kDa, lyofilizace	Bradford	SEC SCX FPLC, SDS/NATIVE-PAGE, IEF	nLC MSMS	X
Marangon et al., 2009	Semillon	hrozno, víno	vysolení ze vzorku o pH 5 (KOH) do 80 % síran amonný	RP-HPLC (TLP, Chitinasy)	SDS-PAGE, LPLC, RP/HIC/SEC HPLC	nLC MSMS	24
van Sluyter et al., 2009	Semillon, Sauvignon blanc	víno	PVPP čištění pH 3 (HCl), filtrace 0.2 µm, SCX LC	RP-HPLC	CE HIC + RP HPLC	nLC MSMS	11
Wigand et al., 2009	komerční vína	víno	dialýza 3,5 kDa, lyofilizace, PVPP čištění	vážení lyofilizované frakce	SDS-PAGE	nLC MSMS	25
Suavage et al., 2010	Chardonnay	víno	bentonit, eluce LSB; fractogel + UF 150 + 5 kDa	Denzitomentricky 1D SDS PAGE (BSA), Bradford	2D ELFO	nLC MSMS	14
Giribaldi et al., 2010	Cabernet Sauvignon	hrozno	drcení v tekutém dusíku, extrakce tris thiomočovina DTT, precipitace TCA a acetonem	2D Quant kit	2D ELFO	nLC MSMS	379/679
Martínez-Esteso et al., 2011	Muscat Hamburg	hrozno	drcení v tekutém dusíku, extrakce do etylacetátu s EtOH, extrakcni pufr, extrakce Tris/fenol, precipitace fenolové frakce MeOH	Bradford	SCX LC	nLC MSMS	830
Vincenzi et al., 2011	Manzoni Bianco	exp. víno + meziprodukty	dialýza + C18 nabohacení, vymrazení, stanovení proteinů precipitace SDS + KCl, rozpuštění peletů	BCA	SDS-PAGE	MSMS	X
Kambiranda et al., 2013	Noble	hrozno	extrakce do 10 TCA s 0.07% 2-ME v acetonu; extrakce do fenolu sat. Tris-HCl, precipitace	Bradford	X	nLC MSMS	522/352
Mainente et al., 2014	Cabernet Sauvignon	víno	PVPP čištění, SDS-KCl extrakce, TCA, precipitace aceton	BCA	2D ELFO	nLC MSMS	23
Vogt et al., 2016	komerční vína	víno	dialýza lyofilizace, extrakce, reextrakce do fenolu, precipitace do octanu amonného v MeOH	X	SDS-PAGE	X	X

Pro extrakci proteinů z precipitátu z hrozna byly srovnány protokoly bez a včetně fázové extrakce organických látek vína do fenolu (Vincent *et al.*, 2006). K extrakci proteinů z vína nebo hroznové šťávy lze použít také vysolení pomocí síranu amonného do 80 % nasycení (Kwon, 2004; Marangon *et al.*, 2009). Inovativní postup zakoncentrování proteinů z vína pomocí adsorpce proteinů na bentonit (150 $g \times hl^{-1}$) s následnou elucí Laemliho pufrem pro SDS-PAGE popsal Sauvage *et al.*, 2009. Tato technika umožňuje

po provedení elektroforetické separace a vizualizace přímé srovnání proteinových profilů vín při využití mililitrových objemů vzorku. Nevýhodou je její omezená účinnost pro vína již dříve vyčiřená bentonitem (Sauvage *et al.*, 2009). Opačný přístup mající za cíl odstranit z vína malé fenolové látky díky jejich adsorpci na PVPP použili v laboratorním měřítku van Sluyter *et al.*, 2009 a Mainente *et al.*, 2014. Pro zakoncentrování proteinů z hrozna je dále využívána ultrafiltrace nebo přímo lyofilizace dialyzovaných vzorků (Tab. 4). Pro izolaci proteinů i z červených vín lze využít postupy Mainente *et al.*, 2014 a Vogt *et al.*, 2016. Vybrané skupiny vinných proteinů lze efektivně izolovat také pomocí preparativní kapalinové chromatografie na kationtoměniči nebo koloně s reverzní fází (Batista *et al.*, 2009; Marangon *et al.*, 2009; van Sluyter, 2009).

5.6. Výsledky – proteiny vína

Výsledky experimentů zabývajících se analýzou experimentálního vína Sauvignon blanc (vzorky A a B, Obr. 13) a ostatních vín, včetně vlivu vybraných proteinů na zákal vína byly publikovány Perutka *et al.*, 2019, přílohy č. 5 a 6 této práce. Zde uvedené výsledky jsou shrnutím a doplněním k zmíněné publikaci, kde jsou uvedeny jako příloha nebo nejsou prezentovány. Na zmíněnou publikaci navázala práce charakterizující cysteinovou proteasu opakovaně nalezenou ve všech vzorcích vín (Perutka a Šebela, 2020, příloha č. 7). Na základě pozvání od prof. Djuro Josice byla publikována kapitola zabývající se falšováním a biochemickou analýzou vína v sekci Food Safety and Foodomics v referenčním sborníku článků Comprehensive Foodomics (Perutka et al., 2021, příloha č. 8).

5.6.1. Charakteristiky porovnávaných vín

Pro všechna studovaná vína bylo stanoveno pH a míra zákalu (Tab. 5). Po dialýze a ultrafiltraci byl stanoven také obsah proteinů. Změření zákalu pro vzorek čerstvé hroznové šťávy nebylo možné z důvodu rychlé oxidace tohoto vzorku projevující se jeho hnědnutím.

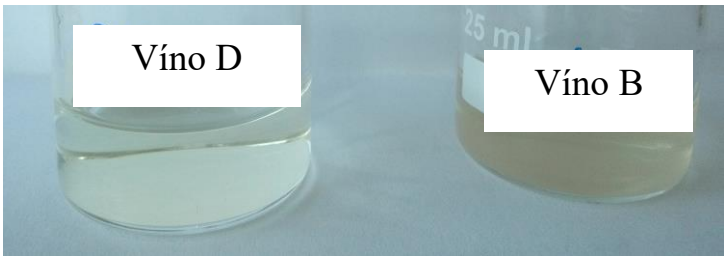

Obr. 13 Porovnání původního zabarvení a průhlednosti vín B a D.

Tab. 5 Charakteristiky analyzovaných vzorků vín.

Stanovené hodnoty obsahu proteinů ve víně stanovené z ultrafiltrátu pomocí měření s BCA a BSA jako standardem. Míra zákalu je měřena jako absorbance při 540 nm a výsledek teplotního testu stability vína uvedený jako změna A při 540 nm před a po provedení testu.

Vzorek vína, odrůda hrozna	Oblast původu hrozna	Charakteristika	pH	obsah proteinů [g·l-1]	A 540	Heat test Δ A 540
A - Experimentální víno, Sauvignon blanc 2015	Mělčany, Jižní Morava, ČR	viditelný zákal, 20 % použitého hrozna napadeno B. cinerea, zápach, nelze aplikovat bentonit, známá historie výroby vína a produkce hrozna	2.2	0.28 ± 0.03	0.391	0.028
B - Experimentální víno, Sauvignon blanc 2015	Mělčany, Jižní Morava, ČR	experimentální víno A stařené 1 rok, zákal, zápach	3.3	0.27 ± 0.02	0.362	0.031
C - Komerční víno, Sauvignon blanc 2016	Francie	suché, bez viditelného zákalu, světlejší barva, bez vůně	3.4	0.22 ± 0.01	0.014	0.002
D - Komerční víno, Ryzlink vlašský, botrytický sběr 2015	Horní Věstonice, Jižní Morava, ČR	sladké, bez viditelného zákalu	3	0.24 ± 0.01	0.019	0.006
E - Komerční víno, Ryzlink vlašský, pozdní sběr 2015	Perná, Jižní Morava, ČR	suché, bez viditelného zákalu, intenzivní žlutooranžová barva, výrazná vůně	3.3	0.27 ± 0.01	0.023	0.003
F - Komerční víno, Ryzlink vlašský, pozdní sběr 2014	Svatobořice-Mistřín, Jižní Morava, ČR	suché, bez viditelného zákalu, nevýrazná barva	3.4	0.29 ± 0.02	0.014	0.002
G - Mladé víno, Irsay Oliver 2018	Rajhradice, Jižní Morava, ČR	bez viditelného zákalu, sladké, neošetřeno bentonitem	3.3	0.13 ± 0.01	0.092	0.011
H - Hroznová šťáva 2018	Jižní Morava, ČR	připraveno lisováním ze stolního hrozna	3.2	0.11 ± 0.01	X	X
Komerční víno, Ryzlink vlašský 2016	Velké Pavlovice, Jižní Morava, ČR	suché, bez viditelného zákalu	3.3	0.58 ± 0.03	0.015	0.001

Pozn.: Historie vzorku vína A. Hrozno bylo sklizeno na konci suchého období během jehož konce se vyskytl silný dešť. Pro výrobu vína bylo použito 20 % hrozna viditelně napadeného *B. cinerea*. Před lisováním byl rmut ponechán 15 h stát. Poté byl přidán disiřičitan draselný do koncentrace 50 $mg \cdot l^{-1}$. Následně byl odstraněn sediment a byly naočkovány kvasinky. Jako výživa pro kvasinky byl přidán sulfát amonný. Fermentace probíhala 8 týdnů.

Proteinové profily byly získány pro všechna vína po rozdělení jejich ultrafiltrátů SDS-PAGE. Následně byly proteiny identifikovány tandemovou hmotnostní spektrometrií. Pro všechny vzorky vín i hroznové šťávy bylo identifikováno mezi 9–28 proteiny viz příloha č. 6. Proteinový profil vín vz. C, E a F zobrazen na obr. 14.

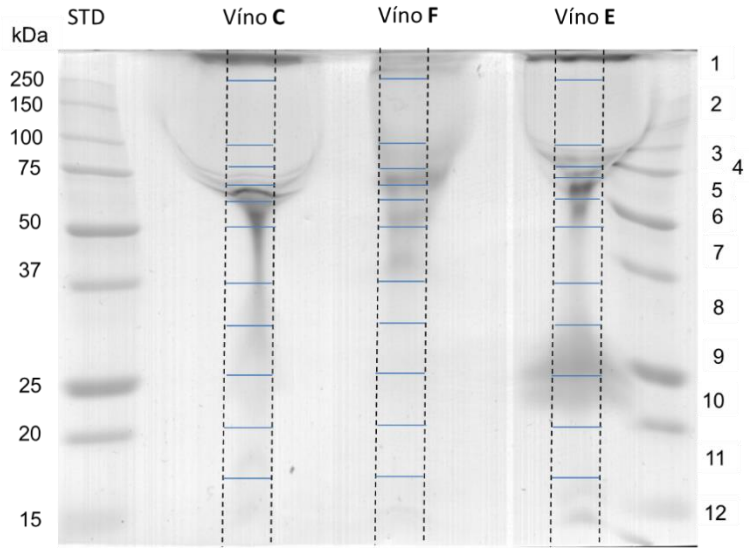

Obr. 14 Proteinový profil koncentrátů vína. SDS-PAGE vzorků vín C, E, F po dialýze a zakoncentrování ultrafiltrací. Na gel naneseno 20 µg vzorků. Vyobrazeno rozdělení na proteinové pásy 1–12 dále použité pro analýzu hmotnostní spektrometrií.

Ze vzorku vína G byly pomocí gelové filtrace izolovány frakce proteinů *V. vinifera* dle jejich AK sekvencí bohatých na prolin: invertasa (gi|225466093, 6,5 % Pro), frakce „thaumatin-like“ proteinů (gi|7406716 a gi|147785114, 7.1 % a 5,0 % Pro), cysteinová proteasa (gi|297740510, 9,8 %) viz příloha č. 6. Tyto frakce byly následně přidány k jinak stabilnímu vínu ryzlink vlašský 2016 přídavkem 50 $\mu g \cdot ml^{-1}$ a znovu byl proveden test teplotní stability. Změna absorbance při 540 nm následně odpovídala nárustu o cca 6 % po přidání proteasy, 4 % v případě invertasy a 16 % po přidání frakce „thaumatin-like“ proteinů. Absolutní změna A_{540} po provedení testu teplotní stability nikdy nepřekročila 0,02 vůči samotnému původnímu vínu.

5.7. Cysteinová proteasa vína

Studie prováděné na proteinech původem z hrozna přetrvávajících i ve víně se věnují omezené skupině dle MW relativně malých zastupců chitinas, TLP, případně LTP souvisejících se zákalem (Ferreira *et al.*, 2001; Marangon *et al.*, 2009). Výsledky proteomických analýz vzorků bílých vín ukazují, že cysteinová proteasa (CYSP,

gi|297740510 a odpovídající delší sekvence XP_002266308 obsahující navíc propetidovou a inhibiční doménu na N-konci proteinu) původem z hrozna s předpokládanou MW 41 kDa byla detegovatelná ve všech vzorcích bez ohledu na odrůdu a stáří. Teoretická MW CYSP neodpovídá hodnotám stanovených SDS-PAGE pro extrakty z vín zobrazující odpovídající proteinový pás v oblasti okolo 200 kDa. Stejná hodnota MW pro CYSP byla zjištěna i při izolaci proteinových frakcí z vína za účelem testování jejich vlivu na stabilitu a zákal. Pro další charakterizaci proto byla CYSP izolována z mladého vína odrůdy Irsay Oliver. Purifikace CYSP zahrnovala dialýzu a ultrafiltraci vína a následnou separaci proteinového koncentrátu pomocí gelové permeační chromatografie při nízkém tlaku na koloně naplněné Sephacrylem S-300 HR (50×2,5 cm, GE Healthcare, Upsalla, Švédsko). Při této chromtografické separaci byla CYSP koeluována s asparaginasou původem z kvasinek (vypočtená MW 35 kDa bez signálního peptidu, gi|767254761) v čase odpovídající molekulám vetším 200 kDa. Toto zjištění potvrzovalo předešlý experiment využívající menší kolonu a vyšší tlak (Perutka et al., 2019). Asparaginasa a CYSP byly následně vzájemně odděleny metodou chromatofokusace na koloně Mono P HR 5/20 (GE Healthcare). Stanovená hodnota p*I* 3,6 pro CYSP se shodovala s teoretickými údaji pro aktivní sekvenci proteasy bez propeptidu a inhibiční domény. Po naštěpení trypsinem a chymotrypsinem byla sekvence CYSP potvrzena pomocí nLC ESI MSMS (Obr. 15).

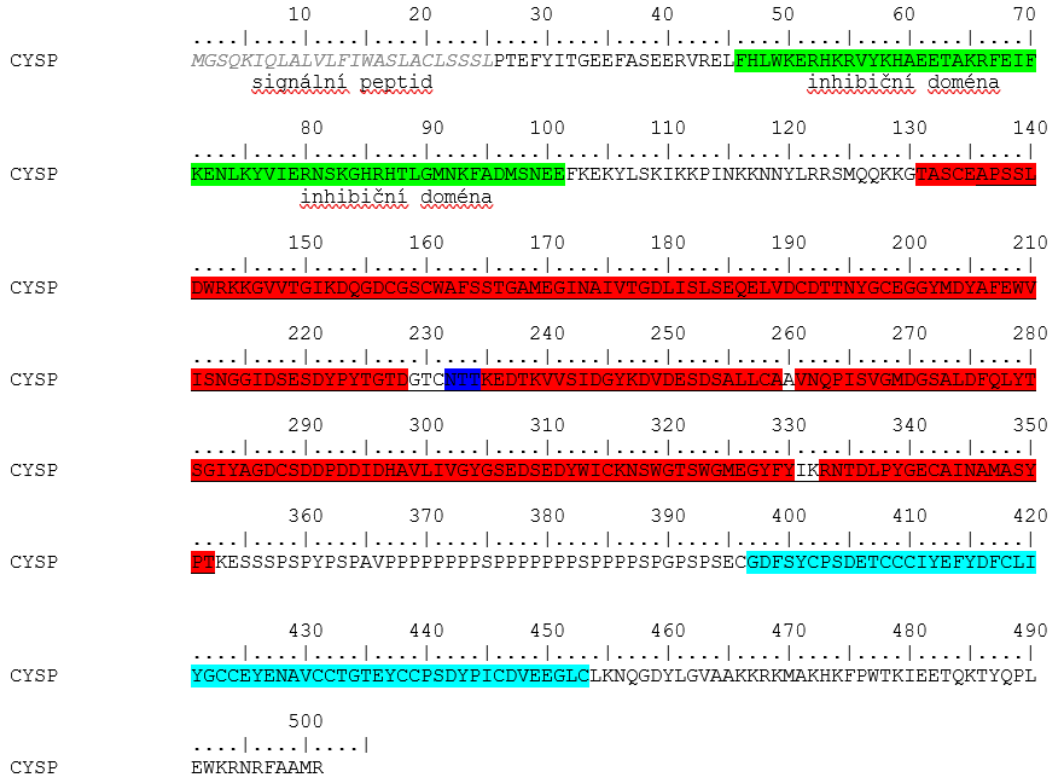

Obr. 15 Proteinová sekvence CYSP z vína (XP_002266308, NCBInr). Modře je vyznačeno místo možné *N*-glykosylace na Asn232. Signální sekvence propeptidu je označena kurzívou šedě. Zeleně je vyznačena sekvence inhibiční domény. Podtržená část sekvence odpovídá regionu funkční domény C1 proteas podobných papainu (pfam00112). Červeně je vyznačena část sekvence přečtené pomocí nLC MSMS po naštěpení CYSP v roztoku trypsinem a chymotrypsinem. Tyrkysovou je označen úsek granulinové domény (smart00277), kterému předchází oblast bohatá na Pro.

Izolace a důkaz proteolytické aktivity neznámé Cys-proteasy s MW 128 kDa původem z hrozna již byla popsána Expósito *et al.*, 1991. Pro CYSP byla stanovena specifická aktivita k redukovanému a alkylovanému BSA po 18 hodinovém štěpení v mravenčanu amonném o pH 3,0 při 37 °C. Množství nehydrolyzovaného BSA zbylého ve směsi bylo stanoveno denzitometricky po provedení SDS-PAGE a obarvení gelu. Specifická aktivita CYSP izolované z vína k BSA byla vypočtena na 0,2 nkat·mg^{-1}. Podobné hodnoty bylo dosaženo při použití stejného postupu také pro CYSP izolovanou z kvasného vinného octa (Rakotonaina, 2020). Přítomnost peptidů odpovídajících CYSP byla již dříve zaznamenána ve víně i v octu (Di Girolamo *et al.*, 2011, Jaeckels *et al.*, 2017). Specifičnost CYSP byla zjištěna po nLC MALDI MSMS analýze produktů štepení směsi proteinových standardů a proteinů extrahovaných z jader ječmene. Štěpení CYSP je nespecifické a nejvíce preferovanými AK na P1 pozici jsou Arg (21–25 %), Lys (17-26%) a Leu (15-20%). Nespecifičnost a vznik produktů štepení již po 10 min inkubaci byly zaznamenány sledováním vzniku štěpných peptidů pomocí MALDI MS ze vzorků CYSP aplikované k polypeptidovým standardům. Dle výsledků sekvenční analýzy CYSP pomocí trypsinu a chymotrypsinu nelze potvrdit přítomnost N-koncové inhibiční ani granulinové domény před C-koncem AK sekvence. Přítomnost granulinové domény umožňující agregaci a vznik oligomeru CYSP by se dala předpokládat na základě podobnosti k charakterizované RD-21 protease z *A. thaliana* a mohla by vysvětlovat zaznamenanou MW (Yamada *et al.*, 2001). Pro CYSP lze předpokládat obsazené glykosylační místo N232, protože nebyly zaznamenány žádné peptidy obsahující tento úsek sekvence. Absenci inhibiční domény prokázala Rakotonaina, 2020, když detegovala CYSP jako gi|297740510 a peptidy odpovídající inhibitoru Cys-proteas gi|296083924 neshodující se s inhibiční sekvencí CYSP. Pravděpodobná přítomnost CYSP spolu s proteinem gi|296083924 byla potvrzena provedením nativní PAGE. Vazba CYSP a inhibitoru byla uvolněna v redukčním prostředí a při SDS-PAGE bylo možné pozorovat

a identifikovat oba proteiny odděleně v oblastech 200 kDa pro CYSP a 11 kDa odpovídající MW inhibitoru (Rakotonaina, 2020).

5.8. Diskuse – proteiny vína

Na základě srovnání proteinových profilů vzorků experimentálního vína se zákalem (vz. A a B) a botrytického vína D bylo nalezena shoda na výrazně redukovaném množství malých PR-proteinů. Malý počet PR-proteinů a minimální signál na SDS-PAGE gelu byl pozorován i pro vzorek vína F vyznačující se nevýraznou barvou. Ve všech těchto případech byla jako marker přítomnosti *B. cinerea* identifikovaná lakasa 2 (gi|15022489). Obsah proteinů ve všech srovnávaných vínech dosahoval 200-300 $mg \cdot l^{-1}$, což odpovídá bežným hodnotám (Pocock *et al.,* 2007). Nižší obsah proteinů v extraktu z hrozna G a mladém víně H pravděpodobně souvisí s ručním zpracováním hrozna, když většina proteinů nacházejících se ve slupce nebyla do vína extrahována (Wigand *et al.,* 2009). Výrazně vyšší kyselost byla zaznamenána pro experimentální zakalené víno A, u kterého byl již při filtraci pozorován vznik krystalků organických kyselin na filtru. Popsaná nízká účinnost aplikovaného bentonitu souvisí s množstvím aplikovaného SO_2. Pro zabránění rozšíření infekce *B. cinerea* je dosažené množství SO_2 odpovídající 50 $mg \cdot l^{-1}$ nedostatečné a růst patogena a aktivitu jeho produktů zcela neinhibuje (Marchal *et al.*, 2006). Polysacharidy produkované *B. cinerea* následně znesnadňují filtraci a čiření vína (Francioli *et al.,* 1999). Jako projev plísně lze označit také nizký obsah malých PR-proteinů v oblasti 20-30 kDa na SDS-PAGE gelech. Tyto proteiny bežně poskytují nejintenzivnější signály a jsou ve víně z odrůdy Sauvignon blanc čiřených bentonitem nejazastoupenější (Esteruelas *et al.,* 2009). K redukci množství PR-proteinů vína nepochyně přispěly i hydrolasy produkované *B. cinerea*. Předpokládán je příspěvek proteas (gi|154310457, gi|154320662, gi|347833309). Výrazného snížení obsahu PR-proteinů ve víně lze dosáhnout aplikací vysokých dávek bentonitu. Odstranění TLP je však dle studie Sauvage *et al.*, 2010 možné maximálně z 80 % jejich celkového obsahu. Proteiny původem z plisně byly po elektroforetické separaci identifikovány v oblastech vyšších MW pro vzorek A (glykosidasa gi|347835718 a Ser-proteasa gi|347833309) a lze předpokládat jejich glykosylaci. Pro rozrušení rostlinné buněčné stěny může sloužit identifikovaná celulasa (gi|48093959). Projevem nežádoucí infekce patogenu na hroznu by mohl být rostlinný protein podobný stellacyaninu (gi|225445553 nebo gi|147780459) objevující se pouze u vzorků vína s nežádoucí botrytidou. Ve vzorku dezertního botrytického vína D nebyl tento protein zaznamenán. Kontrolovaný růst a aktivita *B.*

cinerea jako ušlechtilé plísně, tak sice také značně redukuje množství rostlinných PR-proteinů (vzorek D, příloha č. 6), ale mechanismus vzájemné intereakce mezi rostlinou a plísní může být odlišný. Zvýšená exprese genu pro „stellacyanin-like“ protein byla zaznamenána na listech pepře při růstu patogena *Xanthomonas campestris pv. Vesicatoria* (Jung a Hwang, 2000). Stellacyanin jako dvouelektronový přenašeč by mohl být zapojen do oxidačních procesů úpravy buněčné stěny rostliny v reakci na přítomnost patogenu (Meng *et al.,* 2016). V systému obsahujícím lakasu se nabízí inhibiční působení stellacyaninu omezující radikálovou polymerizaci produktů lakasy a jejich interakci s dalšími rostlinnými strukturami (Yang *et al.*, 2020). Nekontrolovaný růst *B. cinerea* a kompetice o živiny s kvasinkami by mohl být vysvětlením neobvykle dlouhé doby fermentace experimentálního vína. Dokladem zpomaleného metabolismus kvasinek v důsledku nedostatku živin je přítomnost asparaginasy (gi|323346853). Přechod od aerobního k anaerobnímu růstu lze dokládat identifikovanými proteiny spojenými právě s těmito procesy, jako je mannoprotein Tir4 (gi|323352383, Abramova *et al.*, 2001), nebo glykoprotein buněčné stěny Wsc4 (gi|768812869, *Verna et al.*, 1997). Změna v senzorickém profilu vína může být způsobena aktivitou nalezené fosfolipasy B z kvasinek (gi|323336225) nebo aktivitou peroxidasy gi|359478431 původem z *V. vinifera.* Producentem vína zaznamenaná nízká účinnost až nefunkčnost bentonitu k potlačení zákalu vína A může souviset také s velmi nízkým pH tohoto vzorku (Dordoni *et al.*, 2015). K rozšíření plísně nepochybně výrazně napomohlo počasí během posledních dní před sběrem hrozna, kdy byl zaznamenán silný déšť po předchozím velmi suchém období. Po přidání izolovaných frakcí obsahující invertasu, TLP nebo thiolovou proteasu do jinak teplotně stabilního bílého vína nebyl pozorován vznik nestability. Vybrané proteiny vína, všechny bohaté na prolin, proto nelze označit jako primární zdroj zákalu analyzovaného experimentálního vína.

6. PŘEHLED POUŽITÝCH METOD

6.1. Využití pseudotrypsinu pro identifikace jaderných proteinů

6.1.1. Příprava pseudotrypsinu

Výchozím materiálem pro přípravu ψ-trypsinu byl hovězí trypsin (MP Biomedicals, SantaAna, USA). Lyofilizovaný protein 425 mg byl rozpuštěn v 85 ml 20mM hydrogenuhličitanu amonného (Ambic). Po rozpuštění bylo ihned přidáno 2,2 ml 10mM TPCK v ethanolu inhibujícího kontaminující chymotrypsin. Suspenze byla promíchána a po dobu 30 min při 37 °C probíhala inkubace. Následně byl obsah kádinky dialyzován proti 3 l 0,1 % kys. mravenčí (FA). Dialýza probíhala 48 h při 4 °C. Dialyzační roztok FA byl měněn za čerstvý poprvé po 3 h a následně 2× po 15 h. Objem dialyzátu byl zredukován na 40 ml pomocí ultrafiltrace v míchané cele Amicon 8200 (200 ml) za použití 10 kDa „cut-off" membrány (Merck Millipore, Bedford, USA). Pro autolýzu samotného trypsinu byl vzorek pomocí dialýzy proti 20 mM Ambic převeden do bazického prostředí. Dialýza při 4 °C trvala 16 h ve 3 l pufru, přičemž výměna pufru proběhla po prvních 3 h. K dialyzované roztoku byl přidán 0,5M $CaCl_2$ do výsledné 50mM koncentrace a pH vzorku upraveno pomocí 2M NaOH přesně na hodnotu 8,0 a vzorek byl promíchán. Inkubace vedoucí k autolýze trypsinu byla prováděna při 25 °C přes noc (16 h). Po autolýze bylo sníženo pH roztoku na 7,0 přidáním 1M Tris-HCl (pH 7,0) do výsledné 50mM koncentrace a přidán TLCK do obsahu 7,5 mg na 100 mg výchozího trypsinu. Roztok byl promíchán a ponechán stát 105 min. Následovala 48h dialýza proti 0,1% FA jak je uvedeno výše. Dialyzovaný vzorek byl následně ředěn 1:1 100 mM Tris-HCl o pH 7,1 obsahující 20mM $CaCl_2$ a ultrafiltrací zahuštěn z 90 ml na 40 ml, následně byl tento krok opakován při použití 50mM Tris-HCl pufru (pH 7,1) a objem autolyzátu byl zmenšen na výsledných 18,5 ml při pH 7,1. Alikvoty po 2 ml (0,5-1,7 $mg \cdot ml^{-1}$) byly zamrazeny.

6.1.2. Izolace ψ-trypsinu

Separace produktů autolýzy trypsinu byla prováděna na koloně HemaBio 1000SB (7,5×250 mm, Tessek, Praha, ČR) a chromatografickém systému Biologic DuoFlow (Bio-Rad, Hercules, USA), podle upraveného postupu Dyčka *et al.,* 2015. Na kolonu ekvilibrovanou 50 mM Tris-HCl s 10 mM $CaCl_2$ (pH 7,1) byly dávkovány 2 ml alikvoty pomocí nanášecí smyčky a 150 min trvající separace probíhala isokraticky za využití stejného pufru a průtoku 1 $ml \cdot min^{-1}$. Po spuštění separace byl vzorek mezi 2–4 min

nanášen na kolonu, od 4. minuty probíhala separace. Promývací krok mezi jednotlivými chromatografickými běhy nebyl potřeba. Průběh separace byl monitorován pomocí UV-VIS detektoru při sledováním absorbance při 214 a 280 nm a vodivostní cely.

Pro izolaci ψ-trypsinu byla využita i kolona UNO-S12 (15×68 mm, Bio-Rad, USA). Celková doba chromatografického runu byla 75 minut při průtoku 2 $ml \cdot min^{-1}$. Doba samotné separace při lineárním gradientu 1M NaCl v 50mM Tris-HCl s 10 mM $CaCl_2$ pufru (pH 7,1) od 0 do 30 % byla 45 minut. Následovalo skokové navýšení obsahu NaCl na 100% mobilní fáze na 5 min pro vymytí kolony. Mezi jednotlivými chromatografickými běhy nebyl použit další promývací krok. Alternativně byla testována separace stejně připraveného autolyzátu trypsinu pomocí menších 1 ml kolon MonoS5 (Pharmacia, Stockholm, Švédsko) a UnoS1 (Bio-Rad) spojených za sebou. Všechny chromatografické separace probíhaly za stálé teploty při chlazení mobilních fází a kolony na 4 °C.

Frakce odpovídající jednotlivým eluovaným píkům byly manuálně sbírány, dialyzovány 48 h proti 0,1 % FA a pro další použití koncentrovány pomocí ultrafiltrace na 10 kDa „cut-off" membráně (viz. Příprava pseudotrypsinu). Poté byl v jednotlivých frakcích stanoven obsah proteinů metodou využívající kyselinu bicinchoninovou (BCA) za využití BSA a hovězího trypsinu jako standardů (Smith *et al.*, 1985). Pro stanovení ve vzorcích o malém objemu a předpokládaném nízkém obsahu proteinů bylo použito kapkového spektrofotometru („nanodrop"). Takto byla stanovena absorbance při 280 nm a následně vypočten obsah proteinů pomocí molárního extinkčního koeficientu pro trypsin 37560 $dm^3 \cdot mol^{-1} \cdot cm^{-1}$ a MW 23 300 Da.

Obsah získaných frakcí byl po zakoncentrování analyzován pomocí MALDI TOF MS. Metodou dvojité vrstvy bylo na MALDI terčík „steel target" 96 (Bruker Daltonics, Brémy, Německo) naneseno nejprve 0,5 µl saturovaného roztoku SA v ethanolu a ponecháno zaschnout. Na připravenou vrstvu bylo dále aplikováno 0,5 µl popř. 1,0 µl vzorku a 0,5 µl SA rozpuštěné v TA30 (roztok 0,1% kys. trifluoroctové (TFA), smíchané s čistým acetonitrilem (ACN) v poměru 70:30). Pro kalibraci přístroje byl použit proteinový standard 1 (Bruker Daltonics) nanesený na terčík stejným způsobem jako vzorky. Po zaschnutí byly vzorky analyzovány v lineárním módu na spektrometru Microflex LRF (Bruker Daltonics). Pro měření spekter intaktních proteinů bylo toto nastavení; akcelerační napětí: 20.0 kV, napětí pro extrakci: 18,3 kV; napětí na čočkách 7,6 kV; napětí na detektoru 1680 V; zpoždění iontové extrakce: 1000 ns. Spektra byla

získana akumulací signálu po 500 výstřelech laseru s frekvencí 60 Hz. Přístroj byl ovládán pomocí softwaru flexControl a data zpracována v nástroji flexAnalysis 3.3 (vše Bruker Daltonics). Nastavení pro MALDI TOF analýzu na přístroji ultraflextreme (Bruker) bylo následující: rozsah měření 5 – 50 000 Da, Digitizer: 4,00 GS/s; Detector Gain: 50x lineární mód, 3696 V, napětí na iontovém zdroji IS1 – 20 kV, IS2 – 18,7 kV, napětí na čočkách – 5,98 kV. Jako externí kalibrační standard byl použit protein calibration Mix1 5,700-17,000 Da (LaserBio Labs, Valbonne, Francie).

6.1.3. Srovnání štěpění pseudotrypsinu a trypsinu pomocí MALDI TOF MS

Srovnání relativní účinnosti štěpení připraveného ψ-trypsinu, rafinosou modifikovaného hovězího trypsinu (RafBT, Šebela *et al.*, 2006) a komerčních preparátů byly provedeno srovnáním ploch izotopových píků spektra vybraných peptidů BSA. K tomuto účelu byly připraveny 20 pmol vysušené alikvoty dialyzovaného BSA po redukci DTT a alkylaci IAA. Jako interní standard byl připraven digest 20 pmol BSA s 50 ng RafBT štěpený v 20 mM AMBIC rozpuštěném ve vodě obsahující pouze ^{18}O. Štěpení probíhalo 16 h při 37 °C a bylo ukončeno přídavkem 10% FA. Stejným způsobem byly připraveny digesty BSA se všemi trypsiny v běžném pufru. Celkový objem digestu po okyselení činil 20 µl. Před měřením byl ve shodném molárním poměru, vztaženo k výchozímu obsahu BSA, smísen digest interního standardu s digestem v běžném pufru. Poté bylo na na MALDI terčík nakápnuto 0,5 µl směsi. Takto bylo připraveno vždy 5 směsných vzorků vybraného trypsinu a značeného standardu. Každý vzorek byl nanesen 3× na MALDI terčík MSP AnchorChip 96 (Bruker Daltonics) a každý spot byl 3×změřen při akvizici 400 spekter s rozsahem *m/z* 500-4000. Jako matrice byla použita CHCA 5 $mg \cdot ml^{-1}$ v TA70. Získaná spektra byla zpracována softwarem flexAnalysis 3.4, kdy byla automaticky integrovány plochy jednotlivých píku a zaznamenány hodnoty *m/z* a intenzity. Množství jednotlivých peptidů (mpep) vzhledem k standardu značeného peptidu (mISTD), bylo vypočteno jako poměr plochy neznačeného peptidu (Spep a součtu dekonvulovaných ploch píků obsahující ^{18}O značené formy stejného peptidu.

Množství vybraného peptidu (mpep) bylo vypočteno z množství ^{18}O-značeného standardu (mistd) a poměru plochy monoizotopového píku neznačeného peptidu (Spep) a součtu ploch monoizotopových píků obsahující 1 případně 2 ^{18}O atomy (Havliš *et al.*, 2003). Výpočet byl proveden dle vzorce na obr. 15, kde Spep, Ssingle, Sdouble značí plochy izotopových píků *m/z* peptidu, *m/z* +2 Da Ssingle a pro Sdouble *m/z* + 4 Da. Koeficienty izotopového zastoupení f3 a f5 se vztahují právě k píkům Ssingle a Sdouble,

tedy 3. a 5. monoisotopovému píku daného peptidu a byly vypočteny pomocí nástroje MS-Isotope ze sady Protein Prospector software dostupného na http:// prospector.ucsf.edu.

$$\boldsymbol{m}pep = \frac{\boldsymbol{S}pep}{\boldsymbol{S}double + \boldsymbol{S}single \times (1 - f3) + \boldsymbol{S}pep \times (f3^2 - f5 - f3)} \times \boldsymbol{m}istd$$

Obr. 15 Rovnice výpočtu množství peptidu ***m****pep* na základě znalosti izotopového rozdělení a množství použitého ^{18}O-značeného interního standardu ***m****istd*.

6.1.4. Příprava extraktů proteinů z jader ječmene

Pro stanovení specifičnosti štěpení ψ-trypsinu byly využity komplexní vzorky proteinů extrahovaných z 5 milionů jader ječmene izolovaných průtokovou cytometrií a poskytnutých kolegy z Ústavu experimentální biologie AV Olomouc (Petrovská *et al.*, 2014). Nejprve byla jádra převedena z 15 ml zkumavek oplachem 100 µl vodou s následnou centrifugací do 1,5 ml mikrozkumavek. Dále byl sediment jader promyt 2×100 µl vody. Přidáno bylo 50 µl pufru pro štěpení DNasou1 (20 mM Tris-HCl pH 8,3, 2 mM $MgCl_2$). Opakovaným pipetováním a krátkou sonikací byl sediment rozmělněn. Následně byl vzorek inkubován 5 h při 70 °C a třepání na 900 rpm k rozvolnění příčných vazeb vytvořených formaldehydem před izolací jader. Po inkubaci byl vzorek ponechán ochladit a bylo přidáno 10 µl DNasy1 a vzorek byl promíchán pomalým pipetováním. Vzorek byl ponechán 1 h inkubovat při 37 °C bez míchání. Po 1 h bylo přidáno dalších 10 µl DNasy1 a vzorek promíchám opakovaným nasáváním do pipetovací 200 µl špičky. Následovala inkubace přes noc při 37 °C bez třepání. Poté byly vzorky promíchány vortexováním, ochlazeny na ledové lázni a přes noc precipitovány přídavkem 400 µl vychlazeného acetonu v mrazáku (-20 °C, 16 h). Precipitované vzorky byl centrifugovány při 20 000 g 10 min při 4 °C. Získané sedimentybyly rozpuštěny ve 20 µl 2× konc. Laemmliho vzorkového pufru (2XLSB), proběhla sonikace 15 min a promíchání na vortexu. Pro SDS-PAGE byly vzorky povařeny 5 min při 100 °C, ochlazeny na ledové lázni, centrifugovány a supernatant nanesen na gel.

6.1.5. SDS-PAGE

Extrahované proteiny rozpuštěné v 2XLSB byly rozděleny pomocí SDS-PAGE při použití nádobky Mini-Protean (Bio-Rad). Separace probíhala na připraveném vlastním gelu o rozměrech cca 80×65×1 mm a celkovém obsahu 10 % akrylamidu v dělící části a 4 % v části zaostřovací. Elektroforéza probíhala při konstantním napětí 130 V a byla ukončena při doputování barevného pásu bromfenolové modři z Laemmliho pufru

k dolní hraně skla. Gely byl barveny roztokem Coomassie Briliant Blue R-250 (3 g×litr 10% MeOH a 10% kys. octová (HAc) přes noc. Odbarvení pozadí gelů bylo prováděno přes noc roztokem 5 MeOH a 7% HAc). Následně byly gely promyty destilovanou vodu a skenován obraz (ImageScanner, Amersham Biosciences, Uppsala, Švédsko).

6.1.6. Štěpení proteinů v gelu a odsolení peptidů

Separační dráhy proteinů z jednotlivých vzorků na gelu byly rozděleny na navazující úseky, typicky 10–15 frakcí/vzorek, které byly vyřezány skalpelem a zpracovány. Vyřezané proteinové pásy byly rozkrájeny na přibližně 1 mm^3 kostičky a přeneseny do 0,5 ml mikrozkumavky. Dále bylo přidáno 150 µl vody (čistota pro MS), gelové kousky byly 5 min rehydratovány a centrifugovány na dno a roztok vyměněn za odbarvovací směs ACN a 200 µl 100 mM AMBIC (1:1,v/v). Mikrozkumavky se vzorky byly třepány 15 min při 600 rpm při 25 °C. Roztok byl následně odpipetován. V případě přetrvávajícího zabarvení gelových kousků byl tento krok opakován. Po odbarvení bylo přidáno 200 µl čistého ACN a vzorky třepány při 800 rpm po dobu 20 min. Všechen roztok byl po centrifugaci odstraněn a gelové kousky ponechány doschnout v otevřených mikrozkumavkách. Následně bylo přidán 80 µl 10 mM DTT a vzorky umístěny do míchaného termostatu na 30 min, 56 °C, 600 rpm. Po inkubaci byly vzorky ochlazeny na ledu, centrifugovány a odpipetován zbývající roztok. Následně byly gelové kousky dehydratovány čistým ACN viz. výše. K vysušeným gelovým kouskům bylo přidáno 80 µl 55 mM IAA. Míchání s IAA trvalo 20 minut při 25 °C ve tmě. Následně byl zbylý roztok z mikrozkumavek odpipetován a přidáno 200 µl 100 mM AMBIC pro vymytí zbytku použitých činidel. Po 15 minutách třepání při 600 rpm a 25 °C byl všechen roztok odstraněn a gelové kousky dehydratovány pomocí přidání ACN a vysušeny. Poté byl do každé mikrozkumavky, umístěných na ledu, přidán 2 µM roztok RafBT v 50 mM AMIBIC v objemu mírně překrývajícím gelové kousky na dně mikrozkumavek, vzorky promíchány a jemně centrifugovány. Po 20 minutách inkubace byl zkontrolován obsah zkumavek, případně byl doplněn roztok RafBT tak, aby tímto roztokem nasáklé gelové kousky byly ponořeny. Po dalších 20 min bylo přidáno 30 µl 50 mM AMBIC, vzorky promíchány, centrifugovány a umístěny do termostatu vyhřátého na 37 °C. Inkubace probíhala přes noc (18 h) za stálého míchání 500 rpm. Všechny kroky, kromě centrifugace a inkubace zavřených mikrozkumavek byly prováděny v laminárním boxu se zapnutou vnitřní cirkulací vzduchu. Štěpení bylo ukončeno přídavkem směsi 5% FA s ACN v objemovém poměru 1 k 2, běžně v objemu 50 µl a vzorky byly intenzivně míchány 20

min při 25 °C. Poté byl obsah mikrozkumavek centrifugován na dno, všechen roztok přenesen do čistých mikrozkumavek a odpařen při 45 °C ve vakuové centrifuze.

6.1.7. Odsolení vzorků před nLC MSMS analýzou

Peptidové odparky byly rozpuštěny v 0,1% TFA a odsoleny pomocí C18 ZipTip špiček s 0,6 µl sorbentu (Merck Millipore) podle návodu výrobce. Peptidy eluované ze ZipTip špiček byly odpařeny a poté rozpuštěny v 15 µl 0,1% TFA a použity pro nLC MSMS analýzu. K lepšímu rozpuštění odpařených vzorků byla využita ultrazvuková lázeň, kam byly vzorky na 3 min ponořeny a poté opakovaným nasáváním do 10µl špičky promíchány pipetou.

6.1.8. nLC MALDI TOF-TOF MSMS analýza peptidů

Separace odsolené peptidové směsi byla prováděna automaticky na Dionex UltiMate3000 RSLC systému vybaveném C18 předkolonou (100 µm×20 mm, C18 Acclaim PepMap100 5 µm, Thermo Fisher Scientific) a C18 analytickou kolonou (75 µm×150 mm, C18 Acclaim PepMap100 2 µm, Thermo Fisher Scientific) spojeném s automatickým sběračem frakcí Proteineer fc (Bruker Daltonics). Alikvot vzorku o objemu 5 µl byl nanesen na předkolonu v době 5 min. Pro nanesení vzorku byla použita metoda „microliter-pickup“, kdy bylo před a po nasátí vzorku do nástřikové smyčky (20 µl) nasáto injektorem LC systému 5 µl 0,1 % TFA. Složení mobilních fází: nanášení vzorku na předkolonu – 0,05 % TFA s 2 % ACN; separace, mobilní fáze A (MF A) – 0,05 TFA %, B – 0,05 % TFA v 80 % ACN (MF B). Separace přes analytickou kolonu při průtoku 300 $nl \cdot min^{-1}$ probíhala podle následující gradientu: 0–7 min 4% MF B, 7– 5 min do 60% MF B, 45–48 min do 90 % MF B, 48–59 min při 90% MF B, 59–70 min pokles do 4 % MF B. Mezi jednotlivými analýzami byl za každou separací zařazen 20 min ekvilibrační krok při průtoku 4 % MF A. Sběr peptidových frakcí a jejich automatické nanášení na MALDI terčík AnchorChip 384 (Bruker Daltonics) probíhalo od 20. min separace po 17 s intervalech. Celkem bylo posbíráno vždy 120 navazujících frakcí. Eluát byl před nanesením na terčík automaticky smísen s matricí (cca 40 nl vzorku + 380 nl matrice). Složení použitého roztok matrice pro vzorky: 36 µl nasyceného roztoku CHCA v 0,1% TFA s 90 % ACN, 8 µl 10% TFA, 8 µl 100mM $NH_4H_2PO_4$, 748 µl 0,1 % TFA s 95 % ACN. Pro externí kalibraci byla připravena obdobná směs obsahující 748 µl 0,1 % TFA s 85 % ACN namísto 0,1% TFA s 95 % ACN. Z této matrice byl odebrán alikvot 150 µl a smísen s 1 µl peptidového kalibračního standardu 1 připraveného podle pokynů dodavatele (Bruker Daltonics). Po krátkém promíchání bylo 0,5 µl kalibrační směsi

manuálně nakapáno na kalibrační pozice na destičce. Chromatografická separace peptidů, záznam absorbace při 214 nm a dávkování na MALDI terčík bylo řízeno přes software HyStar 3.2 (Bruker Daltonics). Nasledná analýza připravených terčíků se vzorky a standardy pomocí MALDI-TOF/TOF MSMS přístrojem ultraflextreme, Bruker Daltonics) byla prováděna v automatickém módu s následujícími parametry: měření prekurzorů v rozsahu *m/z* 800 – 4000, akumulovány spektra s 2500 výstřely laseru, minimální intenzita signálů pro fragmentaci větší než 800 při poměru signál/šum větší 7. Frekvence pulsu laseru v MS módu 2000 Hz, v MSMS módu 1000 Hz, při LIFT fragmentaci analyzovány pouze fragmenty vybraných prekurzorů při 4000 laserových pulsech, neměřeny znovu MS spektra. Přístroj byl ovládán pomocí softwaru flexControl 3.4 a WarpLC 1.3 (Bruker Daltonics). Data byla prohledána nástrojem ProteinScape 3.1 (Bruker Daltonics) s algoritmem Mascot proti vybrané databázi a volitelných parametrech měření a vyhodnocení. MALDI MSMS spektra byla alternativně prostřednictvím tohoto nástroje exportována do souboru s formátem mgf („mascot generic format“) souboru a prohledána softwarem PEAKS Studio 8 (Bioinformatics Solutions, Waterloo, Kanada).

6.1.9. nLC ESI qTOF MSMS analýza peptidů

Analýza odsolených peptidových směsí pomocí nLC ESI q-TOF systému byla provedena za podmínek a nastavení detailně popsaném v Petrovská *et al., 2014*, kdy však také byla použita metoda nanášení vzorku na kolonu pomocí techniky „microlitre-pickup“ a pro měření bylo využito vždy 5 µl vzorku. Analýzy provedl Mgr. René Lenobel, Ph.D. Poskytnutá data ve formátu mgf byla zpracována pomocí zmíněných nástrojů.

6.2. Extrakce proteinů z trávící šťávy *D. capensis*

Trávící tekutina rosnatky kapské byla sbírána kolegy po indukci její sekrece aplikací 20 µl 2 mM JA na povrch pastí. Po 24 h byly vždy odstřihnuty 3 pasti každé rostliny, z celkem 5 rostlin, a postupně ponořeny do 4 ml 50 mM acetátu sodného na 3 min. Získaný vzorek byl tedy směsí exudátu z 15 pastí (Krausko *et al.,* 2017). Pro extrakci proteinů byly použity alikvoty 100 µl odebraného vzorku, které byly koncentrovány odpařením téměř dosucha ve vakuové centrifuze při 45 °C. Vzniklý lepkavý pelet byl rozsuspendován v 2XLSB.

6.3. Zpracování vína a extrakce proteinů

Elektroforéza SDS-PAGE, zpracování gelů a nLC MALDI-TOF/TOF MSMS analýza probíhaly podle postupů popsaných v kapitole o pseudotrypsinu.

6.3.1. Koncentrování proteinů vína zahuštěním na RVO

Alikvot 200 ml vychlazeného (4 °C) vína A se zákalem byl zfiltrován přes celulosový filtr Whatman Grade 4. Filtrát byl poté zkoncentrován na objem 10 ml pomocí vakuové rotační odparky při 45 °C. Získaný koncentrát byl zfiltrován a precipitován vychlazeným acetonem (-20 °C). Po 60 h inkubace byl vzorek centifugován při 12 500 *g*, 4 °C, po dobu 20 min. Získaný pelet byl rozbit a rozmíchán v čerstvém acetonu a znovu precipitován. Sediment byl ponechán vyschnout a poté byl zmrazen při -20 °C. K odváženému alikvotu sedimentu (0,1 mg) bylo přidáno 200 µl 2XLSB obsahujícího 2-merkaptoethanol a vzorek byl intenzivně promíchán na vortexu dokud nedošlo k rozpuštění úplnému rozpuštění. Poté byl vzorek 5 min zahřát při 100 °C v termobloku. Po ochlazení a jemné centrifugaci byly připraveny 20 µl alikvoty pro SDS PAGE.

6.3.2. Koncentrování proteinů vína ultrafiltrací

Filtrát 100 ml vzorku vín byl dialyzován proti 3 l pufru (100 mM octan amonný, pH 5,0) po dobu 48 h při 4 °C. Dialyzační pufr byl vyměněn každých 16 h. Ultrafiltrací přes 10 kDa „cut-off“ filtr byl dialyzát následně zahuštěn na 2 ml, rozdělen na 0,5 ml alikvoty a zmrazen (-20 °C). Před extrakcí proteinů do 20 µl 2XLB byl alikvot 0,5 ml odpařen při 60 °C ve vakuové centrifuze. Suchý odparek byl rozpuštěn ve 20 µl 2XLB, zahříván 5 min při 100 °C a poté použit pro SDS-PAGE.

6.3.3. Stanovení pH vína

Kyselost vína byla stanovena pomocí pH metru přímo z alikvotu vzorku vína po kalibraci přístroje pomocí standardních pufrů o pH 4 a 7.

6.3.4. Stanovení stability vína a měření zákalu

Míra zákalu vína byla změřena jako absorbance při 540 nm podle Marangon *et al.,* 2011. Náchylnost vína k tvorbě zákalu byla stanovena pomocí teplotního testu stability. V tomto testu je víno nejprve zahříváno na 50 °C po dobu 3 h a následně je ochlazeno na 4 °C a ponecháno v chladu 2 h. Po ukončení inkubace v chladu a dosažení okolní teploty 25 °C je změřena míra zákalu vína. Pokud je rozdíl hodnot míry zákalu naměřený před a po testu menší 0,02 je víno teplotně stabilní (Marangon *et al.* 2011).

6.3.5. Izolace proteinů vína pomocí gelové permeační chromatografie

Koncentrovaný vzorek vína G byl použit jako zdroj proteinových frakcí, které byly získány jeho rozdělením gelovou permeační chromatografií na koloně ENrich SEC 70 (10×300 mm, Bio-Rad) na chromatografu BioLogic Duo-Flow (Bio-Rad). Pro separaci byly využity alikvoty 500 µl ultrafiltrátu vína G. Mobilní fází byl 50 mM acetát amonný. Separace probíhala při průtoku 1 $ml \cdot min^{-1}$ s celkovou dobou běhu 35 min. Pro kalibraci byl použit standard směsi proteinů Gel Filtration Standard #1511901 (Bio-Rad). Získané frakce proteinů odpovídající píkům separace byly manuálně sbírány a zahuštěny ultrafiltrací, viz výše.

6.3.6. Štěpení proteinů z vína v roztoku

Pro ověření proteinového zastoupení ve frakcích z gelové chromatografie bylo provedeno štěpení v roztoku a identifikace přítomných proteinů. Alikvoty izolovaných frakcí z vína G obsahující 50 µg proteinů byly odpařeny ve vakuové centrifuze a následně rozpuštěny 50 µl 25 mM AMBIC. Pro denaturaci bylo přidáno 15 µl 8M močoviny ve stejném pufru a vzorky intenzivně promíchány na vortexu a následně 1 h míchány na třepačce, 800 rpm, při 25 °C. Pro redukci byly přidány 4 µl 55 mM DTT a vzorky inkubovány 30 min při 56 °C na třepačce. Následovala alkylace přidáním 4 µl 330 mM IAA a inkubace 30 min při 25 °C ve tmě na třepačce. Nakonec bylo přidáno 8 µl 55mM DTT a proběhlo doplnění vzorků na objem 200 µl přidáním 25mM AMBIC. Pro štěpení proteinů přes noc při hmotnostním poměru trypsin:proteiny 1:20 byl využit RafBT.

6.3.7. Zpracování dat z MS analýz vína

Získaná data z proteomických analýz vína nahraná do ProteinScape byla prohledána na Mascot serveru 2.4 (Matrix Science) proti vlastní databázi proteinů z *V. vinifera, B. cinerea a S. cerevisiae* obsahující celkem 309 859 proteinových sekvencí z NCBInr databáze a set běžných kontaminantů proteomických experimentů cRAP (ftp://ftp.thegpm.org/fasta/cRAP). Tolerance pro prohledávání spekter byla následující, v případě nLC MALDI MSMS dat byl limit přesnosti měření hmoty prekurzoru 25 ppm, v případě měření iontovou pastí byla tato hodnota 100 ppm. Pro fragmenty bylo povolena tolerance 0,5 Da. Jako štěpící enzym byl zvolen semitrypsin (částečně specifický trypsin) a povoleny 2 vynechaná místa štěpení. Karbamidomethylace Cys byla nastavena jako fixní modifikace a oxidace Met jako variabilní modifikace.

Aminokyselinové sekvence proteinů identifikovaných ve vínech byly analyzovány nástroji SignalP 4.1, NCBI Blast, případně EBI InterProScan. SignalP umožnil určit, zda

protein obsahuje signální sekvenci pro sekreci mimo buňku (Petersen *et al.*, 2011). NCBI Blast a EBI InterProScan umožňují na základě podobnosti dohledat možnou funkci u neznámých proteinů (Johnson *et al.*, 2008; Jones *et al.*, 2014).

6.3.8. nLC ESI-ion trap MSMS analýza peptidů

Alternativou k analýze peptidů pomocí nLC MALDI systému bylo využití iontové pasti Amazon Speed ETD (Bruker Daltonics) s iontovým zdrojem CaptiveSpray (Bruker Daltonics) v online spojení s nLC systémem Dionex UltiMate3000 RSLC. Chromatograf byl vybaven stejným typem kolon jako systém pro přípravu vzorků k MALDI měření. Složení mobilních fází: nanášení vzorku 2% FA; separace MF A – 0,4% FA, MF B – 90% ACN v 0,4% FA. Průběh gradientu kopíroval nastavení systému pro nLC MALDI. Data byla sbírána od 7 minuty analýzy. Rychlost skenování byla 8,100 $u \cdot Sec^{-1}$ v „enhanced resolution“ módu. K fragmentaci prekurzorů bylo použito He. Systém byl ovládán přes Hystar 3.2 a trapControl 7.2 (Bruker Daltonics). Získaná data byla zpracována a exportována do mgf formátu v DataAnalysis 4.2 (Bruker Daltonics).

7. ZÁVĚR

Pseudotrypsin z důvodu větší nespecifičnosti a nižší afinity k bazickým AK produkuje tryptické a často i chymotryptickou aktivitu připomínající peptidy. Po 12 hodinovém štěpení je ve srovnání s hovězím trypsinem účinnost štěpení ψ-trypsinu srovnatelná. Štěpení ψ-trypsinem poskytuje také dostatek tryptických a významný podíl unikátních peptidů pro nLC-MSMS analýzy. Přítomnost unikátních peptidů vzniklých díky menší závislosti štěpení pseudotrypsinu na dostupnosti Arg a Lys původních proteinů umožňuje lepší pokrytí proteinových sekvencí a identifikaci odlišných proteinů. Nízký výtěžek zvolené metody pro izolaci ψ-trypsinu je hlavní překážkou pro jeho další aplikaci. Znalost chování této proteoformy trypsinu k jejímuž vzniku dochází autolýzou hovězího trypsinu při delším štěpení proteinů také částečně vysvětluje přítomnost unikátních nespecifických peptidů v proteomických experimentech.

Proteomická analýza extraktů izolovaných mitotických chromozomů ječmene a následné vyhodnocení pomocí kombinace bioinformatických nástrojů a dostupných informací z databází umožnila nalézt přes 800 proteinů souvisejících právě s rostlinnými chromozomy. V této vyčleněné skupině proteinů byly identifikováni zástupci bežných chromozomálních proteinů jako jsou histony, ale i proteiny související s procesy úprav, oprav, replikace nebo transkripce DNA. Studie publikovaná na základě získaných výsledků je první prací popisující proteom rostlinných chromozomů.

Analýza proteomu trávící tekutiny rosnatky kapské prokázala přítomnost hydrolytických a dalších enzymů použitelných pro rozklad ulovené kořisti. Inicializace trávení vyvolané u rostliny uměle pomocí kys. jasmonové umožnila identifikaci více než 40 proteinů. Identifikované proteiny kopírují svým zastoupením komponenty používané běžnými rostlinami pro jejich obranu, zejména PR-proteiny. K identifikaci přítomných proteinů pouze na základě jejich podobnosti se známými zástupci z rostlinné říše prokazatelně přispělo využití alternativního štěpení pomocí chymotrypsinu poskytující rozmanitější peptidové zastoupení. Identifikované hydrolasy s netradičními strukturami odolávající nízkému pH, které byly predikovány skupinou Butts *et al.,* 2016a a potvrzené experimenty v této práci zahrnutými do publikace Krausko *et al.,* 2017, se pro jejich evoluční původ a možnou praktickou aplikaci jeví jako atraktivní cíle dalšího výzkumu.

Srovnání hlavních komponent proteomu komerčních bílých vín a experimentálního vína se zákalem odhalilo společný znak většiny přítomných proteinů, a to vyšší obsah prolinu v jejich strukturách. Pro takovéto proteiny se dala předpokládat snazší interakce s polyfenoly vína a možná iniciace vzniku zákalu. Vybrané proteiny bohaté na Pro a původem z hrozna jejichž přítomnost byla prokázana ve všech vzorcích vín byly následně izolovány a otestován jejich vliv na stabilitu vína. Test teplotní stability u invertasy, frakce TLP ani cysteinové proteasy neprokázal jejich zásadní příspěvek k nestabilitě vína vedoucí ke vzniku viditelného zákalu. Proteiny a enzymy nalezené v zakaleném experimentálním vínu připraveném z hroznů z části napadených šedou plísní (*B. cinerea*) ukazují jako hlavního viníka zákalu právě tuto patogenní houbu a její nekontrolovaný růst. Na stejného původce zákalu ukazují i charakteristiky tohoto vína, historie jeho původu a výsledky srovnání proteinového zastoupení s ostatními víny. Použitá metodika izolace proteinů z dialyzovaného vína pouze pomocí ultrafiltrace umožnila pomocí SDS-PAGE zachytit a následně hmotnostní spektrometrií identifikovat v jiných studiích přehlížené nebo ztracené velké proteiny a glykoproteiny. Mezi těmito proteiny byla nalezena rostlinná cysteinová proteasa identifikována ve stejné oblasti gelu ve všech analyzovaných vzorcích vín i hroznové šťávy. Tento enzym proto lze zařadit mezi hlavní proteinové složky vína k invertase, chitinasam a TLP. V navazujících pracech byla tato odolná hydrolasa izolována přímo z vína a kvasného octa a charakterizována (Perutka a Šebela, 2020; Rakotonaina, 2020). V obou případech byl získaný enzym stále hydrolyticky aktivní a funkční v kyselém prostředí o pH 3,0 odpovídající pH vína.

SEZNAM ZKRATEK

MALDI	technika ionizace/desorbce laserem prostřednictvím matrice
MS	hmotnostní spektrometrie („mass spectrometry“)
ESI	technika ionizace elektrosprejem
LC	kapalinová chromatografie („liquid chromatography“)
TD metody	„top-down“ metody
FAB	ionizace pomocí rychlého bombardování atomy („fast atom bombardment“)
HCCA (CHCA)	kyselina α-kyano-4-hydroxyskořicová
SA	kyselina sinapová
DHB	2,5-dihydroxybenzoová kyselina
HPA	kyselina 3-hydroxypikolinová
THAP	2,4,6-trihydroxyacetofenon
DAN	1,5-diaminonaftalen
DiFCCA	kyselina 2,4-difluoro-α-kyanoskořicová
PMF	metoda identifikace proteinů pomocí peptidového mapování („peptide mass fingerprinting)
ISD	in source decay
PSD	post source decay
MALDI MSI	zobrazování hmotnostní spektrometrií pomocí MALDI („mass spectrometry imaging“)
TOF	analyzátor doby letu („time of flight“)
SNP	„single nucleotide polymorphisms“
TLCK	N-*p*-tosyl-L-lysin-chlorometyl keton
TPCK	N-*p*-tosyl-L-fenylalanin chlorometyl keton
rRNA	ribozomální RNA
CT	Cajalovo tělíško
SR proteiny	proteiny jádra bohaté na serin a arginin

JP	jaderné póry
NUP	nukleoporiny
ABA	kyselina abscisová
JA	kyselina jasmonová
AMBIC	hydrogenuhličitan amonný
FA	kyselina mravenčí
BCA	kyselina bicinchoninová
BSA	hovězí serový albumin
RafBT	rafinosou modifikovaný hovězí trypsin
DTT	dithiotreitol
IAA	2-jodacetamid
2XLSB	Laemmliho pufr pro vzorky pro elektroforézu, 2× koncentrovaný
HAc	kyselina octová
MF	mobilní fáze
MeOH	metanol
TFA	kyselina trifluoroctová
mgf	datový formát mascot („*mascot generic format"*)
ESI-q-TOF MS	hmotnostní spektrometr vybavený ionizací elektrosprejem, kvadrupólovým analyzátorem a analyzátorem doby letu („*Electrospray ionization quadrupole time-of-flight mass spectrometer"*)
MR	masožravé rostliny
PR proteiny	„*pathogenesis related*" proteiny
OPDA	kyselina oxylipin-12-oxofytodienová
PAL	fenylalaninamoniaklyasa
LTP	proteiny přenášející lipidy („*lipid transfer proteins*")
TLP	proteiny podobné thaumatinu („*thaumatin like proteins*")

SEZNAM LITERATURY

Abramova, N., Sertil, O., Mehta, S., Lowry, C.V., 2001. Reciprocal regulation of anaerobic and aerobic cell wall mannoprotein gene expression in Saccharomyces cerevisiae. *J. Bacteriol.* **183**, 2881-2887.

Aebersold, R.H., Leavitt, J., Saavedra, R.A., Hood, L.E., Kent, S.B., 1987. Internal amino acid sequence analysis of proteins separated by one-or two-dimensional gel electrophoresis after in situ protease digestion on nitrocellulose. *Proc. Natl. Acad. Sci. U.S.A.* **84**, 6970-6974.

Adamec L., 2010. Dark respiration of leaves and traps of terrestrial carnivorous plants: are there greater energetic costs in traps? *Cent. Eur. J. Biol.* **5**, 121–124.

Adamec, L., (1997). Mineral nutrition of carnivorous plants: a review. *Bot. Rev.* **63**, 273–299.

Adamec, L., (2002). Leaf absorption of mineral nutrients in carnivorous plants stimulates root nutrient uptake. *New Phytol.* **155**, 89e100.

Adamec, L., 2013. A comparison of photosynthetic and respiration rates in six aquatic carnivorous Utricularia species differing in morphology. *Aquat. Bot.* **111**, 89-94.

Adlassnig, W., Peroutka, M., Eder, G., Pois, W., Lichtscheidl, I.K., 2005. Ecophysiological observations on Drosophyllum lusitanicum. *Ecol. Res.* **21**, 255–262.

Aebersold, R., Goodlett, D.R., 2001. Mass spectrometry in proteomics. *Chem. Rev.* **101**, 269-296.

Aebersold, R., Mann, M., 2003. Mass spectrometry-based proteomics. *Nature* **422**, 198-207.

Albrethsen, J., 2007. Reproducibility in protein profiling by MALDI-TOF mass spectrometry. *Clin. Chem.* **53**, 852-858.

Alcalde-Eon, C., Garcia-Estevez, I., Puente, V., Rivas-Gonzalo, J.C., Escribano-Bailón, M.T., 2014. Color stabilization of red wines. A chemical and colloidal approach. *J. Agric. Food Chem.* **62**, 6984-6994.

Ali, G.S., Golovkin, M., Reddy, A.S.N., 2003. Nuclear localization andin vivodynamics of a plant-specific serine/arginine-rich protein. *Plant J.* **36**, 883–893.

Altschul, S.F., Wootton, J.C., Gertz, E.M., Agarwala, R., Morgulis, A., Schäffer, A.A., Yu, Y-K., 2005. Protein database searches using compositionally adjusted substitution matrices. *FEBS J.* **272**, 5101–5109.

An, C.-I., Fukusaki, E., Kobayashi, A., 2002. Aspartic proteinases are expressed in pitchers of the carnivorous plant Nepenthes alata Blanco. *Planta* **214**, 661–667.

Aravind, L., Koonin, E.V., (2000). SAP – a putative DNA-binding motif involved in chromosomal organization. *Trends Biochem. Sci.* **25**, 112–114.

Arndt, W., Mitnik, C., Denzler, K.L., White, S., Waters, R., Jacobs, B.L., Rochon, Y., Olson, V.A., Damon, K.I., Langland, J.O., 2012. In Vitro Characterization of a Nineteenth-Century Therapy for Smallpox. *PLoS ONE* **7**, e32610.

Ashton, D.S., Ashcroft, A.E., Beddell, C.R., Cooper, D.J., Green, B.N., Oliver, R.W.A., 1994. On the Analysis of Bovine Trypsin by Electrospray Mass-Spectrometry. *Biochem. Biophys. Res. Commun.* **199**, 694-698.

Athauda, S.B., Matsumoto, K., Rajapakshe, S., Kuribayashi, M., Kojima, M., Kobomura-Yoshida, N., Iwamatsu, A., Shibata, Ch., Inoue, H., Takahashi, K., 2004. Enzymic and structural characterization of nepenthesin, a unique member of a novel sub-family of aspartic proteinases. *Biochem.* **381**, 295–306.

Baker, T.C., Han, J., Borchers, C.H., 2017. Recent advancements in matrix-assisted laser desorption/ionization mass spectrometry imaging. *Curr. Opin. Biotechnol.* **43**, 62-69.

Bannister, A.J., Kouzarides, T., 2011. Regulation of chromatin by histone modifications. *Cell Res.* **21**, 381–395.

Barber, M., Bordoli, R.S., Sedgwick, R.D., Tyler, A.N., 1981. Fast atom bombardment of solids (FAB): A new ion source for mass spectrometry. *J. Chem. Soc., Chem. commun.* **7**, 325-327.

Batista, L., Monteiro, S., Loureiro, V.B., Teixeira, A.R., Ferreira, R.B., 2009. The complexity of protein haze formation in wines. *Food Chem.* **112**, 169-177.

Bauer, F., Pretorius, I.S., 2000. Yeast stress response and fermentation efficiency: how to survive the making of wine. *S. Afr. J. Enol. Vitic*, **21**, 27-51.

Beltran, G., Esteve-Zarzoso, B., Rozès, N., Mas, A., Guillamón, J.M., 2005. Influence of the timing of nitrogen additions during synthetic grape must fermentations on fermentation kinetics and nitrogen consumption. *J. Agric. Food Chem.* **53**, 996-1002.

Benucci, I., Esti, M., Liburdi, K., 2014. Effect of free and immobilised stem bromelain on protein haze in white wine. *Aust. J. Grape Wine Res.* **20**, 347-352.

Benucci, I., Lombardelli, C., Cacciotti, I., Esti, M., 2020. Papain covalently immobilized on chitosan–clay nanocomposite films: application in synthetic and real white wine. *Nanomaterials* **10**, 1622.

Benucci, I., Lombardelli, C., Liburdi, K., Acciaro, G., Zappino, M., Esti, M., 2016. Immobilised native plant cysteine proteases: packed-bed reactor for white wine protein stabilisation. *J. Food Sci. Technol.* **53**, 1130-1139.

Berger, S.L., 2007. The complex language of chromatin regulation during transcription. *Nature* **447**, 407-412.

Beynon, R.J., 2005. The dynamics of the proteome: strategies for measuring protein turnover on a proteome-wide scale. *Brief Funct Genomics* **3**, 382-390.

Biemann, K., Gapp, G., Seibl, J., 1959. Application of mass spectrometry to structure problems. I. Amino acid sequence in peptides. *J. Am. Chem. Soc.* **81**, 2274-2275.

Blavet, N., Uřinovská, J., Jeřábková, H., Chamrád, I., Vrána, J., Lenobel, R., Beinhauer, J., Šebela, M., Doležel, J., Petrovská, B., 2016. UNcleProt (Universal Nuclear Protein database of barley): The first nuclear protein database that distinguishes proteins from different phases of the cell cycle. *Nucleus* **8**, 70–80.

Bolaños-Villegas, P., 2021. The Role of Structural Maintenance of Chromosomes Complexes in Meiosis and Genome Maintenance: Translating Biomedical and Model Plant Research Into Crop Breeding Opportunities. *Front. Plant Sci.* **12**, 563.

Bode, W., Schwager, P., 1975. The single calcium-binding site of crystalline bovine β-trypsin. *FEBS Lett.* **56**, 139-143.

Bodnar, W.M., Blackburn, R.K., Krise, J.M., Moseley, M.A., 2003. Exploiting the complementary nature of LC/MALDI/MS/MS and LC/ESI/MS/MS for increased proteome coverage. *J. Am. Soc. Mass Spectrom.* **14**, 971-979.

Boeglin, M., Fuglsang, A.T., Luu, D.-T., Sentenac, H., Gaillard, I., Chérel, I., 2016. Reduced expression of AtNUP62 nucleoporin gene affects auxin response in Arabidopsis. *BMC Plant Biol.* **16**, 2.

Böhm, J., Scherzer, S., Krol, E., Kreuzer, I., von Meyer, K., Lorey, Ch., Mueller, D.T., Shabala, L., Monte, I., Solano, R., Al-Rasheid, K.A.S., Rennenberg, H., Shabala, S., Neher, E., Hendrich, R., 2016. The Venus flytrap Dionaea muscipula counts prey-induced action potentials to induce sodium uptake. *Curr. Biol.* **26**, 286–295.

Bourgaud, F., Gravot, A., Milesi, S., Gontier, E., 2001. Production of plant secondary metabolites: a historical perspective. *Plant Sci.* **161**, 839–851.

Braud, C., Zheng, W., Xiao, W., 2012. LONO1 encoding a nucleoporin is required for embryogenesis and seed viability in Arabidopsis. *Plant Physiol.* **160**, 823-836.

Brameier, M., Krings, A., MacCallum, R.M., 2007. NucPred—predicting nuclear localization of proteins. *Bioinformatics* **23**, 1159–1160.

Brown, S.L., Stockdale, V.J., Pettolino, F., Pocock, K.F., de Barros Lopes, M., Williams, P.J., Bacic, A., Fincher, G.B., Hoj, P.B., Waters, E.J., 2007. Reducing haziness in white wine by overexpression of Saccharomyces cerevisiae genes YOL155c and YDR055w. *Appl. Microbiol. Biotechnol.* **73**, 1363-1376.

Bruins, A.P., 1998. Mechanistic aspects of electrospray ionization. *J. Chromatogr. A* **794**, 345-357.

Buch, F., Kaman, W.E., Bikker, F.J., Yilamujiang, A., Mithöfer, A., 2015. Nepenthesin Protease Activity Indicates Digestive Fluid Dynamics in Carnivorous Nepenthes Plants. *PLoS One* **10**, e0118853.

Butts, C.T., Bierma, J.C., Martin, R.W., 2016a. Novel proteases from the genome of the carnivorous plant Drosera capensis: Structural prediction and comparative analysis. *Proteins* **84**, 1517–1533.

Butts, C.T., Zhang, X., Kelly, J.E., Roskamp, K.W., Unhelkar, M.H., Freites, J.A., Tahir, S., Martin, R.W., 2016b. Sequence comparison, molecular modeling, and network analysis predict structural diversity in cysteine proteases from the Cape sundew, Drosera capensis. *Comput. Struct. Biotechnol. J.* **14**, 271–282.

Cabaroglu, T., Selli, S., Canbas, A., Lepoutre, J.P., Günata, Z., 2003. Wine flavor enhancement through the use of exogenous fungal glycosidases. *Enzyme Microb. Technol.* **33**, 581-587.

Cantoral, J.M. Collado, I.G., 2011. Filamentous Fungi (Botrytis cinerea). In *Molecular Wine Microbiology*; Santiago, A.V.C., Munoz, R., Garcia, R.G., eds., Chapter 10, (pp 257−277), Academic Press, London, U.K.

Cao, J., Han, X., Zhang, T., Yang, Y., Huang, J., Hu, X., 2014. Genome-wide and molecular evolution analysis of the subtilase gene family in Vitis vinifera. *BMC genomics* **15**, 1-15.

Caprioli, R.M., Farmer, T.B., Gile, J., 1997. Molecular imaging of biological samples: localization of peptides and proteins using MALDI-TOF MS. *Anal. Chem.* **69**, 4751-4760.

Castillo-Sánchez, J.X., García-Falcón, M.S., Garrido, J., Martínez-Carballo, E., Martins-Dias, L.R., Mejuto, X.C., 2008. Phenolic compounds and colour stability of Vinhao wines: Influence of wine-making protocol and fining agents. *Food Chem.* **106**, 18-26.

Cilindre, C., Castro, A.J., Clément, C., Jeandet, P., Marchal, R., 2007. Influence of Botrytis cinerea infection on Champagne wine proteins (characterized by two-dimensional electrophoresis/immunodetection) and wine foaming properties. *Food Chem.* **103**, 139-149.

Cilindre, C., Jégou, S., Hovasse, A., Schaeffer, C., Castro, A.J., Clément, C., Van Dorsselaer A., Jeandet, P., Marchal, R., 2008. Proteomic approach to identify champagne wine proteins as modified by Botrytis cinerea infection. *J. Proteome Res.* **7**, 1199-1208.

Ciska, M., Moreno Díaz de la Espina, S., 2014. The intriguing plant nuclear lamina. *Front. Plant Sci.* **5**, 166.

Claus, H., Sabel, A., König, H., 2014. Wine phenols and laccase: An ambivalent relationship. Ed. Rayess El. Y., In *Wine: Phenolic composition, classification and health benefits*, (pp. 155-185). Nova Publishers

Claydon, M.A., Davey, S.N., Edwards-Jones, V., Gordon, D.B., 1996. The rapid identification of intact microorganisms using mass spectrometry. *Nat. Biotechnol.* **14**, 1584-1586.

Cohen-Kupiec, R., Chet, I., 1998. The molecular biology of chitin digestion. *Curr. Opin. Biotechnol.* **9**, 270-277.

Collier, S., Pendle, A., Boudonck, K., van Rij, T., Dolan, L., Shaw, P., 2006. A Distant Coilin Homologue Is Required for the Formation of Cajal Bodies in Arabidopsis. *Mol. Biol. Cell* **17**, 2942–2951.

Cornett, D.S., Frappier, S.L., Caprioli, R.M., 2008. MALDI-FTICR imaging mass spectrometry of drugs and metabolites in tissue. *Anal. Chem.* **80**, 5648-5653.

Cosme, F., Capão, I., Filipe-Ribeiro, L., Bennett, R.N., Mendes-Faia, A., 2012. Evaluating potential alternatives to potassium caseinate for white wine fining: Effects on physicochemical and sensory characteristics. *LWT* **46**, 382-387.

Cosme, F., Fernandes, C., Ribeiro, T., Filipe-Ribeiro, L., Nunes, F.M., 2020. White wine protein instability: Mechanism, quality control and technological alternatives for wine stabilisation—an overview. *Beverages* **6**, 19.

Cragg, G.M., Newman, D.J., 2013. Natural products: A continuing source of novel drug leads. *Biochim. Biophys. Acta - Gen. Subj.* **1830**, 3670–3695.

Cristobal, A., Marino, F., Post, H., van den Toorn, H.W., Mohammed, S., Heck, A.J., 2017. Toward an optimized workflow for middle-down proteomics. *Anal. Chem.* **89**, 3318-3325.

D'Amato, A., Kravchuk, A. V., Bachi, A., Righetti, P.G., 2010. Noah's nectar: the proteome content of a glass of red wine. *J Proteomics*, **73**, 2370-2377.

Dadáková, K., Havelkova, M., Kurková, B., Tlolková, I., Kasparovsky, T., Zdráhal, Z., Lochman, J., 2015. Proteome and transcript analysis of Vitis vinifera cell cultures subjected to Botrytis cinerea infection. *J proteomics* **119**, 143-153.

Dambrouck, T., Marchal, R., Marchal-Delahaut, L., Parmentier, M., Maujean, A., Jeandet, P., 2003. Immunodetection of proteins from grapes and yeast in a white wine. *J. Agric. Food Chem.* **51**, 2727-2732.

Dau, T., Bartolomucci, G., Rappsilber, J., 2020. Proteomics using protease alternatives to trypsin benefits from sequential digestion with trypsin. *Anal. Chem.* **92**, 9523-9527.

Dempster, A.J., 1925. The Passage of Slow Canal Rays through Hydrogen. *Proc. Natl. Acad. Sci. U. S. A.* **11**, 552.

Di Girolamo, F., D'Amato, A., Righetti, P.G., 2011. Horam nonam exclamavit: sitio. The trace proteome of your daily vinegar. *J Proteomics* **75**, 718-724.

Dick, C.F., Dos-Santos, A.L.A., Meyer-Fernandes, J.R., 2011. Inorganic Phosphate as an Important Regulator of Phosphatases. *Enzyme Res.* **2011**, 1–7.

Doležel, J., Vrána, J., Šafář, J., Bartoš, J., Kubaláková, M., Šimková, H., 2012. Chromosomes in the flow to simplify genome analysis. *Funct. Integr. Genomics* **12**, 397-416.

Doležel, J., Vrána, J., Cápal, P., Kubaláková, M., Burešová, V., Šimková, H., 2014. Advances in plant chromosome genomics. *Biotechnol. Adv.* **32**, 122-136.

Dordoni, R., Colangelo, D., Giribaldi, M., Giuffrida, M.G., De Faveri, D.M., Lambri, M., 2015. Effect of bentonite characteristics on wine proteins, polyphenols, and metals under conditions of different pH. *Am. J. Enol. Vitic.* **66**, 518-530.

Douthwaite, S., Kirpekar, F., 2007. Identifying modifications in RNA by MALDI mass spectrometry. *Meth. Enzym.* **425**, 1-20.

Dreisewerd, K., 2014. Recent methodological advances in MALDI mass spectrometry. *Anal. Bioanal. Chem.* **406**, 2261-227.

Dueñas, M.E., Essner, J.J., Lee, Y.J., 2017. 3D MALDI mass spectrometry imaging of a single cell: spatial mapping of lipids in the embryonic development of zebrafish. *Sci. Rep.* **7**, 1-10.

Dumitriu, G.D., de Lerma, N.L., Luchian, C.E., Cotea, V.V., Peinado, R.A., 2018. Study of the potential use of mesoporous nanomaterials as fining agent to prevent protein haze in white wines and its impact in major volatile aroma compounds and polyols. *Food Chem.* **240**, 751-758.

Duong, V.T., Unhelkar, M.H., Kelly, J.E., Kim, S.H., Butts, C.T., Martin, R.W., 2018. Protein structure networks provide insight into active site flexibility in esterase/lipases from the carnivorous plant Drosera capensis. *Integr Biol (Camb).* **10**, 768-779.

Dupin, I.V., McKinnon, B.M., Ryan, C., Boulay, M., Markides, A.J., Jones, G.P., Williams, J. P., Waters, E.J., 2000. Saccharomyces cerevisiae mannoproteins that protect wine from protein haze: their release during fermentation and lees contact and a proposal for their mechanism of action. *J. Agric. Food Chem.* **48**, 3098-3105.

Durechova, D., Jopcik, M., Rajninec, M., Moravcikova, J., Libantova, J., 2019. Expression of Drosera rotundifolia Chitinase in Transgenic Tobacco Plants Enhanced Their Antifungal Potential. *Mol. Biotechnol.* **61**, 916-928.

Dyčka, F., Franc, V., Frycak, P., Raus, M., Rehulka, P., Lenobel, R., Allmaier, G., Marchetti-Deschmann, M., Šebela, M., 2015. Evaluation of Pseudotrypsin Cleavage Specificity Towards Proteins by MALDI-TOF Mass Spectrometry. *Protein Pept. Lett.* **22**, 1123-1132.

Eberharter, A., Becker, P.B., 2002. Histone acetylation: a switch between repressive and permissive chromatin. *EMBO Rep.* **3**, 224-229.

Edqvist, J., Blomqvist, K., Nieuwland, J., Salminen, T.A., 2018. Plant lipid transfer proteins: are we finally closing in on the roles of these enigmatic proteins? *J. Lipid Res.* **59**, 1374-1382.

Eilenberg, H., Pnini-Cohen, S., Schuster, S., Movtchan, A., Zilberstein, A., 2006. Isolation and characterization of chitinase genes from pitchers of the carnivorous plant Nepenthes khasiana. *J. Exp. Bot.* **57**, 2775–2784

Ellison, A., Adamec, L., 2017. Introduction: what is a carnivorous plant? In *Carnivorous Plants: Physiology, ecology, and evolution*, (pp. 4-6), Oxford University Press.

Escalante-Pérez, M., Krol, E., Stange, A., Geiger, D., Al-Rasheid, K.A., Hause, B., Neher., E., Hedrich, R., 2011. A special pair of phytohormones controls excitability, slow closure, and external stomach formation in the Venus flytrap. *Proc. Natl. Acad. Sci. U.S.A.* **108**, 15492-15497.

Esteruelas, M., Poinsaut, P., Sieczkowski, N., Manteau, S., Fort, M.F., Canals, J.M., Zamora, F., 2009. Characterization of natural haze protein in sauvignon white wine. *Food Chem.* **113**, 28-35.

Esteruelas, M., Kontoudakis, N., Gil, M., Fort, M.F., Canals, J.M., Zamora, F., 2011. Phenolic compounds present in natural haze protein of Sauvignon white wine. *Food Res. Int.* **44**, 77-83.

Expósito, J.M., Gordillo, C.M., Mariño, J.M., Iglesias, J.M., 1991. Purification and characterization of a cysteine protease in Vitis vinifera L. grapes (Macabeo variety). *Food/Nahrung* **35**, 139-142.

Falconer, R.J., Marangon, M., van Sluyter, S.C., Neilson, K., A., Chan, C., Waters, E.J., 2010. Thermal stability of thaumatin-like protein, chitinase, and invertase isolated from Sauvignon blanc and Semillon juice and their role in haze formation in wine. *J. Agric. Food Chem.* **58**, 975-980.

Fasbender, L., Maurer, D., Kreuzwieser, J., Kreuzer, I., Schulze, W.X., Kruse, J., Becker, D., Alfarraj, S., Hedrich, R., Werner, C., Rennenberg, H., 2017. The carnivorous Venus flytrap uses prey-derived amino acid carbon to fuel respiration. *New Phytol.* **214**, 597-606.

Fenn, J.B., Mann, M., Meng, C.K., Wong, S.F., Whitehouse, C.M., 1989. Electrospray ionization for mass spectrometry of large biomolecules. *Science* **246**, 64-71.

Fenselau, C., Demirev, P.A., 2001. Characterization of intact microorganisms by MALDI mass spectrometry. *Mass Spectrom. Rev.* **20**, 157–171.

Ferreira, R.B., Monteiro, S., Piçarra-Pereira, M.A., Tanganho, M.C., Loureiro, V.B., Teixeira, A.R., 2000. Characterization of the proteins from grapes and wines by immunological methods. *Am. J. Enol. Vitic.* **51**, 22-28.

Ferreira, R.B., Piçarra-Pereira, M.A., Monteiro, S., Loureiro, V.B., Teixeira, A.R., 2001. The wine proteins. *Trends Food Sci. Technol* **12**, 230-239.

Figueiredo, J., Costa, G.J., Maia, M., Paulo, O.S., Malhó, R., Sousa Silva, M., Figueiredo, A., 2016. Revisiting Vitis vinifera subtilase gene family: a possible role in grapevine resistance against Plasmopara viticola. *Front. Plant Sci.* **7**, 1783.

Foucault G., Seydoux F., Yon J., 1974. Comparative kinetic properties of α, β and ψ forms of trypsin. Eur. *J. Biochem.* **47**, 295–302.

Francese, S., Bradshaw, R., Flinders, B., Mitchell, C., Bleay, S., Cicero, L., Clench, M.R., 2013. Curcumin: a multipurpose matrix for MALDI mass spectrometry imaging applications. *Anal. Chem.* **85**, 5240-5248.

Francioli, S., Buxaderas, S., Pellerin, P., 1999. Influence of Botrytis cinerea on the polysaccharide composition of Xarel. lo musts and cava base wines. *Am. J. Enol. Vitic.* **50**, 456-460.

Fronk, P., Hartmann, H., Bauer, M., Solem, E., Jaenicke, E., Tenzer, S., Decker, H., 2015. Polyphenoloxidase from Riesling and Dornfelder wine grapes (Vitis vinifera) is a tyrosinase. *Food Chem.* **183**, 49-57.

Fukushima, K., Fang, X., Alvarez-Ponce, D., Cai, H., Carretero-Paulet, C.C., Chang, T.H., Farr, M.K., Fujita, T., Hiwatashi, Y., Hoshi, Y., Imai, T., Kasahara, M., Librado, P., Mao, L., Mori, H., Nishiyama, T., Nozawa, M., Pálfalvi, G., Pollard, S.T., Rozas, J., Sánchez-Gracia, A., Sankoff, D., Shibata, T.F., Shigenobu, S., Sumikawa, N., Uzawa, T., Xie, M., Zheng, C., Pollock, D.D., Albert, V. A., Li, S., Hasebe, M., 2017. Genome of the pitcher plant Cephalotus reveals genetic changes associated with carnivory. *Nat. Ecol. Evol.* **1**, 0059.

Gaascht, F., Dicato, M., Diederich, M., 2013. Venus Flytrap (Dionaea muscipula Solander ex Ellis) Contains Powerful Compounds that Prevent and Cure Cancer. *Front. Oncol.* **3**, 202.

Gallie, D.R., Chang, S.C., 1997. Signal transduction in the carnivorous plant Sarracenia purpurea. *Plant Physiol.* **115**, 1461–1471.

Gao, X., Tan, B.H., Sugrue, R.J., Tang, K., 2012. MALDI Mass Spectrometry for Nucleic Acid Analysis. In *Applications of MALDI-TOF Spectroscopy*, Cai, Z., Liu, S., eds. Topics in Current Chemistry, vol 331. Springer, Berlin, Heidelberg.

Gaspar, L.M., Machado, A., Coutinho, R., Sousa, S., Santos, R., Xavier, A., Figueiredo, M., Teixeira, M.F., Centeno, F., Simões, J., 2019. Development of potential yeast protein extracts for red wine clarification and stabilization. *Front. Microbiol.* **10**, 2310.

Gazzola, D., Vincenzi, S., Marangon, M., Pasini, G., Curioni, A., 2017. Grape seed extract: the first protein-based fining agent endogenous to grapes. *Aust. J. Grape Wine Res.* **23**, 215-225.

Gekenidis, M.T., Studer, P., Wüthrich, S., Brunisholz, R., Drissner, D., 2014. Beyond the matrix-assisted laser desorption ionization (MALDI) biotyping workflow: in search of microorganism-specific tryptic peptides enabling discrimination of subspecies. *Appl. Environ. Microbiol.* **80**, 4234-4241.

Gergely, Z.R., Martinez, D.E., Donohoe, B.S., Mogelsvang, S., Herder, R., Staehelin, L.A., 2018. 3D electron tomographic and biochemical analysis of ER, Golgi and trans Golgi network membrane systems in stimulated Venus flytrap (Dionaea muscipula) glandular cells. *J. Biol. Res. Thessalon.* **25**, 15.

Ghate, N.B., Chaudhuri, D., Das, A., Panja, S., Mandal, N., 2015. An antioxidant extract of the insectivorous plant Drosera burmannii Vahl. alleviates iron-induced oxidative stress and hepatic injury in mice. *PLoS One* **10**, e0128221.

Ghosh, R., Chakrabarti, C., (2008). Crystal structure analysis of NP24-I: a thaumatin-like protein. *Planta* **228**, 883-890.

Giansanti, P., Tsiatsiani, L., Low, T.Y., Heck, A.J.R., 2016. Six alternative proteases for mass spectrometry–based proteomics beyond trypsin. *Nat. Protoc.* **11**, 993–1006.

Gill, N., Hans, C.S., Jackson, S., 2008. An overview of plant chromosome structure. *Cytogenet. Genome Res.* **120**, 194-201.

Gimon, M.E., Preston, L.M., Solouki, T., White, M.A., Russell, D.H., 1992. Are proton transfer reactions of excited states involved in UV laser desorption ionization? *Org. mass spectrom.* **27**, 827-830.

Gindro, K., Berger, V., Godard, S., Voinesco, F., Schnee, S., Viret, O., Alonso-Villaverde, V., 2012. Protease inhibitors decrease the resistance of Vitaceae to Plasmopara viticola. *Plant Physiol. Biochem.* **60**, 74-80.

Girbau, T., Stummer, B.E., Pocock, K.F., Baldock, G.A., Scott, E.S., Waters, E.J., 2004. The effect of Uncinula necator (powdery mildew) and Botrytis cinerea infection of grapes on the levels of haze-forming pathogenesis-related proteins in grape juice and wine. *Aust. J. Grape Wine Res.* **10**, 125-133.

Giribaldi, M., Gény, L., Delrot, S., Schubert, A., 2010. Proteomic analysis of the effects of ABA treatments on ripening Vitis vinifera berries. *J. Exp. Bot.* **61**, 2447-2458.

Giribaldi, M., Perugini, I., Sauvage, F.X., Schubert, A., 2007. Analysis of protein changes during grape berry ripening by 2-DE and MALDI-TOF. *Proteomics* **7**, 3154-3170.

Givnish, T.J., Burkhardt, E.L., Happel, R.E., Weintraub, J.D., 1984. Carnivory in the bromeliad Brocchinia reducta with a cost/benefit model for the general restriction of carnivorous plants to sunny, moist, nutrient poor habitats. *Am. Nat.* **124**, 479–497.

Givnish, T.J., 2015. New evidence on the origin of carnivorous plants. *Proc. Natl. Acad. Sci. U.S.A.* **112**, 10-11.

Givnish, T.J., Sparks, K.W., Hunter, S.J., Pavlovič, A., 2018. Why are plants carnivorous? Cost/benefit analysis, whole-plant growth, and the context-specific advantages of botanical carnivory. In *Carnivorous plants: physiology, ecology, and evolution*, Ellison A.M., Adamec, L., eds, New York: Oxford University Press, 232–255.

Gomès, E., Sagot, E., Gaillard, C., Laquitaine, L., Poinssot, B., Sanejouand, Y.H., Delrot, S., Coutos-Thévenot, P., 2003. Nonspecific lipid-transfer protein genes expression in grape (Vitis sp.) cells in response to fungal elicitor treatments. *Mol. Plant-Microbe Interact.* **16**, 456-464.

Goto, C., Hashizume, S., Fukao, Y., Hara-Nishimura, I., Tamura, K., 2019. Comprehensive nuclear proteome of Arabidopsis obtained by sequential extraction. *Nucleus* **10**, 81-92.

Graham, D.R., Elliott, S.T., Van Eyk, J.E., 2005. Broad-based proteomic strategies: a practical guide to proteomics and functional screening. *J. Physiol.* **563**, 1-9.

Granato, T.M., Piano, F., Nasi, A., Ferranti, P., Iametti, S., Bonomi, F., 2010. Molecular basis of the interaction between proteins of plant origin and proanthocyanidins in a model wine system. *J. Agric. Food Chem.* **58**, 11969-11976.

Grasser, K.D., 2020. The FACT histone chaperone: tuning gene transcription in the chromatin context to modulate plant growth and development. *Front. Plant Sci*. **11**, 85.

Graumann, K., Runions, J., Evans, D.E., 2010. Characterization of SUN-domain proteins at the higher plant nuclear envelope. *Plant J.* **61**, 134–144.

Grenier, J., Potvin, C., Trudel, J., Asselin, A., 1999. Some thaumatin-like proteins hydrolyse polymeric beta-1,3-glucans. *Plant J.* **19**, 473–480.

Griffiths, J., 2008. A brief history of mass spectrometry. *Anal. Chem.* **80**, 5678-5683.

Grimplet, J., Wheatley, M.D., Jouira, H.B., Deluc, L.G., Cramer, G.R., Cushman, J.C., 2009. Proteomic and selected metabolite analysis of grape berry tissues under well-watered and water-deficit stress conditions. *Proteomics* **9**, 2503-2528.

Grossman, E., Medalia, O., Zwerger, M., 2012. Functional Architecture of the Nuclear Pore Complex. *Annu. Rev. Biophys.* **41**, 557–584.

Grover, A., 2012. Plant Chitinases: Genetic Diversity and Physiological Roles. *Crit. Rev. Plant Sci.* **31**, 57–73.

Gu, Y., Zebell, S.G., Liang, Z., Wang, S., Kang, B.-H., Dong, X., 2016. Nuclear Pore Permeabilization Is a Convergent Signaling Event in Effector-Triggered Immunity. *Cell* **166**, 1526–1538.

Guan, Q., Wu, J., Yue, X., Zhang, Y., Zhu, J., 2013. A nuclear calcium-sensing pathway is critical for gene regulation and salt stress tolerance in Arabidopsis. *PLoS Genet.* **9**, e1003755.

Gundersen, G.G., Worman, H.J., 2013. Nuclear positioning. *Cell* **152**, 1376-1389.

Guo, R., Xu, X., Carole, B., Li, X., Gao, M., Zheng, Y., Wang, X., 2013. Genome-wide identification, evolutionary and expression analysis of the aspartic protease gene superfamily in grape. *BMC genomics* **14**, 1-18.

Guo, Z., Zhang, Q., Zou, H., Guo, B., Ni, J., (2003). A Method for the Analysis of Low-Mass Molecules by MALDI-TOF Mass Spectrometry. *Anal. Chem.* **75**, 707–707.

Guth, H., 1997. Identification of character impact odorants of different white wine varieties. *J. Agric. Food Chem.* **45**, 3022-3026.

Guyot, S., Vercauteren, J., Cheynier, V., 1996. Structural determination of colourless and yellow dimers resulting from (+)-catechin coupling catalysed by grape polyphenoloxidase. *Phytochemistry* **42**, 1279-1288.

Haile, Z.M., Malacarne, G., Pilati, S., Sonego, P., Moretto, M., Masuero, D., Vrhovsek, U., Engelen, K., Baraldi, E., Moser, C., 2020. Dual transcriptome and metabolic analysis of Vitis vinifera cv. Pinot Noir berry and Botrytis cinerea during quiescence and egressed infection. *Front. Plant Sci.* **10**, 1704.

Hake, S., Walbot, V., 1980. The genome of *Zea mays*, its organization and homology to related grasses. *Chromosoma* **79,** 251–270.

Hankin, J.A., Barkley, R.M., Murphy, R.C., 2007. Sublimation as a method of matrix application for mass spectrometric imaging. *J. Am. Soc. Mass Spectrom.* **18**, 1646-1652.

Hatano, N., Hamada, T., 2008. Proteome Analysis of Pitcher Fluid of the Carnivorous PlantNepenthes alata. *J. Proteome Res.* **7**, 809–816.

Hatano, N., Hamada, T., 2012. Proteomic analysis of secreted protein induced by a component of prey in pitcher fluid of the carnivorous plant Nepenthes alata. *J. Proteom.* **75**, 4844–4852.

Hattan, S.J., Marchese, J., Khainovski, N., Martin, S., Juhasz, P., 2005. Comparative Study of [Three] LC−MALDI Workflows for the Analysis of Complex Proteomic Samples. *J. Proteome Res.* **4**, 1931–1941.

Havliš, J., Thomas, H., Šebela, M., Shevchenko, A., 2003. Fast-response proteomics by accelerated in-gel digestion of proteins. *Anal. Chem.* **75**, 1300-1306.

He, S., Hider, R., Zhao, J., Tian, B., 2020. Effect of bentonite fining on proteins and phenolic composition of Chardonnay and Sauvignon Blanc wines. *S. Afr. J. Enol. Vitic.* **41**, 113-120.

Hedrich, R., Neher, E., 2018. Venus flytrap: how an excitable, carnivorous plant works. *Trends Plant Sci.* **23**, 220–234.

Heslop-Harrison, Y., Knox, R.B., 1971. A cytochemical study of the leaf-gland enzymes of insec-tivorous plants of the genus Pinguicula. *Planta* **96**, 183–211.

Hetzer, M.W., Walther, T.C., Mattaj, I.W., 2005. Pushing the envelope: structure, function, and dynamics of the nuclear periphery. *Annu. Rev. Cell Dev. Biol.* **21**, 347-380.

Higashi, S., Nakashima, A., Ozaki, H., Abe, M., Uchiumi, T., 1993. Analysis of feeding mechanism in a pitcher of Nepenthes hybrida. *J. Plant Res.* **106**, 47–54.

Hildonen, S., Halvorsen, T.G., Reubsaet, L., 2014. Why less is more when generating tryptic peptides in bottom-up proteomics. *Proteomics* **14**, 2031–2041.

Hirakawa, T., Matsunaga, S., 2019. Characterization of DNA Repair Foci in Root Cells of Arabidopsis in Response to DNA Damage. *Front. Plant Sci.* **10**, 990.

Hodeček, R. Používané metody pro stanovení termolabilních bílkovin v procesu výroby vína a jejich srovnání, Brno, 2016. diplomová práce (Mgr.). Mendelova univerzita v Brně, Zahradnická fakulta.

Hohenstatt, M.L., Mikulski, P., Komarynets, O., Klose, C., Kycia, I., Jeltsch, A., Farrona, S., Schubert, D., 2018. PWWP-DOMAIN INTERACTOR OF POLYCOMBS1 Interacts with Polycomb-Group Proteins and Histones and Regulates Arabidopsis Flowering and Development. *Plant Cell* **30**, 117–133.

Holzlechner, M., Reitschmidt, S., Gruber, S., Zeilinger, S., Marchetti-Deschmann, M., 2016. Visualizing fungal metabolites during mycoparasitic interaction by MALDI mass spectrometry imaging. *Proteomics* **16**, 1742–1746.

Honisch, Ch., Serafim, V., Hennessy, N., Allen, D.J., Ring, Ch.J., Pantoja M., Leonardo, G., Saheer, E., Shah, A.J., Shah, H.N., 2017. Microbial DNA analysis by MALDI-TOF mass spectrometry. In: *MALDI-TOF and Tandem MS for Clinical Microbiology*. Shah, H.N., Gharbia, S.E., eds., (pp. 187-209), Wiley, Oxford.

Hu, X., Wansha, L., Chen, Q., Yang, Y., 2009. Early signals transduction linking the synthesis of jasmonic acid in plant. *Plant Signal. Behav.* **4**, 696-697.

Huang, P., Huang, C.Y., Lin, T.C., Lin, L.E., Yang, E.Lee, C., Hsu, C.C., Chou, P.T., 2020. Toward the rational design of universal dual polarity matrix for MALDI mass spectrometry. *Anal. Chem.* **92**, 7139-7145.

Huang, D.W., Sherman, B.T., Lempicki, R.A., 2009. Bioinformatics enrichment tools: paths toward the comprehensive functional analysis of large gene lists. *Nucleic Acids Res.* **37**, 1–13.

Hughes, C., Ma, B., Lajoie, G.A., 2010. De novo sequencing methods in proteomics. In Proteome Bioinformatics (pp. 105-121). Humana Press.

Chagas, R., Ferreira, L.M., Laia, C.A., Monteiro, S., Ferreira, R.B., 2016. The challenging SO2-mediated chemical build-up of protein aggregates in wines. *Food Chem.* **192**, 460-469.

Chagas, R., Monteiro, S., Ferreira, R.B., 2012. Assessment of potential effects of common fining agents used for white wine protein stabilization. *Am. J. Enol. Vitic.* **63**, 574-578.

Chait, B.T., 2006. Mass spectrometry: bottom-up or top-down? *Science* **314**, 65-66.

Chen, H.S., Rejtar, T., Andreev, V., Moskovets, E., Karger, B.L., 2005. Enhanced characterization of complex proteomic samples using LC−MALDI MS/MS: Exclusion of redundant peptides from MS/MS analysis in replicate runs. *Anal. Chem.* **77**, 7816-7825.

Chen, Y.F., Li, L., Q., Xu, Q., Kong, Y.H., Wang, H., Wu, W.H., 2009. The WRKY6 transcription factor modulates PHOSPHATE1 expression in response to low Pi stress in Arabidopsis. *Plant Cell* **21**, 3554-3566.

Cheng, Y.T., Germain, H., Wiermer, M., Bi, D., Xu, F., Garcia, A.V., Wirthuellerm L., Germain, H., Després, Ch., Parker, J.E., Zhang, Y., Li, X., 2009. Nuclear pore complex component MOS7/Nup88 is required for innate immunity and nuclear accumulation of defense regulators in Arabidopsis. *Plant Cell* **21**, 2503-2516.

Cheynier, V., Basire, N., Rigaud, J., 1989. Mechanism of trans-caffeoyltartaric acid and catechin oxidation in model solutions containing grape polyphenoloxidase. *J. Agric. Food Chem.* **37**, 1069-1071.

Chi, S.M., Nam, D., 2012. WegoLoc: accurate prediction of protein subcellular localization using weighted gene ontology terms. *Bioinformatics* **28**, 1028–1030.

Chinnici, F., Sonni, F., Natali, N., Riponi, C., 2013. Oxidative evolution of (+)-catechin in model white wine solutions containing sulfur dioxide, ascorbic acid or gallotannins. *Food Res. Int.* **51**, 59-65.

Chmelík, J., 2005. Proteomický průvodce. *Chem. listy* **99**, 883-885.

Inagami, T., Sturtevant, J.M., 1960. Nonspecific catalyses by α-chymotrypsin and trypsin. *J. Biol. Chem.* **235**, 1019–1023.

Iniative, A.G., 2000. Analysis of the genome sequence of the flowering plant Arabidopsis thaliana. *Nature* **408**, 796-815.

International Human Genome Sequencing Consortium, 2001. Initial sequencing and analysis of the human genome. *Nature* **409**, 860–921.

Ishisaki, K., Arai, S., Hamada, T., Honda, Y., 2012. Biochemical characterization of a recombinant plant class III chitinase from the pitcher of the carnivorous plant Nepenthes alata. *Carbohydr. Res.* **361**, 170–174.

Jaeckels, N., Tenzer, S., Rosfa, S., Schild, H., Decker, H., Wigand, P., 2013. Purification and structural characterisation of lipid transfer protein from red wine and grapes. *Food Chem.* **138**, 263-269.

Jaeckels, N., Tenzer, S., Rosch, A., Scholten, G., Decker, H., Fronk, P., 2015. β-Glucosidase removal due to bentonite fining during wine making. *Eur. Food Res. Technol.* **241**, 253-262.

Jaeckels, N., Tenzer, S., Meier, M., Will, F., Dietrich, H., Decker, H., Fronk, P., 2017. Influence of bentonite fining on protein composition in wine. *LWT* **75**, 335-343.

Jaffé, K., Blum, M.S., Fales, H.M., Mason, R.T., Cabrera, A., 1995. On insect attractants from pitcher plants of the genus Heliamphora (sarraceniaceae). *J. Chem. Ecol.* **21**, 379–384.

Johnson, M., Zaretskaya, I., Raytselis, Y., Merezhuk, Y., McGinnis, S., Madden, T.L., 2008. NCBI BLAST: a better web interface. *Nucleic Acids Res.* **36**, W5–W9.

Jones, P., Binns, D., Chang, H.Y., Fraser, M., Li, W., McAnulla, C., McWilliam, H., Maslen, J., Mitchell, A., Nuka, G., Pesseat, S., Quinn, A.F., Sangrador-Vegas, A., Scheremetjew, M., Yong, S.Y., Lopez, R., Hunter, S., 2014, InterProScan 5: genome-scale protein function classification. *Bioinformatics* **30**, 1236-1240.

Joyner, J.C., Keuper, K.D., Cowan, J.A., 2013. Analysis of RNA cleavage by MALDI-TOF mass spectrometry. *Nucleic acids res.* **41**, e2-e2.

Jung, H.W., Hwang, B.K., 2000. Isolation, partial sequencing, and expression of pathogenesis-related cDNA genes from pepper leaves infected by Xanthomonas campestris pv. vesicatoria. *Mol. Plant-Microbe Interact.* **13**, 136-142.

Kaku, H., Nishizawa, Y., Ishii-Minami, N., Akimoto-Tomiyama, C., Dohmae, N., Takio, K., Minami E., Shibuya, N., 2006. Plant cells recognize chitin fragments for defense signaling through a plasma membrane receptor. *Proc. Natl. Acad. Sci. U.S.A.* **103**, 11086–11091.

Kambiranda, D., Katam, R., Basha, S.M., Siebert, S., 2014. iTRAQ-based quantitative proteomics of developing and ripening muscadine grape berry. *J. Proteome Res.* **13**, 555-569.

Karas, M., Hillenkamp, F. 1988. Laser desorption ionization of proteins with molecular masses exceeding 10,000 daltons. *Anal. Chem.* **60**, 2299-2301.

Kars, I., Krooshof, G.H., Wagemakers, L., Joosten, R., Benen, J.A., Van Kan, J.A., 2005. Necrotizing activity of five Botrytis cinerea endopolygalacturonases produced in Pichia pastoris. *Plant J.* **43**, 213-225.

Kay, J, Kassell, B., 1971. The autoactivation of trypsinogen. *J. Biol. Chem.* **246**, 6661–6665.

Keil, B., 1971. 8 Trypsin. *In* The enzymes (Vol. 3, pp. 249-275). Academic Press.

Keil-Dlouhá V., Zylber N., Tong N.T., Keil B., 1971b. Cleavage of glucagon by α- and β-trypsin. *FEBS Lett.* **16**, 287–290.

Keil-Dlouhá, V.V., Zylber, N., Imhoff J, Tong, N., Keil, B., 1971a. Proteolytic activity of pseudotrypsin. *FEBS Lett.* **16**, 291-295.

Kellersberger, K.A., Yu, E., Kruppa, G.H., Young, M.M., Fabris, D., 2004. Top-down characterization of nucleic acids modified by structural probes using high-resolution tandem mass spectrometry and automated data interpretation. *Anal. Chem.* **76**, 2438-2445.

Kocáb, O., Jakšová, J., Novák, O., Petřík, I., Lenobel, R., Chamrád, I., Pavlovič, A., 2020. Jasmonate-independent regulation of digestive en-zyme activity in the carnivorous butterwort Pinguicula × Tina. *J. Exp. Bot.* **71**, 3749–3758.

Kompauer, M., Heiles, S., Spengler, B., 2017. Atmospheric pressure MALDI mass spectrometry imaging of tissues and cells at 1.4-μm lateral resolution. *Nat. Methods* **14**, 90-96.

Kováčik, J., Klejdus, B., Repčáková, K., 2012. Phenolic metabolites in carnivorous plants: Inter-specific comparison and physiological studies. *Plant Physiol. Biochem.* **52**, 21–27.

Krausko, M., Perutka, Z., Šebela, M., Šamajová, O., Šamaj, J., Novák, O., Pavlovič, A., 2017. The role of electrical and jasmonate signalling in the recognition of captured prey in the carnivorous sundew plant Drosera capensis. *New Phytol.* **213**, 1818–1835.

Kreuzwieser, J., Scheerer, U., Honsel, A., Kruse, J., Burzlaff, T., Alfarraj, S., Georgiev, P., Schnitzler, J.P., Ghirardi, A., Kreuzer, I., Hedrich, R., Rennenberg, H., 2014. Venus fly trap attracts insects by the release of volatile organic compounds. *J. Exp. Bot.* **65**: 755–766.

Kruse, J., Gao, P., Honsel, A., Kreuzwieser, J., Burzlaff, T., Alfarraj, S., Hedrich, R., Rennenberg, H., 2014. Strategy of nitrogen acquisition and utilization by carnivorous Dionaea muscipula. *Oecologia* **174**, 839–851.

Kunitz, M., 1939. Formation of trypsin from crystalline trypsinogen by means of enterokinase. *J. Gen. Physiol.* **22**, 429–446.

Kupfer, V.M., Vogt, E.I., Siebert, A., Meyer, M., Vogel, R.F., Niessen, L., 2017. Foaming characteristics of the gushing modulating protein PAU5 with detailed investigation on the influence of sparkling wine processing. *Food Res. Int.* **102**, 111-118.

Kwak, K.J., Kim, Y.O., Kang, H., 2005. Characterization of transgenic Arabidopsis plants overexpressing GR-RBP4 under high salinity, dehydration, or cold stress. *J. Exp. Bot.* **56**, 3007-3016.

Kwon, S.W., 2004. Profiling of soluble proteins in wine by nano-high-performance liquid chromatography/tandem mass spectrometry. *J. Agric. Food Chem.* **52**, 7258-7263.

Lacerda, C.D., Teixeira, A.E., de Oliveira, J.S., Silva, S.F., Vasconcelos, A.V.B., Gouveia, D.G., da Silva, A.R., Santoro, M.M., dos Mares-Guia, M.L., Santos, A.M.C., 2014. Gamma trypsin: Purification and physicochemical characterization of a novel bovine trypsin isoform. *Int. J. Biol. Macromol.* **70**, 179–186.

Lambri, M., Dordoni, R., Giribaldi, M., Violetta, M.R., Giuffrida, M.G., 2013. Effect of pH on the protein profile and heat stability of an Italian white wine. *Food Res. Int.* **54**, 1781-1786.

Lambri, M., Dordoni, R., Silva, A., De Faveri, D.M., 2010. Effect of bentonite fining on odor-active compounds in two different white wine styles. *Am. J. Enol. Vitic.* **61**, 225-233.

Lasanta, C., Gómez, J., 2012. Tartrate stabilization of wines. *Trends Food Sci Technol* **28**, 52-59.

Laskay, Ü.A., Lobas, A.A., Srzentić, K., Gorshkov, M.V., Tsybin, Y.O., 2013. Proteome Digestion Specificity Analysis for Rational Design of Extended Bottom-up and Middle-down Proteomics Experiments. *J. Proteome Res.* **12**, 5558–5569.

LeBrasseur, N.D., MacIntosh, G.C., Perez-Amador, M.A., Saitoh, M., Green, P.J., 2002. Local and systemic wound-induction of RNase and nuclease activities in Arabidopsis: RNS1 as a marker for a JA-independent systemic signaling pathway. *Plant J.* **29**, 393–403.

Lee, L., Zhang, Y., Ozar, B., Sensen, C.W., Schriemer, D.C., 2016. Carnivorous Nutrition in Pitcher Plants (Nepenthes spp.) via an Unusual Complement of Endogenous Enzymes. *J. Proteome Res.* **15**, 3108–3117.

Leone, P., Menu-Bouaouiche, L., Peumans, W.J., Payan, F., Barre, A., Roussel, A., Van Damme, E.J.M., Rougé, P., 2006. Resolution of the structure of the allergenic and antifungal banana fruit thaumatin-like protein at 1.7-Å. *Biochimie* **88**, 45-52.

Li, J., Li, C., Lu, S., 2018. Identification and characterization of the cytosine-5 DNA methyltransferase gene family in Salvia miltiorrhiza. *PeerJ* **6**, e4461.

Li, M., Yin, X., Sakata, K., Yang, P., Komatsu, S., 2015. Proteomic Analysis of Phosphoproteins in the Rice Nucleus During the Early Stage of Seed Germination. *J. Proteome Res.* **14**, 2884–2896.

Li, Z., Zhang, S., Han, R., Zhang, H., Li, K., Wang, X., 2019. Infection process and host responses to Elsinoë ampelina, the causal organism of grapevine anthracnose. *Eur. J. Plant Pathol.* **155**, 571-582.

Libiaková, M., Floková, K., Novák, O., Slováková, L., Pavlovič, A., 2014. Abundance of Cysteine Endopeptidase Dionain in Digestive Fluid of Venus Flytrap (Dionaea muscipula Ellis) Is Regulated by Different Stimuli from Prey through Jasmonates. *PLoS ONE* **9**, e104424.

Lilly, M., Bauer, F.F., Lambrechts, M.G., Swiegers, J.H., Cozzolino, D., Pretorius, I.S., 2006. The effect of increased yeast alcohol acetyltransferase and esterase activity on the flavour profiles of wine and distillates. *Yeast* **23**, 641-659.

Liu, Q., Shi, L., Fang, Y., 2012. Dicing bodies. *Plant Physiol.* **158**, 61-66.

Lorković, Z.J., Hilscher, J., Barta, A., 2008. Co-localisation studies of Arabidopsis SR splicing factors reveal different types of speckles in plant cell nuclei. *Exp. Cell Res.* **314**, 3175-3186.

Love, A.J., Yu, C., Petukhova, N.V., Kalinina, N.O., Chen, J., Taliansky, M.E., 2017. Cajal bodies and their role in plant stress and disease responses. *RNA Biol.* **14**, 779–790.

Loza-Muller, L., Rodríguez-Corona, U., Sobol, M., Rodríguez-Zapata, L.C., Hozak, P., Castano, E., 2015. Fibrillarin methylates H2A in RNA polymerase I trans-active promoters in Brassica oleracea. *Front. Plant Sci.* **6**, 976.

Luo, M., Wang, Y.-Y., Liu, X., Yang, S., Lu, Q., Cui, Y., Wu, K., 2012. HD2C interacts with HDA6 and is involved in ABA and salt stress response in Arabidopsis. *J. Exp. Bot.* **63**, 3297–3306.

Luo, Z., van Vuuren, H.J., 2009. Functional analyses of PAU genes in Saccharomyces cerevisiae. *Microbiology* **155**, 4036-4049.

Mainente, F., Zoccatelli, G., Lorenzini, M., Cecconi, D., Vincenzi, S., Rizzi, C., Simonato, B., 2014. Red wine proteins: Two dimensional (2-D) electrophoresis and mass spectrometry analysis. *Food Chem.* **164**, 413-417.

Manteau, S., Abouna, S., Lambert, B., Legendre, L., 2003. Differential regulation by ambient pH of putative virulence factor secretion by the phytopathogenic fungus Botrytis cinerea. *FEMS Microbiol. Ecol.* **43**, 359-366.

Marangon, M., van Sluyter, S.C., Haynes, P.A., Waters, E.J., 2009. Grape and wine proteins: their fractionation by hydrophobic interaction chromatography and identification by chromatographic and proteomic analysis. *J. Agric. Food Chem.* **57**, 4415-4425.

Marangon, M., van Sluyter, S.C., Neilson, K.A., Chan, C., Haynes, P.A., Waters, E.J., Falconer, R.J., 2011. Roles of grape thaumatin-like protein and chitinase in white wine haze formation. *J. Agric. Food Chem.* **59**, 733-740.

Marangon, M., van Sluyter, S.C., Robinson, E.M., Muhlack, R.A., Holt, H.E., Haynes, P.A., Godden, P.W., Smith, P.A., Waters, E.J., 2012. Degradation of white wine haze proteins by Aspergillopepsin I and II during juice flash pasteurization. *Food Chem.* **135**, 1157-1165.

Marangon, M., van Sluyter, S.C., Waters, E.J., Menz, R.I., 2014. Structure of haze forming proteins in white wines: Vitis vinifera thaumatin-like proteins. *PloS one* **9**, e113757.

Marfori, M., Mynott, A., Ellis, J.J., Mehdi, A.M., Saunders, N.F.W., Curmi, P.M., Forwood, J., K., Bodén, M., Kobe, B., 2011. Molecular basis for specificity of nuclear import and prediction of nuclear localization. *Biochim. Biophys. Acta - Mol. Cell Res.* **1813**, 1562–1577.

Marchal, R., Salmon, T., Gonzalez, R., Kemp, B., Vrigneau, C., Williams, P., Doco, T., 2020. Impact of Botrytis cinerea contamination on the characteristics and foamability of yeast macromolecules released during the alcoholic fermentation of a model grape juice. *Molecules* **25**, 472.

Marchal, R., Warchol, M., Cilindre, C., Jeandet, P., 2006. Evidence for protein degradation by Botrytis cinerea and relationships with alteration of synthetic wine foaming properties. *J. Agric. Food Chem.* **54**, 5157-5165.

Marchler-Bauer, A., Bryant, S.H., 2004. CD-search: protein domain annotations on the fly. *Nucleic Acids Res.* **32**, 44598.

Martínez, J.M., Cebrián, G., Álvarez, I., Raso, J., 2016. Release of mannoproteins during Saccharomyces cerevisiae autolysis induced by pulsed electric field. *Front. Microbiol.* **7**, 1435.

Martínez-Esteso, M.J., Casado-Vela, J., Sellés-Marchart, S., Elortza, F., Pedreño, M.A., Bru-Martínez, R., 2011. iTRAQ-based profiling of grape berry exocarp proteins during ripening using a parallel mass spectrometric method. *Mol Biosyst* **7**, 749-765.

Martinez-Esteso, M.J., Sellés-Marchart, S., Vera-Urbina, J.C., Pedreño, M.A., Bru-Martinez, R., 2009. Changes of defense proteins in the extracellular proteome of grapevine (Vitis vinifera cv. Gamay) cell cultures in response to elicitors. *J Proteomics* **73**, 331-341.

Matera, A.G., Shpargel, K.B., 2006. Pumping RNA: nuclear bodybuilding along the RNP pipeline. *Curr. Opin. Cell Biol.* **18**, 317–324.

Mazur, M.J., Spears, B.J., Djajasaputra, A., van der Gragt, M., Vlachakis, G., Beerens, B., Gassmann, W., van den Burg, H.A., 2017. Arabidopsis TCP Transcription Factors Interact with the SUMO Conjugating Machinery in Nuclear Foci. *Front. Plant Sci.* **8**, 2043.

McCombie, G., Knochenmuss, R., 2004. Small-Molecule MALDI Using the Matrix Suppression Effect To Reduce or Eliminate Matrix Background Interferences. *Anal. Chem.* **76**, 4990–4997.

McRae, J.M., Ziora, Z.M., Kassara, S., Cooper, M.A., Smith, P.A., 2015. Ethanol concentration influences the mechanisms of wine tannin interactions with poly (l-proline) in model wine. *J. Agric. Food Chem.* **63**, 4345-4352.

Meier, I., Griffis, A.H., Groves, N.R., Wagner, A., 2016. Regulation of nuclear shape and size in plants. *Curr. Opin. Cell Biol.* **40**, 114–123.

Meisenberg, C., Pinder, S.I., Hopkins, S.R., Wooller, S.K., Benstead-Hume, G., Pearl, F.M.G., Jeggo, P.A., Downs, J.A., 2019. Repression of transcription at DNA breaks requires cohesin throughout interphase and prevents genome instability. *Mol. Cell* **73**, 212–223.

Meng, X., Song, T., Fan, H., Yu, Y., Cui, N., Zhao, J., Meng, K., 2016. A comparative cell wall proteomic analysis of cucumber leaves under Sphaerotheca fuliginea stress. *Acta Physiol. Plant.* **38**, 1-14.

Mierczynska-Vasilev, A., Wahono, S.K., Smith, P.A., Bindon, K., Vasilev, K., 2019. Using zeolites to protein stabilize white wines. *ACS Sustain. Chem. Eng.* **7**, 12240-12247.

Michalko, J., Socha, P., Mészáros, P., Blehová, A., Libantová, J., Moravčíková, J., Matušíková, I., 2013. Glucan-rich diet is digested and taken up by the carnivorous sundew (Drosera rotundifolia L.): implication for a novel role of plant β-1,3-glucanases. *Planta* **238**, 715–725.

Milheiro, J., Filipe-Ribeiro, L., Cosme, F., Nunes, F.M., 2017. A simple, cheap and reliable method for control of 4-ethylphenol and 4-ethylguaiacol in red wines. Screening of fining agents for reducing volatile phenols levels in red wines. *J. Chromat. B* **1041**, 183-190.

Millarini, V., Ignesti, S., Cappelli, S., Ferraro, G., Adessi, A., Zanoni, B., Fratini, E., Domizio, P., 2020. Protection of Wine from Protein Haze Using Schizosaccharomyces japonicus Polysaccharides. *Foods* **9**, 1407.

Millett, J., Foot, G.W., Svensson, B.M., 2015. Nitrogen deposition and prey nitrogen uptake control the nutrition of the carnivorous plant Drosera rotundifolia. *Sci. Total Environ.* **512**, 631-636.

Min, K., Ha, S.C., Hasegawa, P.M., Bressan, R.A., Yun, D.J., Kim, K.K., 2004. Crystal structure of osmotin, a plant antifungal protein. *Proteins* **54**, 170-173.

Mirgorodskaya, O.A., Kozmin, Y.P., Titov, M.I., Körner, R., Sönksen, C.P., Roepstorff, P., 2000. Quantitation of peptides and proteins by matrix-assisted laser desorption/ionization mass spectrometry using 18O-labeled internal standards. *Rapid Commun. Mass Spectrom* **14**, 1226-1232.

Mithöfer, A., 2011. Carnivorous pitcher plants: insights in an old topic. *Phytochemistry* **72**, 1678-1682.

Mithöfer, A., Reichelt, M., Nakamura, Y., 2014. Wound and insect-induced jasmonate accumulation in carnivorous Drosera capensis: two sides of the same coin. *Plant Biol.* **5**, 982–987.

Mody, N.V., Henson, R.D., Hedin, P.A., Kokpol, U., Miles, D.H., 2005. Isolation of the insect paralyzing agent coniine from Sarracenia flava. *Experientia* **32**, 829-830.

Moine-Ledoux, V., Dubourdieu, D., 1999. An invertase fragment responsible for improving the protein stability of dry white wines. *J. Agric. Food Chem.* **79**, 537-543.

Monteiro, S., Barakat, M., Piçarra-Pereira, M.A., Teixeira, A.R., Ferreira, R.B., 2003. Osmotin and thaumatin from grape: a putative general defense mechanism against pathogenic fungi. *Phytopathology* **93**, 1505-1512.

Morohoshi, T., Oikawa, M., Sato, S., Kikuchi, N., Kato, N., Ikeda, T., 2011. Isolation and characterization of novel lipases from a metagenomic library of the microbial community in the pitcher fluid of the carnivorous plant Nepenthes hybrida. *J. Biosci. Bioeng.* **112**, 315–320.

Morris, H.R., Panico, M., Barber, M., Bordoli, R.S., Sedgwick, R.D., Tyler, A. 1981. Fast atom bombardment: a new mass spectrometric method for peptide sequence analysis. *Biochem. Biophys. Res. Commun.* **101**, 623-631.

Mounfield, W.P., Garrett, T.J., 2012. Automated MALDI matrix coating system for multiple tissue samples for imaging mass spectrometry. *J. Am. Soc. Mass Spectrom.* **23**, 563-569.

Nakamura, Y., Reichelt, M., Mayer, V.E., Mithofer, A., 2013. Jasmonates trigger prey-induced formation of outer stomach in carnivorous sundew plants. *Proc. R. Soc. B.* **280**, 20130228.

Narula, K., Datta, A., Chakraborty, N., Chakraborty, S., 2013. Comparative analyses of nuclear proteome: extending its function. *Front. Plant Sci.* **4**, 100.

Ndlovu, T., Buica, A., Bauer, F.F., 2019. Chitinases and thaumatin-like proteins in Sauvignon Blanc and Chardonnay musts during alcoholic fermentation. *Food Microbiol.* **78**, 201-210.

Negri, A.S., Prinsi, B., Rossoni, M., Failla, O., Scienza, A., Cocucci, M., Espen, L., 2008. Proteome changes in the skin of the grape cultivar Barbera among different stages of ripening. *BMC genomics* **9**, 1-19.

Nishimura, E., Kawahara, M., Kodaira, R., Kume, M., Arai, N., Nishikawa, J., Ohyama, T., 2013. S-like ribonuclease gene expression in carnivorous plants. *Planta* **238**, 955–967.

Ogata, C.M., Gordon, P.F., de Vos, A.M., Kim, S.H., 1992. Crystal structure of a sweet tasting protein thaumatin I, at 1· 65 Å resolution. *J. Mol. Biol.* **228**, 893-908.

Ohta, S., Bukowski-Wills, J.C., Sanchez-Pulido, L., de Lima Alves, F., Wood, L., Chen, Z., Platani, M., Fischer, L., Hudson, D.F., Ponting, Ch.P., Fukagawa, F., Earnshaw, W.C., Rappsilber J., 2010. The protein composition of mitotic chromosomes determined using multiclassifier combinatorial proteomics. *Cell* **142**, 810–821.

Okabe, T., Iwakiri, Y., Mori, H., Ogawa, T., Ohyama, T., 2005. An S-like ribonuclease gene is used to generate a trap-leaf enzyme in the carnivorous plant Drosera adelae. *FEBS Lett.* **579**, 5729–5733.

Okuda, T., Fukui, M., Takayanagi, T., Yokotsuka, K., 2006. Characterization of major stable proteins in Chardonnay wine. *Food Sci. Technol. Res.* **12**, 131-136.

Park, Y.J., Luger, K., 2006. The structure of nucleosome assembly protein 1. *Proc. Natl. Acad. Sci. U.S.A.* **103,** 1248-1253.

Palmisano, G., Antonacci, D., Larsen, M.R., 2010. Glycoproteomic profile in wine: a ‘sweet’molecular renaissance. *J. Proteome Res.* **9**, 6148-6159.

Pappin, D.J., Hojrup, P., Bleasby, A.J., 1993. Rapid identification of proteins by peptide-mass fingerprinting. *Curr. Biol.* **3**, 327-332.

Parsons, R., Sunley, R.J., 2001. Nitrogen nutrition and the role of root–shoot nitrogen signalling particularly in symbiotic systems. *J. Exp. Bot.* **52**(suppl_1), 435-443.

Pastorello, E.A., Farioli, L., Pravettoni, V., Ortolani, C., Fortunato, D., Giuffrida, M.G., Garoffo, L.P., Calamari, A.M., Brenna, O., Conti, A., 2003. Identification of grape and wine allergens as an endochitinase 4, a lipid-transfer protein, and a thaumatin. *J. Allergy Clin. Immunol.* **111**, 350-359.

Paszota, P., Escalante-Perez, M., Thomsen, L.R., Risør, M.W., Dembski, A., Sanglas, L., Nielsenm T.A., Karring, H., Thorgersen, I.B., Hedrich, R., Enghild, J.J., Kreuzer, I.,

Pavlovič, A., Demko, V., Hudak, J., 2010. Trap closure and prey retention in Venus flytrap (Dionaea muscipula) temporarily reduces photosynthesis and stimulates respiration. *Ann. Bot.* **105**, 37–44.

Pavlovič, A., Krausko, M., Libiaková, M., Adamec, L., 2014. Feeding on prey increases photosynthetic efficiency in the carnivorous sundew Drosera capensis. *Ann. Bot.* **113**, 69–78.

Pavlovič, A., Mithöfer, A., 2019. Jasmonate signalling in carnivorous plants: Copycat of plant defence mechanisms. *J. Exp. Bot.* **70**, 3379-3389.

Pendle, A.F., Clark, G.P., Boon, R., Lewandowska, D., Lam, Y.W., Andersen, J., Mann, M., Lamond, A.I., Brown, J.W.S., Shaw, P.J., 2005. Proteomic Analysis of the Arabidopsis Nucleolus Suggests Novel Nucleolar Functions. *Mol. Biol. Cell* **16**, 260–269.

Perutka, Z., Šebela, M., 2018. Basis of Mass Spectrometry: Technical Variants. In *The Use of Mass Spectrometry Technology (MALDI-TOF) in Clinical Microbiology*, Cobo, F., ed., (pp. 19-45). Academic Press.

Perutka, Z., Šebela, M., 2018. Pseudotrypsin: A Little-Known Trypsin Proteoform. *Molecules* **23**, 2637.

Perutka, Z., Šufeisl, M., Strnad, M., Šebela, M., 2019. High-proline proteins in experimental hazy white wine produced from partially botrytized grapes. *Biotechnol. Appl. Biochem.* **66**, 398-411.

Perutka, Z., Šebela, M., 2020. Mass spectrometry of peptides and proteins using digestion by a grape cysteine protease at pH 3. *J. Mass Spectrom.* **55**, e4444.

Perutka, Z., Kaduchová, K., Chamrád, I., Beinhauer, J., Lenobel, R., Petrovská, B., Bergougnoux, V., Vrána, J., Pečinka, A., Doležel, J., Šebela, M., 2021. Proteome Analysis of Condensed Barley Mitotic Chromosomes. *Front. Plant Sci.* **12**, 1716.

Petersen, T., Brunak, S., von Heijne, G., Nielsen, H., 2011. SignalP 4.0: discriminating signal peptides from transmembrane regions. *Nat. Methods* **8**, 785–786

Petrovská, B., Šebela, M., Doležel, J., 2015. Inside a plant nucleus: discovering the proteins. *J. Exp. Bot.* **66**, 1627-1640.

Pfeiffer, A., Nagel, M.-K., Popp, C., Wust, F., Bindics, J., Viczian, A., Hiltbrunner, A., Nagy, F., Kunkel, T., Schafer, E., 2012. Interaction with plant transcription factors can mediate nuclear import of phytochrome B. *Proc. Natl. Acad. Sci. U.S.A.* **109**, 5892–5897.

Płachno, B.J., Adamec, L., Lichtscheidl, I.K., Peroutka, M., Adlassnig, W., Vrba, J., 2006. Fluorescence Labelling of Phosphatase Activity in Digestive Glands of Carnivorous Plants. *Plant Biol.* **8**, 813–820.

Ployon, S., Attina, A., Vialaret, J., Walker, A.S., Hirtz, C., Saucier, C., 2020. Laccases 2 & 3 as biomarkers of Botrytis cinerea infection in sweet white wines. *Food Chem.* **315**, 126233.

Pocock, K.F., Hayasaka, Y., Peng, Z., Williams, P.J., Waters, E.J., 1998. The effect of mechanical harvesting and long-distance transport on the concentration of haze-forming proteins in grape juice. *Aust. J. Grape Wine Res.* **4**, 23-29.

Pocock, K.F., Hayasaka, Y., McCarthy, M.G., Waters, E.J., 2000. Thaumatin-like Proteins and Chitinases, the Haze-Forming Proteins of Wine, Accumulate during Ripening of Grape (Vitis v inifera) Berries and Drought Stress Does Not Affect the Final Levels per Berry at Maturity. *J. Agric. Food Chem.* **48**, 1637-1643.

Pocock, K.F., Alexander, G.M., Hayasaka, Y., Jones, P.R., Waters, E.J., 2007. Sulfate a candidate for the missing essential factor that is required for the formation of protein haze in white wine. *J. Agric. Food Chem.* **55**, 1799-1807.

Polgar, L., 1989. Cysteine proteases, In *Mechanisms of protease action*, (pp. 123-125), Boca Raton, FL, USA, CRC Press Inc.

Pontvianne, F., Carpentier, M.-C., Durut, N., Pavlištová, V., Jaške, K., Schořová, Š., Parrinello, H., Rohmer, M., Pikaard, C.S., Fojtová, M., Fajkus, J., Sáez-Vásquez, J., 2016. Identification of Nucleolus-Associated Chromatin Domains Reveals a Role for the Nucleolus in 3D Organization of the A. thaliana Genome. *Cell Rep.* **16**, 1574–1587.

Pozo-Bayón, M.Á., Andújar-Ortiz, I., Moreno-Arribas, M.V., 2009. Scientific evidences beyond the application of inactive dry yeast preparations in winemaking. *Food Res. Int.* **42**, 754-761.

Pradillo, M., Evans, D., Graumann, K., 2019. The nuclear envelope in higher plant mitosis and meiosis. *Nucleus* **10**, 55-66.

Pranada, A.B., Schwarz, G., Kostrzewa, M., 2016. MALDI Biotyping for microorganism identification in clinical microbiology. In Advances in MALDI and Laser-Induced Soft Ionization Mass Spectrometry, (pp. 197-225). Springer, Cham.

Prankevicius, A.B., Cameron, D.M., 1991. Bacterial dinitrogen fixation in the leaf of the northern pitcher plant (Sarracenia purpurea). *Canad. J. Bot.* **69**, 2296-2298.

Pretorius, I.S., 2000. Tailoring wine yeast for the new millennium: novel approaches to the ancient art of winemaking. *Yeast* **16**, 675-729.

Qi, F., Zhang, F., 2020. Cell cycle regulation in the plant response to stress. *Front. Plant Sci.* **10**, 1765.

Rabilloud, T., Chevallet, M., Luche, S., Lelong, C., 2010. Two-dimensional gel electrophoresis in proteomics: Past, present and future. *J proteomics* **73**, 2064-2077.

Raj, G., Kurup, R., Hussain, A.A., Baby, S., 2011. Distribution of naphthoquinones, plumbagin, droserone, and 5-O-methyl droserone in chitin-induced and uninduced Nepenthes khasiana: molecular events in prey capture. *J. Exp. Bot.* **62**, 5429–5436.

Rakotonaina, S. Izolace a charakterizace vybraných proteinů révy vinné (*Vitis vinifera*). Olomouc, 2020. bakalářská práce (Bc.). Univerzita Palackého v Olomouci. Přírodovědecká fakulta.

Ratnayake, S., Stockdale, V., Grafton, S., Munro, P., Robinson, A.L., Pearson, W., McRae, J., M., Bacic, A., 2019. Carrageenans as heat stabilisers of white wine. *Aust. J. Grape Wine Res.* **25**, 439-450.

Reddy, A.S.N., Day, I.S., Gohring, J., Barta, A., 2011. Localization and Dynamics of Nuclear Speckles in Plants. *Plant physiol.* **158**, 67–77.

Renner, T., Specht, C.D., 2012. Molecular and Functional Evolution of Class I Chitinases for Plant Carnivory in the Caryophyllales. *Mol. Biol. Evol.* **29**, 2971–2985.

Resing, K.A., Ahn, N.G., 2005. Proteomics strategies for protein identification. *FEBS Lett.* **579**,

Risør, M.W., Thomsen, L.R., Sanggaard, K.W., Nielsen, T.A., Thøgersen, I.B., Lukassen, M. V., Rossen, L., Garcia-Ferrer, I., Guevara, T., Scavenius, C.,

Meinjohanns, E., Gomis-Ruth, F., X., Enghild, J.J., 2015. Enzymatic and Structural Characterization of the Major Endopeptidase in the Venus Flytrap Digestion Fluid. *J. Biol. Chem.* **291**, 2271–2287.

Rizzi, C., Mainente, F., Pasini, G., Simonato, B., 2016. Hidden exogenous proteins in wine: problems, methods of detection and related legislation-a review. *Czech J. Food Sci.* **34**, 93-104.

Robins, R.J., Juniper, B.E., 1980. The secretory cycle of Dionaea muscipula Ellis. II. Storage and synthesis of the secretory proteins. *New Phytol.* **86**, 297–311.

Robinson, A.L., Adams, D.O., Boss, P.K., Heymann, H., Solomon, P.S., Trengove, R.D., 2012. Influence of geographic origin on the sensory characteristics and wine composition of Vitis vinifera cv. Cabernet Sauvignon wines from Australia. *Am. J. Enol. Vitic.* **63**, 467-476.

Robles, L.M., Deslauriers, S.D., Alvarez, A.A., Larsen, P.B., 2012. A loss-of-function mutation in the nucleoporin AtNUP160 indicates that normal auxin signalling is required for a proper ethylene response in Arabidopsis. *J. Exp. Bot.* **63**, 2231–2241.

Ronald, J., Davis, S.J., 2019. Focusing on the nuclear and subnuclear dynamics of light and circadian signalling. *Plant Cell Environ.* **42**, 2871-2884.

Rothballer, A., Kutay, U., 2013. The diverse functional LINCs of the nuclear envelope to the cytoskeleton and chromatin. *Chromosoma* **122**, 415–429.

Rothkamm, K., Barnard, S., Moquet, J., Ellender, M., Rana, Z., Burdak-Rothkamm, S., 2015. DNA damage foci: Meaning and significance. *Environ. Mol. Mutagen.* **56**, 491–504.

Rottloff, S., Miguel, S., Biteau, F., Nisse, E., Hammann, P., Kuhn, L., Chicher, J., Bazile, V., Gaume, L., Mignard, B., Hehn, A., Bougard, F., 2016. Proteome analysis of digestive fluids in Nepenthes pitchers. *Ann. Bot.* **117**, 479–495.

Rowe, J.D., Harbertson, J.F., Osborne, J.P., Freitag, M., Lim, J., Bakalinsky, A.T., 2010. Systematic identification of yeast proteins extracted into model wine during aging on the yeast lees. *J. Agric. Food Chem.* **58**, 2337-2346.

Rzagalinski, I., Volmer, D.A., 2017. Quantification of low molecular weight compounds by MALDI imaging mass spectrometry–A tutorial review. *Biochim. Biophys. Acta - Proteins Proteom.* **1865**, 726-739.

Řepka, V., Čarná, M., Pavlovkin, J., 2013. Methyl jasmonate-induced cell death in grapevine requires both lipoxygenase activity and functional octadecanoid biosynthetic pathway. *Biologia* **68**, 896-903.

Saganová, M., Bokor, B., Stolárik, T., Pavlovič, A., 2018. Regulation of enzyme activities in carnivorous pitcher plants of the genus Nepenthes. *Planta* **248**, 451-464.

Saito, S., Odagiri, M., Furuya, S., Suzuki, S., Takayanagi, T., 2011. Inhibitory effect of chitinases isolated from Semillon grapes (Vitis vinifera) on growth of grapevine pathogens. *J. Plant Biochem. Biotechnol.* **20**, 47-54.

Salminen, T.A., Blomqvist, K., Edqvist, J., 2016. Lipid transfer proteins: classification, nomenclature, structure, and function. *Planta* **244**, 971-997.

Sandler, B., Murakami, M., Clardy, J., 1998. Atomic structure of the trypsin− aeruginosin 98-B complex. *J. Am. Chem. Soc.* **120**, 595-596.

Sánchez-Vallet, A., Mesters, J.R., Thomma, B.P.H.J., 2015. The battle for chitin recognition in plant-microbe interactions. *FEMS Microbiol. Rev.* **39**, 171–183.

Sanggaard, K.W., 2014. Secreted major Venus flytrap chitinase enables digestion of Arthropod prey. *Biochim. Biophys. Acta - Proteins Proteom.* **1844**, 374–383.

Sarmento, M.R., Oliveira, J.C., Slatner, M., Boulton, R.B., 2000. Influence of intrinsic factors on conventional wine protein stability tests. *Food Control* **11**, 423-432.

Sarry, J.E., Sommerer, N., Sauvage, F.X., Bergoin, A., Rossignol, M., Albagnac, G., Romieu, C., 2004. Grape berry biochemistry revisited upon proteomic analysis of the mesocarp. *Proteomics* **4**, 201-215.

Sauvage, F.X., Bach, B., Moutounet, M., Vernhet, A., 2010. Proteins in white wines: Thermo-sensitivity and differential adsorbtion by bentonite. *Food Chem.* **118**, 26-34.

Scala, J., Lott, K., Schwab, D.W., Semersky, F.E., 1969. Digestive secretion of Dionaea muscipula (Venus's flytrap). *Plant Physiol.* **44**, 367–371.

Simon, L., Voisin, M., Tatout, C., Probst, A.V., 2015. Structure and function of centromeric and pericentromeric heterochromatin in Arabidopsis thaliana. *Front. Plant Sci.* **6**, 1049.

Shaw, J., Love, A.J., Makarova, S.S., Kalinina, N.O., Harrison, B.D., Taliansky, M.E., 2014. Coilin, the signature protein of Cajal bodies, differentially modulates the interactions of plants with viruses in widely different taxa. *Nucleus* **5**, 85–94.

Shaw, P.J., Brown, J.W., 2004. Plant nuclear bodies. *Curr. Opin. Plant Biol.* **7**, 614-620.

Sheridan, M.K., Elias, R.J., 2015. Exogenous acetaldehyde as a tool for modulating wine color and astringency during fermentation. *Food Chem.* **177**, 17-22.

Schäd, S.G., Trcka, J., Vieths, S., Scheurer, S., Conti, A., Bröcker, E.B., Trautmann, A., 2005. Wine anaphylaxis in a German patient: IgE-mediated allergy against a lipid transfer protein of grapes. *Int. Arch. Allergy Immunol.* **136**, 159-164.

Scherzer, S., Böhm, J., Krol, E., Shabala, L., Kreuzer, I., Larisch, C., Bemm, F., Al-Rasheid, K.A.S., Shabala, S., Rennenberg, H., Neher, E., Hedrich, R., 2015. Calcium sensor kinase activates potassium uptake systems in gland cells of Venus flytraps. *Proc. Natl. Acad. Sci. U.S.A.* **112**, 7309-7314.

Scherzer, S., Krol, E., Kreuzer, I., Kruse, J., Escalante-Perez, M., Karl, F., Müller, T., Rennenberg, H., Al-Rascheid, K., A.S., Neher, E., Hedrich, R., 2013. The Dionaea muscipula ammonium channel DmAMT1 provides NH4+ uptake associated with Venus flytrap's prey digestion. *Curr. Biol.* **23**, 1649–1657.

Schubert, I., 2007. Chromosome evolution. *Curr. Opin. Plant Biol.* **10**, 109-115.

Schubert, V., 2009. SMC proteins and their multiple functions in higher plants. *Cytogenet. Genome Res.* **124**, 202-214.

Schulze, W., Frommer, W.B., Ward, J.M., 1999. Transporters for ammonium, amino acids and peptides are expressed in pitchers of the carnivorous plantNepenthes. *Plant J.* **17**, 637–646.

Schulze, W.X., Sanggaard, K.W., Kreuzer, I., Knudsen, A.D., Bemm, F., Thøgersen, I.B., Brautigam, A., Thomsen, L.R., Schliesky, S., Dyrlund, T.F., Escalante-Perez, M., Becker, D., Schultz, J., Karring, H., Weber, A., Hojrup, P., Hendrich, R., Enghild, J.J., 2012. The Protein Composition of the Digestive Fluid from the Venus Flytrap Sheds Light on Prey Digestion Mechanisms. *Mol. Cell Proteomics* **11**, 1306–1319.

Siebert, K.J., Carrasco, A., Lynn, P.Y., 1996. Formation of protein−polyphenol haze in beverages. *J. Agric. Food Chem.* **44**, 1997-2005.

Simpson, R.F., Sefton, M.A., 2007. Origin and fate of 2, 4, 6-trichloroanisole in cork bark and wine corks. *Aust. J. Grape Wine Res.* **13**, 106-116.

Singhal, N., Kumar, M., Kanaujia, P.K., Virdi, J.S., 2015. MALDI-TOF mass spectrometry: an emerging technology for microbial identification and diagnosis. *Front. Microbiol.* **6**, 791.

Siuti, N., Kelleher, N., L., 2007. Decoding protein modifications using top-down mass spectrometry. *Nat. Methods* **4**, 817–821.

Smith, L.M., Kelleher, N.L., 2013. Proteoform: a single term describing protein complexity. *Nat. Methods* **10**, 186-187.

Smith, P.E., Krohn, R.I., Hermanson, G.T., Mallia, A.K., Gartner, F.H., Provenzano, M., Fujimoto, E.K, Goeke, N.M., Olson, B.J, Klenk, D.C., 1985. Measurement of protein using bicinchoninic acid. *Anal. Biochem.* **150**, 76-85.

Smith, R.L., Shaw, E., 1969. Pseudotrypsin: a modified bovine trypsin produced by limited autodigestion. *J. Biol. Chem.* **244**, 4704-4712.

Snowdon, E.M., Bowyer, M.C., Grbin, P.R., Bowyer, P.K., 2006. Mousy off-flavor: a review. *J. Agric. Food Chem.* **54**, 6465-6474.

Solovei, I., Wang, A.S., Thanisch, K., Schmidt, C.S., Krebs, S., Zwerger, M., Cohen, T.V., Devys, D., Foisner, R., Peichl, L., Hermann, H., Blum, H., Engelkamp, D., Stewart, C.L., Leonhart, H., Joffe, B., 2013. LBR and Lamin A/C Sequentially Tether Peripheral Heterochromatin and Inversely Regulate Differentiation. *Cell* **152**, 584–598.

Song, L., Chen, Y., Du, Y., Wang, X., Guo, X., Dong, J., Xiao, D., 2017. Saccharomyces cerevisiae proteinase A excretion and wine making. *World J. Microbiol. Biotechnol.* **33**, 1-12.

Sperschneider, J., Catanzariti, A.M., DeBoer, K., Petre, B., Gardiner, D.M., Singh, K. B., Dodds, P.N., Taylor, J.M., 2017. LOCALIZER: subcellular localization prediction of both plant and effector proteins in the plant cell. *Sci. Rep.* **7**, 1-14.

Spronk, C.A., Tessari, M., Kaan, A.M., Jansen, J.F., Vermeulen, M., Stunnenberg, H. G., Vuister, G.W., 2000. The Mad1–Sin3B interaction involves a novel helical fold. *Nat. struct. biol.* **7**, 1100-1104.

Staples, M., Barofsky, D., 2004. Complementary Use of MALDI and ESI for the HPLC-MS/MS Analysis of DNA-Binding Proteins. *Anal. Chem.* **76**, 5423-5430.

Stephenson, P., Hogan, J., 2006. Cloning and Characterization of a Ribonuclease, a Cysteine Proteinase, and an Aspartic Proteinase from Pitchers of the Carnivorous Plant Nepenthes ventricosa Blanco. *Int. J. Plant Sci.* **167**, 239–248.

Suckau, D., Cornett, D.S., 1998. Protein sequencing by ISD and PSD MALDI-TOF ms. *Analusis* **26**, 18-21.

Suckau, D., Resemann, A., Schuerenberg, M., Hufnagel, P., Franzen, J., Holle, A., 2003. A novel MALDI LIFT-TOF/TOF mass spectrometer for proteomics. *Anal. Bioanal. Chem.* **376**, 952-965.

Sui, Y., McRae, J.M., Wollan, D., Muhlack, R.A., Godden, P., Wilkinson, K.L., 2021. Use of ultrafiltration and proteolytic enzymes as alternative approaches for protein stabilisation of white wine. *Aust. J. Grape Wine Res.* **27**, 234-245.

Swaney, D.L., Wenger, C.D., Coon, J.J., 2010. Value of using multiple proteases for large-scale mass spectrometry-basedproteomics. *J. Proteome Res.* **9**, 1323–1329.

Šebela, M., Štosová, T.Á., Havliš, J., Wielsch, N., Thomas, H., Zdráhal, Z., Shevchenko, A., 2006. Thermostable trypsin conjugates for high-throughput proteomics: synthesis and performance evaluation. *Proteomics* **6**, 2959-2963.

Takahashi, K., Nishii, W., Shibata, C., 2012. The digestive fluid of Drosera indica contains a cysteine endopeptidase ("droserain") similar to dionain from Dionaea muscipula. *Carniv. Pl. Newslett.* **41**, 132-134.

Takahashi, K., Suzuki, T., Nishii, W., Kubota, K., Shibata, S., Isobe, T., Dohmae, N., 2011. A Cysteine Endopeptidase ("Dionain") Is Involved in the Digestive Fluid of Dionaea muscipula (Venus's Fly-trap). *Biosci. Biotechnol. Biochem.* **75**, 346–348.

Tamura, K., Hara-Nishimura, I., 2011. Involvement of the nuclear pore complex in morphology of the plant nucleus. *Nucleus* **2**, 168–172.

Tamura, K., Hara-Nishimura, I., 2014. Functional insights of nucleocytoplasmic transport in plants. *Front. Plant Sci.* **5**, 118.

Tanaka, K., 1987. Detection of high mass molecules by laser desorption time-of-flight mass spectrometry. In *Proceedings of the Second Japan-China Joint Symposium on Mass Spectrometry*, 1987.

Tang, Y., Huang, A., Gu, Y., 2020. Global profiling of plant nuclear membrane proteome in Arabidopsis. *Nat. Plants* **6**, 838–847.

Tattersall, D.B., Van Heeswijck, R., Hoj, P.B., 1997. Identification and characterization of a fruit-specific, thaumatin-like protein that accumulates at very high levels in conjunction with the onset of sugar accumulation and berry softening in grapes. *Plant Physiol.* **114**, 759-769.

ten Have, A., Breuil, W.O., Wubben, J.P., Visser, J., van Kan, J.A., 2001. Botrytis cinerea endopolygalacturonase genes are differentially expressed in various plant tissues. *Fungal Genet. Biol.* **33**, 97-105.

Thomas, A., Charbonneau, J.L., Fournaise, E., Chaurand, P., 2012. Sublimation of new matrix candidates for high spatial resolution imaging mass spectrometry of lipids: enhanced information in both positive and negative polarities after 1, 5-diaminonapthalene deposition. *Anal. Chem.* **84**, 2048-2054.

Thomas, B., Akoulitchev, A.V., 2006. Mass spectrometry of RNA. *Trends Biochem. Sci.* **31**, 173–181.

Thomson, J.J., 1911. XXVI. Rays of positive electricity. *Lond. Edinb. Dublin philos. mag. j. sci.* **21**, 225-249.

Tokunaga, T., Dohmura, A., Takada, N., Ueda, M., 2004. Cytotoxic Antifeedant fromDionaea muscipulaEllis: A Defensive Mechanism of Carnivorous Plants against Predators. *Bull. Chem. Soc. Jpn.* **77**, 537–541.

Tsiatsiani, L., Heck, A.J.R., 2015. Proteomics beyond trypsin. *FEBS J.* **282**, 2612–2626.

Tuteja, N., Tran, N.Q., Dang, H.Q., Tuteja, R. 2011. Plant MCM proteins: role in DNA replication and beyond. *Plant Mol. Biol.* **77**, 537-545.

Tyanova, S., Temu, T., Sinitcyn, P., Carlson, A., Hein, M.Y., Geiger, T., Mann, M., Cox, J., 2016. The Perseus computational platform for comprehensive analysis of (prote)omics data. *Nat. Methods* **13**, 731–740

Ugliano, M., Fedrizzi, B., Siebert, T., Travis, B., Magno, F., Versini, G., Henschke, P.A., 2009. Effect of nitrogen supplementation and Saccharomyces species on hydrogen sulfide and other volatile sulfur compounds in Shiraz fermentation and wine. *J. Agric. Food Chem.* **57**, 4948-4955.

Unhelkar, M.H., Duong, V.T., Enendu, K.N., Kelly, J.E., Tahir, S., Butts, C.T., Martin, R.W., 2017. Structure prediction and network analysis of chitinases from the Cape sundew, Drosera capensis. *Biochim. Biophys. Acta - Gen. Subj.* **1861**, 636–643.

Valaskovic, G.A., Kelleher, N.L., McLafferty, F.W., 1996. Attomole protein characterization by capillary electrophoresis-mass spectrometry. *Science* **273**, 1199-1202.

Valentine, N., Wunschel, S., Wunschel, D., Petersen, C., Wahl, K., 2005. Effect of culture conditions on microorganism identification by matrix-assisted laser desorption ionization mass spectrometry. *Appl. Environ. Microbiol.* **71**, 58-64.

van Rensberg, P., Pretorius, I.S., 2000. Enzymes in Winemaking: Harnessing Natural Catalysts for Efficient Biotransf ormations-A Review. *S. Afr. J. Enol. Vitic.* **21**, 52-73.

van Sluyter, S.C., Marangon, M., Stranks, S.D., Neilson, K.A., Hayasaka, Y., Haynes, P.A., Menz, I.R., Waters, E.J., 2009. Two-step purification of pathogenesis-related proteins from grape juice and crystallization of thaumatin-like proteins. *J. Agric. Food Chem.* **57**, 11376-11382.

van Sluyter, S.C., Warnock, N.I., Schmidt, S., Anderson, P., Van Kan, J.A., Bacic, A., Waters, E.J., 2013. Aspartic acid protease from Botrytis cinerea removes haze-forming proteins during white winemaking. *J. Agric. Food Chem.* **61**, 9705-9711.

van Sluyter, S.C., McRae, J.M., Falconer, R.J., Smith, P.A., Bacic, A., Waters, E.J., Marangon, M., 2015. Wine protein haze: Mechanisms of formation and advances in prevention. *J. Agric. Food Chem.* **63**, 4020-4030.

Vandermarliere, E., Mueller, M., Martens, L., 2013. Getting intimate with trypsin, the leading protease in proteomics. *Mass Spectrom. Rev.* **32**,453–462.

Vanrell, G., Canals, R., Esteruelas, M., Fort, F., Canals, J.M., Zamora, F., 2007. Influence of the use of bentonite as a riddling agent on foam quality and protein fraction of sparkling wines (Cava). *Food Chem.* **104**, 148-155.

Vaysse, P.M., Heeren, R.M., Porta, T., Balluff, B., 2017. Mass spectrometry imaging for clinical research–latest developments, applications, and current limitations. *Analyst* **142**, 2690-2712.

Vegas, A., Scheremetjew, M., Yong, S.Y., Lopez, R., Hunter, S., 2014, InterProScan 5: genome-scale protein function classification. *Bioinformatics* **30**, 1236–1240.

Verna, J., Lodder, A., Lee, K., Vagts, A., Ballester, R., 1997. A family of genes required for maintenance of cell wall integrity and for the stress response in Saccharomyces cerevisiae. *Proc. Natl. Acad. Sci. U.S.A.* **94**, 13804-13809.

Vélez-Bermúdez, I.C., Schmidt, W., 2021. Chromatin enrichment for proteomics in plants (ChEP-P) implicates the histone reader ALFIN-LIKE 6 in jasmonate signalling. *BMC Genom.* **22**, 845.

Vilela-Moura, A., Schuller, D., Mendes-Faia, A., Silva, R.D., Chaves, S.R., Sousa, M.J., Côrte-Real, M., 2011. The impact of acetate metabolism on yeast fermentative performance and wine quality: reduction of volatile acidity of grape musts and wines. *Appl. Microbiol. Biotechnol.* **89**, 271-280.

Vincent, D., Wheatley, M.D., Cramer, G.R., 2006. Optimization of protein extraction and solubilization for mature grape berry clusters. *Electrophoresis* **27**, 1853-1865.

Vincenzi, S., Bierma, J., Wickramasekara, S.I., Curioni, A., Gazzola, D., Bakalinsky, A.T., 2014. Characterization of a grape class IV chitinase. *J. Agric. Food Chem.* **62**, 5660-5668.

Vincenzi, S., Marangon, M., Tolin, S., Curioni, A., 2011. Protein evolution during the early stages of white winemaking and its relations with wine stability. *Aust. J. Grape Wine Res.* **17**, 20-27.

Vincenzi, S., Polesani, M., Curioni, A., 2005. Removal of specific protein components by chitin enhances protein stability in a white wine. *Am. J. Enol. Vitic.* **56**, 246-254.

Vogel, A., Schilling, O., Späth, B., Marchfelder, A., 2005. The tRNase Z family of proteins: physiological functions, substrate specificity and structural properties. *Biol. Chem.* **386**, 1253-1264

Vogt, E.I., Kupfer, V.M., Vogel, R.F., Niessen, L., 2016. A novel preparation technique of red (sparkling) wine for protein analysis. *EuPA Open Proteom.* **11**, 16-19.

Waidmann, S., Kusenda, B., Mayerhofer, J., Mechtler, K., Jonak, C., 2014. A DEK Domain-Containing Protein Modulates Chromatin Structure and Function in Arabidopsis. *Plant Cell* **26**, 4328–4344.

Wang, C.C., Lai, Y.H., Ou, Y.M., Chang, H.T., Wang, Y.S., 2016. Critical factors determining the quantification capability of matrix-assisted laser desorption/ionization–time-of-flight mass spectrometry. *Philos. Trans. R. Soc. A* **374**, 20150371.

Wang, J., Mei, J., Ren, G., 2019. Plant microRNAs: biogenesis, homeostasis, and degradation. *Front. Plant Sci.* **10**, 360.

Wang, X., Jiang, B., Gu, L., Chen, Y., Mora, M., Zhu, M., Noory, E., Wang, Q., Lin, Ch., 2021. A photoregulatory mechanism of the circadian clock in Arabidopsis. *Nat. Plants* **7**, 1397–1408.

Warringer, J., Zörgö, E., Cubillos, F.A., Zia, A., Gjuvsland, A., Simpson, J.T., Forsmark, A., Durbin, R., Omholt, S.W., Louis, E.J., Liti, G., Moses, A., Blomberg, A., 2011. Trait variation in yeast is defined by population history. *PLoS Genet.* **7**, e1002111.

Waters, E.J., Alexander, G., Muhlack, R., Pocock, K.F., Colby, C., O'neill, B.K., Hoj, P.B., Jones, P., 2005. Preventing protein haze in bottled white wine. *Aust. J. Grape Wine Res.* **11**, 215-225.

Weber, P., Steinhart, H., Paschke, A., 2009. Determination of the bovine food allergen casein in white wines by quantitative indirect ELISA, SDS− PAGE, western blot and immunostaining. *J. Agric. Food Chem.* **57**, 8399-8405.

Webster, J., Oxley, D., 2012. Protein identification by MALDI-TOF mass spectrometry. In *Chemical Genomics and Proteomics*, (pp. 227-240). Humana Press.

Wigand, P., Tenzer, S., Schild, H., Decker, H., 2009. Analysis of protein composition of red wine in comparison with rosé and white wines by electrophoresis and high-pressure liquid chromatography−mass spectrometry (HPLC-MS). *J. Agric. Food Chem.* **57**, 4328-4333.

Wilkins, M.R., Sanchez, J.C., Gooley, A.A., Appel, R.D., Humphery-Smith, I., Hochstrasser, D.F., Williams, K.L., 1996. Progress with proteome projects: why all proteins expressed by a genome should be identified and how to do it. *Biotechnol. Genet. Eng. Rev.* **13**, 19-50.

Witt, H., Luck, W., Becker, M., 1999. A signal peptide cleavage site mutation in the cationic trypsinogen gene is strongly associated with chronic pancreatitis. *Gastroenterology* **117**, 7-10.

Wunschel, S.C., Jarman, K.H., Petersen, C.E., Valentine, N.B., Wahl, K.L., Schauki, D., Jakman J., Nelson C.P., White, E., 2005. Bacterial analysis by MALDI-TOF mass spectrometry: An inter-laboratory comparison. *J. Am. Soc. Mass Spectrom.* **16**, 456–462.

Yamada, K., Matsushima, R., Nishimura, M., Hara-Nishimura, I., 2001. A slow maturation of a cysteine protease with a granulin domain in the vacuoles of senescing Arabidopsis leaves. *Plant Physiol.* **127**, 1626.

Yamada, M., Goshima, G., 2018. The KCH kinesin drives nuclear transport and cytoskeletal coalescence to promote tip cell growth in Physcomitrella patens. *Plant Cell* **30**, 1496-1510.

Yan, X., Qiao, H., Zhang, X., Guo, C., Wang, M., Wang, Y., Wang, X., 2017. Analysis of the grape (Vitis vinifera L.) thaumatin-like protein (TLP) gene family and demonstration that TLP29 contributes to disease resistance. *Sci. Rep.* **7**, 1-14.

Yang, J., Caprioli, R.M., 2011. Matrix sublimation/recrystallization for imaging proteins by mass spectrometry at high spatial resolution. *Anal. Chem.* **83**, 5728-5734.

Yates, J.R., 1998. Mass spectrometry and the age of the proteome. *J. Mass Spectrom.* **33**, 1-19.

Yergey, A.L., Coorssen, J.R., Backlund, P.S., Blank, P.S., Humphrey, G.A., Zimmerberg, J., Campbell, J.M., Vestal, M.L., 2002. De novo sequencing of peptides using MALDI/TOF-TOF. *J. Am. Soc. Mass Spectrom.* **13**, 784-791.

Yin, X., Komatsu, S., 2015. Quantitative proteomics of nuclear phosphoproteins in the root tip of soybean during the initial stages of flooding stress. *J. Proteom.* **119**, 183–195.

Younes, B., Cilindre, C., Villaume, S., Parmentier, M., Jeandet, P., Vasserot, Y., 2011. Evidence for an extracellular acid proteolytic activity secreted by living cells of Saccharomyces cerevisiae PlR1: impact on grape proteins. *J. Agric. Food Chem.* **59**, 6239-6246.

Yu, C.S., Cheng, C.W., Su, W.C., Chang, K.C., Huang, S.W., Hwang, J.K., Lu, Ch-H., 2014. CELLO2GO: a web server for protein subCELlular LOcalization prediction with functional gene ontology annotation. *PLoS One* **9**, e99368.

Zemach, A., Kim, M.Y., Hsieh, P.-H., Coleman-Derr, D., Eshed-Williams, L., Thao, K., Harner, S.L., Zilberman, D., 2013. The Arabidopsis Nucleosome Remodeler DDM1 Allows DNA Methyltransferases to Access H1-Containing Heterochromatin. *Cell* **153**, 193–205.

Zenobi, R., Knochenmuss, R., 1998. Ion formation in MALDI mass spectrometry. *Mass Spectrom. Rev.* **17**, 337-366.

Zhang, L., van Kan, J.A., 2013. 14 Pectin as a barrier and nutrient source for fungal plant pathogens. In *Agricultural Applications* (pp. 361-375). Springer, Berlin, Heidelberg.

Zheng, T., Zhang, K., Sadeghnezhad, E., Jiu, S., Zhu, X., Dong, T., Liu, Z., Guan, L., Jia, H., Fang, J., 2020. Chitinase family genes in grape differentially expressed in a manner specific to fruit species in response to Botrytis cinerea. *Mol. Biol. Rep.* **47**, 7349-7363.

Zhong, X.Y., Holzgreve, W., 2009. MALDI-TOF MS in prenatal genomics. *Transfus. Med. Hemotherapy* **36**, 263-272.

Zhou, X., Graumann, K., Wirthmueller, L., Jones, J.D., Meier, I., 2014. Identification of unique SUN-interacting nuclear envelope proteins with diverse functions in plants. *J Cell Biol.* **205**, 677-692.

Zhu, F.M., Du, B., Li, J., 2014. Aroma enhancement and enzymolysis regulation of grape wine using β-glycosidase. *Food Sci. Nutr.* **2**, 139-145.

Zullo, J.M., Demarco, I.A., Piqué-Regi, R., Gaffney, D.J., Epstein, C.B., Spooner, C.J., Luperchio, T.R., Bernstein, B.E., Pritchard, J.K., Reddy, K.L., Singh, H., 2012. DNA Sequence-Dependent Compartmentalization and Silencing of Chromatin at the Nuclear Lamina. *Cell* **149**, 1474-1487.

ŽIVOTOPIS

Osobní údaje

Jméno: Mgr. Zdeněk Perutka
Datum narození: 7. 10. 1990
Adresa: Nádražní 481, Bystřice pod Hostýnem, Česká republika
Tel. č.: +420 733 612 263
E-mail: perutka.zdenek@seznam.cz

Vzdělání

2015 – dosud	Univerzita Palackého v Olomouci Fakulta: Přírodovědecká Studijní obor: Biochemie / doktorské studium
2013 – 2015	Univerzita Palackého v Olomouci Fakulta: Přírodovědecká Studijní obor: Biochemie / magisterské studium
2010 – 2013	Univerzita Palackého v Olomouci Fakulta: Přírodovědecká Studijní obor: Biochemie / bakalářské studium
2002 – 2010	Gymnázium L. Jaroše, Holešov

Pracovní zkušenosti

01/2016 – 01/2022 Univerzita Palackého v Olomouci, Přírodovědecká fakulta
Oddělení biochemie proteinů a proteomiky, Centrum regionu Haná
pro biotechnologický a zemědělský výzkum (1.1.2016 – 31.12.2020)
Katedra biochemie (1.1.2021 – 31.1.2022)
Pozice: vědecký akademický pracovník / Ph.D student

Stáže

10-12/2016 **–** Institut chemických technologií a analytiky, Technická univerzita ve Vídni

11-12/2017 – Oddělení Rostlinné Cytologie a Embryologie**,** Jagellonská univerzita, Krakov

Publikace

Perutka Z., Kaduchová K., Chamrád I., Beinhauer J., Lenobel R., Petrovská B., Bergougnoux V., Vrána J., Pecinka A., Doležel J., Šebela M. (2021) Proteome analysis of condensed barley mitotic chromosomes, Front. Plant Sci. 12, 723674.

Perutka Z., Voženílek V., Šebela M. (2021) Wine contaminations and frauds from the bioanalytical and biochemical points of view. In: Cifuentes, A. (Ed.), Comprehensive Foodomics, vol. 3. Elsevier, pp. 104–116. ISBN: 9780128163955.

Perutka Z., Šebela M. (2020) Mass spectrometry of peptides and proteins using digestion by a grape cysteine protease at pH 3. J. Mass Spectrom. 55, e4444.

Perutka Z., Šufeisl M., Strnad M., Šebela M. (2019) High-proline proteins in experimental hazy white wine produced from partially botrytized grapes. Biotechnol. Appl. Biochem. 66 (3), 398-411.

Perutka Z., Šebela M. (2018) Chapter 2 - Basis of mass spectrometry: Technical variants. In: The Use of Mass Spectrometry Technology (MALDI-TOF) in Clinical Microbiology, Fernando Cobo (Ed.), Academic Press. ISBN 978-0-12-814451-0, pp. 19-45.

Perutka Z., Šebela M. (2018) Pseudotrypsin: a little known trypsin proteoform. Molecules 23, 2637.

Krausko M, **Perutka Z**, Šebela M, Šamajová O, Šamaj J, Novák O, Pavlovič A (2017) The role of electrical and jasmonate signaling in recognition of captured prey in carnivorous sundew plant Drosera capensis. New Phytol. 213, 1818-1835.

Příspěvky na konferencích

Perutka Z., Šufeisl M., Strnad M., Šebela M., Wine proteins –hidden markers of the winemaking process quality? 30th MassSpec Forum Vienna, 19. 2.– 20. 2. 2019, Vídeň, poster č. 13, prezentace formou plakátového sdělení Z. Perutka

Perutka Z., Wine proteins – hidden markers of the winemaking process quality? The Eighth Annual Conference of the Czech Society for Mass Spectrometry, 27. 3 -29. 3. 2019, Olomouc, přednáška ThO-008, prezentace formou přednášky Z. Perutka

Perutka Z., Lenobel R., Šebela M., Grape proteins rich in proline and their effect on wine turbidity, Green for Good V., 10. 6. – 13. 6. 2019, Olomouc, poster č. 63, prezentace formou plakátového sdělení Z. Perutka

Perutka Z., Lenobel R., Šebela M. Pseudotrypsin application in proteomics. 29th MassSpec Forum Vienna, 19. 2.– 21. 2. 2018, Vídeň, poster č. 8

Perutka Z., Lenobel R., Petrovská B., Jeřábková H., Vrána J., Doležel J., Šebela M., Pseudotrypsin application in proteomics, COST 16212, INDEPTH (Impact of

Nuclear Domains On Gene Expression and Plant Traits) Kick Off Meeting, 11. 3.–14. 3. 2018, Clermont-Ferrand, prezentace formou plakátového sdělení Z. Perutka

Perutka Z., Lenobel R, Šebela M., The use of pseudotrypsin in mass spectrometry-based proteomics, 36th Informal Meeting on Mass Spectrometry, 6. 5. - 9. 5. 2018, Kőszeg, prezentace formou přednášky M. Šebela

Perutka Z., Pavlovič A., Šebela M., Green For Good IV, Biotechnology of Plant Products, 19 – 22. 6. 2017, Olomouc, Proteins of Cape sundew deadly glue: from plant defense to killing weapon, poster č. 18, prezentace formou plakátového sdělení Z. Perutka

Perutka Z., Šufeisl M., Strnad M., Šebela M. Protein profiling of a white wine produced from grapes damaged by Botrytis cinerea. The 17th European Biotechnology Congress, 3 – 6. 7. 2016, Krakov, poster P26-2 (příspěvek č. 678), prezentace formou plakátového sdělení Z. Perutka

Pedagogická činnost

Výuka předmětu Praktická cvičení z biochemie, KBC/BCHC

Výuka předmětu Experimentální metody biochemie, KBC/EMB

Vedení bakalářské práce – studentka Simona Rakotonaina, název práce: Izolace a charakterizace vybraných proteinů révy vinné (Vitis vinifera), (práce odevzdána 25. 5. 2020, studijní obor Biochemie)

Vedení bakalářské práce – student Aloise Kozubíka, název práce: Zpracování informací z databázových a predikčních softwarových nástrojů pro anotaci necharakterizovaných proteinů pomocí bioinformatických metod, (práce obhájena 14. 6. 2019, studijní obor Bioinformatika)

Oponentura bakalářské práce – studenta Aleše Kvasničky, Extracelulárně sekretované proteiny a peptidy bakterie *Paenibacillus larvae* (obhajoba 12. 6. 2018)

Spolupráce na přípravě a průběhu Letní školy jaderné proteomiky pořádané na pracovišti Oddělení biochemie proteinů a proteomiky CRH a UEB, Olomouc Proteomic Training School v rámci programu INDEPTH COST Action, 9.-12. 7. 2019.

Příloha 1:

Perutka, Z., Šebela, M., 2018. Basis of Mass Spectrometry: Technical Variants. In *The Use of Mass Spectrometry Technology (MALDI-TOF) in Clinical Microbiology* (pp. 19-45). Academic Press.

CHAPTER TWO

Basis of Mass Spectrometry: Technical Variants

Zdeněk Perutka and Marek Šebela
Department of Protein Biochemistry and Proteomics, Centre of the Region Haná for Biotechnological and Agricultural Research, Faculty of Science, Palacký University, Olomouc, Czech Republic

2.1 OVERVIEW

Chapter 2, Basis of Mass Spectrometry: Technical Variants, provides a definition of mass spectrometry (MS) and describes the history of this analytical technique from the very beginning. Then it summarizes basic components of a mass spectrometer, from which namely mass analyzers are further described in detail together with their combinations in hybrid mass spectrometers. Such instruments are designed to perform tandem MS, which has been used in chemistry and biology to identify and quantify compounds. All possible modes of tandem MS are mentioned as well as common ion activation techniques for the fragmentation of gas-phase ions, which is essential and occurs between different stages of mass analysis. Next, separation techniques hyphenated with MS are discussed, namely gas and liquid chromatography (GC and LC, respectively) and capillary electrophoresis (CE). Hyphenated systems are nowadays almost indispensable for investigations of complex biological samples containing proteins, lipids, or metabolites. Mass spectrometry imaging (MSI) is presented as a tool for direct analyses of biological tissues. The chapter is ended by a part devoted to data representation and management with a focus on free and open source software and data formats. The text is accompanied by a list of the cited literature.

2.2 MS: DEFINITION AND BASIC PRINCIPLES

MS is an analytical technique that measures masses of atoms and molecules after their conversion to charged ions by an ionization process.

The Use of Mass Spectrometry Technology (MALDI-TOF) in Clinical Microbiology.
DOI: https://doi.org/10.1016/B978-0-12-814451-0.00002-2

It is applicable to volatile or nonvolatile samples, polar or nonpolar, solid, liquid, or gaseous. Under specific conditions, MS measurements can also reveal structural or quantitative information. With a modern instrumentation of the current period, it is highly sensitive and typically provides a high resolving power and mass accuracy. Mass spectrometric data for the analyzed compounds (ions) are commonly expressed as the mass-to-charge ratio, m/z (the abbreviation should always be typed in italics), which is the mass of the ion divided by the number of its charges [1]. The total charge is $q = ze$, where e is the elementary charge that equals 1.602×10^{-19} coulomb (C). Hence the SI unit for the expression m/q is $\mathrm{kg \cdot C^{-1}}$. In MS practice, however, the dimensionless m/z is used as it is numerically better related to the unified atomic mass unit (u) or dalton (Da). One unified atomic mass unit (1 u) or 1 Da is defined as 1/12 of the mass of a single ^{12}C atom. The Thomson unit (Th) commemorating Sir Joseph J. Thomson [2] has been used only rarely for m/z values; it is now deprecated. The terms mass spectrometer, mass spectrograph, and mass spectroscope should not be confused with each other. They are not synonymous and the latter two represent rather a historical reminiscence [1]. A mass spectroscope differed from a mass specrograph in its construction as the beam of ions was directed onto a phosphor screen and not to a photographic plate (see in the text section on the history of MS, Section 2.3). The term mass spectroscopy is now discouraged due to the possible confusion with light spectroscopy.

Due to its essential properties, MS plays an important role in many fields of human activities including science, medicine, industry, and public safety sector [3]. In physics, it allows to measure data on particles, elements, materials, energy transfers, dynamics of various processes, etc. It is advantageous for evaluating results of theoretical physical predictions and calculations. MS is probably the most versatile analytical technique in chemistry including biochemistry. Chemists profit, for example, from the accurate measurements of atoms and molecules, structural and quantitative analysis of synthetic and natural compounds, drugs, toxins and pollutants, investigating chemicals processes or fundamentals of gas-phase ion chemistry. Chemical compounds, isotopes, as well as isotope ratios may attract interests of geologists, archeologists, or space researchers. MS is always at hand as an analytical tool. For complex real samples, MS is usually coupled with high-resolution separation techniques (e.g., GC, LC or CE). Medicine and life sciences utilize such hyphenated techniques for a simultaneous separation and detection of compounds in mixtures

originating from biological tissues and fluids. MS is applicable for an efficient amino acid sequencing and related identification of peptides and proteins, quantification of proteins, determination of posttranslational protein modifications, analyses of protein–protein interactions, and composition of protein complexes [4]. Also short oligonucleotides can be efficiently sequenced using MS. Biomolecules (e.g., proteins, peptides, lipids, oligosaccharides, and various metabolites) are amenable to MS-based structural characterizations. For proteins as large molecules, there are indirect methods available involving a covalent crosslinking of adjacent parts of the meandering polypeptide chain or deuterium exchange experiments, which uncover solvent-accessible regions of the three-dimensional structure. These structural studies are helpful to discover functional aspect of proteins. Based on acquiring peptide/protein profile mass spectra using intact cells or spores, MS allows identifying microorganisms, which is useful especially for pathogenic species in clinical microbiology. Industrial applications of MS commonly serve for monitoring of process streams, e.g., in the petroleum or pharmaceutical industry. This introductory overview of the applicability of MS is definitely not complete. We may expect that with future developments, MS will expand to yet unexplored territories to offer new perspectives on solving analytical problems.

2.3 A BRIEF EXCURSION TO THE HISTORY OF MS AND RELATED NOBEL PRIZES

For over than 100 years, MS has gradually been introduced into many scientific disciplines as a reliable tool for molecular analysis. In the light of its current wide applicability, it seems interesting that the history of this analytical technique began in the late 19th century in connection with electrical discharges and electrode rays. Eugen Goldstein (1850–1930), a German physicist, was one of early investigators of discharges in rarefied gases and is credited with his contribution to the discovery of proton [5,6]. He was a student of the famous physician and physicist Hermann Ludwig Ferdinand von Helmholtz (1821–94). In 1886, he reported rays in gas discharges under a low pressure, which traveled from the anode to a perforated cathode through channels in the perforation, exactly opposite to the direction of the negatively charged

cathode rays (i.e. electrons) discovered and studied previously by other scientists (Johann Wilhelm Hittorf, Julius Plücker). Goldstein introduced the term "Kanalstrahlen" (canal rays) for the positively charged anode rays. Wilhelm Wien (1864–1928), another student of Helmholtz, discovered that these rays required much stronger magnetic fields to be deflected compared to cathode rays. He constructed a device that separated particles constituting the positive rays according to their charge and mass [3,7]. Today, most people in the field regard Sir Joseph J. Thomson (1856–1940), the discoverer of electron and Cavendish Professor at the University of Cambridge, as the father of MS. He began with studies on canal rays around 1906 when he was awarded the Nobel Prize in Physics for investigations on the conduction of electricity by gases. He noticed that positive rays showed varying masses reflecting the presence of different gases in the discharge. Thomson is credited with his realization that this new technique would play a profound role in the field of chemical analysis [3,8,9]. In the next two decades, the development of MS occurred in connection with the names Aston, Dempster, and Nier [3]. Francis William Aston (1877–1945) was an assistant of Thompson and in 1912 observed the existence of two isotopes of neon (^{20}Ne and ^{22}Ne) [8,9]. This was the first evidence of isotopes of a stable element. Early devices that measured positive ions were called mass spectrographs as they recorded spectra on a photographic plate. Aston constructed more spectrographs with a gradually increasing performance. They comprised two sectors to improve the resolving power: the electric sector provided energy selection and the other one, magnetic sector, allowed mass separation [10]. With the spectrographs, Aston was able to study isotopes of many elements and was awarded the Nobel Prize in Chemistry in 1922. Arthur Jeffrey Dempster (1886–1950), a Canadian–American physicist at the University of Chicago, built the first modern mass spectrometer in 1918 producing ions (homogeneous in energy) also from solid materials [11]. In the 1930s, Dempster built instruments containing both a direction and velocity focusing. His experimental work led finally to the discovery of the uranium isotope ^{235}U [12].

During the 1940s, MS played an important role in the Manhattan Project, a wartime program involving a preparative-scale separation of the fissionable ^{235}U isotope for atomic bombs [3]. Sector mass spectrometers (calutrons) developed by Ernest Orlando Lawrence (1901–58) at the University of California in Berkeley were used in the uranium enrichment plant in Oak Ridge, Tennessee. Alfred Otto Carl Nier (1911–40)

was another American physicist participating in the Manhattan project, yet he contributed considerably to the conversion of MS from a device used primarily for investigating chemical elements and their isotopes to an analytical tool for chemists. He constructed a simple mass spectrometer with a 60-degree-angle magnetic sector. Interestingly, this instrument was soon applied to track metabolic processes in bacteria via carbon dioxide [13]. MS became ultimately recognized by chemists. The first commercial mass spectrometers for the petroleum industry (to analyze the refining process) were available through the Consolidated Engineering Corporation in 1943 [3,14]. MS applications in organic chemistry commenced in the 1950s and became increasingly popular in the 1960s and 1970s [3]. With its continuous development, new mass analyzers were introduced in this period together with new ionization techniques, e.g., chemical ionization (CI). Wolfgang Paul (1913–93), a physicist from Bonn in Germany, introduced the concept of a quadrupole mass analyzer and ion trap to separate ions without a magnetic field [15]. In 1989, he was awarded for this achievement by sharing the Nobel Prize in Physics with Hans Georg Dehmelt, another researcher on ion traps [3].

MS has emerged as a standard tool for investigating organic compounds [4]. In the 1960s, tandem MS was developed [16], which allowed structural analyses based on reading information from fragmentation patterns of dissociated precursor ion (see further in this chapter). The analyses of compounds in complex mixtures have become much more feasible since the introduction of hyphenated techniques: gas chromatography (GC)–MS in the 1960s and LC-MS in the 1970s. However, for a long time, the use of MS for biological samples with fragile and nonvolatile compounds was marginal because of the lack of suitable ionization techniques [3]. To produce ions from compounds such as porphyrins, oligosaccharides, and peptides, fast atom bombardment (FAB) ionization was introduced in 1981 [17], which was outperformed by electrospray ionization (ESI) [18] and matrix-assisted laser desorption/ionization (MALDI) [19,20] at the end of the 1980s. The discovery of the soft ionization techniques (now typically applied to peptides, proteins, and various metabolites) had an enormous impact on the use of MS in biology and new life science disciplines such as proteomics [3]. This was reflected in awarding the Nobel Prize in Chemistry in 2002 to John Bennett Fenn and Koichi Tanaka. The last two decades provided many improvements in MS instrumentation and data systems. Desorption electrospray ionization (DESI) for sampling under ambient conditions [21] or Orbitrap mass analyzer for high-resolution measurements [22] are two examples to be mentioned at this place.

2.4 BASIC COMPONENTS OF A MASS SPECTROMETER

Fig. 2.1 shows a simplistic scheme of a mass spectrometer. Each instrument consists of several major components: (1) an ion source with a sample inlet, (2) a mass analyzer, (3) a detector, and (4) a data recording and processing system. Indispensable parts are also a vacuum system and controlling electronics [3]. The inlet transfers a sample into the ion source, where sample molecules are converted into gas-phase ions. The ionization chamber is kept in a vacuum, which allows the ions to travel to the analyzer by involving a magnetic or electric field force. There are many possibilities how to ionize chemical or biochemical compounds, some of them are introduced in the next part of this chapter. Based on the amount of the transferred energy, there are soft and hard ionization techniques producing ions with low or high internal energy, respectively [23]. Mass analyzer explores and sorts ions with different properties. It can be used for an overall analysis, or it may function as a filter to select only specific ions for the subsequent analysis and detection. Basic principles of mass analyzers include, e.g., magnetic or electric fields to manipulate the trajectory of ions, utilizing differences in their velocities (when measuring the time of passing the distance in a flight tube) or resonance frequencies (when

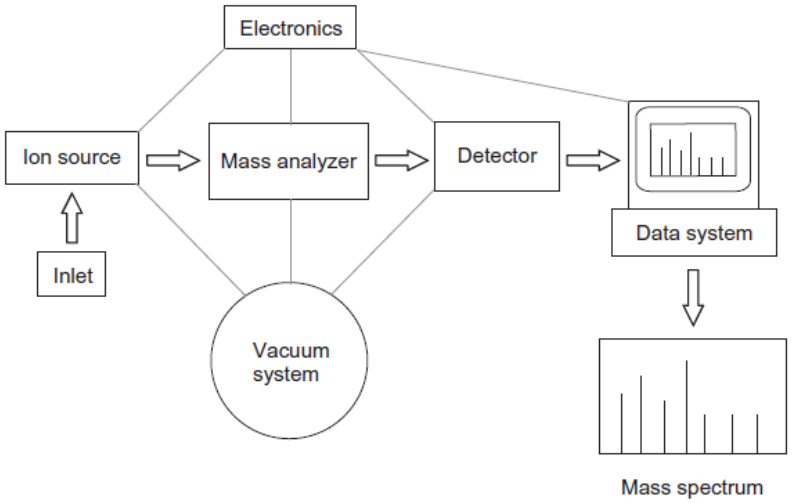

Figure 2.1 *Basic composition of a mass spectrometer. Adapted from Dass C. Basics of mass spectrometry. In: Fundamentals of contemporary mass spectrometry. Hoboken, NJ: John Wiley & Sons, Inc.; 2007. pp. 3–14.*

the ions are trapped inside a trap analyzer and then released) and the principle of ion mobility in the gas phase, which is proportional to the collisional cross section of the respective ion [24,25]. Combining different analyzers inline to separate or fragment and subsequently determine the m/z of the selected ions is a way for how to increase the effectivity and versatility of commercial instruments (see further in this chapter).

The function of a detector is to "visualize" ions, which is done by recording their abundance [25]. There is a recordable electric signal produced, which can be amplified, processed, and displayed by the data system. There are two detector categories: either they detect ions sequentially at one point (focal point detectors) or simultaneously along a plane (focal plane detectors) [25]. Today, common detectors are based on an electron multiplier (EM) [26], which is constructed as a series of discrete dynodes or a continuous dynode (i.e. channel electron multiplier, CEM, in which the surface represents an array of continuous electrodes). Multichannel plate detector is a multichannel version of CEM. The EM principle resides in a multistage electron-releasing cascade initiated by incident ions (coming from the analyzer). In Fourier-transform ion cyclotron resonance (FT-ICR) and Orbitrap mass spectrometers, the detected signal is produced as a record of the image current generated by the oscillating ions inside the analyzer [26]. The most important detector characteristics are its sensitivity, accuracy, resolution, response time, and stability. It is also desirable to have a wide dynamic range and low noise level. The analyzer and detector must be both kept in a high vacuum to work properly. The pressure inside the analyzer reaches around 10^{-8} mbar [3]. To obtain such a value, the spectrometer is equipped with two pumps, typically an auxiliary mechanical membrane or rotary pump, and a turbomolecular pump generating the high vacuum [27]. The analog signals from the detectors are converted into digital information by digitizers. Powerful computers with a large data storage capacity are required for modern MS instrumentation.

2.5 IONIZATION TECHNIQUES IN BIOLOGICAL MS

The classical ionization methods in MS include, for example, electron ionization, CI, photoionization, and FAB. These techniques are not

widely used for studying biological materials but represent pioneering originals, from which many other ionization methods were adapted. The progress in the analysis of biological molecules (including biopolymers such as proteins) has largely been stimulated by the introduction of ESI and MALDI [18–20]. In both cases, the production of ions is achieved with a minimal fragmentation under gentle experimental conditions. A further progress has come with the development of ambient ionization techniques, which facilitate the analysis from real objects outside the mass spectrometer without any extraction of the molecules of interest or pre-treatment of the object itself. DESI and direct analysis in real time (DART) have been reported as the main commercially available representatives of this emerging group [28].

ESI is the most widely used ionization technique for the analysis of samples in a liquid form. In the respective ion source, a sample is ionized at the outlet of the capillary, on which a high voltage is applied (Fig. 2.2). Therefore, these devices can be coupled online to separation techniques in the liquid phase such as LC. The sprayed droplets are dried continuously, and their size is reduced by the stream of a nebulizing gas. The chromatographic solvent (salt-free) carries sample molecules, evaporates rapidly, and the molecules remain inside droplets, which gradually diminish in time. Once the repulsive forces between the molecules overcome the droplet surface tension, it bursts and the charged molecules are released to enter the analyzer [30]. ESI is characteristic by the production of multiply charged ions [18]. This is advantageous for resolving large molecules in mass-range limited analyzers (such as quadrupoles) as they provide lower m/z values. Atmospheric pressure chemical ionization (APCI) represents another soft ionization technique similar to ESI. It is suited to analyze relatively less polar, nonpolar, and heat-stable compounds with masses up to 1500 Da in LC effluents. The ion source contains a heated nebulizer probe, and the emerging droplets and nebulizer gas are converted to a gas stream containing analyte molecules. The ionization region contains a corona discharge. Positive ions of the analyte are formed by a proton transfer from water clusters [31]. The atmospheric pressure photoionization (APPI) is a variation of APCI, in which the initial ionization is achieved by photons [32].

In the case of MALDI (Fig. 2.2), the sample must be first overlaid or mixed with a matrix compound solution and placed onto a conductive target plate. The MALDI probe is introduced into the ion source and irradiated—typically with an ultraviolet (UV) laser. A part of the sample

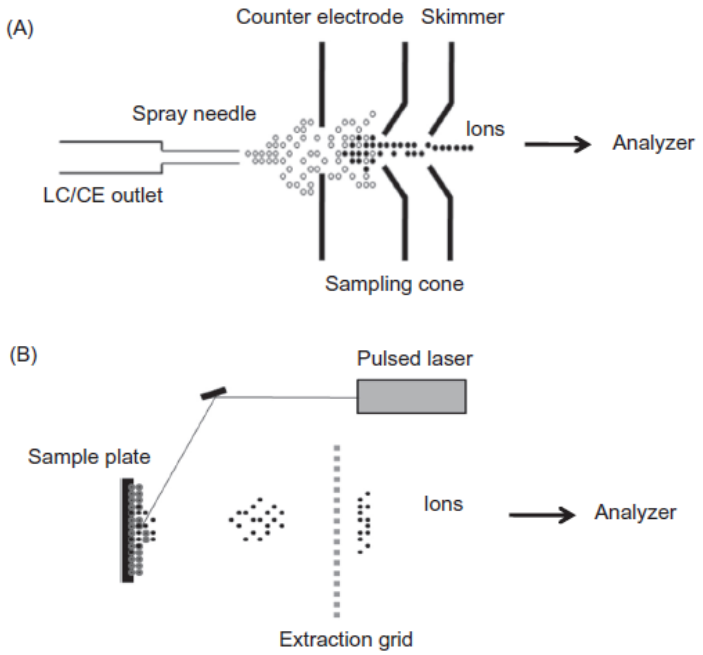

Figure 2.2 ***Common ionization techniques in biological MS.*** (A) The principle of ESI. (B) MALDI. *Adapted from Aebersold R, Mann M. Mass spectrometry-based proteomics. Nature 2003;422:198–207 [29].*

evaporates when the laser energy is absorbed by the matrix. Then the excited matrix ionizes analyte molecules (by definition, analyte is a chemical constituent of a sample that is of interest in an analytical procedure) via a proton transfer. The reverse proton transfer is also possible [33]. This process usually generates singly charged ions. MALDI MS has successfully been applied to the analysis of biomolecules (e.g., proteins, peptides, oligonucleotides, lipids, and sugars), large organic molecules, and polymers [34]. Small organic molecules with a UV-absorbing chromophore such as α-cyano-4-hydroxycinnamic acid (for peptides), 2,5-dihydroxybenzoic acid (for peptides and carbohydrates), sinapinic acid (for proteins), or 3-hydroxypicolinic acid (for oligonucleotides) are routinely used as matrices.

More than 40 ambient ionization technique for MS have been reported, mostly based on the principles of solid–liquid extraction, plasma-based ionization, and non-laser or laser desorption [28]. DESI allows acquiring mass spectra with ordinary samples in their native environment. Small charged solvent droplets are sprayed and directed at the

sample mounted in a holder. As the droplets collide with sample surface structures, ions are released and transferred into a conventional mass spectrometer [35]. DESI is well suited for a rapid tissue analysis [36]. In DART, a gas (typically helium) flows through an electrical discharge, which yields ionized gas, electrons, and excited state atoms/molecules (metastables). With helium, the dominant mechanism of the production of positive analyte ions involves the formation of ionized water clusters and then a proton transfer [37]. DART has been used to analyze a wide range of analytes with a low molecular mass including metabolites, hormones, drugs, synthetic organic compounds, and pigments. Common samples include body fluids or tissues, foods, and beverages.

2.6 MASS ANALYZERS

Mass analyzer is the heart of a mass spectrometer and largely influences the performance of the instrument. Each mass analyzer separates ions according to their m/z ratio and focuses the resolved ions to facilitate their detection. In this regard, the function of this component is similar to the monochromator and lens of a standard spectrophotometer [25]. Currently, several types of mass analyzers are available, which utilize different principles of distinguishing ions. They can be evaluated based on the following parameters (Table 2.1): mass range, resolving power (the ability to distinguish ions that differ only slightly in their mass), mass accuracy (the measured error compared to the accurate mass), sensitivity, speed (how many spectra are acquired in a time unit), linear dynamic range (the range over which ion signal is linear with analyte concentration), transmission efficiency, adaptability (with respect to outfitting with an ionization technique and coupling with a separation technique), and tandem MS capability.

Sector mass spectrometers have been used for the longest time [38]. In principle, they are either single focusing (Fig. 2.3) or double focusing and use a magnetic field or a magnetic plus electrostatic field, respectively. The magnetic analyzer separates ions of different m/z into different beams by bending their trajectories (this is a directional focusing); the electrostatic analyzer selects ions according to their kinetic energy (ions of the same energy are focused at a single point). The double focusing mass

Table 2.1 A comparison of mass analyzers

	Magnetic	Quadrupole	QIT	LIT	TOF	FT-ICR
Mass range (Da)	15,000	4000	4000	4000	Unlimited	$>10^4$
Resolving power	10^2-10^5	4000	10^3-10^4	10^2-10^5	15,000	$>10^6$
Mass accuracy (ppm)	1–5	100	50–100	50–100	5–50	1–5
Abundance sensitivity	10^6-10^9	10^4-10^6	10^3	10^3-10^5	up to 10^6	10^2-10^5
Speed (Hz)	0.1–20	1–20	1–30	1–300	10^1-10^6	$10^{-2}-10^1$
Efficiency (%)	<1	<1–95	<1–50	<1–99	1–100	<1–95
Dynamic range	10^9	10^7	10^2-10^5	10^2-10^5	10^2-10^6	10^2-10^5
MS/MS capability	Excellent	Great	Great	Excellent	Great	Great
LC(CE)-MS adaptability	Poor	Excellent	Excellent	Excellent	Good	Good

Source: Adapted from Dass C. Mass analysis and ion detection. In: Fundamentals of contemporary mass spectrometry. Hoboken, NJ: John Wiley & Sons, Inc.; 2007. pp. 67–117.

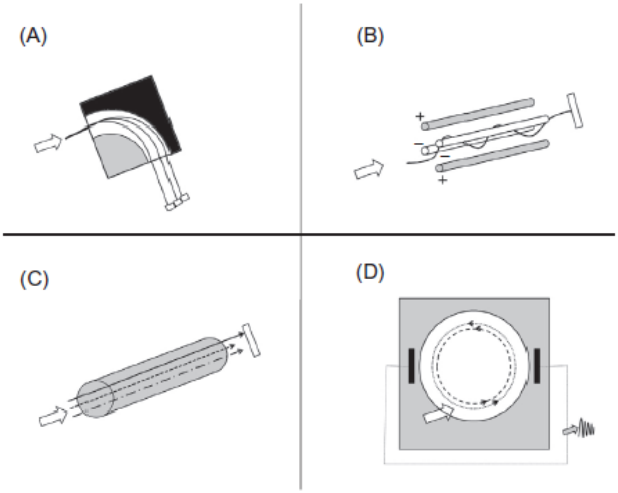

Figure 2.3 ***Mass analyzers.*** (A) Magnetic sector; (B) quadrupole; (C) linear flight tube (TOF); (D) FT-ICR. *Adapted freely from Dass C. Mass analysis and ion detection. In: fundamentals of contemporary mass spectrometry. Hoboken, NJ: John Wiley & Sons, Inc.; 2007. pp. 67–117.*

spectrometers are characterized by a high resolution and mass accuracy [25]. They are suitable, e.g., to study chemical reactions. On the other hand, they are not applicable for a coupling of the instrument with LC. The most common mass analyzer in mass spectrometers is probably a quadrupole [25]. It comprises four parallel metal rods representing electrodes (Fig. 2.3). There are direct current (DC) and radio frequency (RF) potentials applied to these electrodes, which create a high-frequency oscillating electric field. Under a certain combination of defined DC and RF potentials, ions of a specific m/z pass by a stable vibratory motion through the analyzer to reach the detector; other ions follow unstable trajectories and they are deflected. A mass spectrum is then obtained by changing the applied potentials when keeping their ratio constant. Standard quadrupoles provide a relatively low mass range, resolution, and accuracy (Table 2.1). Nevertheless, quadrupole-based instruments can be purchased at a reasonable price; they are sensitive and well suited for ESI and coupling with GC or LC, primarily for the analysis of low-mass compounds in chemistry and biology [39].

A time-of-flight (TOF) mass analyzer separates ions based on the difference in their velocities (Fig. 2.3). It is a long field-free flight tube and has traditionally been combined with a MALDI source [40]. Ions,

produced in pulses, drift in the flight tube, and their velocities are in an inversed function to the square root of the respective m/z values. Classical linear TOF-MS has a poor resolution and is incompatible with continuous ion-beam sources such as electrospray (the latter can be overcome by the use of an orthogonal TOF). To minimize the spatial distribution and kinetic energy spread of ions, and increase resolution in consequence, both delayed extraction and reflectron (reflector) devices are added [25]. The ions formed in the ion source are accelerated by a delayed application of the electrical field to even out their different starting velocities. The reflectron is an energy corrector placed at the end of the flight tube (Fig. 2.4). It consists of ring electrodes with a gradually increased repelling potential, which make a barrier: the higher kinetic energy of an ion,

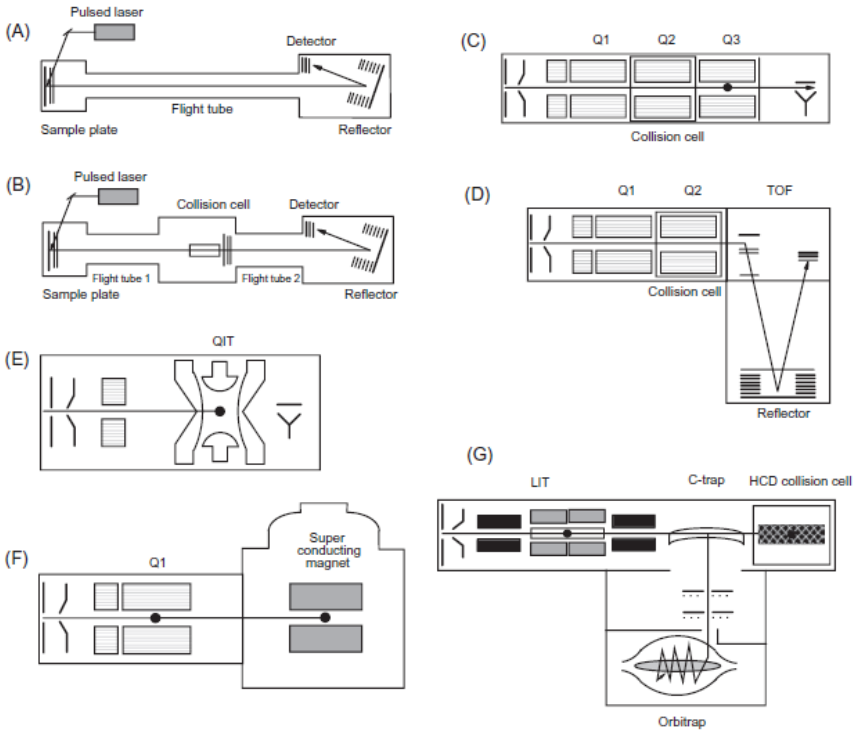

Figure 2.4 ***Mass spectrometers used in proteomics.*** (A) Reflector TOF; (B) time-of-flight reflector time-of-flight (TOF-TOF); (C) triple quadrupole (QqQ) or LIT; (D) quadrupole time-of-flight (Q-TOF); (E) QIT; (F) FT-ICR; (G) LIT-Orbitrap, HCD stands for higher energy collisional dissociation. *Adapted from Aebersold R, Mann M. Mass spectrometry-based proteomics. Nature 2003;422:198–207 [29], except for Panel (G), which is based on a picture by the vendor and made in the style of the others.*

the higher time spend in the reflectron. TOF analyzers theoretically have an unlimited mass range (but in practice it is restricted); they offer a high-spectrum acquisition rate and sensitivity (Table 2.1).

A Paul trap or quadrupole ion trap (QIT) consists of a central ring electrode and two end-cap electrodes (Fig. 2.4). There is an RF potential applied to the ring electrode when the end-cap electrodes are maintained at ground potential. Ions of a broad m/z range are trapped due to the oscillating three-dimensional electric field inside the analyzer, and their motion is then manipulated by increasing the amplitude of the RF potential [41]. This forces the trapped ions to become sequentially unstable, which is accompanied by ejecting them out of the trap for detection. QITs are simple to operate, relatively inexpensive, sensitive, and useful to conduct multistage MS experiments (MS^n) for structural studies. The major drawback is their poor mass accuracy and low dynamic range (Table 2.1). A linear ion trap (LIT) or two-dimensional QIT is made of four parallel rods with hyperbolic profiles; each rod is cut into three axial sections and there is a slit in one of the central rod sections to eject ions (Fig. 2.4). LIT can work as a selective filter or a real trap. Similar to QIT, mass analysis of the trapped ions is performed in the mass-selective instability mode by increasing the RF potential [42]. Compared to QIT, LIT has a higher trapping efficiency, ion storage capacity, and scan speed.

FT−ICR-MS was introduced in the 1970s [43]. The mass analyzer is formed by a cell (Penning trap) placed in a strong magnetic field (Fig. 2.3). The cell is composed of three pairs of opposite plates. Each pair has a different function (trapping, excitation, or detection). Ions are trapped in the cell and excited by an oscillating electric field orthogonal to the magnetic field. The ions excited due to a resonance-based energy transfer rotate in phase-coherent packets and are detected by measuring the image current at the detection plates. The resulting complex time-domain signal is processed to a frequency-domain representation by a Fourier transform. The masses of the ions are resolved by their ion cyclotron frequencies [43]. A typical attribute of FT-ICR-MS is a remarkably high resolving power and a superior mass accuracy. Orbitrap is a new mass analyzer, which was introduced in the 1990s, first commercial instruments then appeared in the 2000s [22]. It is an ion trap with a coaxial barrel-like outer electrode (it is split into halves by an insulating ring) and an axial spindle-like central electrode (Fig. 2.4). Contrary to a conventional ion trap mentioned above, there is no RF potential or magnetic field to keep ions inside an Orbitrap. Instead, ions are trapped in a pure

electrostatic field and forced to cycle in elliptical trajectories around the central electrode; they also move forward and back along the electrode (z-axis). Together a spiral movement pattern is created. The axial component of these oscillations is related to the m/z values of the ions and can be detected as an image current induced between the axial halves of the outer electrode. FT is employed to get oscillation frequencies resulting in accurate m/z values. Another advantage is the high resolution available competing with that of FT-ICR instruments (Table 2.1) and largely surpassing orthogonal TOF analyzers [44].

2.7 TANDEM MS

Tandem MS has been used in chemistry and biology to identify and quantify compounds. It is based on multiple stages of mass analysis, which are coupled either in time or space [45]. If there are two stages, the abbreviation MS/MS or MS^2 is used. For more stages (feasible with ion-trapping instruments), MS^n is a general abbreviation. This technique has largely been perfected since its introduction in the late 1960s. Classical pioneering works included the development of collision-induced dissociation [16] and introduction of the triple quadrupole mass spectrometer [46]. In biological experiments, which utilize the soft ionization techniques ESI and MALDI, abundant structural information can be obtained only by MS/MS [47]. For example, MS/MS-based sequencing analyses of peptides in digests are necessary to get unambiguous data for protein identification. In research projects as well as routine analyses, often there is a need to select ions of a given mass (=precursor ions) for their activation, fragmentation, and mass analysis of the fragmentation products (=product ions). This is commonly applied for elucidating the chemical structure of unknown compounds, identification of target components of complex mixtures, and studying fragmentation pathways. Selective detection of ions providing a given fragment or losing a given neutral is also possible with an appropriate instrumentation [45,48]. Many instruments differing in their construction have become available for this purpose (Table 2.2). There are two types (Fig. 2.4): either with a tandem-in-space setup, where the individual stages of MS/MS are carried out in separate regions (mass analyzers), or a tandem-in-time arrangement, with all steps

Table 2.2 Common instruments applicable for tandem MS

	Q-Q-TOF	TOF-TOF	FT-ICR	Q-Q-Q	QQ-LIT
Resolving power	Good	High	Very high	Low	Low
Mass accuracy	Good	Good	Excellent	Medium	Medium
Dynamic range	Medium	Medium	Medium	High	High
ESI availability	Yes	–	Yes	Yes	Yes
MALDI availability	Optional	Yes	Optional	–	–
Identification	Good	Good	Excellent	Possible	Possible
Quantification	Excellent	Good	Good	Excellent	Excellent
Throughput	High	Very high	High	High	High
Detection of modifications	Possible	Possible	Possible	–	Excellent

Source: Adapted from Domon B, Aebersold R. Mass spectrometry and protein analysis. Science 2006;312:212–17 [49].

performed in the same analyzer by employing a temporal sequence of events [45]. Tandem-in-space instruments comprise several mass analyzers of the same type (e.g., multisector magnetic analyzers, triple quadrupole, TOF/TOF) or they have a hybrid design, in which different mass analyzers are coupled (e.g., magnetic sector–quadrupole, magnetic sector–TOF, quadrupole–TOF, quadrupole–LIT, and quadrupole–FT-ICR). The tandem-in-time variant is the case for ion-trapping instruments such as QIT, LIT, and FT-ICR [48].

There are four scan modes possible on tandem mass spectrometers: product ion scan, precursor ion scan, neutral loss scan, and selected reaction monitoring (SRM) [45]. All four scan modes are available with magnetic sector– and quadrupole-based instruments. TOF/TOF and ion-trapping devices are applicable for the product ion scan only, which is anyway the most common MS/MS experiment: here the selected ions are passed into the collision cell, activated, and induced to fragment [48]. The product ions are then analyzed and the fragmentation data are utilized to deduce structural information of the precursor ion. The precursor ion scan (also parent scan) is done in such an arrangement that the analyzer beyond the collision cell is set to pass exclusively those ions showing a particular (and selected) m/z value. Parent ions, which pass through the first analyzer (a quadrupole for instance), are detected only if they fragment in the collision cell to produce the selected product ion. The neutral loss scan, as in the case of the precursor ion scan, represents a setup

where both analyzers are scanned together with a constant m/z difference. This allows recognizing all ions, which lose a given neutral fragment upon the fragmentation. The SRM approach is similar to acquiring a product-ion scan spectrum, and it is very useful for quantitative measurements because of its specificity. Instead of recording the complete spectrum of fragments, only a specific precursor−product pair is monitored (which means to detect a unique product ion) [50]. Monitoring more than one precursor-to-product transition is expressed by the term multiple reaction monitoring (MRM). Parallel reaction monitoring (PRM) takes the advantage of high-resolution MS. It is based on a quadrupole-Orbitrap platform. Unlike SRM/MRM, which provides one transition at a time, PRM performs parallel detection of all transitions (without the need to select a particular ion pair) in a single analysis. The Orbitrap analyzer scans all product ions with high resolution and high accuracy resulting in the elimination of the background interference and improvement of the detection limit and sensitivity [51].

Ion activation techniques are essential in MS/MS [52]. This is a brief overview: (1) the most common is collision-induced dissociation (CID) also named collisionally activated dissociation (CAD), for which precursor ions are excited by collisions (this can be performed in a high- or low-energy regime) with atoms of an inert gas such as helium or argon; (2) surface-induced dissociation (SID), available on a variety of instruments, where ion activation is achieved by collision with a solid surface (e.g., a metal plate); (3) absorption of UV/infrared photons or absorption of heat: UV photodissociation (PD), infrared multiphoton dissociation (IRMPD), or blackbody-induced radiative dissociation (BIRD), respectively; (4) electron-capture dissociation (ECD), which involves an excitation of protonated precursor by the capture of a low-energy electron and subsequent fragmentation of the resulting odd-electron ion; (5) electron-transfer dissociation (ETD)—the process is similar to ECD but uses an ion−ion reaction where anthracene anions are employed as electron donors. ECD has been primarily a part of FT-ICR instruments and it is solely applicable to the ESI-produced multiply protonated ions. Its applications include peptide sequencing, oligonucleotide sequencing, or identification of protein sites carrying posttranslational modifications such as phosphorylation, glycosylation, and others. Similarly, ETD is typically used to fragment multiply charged peptide ions for studying posttranslational modifications with ion traps.

2.8 SEPARATION TECHNIQUES HYPHENATED WITH MS

To analyze complex samples of the real world such as those from biological tissues, technological processes, and environmental control, the online coupling of MS with a separation device has long been a very successful approach. Commonly, GC, LC, or CE are used, and the respective coupling provides the possibility to increase the information gathered about sample components because of combining the resolving power of the separation technique and performance (particularly with respect to sensitivity and dynamic range) of a mass spectrometer [53]. The physical interconnection between the two instruments requires an interface, which delivers the separated sample components into the ion source. With a proper arrangement, both the resolution of the separation and performance of the mass spectrometer should remain virtually unaffected. The pressure mismatch (in GC–MS) and solvent incompatibility (in the case of LC and CE coupling) are the main issues to be dealt with. Not all mass spectrometers are suitable for the online coupling. Only those, which are characterized by a high scan speed and can tolerate high pressures (e.g., quadrupoles, ion traps, TOF analyzers) are considered optimal [54].

GC–MS is well suited for small in size, volatile, and thermally stable molecules. For larger diameter packed columns and higher carrier gas flows, there are interfaces available such as an open split interface, a jet separator, and a molecular effusion interface [55]. Capillary GC columns can be coupled directly to MS (because a low carrier gas flow is used) and provide a high-resolution separation of complex mixtures. LC and CE are suitable for the separation of mixtures with nonvolatile and thermally labile compounds. The introduction of ESI was an excellent opportunity to couple LC and also CE (as an approach complementary to LC) with MS. As a result, LC–ESI–MS in particular has become the method of choice for many applications including identification and quantification analyses of peptides, lipids, metabolites, drugs, and pesticides [56]. All sizes, from standard analytical high-performance liquid chromatography columns to capillary and nanoscale columns, are applicable for coupling with ESI—MS as there are different types of ESI sources and interfaces available for a wide range of solvent flow rates. Generally, smaller diameter columns are advantageous as they provide increased efficiency of separation. For many biochemical and biological studies, where sample amounts are often limited, capillary/nanoscale columns are

applied [54]. Nanoscale columns are commonly operated at the flow range of 50–500 $nL \cdot min^{-1}$ and attached directly to a nanospray ion source. With analytical and other larger diameter columns operated at higher flow rates (at the level of 100 μL to 1.0 $mL \cdot min^{-1}$), a conventional ESI source (operates at a flow rate of 1–10 $\mu L \cdot min^{-1}$) can be used after a postcolumn flow splitting (e.g., 100:1). LC has also been coupled with MALDI MS [57]. Several constructs have been tried to make online combinations with a postcolumn mixing of the eluate with matrix solution (e.g., using a rotating wheel interface). Nevertheless, an offline approach with depositing eluate fractions on MALDI target in a spotter device after their mixing with a matrix solution has been successfully commercialized [56,57].

In proteomics, for example, reversed-phase LC (RP-LC) on a C18 (octadecyl hydrocarbon-bonded silica stationary phase) column is a standard technique to separate peptides prior to their MS/MS sequencing [54,58]. Besides this mode of separation, affinity chromatography (utilizing a specific affinity interaction of a biomolecule with a ligand immobilized in the stationary phase) or supercritical fluid chromatography (in which the mobile phase is a gas, such as carbon dioxide, liquid-like at a pressure above its critical pressure) can be coupled with MS. When the complexity of a sample is too high, one-dimensional LC is not sufficient to resolve optimally its components [54]. Then a two-dimensional chromatography is chosen, which combines two orthogonal separation steps (the meaning is that these steps represent completely different principles of separation). The second dimension must be faster and MS-compatible solvents have to be used to allow ionization. The most common approach is based on ion-exchange LC and RP-LC, but also size-exclusion chromatography, affinity chromatography, or chromatofocusing can be combined with RP-LC in the second dimension.

Finally, CE has been used in coupling with MS as an alternative to LC-based separations. Currently it is performed in different formats, including capillary zone electrophoresis (the most popular separation technique of this type), capillary gel electrophoresis, capillary isoelectric focusing, capillary isotachophoresis, micellar electrokinetic chromatography, and capillary electrochromatography [59]. The separation is frequently interfaced with ESI or APCI, and the three most practical designs are a sheathless interface, sheath–flow interface, and liquid–junction interface [60]. The CE effluent can also be deposited on MALDI target plate for an offline MS analysis.

2.9 MSI AND OTHER WAYS OF EXAMINING BIOLOGICAL TISSUES

Thanks to the wide range of ionization techniques and availability of high-resolution analyzers, the application of MS encompasses broad science areas in the fields of proteomics, metabolomics, pharmacy, toxicology, environmental applications, isotope analyses, carbon dating, or homeland security. The application of MS in industry is logical for evaluating the quality of raw materials and final products. A bright example is the petrochemical industry [61]. In biology and health sciences, it is now a standard tool for the identification, characterization, and quantification of proteins and organic compounds. MS in clinical diagnostics and toxicology progressively complements spectroscopic or immunoaffinity analytical methods [62]. MSI (also imaging mass spectrometry—IMS) is a technique which allows to investigate spatial molecular distribution in a section of the exact area of a biological sample, typically in a sliced tissue [63]. MSI can provide qualitative as well as quantitative information for a wide variety of compounds such as proteins, peptides, lipids, metabolites, drugs, and others. The final output is a two-dimensional image based on the determined molecular masses. All acquired images from consecutive tissue slices can be combined to a three-dimensional model of the examined object showing the distribution profiles of individual detected compounds [64]. MALDI MS and secondary ion mass spectrometry (SIMS) are the most typical approaches in MSI. Ambient ionization techniques such as DESI, laser ablation electrospray ionization (LAESI), or liquid extraction surface analysis (LESA) represent an alternative [65]. MALDI imaging allows a simultaneous mapping of biological molecules present in thin tissue sections placed on the MALDI probe. The principle is similar to that of scanning microscopy: the whole sample area is set for analysis, divided into closely adjacent positions for laser firing and then sequentially analyzed. Only those instruments with a gentle target displacement and fine laser beam focus can be used. The information obtained by MALDI MSI is suitably complemented by histological and immunological observations, which help to search for molecular markers [66]. The sample preparation procedure is a key step and requires a precise preparation of thin tissue slices, their washing, desalting, and the subsequent application of matrix (sublimation or spraying methods are used to evenly cover the entire surface area of the sample) [67]. Proteins can be

identified directly from the sliced tissue after in situ digestions [68]. The spatial resolution ranges from 5 to 200 μm.

A higher spatial resolution of 50–100 nm can be achieved using SIMS [69]. SIMS was originally used to analyze solid surfaces with a focused primary ion beam and collecting and analyzing the released secondary ions. In biological research, SIMS is applied to study biomolecules with relatively low molecular masses. SIMS instruments work in two different modes: static and dynamic. In the dynamic SIMS, the sample is bombarded constantly by primary ions (Cs^+ or O^-), which causes an excessive analyte fragmentation. An in-depth chemical profile of the observed material can be acquired in this way. Conversely, the static SIMS uses only pulsed primary ion beams to avoid any sample surface distortion and provides the best surface-sensitive molecular resolution [69]. By combining these two SIMS approaches, the analysis by defined layers can be achieved. The first layer of a sample is explored by the soft static mode. Then the analyzed surface is eroded by more invasive atom beams which reveal a lower layer and the process is repeated.

DESI is commonly used for imaging of lipids [70]. Thin-layer chromatography probes used for the separation of organic molecules can be effectively analyzed by DESI MS [65]. By combining the benefits of ESI and MALDI, the hybrid ionization technique matrix-assisted laser desorption electrospray ionization (MALDESI) has been introduced. Here the ions are generated by a laser ablation and electrospray postionization [71]. LAESI combines a mid-infrared laser ablation with a secondary ESI process for samples containing water (liquids or tissues). The laser is tuned to the absorption line of water, but the ejected secondary material is not ionized. Therefore, an ESI source is located above the sample for a post-ablation ionization [72]. LESA represents a different attitude for sampling from tissue specimens. First, the analyte is extracted from the sample surface by a liquid microjunction between the probe and sample. Then the droplet is ionized and analyzed [73]. LESA shows a low spatial resolution, but the noninvasive sampling and easy connectivity to MS analyzers are promising for LESA-based MSI under native conditions.

In addition to MSI, several other interesting approaches for analyzing biological material have been developed on the basis of ambient ionization. Paper spray MS was invented for a fast and direct analysis of molecules such as lipid, hormones, and drugs in tissues without a complicated sample pretreatment. A sample drop (1 μL) is deposited on a triangle shaped paper directed by one of its tips to the MS inlet. For ionization,

both a high voltage and solvent are applied, and the analyte is sprayed from the paper tip into the MS instrument [74]. A more convenient method for tissue analysis is the rapid evaporative ionization mass spectrometry (REIMS) invented for a medical use [75]. This electrosurgical dissection device is combined with an air pump and flexible tubing connected to the ion source. The charged molecules released during the dissection are sucked and transferred to the MS instrument and analyzed in real time. The system is marketed nowadays as "iKnife." REIMS is applicable also for the analysis of intact microorganisms [76]. Nanostructure-initiator MS (NIMS) is a desorption/ionization technique, which uses silicon fibers as laser energy absorbers. The absorption of laser energy results in a fast vaporization of the sample and its ionization. A repeated application of liquid sample on the nanostructure initiator and its drying can be used for analyte enrichment. Small organic molecules such as metabolites can be detected by this approach even in the yoctomole (10^{-24}) range [77].

2.10 MASS SPECTRUM, DATA REPRESENTATION, AND MANAGEMENT

Mass spectrometric experiments involve a sequential use of several software types. First, an acquisition software is employed for acquiring mass spectra and their saving together with metadata of the experiment. The mass spectra are then processed (e.g., with smoothing and peak picking steps) by means of a processing software. Finally, specialized software tools are applied, for example, in proteomics to perform database searches and calculating quantification results. Apart from the proprietary software provided by instrument vendors, there is also both free and open-source software available for MS. To mention a few examples, mMass has been developed for mass spectrometric data analysis and interpretation [78], MaxQuant [79], and Skyline [80] are applicable in quantitative proteomics, OpenChrom is useful for evaluating GC- or LC-MS data [81], and BIOSPEAN allows to compare intact cell MALDI-TOF mass spectra [82].

A common mass spectrum represents a plot of m/z values (on the x-axis) of all detected ions against their abundance ($\sim$ signal intensity; on the y-axis). The most abundant ion is designated a base peak. On a

relative scale, abundances of the other ions are expressed as percentage abundances relative to this peak [3]. Mass spectra can be stored in two major ways: as continuous spectra ("profile-mode") or peak lists ("centroided"). Profile-mode spectra comprise spaced data points and thus each peak has a defined shape. Conversely, a peak list is represented by m/z and intensity pairs extracted from the original peaks. The latter representation saves memory space but substantial information (resolution) is lost [83].

In biological research, MS commonly produces large amounts of data. Mass-spec manufacturers as well as organized user communities have developed various formats for data storage, exchange, and processing. There are many instrument data formats (or the proprietary software generates folders with multiple files) with extensions such as .baf, .fid or .yep (Bruker), .wiff or .t2d (AB Sciex), .qgd (Shimadzu), and .raw (Thermo, Waters), which are not interchangeable and transferable. For database searches using MS/MS data for protein identification, the output files from mass spectrometers are commonly converted into simple text files. The MGF format has been launched by Matrix Science (London, United Kingdom), and it encodes multiple MS/MS spectra in a single file, which is applicable with Mascot, the most common search engine. However, many valuable metadata are lost during the respective conversion [83]. To cope with these disadvantages, attempts appeared in 2003 to introduce a standardized MS data format. The Human Proteome organization (HUPO) has made a big effort via its Proteomics Standards Initiative (PSI) to manage the development of open data formats [83]. All it has started with a requirement to keep most of the information from each experimental run that would easily be accessible by any tool. First, mzData was developed by the PSI itself. Independently, the Institute for Systems Biology (Seattle, The United States) produced mzXML [84]. Because of an inconvenience of having two open formats for preserving the same information, the two institutions have created mzML as a compromise and new format with best features from both mzXML and mzData [85]. For quantitative proteomics analyses, mzQuantML and mzTab formats are currently being developed by the HUPO PSI (http://www.psidev.info).

ACKNOWLEDGMENTS

This work was supported by grant No. LO1204 (National Program of Sustainability I) from the Ministry of Education, Youth and Sports, Czech Republic.

REFERENCES

[1] Price P. Standard definitions of terms relating to mass spectrometry. A report from the Committee on Measurements and Standards of the American Society for Mass Spectrometry. J Am Soc Mass Spectrom 1991;2:336–48.
[2] Cooks RG, Rockwood AL. The "Thomson": suggested unit for mass spectroscopists,. Rapid Commun Mass Spectrom 1991;5:93.
[3] Dass C. Basics of mass spectrometry. In: Fundamentals of contemporary mass spectrometry. Hoboken, NJ: John Wiley & Sons, Inc; 2007. p. 3–14.
[4] Lössl P, M. van de Waterbeemd, Heck AJ. The diverse and expanding role of mass spectrometry in structural and molecular biology. EMBO J 2016;35:2634–57.
[5] Moore CE, Jaselskis B, von Smolinski AJ. The proton. J Chem Educ 1985;62:859–60.
[6] Hedenus M. Eugen Goldstein and his laboratory at Berlin Observatory. Astron Nachr 2002;6:567–9.
[7] Rüchardt E. Zur Entdeckung der Kanalstrahlen vor fünfzig Jahren. Naturwissenschaften 1936;24:57–62.
[8] Thomson JJ. Rays of positive electricity and their application to chemical analyses. In: Thomson JJ, Horton F, editors. Monographs on physics. London: Longmans, Green & Co.; 1913. p. 1–132. Reprinted by the American Society for Mass Spectrometry in 2013.
[9] Thomson JJ. Rays of positive electricity. Proc Roy Soc London 1913;A89:1–20.
[10] Squires G. Francis Aston and the mass spectrograph. Dalton Trans 1998;23:3893–900.
[11] Dempster AJ. A new method of positive ray analysis. Phys Rev 1918;11:316–25.
[12] Allison SK. Arthur Jeffrey Dempster 1886-1950. Biogr Mems Nat Acad Sci 1952;319–33.
[13] Wood HG, Werkman CH, Hemingway A, Nier AO. Heavy carbon as a tracer in bacterial fixation of carbon dioxide. J Biol Chem 1940;135:789–90.
[14] Meyerson S. Reminiscence of the early days of mass spectrometry in the petroleum industry. Org Mass Spectrom 1986;21:197–208.
[15] Paul W, Steinwedel H. Ein neues Massenspektrometer ohne Magnetfeld. Zeitschrift für Naturforschung A 1953;8:448–50.
[16] Jennings KR. Collision-induced decompositions of aromatic molecular ions. Int J Mass Spectrom Ion Phys 1968;1:227–35.
[17] Barber M, Bordoli RS, Sedgwick RD, Tyler AN. Fast atom bombardment of solids as an ion source in mass spectrometry. Nature 1981;293:270–5.
[18] Fenn JB, Mann M, Meng CK, Wong SF, Whitehouse CM. Electrospray ionization for mass spectrometry of large biomolecules. Science 1989;246:64–71.
[19] Karas M, Bachmann D, Bahr U, Hillenkamp F. Matrix-assisted ultraviolet laser desorption of non-volatile compounds. Int J Mass Spectrom Ion Processes 1987;78:53–68.
[20] Tanaka K, Waki H, Ido Y, Akita S, Yoshida Y, Yoshida T. Protein and polymer analyses up to m/z 100 000 by laser ionization time-of-flight mass spectrometry. Rapid Commun Mass Spectrom 1988;2:151–3.
[21] Takats Z, Wiseman JM, Gologan B, Cooks RG. Mass spectrometry sampling under ambient conditions with desorption electrospray ionization. Science 2004;306:471–3.
[22] Makarov A. Electrostatic axially harmonic orbital trapping: high-performance technique of mass analysis. Anal Chem 2000;72:1156–62.
[23] Vékey K. Internal energy effects in mass spectrometry. J Mass Spectrom 1996;31:445–63.

[24] El-Aneed A, Cohen A, Banoub J. Mass spectrometry, review of the basics: electrospray, MALDI, and commonly used mass analyzers. Appl Spectrosc Rev 2009;44:210–30.
[25] Dass C. Mass analysis and ion detection. In: Fundamentals of contemporary mass spectrometry. Hoboken, NJ: John Wiley & Sons, Inc; 2007. p. 67–117.
[26] Kopenaal DW, Barinaga CJ, Denton MB, Sperline RP, Hieftje GM, Schilling GD, et al. MS detectors. Anal Chem 2005;77:418A–27A.
[27] Gross JH. Instrumentation. In: Mass spectrometry: a textbook. 3rd Edition Cham, Switzerland: Springer International Publishing AG; 2017. p. 151–292.
[28] Monge ME, Harris GA, Dwivedi P, Fernández FM. Mass spectrometry: recent advances in direct open air surface sampling/ionization. Chem Rev 2013;113:2269–308.
[29] Aebersold R, Mann M. Mass spectrometry-based proteomics. Nature 2003;422:198–207.
[30] Bruins AP. Mechanistic aspects of electrospray ionization. J Chromatogr A 1998;794:345–57.
[31] Bruins AP. Atmospheric-pressure-ionization mass spectrometry: I. Instrumentation and ionization techniques. Trac-Trends Anal Chem 1994;13:37–43.
[32] Raffaelli A, Saba A. Atmospheric pressure photoionization mass spectrometry. Mass Spectrom Rev 2003;22:318–31.
[33] Zenobi R, Knochenmuss R. Ion formation in MALDI mass spectrometry. Mass Spectrom Rev 1998;17:337–66.
[34] Dreisewerd K. Recent methodological advances in MALDI mass spectrometry. Anal Bioanal Chem 2014;406:2261–78.
[35] Cooks RG, Ouyang Z, Takats Z, Wiseman JM. Detection technologies. Ambient mass spectrometry. Science 2006;311:1566–70.
[36] Wiseman JM, Puolitaival SM, Takáts Z, Cooks RG, Caprioli RM. Mass spectrometric profiling of intact biological tissue by using desorption electrospray ionization. Angew Chem Int Ed 2005;44:7094–7.
[37] Cody RB, Laramée JA, Durst HD. Versatile new ion source for the analysis of materials in open air under ambient conditions. Anal Chem 2005;77:2297–302.
[38] Nier AO. The development of a high resolution mass spectrometer: a reminiscence. J Am Soc Mass Spectrom 1991;2:447–52.
[39] Chernushevich IV, Loboda AV, Thomson B. An introduction to quadrupole–time-of-flight mass spectrometry. J Mass Spectrom 2001;36:849–65.
[40] Wollnik H. History of mass measurements in time-of-flight mass analyzers. Int J Mass Spectrom 2013;349-350:38–46.
[41] March RE. An introduction to quadrupole ion trap mass spectrometry. J Mass Spectrom 1997;32:351–69.
[42] Schwarz JC, Senko MW, Syka JEP. A two-dimensional quadrupole ion trap mass spectrometer. J Am Soc Mass Spectrom 2002;13:659–69.
[43] Marshall AG, Hendrickson CL, Jackson GS. Fourier transform ion cyclotron resonance mass spectrometry: a primer. Mass Spectrom Rev 1998;17:1–35.
[44] Scigelova M, Makarov A. Orbitrap mass analyzer—overview and applications in proteomics. Proteomics 2006;6(Suppl. 2):16–21.
[45] de Hoffmann E. Tandem mass spectrometry: a primer. J Mass Spectrom 1996;31:129–37.
[46] Yost RA, Enke CG. Selected ion fragmentation with a tandem quadrupole mass spectrometer. J Am Chem Soc 1978;100:2274–5.
[47] Cottrell JS. Protein identification using MS/MS data. J Proteomics 2011;74 1842–1851.

[48] Dass C. Tandem mass spectrometry. In: Fundamentals of contemporary mass spectrometry. Hoboken, NJ: John Wiley & Sons, Inc; 2007. p. 119–50.
[49] Domon B, Aebersold R. Mass spectrometry and protein analysis. Science 2006;312:212–17.
[50] Picotti P, Aebersold R. Selected reaction monitoring–based proteomics: workflows, potential, pitfalls and future directions. Nat Methods 2012;9:555–66.
[51] Bourmaud A, Gallien S, Domon B. Parallel reaction monitoring using quadrupole-Orbitrap mass spectrometer: principle and applications. Proteomics 2016;16:2146–59.
[52] Sleno L, Volmer DA. Ion activation methods for tandem mass spectrometry. J Mass Spectrom 2004;39:1091–112.
[53] Tomer KB. Separations combined with mass spectrometry. Chem Rev 2001;101:297–328.
[54] Dass C. Hyphenated separation techniques. In: Fundamentals of contemporary mass spectrometry. Hoboken, NJ: John Wiley & Sons, Inc; 2007. p. 151–94.
[55] Abian J. The coupling of gas and liquid chromatography with mass spectrometry. J Mass Spectrom 1999;34:157–68.
[56] Holčapek M, Jirásko R, Lísa M. Recent developments in liquid chromatography–mass spectrometry and related techniques. J Chromatogr 2012;A 1259:3–15.
[57] Mukhopadhyay R. The automated union of LC and MALDI MS. Anal Chem 2005;77:150A–2A.
[58] Issaq HJ. The role of separation science in proteomics research. Electrophoresis 2001;22:3629–38.
[59] Schmitt-Kopplin P, Frommberger M. Capillary electrophoresis–mass spectrometry: 15 years of developments and applications. Electrophoresis 2003;24:3837–67.
[60] Kostal V, Katzenmeyer J, Arriaga EA. Capillary electrophoresis in bioanalysis. Anal Chem 2008;80:4533–50.
[61] Marshall AG, Rodgers RP. Petroleomics: chemistry of the underworld. Proc Natl Acad Sci USA 2008;105:18090–5.
[62] Vogeser M. Mass spectrometry in the clinical laboratory—challenges for quality assurance. Spectroscopy 2015;13:14–19.
[63] McDonnell LA, Heeren RMA. Imaging mass spectrometry. Mass Spectrom Rev 2007;26:606–43.
[64] Schwamborn K, Caprioli RM. MALDI imaging mass spectrometry—painting molecular pictures. Mol Oncol 2010;4:529–38.
[65] Wu C, Dill AL, Eberlin LS, Cooks RG, Ifa DR. Mass spectrometry imaging under ambient conditions. Mass Spectrom Rev 2012;32:218–43.
[66] Chughtai K, Heeren RMA. Mass spectrometric imaging for biomedical tissue analysis. Chem Rev 2010;110:3237–77.
[67] Chaurand P, Schwartz SA, Reyzer ML, Caprioli RM. Imaging mass spectrometry: principles and potentials. Toxicol Pathol 2005;33:92–101.
[68] Balluff B, Rauser S, Ebert MP, Siveke JT, Höfler H, Walch A. Direct molecular tissue analysis by MALDI imaging mass spectrometry in the field of gastrointestinal disease. Gastroenterology 2012;143:544–9.
[69] Gamble LJ, Anderton CR. Secondary ion mass spectrometry imaging of tissues, cells, and microbial systems. Micros Today 2016;24:24–31.
[70] Ferguson CN, Fowler JWM, Waxer JF, Gatti RA, Loo JA. Mass spectrometry-based tissue imaging of small molecules. advances in experimental medicine and biology. In: Woods A, Darie C, editors. Advancements of Mass Spectrometry in Biomedical Research Advances in Experimental Medicine and Biology, vol 806. Cham, Switzerland: Springer; 2014. p. 283–99.

[71] Robichaud G, Barry JA, Muddiman DC. IR-MALDESI mass spectrometry imaging of biological tissue sections using ice as a matrix. J Am Soc Mass Spectrom 2014;25:319–28.
[72] Nemes P, Vertes A. Laser ablation electrospray ionization for atmospheric pressure, in vivo, and imaging mass spectrometry. Anal Chem 2007;79:8098–106.
[73] Griffiths RL, Creese A, Race AM, Bunch J, Cooper HJ. LESA FAIMS mass spectrometry for the spatial profiling of proteins from tissue. Anal Chem 2016;88:6758–66.
[74] Wang H, Manicke NE, Yang Q, Zheng L, Shi R, Cooks RG, et al. Direct analysis of biological tissue by paper spray mass spectrometry. Anal Chem 2011;83:1197–201.
[75] Balog J, Szaniszlo T, Schaefer KC, Denes J, Lopata A, Godorhazy L, et al. Identification of biological tissues by rapid evaporative ionization mass spectrometry. Anal Chem 2010;82:7343–50.
[76] Strittmatter N, Jones EA, Veselkov KA, Rebec M, Bundy JG, Takats Z. Analysis of intact bacteria using rapid evaporative ionisation mass spectrometry. Chem Commun 2013;49:6188–90.
[77] Greving MP, Patti GJ, Siuzdak G. Nanostructure-initiator mass spectrometry metabolite analysis and imaging. Anal Chem 2011;83:2–7.
[78] Strohalm M, Hassman M, Košata B, Kodíček M. mMass data miner: an open source alternative for mass spectrometric data analysis. Rapid Commun Mass Spectrom 2008;22:905–8.
[79] Cox J, Mann M. MaxQuant enables high peptide identification rates, individualized p.p.b.-range mass accuracies and proteome-wide protein quantification. Nat Biotechnol 2008;26:1367–72.
[80] MacLean B, Tomazela DM, Shulman N, Chambers M, Finney GL, Frewen B, et al. Skyline: an open source document editor for creating and analyzing targeted proteomics experiments. Bioinformatics 2010;26:966–8.
[81] Wenig P, Odermatt J. OpenChrom: a cross-platform open source software for the mass spectrometric analysis of chromatographic data. BMC Bioinform 2010;11:405.
[82] Raus M, Šebela M. BIOSPEAN: a freeware tool for processing spectra from MALDI intact cell/spore mass spectrometry. J Proteomics Bioinform 2013;6:283–7.
[83] Deutsch EW. File formats commonly used in mass spectrometry proteomics. Mol Cell Proteomics 2012;11:1612–21.
[84] Pedrioli PG, Eng JK, Hubley R, Vogelzang M, Deutsch EW, Raught B, et al. A common open representation of mass spectrometry data and its application to proteomics research. Nat Biotechnol 2004;22:1459–66.
[85] Martens L, Chambers M, Sturm M, Kessner D, Levander F, Shofstahl J, et al. mzML—a community standard for mass spectrometry data. Mol Cell Proteomics 2011;10;R110.000133.

Příloha 2:

Perutka, Z., Kaduchová, K., Chamrád, I., Beinhauer, J., Lenobel, R., Petrovská, B., Bergougnoux, V., Vrána, J., Pečinka, A., Doležel, J., Šebela, M., 2021. Proteome Analysis of Condensed Barley Mitotic Chromosomes. *Frontiers in Plant Science* 12, 1716.

frontiers in Plant Science

ORIGINAL RESEARCH
published: 23 August 2021
doi: 10.3389/fpls.2021.723674

Proteome Analysis of Condensed Barley Mitotic Chromosomes

Zdeněk Perutka[1], Kateřina Kaduchová[2], Ivo Chamrád[1], Jana Beinhauer[1], René Lenobel[1], Beáta Petrovská[2], Véronique Bergougnoux[3†], Jan Vrána[2], Ales Pecinka[2], Jaroslav Doležel[2] and Marek Šebela[1]**

[1]Department of Protein Biochemistry and Proteomics, Faculty of Science, Centre of the Region Haná for Biotechnological and Agricultural Research, Palacký University Olomouc, Olomouc, Czechia, [2]Institute of Experimental Botany of the Czech Academy of Sciences, Centre of the Region Haná for Biotechnological and Agricultural Research, Olomouc, Czechia, [3]Department of Molecular Biology, Faculty of Science, Centre of the Region Haná for Biotechnological and Agricultural Research, Palacký University Olomouc, Olomouc, Czechia

OPEN ACCESS

Edited by:
Hans-Peter Mock, Leibniz Institute of Plant Genetics and Crop Plant Research (IPK), Germany

Reviewed by:
Tiago Santana Balbuena, São Paulo State University, Brazil
Xiaojian Yin, China Pharmaceutical University, China

***Correspondence:**
Marek Šebela
marek.sebela@upol.cz
Jaroslav Doležel
dolezel@ueb.cas.cz

†Present address:
Véronique Bergougnoux, Centre of the Region Haná for Biotechnological and Agricultural Research, Czech Advanced Technology and Research Institute (CATRIN), Palacký University Olomouc, Olomouc, Czechia

Specialty section:
This article was submitted to Plant Proteomics and Protein Structural Biology, a section of the journal Frontiers in Plant Science

Received: *11 June 2021*
Accepted: *21 July 2021*
Published: *23 August 2021*

Citation:
Perutka Z, Kaduchová K, Chamrád I, Beinhauer J, Lenobel R, Petrovská B, Bergougnoux V, Vrána J, Pecinka A, Doležel J and Šebela M (2021) Proteome Analysis of Condensed Barley Mitotic Chromosomes. Front. Plant Sci. 12:723674. doi: 10.3389/fpls.2021.723674

Proteins play a major role in the three-dimensional organization of nuclear genome and its function. While histones arrange DNA into a nucleosome fiber, other proteins contribute to higher-order chromatin structures in interphase nuclei, and mitotic/meiotic chromosomes. Despite the key role of proteins in maintaining genome integrity and transferring hereditary information to daughter cells and progenies, the knowledge about their function remains fragmentary. This is particularly true for the proteins of condensed chromosomes and, in particular, chromosomes of plants. Here, we purified barley mitotic metaphase chromosomes by a flow cytometric sorting and characterized their proteins. Peptides from tryptic protein digests were fractionated either on a cation exchanger or reversed-phase microgradient system before liquid chromatography coupled to tandem mass spectrometry. Chromosomal proteins comprising almost 900 identifications were classified based on a combination of software prediction, available database localization information, sequence homology, and domain representation. A biological context evaluation indicated the presence of several groups of abundant proteins including histones, topoisomerase 2, POLYMERASE 2, condensin subunits, and many proteins with chromatin-related functions. Proteins involved in processes related to DNA replication, transcription, and repair as well as nucleolar proteins were found. We have experimentally validated the presence of FIBRILLARIN 1, one of the nucleolar proteins, on metaphase chromosomes, suggesting that plant chromosomes are coated with proteins during mitosis, similar to those of human and animals. These results improve significantly the knowledge of plant chromosomal proteins and provide a basis for their functional characterization and comparative phylogenetic analyses.

Keywords: barley, chromatin, FIBRILLARIN 1, flow cytometric sorting, mass spectrometry, mitotic chromosome, perichromosomal layer, protein prediction

INTRODUCTION

Nuclear DNA in eukaryotes is tightly associated with various proteins to form chromatin (Fierz and Poirer, 2019). The nucleoprotein complex not only participates in DNA packaging so that it fits the small nuclear volume, but also plays an important role in functional organization of DNA in the three-dimensional nuclear space, DNA damage repair, and regulation of gene expression. It also facilitates replication and faithful transmission of hereditary information to

daughter cells during mitosis, and the production of functional gametes in meiosis, which are intricate, highly dynamic and strictly controlled processes. At the beginning of mitosis and meiosis, the interphase chromatin undergoes a series of structural changes that lead to the formation of condensed chromosomes (Antonin and Neumann, 2016).

The organization of condensed chromosomes and their function is determined by a variety of proteins. Structural maintenance of chromosome (SMC) family complexes, including condensin, cohesin, and SMC5/6, modulate the chromosome structure and impact their function during mitosis (Skibbens, 2019). Replicated sister chromatids are tethered together by cohesins. In prophase, condensin II binds DNA and extrudes large initial scaffolding loops (Ganji et al., 2018). In prometaphase, after nuclear envelope breakdown, condensin I binds to chromatin and forms smaller loops for a further compaction, which are nested within the large loops produced by condensin II. Additional proteins were described as condensation factors including topoisomerase II and in mammals also chromosome-associated kinesin KIF4. Moreover, the condensation of chromosomes is facilitated by histone modifications, including phosphorylation and deacetylation (Antonin and Neumann, 2016).

Chromosome condensation was expected to be accompanied by the eviction of proteins involved in the regulation of gene expression, chromatin state, and accessibility (Martínez-Balbás et al., 1995). This was confirmed in the case of epigenetic modifiers that promote transcription (Ginno et al., 2018) and for a majority of polymerase II transcription elongation complexes (Parsons and Spencer, 1997; Ginno et al., 2018). However, repressive modifiers, some polymerase II ternary complexes, and a majority of transcription factors are retained, including core promoter-binding proteins (Parsons and Spencer, 1997; Ginno et al., 2018; Djeghloul et al., 2020). These proteins, collectively called mitotic bookmarking factors, ensure the transfer of gene regulatory information to daughter cells (Festuccia et al., 2016; Raccaud and Suter, 2018; Zaidi et al., 2018). As the accessibility of chromatin to regulatory proteins is not dramatically changed during chromosome condensation (Hsiung et al., 2015; Blythe and Wieschaus, 2016), many genes can be expressed during mitosis (Palozola et al., 2017), implying the association of various proteins and RNAs with the chromatin of condensed chromosomes.

In mammalian models, it has been shown that a perichromosomal layer covering the whole chromosome is established simultaneously with the chromosome condensation except for the centromeric region where the kinetochore complex is formed. This layer represents at least 33% of the protein mass of mitotic chromosomes (Booth et al., 2016) and consists of pre-rRNA and proteins originating mostly from nucleoli, which disassemble during prophase. Stenström et al. (2020) identified 65 nucleolar proteins at the chromosome periphery. This recruitment was temporary as some of the proteins relocated during prometaphase, and the remaining ones were recruited only after metaphase. The proteins transferred during prometaphase included the Ki-67 protein, which has been shown the main organizer of the perichromosomal layer in human and animals (Booth et al., 2014). A series of studies revealed multiple roles of the layer, which include the formation and maintenance of chromosome architecture (Takagi et al., 2016), prevention of chromosome clumping (Cuylen et al., 2016), displacement of cytoplasmic components before nuclear envelope assembly (Cuylen-Haering et al., 2020), and transport of proteins and RNAs and their distribution to daughter nuclei (Sirri et al., 2016). The key role of the perichromosomal layer in chromosome function is reflected by its highly ordered structure (Hayashi et al., 2017), which excludes the formation of this domain by a random attachment of nuclear and cytoplasmic components.

Centromeric regions are the sites for the assembly of kinetochores – large protein complexes that attach chromosomes to spindle microtubules during cell division (Cheeseman, 2014). In vertebrates, the kinetochore consists of over a 100 proteins and comprises two major interaction networks (Pesenti et al., 2018). The constitutive centromere-associated network (CCAN) has 16 subunits and remains associated with centromeric chromatin throughout the cell cycle. The Knl1, Mis12, and Ndc80 network with 10 subunit super-complexes binds to CCAN at early prophase and remains attached during the whole mitosis (Hara and Fukagawa, 2020). Interestingly, the correct function of kinetochore depends on the translocation of the NOL11, WDR43, and Cirhin complex from the nucleoli to the perichromosomal layer. This is required for the centromeric enrichment of Aurora B and the subsequent phosphorylation of histone H3 (Fujimura et al., 2020) and underlines the key role of nucleolar proteins in the function of mitotic chromosomes.

Despite the great progress achieved during the past two decades in identifying and cataloging chromosomal proteins and unraveling their function, many proteins have an unknown function and many may remain to be discovered. The pioneering studies on human cell lines reported a relatively low number of chromosomal proteins, ranging from 60 to 250 (Morrison et al., 2002; Gassmann et al., 2005; Uchiyama et al., 2005; Takata et al., 2007). The first detailed survey by Ohta et al. (2010) revealed approximately 4,000 individual proteins and introduced a bioinformatics approach for statistical analysis to prove the authenticity of protein localization. A combination of six different classifiers by machine learning turned out to be crucial because only 19% of the total identified proteins could be annotated as truly chromosomal. This approach was further developed to detect protein complexes and their relation to chromosome structure and segregation (Ohta et al., 2016a;

Abbreviations: ACN, acetonitrile; ARATH, *Arabidopsis thaliana*; CCAN, centromere-associated network; DAPI, 4',6-diamidine-2'-phenylindole; DTT, dithiothreitol; ESI, electrospray ionization; EYFP, enhanced yellow fluorescent protein; FDR, false discovery rate; FoA, formic acid; GFP, green fluorescent protein; GO, gene ontology; HMG, high mobility group; HORVU, *Hordeum vulgare*; HyD, hybrid detectors; ID, identification; KMN, Knl1, Mis12, and Ndc80 network; nLC, nanoflow liquid chromatography; MALDI, matrix-assisted laser desorption/ionization; MCM, minichromosome maintenance; MG, microgradient; MGF, Mascot generic format; MS, mass spectrometry; MS/MS, tandem mass spectrometry; NSAF, normalized spectral abundance factor; NWC, NOL11, WDR43, and Cirhin complex; PMSF, phenylmethylsulfonyl fluoride; RAF-BT, raffinose-modified bovine trypsin; SDS-PAGE, sodium dodecyl sulfate–polyacrylamide gel electrophoresis; SCX, strong cation exchange; SMC, Structural maintenance of chromosome; TCEP, tris(2-carboxyethyl)phosphine; TFA, trifluoroacetic acid; WT, wild type.

Montaño-Gutierrez et al., 2017), mitosis-specific chromosome phosphorylation events (Ohta et al., 2016b), and components of the chromosomal scaffold (Ohta et al., 2019).

Most of the advances were made by analyzing human and animal chromosomes and very little is known about chromosomal proteins in plants. To date, proteomics studies in plants focused on interphase nuclei (Tan et al., 2007; Bigeard et al., 2014; Petrovská et al., 2014; Zeng and Jiang, 2016; Blavet et al., 2017). One of the reasons for the absence of studies on plant mitotic chromosomes may be a difficulty to obtain highly synchronized plant cell populations in mitosis. Ideally, the studies should be done on purified mitotic chromosomes as this helps to discriminate the "genuine" and functionally significant chromosomal proteins from those isolated from interphase nuclei, which escaped synchronization, and cytoplasmic proteins. However, any preparation of pure fractions of mitotic chromosomes is challenging in plants (Doležel et al., 2012; Zwyrtková et al., 2020).

Here, we report on identification of a large number of proteins from condensed plant mitotic chromosomes. Our interdisciplinary approach comprised the induction of high degree of mitotic synchrony in meristem root-tip cells, purification of chromosomes by flow cytometric sorting, in-solution DNA and protein digestion, liquid chromatography of peptides, high-resolution MS/MS, and adapted multi-classifier data analysis.

MATERIALS AND METHODS

Chemicals

Benzonase® (Cat. No. E1014), DNase I (Cat. No. AMPD1), SOLu-trypsin (Cat. No. EMS0004), dithiothreitol (DTT), iodoacetamide, and tris(2-carboxyethyl)phosphine (TCEP) were from Sigma-Aldrich (Steinheim, Germany), and NEBNext® dsDNA Fragmentase® was from New England Biolabs (Ipswich, MA, United States). Raffinose-modified bovine trypsin (RAF-BT) was prepared as described (Šebela et al., 2006). Chromatography solvents were of LC-MS grade. All other chemicals were from commercial sources and were of analytical purity grade if not stated otherwise.

Flow Cytometric Chromosome Sorting for Proteomic Analysis

Suspensions of intact mitotic metaphase chromosomes were prepared as described by Lysák et al. (1999) with modifications. Briefly, root-tip meristem cells of young seedlings of barley [*Hordeum vulgare* (HORVU) L.] cv. Morex were accumulated in metaphase after treatments with 2 mM hydroxyurea for 18 h, 2.5 μM amiprophos-methyl for 2 h, and ice water (overnight). Synchronized root tips were fixed in 2% (v/v) formaldehyde at 5°C for 15 min and homogenized using a Polytron PT1300D (Kinematica AG, Littau, Switzerland) at 15,000 rpm for 13 s in LB01-P buffer (Petrovská et al., 2014). The resulting chromosome suspension was stained with 2 μg mL^{-1} 4',6-diamidino-2-phenylindole (DAPI) and analyzed at a rate of ~5,000 particles per second using a FACSAria SORP flow cytometer (Becton Dickinson, San José, United States). Sort windows were set on a dot plot of fluorescence pulse area versus fluorescence pulse width to select all seven chromosomes of barley. For proteomic analyses, samples were prepared by sorting a total of 10–11 × 10^6 chromosomes into 15-mL Falcon tubes containing 1 mL LB01-P buffer supplemented with 5 mM phenylmethylsulfonyl fluoride. Flow-sorted chromosomes were pelleted at 2,500 rpm and 4°C for 30 min, and resuspended in ddH_2O.

Protein Extraction Procedure No. 1

The pellets of flow-sorted barley chromosomes were decrosslinked by incubation in 50 μL of 50 mM Tris-HCl, pH 8.0, containing 2 mM $MgCl_2$, at 70°C for 9 h. This was followed by adding 50 μL of the same buffer supplemented with 8 M urea and 10 mM DTT. After adding Benzonase (250 units), DNA was digested at 25°C for 24 h. Similarly, DNase I (20 units) was applied for DNA digestion. In parallel, Fragmentase alone (20 μL) or in a combination with Benzonase (as above) was used. The digestion buffer for Fragmentase was 50 mM Tris-HCl, pH 8.0, containing 15 mM $MgCl_2$, and 50 mM NaCl (pipetted in an amount of 50 μL to the chromosomal pellet). The DNA digestion with Fragmentase proceeded at 37°C for 24 h. The released proteins were recovered by precipitation with chilled acetone (1:4, v/v) at −20°C for 24 h.

Gel Electrophoresis

Protein precipitate from the extraction step (procedure no. 1) was dissolved in 25 μL of Laemmli sample buffer and kept at 60°C for 30 min. Sodium dodecylsulfate polyacrylamide gel electrophoresis (SDS-PAGE) was performed with 10% T/3.3% C resolving and 4% T/3.3% C stacking 1-mM thick vertical gels following a standard protocol (Laemmli, 1970) and using a Mini-Protean II apparatus (Bio-Rad, Hercules, CA, United States). %T stands for the total monomer concentration (in g per 100 mL) and %C stands for weight percentage of crosslinker (*N,N'*-methylenebisacrylamide). The whole protein sample (25 μL) was applied to a sample well at the top of the stacking gel. Electrophoresis was run at 110 V until the marker dye reached the bottom of the resolving gel. Gel staining employed a standard protocol with 0.025% w/v Coomassie Brilliant Blue G-250 in 40% v/v methanol–10% v/v acetic acid (background destaining by 5% v/v methanol–7% v/v acetic acid). Gel images were obtained using an ImageScanner device and Lab Scan 5.0 software (Amersham Biosciences, Uppsala, Sweden).

In-Gel Digestion of Proteins

The sample lane was cut horizontally into 17 sections representing protein fractions (12 stained bands and 5 less stained larger areas) of a different molecular mass. After destaining using 50 mM NH_4HCO_3 in 50% v/v acetonitrile (ACN) for 45 min, proteins were in-gel reduced by 10 mM DTT in 100 mM NH_4HCO_3 and then alkylated by 55 mM iodoacetamide in 100 mM NH_4HCO_3 (Shevchenko et al., 2006). In-gel digestion was performed using RAF-BT (Šebela et al., 2006). Peptides were

extracted from the digests with 5% v/v formic acid (FoA)/ACN, 1:2, v/v (Shevchenko et al., 2006), recovered in test tubes after solvent evaporation in a vacuum centrifuge, and finally purified using C18-StageTips (Rappsilber et al., 2007).

In-Solution Digestion of Proteins No. 1

The entire precipitate from extraction procedure no. 1 was dissolved in 40 µL of 100 mM triethylammonium bicarbonate, pH 8.0, containing 6 M urea and 2 M thiourea. The protein content was then assayed by the bicinchoninic acid method (Smith et al., 1985) after a sample aliquot dilution to decrease the urea concentration to 3 M. Proteins were reduced by TCEP (5 mM, 23°C, 45 min) and alkylated using iodoacetamide (50 mM, 23°C, 30 min). In-solution digestion with RAF-BT was subsequently done using a protein-to-trypsin molar ratio of 20:1.

In-solution digests were fractionated using the StageTips (Rappsilber et al., 2007) containing Empore™ Cation Exchange-SR extraction disks 2251 (3 M Bioanalytical Technologies, St. Paul, MN, United States) or by reversed-phase chromatography in a microgradient (MG) device (Franc et al., 2013a,b). The cation-exchange separation was performed using a stepwise concentration gradient of ammonium acetate (25 mM, 50 mM, 75 mM, 125 mM, and 200 mM) when the total elution was achieved by 5% v/v NH_4OH in 80% v/v ACN. The separate peptide fractions were then recovered in test tubes after solvent evaporation in a vacuum centrifuge and purified using the StageTips with Empore™ C18 extraction disks 2215 (3 M Technologies).

Protein Extraction and In-Solution Digestion Procedure No. 2

A suspension containing 10×10^6 flow-sorted barley chromosomes was repeatedly mixed with 150 µL of mass spectrometry (MS)-quality water for washings. The solid material was collected by a brief centrifugation. Next, the pellet was suspended in 40 µL of 50 mM Tris-HCl, pH 8.0, containing 2 mM $MgCl_2$ and kept at 70°C and 850 rpm for 5 h. Proteins were denatured by the addition of 20 µL of the same buffer containing 8 M urea and 10 mM DTT. The mixture was incubated at 23°C for 1 h before adding 1 µL (250 units) of Benzonase and kept at 23°C without shaking for 18 h. Disulfide reduction was achieved by the addition of 15 µL of 5 mM TCEP and incubation at 23°C for 45 min. This was followed by alkylation of cysteine thiols by adding 15 µL of 50 mM iodoacetamide in 50 mM Tris-HCl, pH 8.0, and incubating at 23°C for 30 min. Protein digestion was performed using 1 µg of SOLu-trypsin in an overall volume of 240 µL of the 50 mM Tris-HCl buffer, pH 8.0, containing $MgCl_2$ at 37°C and 350 rpm for 18 h. The digestion was stopped by adding 2 µL of 50% v/v FoA.

The second sample was the original root-tip homogenate containing chromosomes as used for chromosome flow sorting, and the third sample was a chromosome-depleted fraction (i.e., a homogenate from which chromosomes were removed by flow cytometric sorting). Cell lyzate proteins were obtained from 1 mL of the extract in a 5-mL tube using acetone precipitation (1:4, v/v) at −20°C for 24 h and centrifugation at 20,000 *g* and 4°C for 15 min. The pellet was then suspended in 1 mL of fresh acetone, transferred into a 1.5-mL tube, and collected by centrifugation as above. Further processing of the additional samples followed the protocol for chromosomes with the initial washing step omitted in case of the original root-tip homogenate.

Peptide Quantification Assay

The acidified peptide mixture from procedure no. 2 was spun down at 10,000 *g* for 15 min and the supernatant was transferred into a new tube. Then, the tryptophan content in the peptides was determined using a microarray fluorescence reader Synergy MX (BioTek Instruments, United States) as published by Wisniewski and Gaugaz (2015). Samples of 200 µL were loaded into microtitration plate wells. The instrument parameters were as follows: excitation wavelength of 295 nm and bandwidth of 9.0 nm; emission wavelength of 350 nm and bandwidth of 20.0 nm; gain of 75 units, 10 reads; 20°C; and integration time of 50 µs. The calibration solutions contained 0.01–5.0 µg $µL^{-1}$ tryptophan in the sample buffer with urea. Peptide amounts in the assayed samples were calculated using the assumption that HORVU proteins contain on average 1.95% tryptophan by mass (derived from the UniProt barley protein database, see below for details).

Microgradient Separation of Peptides

Tryptic peptides from the digests were first chromatographed using a MG device (Franc et al., 2013a,b). The peptides in an amount of 4 µg were loaded into an equilibrated microcolumn (250 µm i.d. × 30 mM) made of Kinetex EVO C18 2.6 µm core-shell particles (Phenomenex, 00G-4,725-E0) and desalted by washing with 25 µL of 0.1% v/v TFA. Then, the retained peptides were eluted by a stepwise gradient of 8, 12, 16, 20, 24, 28, 36, and 48% v/v ACN in 20 mM NH_4HCO_3 aspirated into the gas-tight syringe. The eluate was collected in seven consecutive 4-µL fractions. Each fraction was then diluted by 21 µL of 5% v/v FoA for the subsequent MS analysis.

Mass Spectrometry of Peptides

Nanoflow liquid chromatography-tandem mass spectrometry (nLC-MS/MS) analyses were performed on a maXis UHR-Q-TOF mass spectrometer equipped with a nanoelectrospray ion source (Bruker Daltonik) and connected to a Dionex UltiMate3000 RSLCnano liquid chromatograph (Thermo Fisher Scientific, Germering, Germany). Each sample was measured in two runs and the data were pooled. The experimental setup including the reversed-phase analytical column, pre-column, composition of mobile phases, flow rates, gradient programming, and other automated MS and MS/MS data acquisition parameters was the same as described previously (Chamrád et al., 2014).

Data Analysis and Annotation

Raw data were converted into Mascot generic format-formatted files and processed for database searches using PEAKS Studio 10 (Bioinformatics Solutions, Waterloo, ON, Canada). The search

parameters were as follows: mass tolerance for precursor ions and fragments – 50 ppm and 0.05 Da, respectively; enzyme – trypsin (semispecific); the number of missed cleavages – 2; allowed modifications per peptide – up to 3; variable peptide modifications – Met oxidation, Asn/Gln deamidation, protein N-terminal acetylation; and fixed peptide modification – Cys carbamidomethylation. The sequence databases used were barley (HORVU) proteome database downloaded from the UniProtKB (https://www.uniprot.org, 11/10/2020, Proteome ID UP000011116, 189,799 entries; International Barley Genome Sequencing Consortium et al., 2012) and cRAP contaminant database (downloaded from https://www.thegpm.org/crap/ on 11/10/2020). The false discovery rate was set at 1% as a positivity threshold for the peptide-spectrum match plus peptide and protein sequence matches. At least one unique peptide was required for positive protein identification and only the first identification (ID) with the highest –logP score for each protein group was used for the subsequent data evaluation.

The obtained list of IDs matching the set of barley protein sequences was then searched against the UniProtKB/Swiss-Prot database to find *Arabidopsis thaliana* (ARATH) homologs by blastp (protein-protein BLAST; Altschul et al., 2005). Then, the available information on the cellular localization, related gene ontology (GO) terms, molecular mass, and sequence length for each Arabidopsis protein accession was acquired *via* UniProtKB Retrieve/ID mapping tool. A limit of 70% sequence homology was set up for the further search on UniProtKB protein localization information for Arabidopsis homologs. The whole protein FASTA-formatted file was reduced into partial files of 400 IDs for the application of other bioinformatics tools, such as NucPred (Brameier et al., 2007), Localizer (Sperschneider et al., 2017), CELLO2GO (Yu et al., 2014), and WegoLoc (Chi and Nam, 2012). In Localizer, the input was specified as "full plant sequences." The plant BaCelLo dataset and default settings were used in WegoLoc. In CELLO2GO search parameters, the eukaryotic organism option was selected. Also, matching GO terms and other information were obtained by searches using DAVID Functional Annotation Tool (Huang et al., 2009).

Evaluation of Nuclear or Chromosomal Localization

All data obtained from the databases and bioinformatics tools were merged using Perseus v.1.6.10.45 (Tyanova et al., 2016) and further processed in Microsoft Excel 2016. Six groups reflecting the prediction results and UniProtKB information were established to categorize the identified proteins (Search S1). Protein IDs yielding information on a nuclear/chromosomal localization in more than two prediction tools, which possessed a positive record on their nuclear origin in UniProtKB, were marked as "NUCLEAR." Those IDs with more than two nuclear prediction hits and lacking any UniProtKB information on nuclear localization were grouped as "PREDICTED NUCLEAR." Proteins labeled as nuclear/chromosomal by two prediction tools with a reliable record in UniProtKB were classified as "POSSIBLY NUCLEAR." The group "DISCREPANCY UNIPROT" contained IDs with non-nuclear UniProtKB localization information and more than two positive nuclear/chromosomal localization hits from the prediction tools. The group "DISCREPANCY PREDICTION" refers to protein IDs labeled as nuclear in UniProtKB and yielding less than two positive hits from the prediction tools. Finally, proteins classified in the "CYTOSOLIC" group were assigned according to information available on their subcellular localization in UniProtKB for HORVU or the corresponding ARATH protein accessions by searching with tags "cytos," "cytop," "mitoch," "memb," and "recept." One positive hit for nuclear localization was a maximum for this group. The following criteria were used to filter out positive nuclear/chromosomal localizations: Localizer – predicted nuclear localization; NucPred – prediction score $\geq$ 0.50; WegoLoc – predicted localization contains the tag "nucl"; and CELLO2GO – the predicted localization (CP) result contains the tag "nucl" or "chromo." The UniProtKB HORVU IDs and their ARATH homologs were searched for the tags "chromos," "chromat," and "nucl" in the "Subcellular location (CC)" information provided in the database entry. Information on protein domains was obtained using CD-Search (Marchler-Bauer and Bryant, 2004; default settings) and barley FASTA sequences.

Each protein containing at least one functional domain was scored using an in-house made database of domains (inspired by Ohta et al., 2010) based on experiments following the in-solution digestion procedure 2 and MG peptide separation. Finally, it contained 869 domains. Those domains bound to the protein ID groups "NUCLEAR," "PREDICTED NUCLEAR," and "POSSIBLY NUCLEAR" were attributed as nuclear. Domains related to "CYTOSOLIC" proteins were considered false. Each domain for a protein ID was then scored for these attributes. Domains not included in the database were marked as unknown. Comprehensive data combining nuclear prediction hits, information on protein localization in the UniProtKB, and the domain score were re-evaluated (Search S2). Protein IDs with more than three nuclear prediction hits plus the existing nuclear localization information in UniProtKB (barley accessions) and true domain attribute were "NUCLEAR." The same score but the existing nuclear localization information in UniProtKB for ARATH homolog only resulted in "NUCLEAR (BLAST)" classification. Proteins lacking any domain information were classified in the group "UNSUFFICIENT CD INFO." Those with less than three nuclear prediction hits were denoted as "POSSIBLY NUCLEAR." Missing or non-nuclear localizations found for barley and ARATH accessions in the corresponding UniProtKB/Swiss-Prot entries were evaluated as "DISCREPANCY UNIPROT."

Generating Barley EYFP-FIB1 Reporter Line

The CDS sequence of barley *FIBRILLARIN 1* (*FIB1*; HORVU6Hr1G091860), cultivar Golden Promise, was amplified to generate the *ZmUBI1::EYFP-FIBRILLARIN1::T35S* fusion construct. The amplification was achieved with cDNA obtained by a reverse transcription (Transcriptor High Fidelity cDNA Synthesis Kit; Roche) using total RNA isolated from roots (RNeasy kit; Qiagen) with the following primer pair: 5'-ATGAGGGCTCCCATGAGAGG-3' and 5'-CTTTTGCTTC

TTGGGCATCCTGT-3', including the stop codon. *FIB1* CDS was then reamplified with another primer pair 5'- GGGGACA ACTTTGTATAATAAAGTTGTTCACTTTTGCTTCTTGGGC ATCC-3' and 5'- GGGGACAGCTTTCTTGTACAAAGTGGT AATGAGGGCTCCCATGAGAGG-3' containing the attB sites and cloned *via* BP reaction into a *pDONR-P2r-P3* vector by Gateway cloning strategy (Gateway™). The final expression cassette, including *ZmUBI1* promoter, *EYFP-FIB1*, and *T35S* terminator, was subcloned by multisite LR reaction combining three entry vectors *pEN-L4-UBIL-R1*, *pEN-L1-Y-L2*, and *pDONR-P2r-P3* with *FIB1* CDS into the *pH7m34GW* destination vector. All constructs assemblies were verified by Sanger sequencing.

The full construct in *pH7m34GW* vector was transformed into *Agrobacterium tumefaciens* strain AGL1. For barley transformation, immature embryos of the cultivar Golden Promise were dissected and transformed according to the previously described protocol (Marthe et al., 2015). Regenerated plants were genotyped for the presence of *hptII* gene, conferring resistance to hygromycin, by PCR with primer pair 5'-GACGTCTGTCGAGAAGTTTCTG-3' and 5'-CGAGTACTT CTACACAGCCATC-3'. The presence of EYFP-FIB1 fusion protein *in planta* was confirmed by the confocal microscopy using a Leica TCS SP8 STED3X microscope (Leica Microsystems, Wetzlar, Germany), equipped with an HC PL APO CS2 20 ×/0.75 DRY objective, hybrid detectors (HyD), and the Leica Application Suite X (LAS-X) software version 3.5.5 with the Leica Lightning module (Leica, Buffalo Grove, IL, United States).

Isolation of Mitotic Chromosomes for Microscopic Analyses

Preparation of suspensions of mitotic metaphase chromosomes and flow cytometric chromosome sorting was done as described above for the proteomic analyses. However, chromosome suspensions were prepared in LB01 buffer (Doležel et al., 1989) from barley cv. Golden Promise and EYFP-FIB1 transgenic plants, and 10^5 chromosomes were flow sorted into 25 µL of LB01 buffer. 10 µL of the flow-sorted chromosome suspension was pipetted into a 10-µL drop of P5 buffer (Kubaláková et al., 1997) on poly-lysine coated microscopic slides (Thermo Scientific™), air dried for up to 15 min, and stored at −20°C until use. To evaluate the effect of RNA removal, RNase A (Sigma Aldrich) was added to 100 µL aliquots of the flow-sorted chromosome suspensions in LB01 to a final concentration of 0.01 ng μL^{-1} and incubated for 30 min at 16°C prior to pipetting into microscopic slides.

Isolation of Interphase Nuclei for Microscopic Analyses

For the isolation of root-tip meristem cell nuclei, both Golden Promise and EYFP-FIB1 transgenic seeds were surface sterilized as described (Marthe et al., 2015), cold stratified for 2 days at 4°C on a wet paper towel, and germinated for 2 days at 24°C in dark. Suspensions of cell nuclei were prepared following a previous protocol (Doležel et al., 1992) with modifications. Briefly, roots of the young seedlings were fixed in 3% (v/v) formaldehyde in 10 mM Tris buffer with additives (pH 7.5; Doležel et al., 2011) for 15 min on ice plus 5 min on ice/vacuum (500 mBa). Then, they were washed twice in the same buffer for 10 min on ice. About 30 root tips were cut with a razor blade and homogenized in 500 µL P5 buffer (Kubaláková et al., 1997) using Polytron PT1300D homogenizer (Kinematica AG) at 15,000 rpm for 13 s. The homogenate was filtered through a 30 µm nylon mesh and centrifuged at 2,000 *g* and 4°C for 10 min. The supernatant was removed and the pellet containing nuclei was resuspended in 100 µL of the P5 buffer. About 10 µL of the suspension was pipetted into poly-lysine coated slides (Thermo Scientific™), air dried for up to 15 min, and stored at −20°C.

Immunostaining and Microscopy

The immunostaining was performed as described (Jasenčáková et al., 2001). EYFP-FIB1 was detected with primary mouse antisera against FIB1 (1:100; ab4566; Abcam) and secondary antibodies goat anti-mouse-Cy5 (Alexa Fluor® 647; 1:300; A21235; Invitrogen) or with a goat anti-mouse-Cy3 (Alexa Fluor® 546; 1:300; A-11003; Invitrogen) for nuclei or metaphase chromosomes, respectively. Alternatively, EYFP-FIB1 on metaphase chromosomes was detected with rabbit antisera against GFP (1,100; ab290; Abcam) recognizing also EYFP and secondary antibodies goat anti-rabbit-Cy3 (Alexa Fluor® 647; 1:300; A-11010; Invitrogen) for metaphase chromosomes. Nuclei and chromosomes were counterstained with DAPI dihydrochloride (1 µg mL^{-1}) in a Vectashield medium (Vector Laboratories).

Microscopic images were acquired using a Leica TCS SP8 STED3X confocal microscope (Leica Microsystems, Wetzlar, Germany), equipped with an HC PL APO CS2 63 ×/1.40 Oil objective, hybrid detectors, and the LAS-X software version 3.5.5 with the Leica Lightning module (Leica, Buffalo Grove, IL, United States). Confocal images were captured separately in sequential scans, to avoid spectral mixing, using 405 nm (DAPI), 508 nm (EYFP), 557 nm (Alexa Fluor® 546), and 594 nm (Alexa Fluor® 647) laser lines for excitation and appropriate emission spectrum. Pictures were processed in Adobe Photoshop version 12.0 (Adobe Systems).

RESULTS

Gel-Based Identification of Barley Chromosomal Proteins

Our initial experiments followed the protocol used by Petrovská et al. (2014) and Chamrád et al. (2018) to characterize the proteome of barley interphase nuclei. Their procedure included a heat-treatment, nuclease-assisted protein extraction, SDS-PAGE, in-gel proteolytic digestion, and MS/MS-based protein identification. The protein extraction step was facilitated by heat-induced disruption of formaldehyde cross-links to dissociate nuclear/chromosomal proteins from their complexes with DNA. The protocol yielded only 63 barley protein IDs (**Supplementary Table S1**) using 11 million chromosomes. Even though this number was much lower than expected, the

electrophoretic pattern (**Figure 1**) was typical for chromosomal/nuclear preparations with distinct histone bands (Ohta et al., 2010; Petrovská et al., 2014). A majority of the identified proteins had a nuclear/chromosomal localization and related functions. This group included histones and also ribosomal proteins (assigned mostly as non-classified as well as cytosolic proteins according to their localization) and a few DNA/RNA-binding proteins. Other protein IDs included, e.g., abundant enzymes representing components of energy metabolism pathways (glycolysis and oxidative phosphorylation).

Gel-Free Approaches Including Fractionations of Peptide Mixtures

We suspected that the low yield of protein IDs was related to a low protein input (10 million barley chromosomes provided an average protein mass of 4.4 µg). Therefore, the gel-based procedure was replaced by a gel-free protocol. Moreover, DNA digestion was performed differently using a set of nucleases comprising DNase I, Benzonase, and Fragmentase, the latter two were also combined in a single reaction mixture. The recovered proteins were then subjected to tryptic proteolysis and the resulting peptides were fractioned on a strong cation exchanger prior to nanoflow liquid chromatography (nLC)-electrospray ionization (ESI)-MS/MS. **Table 1** shows an overview of all experiments, which are documented in **Supplementary Table S2**. The best results with regard to the number of protein IDs in a single experiment were obtained with the protocol using Benzonase (1169–1531 proteins). This enzyme was employed in all subsequent experiments.

Figure 2 shows the predicted nuclear or non-nuclear localization of all identified proteins attributed in the two-round search approach referred to as S1 and S2 here. Database searches provided an overall number of 4139 protein IDs by combining individual datasets (**Supplementary Table S3**). A total of 674 proteins might be considered nuclear/chromosomal utilizing predictors based on data from gene ontology prediction tools, UniProtKB database annotations, and conserved domain searches. The more stringent search approach S2, which additionally considered information on the presence of a verified nuclear domain in the sequence of each identified protein, clearly confirmed 228 nuclear/chromosomal hits (143 + 62 + 23) and additional 485 entries (428 + 18 + 39) were found less plausible for classification in this category. Some of the latter IDs could not be verified by nuclear domain in S2 search (18 items) or consistent results in both S1 and S2 search (39 items). The reason resides, namely, in a discrepancy found for their localization in the UniProtKB database (i.e., they are not denoted as nuclear – 428 items).

The Panther GO (gene ontology) classification tool was applied to evaluate the identified 674 nuclear/chromosomal barley proteins (including those with the localization annotation discrepancy in UniProtKB) as regards to the attributed protein class name. Arabidopsis homologs (636 in total) were reduced to 293 unique Arabidopsis database entries for the GO classification search referring to 405 original barley proteins IDs (**Supplementary Table S3**). Almost two-thirds of the evaluated IDs belonged to nucleic acids-binding proteins including histones, replication factors, and various DNA/RNA processing enzymes, such as helicases, ligases, methyltransferases,

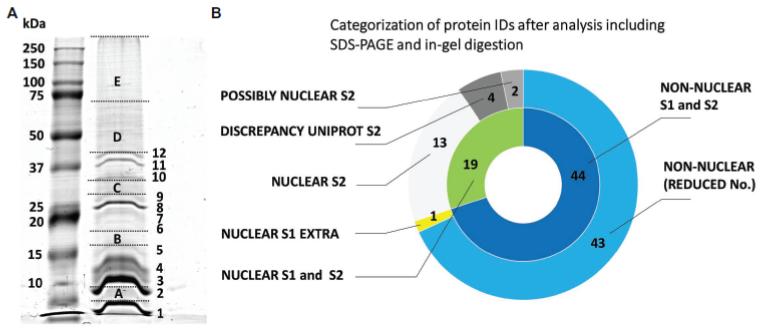

FIGURE 1 | Evaluation of the origin of proteins from mitotic chromosomes identified by GeLC-ESI-Q-TOF MS/MS. **(A)** SDS-PAGE of extracted barley chromosomal proteins (Coomassie Brilliant Blue staining). The separation was achieved in a 10% T/3.3% C resolving polyacrylamide gel. Left lane, protein marker 10–250 kDa (Kaleidoscope Standards, Bio-Rad); right lane, chromosomal proteins. The excised gel fractions and bands are labeled by capital letters A-E and numbers 1–12, respectively; this labeling is used in **Supplementary Table S1** for reference. **(B)** The nested pie chart shows information on the possible nuclear or non-nuclear localization of all identified proteins and their distribution into categories reflecting results of a two-round search approach (S1 and S2) utilizing predictors based on data from gene ontology prediction tools, UniProtKB database annotations and conserved domain searches (NCBI CDD database). The principle of S1 and S2 sorting is elucidated in Materials and Methods. The inner ring shows combined results of the two data search and evaluation procedures. The area labeled "NUCLEAR S1 and S2" refers to the consistently obtained attributes NUCLEAR, PREDICTED NUCLEAR/DISCREPANCY UNIPROT, and POSSIBLY NUCLEAR. The outer ring shows a protein distribution based on the procedure S2 plus an additional non-overlapping hit obtained using S1 ("NUCLEAR S1 EXTRA"). The label "NON-NUCLEAR (REDUCED No.)" refers to subtraction of the non-overlapping hit from the total number of non-nuclear identification.

TABLE 1 | A summary of the results of nLC-ESI-MS/MS analyses yielding protein identification after previous peptide fractionation using strong cation exchanger.

Sample processing prior to before SCX	Matched peptide MS/MS spectra	Mean sequence coverage	Matched peptides	Unique matched peptides	Protein IDs	Possibly nuclear proteins[a]		Nuclear proteins (BLAST)[a]		Nuclear proteins[a]	
						#	%	#	%	#	%
Benzonase and in-sol digestion	60360	20.2	7491	4810	1169	17	1.5	17	1.5	47	4.0
Fragmentase and in-sol digestion	23705	17.8	4354	2943	815	5	0.6	13	1.6	25	3.1
Fragmentase+Benzonase and in-sol digestion	13232	17.1	1981	1,346	435	6	1.4	9	2.1	22	5.1
DNase I and in-sol digestion	67819	18.9	6764	4210	1090	15	1.4	17	1.6	57	5.2
Benzonase and in-sol digestion	37137	15.2	6047	4243	1216	11	0.9	22	1.8	35	2.9
Benzonase and in-sol digestion[b]	50659	19.8	7577	5029	1209	10	0.8	19	1.6	47	3.9
Benzonase and in-sol digestion (no precipitation)	24609	13.2	6873	4885	1436	13	0.9	18	1.3	46	3.2
Benzonase and in-sol digestion (no precipitation)[b]	58019	15	7186	5387	1531	13	0.8	18	1.2	42	2.7
Overall	135009	14.2	18795	13237	4139	31	0.7	62	1.5	143	3.5

[a]*Nuclear localization in data search S2 as attributed to protein IDs using predictors (see Materials and Methods and* ***Supplementary Table S2****).*
[b]*Extraction of chromosomes was performed at pH 9 otherwise it was pH 7.*

topoisomerases, chromatin-remodeling complex ATPase, DNA-directed RNA polymerase subunits, and others. SMC proteins (including cohesins and condensins) were represented by 13 items. Approximately 15% of the IDs were ribosomal proteins, ribosome biogenesis regulators, and translation factors. Chromatin proteins and gene-specific transcription regulators represented roughly 5%. Other attributed nuclear/chromosomal proteins were, e.g., kinetochore proteins, nucleosome assembly proteins, importin, ubiquitin, and ubiquitin-related enzymes.

Another set of experiments involved peptide fractionation using a C18 reversed-phase MG device (Moravcová et al., 2009). This approach has repeatedly been shown very helpful and efficient for a pre-separation of peptides from digests prior to nanoLC-matrix-assisted laser desorption/ionization-MS/MS or nanoLC-ESI-MS/MS analysis (Franc et al., 2013a,b). In that case, each analyzed peptide sample was first separated into seven fractions that were individually subjected to nanoLC-ESI-MS/MS. The obtained results are summarized in **Figure 3**. The total number of unique barley protein IDs was 2941 (**Supplementary Table S4**), from which 398 might be considered nuclear/chromosomal based on the bioinformatics data processing S1 + S2 as already mentioned above using UniProtKB database and prediction tools referring to the appropriate conserved protein domains and attributed gene ontology terms. The search approach S2 confirmed 155 nuclear/chromosomal hits (92 + 43 + 20). Additional 299 entries (243 + 56) were found less plausible for classification in this category, from which the number 56 were inconsistently retrieved results in both S1 and S2 search. A repeated application of the MG separation showed 1193 reproducible protein IDs. They were present in at least two biological replicates, see below, from which 144 were classified as nuclear/chromosomal.

The consensual number of 398 barley protein IDs provided 371 Arabidopsis homologs, which were reduced to 263 unique Arabidopsis database entries for the GO classification search referring to 252 original barley protein IDs (**Supplementary Table S4**). Again, a majority of the evaluated IDs (54%) belonged to nucleic acids-binding proteins including histones, replication/transcription/splicing factors, and various DNA/RNA processing enzymes, such as helicases, ligases, methyltransferases, topoisomerases, chromatin-remodeling complex ATPase, DNA-directed RNA polymerase subunits, and others. SMC proteins were represented by six items. About 16% were ribosomal proteins and translation factors. Chromatin proteins and gene-specific transcription regulators represented roughly 4%. Other attributed nuclear/chromosomal proteins included nucleosome assembly proteins, a kinetochore protein, transporters, and ubiquitin-related enzymes.

Enrichment of Nuclear/Chromosomal Proteins

The experimental workflow with MG pre-separation of peptides was applied to three different sample types: (1) flow-sorted barley chromosomes, (2) original root-tip homogenate as a control, and (3) chromosome-depleted homogenate (chromosomes were removed by flow cytometric sorting).

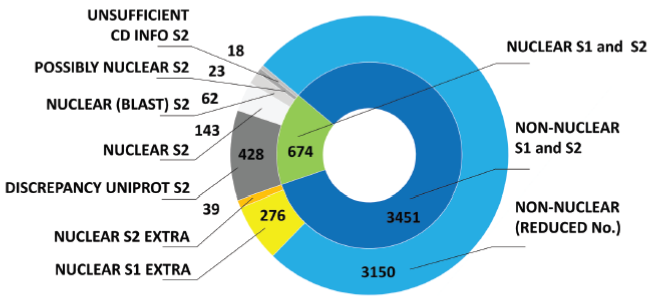

FIGURE 2 | Evaluation of the origin of proteins from mitotic chromosomes identified by nLC-ESI-Q-TOF MS/MS with SCX fractionation of tryptic peptides. The nested pie chart shows information on the possible nuclear or non-nuclear localization of all identified proteins and their distribution into categories reflecting results of a two-round search approach (S1 and S2). The principle of S1 and S2 sorting is provided in Materials and Methods. See the legend to **Figure 1** for elucidation of the attributed categories.

Every sample type was analyzed in three biological replicates and each of them in two technical replicates. The results are summarized in **Figure 4**. Our analyses considered only proteins which were identified in at least two biological replicates. Normalized spectral abundance factor values were chosen as a quantitative measure (Zybailov et al., 2006) for comparison. Proteins verified in S1 + S2 search and categorized as nuclear (and accordingly considered chromosomal) represented 30% of all repetitive IDs for the flow-sorted chromosomes. This was significantly more than ~10% obtained for the control (i.e., the original root-tip homogenate) and the chromosome-depleted fraction. Data analysis confirmed the expected enrichment of nuclear/chromosomal proteins in chromosomes as the percentages for individual search categories were rather similar for all three sample types when comparing the numbers of protein IDs (**Figure 4**). Non-nuclear proteins always represented more than 80% of IDs, and almost 90% were identified in the chromosome-depleted fraction. The category NUCLEAR S2 was the most enriched one and contained histones categorized according to Arabidopsis homology as histones and their variants: H2 (13 IDs), H1 (six IDs), and H3 (three IDs). Next, four DNA helicases were found although three of them are classified as DNA replication licensing factor or minichromosome maintenance (MCM) proteins. Single SMC protein and DNA (cytosine-5)-methyltransferase CHROMOMETHYLASE 3 (CMT3; EC 2.1.1.37) were found in this category, which may reflect the under-representation of characterized barley representatives in the database. Additionally, three chromatin handling proteins, chromatin-remodeling ATPase (2 IDs) and facilitates chromatin transcription complex subunit SSRP1 protein, confirm the presence of predominantly well-characterized DNA-binding proteins or enzymes in this group.

Altogether, a combination of the strong cation exchange (SCX) and MG-related analyses provided a list of 837 unique IDs, which may be considered nuclear/chromosomal based on the applied bioinformatics processing (**Supplementary Table S5**). This group of identified proteins was compared with the content of the UNcleProt barley nuclear protein database (Blavet et al., 2017). Only 311 out of the 837 proteins had matches in the database. **Table 2** shows that a majority of them, categorized by searches according to their names and functional annotations, were DNA-associated proteins (including histones) and RNA-associated proteins as well as proteins attributed to ribosomes. Numerous matched IDs were uncharacterized proteins in the barley proteome but could be assigned by homology to their Arabidopsis counterparts. Many novel protein IDs outside the UNcleProt belonged to the same categories but above that the others were typically chromosomal (e.g., condensin, cohesin, and kinetochore components) or mitosis-related (kinesins).

Localization of FIB1 on Mitotic Chromosomes

Besides the known chromatin proteins, the SCX and MG identified a high number of chromosomal proteins that are not associated with chromatin. A prominent group was represented by nucleolar proteins, including abundant peptides from FIB1. FIB1 is a marker of nucleoli that forms foci of various densities. We have confirmed the localization of FIB1 in nucleoli of barley interphase nuclei by immunostaining and also by constructing a barley reporter line constitutively expressing a translational fusion of EYFP-FIB1 (**Figures 5A,B**). To confirm FIB1 localization on mitotic chromosomes as suggested by the proteomic analysis, we flow-sorted metaphase chromosomes of wild-type and EYFP-FIB1 reporter line into microscopic slides and observed them either directly (EYFP-FIB1) or after immunodetection with the antibodies against FIB1 and/or GFP

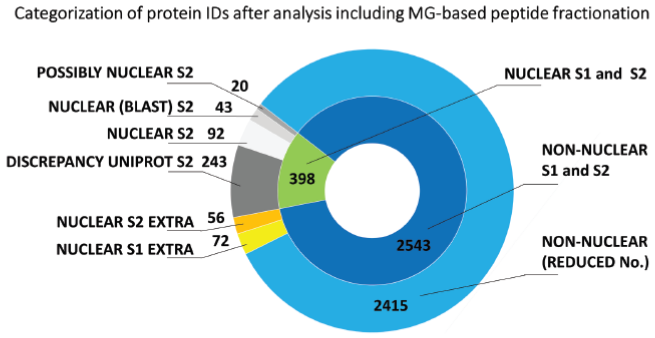

FIGURE 3 | Evaluation of the origin of proteins from mitotic chromosomes identified by nLC-ESI-Q-TOF MS/MS with MG fractionation of tryptic peptides. The nested pie chart shows information on the possible nuclear or non-nuclear localization of all identified proteins and their distribution into categories reflecting results of a two-round search approach (S1 and S2). The principle of S1 and S2 sorting is provided in Materials and Methods. See the legend to **Figure 1** for elucidation of the attributed categories.

(recognizes also EYFP). In all cases, a signal was observed confirming the presence of FIB1 (native or fusion) protein, which was not the case for negative controls when chromosomes were incubated only with a secondary antibody (**Figures 5C–F**). The chromosomes were covered entirely with foci of higher signal intensity. On some chromosomes, we observed even FIB1 localization in the kinetochore-binding region (**Figure 5D**). This observation confirmed that nucleolar protein FIB1 is associated with plant mitotic chromosomes during cell division.

FIB1 is an RNA methyltransferase that functions in complex with other proteins and RNA molecules. Therefore, we asked whether FIB1 is localized on chromosomes as an isolated protein or in complex with RNA. To test this, we treated flow-sorted chromosomes by RNase (**Figure 6**). In both cases, immunolocalized native FIB1 and EYFP-FIB1 fusion protein, RNase A treatment led to the loss of FIB1 signals, suggesting that the entire FIB1 complex including RNA molecules is associated with barley mitotic chromosomes.

DISCUSSION

Flow Cytometry as a Critical Step in Plant Chromosomal Proteomics

We have identified the largest set to date of proteins associated with plant mitotic chromosomes. Barley was chosen as a model plant because its reference genome is available (Mascher et al., 2017) as well as a plethora of transcriptome data (Kintlová et al., 2017; Rapazote-Flores et al., 2019). Its nuclear proteome has been characterized as well (Petrovská et al., 2014; Blavet et al., 2017). Importantly, a well-established method is available for the preparation of suspensions of intact mitotic metaphase chromosomes and their purification by flow cytometric sorting (Lysák et al., 1999). This allowed us to prepare samples enriched for proteins from mitotic metaphase chromosomes. Vertebrate chromosomes, on the other hand, are commonly prepared by a density gradient centrifugation, for example, by applying sucrose and Percoll gradients (Samejima and Earnshaw, 2018). While highly synchronized mitotic cell populations have been used to characterize the proteome of human and animal chromosomes, such a synchrony is hardly reachable with plant tissues.

As chromosomes are released into the cytoplasm during mitosis, it is critical to ensure that the chromosomal protein content is not contaminated by cytoplasmic proteins. As such a contamination cannot be *a priori* avoided, we have identified chromosomal proteins by comparing the results of protein identification in: (1) the original homogenate containing chromosomes plus cellular and tissue debris, (2) chromosomes purified by flow sorting, and (3) chromosome-depleted homogenate containing only cellular and tissue debris. Given that the protocol for preparation of chromosome suspensions (Lysák et al., 1999) includes mild formaldehyde fixation, there is a risk of crosslinking cytoplasmic proteins with those forming the perichromosomal layer. As this should be a random process, it should result in protein clusters of varying size irregularly associated with the chromosome surface. However, only highly regular structures were observed on the surface of flow-sorted barley chromosomes using environmental scanning electron microscopy (V. Neděla, personal communication). Based on this observation and our experimental design, we consider the results obtained in this work as well supported. We categorized all proteins identified in flow-sorted chromosomes using the information obtained from the relevant UniProtKB database records and related DAVID search data, and compared with a previous proteomics analysis of avian chromosomes (Ohta et al., 2010). The comparison showed a good overall agreement as the majority of proteins was classified as nuclear or chromosomal, while uncharacterized proteins represented consistently about 20–25% (**Figure 7**).

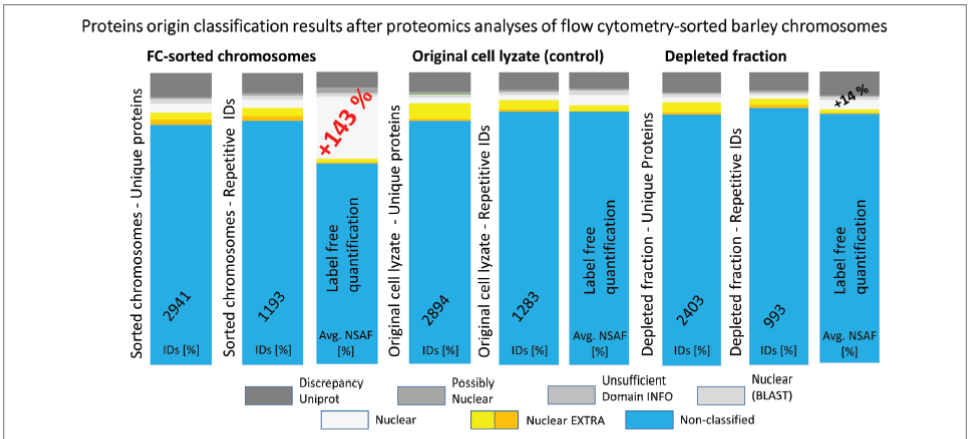

FIGURE 4 | A summary of results obtained from repeated experiments with different starting biological materials. The bar plots show a comparison of protein identification results obtained using MG separation of peptides from tryptic digests followed by nLC-ESI-Q-TOF MS/MS. Three types of biological material were used for the proteomics analyses: flow cytometry-sorted barley chromosomes, original plant cell lyzates (as a control), and depleted fractions after the flow cytometry. Repetitive IDs refer to repeated experiments, where the counted hits were obtained for at least two biological replicates (three biological replicates were analyzed in total, each was run in two technical replicates). The graphics depict percentages of the protein ID categories attributed in S2 search and the corresponding NSAF values.

TABLE 2 | Attributes assigned to the 837 identified barley chromosomal proteins (NUCLEAR S1 + S2).

Searched text string	Novel IDs in chromosomes		Matched nuclear IDs	
	HORVU[a]	ARATH[b]	HORVU[a]	ARATH[b]
Chromosome	11	20	3	13
Chromatin	2	22	2	8
DNA	17	41	17	35
Kinetochor	0	3	0	1
Histon	52	61	62	76
Replicat	6	11	2	11
Mitotic	0	1	0	2
Kinesin	10	12	0	0
Condensin	5	4	0	0
Cohesin	0	4	0	2
Transcript	0	18	3	13
RNA	11	54	7	36
Ribosome	16	35	19	34
Uncharacterized	185	1	88	2

The text strings provided in the first column were applied as "keywords" for searching in the names of barley or homologous Arabidopsis proteins (see ***Supplementary Table S5****). Only 311 out of the 837 proteins matched the original dataset of the barley nuclear protein database UNcleProt (Blavet et al., 2017). The others were thus considered novel IDs.*

[a]HORVU, Hordeum vulgare.

[b]ARATH, Arabidopsis thaliana.

To assess barley chromosomal proteome from a biological point of view, we considered a semi-quantitative nature of our methods and looked at the most relevant proteins and complexes identified. These proteins were classified as nuclear/chromosomal and were ordered decreasingly according to the number of unique identified peptides and analyzed as regards to their biological role based on the existing annotation and homology to Arabidopsis.

Pre-separations of Peptides Prior to nLC–MS/MS to Increase the Protein Identification Rate

In-gel digestion yielded only 63 proteins with 16 classified as nuclear/chromosomal. These proteins comprised almost exclusively histone proteins (H1 to H4) specific to both euchromatin (H3.3, H2A.XB, and H2A.Z) and heterochromatin (H3.1, H2A.W, and H1.2). The heterochromatic variants were generally more frequent, which may correspond to the high proportion of repetitive DNA in the barley genome (Baker et al., 2015). The GTP-binding protein RAN3 (Hv: M0UFI4; At: Q8H156/AT5G55190) was the only non-histone case likely responsible for nucleocytoplasmic protein transport. However, RAN3 most likely does not have a direct DNA-binding activity and the analysis in Arabidopsis identified it as interactor of METHYL-BINDING PROTEIN 5, which is one of four Arabidopsis MBDs binding to 5-methyl cytosine (Yano et al., 2006). In summary, the in-gel digestion method revealed practically only nucleosomal subunits, suggesting a loss of a majority of chromosomal proteins and/or a failure to detect them when using this approach.

The other two methods used, i.e., the SCX and C18 reversed-phase MG, were based on the in-solution isolated chromosomal proteins and differed in the principle of pre-separation of peptide

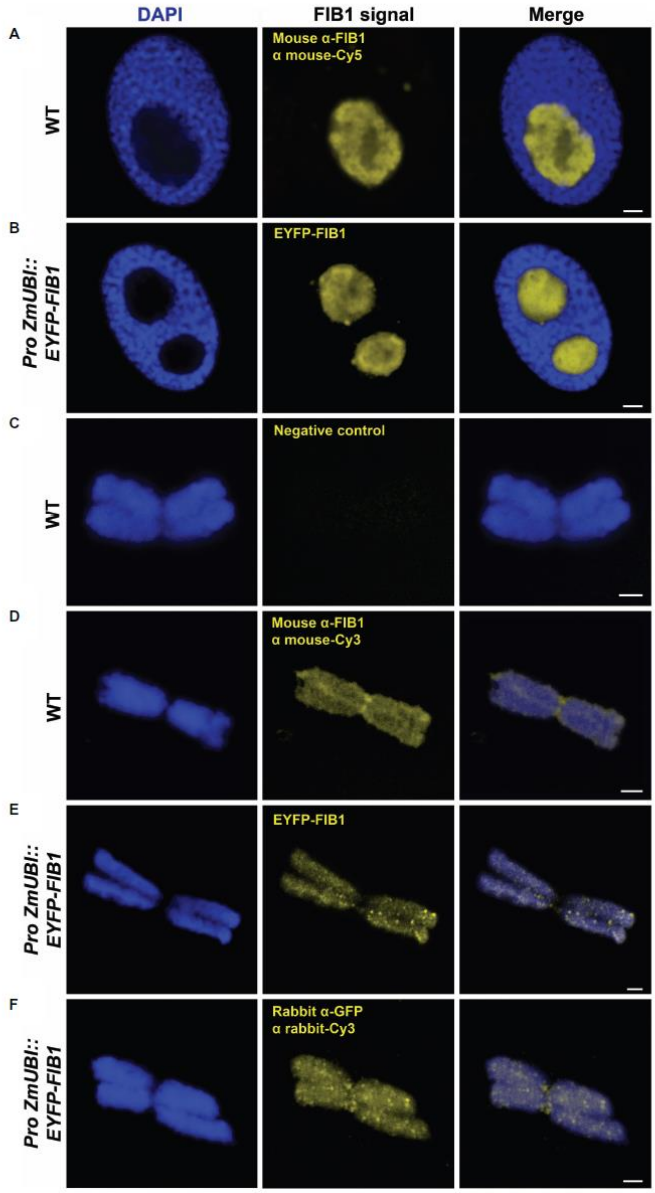

FIGURE 5 | *(Continued)*

FIGURE 5 | Detection of barley FIB1 in interphase nuclei and on metaphase chromosomes. All nuclei and chromosomes were counterstained with DAPI. Unstained regions within interphase nuclei correspond to nucleoli. **(A)** Wild-type (WT) interphase nucleus with FIB1 detected *via* immunolocalization with a specific antibody against FIB1 and secondary fluorochrome-coupled antibody. **(B)** The interphase nucleus of the barley reporter line expressing a translational fusion of the EYFP-FIB1. **(C)** Metaphase chromosome without immunostaining serving as a negative control for autofluorescence in Cy3 channel. **(D)** WT metaphase chromosome with FIB1 detected as described in **(A)**. **(E)** Reporter line metaphase chromosome with direct EYPF-FIB1 signal. **(F)** Reporter line chromosome with EYFP-FIB1 signal enhanced *via* immunolocalization with anti-GFP-Cy3 antibody (recognizing also EYFP). Scale bars = 2 μm.

mixtures. Consistently, around 15% of the obtained protein IDs were classified as nuclear/chromosomal. The lists of the most abundant proteins were very similar for both methods (**Supplementary Tables 3** and **4**). The four most common proteins/complexes (Group 1) were TOPOISOMERASE 2 (TOP2), POLY(ADP-RIBOSE) POLYMERASE 2 (PARP2), various histone proteins, and condensin complex subunits. At the fifth to the seventh position (Group 2), we found inner nuclear envelope protein CROWDED NUCLEI 1 (CRWN1), nucleolar proteins (e.g., FIB1), and subunits of the replication licensing complex MCM MCM2 to MCM7. The remaining positions (Group 3) were more variable between the methods and represented a mix of proteins with various chromatin-related functions. They included chromatin-remodeling ISWI complex factor (CHR11); FACT complex factors (SPT16 and SSRP1 subunits); high mobility group proteins; histone chaperone NAP1,2; DNA repair proteins ZINC 4 FINGER DNA 3'-PHOSPHOESTERASE (ZDP), LIGASE 1 (LIG1) and KU80; and transcriptional gene silencing factors CHG DNA methyltransferase CMT3, CG DNA METHYLTRANSFERASE 1 (MET1), or ARGONAUTE 4.

Based on the spectra of the most abundant chromosomal proteins, we can draw a picture of barley metaphase mitotic chromosome proteins. Using all three methods, we obtained abundant histone proteins, which are the expected component of the highly compact metaphase chromosomes. The frequent presence of histone H1.2 agrees with the transcriptionally inactive chromatin of condensed chromosomes. From the condensin complex, we found mainly the core subunits STRUCTURAL MAINTENANCE OF CHROMOSOMES 2 and 4 (SMC2 and SMC4) and there was only one hit for the cohesin complex, suggesting that the latter is less abundant. To our surprise, the most abundant peptides in both SXC and MG methods originated from TOP2. Although the TOP1 was present, it was less abundant. This indicates frequent sister chromatid intertwinings and/or supercoils that need to be mitigated primarily by the TOP2 and to a lesser extent by the TOP1 activities. The candidates from the Group 2 are intriguing as they represent typical interphase nuclear proteins. CRWN1 is an inner nuclear envelope (NE) protein that interacts with other chromatin-binding proteins and thus mediates chromatin and chromosome organization (Meier et al., 2016; Mikulski et al., 2019). It is tempting to speculate that the complex remains bound to the surface of the chromosome also during mitosis, helping to anchor the centromeric region to the NE. This could, on the one hand, accelerate the kinetics of the division and, on the other hand, help maintaining Rabl chromosome organization found in barley nuclei (Tiang et al., 2012).

A surprising observation concerned the numerous peptides derived from the maintenance complex 2 to 7 (MCM2-7). This complex is typical for DNA replication initiation and elongation during the S-phase of the cell cycle (Tuteja et al., 2011). Currently, no data support a direct role of the MCM2-7 complex during mitosis. Therefore, the MCM2-7 proteins may represent a contamination from the cytoplasm. However, the presence of some other (Group 3) proteins, such as DNA replication coupled maintenance DNA methyltransferases MET1 and CMT3, indicates that some replication-related processes appear during mitosis, possibly at specific DNA repair sites. Furthermore, there is a specific report of MCM function in late mitosis. Other members of Group 3 indicate active transcription (FACT and ISWI complex subunits) and DNA repair. From the DNA repair enzymes, we detected KU80, which acts as a heterodimer with KU70 and stabilizes free DNA ends. In addition, we found ZDP and LIG1, both acting in the excision repair pathways. This indicates a repair of DNA double and single-strand breaks that could arise from the tension during chromosome condensation and/or topoisomerase activity.

Validation of Perichromosomal Location of FIB1

Abundant nucleolar proteins bind to chromosomes after nucleoli disassemble at the onset of mitosis. Several studies have demonstrated the presence of nucleolar proteins over the entire mitosis and their important role in reconstituting a new nucleolus after the mitosis is completed (reviewed in Kalinina et al., 2018). Our proteomic data confirm the idea that at least part of these nucleolar proteins is physically attached to plant mitotic chromosomes, where they presumably contribute to the formation of a perichromosomal layer. We have experimentally validated this localization for the large nucleolar protein FIB1 using multiple approaches. FIB1 is a part of small nuclear ribonucleoprotein complexes involved in the first steps of RNA splicing and processing pre-ribosomal (r)RNAs (Reichow et al., 2007). Sirri et al. (2016) demonstrated that precursor rRNAs associate with the perichromosomal layer of human chromosomes where they serve as binding sites for various nucleolar proteins. In our work, the treatment of barley chromosomes with RNase A resulted in a strong reduction of FIB1 signal. This observation supports the critical role of RNAs in the assembly of perichromosomal layer also in plants and confirms the specific binding of FIB1. The marker of proliferation Ki67 is another nucleolar protein associating with perichromosomal layer in human (Takagi et al., 1999). According to Hayashi et al. (2017), Ki67 functions as a binding scaffold for pre-RNAs to which nucleolar proteins bind. Given the critical role of Ki67 in human, it is surprising that our analyses did not identify Ki67 in the proteome of barley chromosomes. Given the large evolutionary distance between animals and plants, it is possible that a similar role is played by a different and not yet described protein.

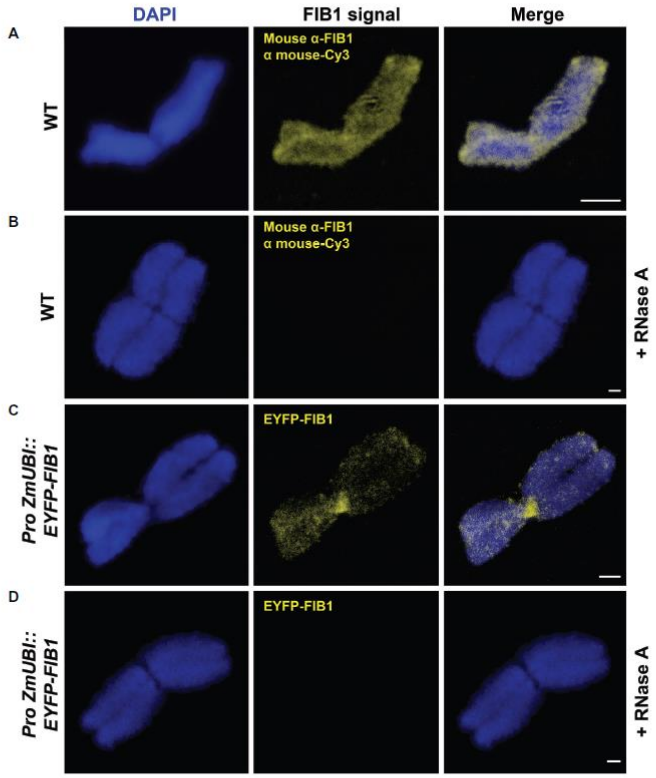

FIGURE 6 | FIB1 is removed from chromosomes by RNase A treatment. All chromosomes were counterstained with DAPI. **(A)** WT flow-sorted chromosome with immunolocalized FIB1. **(B)** Representative chromosome prepared in the same way with additional RNAse A treatment. **(C)** Chromosome from a transgenic reporter line expressing EYFP-FIB1 fusion protein. **(D)** Chromosome from the same material as in **(C)** with additional RNAse A treatment. Scale bars = 2 μm.

CONCLUSION

Our results provide valuable insights into the protein composition of condensed barley chromosomes and support a multi-layer model suggested for human mitotic chromosome (Uchiyama et al., 2005; Takata et al., 2007). This model categorized the identified proteins into separate groups: (1) coating cytoplasmic proteins on chromosome surfaces, (2) a perichromosomal layer comprising RNAs and nucleolar proteins, and (3) chromosome structural and fibrous proteins deeper in the chromosome core. Indeed, we detected the presence of many cytoplasmic proteins in the sorted mitotic barley chromosomes. However, these were excluded by our multi-classifier data analysis as random cellular hitchhikers with no essential functions during mitosis. On the other hand, a large group of nucleolar proteins was assigned as truly chromosomal and this finding, together with an important organizational role of RNA, was further confirmed by immunolocalization experiments. Finally, we included into the list a variety of proteins contributing to the processes of chromosome organization and maintenance. Generally, there were attempts to assign the identified barley proteins to their counterparts in Arabidopsis. In some cases, we could find a high homology for relevant hits supported by experimental data in the literature. Examples are SWITCH/SUCROSE NONFERMENTING (SWI/SNF) chromatin-remodeling complex proteins. Barley SNF protein, UniProtKB access. no. A0A287IBE5, shows 75% sequence similarity to its ARATH homolog Q9FMT4. Barley SWI3C subunit (access. no. A0A287QVR1) is identical at 46%. The possible regulatory function of Arabidopsis SWI3C resides in affecting plant development as its mutations led to lower fertility (Sarnowski et al., 2005). Barley PROLIFERATING CELL NUCLEAR ANTIGEN 2 (PCNA2), access. no. A0A287FZQ3, is largely homologous (sequence similarities

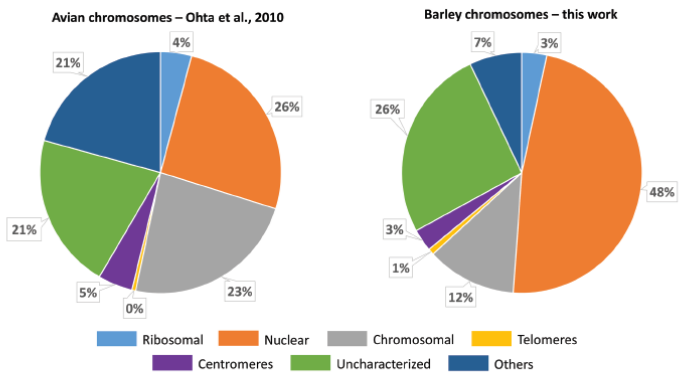

FIGURE 7 | A comparison of the categorization of chromosomal proteins identified for chicken DT40 cells (Ohta et al., 2010) and flow-sorted barley chromosomes (this work). The categorization for barley is derived from information provided in the respective protein names and retrieved by searching in UniProt GO-CC, UniProt Subcellular Localization a DAVID GOTERM-CC data (see **Supplementary Table S5**).

above 80%) to Arabidopsis (Q9ZW35) and human PCNAs (Q6FHF5). This protein is an auxiliary component for DNA polymerase delta and is involved in the replication control. Its interaction partner REPLICATION FACTOR C PROTEIN SUBUNIT 1, which participates in meiotic recombination and crossover formation process (Liu et al., 2013), was identified in several forms in the present proteomics dataset. As exemplified by the missing counterpart of human Ki67, many chromosome-associated proteins that play key roles in plant mitotic pathways remain elusive. Thus, our dataset may serve as a valuable resource for functional characterization of plant chromosomal proteins, their comparative phylogenetic analyses, and ultimately, the development of the next-generation models for the hierarchical organization of plant chromosomes.

DATA AVAILABILITY STATEMENT

The datasets presented in this study can be found in the PRIDE Archive (https://www.ebi.ac.uk/pride/archive/; Perez-Riverol et al., 2019). The accession number is PXD024689.

AUTHOR CONTRIBUTIONS

BP and JV maintained barley plants and purified mitotic chromosomes by flow cytometric sorting. ZP performed all experiments comprising microgradient pre-separation of peptides, he also processed, analyzed, and curated the data, created all figures, and contributed to the original manuscript draft writing. JB carried out all experiments that included in-gel digestion and in-solution digestion followed by SCX pre-separation of peptides. IC partly designed the study and employed the methodologies, he also created the tables and contributed to data processing and writing of the original manuscript draft. RL was responsible for all MS analyses. KK prepared barley transgenic line and performed immunostaining and microscopy. VB coordinated barley transformation. AP evaluated and discussed the biological meaning of the obtained results. JD, MŠ, and AP conceived, conducted, and supervised the study and secured funding. MŠ wrote the original manuscript draft. All authors read, edited, and approved the final manuscript.

FUNDING

This work was supported by the ERDF project "Plants as a tool for sustainable global development" (No. CZ.02.1.01/0.0/0.0/16_019/0000827), MEYS INTER-COST grant LTC18026, and stimulated by the COST action CA16212 "Impact of nuclear domains on gene expression and plant traits."

ACKNOWLEDGMENTS

We thank Petr Cápal, Zdeňka Dubská, Romana Šperková, and Jitka Weiserová for the assistance with flow cytometric sorting of chromosomes and cell nuclei, and Vendula Svobodová and Iva Hradilová with barley transformation and plant regeneration.

SUPPLEMENTARY MATERIAL

The Supplementary material for this article can be found online at https://www.frontiersin.org/articles/10.3389/fpls.2021.723674/full#supplementary-material

REFERENCES

Altschul, S. F., Wootton, J. C., Gertz, E. M., Agarwala, R., Morgulis, A., Schäffer, A. A., et al. (2005). Protein database searches using compositionally adjusted substitution matrices. *FEBS J.* 272, 5101–5109. doi: 10.1111/j.1742-4658.2005.04945.x

Antonin, W., and Neumann, H. (2016). Chromosome condensation and decondensation during mitosis. *Curr. Opin. Cell Biol.* 40, 15–22. doi: 10.1016/j.ceb.2016.01.013

Baker, K., Dhillon, T., Colas, I., Cook, N., Milne, I., Milne, L., et al. (2015). Chromatin state analysis of the barley epigenome reveals a higher-order structure defined by H3K27me1 and H3K27me3 abundance. *Plant J.* 84, 111–124. doi: 10.1111/tpj.12963

Bigeard, J., Rayapuram, N., Bonhomme, L., Hirt, H., and Pflieger, D. (2014). Proteomic and phosphoproteomic analyses of chromatin-associated proteins from *Arabidopsis thaliana*. *Proteomics* 14, 2141–2155. doi: 10.1002/pmic.201400072

Blavet, N., Uřinovská, J., Jeřábková, H., Chamrád, I., Vrána, J., Lenobel, R., et al. (2017). UNcleProt (universal nuclear protein database of barley): The first nuclear protein database that distinguishes proteins from different phases of the cell cycle. *Nucleus* 8, 70–80. doi: 10.1080/19491034.2016.1255391

Blythe, S. A., and Wieschaus, E. F. (2016). Establishment and maintenance of heritable chromatin structure during early drosophila embryogenesis. *eLife* 5:e20148. doi: 10.7554/eLife.20148

Booth, D. G., Beckett, A. J., Molina, O., Samejima, I., Masumoto, H., Kouprina, N., et al. (2016). 3D-CLEM reveals that a major portion of mitotic chromosomes is not chromatin. *Mol. Cell* 64, 790–802. doi: 10.1016/j.molcel.2016.10.009

Booth, D. G., Takagi, M., Sanchez-Pulido, L., Petfalski, E., Vargiu, G., Samejima, K., et al. (2014). Ki-67 is a PP1-interacting protein that organises the mitotic chromosome periphery. *eLife* 3:e01641. doi: 10.7554/eLife.01641

Brameier, M., Krings, A., and MacCallum, R. M. (2007). NucPred—predicting nuclear localization of proteins. *Bioinformatics* 23, 1159–1160. doi: 10.1093/bioinformatics/btm066

Chamrád, I., Simerský, R., Bérešová, L., Strnad, M., Šebela, M., and Lenobel, R. (2014). Proteomic identification of a candidate sequence of wheat cytokinin-binding protein 1. *J. Plant Growth Regul.* 33, 896–902. doi: 10.1007/s00344-014-9419-z

Chamrád, I., Uřinovská, J., Petrovská, B., Jeřábková, H., Lenobel, R., Vrána, J., et al. (2018). Identification of plant nuclear proteins based on a combination of flow sorting, SDS-PAGE, and LC-MS/MS analysis. *Methods Mol. Biol.* 1696, 57–79. doi: 10.1007/978-1-4939-7411-5_4

Cheeseman, I. M. (2014). The kinetochore. *Cold Spring Harb. Perspect. Biol.* 6:a015826. doi: 10.1101/cshperspect.a015826

Chi, S. M., and Nam, D. (2012). WegoLoc: accurate prediction of protein subcellular localization using weighted gene ontology terms. *Bioinformatics* 28, 1028–1030. doi: 10.1093/bioinformatics/bts062

Cuylen, S., Blaukopf, C., Politi, A. Z., Müller-Reichert, T., Neumann, B., Poser, I., et al. (2016). Ki-67 acts as a biological surfactant to disperse mitotic chromosomes. *Nature* 535, 308–312. doi: 10.1038/nature18610

Cuylen-Haering, S., Petrovic, M., Hernandez-Armendariz, A., Schneider, M. W., Samwer, M., Blaukopf, C., et al. (2020). Chromosome clustering by Ki-67 excludes cytoplasm during nuclear assembly. *Nature* 587, 285–290. doi: 10.1038/s41586-020-2672-3

Djeghloul, D., Patel, B., Kramer, H., Dimond, A., Whilding, C., Brown, K., et al. (2020). Identifying proteins bound to native mitotic ESC chromosomes reveals chromatin repressors are important for compaction. *Nat. Commun.* 11, 1–15. doi: 10.1038/s41467-020-17823-z

Doležel, J., Binarová, P., and Lucretti, S. (1989). Analysis of nuclear DNA content in plant cells by flow cytometry. *Biol. Plant.* 31, 113–120. doi: 10.1007/BF02907241

Doležel, J., Kubaláková, M., Číhalíková, J., Suchánková, P., and Šimková, H. (2011). Chromosome analysis and sorting using flow cytometry. *Methods Mol. Biol.* 701, 221–238. doi: 10.1007/978-1-61737-957-4_12

Doležel, J., Sgorbati, S., and Lucretti, S. (1992). Comparison of three DNA fluorochromes for flow cytometric estimation of nuclear DNA content in plants. *Physiol. Plant.* 85, 625–631. doi: 10.1111/j.1399-3054.1992.tb04764.x

Doležel, J., Vrána, J., Šafář, J., Bartoš, J., Kubaláková, M., and Šimková, H. (2012). Chromosomes in the flow to simplify genome analysis. *Funct. Integr. Genomics* 12, 397–416. doi: 10.1007/s10142-012-0293-0

Festuccia, N., Dubois, A., Vandormael-Pournin, S., Tejeda, E. G., Mouren, A., and Bessonnard, S. (2016). Mitotic binding of Esrrb marks key regulatory regions of the pluripotency network. *Nat. Cell Biol.* 18, 1139–1148. doi: 10.1038/ncb3418

Fierz, B., and Poirer, M. G. (2019). Biophysics of chromatin dynamics. *Annu. Rev. Biophys.* 48, 321–345. doi: 10.1146/annurev-biophys-070317-032847

Franc, V., Řehulka, P., Medda, R., Padiglia, A., Floris, G., and Šebela, M. (2013a). Analysis of the glycosylation pattern of plant copper amine oxidases by MALDI-TOF/TOF MS coupled to a manual chromatographic separation of glycans and glycopeptides. *Electrophoresis* 34, 2357–2367. doi: 10.1002/elps.201200622

Franc, V., Řehulka, P., Raus, M., Stulík, J., Novak, J., Renfrow, M. B., et al. (2013b). Elucidating heterogeneity of IgA1 hinge-region *O*-glycosylation by use of MALDI-TOF/TOF mass spectrometry: role of cysteine alkylation during sample processing. *J. Proteomics* 92, 299–312. doi: 10.1016/j.jprot.2013.07.013

Fujimura, A., Hayashi, Y., Kato, K., Kogure, Y., Kameyama, M., Shimamoto, H., et al. (2020). Identification of a novel nucleolar protein complex required for mitotic chromosome segregation through centromeric accumulation of Aurora B. *Nucleic Acids Res.* 48, 6583–6596. doi: 10.1093/nar/gkaa449

Ganji, M., Shaltiel, I. A., Bisht, S., Kim, E., Kalichava, A., Haering, C. H., et al. (2018). Real-time imaging of DNA loop extrusion by condensin. *Science* 360, 102–105. doi: 10.1126/science.aar7831

Gassmann, R., Henzing, A. J., and Earnshaw, W. C. (2005). Novel components of human mitotic chromosomes identified by proteomic analysis of the chromosome scaffold fraction. *Chromosoma* 113, 385–397. doi: 10.1007/s00412-004-0326-0

Ginno, P. A., Burger, L., Seebacher, J., Iesmantavicius, V., and Schübeler, D. (2018). Cell cycle-resolved chromatin proteomics reveals the extent of mitotic preservation of the genomic regulatory landscape. *Nat. Commun.* 9, 1–12. doi: 10.1038/s41467-018-06007-5

Hara, M., and Fukagawa, T. (2020). Dynamics of kinetochore structure and its regulations during mitotic progression. *Cell. Mol. Life Sci.* 77, 1–15. doi: 10.1007/s00018-020-03472-4

Hayashi, Y., Kato, K., and Kimura, K. (2017). The hierarchical structure of the perichromosomal layer comprises Ki67, ribosomal RNAs, and nucleolar proteins. *Biochem. Biophys. Res. Commun.* 493, 1043–1049. doi: 10.1016/j.bbrc.2017.09.092

Hsiung, C. C. S., Morrissey, C. S., Udugama, M., Frank, C. L., Keller, C. A., Baek, S., et al. (2015). Genome accessibility is widely preserved and locally modulated during mitosis. *Genome Res.* 25, 213–225. doi: 10.1101/gr.180646.114

Huang, D. W., Sherman, B. T., and Lempicki, R. A. (2009). Bioinformatics enrichment tools: paths toward the comprehensive functional analysis of large gene lists. *Nucleic Acids Res.* 37, 1–13. doi: 10.1093/nar/gkn923

International Barley Genome Sequencing Consortium, Mayer, K. F. X., Waugh, R., Brown, J. W. S., Schulman, A., Langridge, P., et al. (2012). A physical, genetic and functional sequence assembly of the barley genome. *Nature* 491, 711–716. doi: 10.1038/nature11543

Jasenčáková, Z., Meister, A., and Schubert, I. (2001). Chromatin organization and its relation to replication and histone acetylation during the cell cycle in barley. *Chromosoma* 110, 83–92. doi: 10.1007/s004120100132

Kalinina, N. O., Makarova, S., Makhotenko, A., Love, A. J., and Taliansky, M. (2018). The multiple functions of the nucleolus in plant development, disease and stress responses. *Front. Plant Sci.* 9:132. doi: 10.3389/fpls.2018.00132

Kintlová, M., Blavet, N., Cegan, R., and Hobza, R. (2017). Transcriptome of barley under three different heavy metal stress reaction. *Genom. Data* 13, 15–17. doi: 10.1016/j.gdata.2017.05.016

Kubaláková, M., Macas, J., and Dolezel, J. (1997). Mapping of repeated DNA sequences in plant chromosomes by PRINS and C-PRINS. *Theor. Appl. Genet.* 94, 758–763. doi: 10.1007/s001220050475

Laemmli, U. K. (1970). Cleavage of structural proteins during the assembly of the head of bacteriophage T4. *Nature* 227, 680–685. doi: 10.1038/227680a0

Liu, Y., Deng, Y., Li, G., and Zhao, J. (2013). Replication factor C1 (RFC1) is required for double-strand break repair during meiotic homologous recombination in Arabidopsis. *Plant J.* 73, 154–165. doi: 10.1111/tpj.12024

Lysák, M. A., Číhalíková, J., Kubaláková, M., Šimková, H., Künzel, G., and Doležel, J. (1999). Flow karyotyping and sorting of mitotic chromosomes of barley (*Hordeum vulgare* L.). *Chromosom. Res.* 7, 431–444. doi: 10.1023/A:1009293628638

Marchler-Bauer, A., and Bryant, S. H. (2004). CD-search: protein domain annotations on the fly. *Nucleic Acids Res.* 32, W327–W331. doi: 10.1093/nar/gkh454

Marthe, C., Kumlehn, J., and Hensel, G. (2015). Barley (*Hordeum vulgare* L.) transformation using immature embryos. *Methods Mol. Biol.* 1223, 71–83. doi: 10.1007/978-1-4939-1695-5_6

Martínez-Balbás, M. A., Dey, A., Rabindran, S. K., Ozato, K., and Wu, C. (1995). Displacement of sequence-specific transcription factors from mitotic chromatin. *Cell* 83, 29–38. doi: 10.1016/0092-8674(95)90231-7

Mascher, M., Gundlach, H., Himmelbach, A., Beier, S., Twardziok, S. O., Wicker, T., et al. (2017). A chromosome conformation capture ordered sequence of the barley genome. *Nature* 544, 427–433. doi: 10.1038/nature22043

Meier, I., Griffis, A. H., Groves, N. R., and Wagner, A. (2016). Regulation of nuclear shape and size in plants. *Curr. Opin. Cell Biol.* 40, 114–123. doi: 10.1016/j.ceb.2016.03.005

Mikulski, P., Hohenstatt, M. L., Farrona, S., Smaczniak, C., Stahl, Y., Kaufmann, K., et al. (2019). The chromatin-associated protein PWO1 interacts with plant nuclear Lamin-like components to regulate nuclear size. *Plant Cell* 31, 1141–1154. doi: 10.1105/tpc.18.00663

Montaño-Gutierrez, L. F., Ohta, S., Kustatscher, G., Earnshaw, W. C., and Rappsilber, J. (2017). Nano random forests to mine protein complexes and their relationships in quantitative proteomics data. *Mol. Biol. Cell* 28, 673–680. doi: 10.1091/mbc.E16-06-0370

Moravcová, D., Kahle, V., Řehulková, H., Chmelík, J., and Řehulka, P. (2009). Short monolithic columns for purification and fractionation of peptide samples for matrix-assisted laser desorption/ionization time-of-flight/time-of-flight mass spectrometry analysis in proteomics. *J. Chromatogr. A* 1216, 3629–3636. doi: 10.1016/j.chroma.2009.01.075

Morrison, C., Henzing, A. J., Jensen, O. N., Osheroff, N., Dodson, H., Kandels-Lewis, S. E., et al. (2002). Proteomic analysis of human metaphase chromosomes reveals topoisomerase II alpha as an Aurora B substrate. *Nucleic Acids Res.* 30, 5318–5327. doi: 10.1093/nar/gkf665

Ohta, S., Bukowski-Wills, J. C., Sanchez-Pulido, L., de Lima Alves, F., Wood, L., Chen, Z., et al. (2010). The protein composition of mitotic chromosomes determined using multiclassifier combinatorial proteomics. *Cell* 142, 810–821. doi: 10.1016/j.cell.2010.07.047

Ohta, S., Kimura, M., Takagi, S., Toramoto, I., and Ishihama, Y. (2016b). Identification of mitosis-specific phosphorylation in mitotic chromosome-associated proteins. *J. Proteome Res.* 15, 3331–3341. doi: 10.1021/acs.jproteome.6b00512

Ohta, S., Montaño-Gutierrez, L. F., de Lima Alves, F., Ogawa, H., Toramoto, I., Sato, N., et al. (2016a). Proteomics analysis with a nano random Forest approach reveals novel functional interactions regulated by SMC complexes on mitotic chromosomes. *Mol. Cell. Proteomics* 15, 2802–2818. doi: 10.1074/mcp.m116.057885

Ohta, S., Taniguchi, T., Sato, N., Hamada, M., Taniguchi, H., and Rappsilber, J. (2019). Quantitative proteomics of the mitotic chromosome scaffold reveals the association of BAZ1B with chromosomal axes. *Mol. Cell. Proteomics* 18, 169–181. doi: 10.1074/mcp.RA118.000923

Palozola, K. C., Donahue, G., Liu, H., Grant, G. R., Becker, J. S., Cote, A., et al. (2017). Mitotic transcription and waves of gene reactivation during mitotic exit. *Science* 358, 119–122. doi: 10.1126/science.aal4671

Parsons, G. G., and Spencer, C. A. (1997). Mitotic repression of RNA polymerase II transcription is accompanied by release of transcription elongation complexes. *Mol. Cell. Biol.* 17, 5791–5802. doi: 10.1128/MCB.17.10.5791

Perez-Riverol, Y., Csordas, A., Bai, J., Bernal-Llinares, M., Hewapathirana, S., Kundu, D. J., et al. (2019). The PRIDE database and related tools and resources in 2019: improving support for quantification data. *Nucleic Acids Res.* 47, D442–D450. doi: 10.1093/nar/gky1106

Pesenti, M. E., Prumbaum, D., Auckland, P., Smith, C. M., Faesen, A. C., Petrovic, A., et al. (2018). Reconstitution of a 26-subunit human kinetochore reveals cooperative microtubule binding by CENP-OPQUR and NDC80. *Mol. Cell* 71, 923–939. doi: 10.1016/j.molcel.2018.07.038

Petrovská, B., Jeřábková, H., Chamrád, I., Vrána, J., Lenobel, R., Uřinovská, J., et al. (2014). Proteomic analysis of barley cell nuclei purified by flow sorting. *Cytogenet. Genome Res.* 143, 78–86. doi: 10.1159/000365311

Raccaud, M., and Suter, D. M. (2018). Transcription factor retention on mitotic chromosomes: regulatory mechanisms and impact on cell fate decisions. *FEBS Lett.* 592, 878–887. doi: 10.1002/1873-3468.12828

Rapazote-Flores, P., Bayer, M., Milne, L., Mayer, C. D., Fuller, J., Guo, W., et al. (2019). BaRTv1. 0: an improved barley reference transcript dataset to determine accurate changes in the barley transcriptome using RNA-seq. *BMC Genomics* 20:968. doi: 10.1186/s12864-019-6243-7

Rappsilber, J., Mann, M., and Ishihama, Y. (2007). Protocol for micro-purification, enrichment, pre-fractionation and storage of peptides for proteomics using stagetips. *Nat. Protoc.* 2, 1896–1906. doi: 10.1038/nprot.2007.261

Reichow, S. L., Hamma, T., Ferré-D'Amaré, A. R., and Varani, G. (2007). The structure and function of small nucleolar ribonucleoproteins. *Nucleic Acids Res.* 35, 1452–1464. doi: 10.1093/nar/gkl1172

Samejima, I., and Earnshaw, W. C. (2018). Isolation of mitotic chromosomes from vertebrate cells and characterization of their proteome by mass spectrometry. *Methods Cell Biol.* 144, 329–348. doi: 10.1016/bs.mcb.2018.03.021

Sarnowski, T. J., Ríos, G., Jásik, J., Świeżewski, S., Kaczanowski, S., Li, Y., et al. (2005). SWI3 subunits of putative SWI/SNF chromatin-remodeling complexes play distinct roles during Arabidopsis development. *Plant Cell* 17, 2454–2472. doi: 10.1105/tpc.105.031203

Šebela, M., Štosová, T., Havliš, J., Wielsch, N., Thomas, H., Zdráhal, Z., et al. (2006). Thermostable trypsin conjugates for high-throughput proteomics: synthesis and performance evaluation. *Proteomics* 6, 2959–2963. doi: 10.1002/pmic.200500576

Shevchenko, A., Tomas, H., Havliš, J., Olsen, J. V., and Mann, M. (2006). In-gel digestion for mass spectrometric characterization of proteins and proteomes. *Nat. Protoc.* 1, 2856–2860. doi: 10.1038/nprot.2006.468

Sirri, V., Jourdan, N., Hernandez-Verdun, D., and Roussel, P. (2016). Sharing of mitotic pre-ribosomal particles between daughter cells. *J. Cell Sci.* 129, 1592–1604. doi: 10.1242/jcs.180521

Skibbens, R. V. (2019). Condensins and cohesins – one of these things is not like the other! *J. Cell Sci.* 132:jcs220491. doi: 10.1242/jcs.220491

Smith, P. K., Krohn, R. I., Hermanson, G. T., Mallia, A. K., Gartner, F. H., Provenzano, M. D., et al. (1985). Measurement of protein using bicinchoninic acid. *Anal. Biochem.* 150, 76–85. doi: 10.1016/0003-2697(85)90442-7

Sperschneider, J., Catanzariti, A. M., DeBoer, K., Petre, B., Gardiner, D. M., Singh, K. B., et al. (2017). LOCALIZER: subcellular localization prediction of both plant and effector proteins in the plant cell. *Sci. Rep.* 7:44598. doi: 10.1038/srep44598

Stenström, L., Mahdessian, D., Gnann, C., Cesnik, A. J., Ouyang, W., Leonetti, M. D., et al. (2020). Mapping the nucleolar proteome reveals a spatiotemporal organization related to intrinsic protein disorder. *Mol. Syst. Biol.* 16:e9469. doi: 10.15252/msb.20209469

Takagi, M., Matsuoka, Y., Kurihara, T., and Yoneda, Y. (1999). Chmadrin: a novel Ki-67 antigen-related perichromosomal protein possibly implicated in higher order chromatin structure. *J. Cell Sci.* 112, 2463–2472. doi: 10.1242/jcs.112.15.2463

Takagi, M., Natsume, T., Kanemaki, M. T., and Imamoto, N. (2016). Perichromosomal protein Ki67 supports mitotic chromosome architecture. *Genes Cells* 21, 1113–1124. doi: 10.1111/gtc.12420

Takata, H., Uchiyama, S., Nakamura, N., Nakashima, S., Kobayashi, S., Sone, T., et al. (2007). A comparative proteome analysis of human metaphase chromosomes isolated from two different cell lines reveals a set of conserved chromosome-associated proteins. *Genes Cells* 12, 269–284. doi: 10.1111/j.1365-2443.2007.01051.x

Tan, F., Li, G., Chitteti, B. R., and Peng, Z. (2007). Proteome and phosphoproteome analysis of chromatin associated proteins in rice (*Oryza sativa*). *Proteomics* 7, 4511–4527. doi: 10.1002/pmic.200700580

Tiang, C. L., He, Y., and Pawlowski, W. P. (2012). Chromosome organization and dynamics during interphase, mitosis, and meiosis in plants. *Plant Physiol.* 158, 26–34. doi: 10.1104/pp.111.187161

Tuteja, N., Tran, N. Q., Dang, H. Q., and Tuteja, R. (2011). Plant MCM proteins: role in DNA replication and beyond. *Plant Mol. Biol.* 77, 537–545. doi: 10.1007/s11103-011-9836-3

Tyanova, S., Temu, T., Sinitcyn, P., Carlson, A., Hein, M. Y., Geiger, T., et al. (2016). The Perseus computational platform for comprehensive analysis of (prote)omics data. *Nat. Methods* 13, 731–740. doi: 10.1038/nmeth.3901

Uchiyama, S., Kobayashi, S., Takata, H., Ishihara, T., Hori, N., Higashi, T., et al. (2005). Proteome analysis of human metaphase chromosomes. *J. Biol. Chem.* 280, 16994–17004. doi: 10.1074/jbc.M412774200

Wisniewski, J. R., and Gaugaz, F. Z. (2015). Fast and sensitive total protein and peptide assays for proteomic analysis. *Anal. Chem.* 87, 4110–4116. doi: 10.1021/ac504689z

Yano, A., Kodama, Y., Koike, A., Shinya, T., Kim, H. J., and Matsumoto, M. (2006). Interaction between methyl CpG-binding protein and ran GTPase during cell division in tobacco cultured cells. *Ann. Bot.* 98, 1179–1187. doi: 10.1093/aob/mcl211

Yu, C. S., Cheng, C. W., Su, W. C., Chang, K. C., Huang, S. W., Hwang, J. K., et al. (2014). CELLO2GO: a web server for protein subCELlular LOcalization prediction with functional gene ontology annotation. *PLoS One* 9:e99368. doi: 10.1371/journal.pone.0099368

Zaidi, S. S. E. A., Mukhtar, M. S., and Mansoor, S. (2018). Genome editing: targeting susceptibility genes for plant disease resistance. *Trends Biotechnol.* 36, 898–906. doi: 10.1016/j.tibtech.2018.04.005

Zeng, Z., and Jiang, J. (2016). Isolation and proteomics analysis of barley centromeric chromatin using PICh. *J. Proteome Res.* 15, 1875–1882. doi: 10.1021/acs.jproteome.6b00063

Zwyrtková, J., Šimková, H., and Doležel, J. (2020). Chromosome genomics uncovers plant genome organization and function. *Biotechnol. Adv.* 46:107659. doi: 10.1016/j.biotechadv.2020.107659

Zybailov, B., Mosley, A. L., Sardiu, M. E., Coleman, M. K., Florens, L., and Washburn, M. P. (2006). Statistical analysis of membrane proteome expression changes in *Saccharomyces cerevisiae*. *J. Proteome Res.* 5, 2339–2347. doi: 10.1021/pr060161n

Conflict of Interest: The authors declare that the research was conducted in the absence of any commercial or financial relationships that could be construed as a potential conflict of interest.

Publisher's Note: All claims expressed in this article are solely those of the authors and do not necessarily represent those of their affiliated organizations, or those of the publisher, the editors and the reviewers. Any product that may be evaluated in this article, or claim that may be made by its manufacturer, is not guaranteed or endorsed by the publisher.

Příloha 3:

Seznam nově identifikovaných proteinů z jader ječmene na základě peptidů získaných po štěpení proteinových extraktů pseudotrypsinem.

1/4 Nově identifikované proteiny z jader *H. Vulgare* identifikované nLC ESI MSMS

Vzorek	Protein	-10lgP	Pokrytí sekvence (%)	Počet peptidů	Unikátní peptidy	Avg. Mass	Název proteinu
G1	M0Y7N0_HORVD	171.27	10	21	6	250692	Uncharacterized protein OS=Hordeum vulgare var. distichum PE=4 SV=1
G1	M0W639_HORVD	164.32	10	16	1	202294	Uncharacterized protein OS=Hordeum vulgare var. distichum PE=4 SV=1
G1	M0Z2T0_HORVD	154.07	22	13	5	85727	Uncharacterized protein OS=Hordeum vulgare var. distichum PE=3 SV=1
G1	M0XB66_HORVD	25.12	1	1	1	92465	Uncharacterized protein OS=Hordeum vulgare var. distichum PE=4 SV=1
G1	M0Z1H9_HORVD	54.67	5	2	2	89508	Uncharacterized protein OS=Hordeum vulgare var. distichum PE=3 SV=1
G1	M0V1D0_HORVD	23.06	2	1	1	37166	Uncharacterized protein OS=Hordeum vulgare var. distichum PE=4 SV=1
G1	M0VR00_HORVD	61.15	19	3	2	26989	Uncharacterized protein OS=Hordeum vulgare var. distichum PE=4 SV=1
G1	M0VFN6_HORVD	65.47	7	3	3	57783	Uncharacterized protein OS=Hordeum vulgare var. distichum PE=4 SV=1
G1	M0XD10_HORVD	47.8	3	3	1	105216	Uncharacterized protein OS=Hordeum vulgare var. distichum PE=3 SV=1
G1	M0WPB1_HORVD	43.12	0	1	1	304559	Uncharacterized protein OS=Hordeum vulgare var. distichum PE=4 SV=1
G1	M0YUL8_HORVD	55.34	1	2	2	195852	DNA-directed RNA polymerase OS=Hordeum vulgare var. distichum PE=3 SV=1
G1	F2DC74_HORVD	39.63	3	1	1	47121	Predicted protein OS=Hordeum vulgare var. distichum PE=2 SV=1
G1	M0ZCQ3_HORVD	32.12	2	2	1	78693	Uncharacterized protein OS=Hordeum vulgare var. distichum PE=4 SV=1
G1	M0UKX4_HORVD	55.4	2	2	1	127015	Uncharacterized protein OS=Hordeum vulgare var. distichum PE=4 SV=1
G1	M0W1W4_HORVD	36.47	6	2	2	47533	Uncharacterized protein OS=Hordeum vulgare var. distichum PE=4 SV=1
G1	M0Y5P5_HORVD, M0Y5P7_HORVD	30.79	5	1	1	31216	Uncharacterized protein OS=Hordeum vulgare var. distichum PE=4 SV=1
G1	M0WPU0_HORVD, M0WPU2_HORVD	30.73	1	1	1	74341	Uncharacterized protein OS=Hordeum vulgare var. distichum PE=4 SV=1
G1	F2DS69_HORVD	29.67	1	1	1	79956	Predicted protein OS=Hordeum vulgare var. distichum PE=2 SV=1
G1	M0XH08_HORVD, M0XH09_HORVD	57.66	7	2	2	49920	Uncharacterized protein OS=Hordeum vulgare var. distichum PE=4 SV=1
G1	M0UMB9_HORVD	31.49	2	1	1	60966	Uncharacterized protein OS=Hordeum vulgare var. distichum PE=4 SV=1
G1	M0VLL0_HORVD	20.08	1	1	1	93792	Uncharacterized protein OS=Hordeum vulgare var. distichum PE=4 SV=1
G1	M0XCP1_HORVD	55.48	2	1	1	59401	Uncharacterized protein OS=Hordeum vulgare var. distichum PE=4 SV=1
G1	F2DIB0_HORVD	20.2	1	1	1	124660	Predicted protein OS=Hordeum vulgare var. distichum PE=2 SV=1
G1	M0UEQ2_HORVD	31.16	1	1	1	132398	Uncharacterized protein OS=Hordeum vulgare var. distichum PE=4 SV=1
G1	M0YXZ7_HORVD	31.05	4	1	1	15536	Uncharacterized protein OS=Hordeum vulgare var. distichum PE=4 SV=1
G1	M0XTU7_HORVD	33.4	2	1	1	55959	Uncharacterized protein OS=Hordeum vulgare var. distichum PE=4 SV=1
G1	F2CSK4_HORVD	22.96	4	1	1	37516	Predicted protein OS=Hordeum vulgare var. distichum PE=2 SV=1
G1	M0WXP2_HORVD, M0WXP3_HORVD	20.46	2	1	1	62503	ATP-dependent 6-phosphofructokinase OS=Hordeum vulgare var. distichum GN=PFK PE=3 SV=1
G1	M0UKI9_HORVD	20.87	3	1	1	18414	Uncharacterized protein OS=Hordeum vulgare var. distichum PE=4 SV=1
G1	F2DBD4_HORVD	20.12	3	1	1	34550	Predicted protein OS=Hordeum vulgare var. distichum PE=2 SV=1
G1	M0X951_HORVD	20.55	4	1	1	40055	Uncharacterized protein OS=Hordeum vulgare var. distichum PE=4 SV=1
G1	F2DIC7_HORVD	28.48	6	1	1	30509	Predicted protein OS=Hordeum vulgare var. distichum PE=2 SV=1
G1	M0UL37_HORVD	24.16	12	1	1	18099	Uncharacterized protein OS=Hordeum vulgare var. distichum PE=4 SV=1
G1, G2	M0WZE8_HORVD	143.33	15	7	5	62236	Uncharacterized protein OS=Hordeum vulgare var. distichum PE=3 SV=1
G1, G2	M0UHH0_HORVD	75.52	3	5	1	170937	Cytosine-specific methyltransferase OS=Hordeum vulgare var. distichum PE=3 SV=1
G1, G2	M0WZP4_HORVD	96.21	21	7	7	47154	Uncharacterized protein OS=Hordeum vulgare var. distichum PE=4 SV=1
G1, G2	M0XHS5_HORVD	48.48	12	2	1	30883	Uncharacterized protein OS=Hordeum vulgare var. distichum PE=4 SV=1
G1, G2	M0WVM3_HORVD, M0WVM7_HORVD	48.7	1	1	1	99173	Lipoxygenase OS=Hordeum vulgare var. distichum PE=3 SV=1
G1, G2	M0YG02_HORVD	56.44	1	1	1	104441	Uncharacterized protein OS=Hordeum vulgare var. distichum PE=3 SV=1
G1, G2, S	M0VKL0_HORVD	258.13	73	32	4	7563	Uncharacterized protein OS=Hordeum vulgare var. distichum PE=4 SV=1
G1, G2, S	M0ZCL5_HORVD	240.57	63	27	1	9365	Uncharacterized protein OS=Hordeum vulgare var. distichum PE=4 SV=1
G1, G2, S	M0YSA8_HORVD	176.64	60	13	3	9854	Uncharacterized protein OS=Hordeum vulgare var. distichum PE=4 SV=1
G1, G2, S	M0VKB3_HORVD	265.41	71	26	1	7683	Histone H2A OS=Hordeum vulgare var. distichum PE=3 SV=1
G1, G2, S	M0UU37_HORVD, M0UU36_HORVD	184.89	30	17	2	61464	Uncharacterized protein OS=Hordeum vulgare var. distichum PE=3 SV=1
G1, G2,S	M0WBQ7_HORVD	134.74	28	6	6	7150	Uncharacterized protein OS=Hordeum vulgare var. distichum PE=4 SV=1

2/4 Nově identifikované proteiny z jader *H. Vulgare* identifikované nLC ESI MSMS

Vzorek	Protein	-10lgP	Pokrytí sekvence (%)	Počet peptidů	Unikátní peptidy	Avg. Mass	Název proteinu
G1, S	M0YI84_HORVD	63.94	13	4	3	25147	Uncharacterized protein OS=Hordeum vulgare var. distichum PE=4 SV=1
G1, S	M0WJV7_HORVD	68.41	15	1	1	16570	Uncharacterized protein OS=Hordeum vulgare var. distichum PE=4 SV=1
G2	M0VFA6_HORVD, M0VFA7_HORVD	216.15	55	23	5	10410	Histone H2A OS=Hordeum vulgare var. distichum PE=3 SV=1
G2	M0V7V4_HORVD	222.65	64	19	1	6427	Uncharacterized protein OS=Hordeum vulgare var. distichum PE=4 SV=1
G2	F2CT05_HORVD	211.27	54	23	4	42828	S-adenosylmethionine synthase OS=Hordeum vulgare var. distichum PE=2 SV=1
G2	M0Z2T5_HORVD	181.14	22	17	3	88313	Uncharacterized protein OS=Hordeum vulgare var. distichum PE=3 SV=1
G2	M0YEP9_HORVD	137.99	23	5	5	27616	Uncharacterized protein OS=Hordeum vulgare var. distichum PE=4 SV=1
G2	M0YKC8_HORVD, M0YKD6_HORVD	108.89	19	4	4	29507	Uncharacterized protein OS=Hordeum vulgare var. distichum PE=4 SV=1
G2	M0UHG9_HORVD	75.87	2	3	1	157070	Cytosine-specific methyltransferase OS=Hordeum vulgare var. distichum PE=3 SV=1
G2	M0WA39_HORVD	126.64	14	9	1	85692	Uncharacterized protein OS=Hordeum vulgare var. distichum PE=4 SV=1
G2	M0WEF4_HORVD	37.95	6	2	1	32774	Uncharacterized protein OS=Hordeum vulgare var. distichum PE=4 SV=1
G2	M0XHY6_HORVD	44.06	3	2	2	84688	Uncharacterized protein OS=Hordeum vulgare var. distichum PE=4 SV=1
G2	M0XWU4_HORVD	42.47	15	1	1	11149	Uncharacterized protein OS=Hordeum vulgare var. distichum PE=4 SV=1
G2	F2E2W4_HORVD	26.19	2	1	1	54999	Predicted protein OS=Hordeum vulgare var. distichum PE=2 SV=1
G2	F2D2J5_HORVD	89.66	12	2	2	29880	Predicted protein OS=Hordeum vulgare var. distichum PE=2 SV=1
G2	M0X0I0_HORVD	40.24	1	2	1	119551	Uncharacterized protein OS=Hordeum vulgare var. distichum PE=4 SV=1
G2	M0YGC4_HORVD	65.36	4	2	2	104035	Uncharacterized protein OS=Hordeum vulgare var. distichum PE=4 SV=1
G2	M0Y5T2_HORVD	64.16	5	2	2	66656	Uncharacterized protein OS=Hordeum vulgare var. distichum PE=4 SV=1
G2	M0UWB7_HORVD	77.8	14	2	1	18453	Uncharacterized protein OS=Hordeum vulgare var. distichum PE=3 SV=1
G2	M0Y8N7_HORVD	61.46	3	1	1	45605	Uncharacterized protein OS=Hordeum vulgare var. distichum PE=4 SV=1
G2	M0WED0_HORVD	54.15	2	2	1	85160	Uncharacterized protein OS=Hordeum vulgare var. distichum PE=4 SV=1
G2	M0XBC0_HORVD	41.35	1	1	1	140609	Uncharacterized protein OS=Hordeum vulgare var. distichum PE=4 SV=1
G2	M0V7F0_HORVD	36.53	0	1	1	187573	Uncharacterized protein OS=Hordeum vulgare var. distichum PE=4 SV=1
G2	M0XJS0_HORVD	71.95	2	2	1	121125	Kinesin-like protein OS=Hordeum vulgare var. distichum PE=3 SV=1
G2	M0ZD81_HORVD, M0ZD82_HORVD	43.41	3	2	2	91960	Uncharacterized protein OS=Hordeum vulgare var. distichum PE=4 SV=1
G2	M0ZD82_HORVD	43.41	3	2	2	88612	Uncharacterized protein OS=Hordeum vulgare var. distichum PE=4 SV=1
G2	M0YE09_HORVD	27.93	2	1	1	59653	Uncharacterized protein OS=Hordeum vulgare var. distichum PE=4 SV=1
G2	M0VHZ5_HORVD	25.68	8	1	1	23472	Uncharacterized protein OS=Hordeum vulgare var. distichum PE=4 SV=1
G2	M0WTN5_HORVD	35.67	2	1	1	66031	Uncharacterized protein OS=Hordeum vulgare var. distichum PE=4 SV=1
G2	M0WMR6_HORVD	24.2	3	1	1	46196	Uncharacterized protein OS=Hordeum vulgare var. distichum PE=3 SV=1
G2	F2DE05_HORVD	34.63	3	1	1	90583	Predicted protein OS=Hordeum vulgare var. distichum PE=2 SV=1
G2	F2CYV6_HORVD, M0WZ48_HORVD	21.68	2	1	1	68245	Predicted protein OS=Hordeum vulgare var. distichum PE=2 SV=1
G2	M0VTB3_HORVD	38.29	1	1	1	141258	Uncharacterized protein OS=Hordeum vulgare var. distichum PE=4 SV=1
G2	M0Z996_HORVD	21.45	3	1	1	36999	Uncharacterized protein OS=Hordeum vulgare var. distichum PE=4 SV=1
G2	M0W888_HORVD	44.17	8	1	1	28336	Uncharacterized protein OS=Hordeum vulgare var. distichum PE=4 SV=1
G2	M0UH40_HORVD	30.77	4	1	1	55443	Uncharacterized protein OS=Hordeum vulgare var. distichum PE=3 SV=1
G2	M0XNJ8_HORVD	43.65	2	1	1	82006	Uncharacterized protein OS=Hordeum vulgare var. distichum PE=4 SV=1
G2	M0ZCY2_HORVD, M0ZCY3_HORVD	22.89	2	1	1	64149	Uncharacterized protein OS=Hordeum vulgare var. distichum PE=4 SV=1
G2	M0UF35_HORVD	29.81	2	1	1	97444	Uncharacterized protein OS=Hordeum vulgare var. distichum PE=4 SV=1
G2	M0V4T2_HORVD	21.81	2	1	1	35991	Uncharacterized protein OS=Hordeum vulgare var. distichum PE=4 SV=1
G2	M0UK71_HORVD, M0UK72_HORVD, M0UK73_HORVD	24.45	0	1	1	214095	Uncharacterized protein OS=Hordeum vulgare var. distichum PE=4 SV=1
G2	F2D3N3_HORVD	21.99	2	1	1	29178	Predicted protein OS=Hordeum vulgare var. distichum PE=2 SV=1
G2	M0WE28_HORVD	20.85	3	1	1	39514	Uncharacterized protein OS=Hordeum vulgare var. distichum PE=4 SV=1
G2	M0WPD2_HORVD	29.27	3	1	1	59312	Uncharacterized protein OS=Hordeum vulgare var. distichum PE=4 SV=1
G2	M0YT67_HORVD	29.78	1	1	1	64288	Uncharacterized protein OS=Hordeum vulgare var. distichum PE=4 SV=1
G2	F2DGP4_HORVD	26.69	2	1	1	56595	Predicted protein OS=Hordeum vulgare var. distichum PE=2 SV=1

3/4 Nově identifikované proteiny z jader *H. Vulgare* identifikované nLC ESI MSMS

Vzorek	Protein	-10lgP	Pokrytí sekvence (%)	Počet peptidů	Unikátní peptidy	Avg. Mass	Název proteinu
G2	F2D507_HORVD, M0YB22_HORVD, M0YB23_HORVD	20.91	5	1	1	30372	Predicted protein OS=Hordeum vulgare var. distichum PE=2 SV=1
G2	M0WXF4_HORVD, M0WXF6_HORVD, M0WXF7_HORVD, M0WXF8_HORVD, M0WXG0_HORVD, M0WXG3_HORVD	44.52	7	1	1	25254	Uncharacterized protein OS=Hordeum vulgare var. distichum PE=4 SV=1
G2	M0ZDJ6_HORVD, M0ZDJ8_HORVD, M0ZDJ9_HORVD, M0ZDK1_HORVD, M0ZDK4_HORVD, M0ZDK5_HORVD, M0ZDK8_HORVD	20.34	3	1	1	30166	Uncharacterized protein OS=Hordeum vulgare var. distichum PE=4 SV=1
G2, S	M0W801_HORVD, M0W802_HORVD, M0W803_HORVD, M0W804_HORVD	22.69	5	1	1	32753	Uncharacterized protein OS=Hordeum vulgare var. distichum PE=4 SV=1
G2, S	M0W802_HORVD	22.69	5	1	1	34909	Uncharacterized protein OS=Hordeum vulgare var. distichum PE=4 SV=1
G2, S	M0VXN6_HORVD	45.99	2	1	1	77802	Uncharacterized protein OS=Hordeum vulgare var. distichum PE=4 SV=1
S	M0YSA8_HORVD	200.1	82	18	5	9854	Uncharacterized protein OS=Hordeum vulgare var. distichum PE=4 SV=1
S	M0YHR5_HORVD	134	22	10	10	54268	Uncharacterized protein OS=Hordeum vulgare var. distichum PE=3 SV=1
S	M0ZCU7_HORVD	119.21	25	7	7	21315	Uncharacterized protein OS=Hordeum vulgare var. distichum PE=4 SV=1
S	M0X0M4_HORVD	117.1	8	4	4	48160	Uncharacterized protein OS=Hordeum vulgare var. distichum PE=4 SV=1
S	M0WUU5_HORVD	116.24	19	5	5	34190	Uncharacterized protein OS=Hordeum vulgare var. distichum PE=4 SV=1
S	M0XB67_HORVD	47.76	1	1	1	99944	Uncharacterized protein OS=Hordeum vulgare var. distichum PE=4 SV=1
S	M0Z2T4_HORVD	118.47	8	5	5	76382	Uncharacterized protein OS=Hordeum vulgare var. distichum PE=4 SV=1
S	M0WRH9_HORVD	104.81	6	5	5	123992	Uncharacterized protein OS=Hordeum vulgare var. distichum PE=4 SV=1
S	M0VYE2_HORVD	41.68	1	1	1	56291	Uncharacterized protein OS=Hordeum vulgare var. distichum PE=4 SV=1
S	M0YUD6_HORVD, M0YUD7_HORVD	56.86	2	2	2	96832	Uncharacterized protein OS=Hordeum vulgare var. distichum PE=3 SV=1
S	M0XV63_HORVD, M0XV64_HORVD, M0XV65_HORVD	54.9	1	1	1	142730	Uncharacterized protein OS=Hordeum vulgare var. distichum PE=4 SV=1
S	M0YJ44_HORVD	47.13	1	1	1	107561	Uncharacterized protein OS=Hordeum vulgare var. distichum PE=4 SV=1
S	M0WZF6_HORVD, M0WZF8_HORVD	51.56	1	1	1	167152	Uncharacterized protein OS=Hordeum vulgare var. distichum PE=4 SV=1
S	M0WZF8_HORVD	51.56	1	1	1	168051	Uncharacterized protein OS=Hordeum vulgare var. distichum PE=4 SV=1
S	M0Z980_HORVD	47.6	1	1	1	92987	Uncharacterized protein OS=Hordeum vulgare var. distichum PE=4 SV=1
S	F2DC11_HORVD	48.54	2	1	1	38143	Predicted protein OS=Hordeum vulgare var. distichum PE=2 SV=1
S	M0YC69_HORVD	54.94	4	2	2	71658	Uncharacterized protein OS=Hordeum vulgare var. distichum PE=3 SV=1
S	F2D621_HORVD	48.07	10	3	1	23583	Predicted protein OS=Hordeum vulgare var. distichum PE=2 SV=1
S	M0WVF9_HORVD	39.55	2	2	1	81254	Uncharacterized protein OS=Hordeum vulgare var. distichum PE=4 SV=1
S	F2E609_HORVD	41.53	2	1	1	75893	Predicted protein OS=Hordeum vulgare var. distichum PE=2 SV=1
S	F2DA43_HORVD	50.99	2	1	1	85874	Predicted protein OS=Hordeum vulgare var. distichum PE=2 SV=1
S	M0WWR4_HORVD	36.52	2	1	1	53738	Uncharacterized protein OS=Hordeum vulgare var. distichum PE=4 SV=1
S	M0Y092_HORVD, M0Y093_HORVD	37.37	3	1	1	24869	Uncharacterized protein OS=Hordeum vulgare var. distichum PE=3 SV=1
S	M0WBQ3_HORVD	36.23	32	2	2	16847	Uncharacterized protein OS=Hordeum vulgare var. distichum PE=4 SV=1
S	M0Y5F6_HORVD	42.6	3	1	1	35734	Uncharacterized protein OS=Hordeum vulgare var. distichum PE=3 SV=1
S	M0XB03_HORVD	45.21	2	2	1	69283	Uncharacterized protein OS=Hordeum vulgare var. distichum PE=4 SV=1
S	F2EDJ3_HORVD	29.72	2	1	1	61933	Predicted protein OS=Hordeum vulgare var. distichum PE=2 SV=1
S	M0UFH7_HORVD	33.21	2	1	1	68434	Uncharacterized protein OS=Hordeum vulgare var. distichum PE=4 SV=1
S	M0UFF0_HORVD	35.55	2	2	1	146931	Uncharacterized protein OS=Hordeum vulgare var. distichum PE=4 SV=1
S	M0VLL9_HORVD, M0VLM0_HORVD	30.21	11	1	1	13383	Uncharacterized protein OS=Hordeum vulgare var. distichum PE=4 SV=1
S	M0ZD30_HORVD, M0ZD31_HORVD, M0ZD32_HORVD	25.13	2	1	1	53139	Uncharacterized protein OS=Hordeum vulgare var. distichum PE=3 SV=1
S	M0XC48_HORVD	33.13	2	1	1	45237	Uncharacterized protein OS=Hordeum vulgare var. distichum PE=4 SV=1
S	M0X804_HORVD, M0X808_HORVD	22.54	3	1	1	33111	Uncharacterized protein OS=Hordeum vulgare var. distichum PE=4 SV=1
S	M0VDW1_HORVD	35.06	14	1	1	9507	Uncharacterized protein OS=Hordeum vulgare var. distichum PE=4 SV=1

4/4 Nově identifikované proteiny z jader *H. Vulgare* identifikované nLC ESI MSMS

Vzorek	Protein	-10lgP	Pokrytí sekvence (%)	Počet peptidů	Unikátní peptidy	Avg. Mass	Název proteinu
S	M0W7S2_HORVD	25.54	3	1	1	36240	Uncharacterized protein OS=Hordeum vulgare var. distichum PE=4 SV=1
S	M0XLC8_HORVD	30.41	8	1	1	21284	Uncharacterized protein OS=Hordeum vulgare var. distichum PE=3 SV=1

1/1 Nově identifikované proteiny z jader *H. Vulgare* identifikované nLC MALDI MSMS

Vzorek	Protein	-10lgP	Pokrytí sekvence (%)	Peptidy	Unikátní peptidy	MW	Název proteinu
G1	M0WLK7_HORVD, M0WLK8_HORVD, M0WLK9_HORVD	39.29	2	1	1	51156	Uncharacterized protein OS=Hordeum vulgare var. distichum PE=4 SV=1
G1	M0Y3F1_HORVD, M0Y3F2_HORVD, M0Y3F3_HORVD	45.24	2	1	1	92521	Uncharacterized protein OS=Hordeum vulgare var. distichum PE=3 SV=1
G1	M0WA46_HORVD	22.88	1	1	1	89373	Uncharacterized protein OS=Hordeum vulgare var. distichum PE=4 SV=1
G1	M0WTL8_HORVD	40.65	2	1	1	83457	Uncharacterized protein OS=Hordeum vulgare var. distichum PE=4 SV=1
G1	M0XWU4_HORVD	22.92	15	1	1	11149	Uncharacterized protein OS=Hordeum vulgare var. distichum PE=4 SV=1
G1	M0UFL5_HORVD	38.95	2	1	1	117061	Uncharacterized protein OS=Hordeum vulgare var. distichum PE=4 SV=1
G1	M0W571_HORVD	27.72	7	1	1	26752	Uncharacterized protein OS=Hordeum vulgare var. distichum PE=4 SV=1
G1	M0UEY9_HORVD	25.52	2	1	1	45969	Uncharacterized protein OS=Hordeum vulgare var. distichum PE=4 SV=1
G1	M0XDV5_HORVD	22.75	2	1	1	43936	Uncharacterized protein OS=Hordeum vulgare var. distichum PE=4 SV=1
G1	M0WR96_HORVD	24.47	6	1	1	20124	Uncharacterized protein OS=Hordeum vulgare var. distichum PE=3 SV=1
G1	M0WJV7_HORVD	36.41	9	1	1	16570	Uncharacterized protein OS=Hordeum vulgare var. distichum PE=4 SV=1
G1	M0UKH1_HORVD	26.37	1	1	1	95583	Uncharacterized protein OS=Hordeum vulgare var. distichum PE=4 SV=1
G1	M0VPS2_HORVD	22.96	2	1	1	55288	Uncharacterized protein OS=Hordeum vulgare var. distichum PE=4 SV=1
G1, G2	M0V6J2_HORVD, M0V6J3_HORVD, M0V6J4_HORVD, M0V6J5_HORVD, M0V6J6_HORVD	26.7	1	1	1	223234	Uncharacterized protein OS=Hordeum vulgare var. distichum PE=4 SV=1
G1, G2, S	M0ZCL5_HORVD	220.73	53	17	1	9365	Uncharacterized protein OS=Hordeum vulgare var. distichum PE=4 SV=1
G1, S	M0VKL0_HORVD	241.91	74	22	3	7563	Uncharacterized protein OS=Hordeum vulgare var. distichum PE=4 SV=1
G1, S	M0UWJ1_HORVD, M0UWJ2_HORVD, M0UWJ6_HORVD	22.95	3	1	1	31792	Uncharacterized protein OS=Hordeum vulgare var. distichum PE=4 SV=1
G1, S	M0Y4H3_HORVD, M0Y4H4_HORVD	37.07	2	1	1	86581	Chloride channel protein OS=Hordeum vulgare var. distichum PE=3 SV=1
G2	M0YSA8_HORVD	150.82	27	4	1	9854	Uncharacterized protein OS=Hordeum vulgare var. distichum PE=4 SV=1
G2	M0VXK9_HORVD	27.75	2	1	1	103871	Uncharacterized protein OS=Hordeum vulgare var. distichum PE=4 SV=1
G2	M0UH65_HORVD, M0UH67_HORVD	24.28	1	1	1	74846	Uncharacterized protein OS=Hordeum vulgare var. distichum PE=4 SV=1
G2	M0XVH0_HORVD	27.32	3	1	1	66396	Uncharacterized protein OS=Hordeum vulgare var. distichum PE=4 SV=1
G2	M0UFC8_HORVD, M0UFC9_HORVD, M0UFD0_HORVD M0UFD6_HORVD, M0UFD7_HORVD	24.18	9	1	1	16071	Uncharacterized protein OS=Hordeum vulgare var. distichum PE=4 SV=1
G2	M0YKD2_HORVD	31.99	5	1	1	32630	Uncharacterized protein OS=Hordeum vulgare var. distichum PE=4 SV=1
G2	M0V8V4_HORVD, M0V8V6_HORVD	22.43	4	1	1	52734	Uncharacterized protein OS=Hordeum vulgare var. distichum PE=3 SV=1
G2	M0V8V6_HORVD	22.43	4	1	1	49143	3-oxoacyl-[acyl-carrier-protein] synthase OS=Hordeum vulgare var. distichum PE=3 SV=1
G2	M0YDW1_HORVD	23.74	1	1	1	92871	Serine/threonine-protein kinase OS=Hordeum vulgare var. distichum PE=3 SV=1
G2	M0VXN6_HORVD	36.24	2	1	1	77802	Uncharacterized protein OS=Hordeum vulgare var. distichum PE=4 SV=1
G2	M0WEA7_HORVD	26.02	15	1	1	11891	Uncharacterized protein OS=Hordeum vulgare var. distichum PE=4 SV=1
G2	F2EH42_HORVD	24.84	11	1	1	19055	Predicted protein OS=Hordeum vulgare var. distichum PE=2 SV=1
G2	M0WZE4_HORVD, M0WZE9_HORVD	25.57	2	1	1	60325	Uncharacterized protein OS=Hordeum vulgare var. distichum PE=3 SV=1
G2	F2EED1_HORVD	23.98	4	1	1	47702	Predicted protein OS=Hordeum vulgare var. distichum PE=2 SV=1
G2	M0XWY2_HORVD	23.99	1	1	1	87351	Uncharacterized protein OS=Hordeum vulgare var. distichum PE=4 SV=1
G2, S	F2EGH3_HORVD	22.81	2	1	1	76770	Predicted protein OS=Hordeum vulgare var. distichum PE=2 SV=1
S	M0WLK9_HORVD	33.54	4	1	1	26080	Uncharacterized protein OS=Hordeum vulgare var. distichum PE=4 SV=1
S	M0VUL9_HORVD	21.62	1	1	1	158540	Uncharacterized protein OS=Hordeum vulgare var. distichum PE=4 SV=1
S	M0WHB6_HORVD, M0WHB7_HORVD, M0WHB8_HORVD	28.99	1	1	1	108151	Uncharacterized protein OS=Hordeum vulgare var. distichum PE=4 SV=1
S	M0YL40_HORVD	20.94	2	1	1	65122	Uncharacterized protein OS=Hordeum vulgare var. distichum PE=3 SV=1
S	M0WBQ7_HORVD	46.75	15	1	1	7150	Uncharacterized protein OS=Hordeum vulgare var. distichum PE=4 SV=1
S	M0XBT0_HORVD	33.21	4	1	1	40837	Uncharacterized protein OS=Hordeum vulgare var. distichum PE=4 SV=1
S	M0XWY3_HORVD	22.46	1	1	1	93588	Uncharacterized protein OS=Hordeum vulgare var. distichum PE=4 SV=1
S	M0XVU7_HORVD	20.82	21	1	1	10339	Uncharacterized protein OS=Hordeum vulgare var. distichum PE=4 SV=1

Příloha 4:

Perutka, Z., Šebela, M., 2018. Pseudotrypsin: a little known trypsin proteoform. *Molecules* 23, 2637**.**

molecules

MDPI

Review

Pseudotrypsin: A Little-Known Trypsin Proteoform

Zdeněk Perutka and Marek Šebela *

Department of Protein Biochemistry and Proteomics, Centre of the Region Haná for Biotechnological and Agricultural Research, Faculty of Science, Palacký University, Šlechtitelů 27, 783 71 Olomouc, Czech Republic; Perutka.Zdenek@seznam.cz

* Correspondence: marek.sebela@upol.cz; Tel.: +420-585-634-927

Academic Editor: Paolo Iadarola

Received: 11 September 2018; Accepted: 9 October 2018; Published: 14 October 2018

check for updates

Abstract: Trypsin is the protease of choice for protein sample digestion in proteomics. The most typical active forms are the single-chain β-trypsin and the two-chain α-trypsin, which is produced by a limited autolysis of β-trypsin. An additional intra-chain split leads to pseudotrypsin (ψ-trypsin) with three chains interconnected by disulfide bonds, which can be isolated from the autolyzate by ion-exchange chromatography. Based on experimental data with artificial substrates, peptides, and protein standards, ψ-trypsin shows altered kinetic properties, thermodynamic stability and cleavage site preference (and partly also cleavage specificity) compared to the above-mentioned proteoforms. In our laboratory, we have analyzed the performance of bovine ψ-trypsin in the digestion of protein samples with a different complexity. It cleaves predominantly at the characteristic trypsin cleavage sites. However, in a comparison with common tryptic digestion, non-specific cleavages occur more frequently (mostly after the aromatic residues of Tyr and Phe) and more missed cleavages are generated. Because of the preferential cleavages after the basic residues and more developed side specificity, which is not expected to occur for the major trypsin forms (but may appear anyway because of their autolysis), ψ-trypsin produces valuable information, which is complementary in part to data based on a strictly specific trypsin digestion and thus can be unnoticed following common proteomics protocols.

Keywords: autolysis; chain; cleavage; digestion; peptide; proteoform; pseudotrypsin; specificity; trypsin

1. Cleavage Specificity of Trypsin

Trypsin, a serine protease, is commonly used as an important enzymatic reagent in biochemistry and biology. It is almost indispensable especially for the digestion of protein samples to peptides in bottom-up proteomics [1]. Apart from this application, trypsin is a tool in working with cell cultures. During trypsinization, surface adhesion proteins are degraded, which allows adherent cells to be detached from each other and the walls of plastic containers or plates in which they are being cultured. In industry, interestingly, trypsin is applied to hydrolyze allergenic proteins for the production of hypoallergenic milk [2]. In proteomics, sample digests are typically analyzed for protein identification by nanoflow liquid chromatography coupled to tandem mass spectrometry (nLC-MS/MS). MS-based data on peptides are searched against amino acid sequence databases, which benefits from the relative stringent cleavage specificity of trypsin as the search algorithms incorporate the cleavage rule as a filtering criterion. According to a study with complex samples from 2004, the enzyme cleaves peptide bonds in proteins at pH 8.3 exclusively at the carboxyl end of arginine and lysine residues [3]. This is in agreement with the canonical trypsin cleavage rule postulated a long time ago [4] even though it was built on results obtained at that time only with a limited amount of substrates [5]. Thus, it has long been accepted that trypsin does not cleave before proline and its activity is suppressed either

if a cysteine appears next to Arg/Lys or the basic residue is N- or C-terminally adjacent to an acidic residue. This old rule was questioned when a large data set of 14.5 million MS/MS spectra of peptides from *Shewanella oneidensis* was processed to statistically evaluate the cleavage sites [5]. Interestingly, numerous cleavages before proline were found. Their number was even higher than that referring to the cleavages before cysteine.

An average length of tryptic peptides is 14 amino acids. This number has been deduced from an in silico digestion of human proteins in the UniProt database [1]. Because of this reasonable size as well as the presence of a positive charge at the C-terminal Arg or Lys, which enhances the ionization process in the positive ionization mode, tryptic peptides are highly amenable to mass spectrometric measurements. In fact, there are at least two defined positive charges in tryptic peptides (at both N- and C-termini), which is favorable for a good fragmentation in MS/MS analyses [1,2].

2. Nonspecific and Missed Cleavage Sites

In addition to the cleavages after Arg or Lys, proteomics studies have often reported the formation of semitryptic and nonspecific peptides during the digestion process involving trypsin [1,6]. The semitryptic cleavage assumes that one of the cleavage sites is tryptic, but the other site may be at any residue. A minor chymotrypsin or chymotrypsin-like activity yields nonspecific cleavages C-terminal to phenylalanine, tyrosine, tryptophan, or leucine residues [7]. This can result either from the presence of a chymotrypsin contamination, which is variable in trypsin preparations supplied by different vendors [1], or pseudotrypsin (ψ-trypsin), a product of trypsin autolysis, which possesses such an activity in addition to the characteristic trypsin properties [8]. The presence of nonspecific peptides in tryptic digests (excluding C-terminal peptides) is also elucidated by a secondary non-enzymatic cleavage between Asp and Pro residues yielding peptides with an N-terminal proline. This is because of the lability of the respective bond, which is easily hydrolyzed in solution as well as broken in the gas phase [3].

When the protein substrate is not cleaved to a completion, missed cleavages occur, which make the assignment of experimental data to amino acid sequence databases less specific and straightforward. Missed cleavage sites were investigated for example by matrix-assisted laser desorption/ionization time-of-flight mass spectrometry (MALDI-TOF MS) using human cell line or *Mycobacterium* proteins separated by two-dimensional gel electrophoresis and digested in-gel by a porcine trypsin [9]. The analysis showed that about 90 % of the detected peptides with missed cleavage sites could be attributed to the following sequence motifs: (1) Arg or Lys with a neighboring proline at the C-terminal side, (2) two successive basic residues (Arg-Arg, Arg-Lys, Lys-Arg, Lys-Lys), and (3) Arg or Lys with an aspartic acid or glutamic acid residue at either N-terminal or C-terminal side. When processing peptide MS- and MS/MS-based data by database searches (during which theoretical peptide sequences are generated according to the selected input cleavage rules), the user may, among others, adjust a maximum number of missed cleavage sites. Usually, a setting of 0, 1, or 2 missed cleavages for peptides is recommended. The presence of missed cleavages in tryptic peptides represents a challenge in quantitative MS-based proteomics, which uses peptides as surrogates for their parent proteins [10]. Under optimal conditions, peptides should be stoichiometric with the parent protein to enable accurate quantitation. However, if a protein is digested into multiple overlapping peptides, the specific signal is attenuated and in consequence the quantification becomes underestimated.

There are also side reactions of trypsin known, for example its transpeptidase activity, which yields the addition of a single amino acid (Arg or Lys) to peptides in the reaction mixture. There are also dipeptides added or two longer peptides are combined together. The additions have been described for both N- and C-termini of peptides [7]. However, the incidence of the modified peptides is much lower compared to their unmodified counterparts.

3. Trypsin Forms

Wilhelm Kühne, who discovered trypsin and coined its name in 1876, noticed that the enzyme was produced as an inactive zymogen (trypsinogen) in pancreatic cells [11]. In the 1930s, Moses Kunitz and John H. Northrop elaborated procedures to isolate both trypsinogen and trypsin in crystalline forms, which largely contributed to the development of enzymology [12]. Trypsinogen is stable at acidic pH (2–4). In a neutral or alkaline solution, it is activated by a limited proteolysis catalyzed by either duodenal enteropeptidase (enterokinase) or trypsin itself [4]. Thus, in the latter case, an autocatalytic process occurs. The complete amino acid sequence of bovine trypsinogen was deduced from peptide sequencing experiments by several independent groups in the 1960s [13,14] with later corrections at ambiguous positions (some Asn/Asp and Gln/Glu were not distinguished in early studies because of limitations of the sequencing methods used at that time). In addition to the dominant cationic trypsinogen, a minor anionic trypsinogen is produced in bovine pancreas [15]. The UniProt accession numbers are P00760 (TRY1_BOVIN) and Q29463 (TRY2_BOVIN), respectively; the corresponding mature trypsin sequences share 72% identity.

The cationic trypsinogen sequence spans the length of 229 amino acids (Figure 1). Altogether, there are six disulfide bonds in the molecule connecting the following cysteine residues: 13 and 143, 31 and 47, 115 and 216, 122 and 189, 154 and 168 plus 179 and 203 [14]. By the removal of the N-terminal hexapeptide VDDDDK, the single chain β-trypsin is formed as the predominant product of trypsinogen activation. Trypsin autolysis with a cleavage between Lys-131 and Ser-132 (numbered according to the trypsinogen convention) produces α-trypsin, which has two chains connected by disulfide bonds) [4]. A further cleavage at the bond Lys-176–Asp-177 yields ψ-trypsin with three discrete chains [16]. Another known active trypsin forms include for example the two chain δ-trypsin [17–19] and γ-trypsin [20] with chain splits at the bonds Arg-105–Val-106 and Lys-155–Ser-156, respectively. On the contrary, a cleavage between Lys-49 and Ser-50 has been shown to inactivate the enzyme [18]. More degraded autolysis products are considered inactive [4]. Bovine trypsin is characterized by a molar absorption coefficient ε_{280} of 40,000 mol·L^{-1}·cm^{-1} [21] resulting from the presence of 4 Trp, 10 Tyr, and 12 Cys residues (oxidized to disulfides in the protein) in the sequence. A certain degree of variability in these numbers can be found for trypsin enzymes from different mammalian or other sources of origin [4]. All mentioned variants are often called "trypsin isoforms" in the literature but this is not satisfactory. According to the International Union of Pure and Applied Chemistry (IUPAC), the term isoform refers only to genetic differences and not to a variation at the protein level. Hence, the real isoforms are e.g., the cationic and anionic trypsin. To solve this terminological confusion, the term "proteoform" has recently been introduced, which covers all molecular forms encoded by a single gene, including changes due to genetic variations, alternatively spliced transcripts and posttranslational modifications [22].

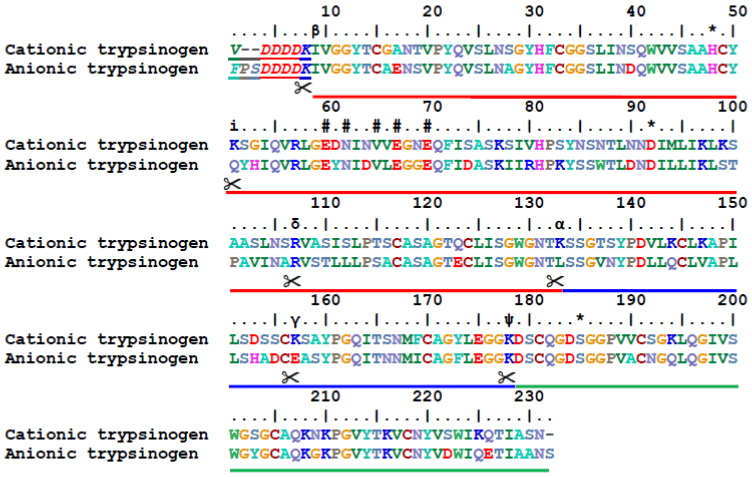

Figure 1. An alignment of the cationic and anionic bovine trypsinogen sequences. Italic letters and a thin underlining at the beginning of the sequences highlight the activation peptides, which are cleaved off during the trypsinogen conversion to mature trypsin. In the ruler line, asterisks (*) indicate active-site residues (the charge relay system, also catalytic triad) and hash (#) symbols mark calcium-binding residues. Greek alphabet letters indicate the cleavage sites in the active single-chain β-trypsin (223 residues), which yield the other trypsin proteoforms (α, γ, δ, and ψ) upon autolysis. The small-case letter 'i' denotes the cleavage site leading to an inactive trypsin variant. All above mentioned cleavage sites are additionally highlighted by a symbol of scissors. Thick red, blue, and green lines indicate individual ψ-trypsin chains. The alignment was made using BioEdit 7.2.5 with trypsinogen sequences obtained from the UniProt database. The accession numbers are P00760 (TRY1_BOVIN, cationic) and Q29463 (TRY2_BOVIN, anionic). The numbering refers to anionic trypsinogen. For cationic trypsinogen, it is shifted towards the canonical numbering by two units up because of the alignment.

4. Pseudotrypsin Purification from the Autolyzate

In the original report from 1969, ψ-trypsin was purified from an autolyzate of bovine trypsin using isocratic ion-exchange chromatography [16]. The autodigestion proceeded at pH 8.0 and 25 °C in the presence of calcium ions for up to 6.5 h. Then N^a-*p*-tosyl-L-lysine-chloromethyl ketone (TLCK), which is an irreversible trypsin inhibitor, was added at pH 7.0 to abolish any detectable activity. After a removal of low-molecular weight compounds from the protein by gel permeation chromatography (1 mM HCl as a mobile phase) and the subsequent lyophilization, the TLCK-treated autolyzate was separated on an Sulfoethyl (SE)-Sephadex C-50 column (1 × 48 cm) in 100 mM Tris-HCl, pH 7.1, containing 20 mM $CaCl_2$. This procedure had previously been developed for a reliable resolving α- and β-trypsin [23]. In this arrangement, ψ-trypsin was eluted prior to the elution of α- and finally β-trypsin. It was found not to contain an alkylation resulting from the TLCK treatment, which was elucidated by its decreased activity towards trypsin substrates [16]. In a similar way, ψ-trypsin was purified on SE-Sephadex C-50 in several other studies. Some differences appeared in the column length, e.g., 1.5 × 150 cm [24], or the authors optimized the composition of the mobile phase by varying sample loading, pH, flow rate and concentration of NaCl [25].

In our laboratory, we used a HEMA-BIO 1000 SB column (0.75 × 25 cm) in a medium-pressure protein liquid chromatography to separate trypsin autolyzate components [8]. The flow rate was adjusted to 2 mL·min^{-1} and the whole time window to resolve isocratically ψ-, α-, and β-trypsin (in

the given order of elution times) at pH 7.1 was 45 min long. We have recently replaced the HEMA-BIO 1000 SB column by a Uno S12 column (15 × 68 mm), which allowed reducing the separation time, at the expense of resolution, but still yielded a pure ψ-trypsin (Figure 2). In this case, however, the use of a gradient elution was necessary—the buffer B contained 1 M NaCl (Perutka et al., unpublished results). In the 1970s, a French group, which studied kinetic properties of ψ-trypsin at that time, developed a convenient purification method based on affinity chromatography [26,27]. The yield was 15–20 % of the initial fully active trypsin. To prepare the affinity column, a trypsin inhibitor from egg-white chicken ovomucoid was attached to aminoethyl-cellulose using glutaraldehyde as a coupling reagent. The equilibration buffer for separation runs was 0.1 M Tris-HCl, containing 50 mM $CaCl_2$, pH 7.1. ψ-Trypsin appeared already in the flow-through fraction (just after the void volume). Thus, it was necessary to include a size-exclusion chromatographic step prior to the affinity separation in order to remove low-molecular-weight contaminants such as peptides. In contrast, the proteoforms α and β remained bound and could be eluted (as an unresolved mixture) by applying an acidic elution buffer of pH 2.3 [27]. This low affinity of ψ-trypsin is in agreement with results on the formation of its complex with pancreatic trypsin inhibitor, where the corresponding dissociation constant was increased by five orders of magnitude compared to that for a mixture of α- and β-trypsin [28].

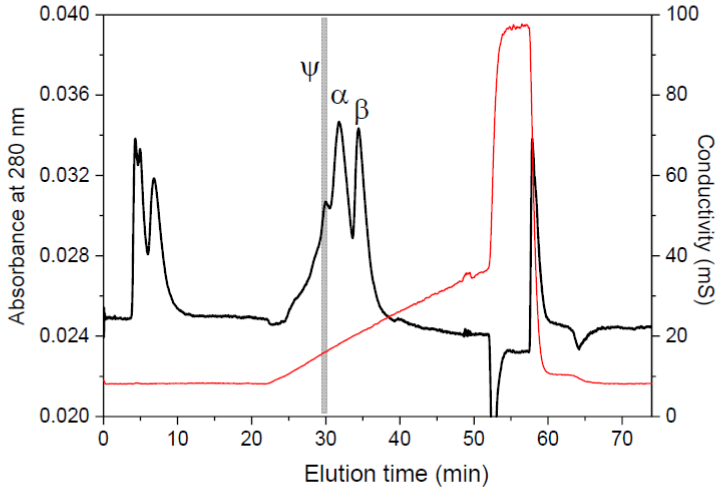

Figure 2. Ion-exchange chromatography of trypsin autolyzate. The depicted separation was performed on a Uno S12 column (15 × 68 mm; Bio-Rad, Hercules, CA, USA) using a linear gradient of NaCl (0–1 M) in 100 mM Tris-HCl, pH 7.1, containing 10 mM $CaCl_2$. The gray box indicates a time window, in which the respective ψ-trypsin fraction was collected. The black line shows absorbance at 280 nm, the red line refers to conductivity of the eluate.

5. Molecular Properties and Structure of Trypsin and Pseudotrypsin

Accurate experimental molecular mass values of bovine ψ-trypsin were first determined by electrospray ionization (ESI)-MS [29,30]. For β-trypsin, α-trypsin, and ψ-trypsin, the following average numbers (relative monoisotopic molecular masses) were obtained in the given order: 23296, 23310, and 23325 [29] or 23294, 23312 and 23328 [30]. These numbers are in accordance with sequence-based calculated values of 23293, 23311, and 23329, respectively [30], which reflect a relative mass difference of 18 resulting from each consecutive autolytic cleavage. For ψ-trypsin, the most recent data are 23332 ± 4 (MALDI-MS) and 23330 ± 0.1 (ESI-MS) [8]. Thus, based on an accurate molecular mass

determination, the purity of ψ-trypsin preparations can easily be evaluated, also to rule out the presence of a chymotrypsin contamination coming from the original trypsin material.

Isoelectric points of proteins can be estimated from their amino acid sequences for example using the software tool ProtParam (https://web.expasy.org/cgi-bin/protparam/). A theoretical p*I* value of the cationic bovine trypsin (Uniprot accession number P00760, positions 24–246) is 8.69. Similarly, for porcine trypsin (Uniprot accession number P00761, positions 9–231), the result is 8.26. Interestingly, higher experimental values of 10.0/10.5 [31,32] were published for the bovine enzyme and 10.2/10.8 for the porcine enzyme [33,34]. For ψ-trypsin, no experimental data on p*I* are available to our knowledge, but similar values could be expected. The anionic bovine trypsin (Uniprot accession number Q29463, positions 24–247) has a theoretical p*I* value of 4.90, which agrees well with an experimental result [35].

Chymotrypsin and trypsin were among first proteins with experimentally determined spatial structures. The crystal structure of bovine chymotrypsin appeared already in 1967 [36] and was refined later on [37]. At that time, a similarity in the three-dimensional folding of trypsin and chymotrypsin could be assumed because of the amino acid sequence homology and matching positions of disulfide bonds. The crystal structures of bovine β-trypsin and trypsinogen were solved in the 1970s [38–40]. Figure 3 shows a view of the trypsin structure (PDB accession code 1AQ7 [41]) visualized using PyMol 1.3. Trypsin is a globular protein. Its overall fold comprises two six-stranded Greek-key β-barrels [42]. The active site with the catalytic triad of amino acids is located between the two barrels. His-57 and Asp-102 belong to the N-terminal barrel whereas Ser-195 originates from the C-terminal barrel (this numbering is according to the chymotrypsinogen convention, see in Walsh and Neurath) [13]. Helices represent only minor secondary structure components, for example at the C-terminus. The enzyme contains a calcium ion, which is important for activity. Its coordination chemistry involves several residues from the calcium-binding loop [38]. The calcium ion interacts with the side-chain oxygens (in the trypsinogen numbering) of Glu-58, Glu-65 (this one via a coordinated water molecule), and Glu-68 plus the carbonyl oxygens of Asn-60 and Val-63. No crystal structure of ψ-trypsin has been solved up to now. As this proteoform contains two chain splits (between: 1. Lys-131 and Ser-132, 2. Lys 176 and Asp-177; according to the trypsinogen numbering), the whole molecule is loosened somehow in comparison to that of β-trypsin. The bond Lys-176—Asp-177 is located close to the anionic binding site (i.e., specificity site: Asp-177, which is the position 189 when expressed in the chymotrypsinogen numbering). Upon the autolytic splitting, the binding site arrangement is disconnected. In consequence, the affinity for polypeptide trypsin substrates is lowered and the cleavage specificity broadened [8,24]. This structural alteration does not prevent from binding of a pancreatic trypsin inhibitor; only the dissociation constant of the enzyme-inhibitor complex is increased [24,28]. ψ-Trypsin still keeps a certain level of specificity, which is based on hydrophobic interactions, as confirmed using synthetic ester substrates [27].

After trypsinogen activation, the new N-terminal residue (Ile-16, in chymotrypsinogen numbering) inserts into a cleft, where it establishes an ion pair (via α-amino group) with Asp-194 next to the catalytic serine. This results in a conformational rearrangement. The amino group of Gly-193 moves into a position, which completes the oxyanion hole at the active site [2]. The hole is formed by the trypsin amide hydrogens of Gly-193 and Ser-195 in favor of stabilization of the developing negative charge on the carbonyl oxygen atom of the cleaved substrates.

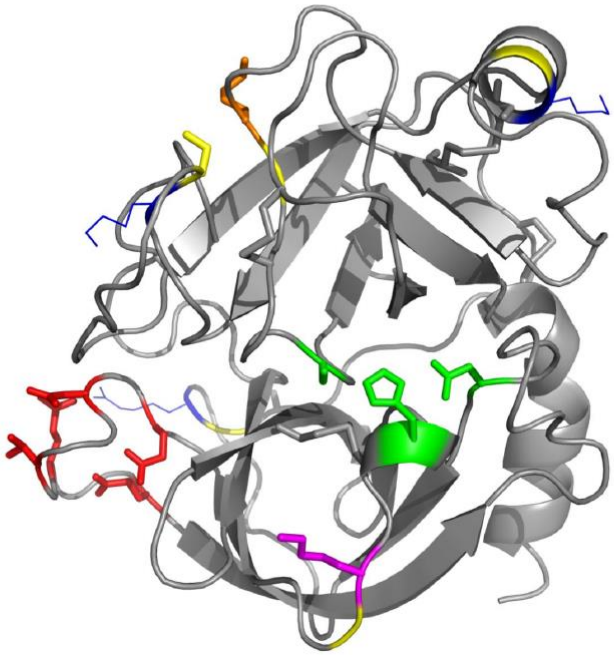

Figure 3. The crystal structure of bovine β-trypsin. This overall view was made in PyMOL 1.3 using a pdb formatted file (accession number 1AQ7 [41]) downloaded from the PDB database (http://www.rcsb.org/pdb). Trypsin fold comprises two β-barrels. The active site with the catalytic triad of amino acids is located between them (in the center of this figure) and highlighted in green. Red color on the bottom left shows the calcium-binding residues. The KD bond, which is cleaved to generate ψ-trypsin is expressed as an orange side chain (Lys-176) at a yellow backbone segment (Asp-177). Blue-line side chains at other yellow segments indicate the presence of the basic residues, where the β-trypsin polypeptide chain is cleaved to produce α-trypsin (Lys-131, above the calcium site and not far away from Lys-176 in this projection), γ-trypsin (Lys-155, top right, in the helix), and δ-trypsin (Arg-105, behind the calcium site). Finally, magenta color at the bottom indicates Lys-49, which is disconnected from Ser-50 to yield the inactive autolytic form.

6. Pseudotrypsin Activity with Artificial Substrates (Enzyme Kinetics)

Compared to α-trypsin and β-trypsin, the overall structural change resulting from the additional intrachain split in ψ-trypsin yields differences in the activity and specificity. This was evaluated already in the 1960s and 1970s by measuring kinetic parameters for low-molecular-weight substrates (Table 1). Smith and Shaw [16] recognized during the chromatographic purification that ψ-trypsin did not show any measurable activity with N^{α}-benzoyl-D,L-arginine-4-nitroanilide (Bz-Arg-pNA) as a substrate under experimental conditions optimized for α-trypsin (i.e., no amidase activity). Nevertheless, they could demonstrate a hydrolytic activity of ψ-trypsin by detecting a stoichiometric incorporation of [^{14}C] diisopropyl fluorophosphate at the active site, which is typical for serine proteases or esterases in general. However, the rate of ^{14}C incorporation was very slow, which indicated a decreased reactivity of ψ-trypsin compared to α-trypsin. Similarly, a slow conversion of the active site titrant *p*-nitrophenyl-*p*′-guanidinobenzoate (NPGB) was observed. Comparative kinetic data measured with several artificial ester substrates are shown in Table 1. For example, the affinity of ψ-trypsin for the

cationic N^{α}-benzoyl-L-arginine ethyl ester (Bz-Arg-OEt) represented by the determined Michaelis constant value is lower by three orders of magnitude than that of α-trypsin [16]. Such a big difference in affinity was observed also for carboxybenzyl-L-lysine esters or N^{α}-*p*-tosyl-L-arginine methyl ester [27]. Not only the affinity, but also the activity (catalytic constant) is often largely different. A typical chymotrypsin substrate N^{α}-acetyl-L-tyrosine ethyl ester (Ac-Tyr-OEt) is hydrolyzed by α-trypsin almost 3000 times faster than by ψ-trypsin (Table 1). At the same time, the respective K_m values are comparable as the binding of this neutral substrate is not affected so much by the disconnection of Asp-177 (the specificity site) in ψ-trypsin [16]. As a consequence of the reduced affinity and activity towards cationic substrates, the efficiency constant values k_{cat}/K_m are decreased by many orders of magnitude (up to 6) for ψ-trypsin [16,27].

Table 1. Kinetic data for bovine α-trypsin and ψ-trypsin with artificial substrates. This table is adapted from Smith and Shaw [16] and completed by results with non-fractionated trypsin [43]. All experiments were performed at pH 8.0 and 25 °C.

Enzyme	Substrate [a]	k_{cat} (s^{-1})	K_m ($mol \cdot L^{-1}$)	K_i ($mol \cdot L^{-1}$)
α-Trypsin	Bz-Arg-OEt (0.05 M $CaCl_2$)	24	2.5×10^{-6}	-
ψ-Trypsin	Bz-Arg-OEt (0.001 M $CaCl_2$)	0.19	1.1×10^{-2}	-
ψ-Trypsin	Bz-Arg-OEt (0.05 M $CaCl_2$, benzamidine)	-	-	3.7×10^{-2}
Trypsin (non-fractionated)	Bz-Arg-OEt (0.025 M $CaCl_2$)	14.6	4.3×10^{-6}	-
α-Trypsin	Ac-Tyr-OEt (0,05 M $CaCl_2$, 10% 2-propanol)	57	6.2×10^{-2}	-
ψ-Trypsin	Ac-Tyr-OEt (0.001 M $CaCl_2$, 10% 2-propanol)	0.02	3.7×10^{-2}	-
Trypsin (non-fractionated)	Ac-Tyr-OEt (0.05 M $CaCl_2$, 5% dioxane)	14.5	4.2×10^{-2}	-
Trypsin (non-fractionated)	Bz-Arg-pNA (benzamidine) [b]	-	-	1.8×10^{-5}

[a] Further information on the composition of the reaction mixture is provided in parentheses; [b] This reaction was performed at pH 8.15 and 15 °C.

Benzamidine has been shown a potent competitive inhibitor of trypsin. It is approximately of the same size as the side chain of lysine and arginine and contains both a positively charged group and hydrophobic moiety in its structure. The K_i value of benzamidine for the reaction of trypsin with Bz-Arg-pNA is 1.8×10^{-5} $mol \cdot L^{-1}$ [4]. In contrast, the binding of the inhibitor to ψ-trypsin is characterized by an increased K_i value 3.7×10^{-2} $mol \cdot L^{-1}$, which is in agreement with the K_m value for the neutral (and thus non-specific) substrate Ac-Tyr-OEt (Table 1). The irreversible trypsin inhibitor TLCK does not inactivate ψ-trypsin at all [16]. Further evidence of the reduced ψ-trypsin affinity to positively charged ligands was observed with a basic pancreatic trypsin inhibitor. The second-order rate constant of the association is decreased by a factor of 16 when ψ-trypsin is used instead of α- and β-trypsin and the dissociation constant is increased by a factor of 1.5×10^5 from 6×10^{-14} $mol \cdot L^{-1}$ (a quasi-irreversible binding in the case of trypsin) to 9×10^{-9} $mol \cdot L^{-1}$. This value is similar to that of chymotrypsin, which also associates with this inhibitor but lacks the trypsin specificity site [28]. When the disulfide bond Cys-179−Cys-203 in trypsin is selectively reduced and the emerged cysteines subsequently carboxymethylated, the resulting enzyme derivative still binds the inhibitor efficiently. Interestingly, the observed kinetic parameters of the association and dissociation correspond to those determined for ψ-trypsin [28].

The reaction mechanism of trypsin is illustrated in Scheme 1 (based on that in [27]) Acylation and deacylation rate constants (k_2 and k_3, respectively) were measured with the active site titrant NPGB and pure bovine α-, β-, and ψ-trypsin preparations [27]. Whereas the acylation rate was found to be 1000 slower for ψ-trypsin than for the other proteoforms at optimum pH, the deacylation rates were rather comparable. A similar difference in the acylation rate was observed with *p*-acetoxyphenylguanidine *p*-toluenesulfonate. This compound belongs to "inverse substrates" as it contains the specific cationic center within the leaving group instead of the acyl moiety [44]. Measurements with different

carboxybenzyl-L-lysine esters (cationic i.e., specific trypsin substrates) indicated that acylation is largely the rate-limiting step for ψ-trypsin contrary to deacetylation as it appears in the case of α-/β-trypsin [27,45]. For neutral (nonspecific) substrates, acylation is rate limiting also for the major proteoforms. The k_{cat} values for ψ-trypsin were found sensitive to the substrate leaving group in contrast to those observed for α-trypsin, which shows that the catalysis by this form is not completely nonspecific and hydrophobic binding subsites are preserved.

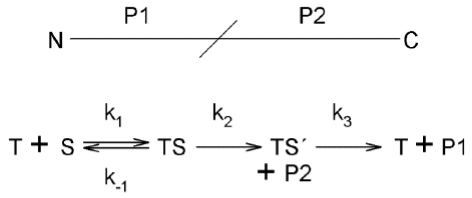

Scheme 1. The reaction mechanism of trypsin. A protein substrate (S) with the indicated N- and C-termini and the cleavage site is cleaved by trypsin (T) into two large peptides or polypeptides P1 and P2. TS stands for a Michaelis trypsin-substrate complex, TS′ represent an acyl-enzyme intermediate. The reaction rate constants are as follows: k_1—enzyme-substrate association rate constant; k_{-1}—enzyme-substrate dissociation rate constant; k_2—enzyme-substrate acylation rate constant; k_3—enzyme-substrate deacylation rate constant; $k_{cat} = k_2k_3/(k_2 + k_3)$. This scheme has been adapted from the reference [27].

7. Cleavage Specificity towards Peptides and Proteins

Both major forms of trypsin (α and β) prefer Arg-X sites to Lys-X sites during the hydrolysis of synthetic as well as polypeptide substrates at an optimal pH of 8–9. The preference ratio is even more pronounced at higher pH values (>pH 10) because the ε-amino group of lysine is largely discharged under these conditions and becomes less attractive [4]. The cleavage specificity of ψ-trypsin towards peptide bonds was first analyzed with two peptide substrates: a mixture of bovine and porcine glucagon and a heptapeptide fragment of the B chain of insulin with a sequence of GFFYTPK [24]. The heptapeptide was selected because of the content of aromatic residues to evaluate whether ψ-trypsin shows a preference similar to that of chymotrypsin. The glucagon sequence contains three canonical trypsin cleavage sites (Lys-12, Arg-17, and Arg-18). In a parallel work, the same group demonstrated that pure α- and β-trypsin preparations did not show any effect on the insulin-derived heptapeptide and carboxy sites of aromatic amino acid residues in glucagon [46]. Conversely to the effect of α-chymotrypsin used as a 1% model contamination in a commercial trypsin preparation (control digest), no effect of ψ-trypsin on the heptapeptide was observed. The digestion of glucagon was performed in 0.1 ammonium carbonate containing 20 mM $CaCl_2$ at pH 8.0 and ψ-trypsin generated the same fragments as it had been observed in the parallel study with α- and β-trypsin. However, the yield of these fragments was lower than those produced by the major forms, indicating its decreased affinity to polypeptides. However, ψ-trypsin showed an additional ability to cleave bonds adjacent to the aromatic amino acids Phe and Trp [24].

Dyčka et al. [8] performed overnight in-gel digestions of six standard proteins with monomer molecular masses of 12–95 kDa (cytochrome *c*, lysozyme, myoglobin, glucose oxidase, serum albumin, and glycogen phosphorylase) using ψ-trypsin, non-fractionated trypsin (treated by *N*-*p*-tosyl-L-phenylalanine chloromethyl ketone—TPCK—to inactivate a possible chymotrypsin contamination) and chymotrypsin to obtain a more complex view of the cleavage specificity. The numbers of sequence-matched peptides with the respective sequence coverage values from nLC-MALDI-MS/MS were similar for ψ-trypsin and trypsin. A majority of the registered ψ-trypsin cleavage sites (77 %) were produced by its action upon the C-termini of Arg and Lys residues (in the case of trypsin, it was 86 %). Additional cleavages appeared particularly after Phe and Tyr residues,

which confirmed the previous data obtained with glucagon [24]. Interestingly, ψ-trypsin provided 1.5-fold higher number of peptides containing missed cleavage (Arg and Lys) sites, which probably results from the lower substrate binding ability of this proteoform [8].

8. The Use of Pseudotrypsin for Protein Identification in Proteomics

At the present time, ψ-trypsin is not commonly used in biochemistry and proteomics as it is not commercially available and its purification takes a few days with a low yield of pure protein at the end. From 200 mg of bovine trypsin as a starting material [8], only milligrams of the final product could be obtained. The applicability of ψ-trypsin has a potential in protein identification experiments involving ESI- or MALDI-MS/MS as it generates more peptides with missed cleavage sites than native trypsin and also nonspecific peptides terminated mainly by Phe and Tyr residues (resembling partially the chymotrypsin mode of action). In consequence, higher sequence coverage values and increased number of matched peptides can be achieved. Interestingly, pseudotrypsin has been hypothesized to cause the cleavage of a Cys–Gly bond in NDRG1 protein [47]. Another possibility of application resides in studying posttranslational modifications. Such a modification may under a common routine interfere with trypsin digestion, for example when a phosphorylation occurs close to an arginine or lysine, and would then require selecting of another protease [48]. On the other hand, for its broader cleavage specificity, ψ-trypsin is not recommendable for mass spectrometry-based protein quantification experiments [49] because of the possible distribution of the same predicted canonical cleavage site in more peptides (multiple cleavage products due to missed cleavages or additional cleavage sites).

A comparative in-gel digestion of a gel fraction of rat urine proteins resulted in 22 identifications after the use of ψ-trypsin. The same number was reached with a commercial non-fractionated trypsin, but only 17 were identified in both cases. Hence a simple combination of the two digestions provided about 20 % more identification [8]. The total number of the matched peptides was 233 and 199, respectively. The numbers of the cleaved Arg and Lys sites were comparable (around 130); in the case of Phe and Tyr site cleavages, two times more peptides were produced by ψ-trypsin. Recently, this proteoform was applied to analyze nuclear proteins after a DNase treatment of barley nuclei and sodium dodecyl sulfate polyacrylamide gel electrophoresis of the released protein material (Perutka et al., unpublished results). Peptides from the digests were analyzed by MALDI and ESI MS/MS and the results compared with parallel tryptic digestions. The identified nonspecific peptides in the ψ-tryptic digests represented 15–20 % of the total peptide number (compared to 7 % for a standard trypsin). In agreement with previous reports [8,24], peptides with C-terminal Tyr and Phe residues (and also Leu) were found in a significant percentage representation but were only minor to those resulting from the characteristic trypsin cleavage after the basic Arg and Lys residues (Figure 4). The higher number of Arg-ending over Lys-ending peptides in the MALDI-TOF/TOF MS/MS results (but not in the ESI-based results; not shown) probably reflected the fact that Arg-peptides provide more intense signals in MALDI-TOF MS [50], and thus they are preferably selected for the subsequent data-dependent fragmentation. Database searches allowed identifying novel proteins which had not previously been recognized based on standard tryptic peptides and deposited in the database UNcleProt [51]. They accounted for around 10 % of all identifications. The digestion performance of ψ-trypsin was compared relatively to that of a commercial trypsin using MALDI-TOF MS-based quantification of bovine serum albumin peptides (Perutka et al., unpublished results). Tryptic digestion was performed in a buffer made of $H_2{}^{18}O$ [52]. During proteolysis, labeled standards were generated by incorporating ^{18}O isotope into the carbonyl group of the nascent peptides. The ψ-tryptic digest was made in a buffered $H_2{}^{16}O$ and then mixed equivolumetrically with the labeled standards. The ratios of non-labeled versus labeled peptides were calculated from the areas of isotopically resolved peaks in MALDI-TOF MS spectra. As a result, the observed overall overnight digestion performance of ψ-trypsin was found lower by around 20 %.

P1 amino acid	G	A	P	V	L	I	M	F	W	Y	S	T	C	N	Q	K	H	R	D	E
side chain	Nonpolar							Aromatic			Polar					Basic			Acidic	
Ψ-trypsin	2.0%	0.9%	0.3%	0.5%	2.2%	0.1%	0.9%	2.1%	0.4%	4.2%	0.7%	0.6%	0.0%	1.1%	0.4%	32.7%	0.4%	49.2%	1.2%	0.1%
α/β trypsin	0.8%	0.2%	0.0%	0.2%	1.1%	0.0%	0.0%	2.4%	0.0%	2.1%	0.0%	0.1%	0.0%	0.7%	0.0%	31.3%	0.5%	60.5%	0.1%	0.0%

Figure 4. C-terminal amino acids (P1 cleavage site) of peptides in ψ-tryptic and tryptic digests. This table summarizes results obtained after in-gel digestions of barley nuclear proteins. The percentage values were averaged from data for almost 40 distinct protein fraction samples. MALDI TOF/TOF MS/MS allowed to identify 1199 and 1238 peptides, respectively. PEAKS Studio 8 software (Bioinformatics Solutions, Waterloo, ON, Canada) was used to process the MGF-formatted files by searching against a *Hordeum vulgare* protein sequence database downloaded from the National Center for Biotechnology Information, USA, at 1% peptide false discovery rate (Perutka, Z. et al.; unpublished results). Peptide sequences containing C-termini of the identified proteins were not included in the calculation.

9. Concluding Remarks

Early studies identified ψ-trypsin as a proteoform resulting from trypsin autolysis. Amino acid analyses of its polypeptide chains revealed the existence of an additional split between Lys-176 and Asp-177 compared to the primary structure of α-trypsin. The enzyme can be obtained from a trypsin autolyzate by ion exchange chromatography. Purification protocols that are available utilize one of the characteristic features of ψ-trypsin: in contrast to α- or β-trypsin, it is not modified by the trypsin inactivator TLCK and shows a minimum retention on cation exchangers such as Sulfoethyl-Sephadex.

Enzyme kinetics studies with synthetic amino acid esters demonstrated a largely decreased affinity and activity towards cationic substrates. This has been elucidated by the presence of the characteristic chain split, which disconnects the specificity site (Asp-177) from the active site (Ser-183, His-46, Asp-90; all indicated according to the trypsinogen numbering convention). The reaction mechanism of ψ-trypsin with specific substrates differs from that of α- or β-trypsin in the rate limiting step. No crystal structure of ψ-trypsin has been solved yet, but the anticipated existence of the modified ('neutral') active site and the ability to hydrolyze tyrosine-derived ester substrates lead to cleavages characteristic of chymotrypsin. So far, only a few studies have focused on the digestion of peptides and proteins by ψ-trypsin. These studies have confirmed its preferential action on Arg and Lys residues but also at Phe and Tyr residues (which is typical for chymotrypsin) as minor cleavage sites. The produced peptides contain frequent missed cleavages because of the absent specificity and reduced affinity towards the cationic sites. However, overnight digestions of protein samples provide enough peptides for identification experiments involving nLC-MALDI or nLC-ESI MS/MS. Subsequently, combining data from tryptic and ψ-tryptic digestions has been shown to be advantageous in order to increase the number of matched peptides and sequence coverage values. Furthermore, peptides with missed cleavage sites could be beneficial for studying posttranslational modifications of proteins.

ψ-Trypsin should not be used as an equivalent substitute of trypsin or chymotrypsin and, in fact, there is no need to do it. However, as it makes preferential cleavages after basic Arg and Lys residues and has a more developed side specificity for aromatic and Leu residues, which is not expected to occur for pure major trypsin forms α and β (but may appear anyway because of their autolysis), it produces valuable complementary information. The unavailability of any commercial material represents a big obstacle for the application of ψ-trypsin in common proteomics research. On the other hand, a single-step affinity chromatographic method has already been introduced [27], which could make the preparation of the enzyme easier (after a revision and transformation with the use of modern chromatographic materials).

Author Contributions: Marek Šebela came with the idea, wrote the Sections 1–5 and finally edited the whole text, Zdeněk Perutka wrote the Sections 6–9 and provided some of his unpublished results.

Funding: This work was supported by grant no. LO1204 (National Program of Sustainability I) from the Ministry of Education, Youth and Sports, Czech Republic.

Conflicts of Interest: The authors declare that there is no conflict of interests.

Abbreviations

Ac-Tyr-OEt	N^{α}-acetyl-L-tyrosine ethyl ester
Bz-Arg-OEt	N^{α}-benzoyl-L-arginine ethyl ester
Bz-Arg-pNA	N^{α}-benzoyl-D,L-arginine-4-nitroanilide
ESI	electrospray ionization
IUPAC	International Union of Pure and Applied Chemistry
MALDI	matrix-assisted laser desorption/ionization
MS	mass spectrometry
MS/MS	tandem mass spectrometry
NPGB	*p*-nitrophenyl-*p*′-guanidinobenzoate
nLC	nanoflow liquid chromatography
PDB	Protein Data Bank
SE-Sephadex	Sulfoethyl-Sephadex
TLCK	N^{α}-*p*-tosyl-L-lysine-chloromethyl ketone
TOF	time-of-flight
TPCK	*N*-*p*-tosyl-L-phenylalanine chloromethyl ketone

References

1. Burkhart, J.M.; Schumbrutzki, C.; Wortelkamp, S.; Sickman, A.; Zahedi, R.P. Systematic and quantitative comparison of digest efficiency and specificity reveals the impact of trypsin quality on MS-based proteomics. *J. Proteom.* **2012**, *75*, 1454–1462. [CrossRef] [PubMed]
2. Vandermarliere, E.; Mueller, M.; Martens, L. Getting intimate with trypsin. The leading protease in proteomics. *Mass Spectrom. Rev.* **2013**, *32*, 453–465. [CrossRef] [PubMed]
3. Olsen, J.V.; Ong, S.E.; Mann, M. Trypsin cleaves exclusively C-terminal to arginine and lysine residues. *Mol. Cell. Proteom.* **2004**, *3*, 608–614. [CrossRef] [PubMed]
4. Keil, B. Trypsin. *Enzymes* **1971**, *3*, 249–275. [CrossRef]
5. Rodriguez, J.; Gupta, N.; Smith, R.D.; Pevzner, P.A. Does trypsin cut before proline? *J. Proteom. Res.* **2008**, *7*, 300–305. [CrossRef] [PubMed]
6. Picotti, P.; Aebersold, R.; Domon, B. The implications of proteolytic background for shotgun proteomics. *Mol. Cell. Proteom.* **2007**, *6*, 1589–1598. [CrossRef] [PubMed]
7. Schaefer, H.; Chamrad, D.C.; Marcus, K.; Reidegeld, K.A.; Blüggel, M.; Meyer, H.E. Tryptic transpeptidation products observed in proteome analysis by liquid chromatography-tandem mass spectrometry. *Proteomics* **2005**, *5*, 846–852. [CrossRef] [PubMed]
8. Dyčka, F.; Franc, V.; Fryčák, P.; Raus, M.; Řehulka, P.; Lenobel, R.; Allmaier, G.; Marchetti-Deschmann, M.; Šebela, M. Evaluation of pseudotrypsin cleavage specificity towards proteins by MALDI-TOF mass spectrometry. *Protein Pept. Lett.* **2015**, *22*, 1123–1132. [CrossRef] [PubMed]
9. Thiede, B.; Lamer, S.; Mattow, J.; Siejak, F.; Dimmler, C.; Rudel, T.; Jungblut, P.R. Analysis of missed cleavage sites, tryptophan oxidation and N-terminal pyroglutamylation after in-gel tryptic digestion. *Rapid Commun. Mass Spectrom.* **2000**, *14*, 496–502. [CrossRef]
10. Lawless, C.; Hubbard, S.J. Prediction of missed proteolytic cleavages for the selection of surrogate peptides for quantitative proteomics. *OMICS* **2012**, *16*, 449–456. [CrossRef] [PubMed]
11. Kühne, W. *Über das Trypsin (Enzym des Pankreas). Verhandlungen des Naturhistorisch-medizinischen Vereins zu Heidelberg*; Carl Winter's Universitätsbuchhandlung: Heidelberg, Germany, 1877; Volume 1, pp. 194–198, reprinted in *FEBS Lett.* **1976**, *62*, E8–E12. [CrossRef]
12. Kunitz, M.; Northrop, J.H. Isolation from beef pancreas of crystalline trypsinogen, trypsin, a trypsin inhibitor, and an inhibitor-trypsin compound. *J. Gen. Physiol.* **1936**, *19*, 991–1007. [CrossRef] [PubMed]

13. Walsh, K.A.; Neurath, H. Trypsinogen and chymotrypsinogen as homologous proteins. *Proc. Natl. Acad. Sci. USA* **1964**, *52*, 884–889. [CrossRef] [PubMed]
14. Mikeš, O.; Holeyšovský, V.; Tomášek, V.; Šorm, F. Covalent structure of bovine trypsinogen. The position of remaining amides. *Biochem. Biophys. Res. Commun.* **1966**, *24*, 346–352. [CrossRef]
15. Puigserver, A.; Desnuelle, P. Identification of an anionic trypsinogen in bovine pancreas. *Biochim. Biophys. Acta* **1971**, *236*, 499–502. [CrossRef]
16. Smith, R.L.; Shaw, E. Pseudotrypsin. A modified bovine trypsin produced by limited autodigestion. *J. Biol. Chem.* **1969**, *244*, 4704–4712. [PubMed]
17. Maroux, S.; Rovery, M.; Desnuelle, P. An autolyzed and still active form of bovine trypsin. *Biochim. Biophys. Acta* **1967**, *140*, 377–380. [CrossRef]
18. Maroux, S.; Desnuelle, P. On some autolyzed derivatives of bovine trypsin. *Biochim. Biophys. Acta* **1969**, *181*, 59–72. [CrossRef]
19. Kumazaki, T.; Ishi, S. Characterization of active derivatives produced by acetamidination and selective autolysis of bovine trypsin. *J. Biochem.* **1979**, *85*, 581–590. [CrossRef] [PubMed]
20. Lacerda, C.D.; Teixeira, A.E.; de Oliveira, J.S.; Silva, S.F.; Vasconcelos, A.V.B.; Gouveia, D.G.; da Silva, A.R.; Santoro, M.M.; dos Mares-Guia, M.L.; Santos, A.M.C. Gamma trypsin: Purification and physicochemical characterization of a novel bovine trypsin isoform. *Int. J. Biol. Macromol.* **2014**, *70*, 179–186. [CrossRef] [PubMed]
21. Walsh, K.A.; Wilcox, P.E. Serine proteases. *Methods Enzymol.* **1970**, *19*, 31–41. [CrossRef]
22. Smith, L.M.; Kelleher, N.L. The Consortium for Top Down Proteomics. Proteoform: A single term describing protein complexity. *Nat. Methods* **2013**, *10*, 186–187. [CrossRef] [PubMed]
23. Schroeder, D.D.; Shaw, E. Chromatography of trypsin and its derivatives. Characterization of a new active form of bovine trypsin. *J. Biol. Chem.* **1968**, *243*, 2943–2949. [PubMed]
24. Keil-Dlouhá, V.V.; Zylber, N.; Imhoff, J.M.; Tong, N.T.; Keil, B. Proteolytic activity of pseudotrypsin. *FEBS Lett.* **1971**, *16*, 291–295. [CrossRef]
25. Santos, A.M.C.; Oliveira, J.S.D.; Bittar, E.R.; Silva, A.L.D.; Guia, M.L.D.M.; Bemquerer, M.P.; Santoro, M.M. Improved purification process of β-and α-trypsin isoforms by ion-exchange chromatography. *Braz. Arch. Biol. Technol.* **2008**, *51*, 511–521. [CrossRef]
26. Foucault, G.; Kellershohn, N.; Seydoux, F.; Yon, J.; Parquet, C.; Arrio, B. Comparative study of some conformational properties of α, β and ψ trypsins. *Biochimie* **1974**, *56*, 1343–1350. [CrossRef]
27. Foucault, G.; Seydoux, F.; Yon, J. Comparative kinetic properties of α, β and ψ forms of trypsin. *Eur. J. Biochem.* **1974**, *47*, 295–302. [CrossRef] [PubMed]
28. Vincent, J.P.; Lazdunski, M. Trypsin-pancreatic trypsin Inhibitor association. Dynamics of the interaction and role of disulfide bridges. *Biochemistry* **1972**, *11*, 2967–2977. [CrossRef] [PubMed]
29. Chowdhury, S.K.; Chait, B.T. Analysis of mixtures of closely related forms of bovine trypsin by electrospray ionization mass spectrometry: Use of charge state distributions to resolve ions of the different forms. *Biochem. Biophys. Res. Commun.* **1990**, *173*, 927–931. [CrossRef]
30. Ashton, D.S.; Ashcroft, A.E.; Beddell, C.R.; Cooper, D.J.; Green, B.N.; Oliver, R.W.A. On the analysis of bovine trypsin by electrospray-mass spectrometry. *Biochem. Biophys. Res. Commun.* **1994**, *199*, 694–698. [CrossRef] [PubMed]
31. Cunningham, L.W. Molecular-kinetic properties of crystalline diisopropyl phosphoryl trypsin. *J. Biol. Chem.* **1954**, *211*, 13–19. [PubMed]
32. Günther, A.R.; Santoro, M.M.; Rogana, E. pH titration of native and unfolded β-trypsin: Evaluation of the $\Delta\Delta G^0$ titration and the carboxyl pK values. *Braz. J. Med. Biol. Res.* **1997**, *30*, 1281–1286. [CrossRef] [PubMed]
33. Buck, F.F.; Vithayathil, A.J.; Bier, M.; Nord, F.F. On the mechanism of enzyme action. LXXIII. Studies on trypsins from beef, sheep and pig pancreas. *Arch. Biochem. Biophys.* **1962**, *97*, 417–424. [CrossRef]
34. Travis, J.; Liener, I.E. The crystallization and partial characterization of porcine trypsin. *J. Biol. Chem.* **1965**, *240*, 1962–1966. [PubMed]
35. Ianucci, N.B.; Albanesi, G.J.; Marani, M.M.; Fernández Lahore, H.M.; Cascone, O.; Camperi, S.A. Isolation of trypsin from bovine pancreas using immobilized benzamidine and peptide CTPR ligands in expanded beds. *Sep. Sci. Technol.* **2007**, *40*, 3277–3287. [CrossRef]
36. Matthews, B.W.; Sigler, P.B.; Henderson, R.; Blow, D.M. The three-dimensional structure of tosyl-α-chymotrypsin. *Nature* **1967**, *214*, 652–656. [CrossRef] [PubMed]

37. Birktoft, J.J.; Blow, D.M. Structure of crystalline α-chymotrypsin: V. The atomic structure of tosyl-α-chymotrypsin at 2 Å resolution. *J. Mol. Biol.* **1972**, *68*, 187–240. [CrossRef]
38. Bode, W.; Schwager, P. The refined crystal structure of bovine β-trypsin at 1.8 Å resolution. II. Crystallographic refinement, calcium binding site, benzamidine binding site and active site at pH 7.0. *J. Mol. Biol.* **1975**, *98*, 693–717. [CrossRef]
39. Bode, W.; Fehlhammer, H.; Huber, R. Crystal structure of bovine trypsinogen at 1.8 Å resolution. I. Data collection, application of Patterson search techniques and preliminary structural interpretation. *J. Mol. Biol.* **1976**, *106*, 325–335. [CrossRef]
40. Fehlhammer, H.; Bode, W.; Huber, R. Crystal structure of bovine trypsinogen at 1.8 Å resolution. II. Crystallographic refinement, refined crystal structure and comparison with bovine trypsin. *J. Mol. Biol.* **1977**, *111*, 415–438. [CrossRef]
41. Sandler, B.; Murakami, M.; Clardy, J. Atomic structure of the trypsin-aeruginosin 98-B complex. *J. Am. Chem. Soc.* **1998**, *120*, 595–596. [CrossRef]
42. Page, M.J.; Di Cera, E. Combinatorial enzyme design probes allostery and cooperativity in the trypsin fold. *J. Mol. Biol.* **2010**, *399*, 306–319. [CrossRef] [PubMed]
43. Inagami, T.; Sturtevant, J.M. Nonspecific catalyses by α-chymotrypsin and trypsin. *J. Biol. Chem.* **1960**, *235*, 1019–1023. [PubMed]
44. Nakano, M.; Tanizawa, K.; Nozawa, M.; Kanaoka, Y. Efficient tryptic hydrolysis of aryl esters with a cationic center in the leaving group. Further characterization of "inverse substrates". *Chem. Pharm. Bull.* **1980**, *28*, 2212–2216. [CrossRef]
45. Seydoux, F.; Yon, J. On the specificity of tryptic catalysis. *Biochem. Biophys. Res. Commun.* **1971**, *44*, 745–751. [CrossRef]
46. Keil-Dlouhá, V.; Zylber, N.; Tong, N.T.; Keil, B. Cleavage of glucagon by α- and β-trypsin. *FEBS Lett.* **1971**, *16*, 287–290. [CrossRef]
47. Ghalayini, M.K.; Dong, Q.; Richardson, D.R.; Assinder, S.J. Proteolytic cleavage and truncation of NDRG1 in human prostate cancer cells, but not normal prostate epithelial cells. *Biosci. Rep.* **2013**, *33*, e00042. [CrossRef] [PubMed]
48. Kirkpatrick, D.S.; Gerber, S.A.; Gygi, S.P. The absolute quantification strategy: A general procedure for the quantification of proteins and post-translational modifications. *Methods* **2005**, *35*, 265–273. [CrossRef] [PubMed]
49. Nigam, A.; Subramanian, M.; Rajanna, P.K. Non-specific digestion artifacts of bovine trypsin exemplified with surrogate peptides for endogenous protein quantitation. *Chromatographia* **2018**, *81*, 57–64. [CrossRef]
50. Krause, E.; Wenschuh, H.; Jungblut, P.R. The dominance of arginine-containing peptides in MALDI-derived tryptic mass fingerprints of proteins. *Anal. Chem.* **1999**, *71*, 4160–4165. [CrossRef] [PubMed]
51. Blavet, N.; Uřinovská, J.; Jeřábková, H.; Chamrád, I.; Vrána, H.; Lenobel, R.; Beinhauer, J.; Šebela, M.; Doležel, J.; Petrovská, B. UNcleProt (Universal Nuclear Protein database of barley): The first nuclear protein database that distinguishes proteins from different phases of the cell cycle. *Nucleus* **2016**, *8*, 70–80. [CrossRef] [PubMed]
52. Havliš, J.; Thomas, H.; Šebela, M.; Shevchenko, A. Fast-response proteomics by accelerated in-gel digestion of proteins. *Anal. Chem.* **2003**, *75*, 1300–1306. [CrossRef] [PubMed]

Příloha 5:

Perutka, Z., Šufeisl, M., Strnad, M., Šebela, M., 2019. High-proline proteins in experimental hazy white wine produced from partially botrytized grapes. *Biotechnology and Applied Biochemistry* 66, 398-411.

High-proline proteins in experimental hazy white wine produced from partially botrytized grapes

Zdeněk Perutka [1]
Miloslav Šufeisl [2]
Miroslav Strnad [3]
Marek Šebela [1*]

[1] Department of Protein Biochemistry and Proteomics, Centre of the Region Haná for Biotechnological and Agricultural Research, Faculty of Science, Palacký University, Olomouc, Czech Republic

[2] Šufeisl Winery, Oslavany, Czech Republic

[3] Laboratory of Growth Regulators, Palacký University and Institute of Experimental Botany AS CR, Olomouc, Czech Republic

Abstract

Undesirable effects of the pathogen *Botrytis cinerea* include reduced quality and quantity of wine grapes. Winemaking is also complicated by the formation of a protein haze in white wines and oxidative browning of red wines. We analyzed proteins in experimental Moravian white wines characterized by their instability and haze formation in bottles during storage despite prior bentonite treatment. To study the relationship of wine proteins and haze, we carried out proteomics on hazy and clear white wines produced with partly or largely botrytized grapes and standard reference wines. Wine proteins were identified after their extraction, electrophoresis, and tryptic digestion by reversed-phase liquid chromatography of peptides, coupled with tandem mass spectrometry. Plant defense proteins, yeast glycoproteins, and various enzymes from Botrytis, particularly hydrolases, were found. As the content of the known haze-active thaumatin-like proteins and chitinases was visually low on stained gels (missing bands) compared to previous studies with unfined wines, other proteins are discussed in terms of the haze formation. As the main novelty, this work reveals the role of high proline-containing proteins in the propensity of white wines to turbidity following prior Botrytis damage of grapes.

Volume 00, Number 0, Pages 1–15, 2019

Keywords: *Botrytis cinerea, proline, proteomics, wine haze, thaumatin, yeast*

1. Introduction

Gray or blue molds (*Botrytis* and *Penicillium* species, respectively) and downy or powdery mildews (*Plasmopara* and *Oidium* plus *Erisyphe* species, respectively) are common grape pests [1]. Apart from associated economic losses and technological challenges for winemakers, pathogen products alter the chemical composition of the grapes, which affects the sensory properties of the resulting wine [2]. In the host plant, pathogenesis induces the production of specific defense-related molecules such as low-molecular-weight phytoalexins and pathogenesis-related (PR) proteins [3]. Chitinases, thaumatin-like proteins (TLPs) and lipid-transfer protein (LTP) are typical PR proteins in the juice and wine [4–6]. Other wine proteins originating from grapevine (*Vitis vinifera*) are, for example, invertase 1, β-1,3-glucanase, enzymes of carbohydrate metabolism, various glycoproteins, and proteoglycans [6]. Wine proteome also includes *Saccharomyces cerevisiae* proteins, which are released by yeast autolysis [7].

The amount of protein in wine is generally lower than that in juice, mainly due to proteolysis and denaturation of the grape proteins during fermentation, which is caused by proteases and changes in pH [7, 8]. The protein-level effects of pathogen infection of grapes [9, 10], grapevine leaves [11, 12],

Abbreviations: *ACN, acetonitrile; CHCA, α-cyano-4-hydroxycinnamic acid; ESI, electrospray ionization; FoA, formic acid; LC, liquid chromatography; LTP, lipid transfer protein; MALDI-TOF, matrix-assisted laser desorption/ionization time-of-flight; MS, mass spectrometry; MS/MS, tandem mass spectrometry; PR proteins, pathogenesis-related proteins; TFA, trifluoroacetic acid; TLP, thaumatin-like protein.*

*Address for correspondence: Prof. Marek Šebela, Department of Protein Biochemistry and Proteomics, Centre of the Region Haná for Biotechnological and Agricultural Research, Faculty of Science, Palacký University, Olomouc, Czech Republic. Tel. +420 585634927; e-mail: marek.sebela@upol.cz.

Additional supporting information may be found online in the Supporting Information section at the end of the article.

Received 4 September 2018; accepted 1 February 2019

DOI: 10.1002/bab.1736

Published online in Wiley Online Library (wileyonlinelibrary.com)

trunk [13], and cell cultures [14] have been studied. Processing of Botrytis-infected grapes yields juice, which is reduced in PR protein content due to proteolytic degradation by enzymes released from the fungus [7, 8]. In addition, fungal oxidases (e.g., laccase) can affect the organoleptic characteristics of wine such as color, taste, and aroma [1, 2]. The chemical composition of wine can also be modified by adding enzymes during the winemaking process [15–17]. An example is the application of β-glycosidases for the release of free terpenoids from their glycoside forms in the juice to enhance grape variety flavors [18].

A number of studies on wine have sought a connection between the protein content and haze formation [19]. Both temperature and pH were found to be important factors influencing the behavior of wine proteins. A combination of low pH and temperature over 40 °C accelerates the release of proteins from natural structures and leads to the formation of aggregates [20, 21]. The proportional content of PR proteins in grape juice increases during the maturation period [22] and the association with haze formation processes has been well documented [7, 8, 19]. Common methods for wine stabilization and clarification utilize bentonite or chitosan for removing positively charged molecules. Egg yolk, gelatin, and collagen are used for eliminating excess tannins and other negatively charged molecules and other applications include, for example, milk casein and polyvinylpolypyrrolidone [23]. On their release, yeast mannoproteins are also able to reduce the visible protein haze in white wine [24, 25]. The application of an acid protease for deproteinization during the winemaking process caused a significant loss of haze forming proteins in wine [26].

In this study, we analyzed the proteins in experimental Moravian wines characterized by instability and haze formation in bottles during storage. As these wines had been produced from grapes affected in part by a Botrytis infection and treated by bentonite, we were interested in differences in the protein composition compared with clear white wines including samples produced from totally botrytized grapes. Wine proteins were extracted, separated by gel electrophoresis, and after digestion, subjected to parallel identifications using nanoLC coupled either with matrix-assisted laser desorption/ionization (MALDI) or electrospray ionization tandem mass spectrometry (ESI MS/MS).

2. Materials and Methods

2.1. Wine samples

The experimental white wine (sample A) was produced from a combination of musts made of healthy grapes and grapes naturally affected by *B. cinerea* (20% of the latter). The grapes (Sauvignon Blanc variety) were harvested in the wine region of Mělčany (South Moravia, Czech Republic). The weather over the entire vegetative period was very warm and dry with the exception of one short, heavy rainfall at the end of the vegetation period. During the wine production, the grape mash was left to ripen (to release the aromatic compounds in the grape skins) for 15 H. Sulfur dioxide was then applied as potassium metabisulfite to achieve a free 50 mg L^{-1} concentration in the must. Dregs were removed by sedimentation and yeasts were inoculated. Ammonium sulfate was added as a nutrient for the yeasts. The fermentation process lasted 8 weeks. The resulting wine was characterized by instability, accompanied by haze formation, which could not be removed by the standard use of bentonite. For comparison, another sample (sample B) of the unstable Sauvignon Blanc white wine from the same year and place of origin was used but with a period of maturation longer by 1 year.

The experimental set was extended by reference white wines purchased in local shops: (1) sample C: Sauvignon Blanc, no haze, dry, 2016 (France); (2) sample D: Welschriesling, selection of botrytized grapes, no haze, sweet, 2015 (Horní Věstonice, South Moravia); (3) sample E: Welschriesling, late harvest, no haze, dry, 2015 (Perná, South Moravia); (4) sample F: Welschriesling, late harvest, no haze, dry, 2014 (Svatobořice-Mistřín, South Moravia). This collection of wines was intended to make up a non-haze botrytis Sauvignon wine as well as Welschriesling, which is most typical for a South Moravian terroir similar to that of samples A and B. No information was available on the possible bentonite fining of the purchased wines but it was very probable, an assumption that was important for valid comparison with samples A and B. Sample G was a nouveau non-hazy unfined wine produced in 2018 from grapes of the Irsai Oliver variety (Rajhradice, South Moravia; 8 weeks of fermentation). Finally, sample H was represented by a juice (150 mL) freshly pressed from 200 g of table grapes purchased in a local shop.

2.2. Chemicals

All chemicals used for sample processing and analyses were commercial products of either LC–MS quality (solvents for liquid chromatography coupled with mass spectrometry) or at least analytical purity grade. Special chemicals for MALDI-TOF mass spectrometry such as matrix compounds or peptide calibration standards were purchased from Bruker Daltonik (Bremen, Germany).

2.3. Basic wine characterization

Wine pH was determined using a standard pH meter calibrated with two reference buffers of pH 7.0 and 4.0. The turbidity of the analyzed wines was measured at 540 nm on a spectrophotometer and expressed in A_{540} values [27].

2.4. Protein extraction

A sample of 200 mL of the white wine A was filtered through a Whatman Grade 4 cellulose filter (pore size of 20–25 μm) at 4 °C to remove coarse solid particles and concentrated to a final volume of 10 mL on a rotary vacuum evaporator at 45 °C. The concentrate was filtered and its protein content precipitated by adding four volumes of chilled acetone (–20 °C) and incubating at –20 °C for 60 H. After precipitation, the sample was centrifuged (12,500*g*, 4 °C, 20 Min), the sediment was crushed by a glass rod and the acetone precipitation and

centrifugation were repeated. The collected sediment was then stored at –20 °C until use. The precipitated proteins were extracted into 200 μL of 2× Laemmli sample buffer containing 2-mercaptoethanol and heated at 100 °C for 5 Min. Finally, after centrifugation to remove insoluble particles, 20-μL aliquots of the extract were used for sample loading in SDS-PAGE.

Alternatively, another wine aliquot of 100 mL was filtered and dialyzed against 0.1 mol L^{-1} ammonium acetate buffer, pH 5.0, at 4 °C for 48 H; the cold buffer was exchanged every 16 H. The dialyzed sample was concentrated by ultrafiltration with a 10-kDa membrane filter down to a volume of 2 mL and stored frozen at –20 °C. Prior to SDS-PAGE, an aliquot of 500 μL of the concentrate was dried in a vacuum concentrator. It was then dissolved in 20 μL of the 2× Laemmli sample buffer with 2-mercaptoethanol, heated at 100 °C for 5 Min and centrifuged. This amount was then used for sample loading on polyacrylamide gels. The other samples (B–H) were processed only via this dialysis-plus-ultrafiltration procedure.

2.5. Protein assay and gel chromatography

The protein concentration of the wine samples was determined from triplicates on a spectrophotometer using the bicinchoninic acid assay [28]. Bovine serum albumin was used as a standard and the calibration amounts were between 5 and 50 μg. After ultrafiltration, the concentrated proteins from sample G were separated in 500 μL-aliquots by gel chromatography under native conditions using an ENrich SEC 70 column, 10 × 300 mm (Bio-Rad, Hercules, CA, USA). The column was attached to and operated with a BioLogic Duo-Flow medium pressure liquid chromatograph (Bio-Rad). The flow rate of the mobile phase (50 mmol L^{-1} ammonium acetate, pH 6.0) was 1 mL Min^{-1}. Protein fractions were collected, pooled, and concentrated by ultrafiltration using 10-kDa cut off centrifugal filters (Merck Millipore, Tullagreen-Carrigtwohill, Ireland). On evaporation of the buffer in a vacuum centrifuge, the proteins (50 μg; first dissolved in 50 μL of 25 mmol L^{-1} NH_4HCO_3) were in-solution digested by raffinose-modified trypsin [29] in a weight ratio of 1:20 after a denaturation step with urea (8 mol L^{-1}; 15 μL), reduction by dithiothreitol (55 mmol L^{-1}, 4 μL, 56 °C, 30 Min), alkylation by iodoacetamide in the dark (330 mmol L^{-1}, 4 μL, 30 Min), second reduction by dithiothreitol (55 mmol L^{-1}, 8 μL), and a final dilution to 200 μL by 25 mmol L^{-1} NH_4HCO_3.

2.6. SDS-PAGE and protein in-gel digestion

SDS-PAGE separation of wine proteins was performed using 10% running gels and 4% stacking gels [30] in a Mini-Protean unit (Bio-Rad). Electrophoresis was run at 130 V until the dye front reached the bottom of the gel slab. Proteins in gels were stained with Coomassie Brilliant Blue R-250 [31]; 5% (v/v) methanol with 7% (v/v) acetic acid was used for background destaining. The gels were finally rinsed with water and the sample lane divided by a lancet into 10–12 consecutive vertical parts ("fractions"). An in-gel digestion procedure followed [32]. In brief, the excised and chopped protein bands were destained by 100 mmol L^{-1} NH_4HCO_3/acetonitrile (ACN), 1:1, v/v, for 1 H. The solvent was then removed and the gel particles shrunk in neat ACN, reduced by 10 mmol L^{-1} dithiothreitol in 100 mmol L^{-1} NH_4HCO_3 at 56 °C for 30 Min, chilled on ice, shrunk in ACN, alkylated by 55 mmol L^{-1} iodoacetamide at laboratory temperature in the dark for 20 Min and washed by vortexing in 100 mmol L^{-1} NH_4HCO_3. After a final shrinking in ACN, the digestion step was conducted with raffinose-modified trypsin at 37 °C overnight. The trypsin solution with a concentration of 2 μmol L^{-1} was made in 50 mmol L^{-1} NH_4HCO_3 [29]. Peptides were extracted by adding 5% (v/v) formic acid (FoA)/ACN, 1:2, v/v, and recovered in a vacuum centrifuge. Finally, they were dissolved in 15 μL of 0.1% (v/v) trifluoroacetic acid (TFA), desalted using C-18 ZipTips (Merck Millipore) as instructed by the manufacturer, and reconstituted in 15 μL of 0.1% (v/v) TFA.

2.7. nanoLC–MALDI MS/MS analysis

The system used consisted of an ultrafleXtreme MALDI-TOF/TOF mass spectrometer equipped with a smartbeam-II laser of a repetition rate up to 2 kHz (Bruker Daltonik) and operated in offline coupling with a Dionex UltiMate3000 RSLCnano liquid chromatograph (Thermo Fisher Scientific, Germering, Germany) connected to a Proteineer fc II fraction collector (Bruker Daltonik). Eluted fractions were collected on MTP AnchorChip™ 800-384 MALDI targets (Bruker Daltonik).

Peptide sample aliquots (5 μL) were injected from the autosampler onto a Nano Trap precolumn (100 μm × 20 mm) for preconcentration and then separated on an analytical column (75 μm × 150 mm). The columns were packed with Acclaim PepMap100 C18 particles (5 and 2 μm, respectively; Thermo Fisher Scientific). The flow rate of the loading solvent was 10 μL Min^{-1}; both the preconcentration and separation on the analytical column were achieved in a run time of 70 Min at a constant flow rate of 300 nL Min^{-1}. The mobile phase A was 0.05% (v/v) TFA and mobile phase B was 80% (v/v) ACN/0.05% (v/v) TFA; the loading solvent was 2% (v/v) ACN/0.05% (v/v) TFA. The gradient was programmed as follows: 0 Min, 4% B; 7 Min, 4% B; 48 Min, 60% B; 51 Min, 96% B; 56 Min, 96% B; 59 Min, 4% B; 70 Min, 4% B. Before and after sample injection, 5 μL of 0.1% (v/v) TFA was picked up into the loading loop. The eluate was collected in 17-Sec fractions starting from 20 Min and spotted after mixing with a matrix solution (α-cyano-4-hydroxycinnamic acid, CHCA: 2.5 mg mL^{-1} in 90% v/v ACN containing 0.1% v/v TFA and 1 mM diammonium hydrogen phosphate) onto an AnchorChip 800-384 target plate, 120 fractions of each sample were automatically deposited onto the target plate by fraction collector. Peptide Calibration Standard II (Bruker) with CHCA matrix (in 80% v/v ACN but with the same additives) was applied manually by the dried-droplet technique. The chromatograph and spotter were controlled by HyStar 3.2 (Bruker Daltonik). The mass spectrometer was controlled by flexControl 3.4 for acquisition, flexAnalysis 3.4 for spectra processing and WarpLC 1.3 for automatic measurement of nanoLC–MALDI fractions (all software by Bruker Daltonik). MS spectra were acquired in automatic mode with the laser firing

rate set at 2,000 Hz and summed over 2,500 satisfactory shots. In MS/MS mode, the following acquisition method settings were applied: primary choice mass range (of precursors): 800–3,000, number of precursor masses: 10; peak intensity: >800; peak quality factor: >30; signal/noise: >7; FAST minimal fragment mass: 250; LIFT: measure fragments only.

2.8. nanoLC–ESI MS/MS analysis

Aliquots (5 μL) of the desalted peptide samples in 0.1% TFA were additionally separated by means of the same runs on Dionex UltiMate3000 RSLCnano liquid chromatograph but coupled in this case to an amaZon speed ETD ion trap equipped with a CaptiveSpray ion source (Bruker Daltonik). The mobile phase A was 0.4% (v/v) FoA and mobile phase B was 90% (v/v) ACN/0.4% (v/v) FoA; the loading solvent was 2% (v/v) FoA. The scan speed was 8,100 u Sec^{-1} for both MS and MS/MS; acquisition was performed with collision-induced fragmentation of precursors (helium as a collision gas). The mass spectrometer was controlled by trapControl 7.2 and HyStar 3.2, data were processed by DataAnalysis 4.2 (all software by Bruker Daltonik) and stored as MGF-formatted files.

2.9. Bioinformatic analysis

MS and MS/MS data from nanoLC–MALDI experiments processed by flexAnalysis 3.4 (Bruker Daltonik) were uploaded to ProteinScape 3.1 (Bruker Daltonik) and searched via Mascot Server 2.4 (Matrix Science, London, UK) against a custom database containing protein sequences for *Botrytis cinerea* (45,457 items), *S. cerevisiae* (171,837 items), and *V. vinifera* (92,565 items), all downloaded from the NCBInr database, plus sequences of common protein contaminants. The MGF-formatted files from the ion trap were similarly analyzed. The search parameters included no taxonomy, a mass tolerance of ±25 ppm for precursors (±100 ppm for the ion trap data) and ±0.5 Da for fragments; semi-trypsin was set as an enzyme with two missed cleavages allowed. Carbamidomethylation of cysteine was a fixed modification and Met oxidation was a variable modification.

The SignalP 4.1 server was used to evaluate whether the identified proteins are secreted or intracellular [33]. Possible functions for yet unknown proteins were predicted using NCBI Blast [34] and EBI InterProScan (http://www.ebi.ac.uk/interpro/search/sequence-search) sequence search tools [35].

3. Results and Discussion

3.1. Basic characterization of wine and juice samples

Wine proteins from sample A were obtained by two methods: using direct acetone precipitation or by ultrafiltration of its dialyzate. For samples B–H, only the second procedure was used as it was found to be optimal (see further). A low pH value of 2.2 was determined for wine A which contained a high quantity of organic acids, recognized during the initial filtration when white acid crystals were collected on a cellulose filter. The protein concentration in the filtrate of sample A was 2.12 ± 0.13 g L^{-1}, but this value was obviously overestimated. The protein content of the original sample recalculated from values measured with a dissolved precipitate was only 0.28 ± 0.03 g L^{-1}. This difference may be attributed to the confounding effects of non-proteinaceous components of the wine. The other samples were characterized by pH values of 3.3 (B), 3.4 (C), 3.0 (D), 3.3 (E), 3.4 (F), 3.3 (G), and 3.2 (H). The protein content after dialysis was 0.27 ± 0.01 (B), 0.22 ± 0.01 (C), 0.24 ± 0.01 (D), 0.27 ± 0.02 (E), and 0.29 ± 0.02 g L^{-1} (F). All numbers refer to residual proteins after bentonite fining. This sorbent is well known for not equally removing all wine proteins and, as a cation exchanger, it also binds other wine components that compete with the protein binding [7]. The unfined nouveau wine (G) and unfermented juice (H) showed a lower protein content of 0.13 and 0.10 g L^{-1} (±0.01 g L^{-1}).

The protein concentration determined after purification by precipitation or after the removal of interfering compounds by dialysis, appears within the normal range (up to 500 mg L^{-1}) [27]. Higher concentration of gluconic acid and lowered ethanol production during fermentation, necessitating a longer yeast fermentation step in consequence, are characteristic of invasion of grape berries by *B. cinerea* [36]. Grape peroxidases play an important role in the oxidation metabolism of phenols during grape maturation. Efficient endogenous pectinase activity is necessary for the degradation of grape pectin, which facilitates the clarification of the wine. Sulfur dioxide (SO_2) has a negative effect on the activity of these enzymes and this deters its use in inhibiting the growth of microorganisms in must [18]. The application of SO_2 (as potassium metabisulfite) at the above-mentioned level of 50 mg L^{-1} has no inhibitory effect on proteases originating from *B. cinerea* in either must or wine [37]. The enzyme activities of phenol oxidases are only slightly reduced under these conditions [38]. The measured turbidity of the hazy wines was high, average values ($n = 5$) at 540 nm of 0.391 and 0.362 were determined for samples A and B, respectively, whereas the non-hazy wines C–F provided substantially lower values of 0.011–0.023. Only for sample G—unfined wine—was a value of 0.092 measured.

3.2. Gel electrophoresis of wine proteins

The wine proteins recovered after the precipitation or ultrafiltration procedures with sample A were subjected to SDS-PAGE for separation under denaturing conditions according to the molecular mass (Fig. 1). In contrast to the acetone precipitation, the use of dialysis prior to protein extraction resulted in an undisturbed protein band pattern. For this reason, the latter protocol was considered more reliable and applied to all other samples. The resulting staining patterns of the gels for the two protocols showed a few similar protein zones particularly in areas corresponding to molecular masses above 94 kDa or around 66 kDa but differences for masses of 66–94 kDa and below 45 kDa (Fig. 1). Proteins with molecular masses of around 60–65 kDa have known resistance to common bentonite treatment and thus they remain in protein-stabilized wines [8].

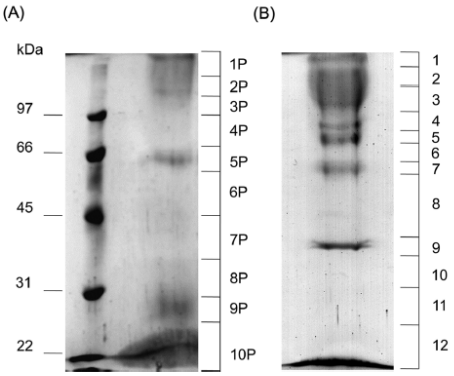

FIG. 1 *SDS-PAGE separation of proteins from the hazy white wine (sample A). Photographs show Coomassie-stained 10% resolving gels run after (A) vacuum evaporation-based or (B) dialysis and ultrafiltration-based protein extraction protocols. The left-side numbers (molecular mass values in kDa) refer to the protein marker used (low range standards, Cat. No. 161–0304; Bio-Rad); the corresponding stained bands are visible in panel (A). The right-side numbers 1P-10P (P stands for "precipitate") and 1–12 indicate the extension of the sliced gel fractions subjected to the process of in-gel digestion of proteins with modified trypsin. Sample loads are specified in section Materials and Methods.*

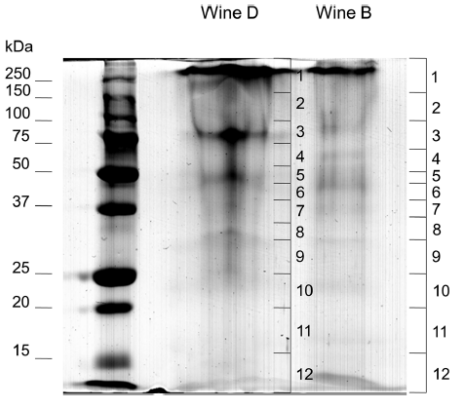

FIG. 2 *SDS-PAGE separation of wine proteins (samples B and D). This photograph shows a Coomassie-stained 10% resolving gel with proteins obtained from the hazy white wine B (Sauvignon Blanc) and botrytized white wine D (Welschriesling) as indicated at the respective separation lanes. The left-side numbers (molecular mass values in kDa) refer to the protein marker separated in the left lane (Precision Plus Protein Standards, Cat. No. 161–0373; Bio-Rad). The right-side numbers 1–12 indicate the extension of the sliced gel fractions subjected to the process of in-gel digestion of proteins with modified trypsin. Sample loads are specified in section Materials and Methods.*

No straightforward comparison of our results with those obtained previously for clear white wines of standard quality is possible. For instance, the lack of major PR-proteins bands typical for Sauvignon Blanc grape variety was registered in the area between 20 and 30 kDa (obviously because of the bentonite fining and/or enzyme degradation related to the presence of Botrytis) and this contrasts with the results of Esteruelas et al. [39]. The separation of proteins from the hazy wine B and non-hazy botrytized wine D is documented in Fig. 2. In the case of sample D, a disturbance of the visualized protein bands could not be overcome by preceding dialysis and this probably reflects the presence of largely glycosylated proteins such as mannosidase and glycoside hydrolase (see Section 3.4.). Again, a majority of the Coomassie-stained protein bands appeared at positions corresponding to molecular masses above 50 kDa. Conversely, both the unfined wine (G) and grape juice (H) contained a large quantity of PR proteins (Fig. 3).

Horizontal gel slices from sample lanes representing individual fractions were then processed for in-gel digestion prior to nanoLC–MS/MS. This strategy was preferred to those with an in-solution digestion given the possibility of combining the protein solubilizing and dissociation power of Laemmli sample buffer and, resolving power of SDS-PAGE [30, 40].

3.3. Identification of proteins in the hazy wine

Protein identification for the hazy sample A were performed after in-gel digestion and nanoLC separations of peptides from the digests. A total of 28 proteins were identified by searching the obtained MS/MS data against the custom sequence database with grape, yeast and Botrytis proteins. Of these, nine were grape proteins (Table 1), seven originating in Botrytis (Table 2), and 12 were from the yeast (Table 3). More details on the identified proteins are provided in Supplementary Table S1. Supplementary Fig. S1 shows an example of the acquired peptide MS/MS spectrum. Most of the identified yeast proteins came from gel slices nos. 1, 2, and 3. The appearance at the top of the gel referring to higher molecular masses suggests glycosylation. The prediction server SignalP 4.1 revealed the presence of signal peptide sequences for an extracellular localization. Four of the seven identified Botrytis proteins were extracellular hydrolases secreted to degrade the grape structures. Several typical grape proteins in wine were identified including, for example, a vacuolar invertase and other enzymes (hydrolases and oxidoreductases) plus a TLP and LTP. The vacuolar invertase (gi: 1839578) was found in white as well as red wine [41, 42]. The sequence homology of this enzyme with another

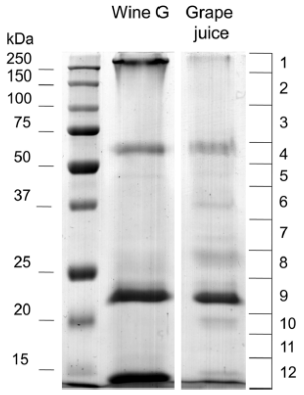

FIG. 3 *SDS-PAGE separation of wine and juice proteins (samples G and H). This photograph shows a Coomassie-stained 10% resolving gel with proteins obtained from the nouveau white wine G (Irsai Oliver), on the left, and fresh grape juice H, on the right. The left-side numbers (molecular mass values in kDa) refer to the protein marker (Precision Plus Protein Standards, Cat. No. 161–0373; Bio-Rad). The right-side numbers 1–12 indicate the extension of the sliced gel fractions subjected to the process of in-gel digestion of proteins with modified trypsin. Sample loads are specified in section Materials and Methods.*

identified invertase protein (gi: 225466093) is 96.6%. Plant invertases convert sucrose to glucose and fructose. A reduction in the number of grape invertase isoforms was observed in a botrytized wine [41]. Plant LTPs are characterized as small PR-14 family glycoproteins originating from the grape skin [42]. High tolerance to *B. cinerea* was achieved after exogenous application of LTP4 and jasmonic acid on grapevine plantlets [43]. TLPs and plant chitinases are the major proteins present in white wines [44]. The antifungal effects of grape TLPs are not clear [7]. The content of these PR-proteins in grapes may be induced on infection but the increased level of plant defense proteins may not be detected because of the activity of mold proteolytic enzymes [44]. The fragment of an unnamed plant protein (gi: 297740510; slice no.2) is predicted to be an active form of a glycosylated thiol protease. The formation of plant cysteine proteases could be induced by mold products in a plant defense reaction as reviewed previously [45]. To the best of our knowledge, only one grape cysteine protease has been characterized to date [46].

Yeasts respond to chemical and physical environmental changes that occur during wine fermentation by adaptation of their cell wall structures. The identified Wsc4 protein (gi: 768812869; the sequence contains seven potential *N*-glycosylation sites), may mediate intracellular responses to environmental stress [47]. The transglycosidase Crh1 protein (gi: 323354858) plays a key role in the cell wall construction [48]. Yeast Tir4 mannoprotein (gi: 323352383) found in gel slice no. 1 is involved in anaerobic adaptation [49]. A positive effect of heavily mannosylated proteins against haze formation in white wines has been described [24]. The production of Ygp1 protein (gi: 323346853), functionally annotated as an extracellular asparaginase, can be assumed at an advanced stage of fermentation after consumption of the supplied nitrogen. The Plb2 protein (gi: 323336225) is involved in the formation of ethyl esters that contribute to wine flavor [50]. Also, the identified peroxidase (gi: 359478431) may degrade the anthocyanins in the wine and change its sensory characteristics [51]. This enzyme can also be formed during heat stress [52].

Laccase 2 (gi: 15022489) was identified as a marker of the Botrytis invasion. Laccase oxidizes wine phenols to quinones, which may then interact with other organic compounds and proteins [53]. For laccase activity, specific glucans produced by Botrytis are necessary [54]. Additionally, these glucans trigger increase in the formation of acetic acid during fermentation [55]. The other identified mold enzymes, disrupt plant cell walls during the pathogenesis. Glycoside hydrolase (gi: 347835718) with a relatively high molecular mass of 109 kDa was detected in gel slice no.2. The identified hypothetical protein BC1G_09079 (gi: 154304407) was found to be a beta-1,3-glucanase (slice no. 8). A precursor of endo-beta-1,4-glucanase (gi: 48093959) was assigned in the slice no. 9. These three enzymes are assumed to be extracellular.

For sample B, 19 proteins were identified, typically from the yeast and Botrytis. Five proteins originated from grapevine (Supplementary Table S1). The identifications were consistent with sample A in 12 items including invertase, cysteine protease and thaumatin from grapevine, several Botrytis enzymes (glycoside hydrolase, laccase, and serine protease) and many yeast proteins.

3.4. Identification of proteins in other wine samples

The non-hazy botrytized wine D apparently did not contain yeast proteins and the vast majority of its protein components originated naturally from Botrytis. Altogether, 18 identifications were achieved (Supplementary Table S2). In comparison with samples A and B, the botrytized wine D provided a substantially reduced number of proteins with more than 5% of proline residues in their sequence (Fig. 4 and Supplementary Tables S1 and S2). Instead, it contained a higher portion of different hydrolytic enzymes. The non-hazy standard white wines C, E, and F were found to contain grapevine, yeast, and Botrytis proteins and the number of identifications was between 13 and 17 using nanoLC–MALDI (Supplementary Table S3). Proteases were abundant among them, which indicates a high level of degradation of proteolysis-susceptible components. Proteins high in proline were represented in the lists (including TLPs), but fewer than the hazy wine samples (Fig. 5). Interestingly, of the other proteins identified in sample F, hyphally regulated cell wall mannoprotein (gi: 323309306)

TABLE 1 *A list of* Vitis vinifera *proteins identified in the hazy Sauvignon Blanc wine (sample A)*

Protein number	*Ionization technique*	*Gel slice number*	*Organism*	*Accession number (NCBInr)*	*Protein function*	*Signal peptide prediction (D score values provided by the Signal P 4.1 server)*	*MW (kDa)*	*pI*	*Score*	*Number of sequenced peptides*	*Sequence coverage (%)*	*Proline content (%)*	*RMS90 (ppm)*
1	MALDI	1	*V. vinifera*	gi|731438691	Lipid transfer	0.757	14.7	4.2	95.1	1	9.7	8.5	2.51
	ESI	2							97.5	2	9.7		78.61
	ESI	2P		gi|147834849		0.773	14.8	4.2	172.7	3	17.2	8.8	48.82
2	MALDI	2	*V. vinifera*	gi|297740510	Cysteine protease	0.106	41.1	4.2	1539.9	22	25.7	9.8	3.91
	ESI								1236.0	20	25.7		56.49
	ESI	2P							957.6	15	20.4		50.24
3	MALDI	2	*V. vinifera*	gi|225445553	Stellacyanin, electron transfer	0.836	30.7	5.1	408.6	6	12.8	6.6	3.00
	ESI								407.7	6	17.1		48.50
	ESI	3P							407.6	6	17.1		56.58
4	MALDI	7	*V. vinifera*	gi|225466093	Invertase	0.122	72.0	4.6	993.6	15	15.6	6.5	5.50
	ESI			gi|1839578		0.124	71.5		972.9	16	17.1	6.2	46.11
	ESI	5P							893.9	13	19.3		43.10
5	MALDI	8	*V. vinifera*	gi|359478431	Secreted peroxidase	0.764	36.5	4.4	162.4	3	7.9	3.8	2.55
	ESI								179.4	3	10.8		63.47
6	ESI	8P	*V. vinifera*	gi|2306813	Chitinase	0.928	27.5	5.4	362.5	6	15.9	2.0	66.90
7	ESI	9P	*V. vinifera*	gi|520729528	Thaumatin-like protein	0.167	21.3	4.8	206.6	4	18.7	7.6	64.99
8	ESI	9P	*V. vinifera*	gi|147785114	Thaumatin-like protein	0.784	23.9	4.6	632.7	11	41.3	4.5	53.21
9	MALDI	12	*V. vinifera*	gi|296084197	Invertase (fragment)	0.127	60.5	4.4	822.3	12	12.5	5.7	2.53
	ESI								710.8	11	12.9		58.76

RMS90 stands for root mean square value.

TABLE 2

A list of Botrytis cinerea *proteins identified in the hazy Sauvignon Blanc wine (sample A)*

Protein number	*Ionization technique*	*Gel slice number*	*Organism*	*Accession number (NCBInr)*	*Protein function*	*Signal peptide prediction (D score values provided by the Signal P 4.1 server)*	*MW (kDa)*	*pI*	*Score*	*Number of sequenced peptides*	*Sequence coverage (%)*	*Proline content (%)*	*RMS90 (ppm)*
1	MALDI	2	*B. cinerea*	gi|347835718	Glycoside hydrolase	0.733	109.3	4.5	467.8	9	9.7	5.7	4.14
	ESI								347.5	7	9.2		53.75
2	MALDI	3	*B. cinerea*	gi|347833309	Serine carboxypeptidase	0.779	60.8	4.7	395.5	5	12.3	7.7	4.65
	ESI								214.3	5	11.9		56.52
3	ESI	3P	*B. cinerea*	gi|154291355	Extracellular membrane protein	0.879	20.2	4.3	137.9	2	12.6	8.1	33.06
4	MALDI	5	*B. cinerea*	gi|154300984	Cell wall organisation protein	0.770	41.1	4.3	190.8	4	12.7	2.9	6.27
	ESI								421.5	7	12.4		60.03
5	MALDI	5	*B. cinerea*	gi|15022489	Laccase	0.703	63.4	4.5	860.2	15	22.2	5.2	4.78
	ESI								1257.5	20	25.3		59.68
	ESI	4P							125.2	2	3.8		46.51
6	MALDI	8	*B. cinerea*	gi|154304407	Beta-1,3-glucanase	0.667	44.1	4.3	72.2	2	6.6	3.2	1.59
	ESI	8							122.8	2	5.7		67.04
7	MALDI	10	*B. cinerea*	gi|48093959	Cellulase	0.764	44.2	4.2	156.3	2	9.0	3.2	10.66
	ESI	9							133.7	3	5.7		79.92

RMS90 stands for root mean square value.

TABLE 3 *A list of* Saccharomyces cerevisiae *proteins identified in the hazy Sauvignon Blanc wine (sample A)*

Protein number	*Ionization technique*	*Gel slice number*	*Organism*	*Accession number (NCBInr)*	*Protein function*	*Signal peptide prediction (D score values provided by the Signal P 4.1 server)*	*MW (kDa)*	*pI*	*Score*	*Number of sequenced peptides*	*Sequence coverage (%)*	*Proline content (%)*	*RMS90 (ppm)*
1	MALDI	1	*S. cerevisiae*	gi|323346853	Asparaginase	0.818	37.3	5.3	1354.0	15	28.0	5.1	3.52
	ESI			gi|323335922					1194.4	16	25.4	5.1	74.52
	ESI	1P							956.3	13	24.6		60.29
2	MALDI	1	*S. cerevisiae*	gi|323331721	Stress-induced protein	0.712	16.4	3.9	325.1	4	18.5	4.4	6.18
	ESI								231.5	4	19.7		74.70
	ESI	1P		gi|323352383		0.713	41.9	7.2	226.1	5	7.4	13.1	48.13
3	ESI	1P	*S. cerevisiae*	gi|323307336	Yeast mannoprotein	0.652	69.0	6.2	270.0	4	3.8	2.7	43.63
4	MALDI	1	*S. cerevisiae*	gi|207342449	Phospholipase B	0.462	59.8	4.4	1361.9	19	29.8	4.5	3.35
	ESI	2		gi|323336225			75.4	4.5	566.3	10	16.6	4.1	64.63
	ESI	2P		gi|207342449			59.8	4.4	226.5	5	10.4	4.5	74.29
5	MALDI	2	*S. cerevisiae*	gi|768812869	Cell wall integrity stress response protein	0.803	63.7	6.0	104.2	1	2.8	5.7	1.02
	ESI								95.1	1	2.8		80.60
6	MALDI	2	*S. cerevisiae*	gi|190406234	Stress-induced cell wall mannoprotein	0.803	24.3	4.3	431.0	4	11.4	1.8	7.35
	ESI	3							420.3	5	11.4		57.28
	ESI	4P							247.4	3	11.4		60.29

(*Continued*)

TABLE 3 *Continued*

Protein number	Ionization technique	Gel slice number	Organism	Accession number (NCBInr)	Protein function	Signal peptide prediction (D score values provided by the Signal P 4.1 server)	MW (kDa)	pI	Score	Number of sequenced peptides	Sequence coverage (%)	Proline content (%)	RMS90 (ppm)
7	MALDI	3	*S. cerevisiae*	gi|207344997	Transglycosidase	0.699	51.3	4.4	535.8	10	17.7	2.8	5.15
	ESI			gi|323354858			45.6	4.5	410.5	6	13.4	3.2	62.97
	ESI	3P							671.6	13	21.0		51.03
8	MALDI	3	*S. cerevisiae*	gi|190408747	Histidine phosphatase	0.456	52.8	4.4	555.2	8	20.3	3.1	5.47
	ESI			gi|762051192		0.575	52.7	4.5	513.6	8	20.3	3.1	55.74
	ESI	3P							128.2	2	7.1		57.99
9	MALDI	3	*S. cerevisiae*	gi|323356058	Histidine phosphatase	0.495	52.8	4.7	494.4	9	15.6	2.9	2.46
	ESI			gi|323310064			47.3	4.6	515.9	12	23.3	3.2	71.91
10	ESI	4P	*S. cerevisiae*	gi|207342034	Beta-1,3-glucanosyltransferase	0.146	48.3	4.4	128.0	2	5.5	2.4	14.22
11	ESI	6P	*S. cerevisiae*	gi|767173549	Cell wall protein	0.773	24.2	4.5	121.5	3	18.0	1.8	19.18
12	MALDI	9	*S. cerevisiae*	gi|207344015	Cell wall-associated protein	0.712	34.2	4.2	131.2	1	5.3	3.8	2.78
	ESI								129.8	2	5.3		53.02

RMS90 stands for root mean square value.

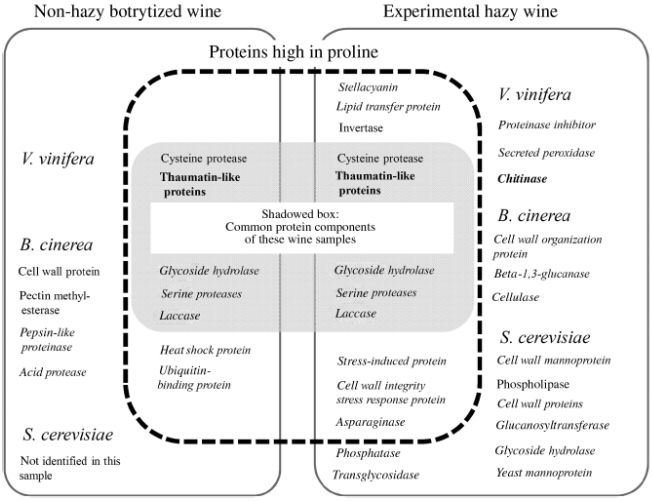

FIG. 4 *Proteins identified in the analyzed non-hazy botrytized white wine and experimental hazy white wine. A diagram is shown, which summarizes all identifications and points out proteins high in proline in the samples A (Sauvignon Blanc) and D (Welschriesling). Proteins predicted as extracellular are highlighted by italicized names. Typical haze-active proteins are highlighted in bold. For details see Supplementary Tables S1 and S2.*

had eight potential glycosylation sites, six of which were predicted to be occupied with a very high probability. Its mannosylation may contribute to the processes preventing haze formation: yeast mannoproteins seem to compete with haze-active proteins for wine component(s) required for the formation of large insoluble protein aggregates [24].

The nouveau white wine (sample G) and grape juice (sample H) showed a high natural content of invertase and TLPs, which could be deduced from the strong intensity of the corresponding protein bands on polyacrylamide gels (Fig. 3; fractions 4 and 9, respectively) as well as from the number of sequenced peptides in nanoLC–ESI–MS/MS analysis. The samples also contained other PR-proteins such as chitinase and glucanase (Supplementary Table S4). Fractions containing cysteine protease, invertase, and TLPs were obtained by gel chromatography of the dialyzed and ultrafiltrated sample G (Fig. 6) and applied in the heat stability test according to Marangon et al. [27]. A stable commercial white wine (Welschriesling, 2016) with a protein content of 58 mg L^{-1} had an absorbance value of 0.015 at 540 nm. After heating at 50 °C for 3 H and cooling on ice for 2 H, this increased to 0.016, which is well below the difference of >0.02 considered the limit for instability [27]. By adding the cysteine protease, invertase and TLPs protein fractions in a concentration of 50 mg mL^{-1}, the resulting A_{540} was shifted to values of 0.018, 0.018, and 0.020. The difference values towards the control of 0.002, 0.002, and 0.004, respectively, were comparable (in the same milli absorbance units) with previous heat test data measured with chitinase and TLPs [27].

3.5. The role of proteins in wine haze formation

The process of haze formation and the significance of proteins, sulfate ions, and organic compounds in white wine have recently been reviewed [19]. For the studied hazy wine, a mild desiccation of the grapes during ripening in dry summer resulted in the relatively high measured protein content. The growing conditions of the grapes partially affected by Botrytis were then reflected in the composition of the identified proteins. The low pH in sample A (a standard pH value for white wines is around 3–4 [56], would itself induce protein aggregation and precipitation. Various compounds produced by Botrytis such as high-molecular-weight glucans could reduce the value of bentonite for wine refinement. We confirmed this in a trial experiment and the subsequent use of bentonite suspensions for protein extraction [57], which resulted in missing protein bands on gels (not shown).

The formation of haze is not predictable based on the total protein content [44]. There are several factors which have to be considered for a discussion of the protein instability of the analyzed hazy wine after ineffective bentonite fining. First, the most typical cause of haze in beer, wine, and fruit juices is protein–polyphenol interactions [58]. Second, PR proteins such as TLPs and chitinases have been implicated in the haze formation induced at elevated temperatures (over 30 °C) that

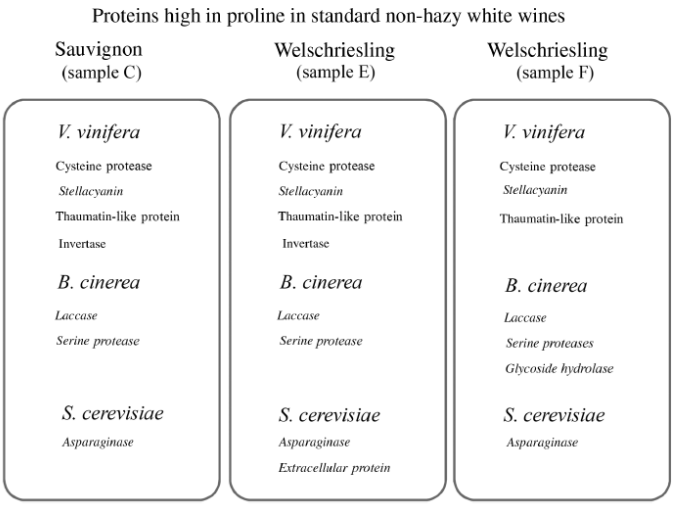

FIG. 5 *Proteins high in their proline content from standard non-hazy white wines. A diagram is shown, which summarizes proteins high in proline identified in the samples C, E, and F (standard non-hazy Sauvignon Blanc or Welschriesling white wines). Proteins predicted as extracellular are highlighted by italicized names. For details see Supplementary Table S3.*

can occur during storage and transportation [27, 59]. Third, TLPs and chitinases are thermally unstable and prone to aggregation and precipitation [27]. Finally, it is important to note that wine instability results from a complex interplay between proteins, chemical and physical factors.

The haze-forming proteins are similar in wines vinified from different grapevine varieties. They are stable in the acidic pH of wine and show proteolytic resistance [56]. During the production of beer and wine, both proteins and polyphenols are extracted and their nature, concentrations, and mutual ratios may combine to yield a haze. In beer, the molecular principle of haze formation resides in the binding of polyphenols to proline-rich barley storage proteins (hordeins), which results in visible aggregates known as a chill-haze [60]. In wine, haze-active phenolic compounds, polysaccharides, and sulfate are critical. But the important role of proteins that survive the winemaking process particularly chitinases has also been demonstrated [27]. The ratio between polyphenols and proline-rich proteins is critical for the size of aggregates in beer [58]. Haze formation in wine depends on the size of the phenolic compounds present: compared with small phenolics, a lower quantity of high-molecular-weight polyphenols is enough to form visible aggregates with wine proteins. After mold invasion, more than 50 % of polyphenols originating from the skin of Merlot variety grapes can be degraded [61]. Nevertheless, botrytized white wines are characterized by higher levels of polyphenolic compounds than standard wines [62]. Thus, we could expect the polyphenol content in the hazy wine analyzed, to be changed by the action of gray mold and that this could contribute to haze formation.

PR proteins were identified in samples A and B. This could partially answer the question of the origin of the instability despite the bentonite fining, but they were obviously much less represented than in the juice or nouveau wine (Fig. 1 versus Fig. 3). In the presence of Botrytis-produced proteolytic enzymes, these proteins had to be effectively degraded [26]. This has clearly been demonstrated by the protein profile of the botrytized wine D, where grapevine proteins constituted only a minor component compared with the prevailing presence of extracellular Botrytis proteins. For this reason, other ways of protein haze formation have to be considered. Interestingly, in looking at the amino acid composition of all identified proteins (i.e., including also those from the yeast and Botrytis), we discovered that half of them contained more than 5% of proline in their sequences (Tables 1–3 and Supplementary Table S1). The average proline content of proteins in the UniProt/Swiss-Prot database is lower than 5% [63]. Due to the higher content of proline, the above-mentioned proteins must be more resistant to proteolysis and can bind polyphenols. The grape TLP (gi: 520729528) contains 7.6% of Pro in its sequence. The high proline representation in TLPs may contribute to their physical tolerance and refolding ability [64]. Interestingly, certain proline-rich proteins increase in grapes at the onset of ripening [65]. *V. vinifera* cysteine protease (gi: 297740510) differs from

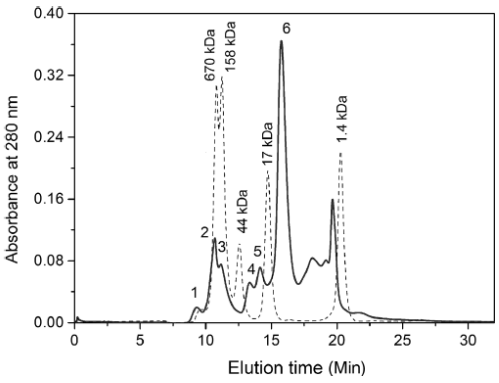

FIG. 6 *Gel chromatography of wine proteins. Wine sample G proteins were dialyzed, concentrated by ultrafiltration, and separated by gel permeation chromatography on ENrich SEC 70 column, 10 × 300 mm (Bio-Rad). The mobile phase was 50 mmol L^{-1} ammonium acetate; the flow rate was 1 mL Min^{-1}. The sample chromatogram is highlighted in red, whereas the separation of protein standards (Cat. No. 151–1901; Bio-Rad) is shown by a dashed line with the indicated molecular mass values. The collected protein fractions are labeled with Arabic numerals and contained as major components: 1, yeast asparaginase (Ygp1); 2, cysteine protease; 3, invertase; 4, glucanase; 5, TLPs; and 6, chitinase.*

the other proteins with a high proline content by the presence of two proline repetitions in its sequence (residues 243–250, 252–258) plus a PPPP segment (260–263). This is real proline-rich protein in the true sense of the word resembling the structure of polyvinylpyrrolidone, a polyphenol precipitant, by the accumulated proline residues.

The grape chitinase (gi: 2306813) contains only 2.1% of Pro and the described lower thermal and proteolytic resistance compared with those of plant TLPs [27] is consistent with this observation. Conversely, there is high proline content in grape invertase (gi: 225466093; gi: 1839578; above 6%), which has been assigned to haze-inactive proteins [26]. This group also includes the identified yeast mannoproteins or cell wall glycoproteins [26] such as Tir4, Cwp1, and Hpf1 (see in Supplementary Table S1). Invertase, because of its high thermal stability, should not participate in the haze formation under normal conditions [27], but this might change owing to the presence of yeast and Botrytis products including proteins. We attempted to demonstrate that the separated fractions with cysteine protease or invertase might contribute to the haze under model conditions of the heat stability test. Although their effect is less evident than that of TLPs, it is not insignificant.

It has already been shown that bentonite does not have full ability to remove proteins from wine prior to bottling. In order to minimize the risk of haze formation, the development of other technologies for wine deproteinization is paramount, for example, with the involvement of a potent proteolysis [26], in addition to keeping optimal temperatures during transport and storage of bottled wine.

4. Conclusions

We demonstrated and discussed a number of biochemical factors that all contributed to the formation of haze in the white wine produced from grapes partially damaged by *B. cinerea*: (1) low pH and presence of compounds related to Botrytis infection; (2) the presence of grape TLPs and chitinase known as haze-active proteins; (3) the presence of other proteins with a high proline content, which may interact with phenolic compounds and contribute to the haze. The main value of this study is explication of the role of such proteins in the propensity of white wine to turbidity suggesting a direction for future research of the wine haze phenomenon.

5. Acknowledgements

This work was supported by grant no. LO1204 from the Ministry of Education, Youth and Sports, Czech Republic (the National Program of Sustainability I). Dr. Alexander Oulton is thanked for critical reading the manuscript.

The authors declare no conflict of interest.

6. References

[1] Jackson, R. S. (2008) Wine Science, Principles and Applications, 3rd ed., Academic Press, New York.
[2] Li, H., Guo, A., and Wang, H. (2008) Food Chem. 108, 1–13.
[3] Enoki, S., and Suzuki, S., in Morata, A., Loira, I., Eds. (2016) Grape and Wine Biotechnology. pp. 43–57, IntechOpen, London.
[4] Marangon, M., Van Sluyter, S. C., Haynes, P. A., and Waters, E. J. (2009) J. Agric. Food Chem. 57, 4415–4425.
[5] Van Sluyter, S. C., Marangon, M., Stranks, S. D., Neilson, K. A., Haynes, P. A., Hayasaka, Y., Menz, R. I., and Waters, E. J. (2009) J. Agric. Food Chem. 57, 11376–11382.
[6] Giribaldi, M., and Giuffrida, M.G. (2010) J. Proteomics 73, 1647–1655.
[7] Ferreira, R. B., Piçarra-Pereira, M. A., Monteiro, S., Loureiro, V. B., and Teixeira, A. R. (2001) Trends Food Sci. Technol. 12, 230–239.
[8] Waters, E. J., and Colby, C. B., in Moreno-Arribas, M. V., Polo, M. C., Eds. (2009) Wine Chemistry and Biochemistry. pp. 213–230, Springer.
[9] Lorenzini, M., Millioni, R., Franchin, C., Zapparoli, G., Arrigoni, G., and Simonato, B. (2015) Food Chem. 179, 170–174.
[10] Lorenzini, M., Mainente, F, Zapparoli, G., Cecconi, D., and Simonato, B. (2016) Food Chem. 199, 639–647.
[11] Marsh, E., Alvarez, S., Hicks, L. M., Barbazuk, W. B., Qiu, W., Kovacs, L., and Schachtman, D. (2010) Proteomics 10, 2057–2064.
[12] Milli, A., Cecconi, D., Bortesi, L., Persi, A., Rinalducci, S., Zamboni, A., Zoccatelli, G., Lovato, A., Zolla, L., and Polverari, A. (2012) J. Proteomics 75, 1284–1302.
[13] Spagnolo, A., Magnin-Robert, M., Alayi, T. D., Cilindre, C., Mercier, L., Schaeffer-Reiss, C., Van Dorsselaer, A., Clément, C., and Fontaine, F. (2012) J. Proteome Res. 11, 461–475.

[14] Dadakova, K., Havelkova, M., Kurkova, B., Tlolkova, I., Kasparovsky, T., Zdrahal, Z., and Lochman, J. (2015) J. Proteomics 119, 143–153.
[15] Gueguen, Y., Chemardin, P., Pien, S., Arnaud, A., and Galzy, P. (1997) J. Biotechnol. 55, 151–156.
[16] Martino, A., Schiraldi, C., Di Lazzaro, A., Fiume, I., Spagna, G., Pifferi, P. G., and De Rosa, M. (2000) Process Biochem. 36, 93–102.
[17] Younes, B., Cilindre, C., Jeandet, P., and Vasserot, Y. (2013) Food Res. Int. 54, 1298–1301.
[18] Van Rensburg, P., and Pretorius, I. S. (2000) S. Afr. J. Enol. Vitic. 21, 52–73.
[19] Van Sluyter, S. C., McRae, J. M, Falconer, R. J., Smith, P. A., Bacic, A., Waters, E. J., and Marangon, M. (2015) J. Agric. Food Chem. 63, 4020–4030.
[20] Dufrechou, M., Sauvage, F. X., Bach, B., and Vernhet, A. (2010) J. Agric. Food Chem. 58, 10209–10218.
[21] Dufrechou, M., Poncet-Legrand, C., Sauvage, F. X., and Vernhet, A. (2012) J. Agric. Food Chem. 60, 1308–1319.
[22] Kambiranda, D., Katam, R., Basha, S. M., and Siebert, S. (2014) J. Proteome Res. 13, 555–569.
[23] Cosme, F., Ricardo-da-Silva, J. M., and Laureano, O. (2007) Ital. J. Food Sci. 19, 39–56.
[24] Dupin, I. V., McKinnon, B. M., Ryan, C., Boulay, M., Markides, A. J., Jones, G. P., Williams, P. J., and Waters, E. J. (2000) J. Agric. Food Chem. 48, 3098–3105.
[25] Gonzalez-Ramos, D., Cebollero, E., and Gonzalez, R. (2008) Appl. Environ. Microbiol. 74, 5533–5540.
[26] Van Sluyter, S. C., Warnock, N. I., Schmidt, S., Anderson, P., van Kan, J. A. L., Bacic, A., and Waters, E. J. (2013) J. Agric. Food Chem. 61, 9705–9711.
[27] Marangon, M., Van Sluyter, S. C., Neilson, K. A., Chan, C., Haynes, P. A., Waters, E. J., and Falconer, R. J. (2011) J. Agric. Food Chem. 59, 733–740.
[28] Smith, P. K., Krohn, R. I., Hermanson, G. T., Mallia, A. K., Gartner, F. H., Provenzano, M. D., Fujimoto, E. K., Goeke, N. M., Olson, B. J., and Klenk, D. C. (1985) Anal. Biochem. 150, 76–85.
[29] Šebela, M., Štosová, T., Havliš, J., Wielsch, N., Thomas, H., Zdráhal, Z., and Shevchenko, A. (2006) Proteomics 6, 2959–2963.
[30] Laemmli, U. K. (1970) Nature 227, 680–685.
[31] Bennett, J., and Scott, K. J. (1971) Anal. Biochem. 43, 173–182.
[32] Shevchenko, A., Chernushevich, I., Wilm, M., and Mann, M. (2000) Methods Mol. Biol. 146, 1–16.
[33] Petersen, T. N., Brunak, S., von Heijne, G., and Nielsen, H. (2011) Nat. Methods 8, 785–786.
[34] Johnson, M., Zaretskaya, I., Raytselis, Y., Merezhuk, Y., McGinnis, S., and Madden, T. L. (2008) Nucleic Acids Res. 36, W5-W9.
[35] Jones, P., Binns, D., Chang, H. Y., Fraser, M., Li, W., McAnulla, C., McWilliam, H., Maslen, J., Mitchell, A., Nuka, G., Pesseat, S., Quinn, A. F., Sangrador-Vegas, A., Scheremetjew, M., Yong, S. Y., Lopez, R., and Hunter, S. (2014) Bioinformatics 30, 1236–1240.
[36] Ribéreau-Gayon, P., Glories, Y., Maujean, A., and Dubourdieu, D. (2006) Handbook of Enology. Volume 2—The Chemistry of Wine: Stabilization and Treatments, 2nd ed., J. Wiley & Sons, Chichester.
[37] Marchal, R., Warchol, M., Cilindre, C., and Jeandet, P. (2006) J. Agric. Food Chem. 54, 5157–5165.
[38] Dubernet, M., and Ribéreau-Gayon, P. (1974) Vitis 1, 233-244.
[39] Esteruelas, M., Poinsaut, P., Sieczkowski, N., Manteau, S., Fort, M. F., Canals, J. M., and Zamora, F. (2009) Am. J. Enol. Vitic. 60, 302–311.
[40] Karlsson, J. O., Ostwald, K., Kåbjörn, C., and Andersson, M. (1994) Anal. Biochem. 219, 144–146.
[41] Cilindre, C., Jégou, S., Hovasse, A., Schaeffer, C., Castro, A. J., Clément, C., Van Dorsselaer, A., Jeandet, P., and Marchal, R. (2008) J. Proteome Res. 7, 1199–1208.
[42] Wigand, P., Tenzer, S., Schild, H., and Decker, H. (2009) J. Agric. Food Chem. 57, 4328–4333.
[43] Girault, T., François, J., Rogniaux, H., Pascal, S., Delrot, S., Coutos-Thévenot, P., and Gomès, E. (2008) Plant Physiol. Biochem. 46, 140–149.
[44] Waters, E. J., Alexander, G., Muhlack, R., Pocock, K. F., Colby, C., O'Neill, B. K., Høj, P. B., and Jones, P. (2005) Aust. J. Grape Wine Res. 11, 215–225.
[45] Jashni, M. K., Mehrabi, R., Collemare, J., Mesarich, C. H., and de Wit, P . J. (2015) Front. Plant Sci. 6, 584.
[46] Expósito, J. M., Gordillo, C. M., Mariño, J. I. M., and Iglesias, J. L. M. (1991) Nahrung 35, 139–142.
[47] Verna, J., Lodder, A., Lee, K., Vagts, A., and Ballester, R. (1997) Proc. Natl. Acad. Sci. U.S.A. 94, 13804–13809.
[48] Rodriguez-Peña, J. M., Cid, V. J., Arroyo, J., and Nombela, C. (2000) Mol. Cell. Biol. 20, 3245–3255.
[49] Abramova, N., Sertil, O., Mehta, S., and Lowry, C. V. (2001) J. Bacteriol. 183, 2881–2887.
[50] Steyer, D., Ambroset, C., Brion, C., Claudel, P., Delobel, P., Sanchez, I., Erny, C., Blondin, B., Karst, F., and Legras, J. L. (2012) BMC Genomics 13, 573.
[51] Calderón, A. A., Garcia-Florenciano, E., Muñoz, R., and Barceló R. A. (1992) Vitis 31, 139–147.
[52] Mori, K., Goto-Yamamoto, N., Kitayama, M., and Hashizume, K. (2007) J. Exp. Bot. 58, 1935–1945.
[53] El Rayess, and Y., Ed. (2014) Wine: Phenolic Composition, Classification and Health Benefits, Nova Science Publishers Inc., New York, pp. 155–186.
[54] Gil-ad, N. L., Bar-Nun, N., and Mayer, A. M. (2001) FEMS Microbiol. Lett. 199, 109–113.
[55] Donèche, B. J., in Fleet, G. H. Ed. (1993) Wine Microbiology and Biotechnology. pp. 327–351, Harwood Academic Publishers, Chur.
[56] Waters, E. J., Shirley, N. J., and Williams, P. J. (1996) J. Agric. Food Chem. 44, 3–5.
[57] Sauvage, F. X., Bach, B., Moutounet, M., and Vernhet, A. (2010) Food Chem. 118, 26–34.
[58] Siebert, K. J. (1999) J. Agric. Food Chem. 47, 353–362.
[59] Pocock, K. F., Hayasaka, Y., McCarthy, M. G., and Waters, E.J. (2000) J. Agric. Food Chem. 48, 1637–1643.
[60] Lopez, M., and Edens, L. (2005) J. Agric. Food Chem. 53, 7944–7949.
[61] Ky, I., Lorrain, B., Jourdes, M., Pasquier, G., Fermaud, M., Gény, L., Rey, P., Doneche, B., and Teissedre, P. L. (2012) Aust. J. Grape Wine Res. 18, 215–226.
[62] Pour Nikfardjam, M. S., László, G., and Dietrich, H. (2006) Food Chem. 96, 74–79.
[63] Kovacs, E., Tompa, P., Liliom, K., and Kalmar, L. (2010) Proc. Natl. Acad. Sci. U.S.A. 107, 5429–5434.
[64] Marangon, M., Van Sluyter, S. C., Waters, E. J., and Menz, R. I. (2014) PLoS ONE 9, e113757.
[65] Davies, C., and Robinson, S. P. (2000) Plant Physiol. 12, 803–812.

Příloha 6:

Seznamy proteinů identifikovaných ve vínech a informace o obsahu prolinu v nalezených proteinech. Výsledková příloha k Perutka *et al.*, 2019.

Perutka *et al.*, 2019, Proteins identified in hazy Sauvignon Blanc wine, sample A, part 1/2

Protein number	Ionization technique	Gel slice number	Organism	Accession number (NCBInr)	Protein name	Protein function	Signal peptide prediction (D-score values provided by the Signal P 4.1 server)	MW [kDa]	pI	Score	Number of sequenced peptides	Sequence coverage [%]	Sequence coverage [%]	Proline content [%]	RMS90 [ppm]
1	MALDI	1	Vitis vinifera	gi|731438691	PREDICTED: probable non-specific lipid-transfer protein AKCS9 [Vitis vinifera]	lipid transfer	0.757	14.07	4.02	95.1	1	9.07	9.07	8.5	2.5
	ESI	2								97.5	2	9.07	9.07		78.6
	ESI	2P		gi|147834849	hypothetical protein VITISV_043508 [Vitis vinifera]		0.773	14.08	4.02	172.7	3	17.02	17.02	8.8	48.8
2	MALDI	2	Vitis vinifera	gi|297740510	unnamed protein product, partial [Vitis vinifera]	cysteine protease	0.106	41.10	4.02	1539.9	22	25.07	25.07	9.8	3.9
	ESI									1236	20	25.07	25.07		56.5
	ESI	2P								957.6	15	20.04	20.04		50.2
3	MALDI	2	Vitis vinifera	gi|225445553	PREDICTED: blue copper protein [Vitis vinifera]	stellacyanin, electron transfer	0.836	30.07	5.01	408.6	6	12.08	12.08	6.6	3
	ESI									407.7	6	17.01	17.01		48.5
	ESI	3P								407.6	6	17.01	17.01		56.6
4	MALDI	7	Vitis vinifera	gi|225466093	PREDICTED: beta-fructofuranosidase, soluble isoenzyme I-like [Vitis vinifera]	invertase	0.122	72.00	4.06	993.6	15	15.06	15.06	6.5	5.5
	MALDI				vacuolar invertase 1, GIN1 [Vitis vinifera=grape berries, Sultana, berries, Peptide, 642 aa]					972.9	16	17.01	17.01		46.1
	ESI	5P		gi|1839578			0.124	71.50		893.9	13	19.03	19.03	6.2	43.1
5	MALDI	8	Vitis vinifera	gi|359478431	PREDICTED: peroxidase A2 [Vitis vinifera]	secreted peroxidase	0.764	36.50	4.04	162.4	3	7.09	7.09	3.8	2.6
	ESI									179.4	3	10.08	10.08		63.5
6	ESI	8P	Vitis vinifera	gi|2306813	class IV endochitinase [Vitis vinifera]	chitinase	0.928	27.05	5.04	362.5	6	15.09	15.09	2.1	66.5
7	ESI	9P	Vitis vinifera	gi|520729528	Chain A, Structure Of Haze Forming Proteins In White Wines: Vitis Vinifera Thaumatin-like Proteins	thaumatin-like protein	0.167	21.03	4.08	206.6	4	18.07	18.07	7.6	65
8	ESI	9P	Vitis vinifera	gi|147785114	hypothetical protein VITISV_021587 [Vitis vinifera]	thaumatin-like protein	0.784	23.09	4.06	632.7	11	41.30	41.30	4.5	53.2
9	MALDI	12	Vitis vinifera	gi|296084197	unnamed protein product, partial [Vitis vinifera]	invertase (fragment)	0.127	60.50	4.04	822.3	12	12.05	12.05	5.7	2.5
	ESI									710.8	11	12.09	12.09		58.8
10	MALDI	2	Botrytis cinerea	gi|347835718	glycoside hydrolase family 31 protein [Botrytis cinerea T4]	glycoside hydrolase	0.733	109.30	4.05	467.8	9	9.07	9.07	5.7	4.1
	ESI									347.5	7	9.02	9.02		53.8
11	MALDI	3	Botrytis cinerea	gi|347833309	similar to serine carboxypeptidase (CpdS) (secreted protein) [Botrytis cinerea T4]	serine carboxypeptidase	0.779	60.80	4.07	395.5	5	12.03	12.03	7.7	4.7
	ESI									214.3	5	11.09	11.09		56.5
12	ESI	3P	Botrytis cinerea	gi|154291355	predicted protein [Botrytis cinerea B05.10]	extracellular membrane protein	0.879	20.02	4.03	137.9	2	12.06	12.06	8.1	33.1
13	MALDI	5	Botrytis cinerea	gi|154300984	hypothetical protein BC1G_10630 [Botrytis cinerea B05.10]	cell wall organisation protein	0.770	41.10	4.03	190.8	4	12.07	12.07	2.9	6.3
	ESI									421.5	7	12.04	12.04		60
14	MALDI	5	Botrytis cinerea	gi|15022489	laccase 2 [Botrytis cinerea]	laccase	0.703	63.40	4.05	860.2	15	22.02	22.02	5.2	4.8
	ESI									1257.5	20	25.03	25.03		59.7
	ESI	4P								125.2	2	3.08	3.08		46.5
15	MALDI	8	Botrytis cinerea	gi|154304407	hypothetical protein BC1G_09079 [Botrytis cinerea B05.10]	beta-1,3-glucanase	0.667	44.10	4.03	72.2	2	6.06	6.06	3.2	1.6
	ESI	8								122.8	2	5.07	5.07		67
16	MALDI	10	Botrytis cinerea	gi|48093959	endo-beta-1,4-glucanase precursor [Botrytis cinerea]	cellulase	0.764	44.20	4.02	156.3	2	9.00	9.00	3.2	10.7
	ESI	9								133.7	3	5.07	5.07		79.9

Perutka *et al.*, 2019, Proteins identified in hazy Sauvignon Blanc wine, sample A, part 2/2

Protein number	Ionization technique	Gel slice number	Organism	Accession number (NCBInr)	Protein name	Protein function	Signal peptide prediction (D-score values provided by the Signal P 4.1 server)	MW [kDa]	pI	Score	Number of sequenced peptides	Sequence coverage [%]	Sequence coverage [%]	Proline content [%]	RMS90 [ppm]
17	MALDI	1	Saccharomyces cerevisiae	gi|323346853	Ygp1p [Saccharomyces	asparaginase	0.818	37.30	5.03	1354	15	28.00	28.00	5.1	3.5
	ESI			gi|323335922	cerevisiae]					1194.4	16	25.04	25.04		74.5
	ESI	1P								956.3	13	24.06	24.06	5.1	60.3
18	MALDI	1	Saccharomyces cerevisiae	gi|323331721	Tir4p [Saccharomyces cerevisiae AWRI796]	stress induced protein	0.712	16.04	3.09	325.1	4	18.05	18.05	4.4	6.2
	ESI									231.5	4	19.07	19.07		74.7
	ESI	1P		gi|323352383	Tir4p [Saccharomyces cerevisiae VL3]		0.713	41.90	7.02	226.1	5	7.04	7.04	13.1	48.1
19	ESI	1P	Saccharomyces cerevisiae	gi|323307336	Hpf1p [Saccharomyces cerevisiae FostersO]	yeast mannoprotein	0.652	69.00	6.02	270	4	3.08	3.08	2.7	43.6
20	MALDI	1	Saccharomyces cerevisiae	gi|207342449	YMR006Cp-like protein [Saccharomyces cerevisiae AWRI1631]	phospholipase B	0.462	59.80	4.04	1361.9	19	29.08	29.08	4.5	3.4
	ESI	2		gi|323336225	Plb2p [Saccharomyces cerevisiae Vin13]			75.40	4.05	566.3	10	16.06	16.06	4.1	64.6
	ESI	2P		gi|207342449	YMR006Cp-like protein [Saccharomyces cerevisiae AWRI1631]			59.80	4.04	226.5	5	10.04	10.04	4.5	74.3
21	MALDI	2	Saccharomyces cerevisiae	gi|768812869	Wsc4p [Saccharomyces cerevisiae YJM1250]	cell wall integrity stress response protein	0.803	63.70	6.00	104.2	1	2.08	2.08	5.7	1
	ESI									95.1	1	2.08	2.08		80.6
22	MALDI	2	Saccharomyces cerevisiae	gi|190406234	hypothetical protein SCRG_05191 [Saccharomyces cerevisiae RM11-1a]	stress induced cell wall mannoprotein	0.803	24.03	4.03	431	4	11.04	11.04	1.8	7.4
	ESI	3								420.3	5	11.04	11.04		57.3
	ESI	4P								247.4	3	11.04	11.04		60.3
23	MALDI	3	Saccaromyces cerevisiae	gi|207344997	YGR189Cp-like protein [Saccharomyces cerevisiae AWRI1631]	transglycosidase	0.699	51.30	4.04	535.8	10	17.07	17.07	2.8	5.2
	ESI			gi|323354858	Crh1p [Saccharomyces cerevisiae VL3]			45.60	4.05	410.5	6	13.04	13.04	3.2	63
	ESI	3P								671.6	13	21.00	21.00		51
24	MALDI	3	Saccharomyces cerevisiae	gi|190408747	acid phosphatase [Saccharomyces cerevisiae RM11-1a]	histidine phosphatase	0.456	52.80	4.04	555.2	8	20.03	20.03	3.1	5.5
	ESI									513.6	8	20.03	20.03		55.7
	ESI	3P		gi|762051192	Pho3p [Saccharomyces cerevisiae YJM1418]		0.575	52.70	4.05	128.2	2	7.01	7.01	3.1	58
25	MALDI	3	Saccharomyces cerevisiae	gi|323356058	Pho5p [Saccharomyces cerevisiae VL3]	histidine phosphatase	0.495	52.80	4.07	494.4	9	15.06	15.06	2.9	2.5
	ESI			gi|323310064	Pho5p [Saccharomyces cerevisiae FostersO]			47.30	4.06	515.9	12	23.03	23.03	3.2	71.9
26	ESI	4P	Saccharomyces cerevisiae	gi|207342034	YMR307Wp-like protein [Saccharomyces cerevisiae AWRI1631]	beta-1,3-glucanosyltransferase	0.146	48.30	4.04	128	2	5.05	5.05	2.4	14.2
27	ESI	6P	Saccharomyces cerevisiae	gi|767173549	Cwp1p [Saccharomyces cerevisiae YJM1385]	cell wall protein	0.773	24.02	4.05	121.5	3	18.00	18.00	1.8	19.2
28	MALDI	9	Saccharomyces cerevisiae	gi|207344015	YJL078Cp-like protein [Saccharomyces cerevisiae AWRI1631]	cell wall-associated protein	0.712	34.20	4.02	131.2	1	5.03	5.03	3.8	2.8
	ESI									129.8	2	5.03	5.03		53

Perutka *et al.*, 2019, Proteins identified in hazy Sauvignon Blanc wine, sample B

Protein number	Ionization technique	Gel slice number	Organism	Accession number (NCBInr)	Protein name	Protein function	Signal peptide prediction (D-score values provided by the Signal P 4.1 server)	MW [kDa]	pI	Score	Number of sequenced peptides	Sequence coverage [%]	Proline content [%]	RMS90 [ppm]
1	M	1	Vitis vinifera	gi|297740510	unnamed protein product, partial	cysteine protease	0.106	41.1	4.2	1053.9	13	21.5	9.8	8.12
	E									1787.2	27	26.5		22.58
2	M	2	Vitis vinifera	gi|225445553	PREDICTED: blue copper protein	stellacyanin	0.836	30.7	5.1	224.2	3	12.4	6.6	6.45
	E			gi|147780459	hypothetical protein VITISV_018636, partial		0.836	31.8	5.9	446.1	6	16.7	7.4	26.17
3	M	9	Vitis vinifera	gi|225466093	PREDICTED: beta-fructofuranosidase, soluble isoenzyme I isoform X1	invertase	0.122	72.0	4.6	474.6	7	13.3	6.5	6.87
	E			gi|296084197	unnamed protein product, partial		0.127	60.5	4.4	1076.5	15	23.4	5.7	30.04
4	M	9	Vitis vinifera	gi|7406714	putative thaumatin-like protein, partial	thaumatin	0.151	20.1	4.5	84.9	1	6.3	6.8	9.05
	E									149.9	4	38.9		9.24
5	M	11	Vitis vinifera	gi|359495539	PREDICTED: cysteine proteinase inhibitor 1	cysteine proteinase inhibitor	0.920	13.0	6.6	157.5	1	15.3	3.2	0.87
	E	12								256.7	3	27.1		24.2
6	M	2	Botrytis cinerea	gi|347835718	glycoside hydrolase family 31 protein	glycoside hydrolase	0.733	109.3	4.5	153.5	3	3.6	5.8	13.64
	E									389.3	7	9		31.99
7	M	2	Botrytis cinerea	gi|154310457	hypothetical protein BC1G_07149	serine carboxypeptidase	0.357	61.8	4.6	158.1	2	3.9	7.1	6.88
	E									115.4	2	3.9		66.94
8	M	2	Botrytis cinerea	gi|154320662	hypothetical protein BC1G_01803	serine protease	0.714	70.0	4.7	920.7	8	6.5	7.1	6.09
	E									520.3	9	11.9		11.95
9	M	3	Botrytis cinerea	gi|347833309	similar to serine carboxypeptidase (CpdS)	serine protease	0.779	60.8	4.7	575.8	8	13	7.7	4.63
	E	2								523.4	10	25		14.92
10	M	5	Botrytis cinerea	gi|15022489	laccase 2	laccase	0.703	63.4	4.5	903.8	11	21	5.2	5.41
	E									1428.5	23	28.1		28.64
11	M	8	Botrytis cinerea	gi|154320159	predicted protein	x unknown	0.869	17.2	3.9	176.5	2	17.3	4.9	3.11
	E	9								189.2	2	17.3		31.28
12	M	1	Saccharomyces cerevisiae	gi|767254761	Ygp1p	asparaginase	0.818	37.2	5.3	459.1	4	5.1	5.1	7.13
	E			gi|767229366			0.816	37.3	5.3	649.7	11	24.6	5.1	19.61
13	M	1	Saccharomyces cerevisiae	gi|190406234	hypothetical protein SCRG_05191	stress induced cell-wall mannoprotein	0.803	24.3	4.3	240	2	11.4	1.8	1.56
	E	2								398.5	5	11.4		34.54
14	M	1	Saccharomyces cerevisiae	gi|207342449	YMR006Cp-like protein	phospholipase	0.462	59.8	4.4	193.4	2	6.9	4.5	3.43
	E	2		gi|256273487	Plb2p		0.462	75.5	4.5	566.3	9	13.5	4.0	23.62
15	M	2	Saccharomyces cerevisiae	gi|762051192	Pho3p	phosphatase	0.575	52.7	4.4	162.8	2	5.4	3.1	6.34
	E			gi|323338655			0.658	52.8	4.4	320.7	6	16.5	3.1	32.98
16	M	2	Saccharomyces cerevisiae	gi|323310064	Pho5p, partial	acid phosphatase	0.495	47.3	4.6	97.4	2	4.8	3.2	9.66
	E									198.6	4	6.7		36.36
17	M	3	Saccharomyces cerevisiae	gi|323332206	Gas1p	glucanosyl-transferase	0.730	52.3	4.4	277.5	4	6.9	3.1	2.37
	E			gi|767204492			0.730	59.5	4.5	541.1	9	16.8	2.6	21.1
18	M	4	Saccharomyces cerevisiae	gi|323338696	Tos1p	putative glycoside hydrolase	0.690	42.7	4.7	158.1	2	7.7	3.2	4.95
	E									410.2	6	20.8		38.4
19	M	3	Saccharomyces cerevisiae	gi|323346603	Gas5p	glucanosyl-transferase	0.670	51.8	4.5	86.1	2	4.1	3.5	10.12
	E			gi|259149455			0.622	51.2	4.5	211.5	4	5.5	3.5	41.61

Perutka *et al.*, 2019, Proteins identified in standard clear white wine, sample C

Protein number	Ionization technique	Gel slice number	Organism	Accession number (NCBInr)	Protein name	Protein function	Signal peptide prediction (D-score values provided by the Signal P 4.1 server)	MW [kDa]	p*I*	Score	Number of sequenced peptides	Sequence coverage [%]	Proline content [%]	RMS90 [ppm]
1	MALDI	1	Vitis vinifera	gi|297740510	unnamed protein product, partial	cysteine protease	0.106	41.1	4.2	802.1	11	17.8	9.8	4.92
2	MALDI	2	Vitis vinifera	gi|225445553	PREDICTED: blue copper protein	stellacyanin	0.836	30.7	5.1	360.7	5	12.8	6.6	5.13
3	MALDI	5	Vitis vinifera	gi|225466093	PREDICTED: beta-fructofuranosidase, soluble isoenzyme I-like	invertase	0.122	72	4.6	1189.5	15	25.7	6.5	6.51
4	MALDI	8	Vitis vinifera	gi|147789487	hypothetical protein VITISV_001194	thaumatin	0.885	24.2	8.5	174.2	2	7.1	7.0	13.79
5	MALDI	9	Vitis vinifera	gi|605603680	Chain A, Structure Of Haze Forming Proteins In White Wines: Vitis Vinifera Thaumatin-like Proteins	thaumatin	0.192	21.2	4.5	423.1	5	28.9	5.0	11.67
6	MALDI	9	Vitis vinifera	gi|520729528	Chain A, Structure Of Haze Forming Proteins In White Wines: Vitis Vinifera Thaumatin-like Proteins	thaumatin	0.167	21.3	4.8	98.5	1	6.1	7.6	19.84
7	MALDI	3	Botrytis cinerea	gi|347833309	similar to serine carboxypeptidase (CpdS)	serine protease	0.779	60.8	4.7	131	2	6.3	7.7	6.97
8	MALDI	5	Botrytis cinerea	gi|15022489	laccase 2	laccase	0.703	63.4	4.5	595.5	8	14.3	5.2	3.88
9	MALDI	9	Botrytis cinerea	gi|374094008	acid protease 1, partial	acid protease	0.596	22.7	4.7	169.6	2	13.1	2.9	14.91
10	MALDI	1	Saccharomyces cerevisiae	gi|767254761	Ygp1p	asparaginase	0.818	37.2	5.3	551.6	6	11	5.1	7.97
11	MALDI	1	Saccharomyces cerevisiae	gi|190406234	hypothetical protein SCRG_05191	stress induced cell-wall mannoprotein	0.803	24.3	4.3	212.9	2	11.4	1.8	2.02
12	MALDI	2	Saccharomyces cerevisiae	gi|323348454	Crh1p	transglycosidase	0.699	51.5	4.5	243.3	3	6.9	3.0	9.87
13	MALDI	5	Saccharomyces cerevisiae	gi|4814	YJU1, partial	cell-wall protein	0.099	21.9	4.4	199.6	2	14.4	1.9	5.53

Perutka *et al.*, 2019, Proteins identified in non-hazy botrytized Welschriesling wine, sample D

Protein number	Ionization technique	Gel slice number	Organism	Accession number (NCBInr)	Protein name	Protein function	Signal peptide prediction (D-score values provided by the Signal P 4.1 server)	MW [kDa]	p*I*	Score	Number of sequenced peptides	Sequence coverage [%]	Proline content [%]	RMS90 [ppm]
1	MALDI ESI	1	Vitis vinifera	gi|297740510	unnamed protein product, partial	cysteine protease	0.106	41.1	4.2	1305.7 2467	15 39	25.5 32.9	9.8	9.28 22.53
2	MALDI ESI	9	Vitis vinifera	gi|7406714 gi|147785114	putative thaumatin-like protein, partial hypothetical protein VITISV_021587	thaumatin partial thaumatin	0.151 0.784	20.1 23.9	4.5 4.6	355.7 642.8	4 9	30.5 42.2	6.8 4.5	15.66 28.08
	ESI			gi|147789487	hypothetical protein VITISV_001194	thaumatin	0.885	24.2	8.5	133	2	7.1	7.0	32.11
3	MALDI ESI	1	Botrytis cinerea	gi|347835718 gi|154295712	glycoside hydrolase family 31 protein hypothetical protein BC1G_12859	glycoside hydrolase	0.733 0.736	109.3 109.3	4.5 4.5	438.3 919.6	6 15	7.2 17.7	5.7 5.8	11.69 21.39
4	MALDI ESI	1	Botrytis cinerea	gi|472238473	putative alpha mannosidase family protein	glycoside hydrolase	0.703	91.6	4.8	88.2 274.6	3 4	3.8 4.6	5.5	4.9 37.91
5	MALDI ESI	1	Botrytis cinerea	gi|154320662	hypothetical protein BC1G_01803	serine protease	0.714	70	4.7	1221.9 1148.9	9 17	8 17.6	7.1	9.25 19.99
6	MALDI ESI	3 2	Botrytis cinerea	gi|154309609	hypothetical protein BC1G_07275	possible peptidase	0.841	82.3	4.6	202.1 402.8	3 5	4.4 7.4	5.3	9.44 34.1
7	MALDI ESI	4	Botrytis cinerea	gi|154321738	hypothetical protein BC1G_01016	possible heatshock protein	0.737	21.8	4	140.1 325.6	2 5	12.4 17.3	5.5	3.26 59.32
8	MALDI ESI	3	Botrytis cinerea	gi|154316249 gi|347836387	hypothetical protein BC1G_03710 similar to carboxypeptidase, partial sequence	serine protease	0.644 0.646	63 64.9	4.4 4.6	831.5 1080.5	9 17	15.7 21.7	4.9 4.9	8.87 15.64
9	MALDI ESI	5	Botrytis cinerea	gi|15022489	laccase 2	laccase	0.703	63.4	4.5	1547.8 3175.2	18 45	28.4 48.5	5.2	6.42 22.43
10	MALDI ESI	3	Botrytis cinerea	gi|154310457	hypothetical protein BC1G_07149	serine protease	0.357	61.8	4.6	130 160.5	2 2	3.9 5.2	7.1	4.76 38.57
11	MALDI ESI	3	Botrytis cinerea	gi|347833309	similar to serine carboxypeptidase (CpdS)	serine protease	0.779	60.8	4.7	1129.6 1294	12 22	14.5 33.1	7.7	8.54 27.35
12	MALDI ESI	4	Botrytis cinerea	gi|154300984	hypothetical protein BC1G_10630	GPI-anchored cell wall organization protein	0.77	41.1	4.3	198.2 303.5	2 5	7.2 12.2	2.9	2.74 40.59
13	MALDI ESI	4	Botrytis cinerea	gi|18307424	pectin methylesterase [Botrytis cinerea]	pectin methylesterase	0.878	38	4.4	213.3 504.6	3 8	11.5 19.3	3.3	13.95 33.35
14	MALDI ESI	6	Botrytis cinerea	gi|154317922	hypothetical protein BC1G_02944	serine protease	0.782	61.7	4.8	159.9 1030.8	2 16	4.9 26.4	5.1	8.18 27.13
15	MALDI ESI	6	Botrytis cinerea	gi|347827471	similar to GPI anchored cell wall protein	Ubiquitin 3 binding protein	0.623	36.8	4.4	99.3 273.7	1 5	3.4 14.6	6.7	2.09 41.78
16	MALDI ESI	8	Botrytis cinerea	gi|114149215	aspartic proteinase precursor, partial	pepsin-like proteinase secreted from pathogen to degrade host proteins	0.562	50.5	4.4	241.1 158.2	2 3	4.6 11	3.7	0.51 15.81
17	MALDI ESI	9 8	Botrytis cinerea	gi|154320159	predicted protein	x unknown	0.869	17.2	3.9	227.1 426.4	2 6	17.3 27.2	4.9	8.73 41.15
18	MALDI ESI	9	Botrytis cinerea	gi|374094008	acid protease 1, partial	acid protease	0.596	22.7	4.7	175.3 317.1	2 4	13.1 34.2	2.9	6.28 53.84

Perutka *et al.*, 2019, Proteins identified in standard clear white wines, sample E

Protein number	Ionization technique	Gel slice number	Organism	Accession number (NCBInr)	Protein name	Protein function	Signal peptide prediction (D-score values provided by the Signal P 4.1 server)	MW [kDa]	pI	Score	Number of sequenced peptides	Sequence coverage [%]	Proline content [%]	RMS90 [ppm]
1	MALDI	2	Vitis vinifera	gi|297740510	unnamed protein product, partial	cysteine protease	0.106	41.1	4.2	1079.4	12	17.8	9.8	5.39
2	MALDI	4	Vitis vinifera	gi|225445553	PREDICTED: blue copper protein	stellacyanin	0.836	30.7	5.1	337.9	5	12.4	6.6	1.56
3	MALDI	5	Vitis vinifera	gi|296084197	unnamed protein product, partial	invertase	0.127	60.5	4.4	800.9	9	19.2	5.7	7.75
4	MALDI	8	Vitis vinifera	gi|147789487	hypothetical protein VITISV_001194	thaumatin	0.885	24.2	8.5	206.6	2	7.1	7.0	14.75
5	MALDI	9	Vitis vinifera	gi|605603680	Chain A, Structure Of Haze Forming Proteins In White Wines: Vitis Vinifera Thaumatin-like Proteins	thaumatin	0.192	21.2	4.5	614.3	7	36.3	5.0	2.68
6	MALDI	12	Vitis vinifera	gi|147784001	hypothetical protein VITISV_041168	PR-4 protein	0.879	12.6	9.4	111.3	1	13.7	4.2	6.36
7	MALDI	4	Botrytis cinerea	gi|154320662	hypothetical protein BC1G_01803	sedolisin peptidase	0.714	70	4.7	210.2	2	2.5	7.1	0.3
8	MALDI	4	Botrytis cinerea	gi|154310457	hypothetical protein BC1G_07149	serine protease	0.357	61.8	4.6	107.7	2	3.9	7.1	6.03
9	MALDI	5	Botrytis cinerea	gi|15022489	laccase 2	laccase	0.703	63.4	4.5	520.4	6	11.4	5.2	6.45
10	MALDI	5	Botrytis cinerea	gi|347833309	similar to serine carboxypeptidase (CpdS)	serine protease	0.779	60.8	4.7	203.7	2	6.3	7.7	9.28
11	MALDI	1	Saccharomyces cerevisiae	gi|323354858	Crh1p	transglycosidase	0.699	45.6	4.5	230.6	3	7.8	3.2	6.34
12	MALDI	2	Saccharomyces cerevisiae	gi|190408245	lysophospholipase	phospholipase	0.462	75.4	4.5	598.2	6	12.7	4.1	7.35
13	MALDI	2	Saccharomyces cerevisiae	gi|767254761	Ygp1p	asparaginase	0.818	37.2	5.3	268.8	2	4.8	5.1	9.32
14	MALDI	3	Saccharomyces cerevisiae	gi|190406234	hypothetical protein SCRG_05191	stress induced cell-wall protein	0.803	24.3	4.3	231.4	2	11.4	1.8	5.45
15	MALDI	5	Saccharomyces cerevisiae	gi|766436800	Pry1p	extracellular protein	0.766	29.8	4.4	144	2	10	4.8	8.63
16	MALDI	6	Saccharomyces cerevisiae	gi|323304370	Pry3p	extracellular protein	0.712	92.7	4.5	607.2	5	5.8	3.2	11.11
17	MALDI	5	Saccharomyces cerevisiae	gi|323305979	Tos1p	putative glycosidase	0.824	44.2	4.6	396.5	5	14.5	2.8	6.96

Perutka *et al.*, 2019, Proteins identified in standard clear white wines, sample F

Protein number	Ionization technique	Gel slice number	Organism	Accession number (NCBInr)	Protein name	Protein function	Signal peptide prediction (D-score values provided by the Signal P 4.1 server)	MW [kDa]	*pI*	Score	Number of sequenced peptides	Sequence coverage [%]	Proline content [%]	RMS90 [ppm]
1	MALDI	2	Vitis vinifera	gi|297740510	unnamed protein product, partial	cysteine protease	0.106	41.1	4.2	634	7	16.7	9.8	4.48
2	MALDI	2	Vitis vinifera	gi|225445553	PREDICTED: blue copper protein	stellacyanin	0.836	30.7	5.1	159.1	2	7.7	6.6	5.11
3	MALDI	10	Vitis vinifera	gi|7406714	putative thaumatin-like protein, partial	thaumatin	0.151	20.1	4.5	191	2	15.3	6.8	15.36
4	MALDI	1	Botrytis cinerea	gi|347835718	glycoside hydrolase family 31 protein	glycoside hydrolase	0.733	109.3	4.5	243.4	3	3.6	5.7	2.61
5	MALDI	2	Botrytis cinerea	gi|154320662	hypothetical protein BC1G_01803	serine protease	0.714	70	4.7	439.7	4	4.8	7.1	5.3
6	MALDI	5	Botrytis cinerea	gi|15022489	laccase 2	laccase	0.703	63.4	4.5	1250.3	13	22.9	5.2	8.96
7	MALDI	5	Botrytis cinerea	gi|347833309	similar to serine carboxypeptidase (CpdS)	serine protease	0.779	60.8	4.7	500.5	5	13	7.7	6.41
8	MALDI	5	Botrytis cinerea	gi|154310457	hypothetical protein BC1G_07149	serine protease	0.357	61.8	4.6	176.2	2	3.9	7.1	12.47
9	MALDI	6	Botrytis cinerea	gi|154316249	hypothetical protein BC1G_03710	serine protease	0.646	63	4.4	118.5	2	2.4	4.9	11.31
10	MALDI	7	Botrytis cinerea	gi|48093959	endo-beta-1,4-glucanase precursor	cellulase	0.764	44.2	4.2	166.5	1	6.1	3.2	7.76
11	MALDI	1	Saccharomyces cerevisiae	gi|190408245	lysophospholipase	lysophospho-lipase	0.462	75.4	4.5	706.5	7	13.5	4.1	8.29
12	MALDI	1	Saccharomyces cerevisiae	gi|323307336	Hpf1p	hyphally regulated cell wall mannoprotein	0.652	69	6.2	482.3	5	9.4	2.8	7.64
13	MALDI	1	Saccharomyces cerevisiae	gi|323309306	YAR066W-like protein	hyphally regulated cell wall mannoprotein	0.647	63.8	4.5	136.7	2	5.1	2.5	4.05
14	MALDI	2	Saccharomyces cerevisiae	gi|767254761	Ygp1p	asparaginase	0.818	37.2	5.3	616.8	5	7.6	5.1	14.94
15	MALDI	2	Saccharomyces cerevisiae	gi|190406234	hypothetical protein SCRG_05191	Tir, cell-wall protein	0.803	24.3	4.3	308.9	3	11.4	1.8	6.9
16	MALDI	3	Saccharomyces cerevisiae	gi|584368899	Hpf1p, partial	hyphally regulated cell wall mannoprotein	0.659	75	4.1	811.8	8	11.3	4.5	3.32

Perutka *et al.*, 2019, Proteins identified in a nouveau wine, sample G

Protein number	Ionization technique	Gel slice number	Organism	Accession number (NCBInr)	Protein name	Protein function	Signal peptide prediction (D-score values provided by the Signal P 4.1 server)	MW [kDa]	pI	Score	Number of sequenced peptides	Sequence coverage [%]	Proline content [%]	RMS90 [ppm]
1	ESI	1	Vitis vinifera	gi|297740510	unnamed protein product, partial	cysteine protease	0.106	41.1	4.2	1238.2	24	25.5	9.8	58.0
2	ESI	4	Vitis vinifera	gi|225466093	PREDICTED: beta-fructofuranosidase, soluble isoenzyme I-like	invertase	0.122	72.0	4.6	1559.4	30	27.4	6.5	47.1
3	ESI	9	Vitis vinifera	gi|7406716	putative thaumatin-like protein	thaumatin	0.777	24.0	4.9	889.0	14	49.1	7.1	51.8
4	ESI	9	Vitis vinifera	gi|147785114	hypothetical protein VITISV_021587	thaumatin	0.784	23.9	4.6	481.1	9	40.0	5.0	50.0
5	ESI	11	Vitis vinifera	gi|225453022	PREDICTED: pathogenesis-related protein PR-4	PR4 protein, chitinase	0.879	15.1	8.1	487.0	7	37.8	3.3	45.0
6	ESI	12	Vitis vinifera	gi|225441373	PREDICTED: glucan endo-1,3-beta-glucosidase	glucosidase	0.743	36.7	8.5	272.1	6	21.5	5.5	63.8
7	ESI	1	Saccharomyces cerevisiae	gi|767254761	Ygp1p	asparaginase	0.818	37.2	5.3	220.5	4	11.9	5.1	39.9
8	ESI	6	Saccharomyces cerevisiae	gi|323308946	Crh1p	transglycosidase	0.699	53.4	4.5	133.2	3	7.6	2.8	50.2
9	ESI	12	Saccharomyces cerevisiae	gi|323303769	Fks1p	1,3-glucan synthase	0.101	214.8	6.8	249.2	6	1.8	4.6	60.2

Perutka *et al.*, 2019, Proteins identified in a grape juice, sample H

Protein number	Ionization technique	Gel slice number	Organism	Accession number (NCBInr)	Protein name	Protein function	Signal peptide prediction (D-score values provided by the Signal P 4.1 server)	MW [kDa]	pI	Score	Number of sequenced peptides	Sequence coverage [%]	Proline content [%]	RMS90 [ppm]
1	ESI	1 (5)	Vitis vinifera	gi|297740510	unnamed protein product, partial	cysteine protease	0.106	41.1	4.2	345.4	5	16.2	5.7	64.0
2	ESI	1	Vitis vinifera	gi|302141828	unnamed protein product, partial	LysM domain protein, pathogen interaction	0.133	42.8	5.1	122.0	3	8.6	8.3	55.0
3	ESI	2	Vitis vinifera	gi|147825156	hypothetical protein VITISV_034156	PPR2 protein	0.114	59.6	7.0	130.2	2	1.9	3.2	51.2
4	ESI	4	Vitis vinifera	gi|296084197	unnamed protein product, partial	invertase	0.127	60.5	4.4	927.4	17	25.6	5.7	64.4
5	ESI	4	Vitis vinifera	gi|297744095	unnamed protein product, partial	unknown	0.133	49.9	5.5	196.9	4	11.6	7.8	58.3
6	ESI	4	Vitis vinifera	gi|147811111	hypothetical protein VITISV_027762	Glycerophosphodiester phosphodiesterase	0.938	70.4	5.5	115.1	3	4.8	4.0	81.2
7	ESI	5	Vitis vinifera	gi|296084540	unnamed protein product, partial	glycoside hydrolase, heparanase	0.838	58.6	6.3	123.8	2	3.9	4.1	77.3
8	ESI	6	Vitis vinifera	gi|147766674	hypothetical protein VITISV_035472	polyphenol oxidase, tyrosinase	0.183	67.4	6.0	325.2	7	10.7	7.2	38.8
9	ESI	6	Vitis vinifera	gi|297736730	unnamed protein product, partial	polyphenol oxidase, tyrosinase	0.194	51.5	5.7	168.2	4	9.9	7.3	64.9
10	ESI	6	Vitis vinifera	gi|297739731	unnamed protein product, partial	polygalacturonase inhibitor	0.756	35.5	9.0	114.1	2	7.5	7.2	70.7
11	ESI	7	Vitis vinifera	gi|2306813	class IV endochitinase	chitinase	0.928	27.5	5.4	640.7	13	35.6	2.0	66.8
12	ESI	7	Vitis vinifera	gi|225441373	PREDICTED: glucan endo-1,3-beta-glucosidase	glucosidase	0.743	36.7	8.5	308.0	5	15.0	5.5	59.3
13	ESI	7	Vitis vinifera	gi|147790682	hypothetical protein VITISV_001146	cysteine protease	0.930	51.5	5.1	232.5	3	9.2	4.5	62.6
14	ESI	8	Vitis vinifera	gi|147787076	hypothetical protein VITISV_033131	chitinase	0.920	28.0	4.7	529.7	9	22.3	2.4	62.3
15	ESI	9	Vitis vinifera	gi|7406716	putative thaumatin-like protein	thaumatin	0.777	24.0	4.9	641.6	10	47.7	7.1	70.6
16	ESI	9	Vitis vinifera	gi|33329390	thaumatin-like protein [Vitis vinifera]	thaumatin	0.847	23.9	4.7	241.6	4	18.2	5.5	63.3
17	ESI	12	Vitis vinifera	gi|147768392	hypothetical protein VITISV_031522	cysteine proteinase inhibitor	0.098	11.2	5.6	262.2	6	55.4	3.0	63.3
18	ESI	12	Vitis vinifera	gi|3511147	PR-4 type protein	PR4 protein, chitinase	0.879	15.2	5.5	192.6	2	11.2	3.3	76.2

Příloha 7:

Perutka, Z., Šebela, M., 2020. Mass spectrometry of peptides and proteins using digestion by a grape cysteine protease at pH 3. *Journal of Mass Spectrometry* 55, e4444.

Received: 17 July 2019 | Revised: 6 September 2019 | Accepted: 9 September 2019
DOI: 10.1002/jms.4444

SPECIAL ISSUE - RESEARCH ARTICLE

WILEY Journal of MASS SPECTROMETRY

Mass spectrometry of peptides and proteins using digestion by a grape cysteine protease at pH 3

Zdeněk Perutka | Marek Šebela

Department of Protein Biochemistry and Proteomics, Centre of the Region Haná for Biotechnological and Agricultural Research, Faculty of Science, Palacký University, Šlechtitelů 27, Olomouc CZ-783 71, Czech Republic

Correspondence
Marek Šebela, Department of Protein Biochemistry and Proteomics, Centre of the Region Haná for Biotechnological and Agricultural Research, Faculty of Science, Palacký University, Šlechtitelů 27, Olomouc CZ-783 71, Czech Republic.
Email: marek.sebela@upol.cz

Funding information
ERDF project "Plants as a tool for sustainable global development", Grant/Award Number: CZ.02.1.01/0.0/0.0/16_019/0000827

Abstract

Cysteine protease from grapevine (*Vitis vinifera*) belongs to those resistant proteins, which survive the process of vinification and can therefore be detected as wine components. Its amino acid sequence shows a homology to other members of the papain family, but the enzyme has only partially been explored so far. In order to get more biochemical information with the help of mass spectrometry (MS), wine proteins were collected by ultrafiltration and separated by gel permeation chromatography. The purified enzyme surprisingly displayed a high molecular mass value of around 200 kDa, indicating a possible oligomeric status and aggregation, as it entered only negligibly the separating 10% gel during polyacrylamide gel electrophoresis. The isoelectric point (pI) value of 3.6 was determined by chromatofocusing. Matrix-assisted laser desorption/ionization (MALDI)-MS was employed to evaluate the cleavage specificity and usefulness of the isolated cysteine protease in protein and peptide research. A potential applicability could be anticipated from the efficient digestion performance in volatile ammonium formate buffers at pH 3. Common peptides were digested and the resulting products analyzed by MS/MS sequencing. Then, mixtures of protein standards and extracted barley nuclear proteins were processed in the same way. Grape cysteine protease is nonspecific but shows a certain preference for Arg, Lys, and also Leu residues. Compared with papain, it seems not to require fully the presence of a large hydrophobic residue adjacent to that at the cleavage site. The enzyme is suitable for protein research as it produces peptides of a reasonable length in acidic pH.

KEYWORDS

cysteine protease, digestion, liquid chromatography, papain, peptide, RD21

1 | INTRODUCTION

The protein content of wine may reach several hundred milligrams per liter.[1] Yet, the soluble proteins represent only a minor wine constituent compared with the concentration of ethanol, organic acids, sugars, and glycerol.[2] They originate primarily not only from the grape pulp but also from the autolyzed winemaking yeast. Many proteins become precipitated at the end of fermentation. Those that remain after the vinification process are highly resistant to proteolysis and low pH of around 3 of the final product. It has been shown that wines vinified from different grapevine varieties contain similar soluble proteins.[3] A major group consists of chitinases and

Abbreviations: ACTH, adrenocorticotropic hormone; BSA, bovine serum albumin; CHCA, alpha-cyano-4-hydroxycinnamic acid; CYSP, cysteine protease; FDR, false discovery rate; PR, pathogenesis-related; RD21, responsive-to-desiccation (protein) 21; TCEP, tris(2-carboxyethyl)phosphine; TLP, thaumatin-like protein

thaumatin-like proteins (TLPs), which possess molecular masses in the range of 20 to 30 kDa. They belong to pathogenesis-related proteins (PR proteins): PR-3 and PR-5 family, respectively.[4] PR proteins are produced by plants as a part of defense mechanisms against fungal pathogens. Chitinases and TLPs are known as haze-active and thus responsible for the unattractive turbidity (haze) and proteinaceous sediments of bottled wine.[3] In principle, elevated temperatures induce a structural unfolding of the haze-active proteins and their association with nearby proteins or other wine components to form aggregates.[5] Other grape proteins detected in wine include, eg, lipid transfer protein, osmotin, peroxidase, stellacyanin, and vacuolar invertase. A grape cysteine protease (CYSP) was also found. Yeast (*Saccharomyces cerevisiae*) cells release not only hydrolases (asparaginase, glycosidase, phospholipase, and phosphatase) but also a haze-protective yeast mannoprotein. Laccase, proteases, and other hydrolases reflect the infection of grapes by *Botrytis cinerea*.[6-8]

The sequence of CYSP (NCBI Protein database accession number CBI30692) is largely homologous to those of many other plant CYSPs from the papain family (Figure S1) including for example the RD21 enzyme (the abbreviation comes from "Responsive-to-Desiccation") from *Arabidopsis thaliana*[9] or oryzains from rice.[10] CYSPs (EC 3.4.22) function via the formation of a thioester intermediate between the substrate's acyl part and the catalytic thiol group at the active site.[11] Papain cleavage specificity is based on binding of a bulky nonpolar residue (eg, Leu, Phe, or Val) at the P2 position in substrates. At the P1 position (the cleaved bond appears between P1 and P1′), papain rather prefers Arg but generally the enzyme has a broad specificity.[12,13] Similarly, proteolytic assays with peptides show that RD21-like enzymes prefer aromatic and hydrophobic residues at the P2 position.[14] The biological role of papain has not yet been well defined. But its presence in the latex and fruit of papaya as well as promiscuous cleavage specificity indicates the possible involvement in plant protection mechanisms against pests and fungi.[13] Indeed, many experimental evidences such as the results of knockout studies of the corresponding genes, inhibitions by pathogen effectors, induction of defense responses, and cell death plus a coreceptor role in signaling support the role of papain-like CYSPs as central hubs of plant immunity.[15,16] A CYSP was previously partially purified from white grapes of the Macabeo variety using a polyvinyl pyrrolidone treatment of the grape extract followed by ultrafiltration and gel permeation chromatography.[17] Polyacrylamide gel electrophoresis yielded a molecular mass value of 128 kDa, and the enzyme showed a pH optimum of 2.5.

In this work, we partially purified CYSP from a relatively large volume of white wine to analyze its biochemical properties and evaluate the cleavage specificity and applicability in mass spectrometry (MS) of proteins and peptides. The purification procedure combined ultrafiltration and liquid chromatography (LC). Both the molecular mass and isoelectric point values were determined. The enzyme is highly active at pH 3, which corresponds to the pH value of wine and digests peptides and proteins with low cleavage specificity. But anyway, it shows a preference for the C-termini of Arg, Lys, and Leu.

2 | MATERIALS AND METHODS

2.1 | Chemicals and protein material

Alpha-cyano-4-hydroxycinnamic acid (CHCA), angiotensin II, adrenocorticotropic hormone (ACTH) fragment 18-39, somatostatin-28, and Peptide Calibration Standard II were from Bruker Daltonik (Bremen Germany). β-Amylase from sweet potato, apoferritin from horse spleen, Benzonase (Cat. No. E1014), bovine pancreatic insulin, bovine serum albumin (BSA), bovine thyroglobulin, chicken lysozyme, chicken ovalbumin, cytochrome *c* from horse heart, myoglobin from horse heart, rabbit glycogen phosphorylase b and SOLu-Trypsin were from Sigma-Aldrich Chemie (Steinheim, Germany). The same vendor provided also dithiothreitol, iodoacetamide, and tris(2-carboxyethyl)phosphine (TCEP) hydrochloride. Alpha-chymotrypsin (Cat. No. 100451) was purchased from MP Biomedicals (Illkirch, France). Trifluoroacetic acid (TFA) and LC-MS grade solvents for LC of peptides (acetonitrile and water) were purchased from Merck (Darmstadt, Germany). All other chemicals were of the analytical purity grade.

2.2 | Ultrafiltration of wine

A nouveau unfined white wine made of grapes of the Irsai Oliver variety and originating from Rajhradice, South Moravia (Czech Republic), was centrifuged at 4200 *g* for 1 hour and then processed for protein isolation. In the first step, an ultrafiltration using 10-kDa cutoff filters was performed at laboratory temperature to reduce the volume from 4630 to 400 mL. The concentrated wine was subjected to a dialysis against 50-mM ammonium acetate for 48 hours when the dialysis buffer was replaced two times. Then the ultrafiltration continued to reach a final volume of 13 mL with a protein content of 15 mg mL^{-1}.

2.3 | Chromatographic purification of grape CYSP

The dialyzed and ultrafiltered wine proteins were separated by gel permeation chromatography on a Sepharyl S-300 HR (GE Healthcare, Uppsala, Sweden) column (2.5 cm i.d. × 50 cm) attached to a BioLogic LP low-pressure chromatography system (Bio-Rad, Hercules, CA, USA). The column was equilibrated in 50-mM ammonium acetate and operated at a flow rate of 2 mL min^{-1}. Each single run lasted for 180 minutes and was monitored at 280 nm. The respective protein load was 2 mL at a concentration of 15 mg mL^{-1}. The eluate was collected in five fractions according to the peaks observed in the chromatogram. The collected material was concentrated by ultrafiltration with a 10-kDa cutoff filter and the presence of CYSP in the respective fraction was confirmed by gel-based proteomics using nanoflow LC (nanoLC) coupled to matrix-assisted laser desorption/ionization (MALDI)- time-of-flight (TOF)/TOF MS/MS.[18] Alternatively to the cited protocol with modified bovine trypsin, SOLu-Trypsin (Sigma-Aldrich) and chymotrypsin were used for digestions. The above ultrafiltrate containing CYSP (referred to as the CYSP working solution from here on; 2 mg mL^{-1} protein) was further

separated by chromatofocusing for pI determination[19,20] on a Mono P HR 5/20 column (GE Healthcare) attached to a BioLogic Duo-Flow medium-pressure chromatographic system (Bio-Rad) equipped additionally with a QuadTec UV-Vis detector and pH-monitoring cell (Bio-Rad). The loading buffer used was 25-mM Bis-Tris adjusted to pH 7.0 by iminodiacetic acid. The elution buffers 1 and 2 contained 10% (v/v) Polybuffer 74 (GE Healthcare) adjusted to pH 4.0 and 3.0, respectively, by iminodiacetic acid. CYSP sample was thoroughly dialyzed against the loading buffer prior to chromatofocusing. The column was regenerated by repeated injections of 5-M NaOH (500 μL) and equilibrated in the loading buffer at a flow rate of 0.5 mL min^{-1}; the same flow rate was used for all separations. Each run had duration of 60 minutes. After sample injection (500-μL loop; 2 mg mL^{-1} protein content), the chromatography continued with the elution buffer 1 in the time window of 5 to 38 minutes and then with the elution buffer 2 during 38 to 60 minutes. The separation was monitored by absorption at 280 nm and by the pH of the eluate. Protein fractions were pooled and the solvent evaporated in a vacuum centrifuge. Then a protein aliquot (approximately 50 μg) was dissolved in 50 μL of 100-mM NH_4HCO_3 and mixed with 15 μL of 8-M urea for denaturation, which was followed by the addition of 4 μL of 55-mM dithiothreitol for disulfide reduction. The solution was incubated at 56°C for 30 minutes and then cooled down on ice. An alkylation step followed at laboratory temperature when 4 μL of 330-mM iodoacetamide were added and the solution incubated in the dark for 30 minutes. Final consecutive additions included 8 μL of 55-mM dithiothreitol and 118 μL of 100-mM NH_4HCO_3. The digestion was initiated by adding 1 μg of a modified trypsin[21] and continued at 37°C and 400 revolutions per minute (RPM) for 18 hours. Centrifugation at 10 000 *g* for 10 minutes followed. The supernatant was divided into 100-μL aliquots and evaporated in a vacuum centrifuge. The recovered tryptic peptides from a single aliquot were dissolved in 15 μL of 0.1% TFA by a short sonication step prior to desalting using ZipTip C18 pipette tips (Merck-Millipore, Carrigtwohill, Ireland). Finally, the sample was reconstituted in 15 μL of the same solvent and analyzed by nanoLC-MALDI-TOF/TOF MS/MS (see at the end of Section 2).

2.4 | Protein assay, protease activity assay, and SDS-PAGE

Protein concentration was determined by a spectrophotometric method with bicinchoninic acid[22] using BSA as a calibration standard. To estimate CYSP activity, BSA (100-μg aliquots), after a previous reduction with dithiothreitol and alkylation with iodoacetamide, was digested by CYSP added in different protease-to-substrate mass ratios (1:10, 1:50, 1:100, 1:500, 1:1000, 1:5000, 1:10 000, and 1:50 000). The reactions were conducted in 50-mM ammonium formate, pH 3.0, at 37°C for 18 hours. This was based on the previously described pH optimum of grape protease of 2.5[17] and considering the availability of ammonium formate as a volatile buffer for pH 3.0, which is a typical pH value of wine[8]. The time period of 18 hours was based on standard procedures of overnight protein digestions. Then the reaction mixtures were subjected to sodium dodecyl sulfate polyacrylamide gel electrophoresis (SDS-PAGE) (20-μg sample loads—calculated to the initial protein content). The remaining protein substrate after the digestion was evaluated and compared with an undigested control by reading the intensity of the respective BSA band on scanned gel images using GelAnalyzer 2010 software (developed by Istvan Lazar, http://gelanalyzer.com). SDS-PAGE was routinely performed in a discontinuous system according to Laemmli[23] using 4% stacking and 10% resolving polyacrylamide gels (1-mm thick). The electrophoresis took place in a Mini-Protean II apparatus (Bio-Rad) under a constant voltage of 110 V until the marker dye reached the bottom of the gel slab. After electrophoresis, the gels were stained by Bio-Safe Coomassie Stain (Bio-Rad).

2.5 | Peptide digestions by grape CYSP

Peptide substrates (angiotensin II, ACTH fragment, insulin, and somatostatin) were each dissolved in LC-MS grade water to make stock solutions of 750 to 1000 pmol μL^{-1}. The stock solutions were diluted in 50-mM ammonium formate, pH 3.0, to achieve final peptide concentrations of 3 to 4 pmol μL^{-1}. The CYSP working solution (1 μL) was added to a volume of 25 μL of the diluted peptide solution and the mixture was incubated at 37°C for 30 minutes. This time period was selected to achieve a complete or advanced digestion of the analyzed peptide. Then the solvent was evaporated in a vacuum centrifuge and the collected peptide fragments were dissolved in 20 μL of 0.1% TFA (5-minute sonication), desalted using ZipTip C18 pipette tips (Merck-Millipore) and analyzed by MALDI-TOF/TOF MS/MS analyses (see at the end of this section).

2.6 | Protein digestions by grape CYSP

A model protein mixture was prepared by dissolving BSA, bovine thyroglobulin, chicken lysozyme, chicken ovalbumin, equine apoferritin, equine cytochrome *c*, equine myoglobin, rabbit glycogen phosphorylase b, and sweet potato β-amylase in LC-MS grade water. The final concentration of each protein in the mixture was 0.11 mg mL^{-1}. Then the in-solution reduction and alkylation steps were performed as described above. Additionally, 1 μL of 50% formic acid ensured acidification plus 118 μL of 50-mM amonnium formate, pH 3.0, were added instead of 50-mM NH_4HCO_3. CYSP (1 μL of the working solution) was used, and the proteins were digested at 37°C and 400 RPM for 18 hours. After a centrifugation at 10 000 *g* for 10 minutes, the supernatant was divided into two aliquots (100 μL) and evaporated in a vacuum centrifuge. The collected peptides were dissolved in 20 μL of 0.1% TFA (5-minute sonication) and desalted using ZipTip C18 pipette tips (Merck-Millipore). The desalted peptide mixture was diluted 10 times prior to nanoLC-MALDI-TOF/TOF MS/MS analysis (see at the end of this section).

Barley nuclear proteins were extracted from 10 million G2-phase nuclei collected by flow cytometry as described previously.[18] The nuclei were suspended in 40 μL of the Benzonase digestion buffer (50-mM Tris-HCl, 2-mM $MgCl_2$, pH 8.0), sonicated for 15 minutes and incubated at 70°C and 900 RPM for 5 hours. The sample was

cooled down, and 20 µL of 8-M urea and 10-mM dithiothreitol in the Benzonase digestion buffer were added. This was followed by incubation at 25°C and 950 RPM for 1 hour. After mixing by a pipette with repeated aspiration and release of the suspension, DNA digestion was initiated by adding 0.5 µL of the commercial Benzonase solution and continued at 25°C overnight. The tube content was spun down, and the proteins reduced by adding 15 µL of 5-mM TCEP in 50-mM Tris-HCl, pH 8.0, followed by incubation at 25°C and 400 RPM for 45 minutes. Next, cysteine alkylation was achieved by adding 15 µL of 50-mM iodoacetamide in 50-mM Tris-HCl, pH 8.0, and incubation in the dark at 25°C for 30 minutes. The reaction mixture was then acidified by 0.5 µL of 50% formic acid and diluted with 150 µL of 50-mM ammonium formate, pH 3.0. The CYSP working solution (1 µL) was added, and the proteins are digested at 37°C and 400 RPM for 18 hours. After a centrifugation at 10 000 *g* for 10 minutes, the supernatant was evaporated in a vacuum centrifuge. The collected peptides were reconstituted in 20 µL of 0.1% TFA (5-minute sonication), desalted using ZipTip C18 pipette tips (Merck-Millipore) and then analyzed by nanoMALDI-TOF/TOF MS/MS (see at the end of this section).

2.7 | MS of peptides

Mass spectrometric analyses were performed on an ultrafleXtreme MALDI-TOF/TOF mass spectrometer equipped with smartbeam-II laser providing a repetition rate of up to 2000 Hz (Bruker Daltonik). A Dionex UltiMate3000 RSLCnano liquid chromatograph (Thermo Fisher Scientific, Germering, Germany) connected to a Proteineer fc II fraction collection device (Bruker Daltonik) was used for nanoLC-MALDI TOF/TOF MS/MS. The experimental setup including the analytical column, pre-column, composition of mobile phases, flow rates, gradient programming, and collecting of the eluate on the MALDI target plate as well as the automated MS and MS/MS data acquisitions were the same as described previously.[18] Database searches were performed either using ProteinScape 3.1 (Bruker Daltonik) and Mascot Server 2.4 (Matrix Science, London, UK) or PEAKS Studio 8 (Bioinformatics Solutions, Waterloo, ON, Canada) software. A Microflex LRF20 MALDI-TOF mass spectrometer (Bruker Daltonik) was used for a fast evaluation of digestion mixtures.

3 | RESULTS AND DISCUSSION

The proteins isolated by ultrafiltration from the Irsai Oliver white wine sample were separated by gel permeation chromatography on Sephacryl S-300 HR and collected in five fractions (Figure 1A). Fraction 2 contained grape CYSP, which could be confirmed by nanoLC-MALDI-TOF/TOF MS/MS (NCBI Protein accession number: CBI30692 and gi|297740510) after SDS-PAGE and in-gel digestion (Table S1). A molecular mass value of 190 kDa was estimated from the elution time of fraction 2 and a column calibration made with protein markers (not shown). During repeated separations, fraction 2 was collected starting from the elution time of 56 minutes representing a boundary with the partially overlapping fraction 1. The total protein yield was 6 mg. The enzyme could not be separated completely from a yeast asparaginase (EC 3.5.1.1; NCBI Protein accession number: AJT33259 and gi|767254761) prevailing in fraction 1. Records in the literature describe asparaginases as oligomeric proteins.[24] A high molecular mass value of 800 kDa has been published for the secreted and glycosylated enzyme from *S. cerevisiae*,[25] and elucidated by an aggregation of the oligomers.[24] Recently, a monomer mass of 45 kDa was reported, which is higher than a sequence-based prediction of 37.5 kDa because of the glycosylation.[26] Both CYSP and asparaginase provided two closely associated bands on the polyacrylamide gel (Figure 1B). It seems that CYSP also forms oligomers and because of its potential glycosylation it might aggregate as well. We always identified CYSP at the top of polyacrylamide gels for different wine samples in our previous work on wine proteins,[8] and the first published experimental evidence suggested a molecular mass value of 128 kDa.[17] A homologous protease RD21 isolated from daikon radish (*Raphanus sativus*) was found to form aggregates involving trimers and tetramers.[27] Interestingly, CYSP-based peptides could be detected by MS/MS also for fraction 3, which would correspond to a molecular mass of around 30 kDa.

The amino acid sequence deposited under the accession number CBI30692 in the NCBI protein database comprises 377 amino acids (Figure S2). It comes from the results of a *Vitis vinifera* genome sequencing project.[28] A bioinformatic analysis by the database administration revealed the presence of the coding region for a mature CYSP (positions 12-228; 217 amino acids in length) providing a theoretical molecular mass value of 23.5 kDa and isoelectric point (*pI*) of 3.6. Additionally, a granulin domain is present (positions 273-329) plus a region with proline repetitions (positions 243-263). The CYSP coding region contains a single potential *N*-glycosylation site. The whole sequence is completely identical with a major part of another sequence deposited under the accession number XP_002266308 and comprising 501 amino acids, which has been assembled by an automated computational analysis (Figure S2). At the N-terminus, this longer sequence additionally contains a signal peptide (positions 1-24, as determined using SignalP: http://www.cbs.dtu.dk/services/SignalP/) and a propeptide with cathepsin inhibitor domain, both similar to some other premature papain-like enzymes. It seems, based on an analogy with Arabidopsis RD21 protein,[29] that the grape CYSP is also synthesized as a pro-protein of around 56 kDa, which is further processed via an intermediate (approximately 40 kDa) containing the granulin part to the mature enzyme. It has been shown that the granulin domain mediates formation of aggregates, which prevent from efficient maturation.[29] Visualized CYSP bands on SDS-PAGE gels (Figure 1B) were used for in-gel protein digestions with SOLu trypsin, raffinose modified-trypsin,[21] or chymotrypsin. The peptide sequences, which were subsequently obtained by nanoIC-MALDI-TOF/TOF MS/MS of the in-gel digests, covered largely the coding region of CYSP but not at all the propeptide and granulin domain sequences. This would clearly indicate the presence of mature CYSP in wine.

The isoelectric point of 3.6 of the isolated CYSP was experimentally determined by means of chromatofocusing (Figure 2), and it is

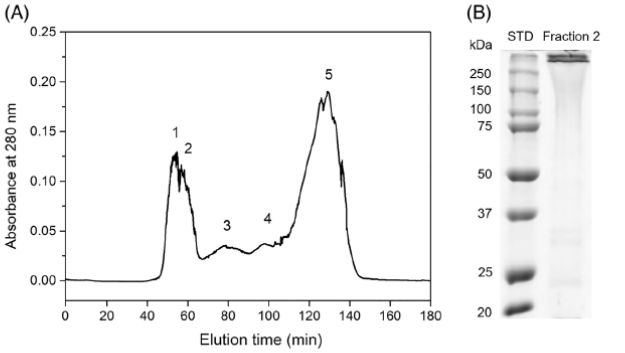

FIGURE 1 Gel permeation chromatography of wine proteins. A, shows a representative chromatogram; the sample load was 30 mg at a flow rate of 2 mL min^{-1} of the mobile phase (50-mM ammonium acetate). B, depicts a 10% SDS-PAGE gel with proteins separated from fraction 2 obtained by the chromatography. The gel was stained using Bio-Safe Coomassie Stain (Bio-Rad); from the left: protein standards (Precision Plus, Bio-Rad) with the indicated molecular mass and a fraction-2 sample (15 µg). The sample was separated into two bands containing yeast asparaginase (top) and CYSP (bottom).

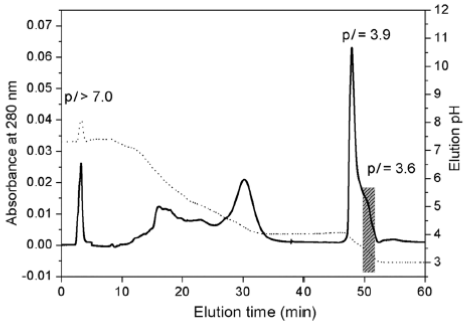

FIGURE 2 Chromatofocusing of grape CYSP. Enzyme sample was first obtained by gel permeation chromatography (see in Figure 1) and then separated in linear pH gradient (shown as a dotted line) produced using Polybuffer 74 on Mono P column. The flow rate was 0.5 mL min^{-1}, 1 mg of sample was loaded. Fraction containing CYSP was collected as indicated by a hatched and shadowed box; a *pI* value of 3.6 was deduced. Yeast asparaginase was coeluted and showed a *pI* value of 3.9.

consistent with the abovementioned theoretical prediction from the coding sequence. At the same time, the procedure appeared very efficient for a final purification of the enzyme. But we preferred the CYSP preparation after gel permeation chromatography for further experiments involving MS analyses because of the presence of low-molecular-weight ampholytes in the elution buffer during chromatofocusing, which could disturb if not completely removed, e.g., by dialysis. The contaminating yeast asparaginase (EC 3.5.1.1) in principle cannot interfere in proteolytic reactions. The reaction mechanism of asparaginase does not involve hydrolysis of a peptide bond. Instead, the enzyme acts on free asparagine yielding aspartate and ammonia. Moreover, it shows neutral or slightly basic pH optimum[24].

The activity of CYSP was evaluated by monitoring a protein digestion in time using SDS-PAGE. BSA aliquots were incubated at 37°C for 18 hours after applying different CYSP-to-BSA mass ratios, and the amount of the digested protein was calculated based on the intensity ("volume") of the corresponding Coomassie-stained BSA bands (Figure 3). It can be seen that the ratios from 1:10 to 1:100 resulted in a complete BSA degradation at the protein level. For those samples, where a BSA band was still visible after incubation (1:500-1:50 000), the decreased staining intensity compared with undigested control allowed calculating of the specific activity yielding an average value of 0.2 nkat mg^{-1}. This is impressive considering that the grape enzyme is active despite the vinification procedure and storage of the nouveau wine for several months prior to its isolation. Such stability is advantageous when considering the use of CYSP for laboratory purposes.

MS experiments were conducted to check the performance and specificity of CYSP in peptidolytic and proteolytic reactions. First, a few peptide standards were chosen including ACTH, angiotensin II, insulin, and somatostatin-28. The obtained results are illustrated in Figures S3 and 4. ACTH fragment 18-39 (RPVKVYPNGAEDESAEAFPLEF; *m/z* 2465.2) was digested completely to yield small fragments. Only short digestion times (10 minutes) allowed to see larger fragments corresponding e.g. to peptides with *m/z* 1344.7 (RPVKVYPNGAED) and 1631.8 (RPVKVYPNGAEDESA). Angiotensin II (DRVYIHPF; *m/z* 1046.6) was cleaved after the arginine, valine, and tyrosine residues as confirmed by the following fragment peptides: VYIHPF (*m/z* 775.4), YIHPF (*m/z* 676.3), and IHPF (*m/z* 513.3) plus DRVY (*m/z* 552.3), respectively. Somatostatin-28 (SANSNPAMAPRERKAGCKNFFWKTFTSC, with a disulfide bridge, *m/z* 3147.5) was hydrolyzed by CYSP after the first lysine residue producing a disulfide-containing peptide (K)↓AGCKNFFWKTFTSC (*m/z* 1637.8) as a major fragment. Another somatostatin fragments (Figure 4) corresponded to disulfide-containing peptides (R)↓KAGCKNFFWKTFTSC (*m/z* 1765.9) and (G)↓CKNFFWKTFTSC (*m/z* 1509.8). Many peptides were observed in the digest of insulin (*m/z* 5734.6). They appeared in the *m/z* range of 850 to 2800, eg, *m/z* 1272.6 yielding the sequence of (C)↓GERGFFYTPKA↓(R). The peptide digestion results indicated non-specific cleavages with a limited preference for the basic residues Arg and Lys at the substrate position P1. The broad cleavage preference of CYSP was investigated in more detail by performing proteolytic treatment of a model and real mixture

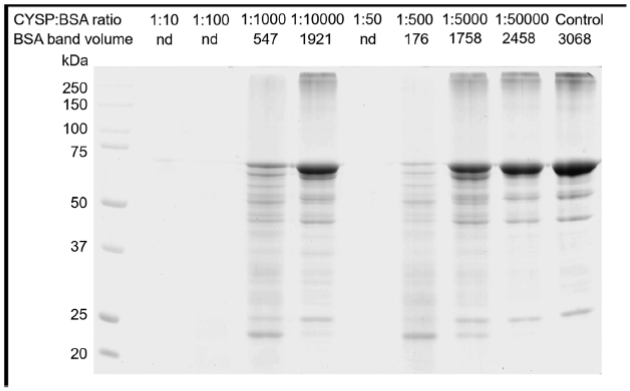

FIGURE 3 Activity assay of grape cysteine protease (CYSP). Bovine serum albumin (BSA) aliquots were mixed with CYSP at different protease-to-sample mass ratios and digested in solution at 37°C. Then the reaction mixtures were separated by SDS-PAGE, and the disappearance of the BSA band was quantified to calculate the corresponding specific activity value. The ratios of the reactants and scanned BSA band volumes are provided at the top of each sample separation lane. STD abbreviation denotes the separation lane of protein standards (Precision Plus, Bio-Rad); the respective molecular masses are indicated on the left.

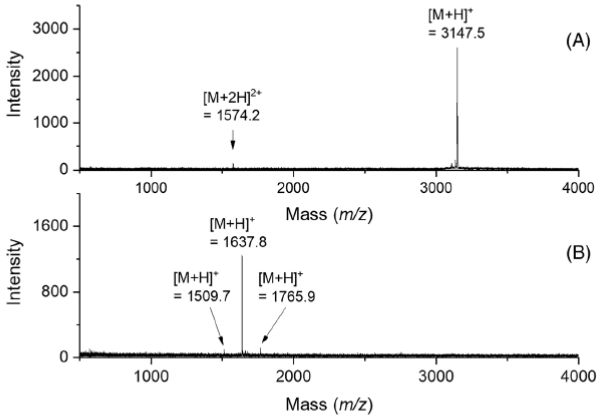

FIGURE 4 MALDI-TOF MS of somatostatin-28 and its fragments generated by grape CYSP. A, provides a mass spectrum of intact somatostatin; B, shows somatostatin fragments after the digestion. Both spectra were acquired on Microflex LRF20 MALDI-TOF mass spectrometer operating in the linear positive ion mode. CHCA served as a matrix, it was dissolved to a concentration of 5 mg mL^{-1} in acetonitrile: 2.5% trifluoroacetic acid, 7:3, v/v. The sample was deposited using a standard dried-droplet technique.

of proteins. The former sample contained nine proteins spanning a large molecular mass range of 12 to 670 kDa; the latter one was composed of proteins extracted from barley nuclei sorted by flow cytometry (Table S1). The digestion was followed by nanoLC-MALDI-TOF/TOF MS/MS analyses: 342 peptides (peptide-to-spectrum matches with an FDR of 0.9 %) were identified for the digested model mixture and 148 (FDR of 0.8 %) for the sample of barley nuclear proteins. An average peptide length was 13 amino acids, whereas a minimum length was six amino acids. Table 1 shows an overview of amino acid residues identified at the positions P1 and P2 in investigated protein substrates when the cleavage site is defined between P1 and P1′ according to the established terminology (… P3-P2-P1↓P1′-P2′-P3′ … .).[11] The obtained results were compared with numbers downloaded from the MEROPS database (https://www.ebi.ac.uk/merops/) for papain and a protease RD21. CYSP preferentially cleaves at the carboxyl side of Arg, similarly to papain and RD21.[13,14] Lys and Leu are also preferred. In fact, the enzyme accepts almost all other amino acids at the P1 position but with a significantly lower incidence compared with the mentioned group of three. As regards to the P2 position, the downloaded MEROPS data for papain and RD21 show Leu as the most frequent residue followed by Phe and Val. For CYSP, the P2 position seems to be less strictly required to be occupied by a narrow group of hydrophobic residues. Gly, Ala, Ile, Tyr, Ser, Thr, Asn, and Glu (not charged at pH 3.0) were markedly represented.

To summarize and conclude, a native grape CYSP can be isolated from wine by ultrafiltration and gel chromatography in a sufficient purity, which allows its further use in digesting proteins and peptides for MS-based research purposes. The enzyme is very stable as it survives the whole vinification process and persists in stored wine for a long time. It is highly active at pH 3, which is a common pH value of wine,[8] and thus applicable in volatile ammonium formate buffers. This would be an advantage as the acidic pH may be useful in specific

TABLE 1 The cleavage site preference of grape CYSP

	Amino Acid																		
P1 or P2 substrate position	G	P	A	V	L	I	M	F	Y	W	S	T	C	N	Q	D	E	K	R	H
P1 (*model mix*), CYSP	15	3	18	2	50	6	4	18	14	2	8	12	7	9	9	14	16	58	70	1
P2 (*model mix*), CYSP	31	5	31	23	26	22	7	9	8	5	23	36	2	23	10	10	31	17	14	3
P1 (*barley nuclear*), CYSP	6	1	5	0	27	0	0	13	8	0	1	0	0	3	0	2	0	36	35	1
P2 (*barley nuclear*), CYSP	14	3	13	16	8	16	0	8	12	0	8	3	0	3	0	2	8	16	6	2
P1, MEROPS, papain	6	1	3	2	6	1	4	10	3	1	2	4	2	3	1	2	2	1	28	3
P2, MEROPS, papain	1	2	3	6	36	1	3	8	4	1	1	5	1	1	1	1	3	2	2	2
P1, MEROPS, RD21	0	0	0	0	0	0	0	1	0	0	1	2	0	0	1	1	0	3	10	0
P2, MEROPS, RD21	1	0	1	4	4	0	0	3	0	0	1	0	0	0	0	0	0	2	3	0

Note. The table provides incidence numbers deduced from the experimental results with model protein mixture and barley nuclear proteins (almost 500 peptides were analyzed). The data for papain and RD21 were retrieved from the MEROPS database (https://www.ebi.ac.uk/merops/). Shadowing indicates the most preferred residues at the P1 and P2 substrate positions.

Abbreviation: CYSP, cysteine protease.

cases. The enzyme is homologous to papain as well as other enzymes from the papain-like family (Figure S1). Similarly to papain and RD21 protease, it is nonspecific but preferentially produces peptides terminated with an arginine residue, but frequently also with Lys and Leu residues. It seems that, contrary to papain, there is no strict rule for the presence of a large hydrophobic residue at the P2 substrate position (next to that at the cleavage site on the N-terminal side). Finally, this work shows a novelty in the field of sample proteolysis in proteomics. Specific proteases are no more unsubstitutable for protein identifications because of the development of fast LC-MS/MS systems for data-independent analyses and novel database searching algorithms.

ACKNOWLEDGEMENTS

This work was supported from ERDF project "Plants as a tool for sustainable global development" (No. CZ.02.1.01/0.0/0.0/16_019/0000827). Dr Beáta Petrovská from the Institute of Experimental Botany, Czech Academy of Sciences, is thanked for providing us with barley nuclei.

ORCID

Zdeněk Perutka https://orcid.org/0000-0002-5105-2236
Marek Šebela https://orcid.org/0000-0001-9835-1375

REFERENCES

1. Ferreira RB, Piçarra-Pereira MA, Monteiro S, Loureiro VB, Teixeira AR. The wine proteins. *Trends Food Sci. Technol.* 2001;12:230. https://doi.org/10.1016/S0924-2244(01)00080-2
2. Jackson RS. *Wine Science: Principles and Applications.* Amsterdam: Academic Press; 2008.
3. Waters EJ, Shirley NJ, Williams PJ. Nuisance proteins of wine are grape pathogenesis-related proteins. *J. Agric. Food Chem.* 1996;44:3. https://doi.org/10.1021/jf9505584
4. Enoki S, Suzuki S. In: Morata A, Loira I, eds. *Grape and Wine Biotechnology*. London: IntechOpen; 2017:43-57.
5. Marangon M, Van Sluyter SC, Waters EJ, Menz RI. Structure of haze forming proteins in white wines: *Vitis vinifera* thaumatin-like proteins. *PLoS ONE.* 2014;9:e113757. https://doi.org/10.1371/journal.pone.0113757
6. Kwon SW. Profiling of soluble proteins in wine by nano-high-performance liquid chromatography/tandem mass spectrometry. *J. Agric. Food Chem.* 2004;52:7258. https://doi.org/10.1021/jf048940g
7. Marangon M, Van Sluyter SC, Haynes PA, Waters EJ. Grape and wine proteins: their fractionation by hydrophobic interaction chromatography and identification by chromatographic and proteomic analysis. *J. Agric. Food Chem.* 2009;57:4415. https://doi.org/10.1021/jf9000742
8. Perutka Z, Šufeisl M, Strnad M, Šebela M. High-proline proteins in experimental hazy white wine produced from partially botrytized grapes. *Biotechnol. Appl. Biochem.* 2019;66:398. https://doi.org/10.1002/bab.1736
9. Koizumi M, Yamaguchi-Shinozaki K, Tsuji H, Shinozaki K. Structure and expression of two genes that encode distinct drought-inducible cysteine proteinases in *Arabidopsis thaliana*. *Gene*. 1993;129:175. https://doi.org/10.1016/0378-1119(93)90266-6
10. Watanabe H, Abe K, Emori Y, Hosoyama H, Arai S. Molecular cloning and gibberellin-induced expression of multiple cysteine proteinases of rice seeds (oryzains). *J. Biol. Chem.* 1991;266:16897.
11. Dunn BM. In: Beynon R, Bond JS, eds. *Proteolytic Enzymes. A Practical Approach*. Oxford: Oxford University Press; 2001:77-104.
12. Glazer AN, Smith EL. In: Boyer PD, ed. *The Enzymes*. Vol.III New York: Academic Press; 1971:501-546.
13. Storer AC, Ménard R. in *Handbook of Proteolytic Enzymes*, (Eds. Barrett A, Rawlings N, Woessner J), Academic Press, Amsterdam, 2013, pp. 1858-1861. https://doi.org/10.1016/B978-0-12-382219-2.00418-X
14. van der Hoorn RAL. in *Handbook of Proteolytic Enzymes*, (Eds. Barrett A, Rawlings N, Woessner J), Academic Press, Amsterdam, 2013, pp. 1892-1896. https://doi.org/10.1016/B978-0-12-382219-2.00432-4
15. Misas-Villamil JC, van der Hoorn RAL, Doechlemann G. Papain-like cysteine proteases as hubs in plant immunity. *New Phytol.* 2016;212:799. https://doi.org/10.1111/nph.14117
16. Shindo T, Misas-Villamil JC, Hörger A, Song J, van der Hoorn RAL. A role in immunity for Arabidopsis cysteine protease RD21, the ortholog of the tomato immune protease C14. *PLoS ONE.* 2012;7:e29317. https://doi.org/10.1371/journal.pone.0029317

17. Expósito JM, Cordillo CM, Mariño JIM, Iglesias JLM. Purification and characterization of a cysteine protease in *Vitis vinifera L.* grapes (Macabeo variety). *Food/Nahrung*. 1991;2:139. https://doi.org/10.1002/food.19910350204

18. Petrovská B, Jeřábková H, Chamrád I, et al. *Cytogenet. Genome Res.* 2014;143:78. https://doi.org/10.1159/000365311

19. Sluyterman LAAE, Elgersma O. Chromatofocusing: Isoelectric focusing on ion-exchange columns. *I. General principles. J. Chrom.* 1978;150:17. https://doi.org/10.1016/S0021-9673(01)92092-8

20. Sluyterman LAAE, Wijdeness J. Chromatofocusing: Isoelectric focusing on ion-exchange columns. *II. Experimental verification. J. Chrom.* 1978;150:31. https://doi.org/10.1016/S0021-9673(01)92093-X

21. Šebela M, Štosová T, Havliš J, et al. Thermostable trypsin conjugates for high-throughput proteomics: synthesis and performance evaluation. *Proteomics*. 2006;6:2959. https://doi.org/10.1002/pmic.200500576

22. Smith PK, Krohn RI, Hermanson GT, et al. Measurement of protein using bicinchoninic acid. *Anal. Biochem.* 1985;150:76. https://doi.org/10.1016/0003-2697(85)90442-7

23. Laemmli UK. Cleavage of structural proteins during the assembly of the head of bacteriophage T4. *Nature*. 1970;227:680. https://doi.org/10.1038/227680a0DO

24. Wriston JC Jr. Asparaginase. *Methods Enzymol.* 1985;113:608. https://doi.org/10.1016/S0076-6879(85)13082-X

25. Dunlop PC, Meyer GM, Ban D, Roon RJ. Characterization of two forms of asparaginase in *Saccharomyces cerevisiae*. *J. Biol. Chem.* 1978;253:1297.

26. Ferrara MA, Severino NMB, Valente RH, Perales J, Bon EPB. High-yield extraction of periplasmic asparaginase produced by recombinant *Pichia pastoris* harbouring the *Saccharomyces cerevisiae ASP3* gene. *Enzyme Microb. Technol.* 2010;47:71. https://doi.org/10.1016/j.enzmictec.2010.05.001

27. Kikuchi Y, Saika H, Yuasa K, Nagahama M, Tsuji A. Isolation and biochemical characterization of two forms of RD21 from cotyledons of daikon radish (*Raphanus sativus*). *J. Biochem.* 2008;144:789. https://doi.org/10.1093/jb/mvn132

28. Jaillon O, Aury JM, Noel B, et al. The grapevine genome sequence suggests ancestral hexaploidization in major angiosperm phyla. *Nature*. 2007;449:463. https://doi.org/10.1038/nature06148

29. Yamada K, Matsushima R, Nishimura M, Hara-Nishimura I. A slow maturation of a cysteine protease with a granulin domain in the vacuoles of senescing Arabidopsis leaves. *Plant Physiol.* 2001;127:1626. https://doi.org/10.1104/pp.010551

SUPPORTING INFORMATION

Additional supporting information may be found online in the Supporting Information section at the end of the article.

How to cite this article: Perutka Z, Šebela M. Mass spectrometry of peptides and proteins using digestion by a grape cysteine protease at pH 3. *J Mass Spectrom.* 2020;55:e4444. https://doi.org/10.1002/jms.4444

Příloha 8:

Perutka, Z., Voženílek, V., Šebela, M., 2021. Wine Contaminations and Frauds From the Bioanalytical and Biochemical Points of View. In *Comprehensive Foodomics* Vol. 3, (pp. 104-116). Elsevier.

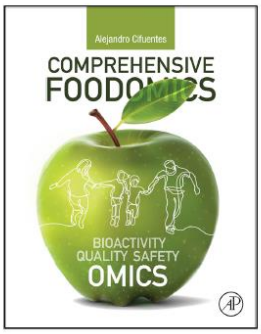

From Perutka, Z., Voženílek, V., Šebela, M., 2021. Wine Contaminations and Frauds From the Bioanalytical and Biochemical Points of View. In: Cifuentes, A. (Ed.), Comprehensive Foodomics, vol. 3. Elsevier, pp. 104–116.
ISBN: 9780128163955

Elsevier

3.09 Wine Contaminations and Frauds From the Bioanalytical and Biochemical Points of View

Zdeněk Peruťka[a], Vít Voženílek[b], and Marek Šebela[a], [a]Department of Protein Biochemistry and Proteomics, Centre of the Region Haná for Biotechnological and Agricultural Research, Faculty of Science, Palacký University, Olomouc, Czech Republic; and [b]Department of Geoinformatics, Faculty of Science, Palacký University, Olomouc, Czech Republic

3.09.1	Geographical Authenticity of Wine	104
3.09.2	Accidental Wine Contaminations	105
3.09.3	Validation of Conformity to Regulations of Wine Production	107
3.09.4	Analysis of Authenticity and Adulteration	108
3.09.5	Wine Proteins	110
3.09.6	Conclusions	113
Acknowledgments		114
References		114

List of abbreviations:

AC Appellation Control
AGP Arabinogalactan-protein
AOC Appellation d'Origine Contrôlée
AVA Approved Viticultural Areas
EA Elemental analysis
ESI Electrospray ionization
GC–MS Gas chromatography coupled to mass spectrometry
GI Geographical Indication
HPLC High performance liquid chromatography
IRMS Isotope ratio mass spectrometry
LC-MS Liquid chromatography coupled to mass spectrometry
MALDI-TOF Matrix-assisted laser desorption/ionization time-of-flight
MS Mass spectrometry
OTA Ochratoxin
PCA Principal component analysis
PDO Protected Designation of Origin
PGI Protected Geographical Indication
PR proteins Pathogenesis-related proteins
QbA Qualitätswein bestimmter Anbaugebiete
SIRA Stable isotope ratio analysis
SNIF-NMR Site-specific natural isotopic fractionation-nuclear magnetic resonance
TCA 2,4,6-trichloroanisol
TLP Thaumatin-like protein
VDQS Vins Délimités de Qualité Supérieure
VOC Víno originální certifikace
VQA Vintners Quality Alliance

3.09.1 Geographical Authenticity of Wine

Wine quality standards in the European Union (EU) are subjected to EU and governmental regulations, which are tailored to the needs of each member country. These regulations cover many aspects ranging from what grape varieties can be grown for wine production to the rules of selling and consumption of wine (Jackson, 2008, pp. 577–640). Until 2008, two wine quality categories were recognized in the EU: Quality Wine Produced in a Specific Region (QWPSR) and Table Wine. Then they were replaced with

Comprehensive Foodomics, 2021, 104–116

PDO (Protected Designation of Origin) and PGI (Protected Geographical Indication) categories, which have been well described elsewhere (Meloni and Swinnen, 2013; Di Vita et al., 2019). Within this system, each EU country has its own quality categories, which correspond to PDO and PGI (wine appellations). PGI production rules are less stringent than those bound to PDO. One of the aims for introducing PGI was to avoid the term "table wine", along with its connotations of a low quality product. The related EU legislation attempts to prevent from any improper use of PDO and PGI protected names. In principle, PDO and PGI labels are applicable not only to wine, but to all foods and beverages. PDO refers to the production, processing and preparation, which all essentially depend on a particular region with specific geographical characteristics (including local geological and climate aspects) and recognized know-how plus other human factors. This is in accordance with a common belief that the local soil and vineyard topoclimate are responsible for distinctive attributes of wines from small delimited regions (Vondráková et al., 2013). On the other hand, a PGI product is closely linked to the geographical area in which it is produced, processed and prepared. It has certain reputation, quality or feature attributable to this area and thus at least one phase of the production process must occur there.

Except for the description of the delimited territory, Appellation Control (AC) laws may apply to the regulation of grape varietal use, maximum grape yields, alcohol content, and other quality factors. Many AC laws also regulate vineyard and production practices in addition to the geographical indication and grape authenticity. Periodic chemical and sensory evaluation tests are also applied. However, the system of AC laws cannot guarantee quality as such and should not be misinterpreted in this way (Jackson, 2008, pp. 577–640). Local producers simply cannot control what happens with the bottled wine after it is shipped out of the winery. Geographical indications may generate value added, especially at the consumer and retailer levels, while the effects on the economic performance of producers are more heterogeneous and dependent on specific local conditions (Cei et al., 2018). But there are also criticisms that any rigidness in the regulation rules may obstruct viticultural flexibility, technological innovations and introduction of modern modifications to the traditional practice.

The first complex national AC laws were established in France in the 1930s (Jackson, 2008, pp. 577–640) with the aim to assure the authenticity and increase the reputation of French regional wines as well as to preclude the usage of registered names elsewhere. This AC system originally comprised a single category (*Appellation d'Origine Contrôlée*, AOC) prior to its extension by including the less distinguished categories of *Vins Délimités de Qualité Supérieure* (VDQS, which has gradually been upgraded to the AOC category since then), *Vins de Pays* and *Vins de Table*. An important part of the AOC regulations is the concept of *terroir* (unique vineyard site) which is based on local soil and climatic conditions. For historical reasons, a few regions also use the *cru classé* ranking of vineyards or wineries. Many other European countries established their AC laws based on the French AOC classification (Jackson, 2008, pp. 577–640). Typical examples are the *Denominazione di Origine Controllata* and *Denominazione di Origine Controllata e Garantita* in Italy (also sensory properties are guaranteed in the latter case) (Fregoni, 1992), *Denominación de Origen* in Spain, *Denominação de Origem Controlada* in Portugal and *Districtus Austriae Controllatus* in Austria. The German system separates geographical and quality aspects. There are two major categories of wine in Germany, *Landwein* and quality wine, which is in accordance with the general EU regulation. The least demanding quality wine as regards to the grape maturity is the category *Qualitätswein bestimmter Anbaugebiete* (QbA). The superior quality level, *Prädikatswein* (quality wine with specific attributes), is classified in more categories based on the ripeness of the grapes (because Germany's climate makes it a challenge to ripen grapes fully) (Jackson, 2008, pp. 577–640). The legislation of the Czech Republic (the approved Czech wine-producing regions are shown in Fig. 1; Hájková et al., 2012) recognizes quality and superior quality wines (the latter with a classification similar to that in Germany), as well as quality wines with a geographical indication (*Víno originální certifikace*, VOC) (Andrusiów, 2015).

Outside Europe, South Africa is an example of establishing a comprehensive AC system, which resembles in part the European legislation, but simultaneously follows its own concepts. Precisely, the geographical designation appears in a hierarchy of several levels from regions to individual vineyards. The Australian legislation uses the term Geographical Indication (GI) for wine-producing regions, which emphasizes the authenticity of grapes. The appellations in the United States are based on Approved Viticultural Areas (AVAs). There is no stringent control of the cultivars as well as viticultural and vinicultural practices (Jackson, 2008, pp. 577–640), which documents that the regulation is primarily directed to the authenticity and not to quality concerns. In Canada, the province of British Columbia has implemented its AC laws. The second wine-producing province, Ontario, has a similar but voluntary regulation system, which is administered by Vintners Quality Alliance (VQA). It is based on permitted cultivars, sensory tests and several protected viticultural areas (Jackson, 2008, pp. 577–640).

3.09.2 Accidental Wine Contaminations

There are two ways how contaminants can appear in wine. First, the technological pollutants and additives used during the wine-making process must inevitably appear in wine. Second, the contamination includes environmental and microbiological agents and their byproducts. For example, air-spread fertilizers, engine exhausts and other human products contaminate grapes before the harvest (Bertrand and Beloqui, 2009; He et al., 2016; Machado et al., 2016). The composition of vineyard soil influences wine in a similar way (Jackson and Lombard, 1993). Any grape contact with extraneous materials during harvest and vinification processes is imprinted in the juice composition. Nowadays, analytical methods are sensitive enough, which even allows detection of traces of hydrocarbons from oil or fuel that originate from vineyard machinery, in final wines (Bertrand and Beloqui, 2009). Similarly, the use of additives, plastic boxes and containers, preservatives, stabilizers or clarifying agents is detectable in wine or must. Even alterations in the isotope composition of elements have been detected in wines produced since the Fukushima accident in 2011 as well as previous global nuclear incidents (Perrot et al., 2012). Modern analytical techniques are sensitive and accurate

Figure 1 The wine-producing regions of the Czech Republic. Information was adapted from Hájková, L., Voženílek, V., Tolasz, 2012. Atlas Fenologických PoměrŮ Česka (Atlas of the Phenological Conditions in Czechia). Czech Hydrometeorological Institute and Palacký University in Olomouc, Prague-Olomouc.

enough to reveal the presence of pesticide residues in grapes, typically of insecticides and fungicides that are used to control pests and diseases, respectively, in vineyards. The maximum residue levels in grapes mostly range between 0.01 mg kg^{-1} and 5 mg kg^{-1}. The analytical aspects of pesticides in grapes have thoroughly been reviewed elsewhere (Cabras and Caboni, 2008, pp. 227–248; Grimalt and Dehouck, 2016) and are out of the scope of this chapter.

In addition, grape juice and pulp are occupied by microorganisms coming from the surface of wine berries and production environment and surfaces (Barata et al., 2012). Interestingly, the common vine pathogenic fungus *Botrytis cinerea*, can act either as the noble rot or it can degrade grapes in the form of gray mold infection (Fournier et al., 2013). Furthermore, compounds produced by pests and microbe-metabolized chemicals, such as insecticides, are also released into the grape juice (Bertrand and Beloqui, 2009). The level of ochratoxin A (OTA), produced by *Aspergillus* and *Penicillium* species, is monitored in grapes and related products (Belli et al., 2002). The mycotoxin has been shown nephrotoxic and hepatotoxic and classified as a possible human carcinogen (Petzinger and Ziegler, 2000). The maximum limit for OTA concentration in the European Union is 2.0 ng l^{-1}; higher incidence and levels of contamination have been found in dessert wines (Mateo et al., 2007). The fungi producing OTA occupy grapes starting from an early stage of their development. OTA concentration is increased during grape crushing or wounding. The pathogen *Dekkera bruxellensis* inhabits oak casks and produces a variety of vinyl pyrrolidons. These compounds, e.g. 2-acetyl-3,4,5-tetrahydropyridine, may cause the unfavorable mousy flavor of wine (Grbin et al., 2007). Additionally, red wine vinyl phenols derived from hydroxycinnamic acid and metabolized by that yeast strain taint wine aroma by the smell of horse sweat (Petrozziello et al., 2014). *Alternaria* species also belong to the grapevine mycobiota producing harmful chemicals (Scott et al., 2006). Their products, such as alternariol and alternariol monomethyl ether, both non-specific mycotoxins, may be detected in wine produced from infected grapes (Meena et al., 2017). To prevent from the microbial spoilage, sulfur dioxide is traditionally used in winemaking as an antioxidant agent (Ough and Crowell, 1987). The killer toxins of *Candida pyralidae* may act against wine pathogens without affecting the fermentation process (Mehlomakulu et al., 2014).

Fining and clarifying agents such as casein, egg yolk, chitosan, isinglass or gluten are other unnatural substances that may be found in wine. All these adsorbents are added to precipitate and remove phenolic and tannin compounds from wine; however, their presence is undesirable because of allergenicity (D'Amato et al., 2010). In addition, it seems that native grape proteins e.g. thaumatin-like proteins or chitinases and, especially, lipid transfer proteins, might also be responsible for consumer intolerance reactions (Jaeckels et al., 2015). The bottlenecks are the potential source of wine contamination by TCA (2,4,6-trichloroanisol) and TBA (2,4,6-tribromoanisol) that cause cork taint (Buser et al., 1982). These compounds are developed in cork stoppers during the wood bleaching process or may be absorbed into the material during storage. Occasionally, contaminated wooden casks may be the source of TCA in wine (Capone et al., 2002).

Metal ions are indispensable for enzymatic wine fermentation processes. The vineyard location, soil type, agricultural chemicals or fumes affect the wine levels of Na, K, Ca, Cu, Cd, Mn, Pb and Zn. However, the amount of these elements changes significantly

after the application of bentonite (Pyrzyńska, 2004; Kment et al., 2005). The pipes and tanks used for wine transport are the possible sources of metals such as Cr, Cu, Fe or Zn (Pyrzyńska, 2004). Historically, lead was the only material used for cooking pots or pipes. Moreover, already in the Roman era, wines were sweetened by lead acetate (Järup, 2003). At present, any application of heavy metals such as lead in wine industry, including the metal bottle caps, is of course forbidden. A high concentration of calcium, which originates from the bentonite fining treatment, could cause the precipitation of organic salts in wine. Elevated levels of natural grape elements potassium and aluminum are found for the same reason (Pyrzyńska, 2004). The removal of hydrogen sulfide by copper (II) sulfate may result in wine browning, which is initiated by an excess of copper as well as iron and manganese ions. Non-declared application of sulfur is classified as a kind of wine fraud (Martínez-Sierra et al., 2010). Apart from the copper sulfate additions, grapevine pesticides are the major sources of the unnatural copper in wine (He et al., 2016; Machado et al., 2016). The winemaking and cellar equipment made from nickel and chromium steels typically appears in a long-lasting contact with wine and thus it could raise their levels. Lithium is used as a denaturing agent for fraud wines in Italy (Pyrzyńska, 2004). Wine plastering (adding plaster to wine) was a traditional practice to protect wine from temperature changes during its transportation in the 19th century (Stanziani, 2009). The addition of gypsum or calcium sulfate also clarifies wine and regulates its acidity. Intentional wine additives such as sweeteners or colorants are discussed in the next chapter section.

3.09.3 Validation of Conformity to Regulations of Wine Production

Wine laws regulate the use of local brands, product composition and vinification processes. Grape variety mixing is one of the most controlled and regulated issue. The use of any undeclared variety is classified as a kind of wine adulteration. On the other hand, wine blending allows mixing of grapes and wines in a legal way (Ferrier and Block, 2001). Blended wines are characteristic for some wine-producing areas (Bordeaux, France) and grape varieties (Jackson, 2008, pp. 520–576), but this procedure can easily be misused. For instance, a more valuable wine is diluted with a cheaper one, or worthy grapes are blended with others and the product is declared as the original (Ferrier and Block, 2001). As an example, over 1,3 million liters of a mixture of Italian Sangiovese and inferior Lancellota wine declared as Brunello di Montalcino DOCG were seized in 2008 (Holmberg, 2010). Furthermore, sherry, port or vermouth are all legally produced by registered recipes, which include both the wine mixing and addition of alcohol and various botanicals. Typical characteristics of these wines are the use of grape varieties providing distinctive color and fortification by a wine distillate with alcohol volume content over 70% (Jackson, 2008, pp. 520–576). On the other hand, the increased sugar content is achieved by stopping fermentation prematurely, or by applying partially dried grapes. The volume content of alcohol reaches about 20%, which indicates that fortified wine cannot be produced by a natural fermentation process. Historically, an illegal blending of wines with Italian, Spanish or Algerian imports was practiced to overcome the period of phylloxera invasion and limited wine production in France in the 19th century (Stanziani, 2009). Nowadays, wine adulteration techniques are much more sophisticated, although basic practices such as a coloring, dilution with water and mislabeling are still frequently used.

In the case of cheap low-alcohol wines, methanol may be misused to increase the total alcohol content. The natural level of methanol in wine differs for white or red wines, however, the respective limits are set to 250 mg l^{-1} and 400 mg l^{-1} (Hodson et al., 2017). Wines tainted with poisonous quantities of industrial methanol were found in Italy in 1985. More than 20 people died in consequence (Stöckl, 2006). Another story started, when Austrian wine producers added diethylene glycol into wine to increase its sweetness. This "antifreeze-scandal" resulted in a 90% drop of the Austrian wine export in 1986 (Stöckl, 2006; Holmberg, 2010). Glycerol acts as a natural wine sweetener. The compound is produced during wine fermentation as the major ethanol by-product in concentrations of up to 10 g l^{-1} (Šehović et al., 2004). Synthetic glycerol can be revealed by positive identification of the technological contaminants such as methoxy-1,2-propanediol, and cyclic diglycerols (Dixit et al., 2005). Unnatural sweeteners such as acesulfame-K, aspartame, sodium cyclamate or saccharin are prohibited adulterants of table wines (Geana et al., 2012). Sugar addition, in any form, to the must before fermentation is banned in most countries and its application is approved only as bad-weather compensation. Grape sugar is metabolized into ethanol and the original $^{13}C/^{12}C$ ratio is preserved after fermentation (Weber et al., 1997). Interestingly, the carbon isotope ratio differs for grapes and other sugar sources. Products derived from C4 plants (such as corn and sugar cane) have higher ^{13}C content compared to a C3 plant (grape). The stable isotope ratio analysis (SIRA; see the next text section) can detect these changes, identify the way of wine adulteration and quantify the content of adulterants (Christoph et al., 2015). The sugar addition in the form of fructose-rich corn syrup may be indicated by the presence of 5-(hydroxymethyl)-2-furaldehyde (Geana et al., 2016). Dark berries are used to improve the color of red wines that are poor in anthocyanins or for a coloring of white grape juices. Mixing grapes and elderberries is one of the middle age originated practices. A more elaborated strategy resides in the addition of extracts from black rice or a different dark grape variety (von Baer et al., 2008). The use of synthetic colorants may even be hazardous for consumers. The most known artificial wine color boosters are Azorubine (E122), Amaranth (E123), Ponceau 4R (E124), Erythrosine (E127), Allura Red AC (E129) or Carmine (E120) for red wines and yellow pigments such as Tartrazine (E102), Quinoline and Sunset Yellows (E104 and E110, respectively) for white wines (Virtanen et al., 1999; Geana et al., 2016). Brilliant Blue FCF (E133) was recently detected in Vindigo and Imajyne blue wines on the French market (Galaup et al., 2019). High-performance liquid chromatography (HPLC) is commonly used to determine colorants by searching for their defined chemical markers (Virtanen et al., 1999).

Dilution of wine by water is a serious problem as there is no simple method for the detection of this fraud (Dordevic et al., 2013). The only possibility available is measuring the 18O/16O isotope ratio (Christoph et al., 2015). In the case of red wine, both a lower anthocyanin content and unnatural color may indicate a fraud (Geana et al., 2016). On the other hand, blending

grapes with a juice made of fruits rich in sugar adjusts the volume of the final wine with a minimum effect on its ethanol level. Detection of sorbitol above its natural concentrations of 100–1000 mg l^{-1} is an indicator (Burda and Collins, 1991). The simultaneous positive identification of chlorogenic acid then confirms the use of apple juice (Dennis et al., 1994). The level of organic acids in wine causes the tart, a refreshing taste (Jackson, 2008, pp. 332–417). Tartaric acid, the primary acidic wine component, maintains the chemical stability of wine. Malic acid reduces the pH of grapes and protects them during veraison (Jackson, 2008, pp. 332–417). Monitoring the above-mentioned organic acids and changes in their concentration during the vinification process helps to control it and determine the date of harvest (Mato et al., 2005; do Nascimento Silva et al., 2015). Furthermore, alteration in the concentrations of lactic and acetic acids produced by fermentation is indicative of a wrong manipulation or wine defect due to microbes (do Nascimento Silva et al., 2015).

Aging of red wines in oak casks, which has been used since the Roman era, improves the flavor and character much more than a simple aging in steel or plastic containers. A few dozen years old barrels are very valuable, and thus substitutes are used. The application of wood pellets combined with a controlled barrel ventilation and simulation of leaks during maturation imitates and accelerates wine aging (Garde-Cerdán and Ancín-Azpilicueta, 2006). The origin of carbon dioxide distinguishes naturally produced sparkling wines (Champagne, Cava) from cheap carbonated wines. The determination of the carbon isotope ratio is carried out if a counterfeit is suspected, similarly as for the wine ethanol (Christoph et al., 2015). Mislabeling on the bottle is the simplest method of wine fraud (Holmberg, 2010). Organized chains of wine resellers help to hide this practice (Bevin et al., 2006). Mislabeled bottles are sold at a higher price, which is certainly unjustified. To prevent this fraud, information on quality and quantity of wine produced from each vineyard would necessarily need to be available for an individual check (Bevin et al., 2006). The most elaborated kind of wine fraud is the production of limited collectable wine fakes. The premium collectable wines produced with a combination of appropriate bottles and labels may be priced by thousands of dollars (Lecat et al., 2017). The story about Rudi Kurniawan, the illegal American wine collector and professional fraudster, arrested for faking and selling more then 10 000 wine bottles in an overall price reaching hundreds millions of dollars, is a real illustration of the lucrative area of wine market (Lecat et al., 2017). It was estimated that the share of counterfeit wine sales on the European market is more than 10% (Holmberg, 2010), reaching over € 1.3 billion in 2015 (Lecat et al., 2017).

3.09.4 Analysis of Authenticity and Adulteration

Both geographic and varietal identity of wine is very important for consumers as they expect it goes hand in hand with quality. Regional wines can be differentiated reliably by a chemical analysis, while human sensory evaluation can fail in the correct identification, as it is not sufficiently precise. Another disadvantage of the latter approach is that it cannot be automated. The geographic authenticity of wines can be validated using discriminative procedures that are based, for example, on differences in the distribution and relative proportion of isotopes of several chemical elements, typically $^{2}H/^{1}H$, $^{13}C/^{12}C$, and $^{18}O/^{16}O$. The analyzed isotope ratios for water, sugar, organic acids and fermentation products (ethanol or glycerol) are influenced by abiotic and biotic fractionation processes (Christoph et al., 2015). In consequence, stable isotope patterns actually represent unique signatures for a certain vintage or place of origin. The environmental factors are related to thermodynamic and/or kinetic isotope effects during water evaporation, plus condensation and ^{18}O equilibration between water and carbon dioxide. The enrichment or depletion of the heavier stable isotopes ^{2}H and ^{18}O in precipitation water depends on: (1) latitude and altitude, (2) distance from the coast, (3) temperature and (4) rainfall amount. For example, ocean water contains more ^{18}O than clouds (Bréas et al., 1994). Transpiration through the leaf stomata or grape skin leads to the enrichment of both ^{2}H and ^{18}O in grapes or leaf water, which is influenced by relative humidity, sun exposure and viticultural practices (irrigation, maturation period, harvest timing). Another example of tracing the geographic authenticity and provenance of wine is the use of $^{87}Sr/^{86}Sr$ ratio (Almeida and Vasconcelos, 2004). From all natural strontium isotopes, only ^{87}Sr is radiogenic as it arises from the radioactive decay of ^{87}Rb. The abundance of radiogenic isotopes in minerals and rocks depends on the geological age and, consequently, it is connected to the respective geographic location. Each soil in vineyards is thus expected to have its own fingerprint strontium isotope composition, which may reliably be traceable by high-precision analytical methods. On the other hand, it has repeatedly been shown that no change in the $^{87}Sr/^{86}Sr$ ratio occurs as a result of the winemaking process (Almeida and Vasconcelos, 2004; Marchionni et al., 2016). The geographic origin can successfully be traced by infrared spectroscopy. The use of mid- or near-infrared spectroscopy to differentiate Cabernet Sauvignon wines from Australia, Chile and China provided more than 90% of reliably assigned samples (Hu et al., 2019).

Biotic isotope fractionation processes involve the action of enzymes. An example of the carbon $^{13}C/^{12}C$ isotope discrimination is known to occur within the process of CO_2 fixation during photosynthesis (Christoph et al., 2015). As regards to the product molecule in this reaction, two characteristic groups, C3 and C4 plants, have been established based on the production of phosphoglycerate (a C3 molecule) and oxaloacetate (a C4 molecule), respectively. The reaction of ribulose-bisphosphate carboxylase causes that the isotopic signature of C3 plants (e.g. grapevine, sugar beet, pea or wheat) shows higher degree of ^{13}C depletion compared to C4 plants (e.g. maize, sugar cane or millet), where the primary fixation enzyme is phosphoenolpyruvate carboxylase. Another isotope depletion effect has been described for deuterium and C3 plants. The addition of sugar to must or young wine (so-called chaptalization) is not allowed in many countries because of wine quality and authenticity, or it is permitted under a strict regulation for low-quality wine categories (Jackson, 2008, pp. 577–640). Sucrose or invert sugar, which is possibly added, is fermented to ethanol. The degree of chaptalization is therefore detected by distinguishing between the ethanol molecules originated from grapes or non-grape sources. This is usually done by determining the ratio of $^{13}C/^{12}C$ in ethanol (Martin, 1990). The $^{13}C/^{12}C$ isotope ratio, which

well characterizes the origin, can also be used to detect other organic compounds such as glycerol or carboxylic acids that are authentic in wine but may become subjects of adulteration (Christoph et al., 2015). The process of glucose fermentation is accompanied by the incorporation of hydrogen atoms from glucose and water into the molecule of ethanol, which can be confirmed using fully deuterated glucose or D_2O (Saur et al., 1968). It has been shown that the incorporation of deuterium from the two molecules is different. A majority of the sugar-based deuterium appears in the methyl group, whereas the water-based deuterium goes mostly to the methylene group. This transfer can be monitored by the use of SNIF-NMR (site-specific natural isotopic fractionation-nuclear magnetic resonance) (Martin and Martin, 1981), which has been adopted as an official method for wine analysis in the European Union (Cagliani et al., 2009, pp. 143–188). Here the determined $(D/H)_I$ ratio refers to the ethanol methyl group, whereas the $(D/H)_{II}$ ratio reflects the status of the methylene group. Finally, the R value is calculated from experimental results as a parameter applicable for authenticity evaluation: $R = 2\ (D/H)_{II}/(D/H)_I$. This method has its limitations for wine as the $(D/H)_{II}$ value is influenced by the conditions of fermentation – yeast strain and temperature (Fauhl and Wittkowski, 2000), but anyway, it is generally applicable in food analysis (Ciepelowski et al., 2018).

The isotopic ratio of wine molecules (ethanol, but also glucose, acids and wine water) can be determined conveniently by isotope ratio mass spectrometry (IRMS), which utilizes conversion of the analyzed compounds into gases by a combustion or pyrolysis. As an advantage, the sample quantity for IRMS is much lower than for NMR. Generally, analysis of stable isotopes for the assessment of food authenticity and quality is termed stable isotope ratio analysis (SIRA). But the term usually refers to IRMS as an experimental technique (Camin et al., 2016). Modern instruments for IRMS with high accuracy, precision and sensitivity are based on an electron ionization source, magnetic sector analyzer and a multi-collector detection arrangement with Faraday cups (Fig. 2).

There are several different interfaces available for introducing the analyzed sample. The most common are those when IRMS is coupled to an elemental analyzer (Fig. 2) or gas chromatograph (Muccio and Jackson, 2009). Gas chromatography coupled to mass spectrometry (GC–MS) is used mostly for volatile samples; initial non-volatiles, such as amino acids, can be derivatized, for example to yield *N*-acetylmethyl esters. Generally, the most optimal derivatization adds only the fewest possible number of new

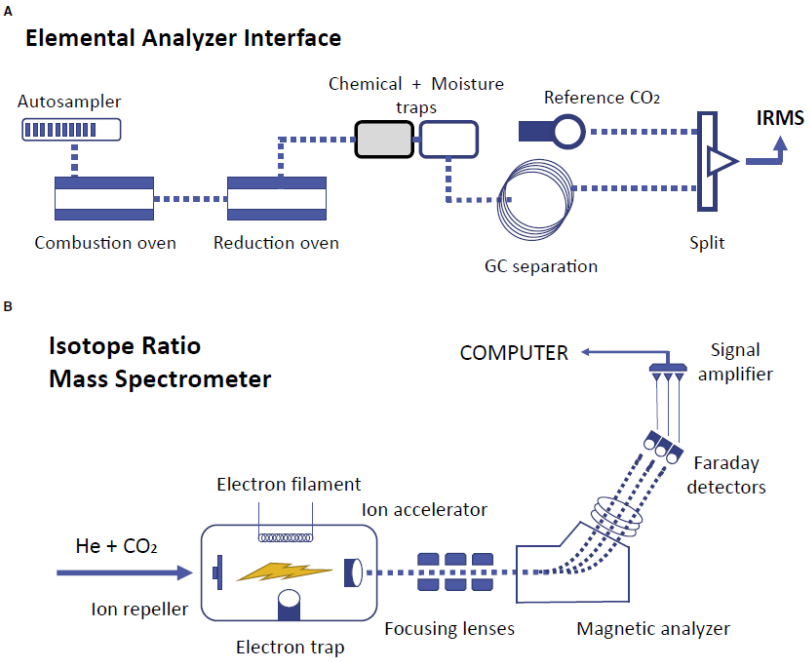

Figure 2 IRMS instrumentation: panel A, elemental analyzer; panel B, isotope-ratio mass spectrometer. The schemes were adapted from Muccio, Z., Jackson, G. P., 2009. Isotope ratio mass spectrometry. Analyst 134, 213-222. DOI: 10.1039/B808232D.

carbon atoms to minimize $\delta^{13}C$ errors [$\delta = 1000\ (R_{sample} - R_{standard})/R_{standard}$, where R is the abundance ratio of the minor (heavier) isotope to the major (lighter) isotope]. Coupling to liquid chromatography (LC) is less frequent but a commercial system is already available on the market and has been shown reliable for wine analysis (Cabañero et al., 2008). Elemental analysis (EA) yields only an average isotopic value of the entire sample (solid or liquid). Usually, $^{13}C/^{12}C$ isotope ratio is analyzed. Here, after the sample combustion, the produced CO_2 is separated from nitrogen and oxygen. Chromatographic sample separations prior to IRMS provide higher discriminative power and hence they are applicable to complex mixtures (Muccio and Jackson, 2009). In the commercial interface for coupling HPLC to IRMS, organic compounds in the eluate are converted to CO_2 by an oxidizing agent (e.g. ammonium peroxodisulfate) in the presence of a catalyst. Wine analysis by $^{13}C/^{12}C$ ratio measurements using EA coupled to IRMS is based on the contained ethanol and its preceding extraction by a distillation (Bréas et al., 1994). The residual water from the distillation is utilized to analyze $^{18}O/^{16}O$ ratios after a prolonged equilibration with CO_2. The equilibrated CO_2 samples are processed by IRMS and compared with a reference CO_2 gas.

Phenolic compounds represent well-known natural wine components. They are produced as secondary metabolites in the grapevine and are extracted during the winemaking process, mostly from grape skin, but also from the flesh and seeds (Gonzalez-Nevez et al., 2012). According to the chemical structure, two major groups are recognized, namely flavonoids (including flavonols, flavanols – catechins, and anthocyanins) and non-flavonoids such as derivatives of hydroxybenzoic or hydroxycinnamic acids (Jackson, 2008, pp. 270–331). Interestingly, wines matured in oak barrels show elevated levels of ellagic acid that comes from hydrolyzable wood tannins. Flavonoids are much more contained in red wines than in white wines and comprise three characteristic rings in their structure: two phenolic rings (A and B) are interconnected by a central oxygen-containing heterocyclic (pyran) ring C; Fig. 3.

They exist as free, conjugated (commonly to sugars as glycosides or to acids as esters) and polymeric compounds, e.g. tannins (Panche et al., 2016). Flavonoids are stored in the central vacuole of the producing cells and are believed to function as defense molecules against microbes, pests and herbivores. The biosynthesis of phenolic compounds starts at phenylalanine (phenylpropanoid pathway) or acetic acid (polyketide pathway); in the case of flavonoids, both these routes are finally combined (Yu and Jez, 2008). Anthocyanins (Fig. 3), glycosides of flavonoid anthocyanidins, are known as the determinants of the characteristic color of red wine, which is influenced in its hue by the hydroxylation pattern of the B ring. Grapevine cultivars synthesize only monoglucosidic anthocyanins, whereas first generation interspecies crossbreeds additionally produce diglucosides which presence in red wines has been suggested to indicate the use of hybrid grapes (Jackson, 2008, pp. 270–331). Anyway, phenolics in wine can successfully be utilized for the assessment of its authenticity: differences in their proportion and amount are attributable to the varietal type, maturity as well as geographic origin (Gonzalez-Neves et al., 2012). HPLC has been established as a powerful separation technique for fingerprinting of wine anthocyanins when coupled to a spectroscopic or mass spectrometric detection (Kumšta et al., 2014; Papoušková et al., 2011). When analytical results are processed in a table, the determined concentrations of individual anthocyanins (columns in the data matrix, i.e. variables) are correlated with the respective wine samples characterized by their grape variety and/or geographic origin (rows in the matrix, i.e. observations) (Papoušková et al., 2011). This data set is subjected to a multivariate statistical analysis, commonly using principal component analysis (PCA), which is applied to reduce the dimension of multivariate data sets and provide a low-dimensional plot instead of the given multivariate table. This plot then reveals groups of observations and allows uncovering of the existing relationships (Eriksson et al., 2013, pp. 33–54). PCA is done by an orthogonal transformation of the original correlated values into a set of new linearly uncorrelated variables (principal components). The first principal component has the largest possible variance. Succeeding components are of largest variance possible at their orthogonality to the preceding components. A direct and fast but not quantitative fingerprinting of anthocyanins from wine and grape samples without any previous chromatographic separation or enrichment steps is feasible using matrix-assisted laser desorption/ionization time-of-flight mass spectrometry (MALDI-TOF). 2,5-Dihydroxybenzoic acid has been repeatedly shown as an optimal matrix compound for this purpose (Carpentieri et al., 2007; Ivanova et al., 2011). Similarly, ESI-MS fingerprinting in the negative ion mode with a direct injection of wine and must has been found useful for quality control during and after fermentation. The method allowed a varietal traceability based on diagnostic signals of low-molecular-weight compounds. Must and wine samples could be reliably distinguished: none of the observed marker ions for the unfermented must samples assigned to sugar molecules was found in wine. Also a sucrose or must addition to wine was recognizable in this way (Catharino et al., 2006).

3.09.5 Wine Proteins

Proteins represent only a minor constituent of wine (the amount is generally from tens to several hundred milligrams per liter), but they contribute significantly to its quality because of affecting clarity and stability. There is a particular importance for champagne wines because of their role in the formation and persistence of foam in a glass (Ferreira et al., 2001). Wine proteins originate from the grapevine and yeast and are stable enough to survive the vinification process and low pH of around 3 of the final product. In the case of an infection of the harvested grapes by pathogens such as *Botrytis cinerea* (a fungus), also pathogen-derived proteins are clearly detectable (Kwon, 2004; Perutka et al., 2019). Wines are essentially composed of identical protein groups. A majority of wine proteins fall in the molecular mass range of around 20–30 kDa. This specific group particularly contains grape chitinases and thaumatin-like proteins (TLPs), which belong to pathogenesis-related proteins (PR proteins): PR-3 and PR-5 family, respectively (Table 1) (Enoki and Suzuki, 2016).

The PR proteins are known as haze-active and thus responsible for the unattractive turbidity (haze) and proteinaceous sediments of bottled wine. They are soluble under acidic conditions and highly resistant to proteolysis or a bentonite treatment, which is

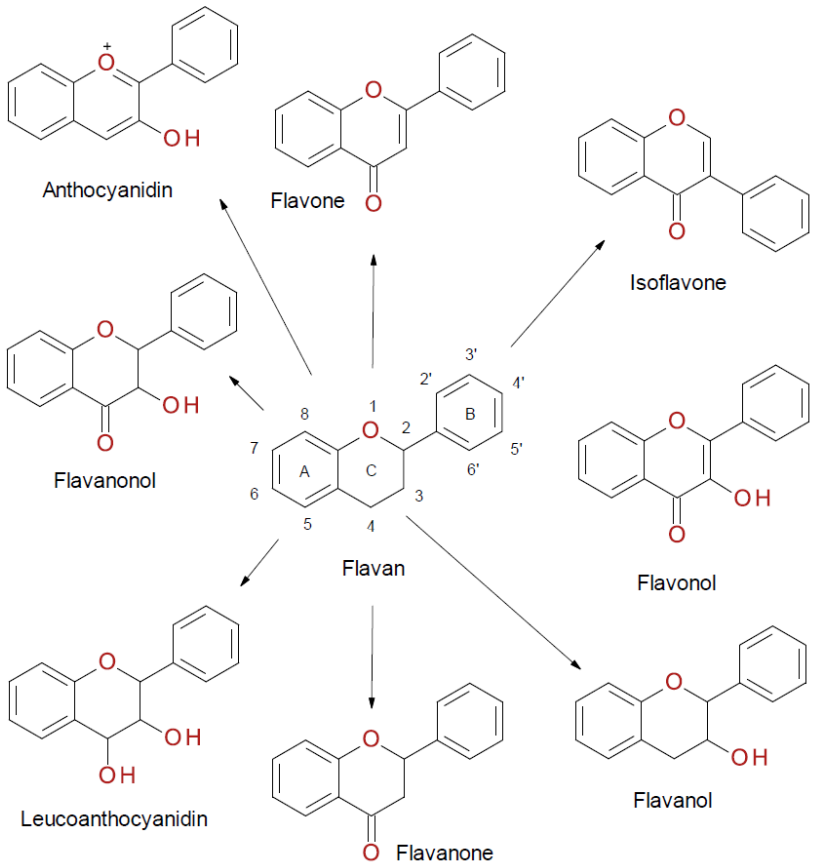

Figure 3 Flavonoid compounds. All chemical formulas were adapted from Jackson, R. S., 2008. Wine Science: Principles and Applications, third ed. Academic Press, Amsterdam, pp. 270–331 and Panche, A. N., Diwan, A. D., Chandra, S. R., 2016. Flavonoids: an overview. J. Nutr. Sci. 5, e47. DOI: 10.1017/jns.2016.41.

commonly applied to prevent haze formation (Waters et al., 1996; Ferreira et al., 2001). Despite the sequence similarity of TLPs to genuine thaumatins, intensively sweet proteins, it is unlikely that they would contribute to the sweetness of wine. The protein content of grape juice differs from that of the final wine. Most of the grape proteins are lost during vinification, primarily because of the fermentation (Ferreira et al., 2000). PR proteins are produced at the onset of ripening (veraison, berry softening) in parallel with the growing accumulation of sugars. They are generally increased in plants as a consequence of pathogen attack or wounding process. Mature grapes harvested at the same place in several successive years accumulate the same set of PR proteins but in different proportions reflecting a variability of the encountered stress conditions (Ferreira et al., 2001). Chitinases and TLPs are highly conserved but exist in more isoforms, which slightly differ in their molecular masses. It has been shown that such mass differences may be useful for an MS-based varietal differentiation (Hayasaka et al., 2001). Biochemical experiments (e.g. N-terminal sequencing) revealed that the similar proteins are possibly derived from a few common precursors undergoing a limited proteolytic processing, which occurs at the end of grape maturation or during vinification. Other *Vitis vinifera* proteins (Fig. 4), which have been identified in wine, include e.g. vacuolar invertase, cysteine protease, lipid transfer protein, osmotin and stellacyanin (Kwon, 2004;

Table 1 PR-proteins in wine

PR-protein family	*Property*	*Function/target site*
PR-1	Antifungal	Unknown
PR-2	β-1,3-Glucanase	Cell wall (β-1,3-glucan)
PR-3	Chitinase (types I, II, IV, V, VI, and VII)	Cell wall (chitin)
PR-4	Chitinase (types I and II)	Cell wall (chitin)
PR-5	Thaumatin-like	Plasma membrane
PR-10	Ribonuclease (like)	RNA
PR-14	Lipid-transfer protein	Involvement in defense signaling pathway
PR-15	Oxalate oxidase	H_2O_2 production with antimicrobial activity
PR-16	Oxalate oxidase-like protein	H_2O_2 production with antimicrobial activity

The table was adapted from Enoki, S., Suzuki, S., 2016. Pathogenesis-related proteins in grape. In: Morata, A., Loira, I. (Eds.), Grape and Wine Biotechnology, pp 43–57. IntechOpen, London.

Marangon et al., 2009; Perutka et al., 2019). Invertase is generally considered haze-inactive as it is more stable than TLPs and chitinases (Marangon et al., 2011).

But recently, high-proline proteins were suggested to contribute to the haze formation in wine produced from partially botrytized grapes (Perutka et al., 2019).

Protein instability of white wines is one of the most common non-microbial wine defects. It is caused by improper storage and transportation conditions: especially elevated temperature induces a structural unfolding of haze-active proteins and their association with nearby proteins or other wine components to form aggregates. The mechanism resides in the presence of newly exposed amino acid side chains (originally hidden in the protein core), which become free to associate as a result of the unfolding process (Marangon et al., 2014). But the development of haze does not depend solely on proteins. Additionally it is influenced by other factors such as the content of polyphenols and polysaccharides as well as wine pH (Mesquíta et al., 2001). Previous routine used to determine the protein content of wine via the total nitrogen by Kjeldahl's method. Various methods have been described to evaluate wine stability including spectrophotometric heat tests (Hsu and Heatherbell, 1987). Yeast mannoproteins, grape

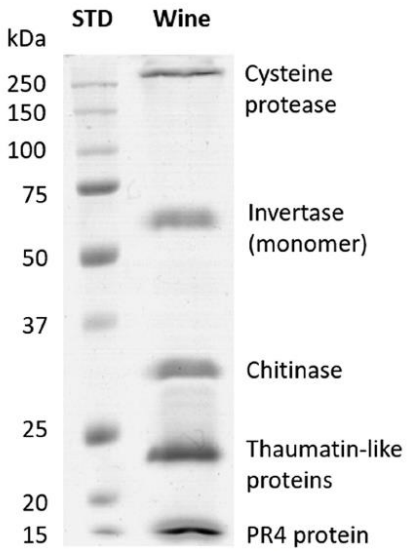

Figure 4 Sodium dodecylsulfate-polyacrylamide gel electrophoresis of wine proteins. The sample was obtained by concentrating a nouveau white wine using ultrafiltration with a 10-kDa cut off filter. From the left, protein standards with the indicated molecular mass, wine proteins; the gel was stained with Bio-Safe Coomassie Stain (Bio-Rad, Hercules, CA, USA). The annotation provided on the right comes from the results of nanoLC-MALDI-TOF/TOF MS/MS analyses after in-gel digestion of the respective proteins visualized as bands by the staining (Perutka, Z. and Šebela, M.; unpublished results).

arabinogalactan-proteins (AGPs) and other polysaccharide compounds (e.g. rhamnogalacturonan), which carry negative charges in the pH conditions of wine, may establish charge interactions with other wine components and produce complexes (Vernhet et al., 1996). Some of them are considered haze-protective (Waters et al., 1994). Hence the addition of polysaccharides to wine may represent an alternative to the removal of haze-forming wine proteins using bentonite adsorption or proteolysis. Their effect resides in decreasing the particle size of the haze rather than preventing protein aggregation (Waters et al., 2005). Young red wines are treated for colloidal stabilization with *Acacia senegal* gum (Acacia gum). It contains highly glycosylated hydroxyproline-rich AGPs, which bind to polyphenols. Interestingly, it has been demonstrated that the more the AGPs are rich in their protein content, the more effective stabilizers they are (Nigen et al., 2019).

Botrytis (gray mold) infection of grapes yields reduced protein levels in the juice. This observation has been elucidated by the presence of proteolytic enzymes from *B. cinerea*, which degrade grape proteins (Marchal et al., 1998). Wines made from Botrytis-infected grapes are markedly depleted in the *Saccharomyces cerevisiae* protein Seripauperin-5 (~17 kDa). The absence of this protein has also been observed for gushing sparkling wines and thus suggested as a biomarker of gushing (Kupfer et al., 2017). Recently, white wines of the Sauvignon and Welschriesling varieties were analyzed for their protein content by MS-based proteomics. The Sauvignon wine was made from grapes partially (and non-intentionally) damaged by *B. cinerea*, whereas the Welschriesling wine was a specific product obtained from fully botrytized bunches (Perutka et al., 2019). Interestingly, whereas the former sample contained *V. vinifera*, *S. cerevisiae*, and *B. cinerea* proteins, the protein content of the latter one was in a vast majority composed of *B. cinerea* proteins. Except for the oxidoreducing enzyme laccase acting on diphenols, which is known as a virulence factor (Buddhika, 2017), numerous hydrolytic enzymes (proteases, peptidases, esterases and glycoside hydrolases) were found. Thus, it is obvious that the exclusive or partial contribution of *B. cinerea* proteins to the total protein content of a wine may represent a clear marker of the input quality of grapes.

Wine proteomics studies have used numerous methods including sample treatment with a semi-permeable membrane (dialysis, ultrafiltration), 1-D or 2-D gel electrophoresis, isoelectric focusing, solid phase extraction, and liquid chromatography (advantageous namely for peptides from proteins digests). More than 300 proteins were identified in a Chardonnay wine using 2-D electrophoresis of chromatographic fractions, blotting and N-terminal Edman sequencing (Okuda et al., 2006). The efficiency of capillary electrophoresis and HPLC has successfully been combined with the accuracy, sensitivity and resolving power of MS. Both electrospray ionization (ESI) and MALDI are applicable for the characterization and identification of wine proteins (Flamini and Rosso, 2006). For published fingerprinting analyses, wine samples were either applied directly without any previous treatment or processed to achieve a preconcentration of proteins and removal of interfering compounds: (1) ultrafiltered, (2) dialyzed plus lyophilized, or (3) subjected to a precipitation step with organic solvents (Nunes-Miranda et al., 2013). So far, MALDI-TOF mass spectrometric fingerprinting has predominantly been employed for white wine samples as red wines are more complex and challenging for the extraction of peptides and proteins. The first report on the use of MALDI-TOF MS for analyzing wine proteins appeared already in 1996 (Szilágyi et al., 1996). In that study, protein ions were observed in the *m/z* region from 5000 to 25,000. The authors emphasized the presence of glycoproteins as deduced from the observed signal series, where neighboring peaks were spaced by a mass difference of one hexose unit. The analysis of two different wine types (Chardonnay and Sauvignon) indicated obvious discriminative capabilities of protein fingerprint mass spectra. Since that time, many experimental methods involving MALDI-TOF MS have been developed and optimized for white wines (Nunes-Miranda et al., 2012; Rešetar et al., 2015) as well as red wines (Vogt et al., 2016).

The aim of national integrated food control systems is not restricted only to the detection of risky products (for food safety) as they largely contribute also to the assurance of quality and authenticity. In the case of wine, quality products are made from grapes of a relatively low number of varieties. High quality white wines from the Italian region Campania produced from different *V. vinifera* cultivars were analyzed by MALDI-TOF MS to develop a rapid method for quality and authenticity tracing (Chambery et al., 2009). The principle was based on a protein extraction step (using chloroform/methanol, 1:1, v/v) followed by dissolving of the collected proteins and the subsequent whole-extract tryptic digestion. The obtained peptides were subjected to MS measurements for acquiring peptide profiles, which revealed the presence of common diagnostic ions as well as differences utilizable for a discrimination of samples. Measuring with peptides instead of intact proteins resulted in higher sensitivity. Fingerprint mass spectra were converted to a graphical bar code-like representation ("mass codes"), which was suggested as a tool for fast wine monitoring (Chambery et al., 2009). The fingerprinting studies have clearly demonstrated their applicability, but a real practical use is still very limited. Commonly, a small number of samples are analyzed, which precludes meaningful statistics. There is also no centralized reference database available (Nunes-Miranda et al., 2013).

3.09.6 Conclusions

Drinking wine on the occasion of ceremonials, celebrations, parties and other festive events as well as for pleasure on ordinary days represents a long lasting tradition in the society. Consumers often look for wine of a high or at least good standard quality and they expect adequate purchasing costs. In addition, they decide based on bottle labels as the producer name and place of origin is often perceived as a guarantee of satisfaction. This is the reason why the control system has been established in many countries to monitor quality and protect authenticity. Wine frauds especially adulterations not only dissatisfy customers. The use of harmful colorants or sweeteners brings health risks. It is also obvious that imitations and label frauds may damage the reputation and cause economic losses of conscientious producers.

Comprehensive Foodomics, 2021, 104–116

Modern bioanalytical and biochemical methods employed in wine analysis can detect natural inorganic and organic constituents, unnatural additives, contaminants and adulterants. They are well suited for both quality control and detection of wine frauds or legislation and best practice non-conformities. NMR and IRMS are of eminent importance in the determination of isotope ratios on the way to evaluation of the geographical authenticity of wine. Additionally, the isotope profile of wine compounds such as ethanol, glucose, glycerol, carboxylic acids and wine water may confirm or disprove suspicions as regards to a potential adulteration. MALDI-TOF mass spectrometric fingerprinting of anthocyanins allows an easy, direct and fast differentiation of grape varieties. MS detection of wine constituents is commonly coupled to efficient sample separation techniques such as LC or GC. On the other hand, gel electrophoresis is well applicable to analyze wine proteins. It has been shown that PR proteins (thaumatin-like proteins are chitinases) are prone to a thermally-induced aggregation, which leads to the formation of haze in bottled wine. But wine contains not only grape and yeast proteins. Excessive damage of grapes by the pathogen *B. cinerea* is reflected in the presence of related fungal proteins. Thus wine proteomics analyses may provide data on the quality of the input grape material.

Acknowledgments

This work was supported from ERDF project "Plants as a tool for sustainable global development" (No. CZ.02.1.01/0.0/0.0/16_019/0000827).

References

Almeida, C.M.R., Vasconcelos, M.T.S.D., 2004. Does winemaking process influence the wine $^{87}Sr/^{86}Sr$? A case study. Food Chem. 85, 7–12. https://doi.org/10.1016/j.foodchem.2003.05.003.

Andrusiów, S., 2015. Vina Originální Certifikace (Original Certification Wines). Bachelor Thesis. Faculty of Horticulture, Mendel University in Brno, Lednice (Czech Republic).

Barata, A., Malfeito-Ferreira, M., Loureiro, V., 2012. The microbial ecology of wine grape berries. Int. J. Food Microbiol. 153, 243–259. https://doi.org/10.1016/j.ijfoodmicro.2011.11.025.

Belli, N., Marin, S., Sanchis, V., Ramos, A.J., 2002. Review: ochratoxin A (OTA) in wines, musts and grape juices: occurrence, regulations and methods of analysis. Food Sci. Technol. Int. 8, 325–335. https://doi.org/10.1106/108201302031863.

Bertrand, A., Beloqui, A.A., 2009. Aromatic spoilage of wines by raw materials and enological products. In: Moreno-Arribas, M.V., Polo, M.C. (Eds.), Wine Chemistry and Biochemistry. Springer, New York, pp. 595–613.

Bevin, C.J., Fergusson, A.J., Perry, W.B., Janik, L.J., Cozzolino, D., 2006. Development of a rapid "fingerprinting" system for wine authenticity by mid-infrared spectroscopy. J. Agric. Food Chem. 54, 9713–9718. https://doi.org/10.1021/jf062265o.

Bréas, O., Reniero, F., Serrini, G., 1994. Isotope ratio mass spectrometry: analysis of wines from different European countries. Rapid Commun. Mass Spectrom. 8, 967–970. https://doi.org/10.1002/rcm.1290081212.

Buddhika, A., 2017. Role of Laccase as a Virulence Factor in the Infection of Grapes by Botrytis Cinerea. Doctoral thesis. School of Agricultural and Wine Sciences, Charles Sturt University, Waga Waga (Australia).

Burda, K., Collins, M., 1991. Adulteration of wine with sorbitol and apple juice. J. Food Protect. 54, 381–382. https://doi.org/10.4315/0362-028X-54.5.381.

Buser, H.R., Zanier, C., Tanner, H., 1982. Identification of 2,4,6-trichloroanisole as a potent compound causing cork taint in wine. J. Agric. Food Chem. 30, 359–362. https://doi.org/10.1021/jf00110a037.

Cabañero, A.I., Recio, J.L., Rupérez, M., 2008. Isotope ratio mass spectrometry coupled to liquid and gas chromatography for wine ethanol characterization. Rapid Commun. Mass Spectrom. 22, 3111–3118. https://doi.org/10.1002/rcm.3711.

Cabras, P., Caboni, P., 2008. Analysis of pesticide residues in grape and wine. In: Flamini, R. (Ed.), Hyphenated Techniques in Grape and Wine Chemistry. John Wiley & Sons, Chichester, pp. 227–248. https://doi.org/10.1002/9780470754320.ch6.

Cagliani, L., Scano, P., Consonni, R., 2009. NMR spectroscopy. In: Franca, A.S., Nollet, L.M.L. (Eds.), Spectroscopic Methods in Food Analysis. CRC Press, Boca Raton, pp. 143–188.

Camin, F., Bontempo, L., Perini, M., Piasentier, E., 2016. Stable isotope ratio analysis for assessing the authenticity of food of animal origin. Compr. Rev. Food Sci. Food Saf. 15, 868–877. https://doi.org/10.1111/1541-4337.12219.

Capone, D.L., Skouroumounis, G.K., Sefton, M.A., 2002. Permeation of 2, 4, 6-trichloroanisole through cork closures in wine bottles. Aust. J. Grape Wine Res. 8, 196–199. https://doi.org/10.1111/j.1755-0238.2002.tb00256.x.

Carpentieri, A., Marino, G., Amoresano, A., 2007. Rapid fingerprinting of red wines by MALDI mass spectrometry. Anal. Bioanal. Chem. 389, 969–982. https://doi.org/10.1007/s00216-007-1476-8.

Catharino, R.R., Cunha, I.B.S., Fogaça, A.O., et al., 2006. Characterization of must and wine of six varieties of grapes by direct infusion electrospray ionization mass spectrometry. J. Mass Spectrom. 41, 185–190. https://doi.org/10.1002/jms.976.

Cei, L., Defrancesco, E., Stefani, G., 2018. From geographical indications to rural development: a review of the economic effects of European Union policy. Sustainability 10, 3745. https://doi.org/10.3390/su10103745.

Chambery, A., del Monaco, G., Di Maro, A., Parente, A., 2009. Peptide fingerprint of high quality Campania white wines by MALDI-TOF mass spectrometry. Food Chem. 113, 1283–1289. https://doi.org/10.1016/j.foodchem.2008.08.031.

Christoph, N., Hermann, A., Wachter, H., 2015. 25 years authentication of wine with stable isotope analysis in the European Union – review and outlook. In: BIO Web of Conferences, vol. 5, p. 02020. https://doi.org/10.1051/bioconf/20150502020.

Ciepielowski, G., Pacholczyk-Sienicka, B., Fraczek, T., et al., 2018. Comparison of quantitative NMR and IRMS for the authentication of 'polish vodka'. J. Sci. Food Agric. 99, 263–268. https://doi.org/10.1002/jsfa.9168.

D'Amato, A., Kravchuk, A.V., Bachi, A., Righetti, P.G., 2010. Noah's nectar: the proteome content of a glass of red wine. J. Proteom. 73, 2370–2377. https://doi.org/10.1016/j.jprot.2010.08.010.

Dennis, M.J., Massey, R.C., Bigwood, T., 1994. Investigation of the sorbitol content of wines and an assessment of its authenticity using stable isotope ratio mass spectrometry. Analyst 119, 2057–2060. https://doi.org/10.1039/an9941902057.

Di Vita, G., Caracciolo, F., Brun, F., D'Amico, M., 2019. Picking out a wine: consumer motivation behind different quality wines choice. Wine Econ. Policy 8, 16–27. https://doi.org/10.1016/j.wep.2019.02.002.

Dixit, V., Tewari, J.C., Cho, B.K., Irudayaraj, J.M.K., 2005. Identification and quantification of industrial grade glycerol adulteration in red wine with Fourier transform infrared spectroscopy using chemometrics and artificial neural networks. Appl. Spectrosc. 59, 1553–1561. https://doi.org/10.1366/00037020577514263.

do Nascimento Silva, F.L., Schmidt, E.M., Messias, C.L., Eberlin, M.N., Sawaya, A.C.H.F., 2015. Quantitation of organic acids in wine and grapes by direct infusion electrospray ionization mass spectrometry. Anal. Methods 7, 53–62. https://doi.org/10.1039/C4AY00114A.
Dordevic, N., Camin, F., Marianella, R.M., et al., 2013. Detecting the addition of sugar and water to wine. Aust. J. Grape Wine Res. 19, 324–330. https://doi.org/10.1111/ajgw.12043.
Enoki, S., Suzuki, S., 2016. Pathogenesis-related proteins in grape. In: Morata, A., Loira, I. (Eds.), Grape and Wine Biotechnology. IntechOpen, London, pp. 43–57.
Eriksson, L., Byrne, T., Johansson, E., Trygg, J., Vikström, C., 2013. Multi- and Megavariate Data Analysis. Basic Principles and Applications, third ed. Umetrics Academy, Umeå.
Fauhl, C., Wittkowski, R., 2000. Oenological influences on the D/H ratios of wine ethanol. J. Agric. Food Chem. 48, 3979–3984. https://doi.org/10.1021/jf000251r.
Ferreira, R.B., Monteiro, S., Piçarra-Pereira, M.A., et al., 2000. Characterization of the proteins from grapes and wines by immunological methods. Am. J. Enol. Vitic. 51, 22–28.
Ferreira, R.B., Piçarra-Pereira, M.A., Monteiro, S., Loureiro, V.B., Teixeira, A.R., 2001. The wine proteins. Trends Food Sci. Technol. 12, 230–239. https://doi.org/10.1016/S0924-2244(01)00080-2.
Ferrier, J.G., Block, D.E., 2001. Neural-network-assisted optimization of wine blending based on sensory analysis. Am. J. Enol. Vitic. 52, 386–395.
Flamini, R., De Rosso, M., 2006. Mass spectrometry in the analysis of grape and wine protein. Expet Rev. Proteomics 3, 321–331. https://doi.org/10.1586/14789450.3.3.321.
Fournier, E., Gladieux, P., Giraud, T., 2013. The 'Dr Jekyll and Mr Hyde fungus': noble rot versus gray mold symptoms of *Botrytis cinerea* on grapes. Evol. Appl. 6, 960–969. https://doi.org/10.1111/eva.12079.
Fregoni, M., 1992. Changes to Italy's wine legislation: the *Nuova disciplina delle denomination d'origine dei vini*. J. Wine Res. 3, 123–136. https://doi.org/10.1080/09571269208717925.
Galaup, C., Auriel, L., Dubs, J., Dehoux, C., et al., 2019. Blue wine, a color obtained with synthetic blue dye addition: two case studies. Eur. Food Res. Technol. 245, 1777–1782. https://doi.org/10.1007/s00217-019-03295-z.
Garde-Cerdán, T., Ancín-Azpilicueta, C., 2006. Review of quality factors on wine ageing in oak barrels. Trends Food Sci. Technol. 17, 438–447. https://doi.org/10.1016/j.tifs.2006.01.008.
Geana, E.I., Iordache, A.M., Ionete, R.E., 2012. Simultaneous determination of artificial sweeteners in possible counterfeited wines, using high performance liquid chromatography with DAD detection. Ovidius Univ. Ann. Chem. 23, 77–81. https://doi.org/10.2478/v10310-012-0012-7.
Geana, E.I., Popescu, R., Costinel, D., et al., 2016. Verifying the red wines adulteration through isotopic and chromatographic investigations coupled with multivariate statistic interpretation of the data. Food Contr. 62, 1–9. https://doi.org/10.1016/j.foodcont.2015.10.003.
Gonzales-Neves, G., Gil, G., Favre, G., Ferrer, M., 2012. Influence of grape composition and winemaking on the anthocyanin composition of red wines of Tannat. Int. J. Food Sci. Technol. 47, 900–909. https://doi.org/10.1111/j.1365-2621.2011.02920.x.
Grbin, P.R., Herderich, M., Markides, A., Lee, T.H., Henschke, P.A., 2007. The role of lysine amino nitrogen in the biosynthesis of mousy off-flavor compounds by *Dekkera anomala*. J. Agric. Food Chem. 55, 10872–10879. https://doi.org/10.1021/jf071243e.
Grimalt, S., Dehouck, P., 2016. Review of analytical methods for the determination of pesticide residues in grapes. J. Chromatogr. A 1433, 1–23. https://doi.org/10.1016/j.chroma.2015.12.076.
Hájková, L., Voženílek, V., Tolasz, R., 2012. Atlas Fenologických PoměrŮ Česka (Atlas of the Phenological Conditions in Czechia). Czech Hydrometeorological Institute and Palacký University in Olomouc, Prague-Olomouc.
Hayasaka, Y., Adams, K.S., Pocock, K.F., et al., 2001. Use of electrospray mass spectrometry for mass determination of grape (*Vitis vinifera*) juice proteins: a potential tool for varietal differentiation. J. Agric. Food Chem. 49, 1830–1839. https://doi.org/10.1021/jf001163+.
He, Z., Xu, Y., Wang, L., et al., 2016. Wide-scope screening and quantification of 50 pesticides in wine by liquid chromatography/quadrupole time-of-flight mass spectrometry combined with liquid chromatography/quadrupole linear ion trap mass spectrometry. Food Chem. 196, 1248–1255. https://doi.org/10.1016/j.foodchem.2015.10.042.
Hodson, G., Wilkes, E., Azevedo, S., Battaglene, T., 2017. Methanol in wine. In: BIO Web of Conferences, vol. 9, p. 02028. https://doi.org/10.1051/bioconf/20170902028.
Holmberg, L., 2010. Wine fraud. Int. J. Wine Res. 2, 105–113. https://doi.org/10.2147/ijwr.s14102.
Hsu, J.C., Heatherbell, D.A., 1987. Heat-unstable proteins in wine. I. Characterization and removal by bentonite fining and heat treatment. Am. J. Enol. Vitic. 38, 11–16.
Hu, X.Z., Liu, S.Q., Li, X.H., et al., 2019. Geographical origin traceability of Cabernet Sauvignon wines based on infrared fingerprint technology combined with chemometrics. Sci. Rep. 9, 8256. https://doi.org/10.1038/s41598-019-44521-8.
Ivanova, V., Dörnyei, A., Stefova, M., et al., 2011. Rapid MALDI-TOF-MS detection of anthocyanins in wine and grape using different matrices. Food Anal. Methods 4, 108–115. https://doi.org/10.1007/s12161-010-9143-7.
Jaeckels, N., Bellinghausen, I., Fronk, P., et al., 2015. Assessment of sensitization to grape and wine allergens as possible causes of adverse reactions to wine: a pilot study. Clin. Transl. Allergy 5, 21. https://doi.org/10.1186/s13601-015-0065-8.
Jackson, R.S., 2008. Wine Science: Principles and Applications, third ed. Academic Press, Amsterdam.
Jackson, D.I., Lombard, P.B., 1993. Environmental and management practices affecting grape composition and wine quality-a review. Am. J. Enol. Vitic. 44, 409–430.
Järup, L., 2003. Hazards of heavy metal contamination. Br. Med. Bull. 68, 167–182. https://doi.org/10.1093/bmb/ldg032.
Kment, P., Mihaljevič, M., Ettler, V., et al., 2005. Differentiation of Czech wines using multielement composition – a comparison with vineyard soil. Food Chem. 91, 157–165. https://doi.org/10.1016/j.foodchem.2004.06.010.
Kumšta, M., Pavloušek, P., Kárník, P., 2014. Use of anthocyanin profiles when differentiating individual varietal wines and terroirs. Food Technol. Biotechnol. 52, 383–390. https://doi.org/10.17113/ftb.52.04.14.3650.
Kupfer, V.M., Vogt, E.I., Ziegler, T., Vogel, R.F., Niessen, R., 2017. Comparative protein profile analysis of wines made from *Botrytis cinerea* infected and healthy grapes reveals a novel biomarker for gushing in sparkling wine. Food Res. Int. 99, 501–509. https://doi.org/10.1016/j.foodres.2017.06.004.
Kwon, S.W., 2004. Profiling of soluble proteins in wine by nano-high-performance liquid chromatography/tandem mass spectrometry. J. Agric. Food Chem. 52, 7258–7263. https://doi.org/10.1021/jf048940g.
Lecat, B., Brouard, J., Chapuis, C., 2017. Fraud and counterfeit wines in France: an overview and perspectives. Br. Food J. 119, 84–104. https://doi.org/10.1108/BFJ-09-2016-0398.
Machado, A.F., Militão, S., Sarubbi, M.M., Brandelli, A., 2016. Pesticide residues screening in wine by mass spectrometry. In: BIO Web of Conferences, vol. 7, p. 4004. https://doi.org/10.1051/bioconf/20160704004.
Marangon, M., Van Sluyter, S.C., Haynes, P.A., Waters, E.J., 2009. Grape and wine proteins: their fractionation by hydrophobic interaction chromatography and identification by chromatographic and proteomic analysis. J. Agric. Food Chem. 57, 4415–4425. https://doi.org/10.1021/jf9000742.
Marangon, M., Van Sluyter, S.C., Neilson, K.A., et al., 2011. Roles of grape thaumatin-like protein and chitinase in white wine haze formation. J. Agric. Food Chem. 59, 733–740. https://doi.org/10.1021/jf1038234.
Marangon, M., Van Sluyter, S.C., Waters, E.J., Menz, R.I., 2014. Structure of haze forming proteins in white wines: *Vitis vinifera* thaumatin-like proteins. PLoS One 9, e113757. https://doi.org/10.1371/journal.pone.0113757.
Marchal, R., Berthier, L., Legendre, L., et al., 1998. Effects of *Botrytis cinerea* infection on the must protein electrophoretic characteristics. J. Agric. Food Chem. 46, 4945–4949. https://doi.org/10.1021/jf980453b.
Marchionni, S., Buccianti, A., Bollati, A., et al., 2016. Conservation of isotopic ratios during the winemaking process of "Red" wines to validate their use as geographic tracer. Food Chem. 190, 7–12. https://doi.org/10.1016/j.foodchem.2015.06.026.
Martin, G.J., 1990. The chemistry of chaptalization. Endeavour 14, 137–143. https://doi.org/10.1016/0160-9327(90)90007-E.
Martin, G.J., Martin, M.L., 1981. Deuterium labeling at the natural abundance level as studied by high field quantitative ^{2}H NMR. Tetrahedron Lett. 22, 3525–3528. https://doi.org/10.1016/S0040-4039(01)81948-1.

Martínez-Sierra, J.G., Moreno Sanz, F., Herrero Espílez, P., et al., 2010. Evaluation of different analytical strategies for the quantification of sulfur-containing biomolecules by HPLC-ICP-MS: application to the characterisation of ^{34}S-labelled yeast. J. Anal. At. Spectrom. 25, 989–997. https://doi.org/10.1039/B925366A.
Mateo, R., Medina, Á., Mateo, E.M., Mateo, F., Jiménez, M., 2007. An overview of ochratoxin A in beer and wine. Int. J. Food Microbiol. 119, 79–83. https://doi.org/10.1016/j.ijfoodmicro.2007.07.029.
Mato, I., Suárez-Luque, S., Huidobro, J.F., 2005. A review of the analytical methods to determine organic acids in grape juices and wines. Food Res. Int. 38, 1175–1188. https://doi.org/10.1016/j.foodres.2005.04.007.
Meena, M., Gupta, S.K., Swapnil, P., et al., 2017. *Alternaria* toxins: potential virulence factors and genes related to pathogenesis. Front. Microbiol. 8, 1451. https://doi.org/10.3389/fmicb.2017.01451.
Mehlomakulu, N.N., Setati, M.E., Divol, B., 2014. Characterization of novel killer toxins secreted by wine-related non-*Saccharomyces* yeasts and their action on *Brettanomyces* spp. Int. J. Food Microbiol. 188, 83–91. https://doi.org/10.1016/j.ijfoodmicro.2014.07.015.
Meloni, G., Swinnen, J., 2013. The Political economy of European wine regulations. J.Wine Econ. 8, 244–284. https://doi.org/10.1017/jwe.2013.33.
Mesquita, P.R., Piçarra-Pereira, M.A., Monteiro, S., et al., 2001. Effect of wine composition on protein stability. Am. J. Enol. Vitic. 52, 324–330.
Muccio, Z., Jackson, G.P., 2009. Isotope ratio mass spectrometry. Analyst 134, 213–222. https://doi.org/10.1039/B808232D.
Nigen, M., Valiente, R.A., Iturmendi, N., et al., 2019. The colloidal stabilization of young red wine by Acacia *senegal* gum: the involvement of the protein backbone from the protein-rich arabinogalactan-proteins. Food Hydrocoll. 97, 105176. https://doi.org/10.1016/j.foodhyd.2019.105176.
Nunes-Miranda, J.D., Santos, H.M., Reboiro-Jato, M., et al., 2012. Direct matrix assisted laser desorption ionization mass spectrometry-based analysis of wine as a powerful tool for classification purposes. Talanta 91, 72–76. https://doi.org/10.1016/j.talanta.2012.01.017.
Nunes-Miranda, J.D., Igrejas, G., Araujo, E., Reboiro-Jato, M., Capelo, J.L., 2013. Mass spectrometry-based fingerprinting of proteins & peptides in wine quality control: a critical overview. Crit. Rev. Food Sci. Nutr. 53, 751–759. https://doi.org/10.1080/10408398.2011.557514.
Okuda, T., Fukui, M., Takayanagi, T., Yokotsuka, K., 2006. Characterization of major stable proteins in Chardonnay wine. Food Sci. Technol. Res. 12, 131–136. https://doi.org/10.3136/fstr.12.131.
Ough, C.S., Crowell, E.A., 1987. Use of sulfur dioxide in winemaking. J. Food Sci. 52, 386–388. https://doi.org/10.1111/j.1365-2621.1987.tb06620.x.
Panche, A.N., Diwan, A.D., Chandra, S.R., 2016. Flavonoids: an overview. J. Nutr. Sci. 5, e47. https://doi.org/10.1017/jns.2016.41.
Papoušková, B., Bednář, P., Hron, K., et al., 2011. Advanced liquid chromatography/mass spectrometry profiling of anthocyanins in relation to set of red wine varieties certified in Czech Republic. J. Chromatogr. A 1218, 7581–7591. https://doi.org/10.1016/j.chroma.2011.07.027.
Perrot, F., Hubert, P., Marquet, C., et al., 2012. Evidence of ^{131}I and ^{134,137}Cs activities in Bordeaux, France due to the Fukushima nuclear accident. J. Environ. Radioact. 114, 61–65. https://doi.org/10.1016/j.jenvrad.2011.12.026.
Perutka, Z., Šufeisl, M., Strnad, M., Šebela, M., 2019. High-proline proteins in experimental hazy white wine produced from partially botrytized grapes. Biotechnol. Appl. Biochem. 66, 398–411. https://doi.org/10.1002/bab.1736.
Petrozziello, M., Asproudi, A., Guaita, M., et al., 2014. Influence of the matrix composition on the volatility and sensory perception of 4-ethylphenol and 4-ethylguaiacol in model wine solutions. Food Chem. 149, 197–202. https://doi.org/10.1016/j.foodchem.2013.10.098.
Petzinger, E., Ziegler, K., 2000. Ochratoxin A from a toxicological perspective. J. Vet. Pharmacol. Therapeut. 23, 91–98. https://doi.org/10.1046/j.1365-2885.2000.00244.x.
Pyrzyńska, K., 2004. Analytical methods for the determination of trace metals in wine. Crit. Rev. Anal. Chem. 34, 69–83. https://doi.org/10.1080/10408340490475858.
Rešetar, D., Marchetti-Deschmann, M., Allmaier, G., Peter Katalinić, J., Kraljević Pavelić, S., 2015. Matrix assisted laser desorption ionization mass spectrometry linear time-of-flight method for white wine fingerprinting and classification. Food Contr. 64, 157–164. https://doi.org/10.1016/j.foodcont.2015.12.035.
Saur, W.K., Crespi, H.L., Halevi, E.A., Katz, J.J., 1968. Deuterium isotope effects in the fermentation of hexoses to ethanol by *Saccharomyces cerevisiae*. I. Hydrogen exchange in the glycolytic pathway. Biochemistry 7, 3529–3536. https://doi.org/10.1021/bi00850a030.
Scott, P.M., Lawrence, G.A., Lau, B.P.Y., 2006. Analysis of wines, grape juices and cranberry juices for *Alternaria* toxins. Mycotoxin Res. 22, 142–147. https://doi.org/10.1007/BF02956778.
Šehović, Đ., Petravić, V., Marić, V., 2004. Glycerol and wine industry. Glycerol determination in grape must and wine. Kem. Ind. 53, 505–516. https://doi.org/10.15255/KUI.2003.025.
Stanziani, A., 2009. Information, quality and legal rules: wine adulteration in nineteenth century France. Bus. Hist. 51, 268–291. https://doi.org/10.1080/00076790902726616.
Stöckl, A., 2006. Austrian wine: developments after the wine scandal of 1985 and its current situation. In: 3rd International Wine Business Research Conference (6-7-8 July 2006). Montpellier.
Szilágyi, Z., Vas, G., Mády, G., Vékey, K., 1996. Investigation of macromolecules in wines by matrix-assisted laser desorption/ionization time-of-flight mass spectrometry. Rapid Commun. Mass Spectrom. 10, 1141–1143. https://doi.org/10.1002/(SICI)1097-0231(19960715)10:9<1141::AID-RCM607>3.0.CO;2-4.
Vernhet, A., Pellerin, P., Prieur, C., Osmianski, J., Moutounet, M., 1996. Charge properties of some grape and wine polysaccharide and polyphenolic fractions. Am. J. Enol. Vitic. 47, 25–29.
Virtanen, S., Ali-Mattila, E., Lehtonen, P., 1999. Determination of synthetic colorants and natural carmine in wines. OENO One 33, 145–147. https://doi.org/10.20870/oeno-one.1999.33.3.1027.
von Baer, D., Rentzsch, M., Hitschfeld, M.A., et al., 2008. Relevance of chromatographic efficiency in varietal authenticity verification of red wines based on their anthocyanin profiles: interference of pyranoanthocyanins formed during wine ageing. Anal. Chim. Acta 621, 52–56. https://doi.org/10.1016/j.aca.2007.11.034.
Vondráková, A., Vávra, A., Voženílek, V., 2013. Climatic regions of the Czech republic. J. Maps 9, 425–430. https://doi.org/10.1080/17445647.2013.800827.
Vogt, E.I., Kupfer, V.M., Vogel, R.F., Niessen, L., 2016. A novel preparation technique of red (sparkling) wine for protein analysis. EuPA Open Proteom. 11, 16–19. https://doi.org/10.1016/j.euprot.2016.03.001.
Waters, E.J., Alexander, G., Muhlack, R., et al., 2005. Preventing protein haze in bottled white wine. Aust. J. Grape Wine Res. 11, 215–225. https://doi.org/10.1111/j.1755-0238.2005.tb00289.x.
Waters, E.J., Pellerin, P., Brillouet, J.M., 1994. A *Saccharomyces* mannoprotein that protects wine from protein haze. Carbohydr. Polym. 23, 185–191. https://doi.org/10.1016/0144-8617(94)90101-5.
Waters, E.J., Shirley, N.J., Williams, P.J., 1996. Nuisance proteins of wine are grape pathogenesis-related proteins. J. Agric. Food Chem. 44, 3–5. https://doi.org/10.1021/jf9505584.
Weber, D., Rossmann, A., Schwarz, S., Schmidt, H.L., 1997. Correlations of carbon isotope ratios of wine ingredients for the improved detection of adulterations I. Organic acids and ethanol. Z. Lebensm. -Forsch. A 205, 158–164. https://doi.org/10.1007/s002170050145.
Yu, O., Jez, J.M., 2008. Nature's assembly line: biosynthesis of simple phenylpropanoids and polyketides. Plant J. 54, 750–762. https://doi.org/10.1111/j.1365-313X.2008.03436.x.